

WITHDRAWN
University of
Illinois Library
at Urbana-Champaign



LIBRARY
OF THE
UNIVERSITY
OF ILLINOIS

539.3

C54a3

cop. 3

REMOTE STORAGE



^A
Return this book on or before the
Latest Date stamped below.

University of Illinois Library

DUE

AP

~~DEC 20 1962~~

~~JAN 9 1964~~

~~MAR 10 1964~~

~~APR 10 1964~~

~~DEC 1 1964~~

~~APR 17 1965~~

~~MAY 18 1965~~

~~OCT 19 1965~~

~~APR 23 1966~~

~~MAY 7 1966~~

~~JUN 10 1966~~

~~OCT 12 1966~~

OCT 09 1980

OCT 09 1980

2-1
INTERNATIONAL SERIES IN PHYSICS

LEE A. DuBRIDGE, CONSULTING EDITOR

APPLIED X-RAYS

INTERNATIONAL SERIES IN PHYSICS

LEE A. DuBRIDGE, *Consulting Editor*

- Bacher and Goudsmit*—ATOMIC ENERGY STATES
Bitter—INTRODUCTION TO FERROMAGNETISM
Clark—APPLIED X-RAYS
Condon and Morse—QUANTUM MECHANICS
Curtis—ELECTRICAL MEASUREMENTS
Davey—CRYSTAL STRUCTURE AND ITS APPLICATIONS
Edwards—ANALYTIC AND VECTOR MECHANICS
Eldridge—THE PHYSICAL BASIS OF THINGS
Hardy and Perrin—THE PRINCIPLES OF OPTICS
Harnwell—PRINCIPLES OF ELECTRICITY AND ELECTRO-
MAGNETISM
Harnwell and Livingood—EXPERIMENTAL ATOMIC PHYSICS
Houston—PRINCIPLES OF MATHEMATICAL PHYSICS
Hughes and DuBridge—PHOTOELECTRIC PHENOMENA
Hund—HIGH-FREQUENCY MEASUREMENTS
Hund—PHENOMENA IN HIGH-FREQUENCY SYSTEMS
Kemble—THE FUNDAMENTAL PRINCIPLES OF QUANTUM
MECHANICS
Kennard—KINETIC THEORY OF GASES
Koller—THE PHYSICS OF ELECTRON TUBES
Morse—VIBRATION AND SOUND
Muskat—THE FLOW OF HOMOGENEOUS FLUIDS THROUGH
POROUS MEDIA
Pauling and Goudsmit—THE STRUCTURE OF LINE SPECTRA
Richtmyer—INTRODUCTION TO MODERN PHYSICS
Ruark and Urey—ATOMS, MOLECULES AND QUANTA
Slater—INTRODUCTION TO CHEMICAL PHYSICS
Slater and Frank—INTRODUCTION TO THEORETICAL
PHYSICS
Smythe—STATIC AND DYNAMIC ELECTRICITY
White—INTRODUCTION TO ATOMIC SPECTRA
Williams—MAGNETIC PHENOMENA
-

Dr. F. K. Richtmyer was consulting editor of the series from its inception in 1929 until his death in 1939.

LIBRARY
UNIVERSITY OF ILLINOIS
AT URBANA

APPLIED X-RAYS

BY

GEORGE L. CLARK, PH.D., D.Sc.

Professor of Chemistry, University of Illinois

THIRD EDITION

McGRAW-HILL BOOK COMPANY, INC.

NEW YORK AND LONDON

1940

COPYRIGHT, 1927, 1932, 1940, BY THE
MCGRAW-HILL BOOK COMPANY, INC.

PRINTED IN THE UNITED STATES OF AMERICA

*All rights reserved. This book, or
parts thereof, may not be reproduced
in any form without permission of
the publishers.*

THE MAPLE PRESS COMPANY, YORK, PA.

CLARK
JUN 1 1961
REMOTE STORAGE

*To Those Whose Faith, Inspiration, and Teaching Have
Been the Principal Challenge to This Effort:*

MY MOTHER AND FATHER

MY WIFE

DEAN WILLIAM MARTIN BLANCHARD *of DePauw University*

The Late PROFESSOR WILLIAM DUANE *of Harvard University*

SIR WILLIAM HENRY BRAGG

1140201

PREFACE TO THE THIRD EDITION

Eight more years have passed, and now we may begin to recognize signs of maturity in the young and ever-growing, multifold science of x-rays. These eight years since the appearance of the second edition of this book have been filled with intense research activities, industrial and chemical achievement, widening interest in and acceptance of the truth as it is disclosed by the invisible rays of Roentgen's discovery forty-five years ago. Since 1932, there has come into clearer relief a classification of applications of astounding scope—physics, electrical engineering, spectroscopy and atomic structure, chemical analysis, medical, industrial, and artistic diagnosis, photochemistry, genetics, biological identification, cancer therapy, crystallography, crystal chemistry, and ultimate fine-structure analysis of the inorganic and living world, from dust to a chromosome. We have become familiar now with million-and-a-half-volt x-ray tubes; tubes with rotating targets; tuned resonance transformers; vector model atoms; oranges, candy, canned fruit, frozen peas, subjected to routine x-ray examination in the interest always of quality; x-rays indispensable in the art gallery; activated water molecules and a new photochemistry; a tremendously impressive list of biological effects including a bombardment of living cells so that they swell by osmosis and burst; powerful new methods and concepts in analysis of ultimate crystalline and molecular structure from diffraction patterns; molecules in a sense drawing their own contour maps—and the rise of a new crystal chemistry; the downfall of the classical and rigid concepts of the chemical formula and the law of definite proportions for the solid state; a fascinatingly orderly science of architectural disorder in crystals, strange as it may seem; minerals, soils, clays, ceramics, and cements with a scheme of simplicity previously obscured by superficial and apparently hopeless complexity; perhaps greatest of all, the development of structure, synthesis, behavior, and use of materials with giant molecules—nylon, safety-glass plastics, synthetic rubber and native rubber, cellulose with its bendable

joint fringes, and the most important molecules in life, the proteins, culminating in living nerve, viruses, and elupein thymonucleate, which comes so near to the chromosome.

And so there is no apology for presenting the 1940 story of applied x-rays. It was useless to retain more than mere fragments of the 1932 version. The experiences of eighteen years of x-ray research and the teaching of a course in applied x-rays to graduate students for a dozen years have led, through many changes, finally to a logic of integrated presentation, which is at least partially satisfactory.

It has been necessary to bring the subject matter up to date, and this has involved not only expansion but also a changing viewpoint. For there is not so much need any longer for somewhat superficial missionary effort as for deepening interest to the point where the reader shall be eager to take for himself the steps toward the fundamental principles of interpretation of x-ray results. This is no small or easy task, but it has been attempted; and it is in this more rigorous and quantitative treatment that this new edition differs most markedly from the preceding one. And yet it is hoped that this effort to make the book more sufficient unto itself will not detract from the original intention, in 1926, of portraying x-rays as a great practical research tool in industry. It is our experience that every executive or scientist who finds himself interested in the possibilities of x-ray research or testing wants to make the effort really to understand, for example, what a diffraction pattern really means. The result is less mystery and a more usable knowledge.

Probably the greatest source of aid in improving logic, choice of material, and presentation—and it is sincerely hoped that these have been improved—has been the friendly counsel, constructive criticism, and personal inspiration received during a visit in 1938 to 41 x-ray laboratories in Europe. Colleagues whose names in the literature are almost synonymous with x-ray science became living, hospitable personalities. The author will forever remain indebted to this cherished group, especially to Sir William Bragg, Profs. W. L. Bragg, Astbury, Ewald, Wooster, Bernal, Shearer, Bradley, and Dorothy Crowfoot in England; Dr. Rawlins on behalf of the National Art Gallery, London; Dr. Fournier of the French Air Ministry in Paris; Prof. Trillat of Besançon; Profs. von Laue of Berlin, Schiebold of Leipzig, Glocker and Graf of

Stuttgart, Simon of Dresden, Mark, Kratky, Eirich, and Halla of Vienna, Meyer of Geneva, Rollier of Milan, and many others. Grateful acknowledgment is made to the French Air Ministry and the National Art Gallery of London for the very unusual privilege of reproducing choice photographs, which they have generously provided.

For invaluable and loyal help, without which the task would have been vastly more difficult, the author is, most of all, indebted to his immediate associates in the X-ray Laboratory at the University of Illinois, Drs. S. T. Gross, J. N. Mrgudich, and W. F. Bradley; and to one of the best and most enthusiastic groups of graduate students imaginable, not only because of their own creative research efforts in the field, but also because they have listened as severe, but constructive, critics to this manuscript. In the untimely death of Dean F. K. Richtmyer, Editor of the International Series in Physics, before this revision could be submitted for his judicious appraisal, the author has suffered with so many others a deep personal loss.

It is again impossible to give justly due credit specifically to so many utilized sources of material and to generous contributions of photographs. Thousands of papers have been examined. (Available reprints of papers since 1932, in the field of cellulose alone, make a file nearly two feet thick.) Especially helpful and heavily drawn upon have been the delightfully written "Crystal Chemistry" by Evans (Cambridge University Press), and also "Crystal Chemistry," by Stillwell, "The Nature of the Chemical Bond" by Pauling, the "Biography of Roentgen" by Glasser, and newer x-ray treatises by Glocker and Halla and Mark. These, and many other contributions, have made the subject what it is in 1940 and what it will be in the future.

GEORGE L. CLARK.

URBANA, ILL.,
May, 1940.

PREFACE TO THE FIRST EDITION

The primary motive underlying the preparation of this book is the presentation of x-rays as a new tool for industry.

The thirty-year-old science of x-rays is now broadening from the stage of pure or academic science to that of applied or industrial science. It has already to its credit a notable record of practical achievement.

There are, therefore, several interwoven phases of the science of x-rays, none of which can be neglected in the consideration of practical applications. The spectroscopy of x-rays, involving the measurement of radiation wave lengths, has been of immeasurable assistance to the physicist in his searching of atomic structures and of the interrelationships between matter and radiant energy. This phase of the science has found excellent expression in several books, particularly the authoritative exposition, recently translated into English, of the master experimenter and Nobel Prize recipient, Manne Siegbahn.

Scarcely more than twelve years ago, von Laue and the Braggs reasoned that the use of crystals should make it possible to measure wave lengths of x-rays, and hence that x-rays of known wave lengths might render possible the analysis of crystals of unknown ultimate structures. The complete verification of this prediction has led to the foundation of a chemical, physical, and engineering science of the solid state, which has yielded beyond all expectations exact knowledge of a previously little known subject. On this phase of the science of x-rays, again, excellent books have been written by the great pioneer Braggs, Ewald, Wyckoff, and others.

Now the science enters the industrial phase. This book aims to tell what this new tool is, how it may be used, what results it produces, why it can be applied to practical problems of everyday life and how industry is beginning to use it now. The book is the expression of a conviction that x-ray research and control methods can now and in the future be of invaluable service in the solution of problems of constitution and practical behavior of

metals and alloys of every kind, of catalysts, textile fibers (cotton, flax, jute, ramie, sisal, hemp, silk, wool, rayon), rubber, balata, gutta percha, resins, varnishes, lacquers, paints, pigments, dyes, enamels, carbon black, inorganic and organic chemicals, waxes, greases, soaps, oils, liquids of all kinds, dielectrics, storage battery oxides, colloidal metals and gels, patent leather, glass and its substitutes, gelatine, adhesives, abrasives, lime, plaster of paris, cement, ceramics, sugars, starches, biological systems, coal, gems, and numerous other substances.

I have tried to give the reader, whether he be the industrial executive or research director who is seeking to learn of a new method of attacking his problems, or the inquiring student or layman, a true and understandable survey of x-ray science as it is known to-day. This is not a handbook for the complete and precise determination by experts of wave lengths or crystal structures, but an outline of information for the intelligent inquirer who may himself never conduct a single x-ray experiment. I have hoped to make of it a missionary, which must speak an understandable language and have at hand the foundation facts to support its case.

The subject matter falls into a natural arrangement in three parts. The first eight chapters present the fundamental physics of x-rays; Chapters IX to XII cover the properties and applications of the radiation as such; the remaining chapters are concerned with the application to the study of crystalline structure.

Free usage has been made of most of the published books on x-rays. These include, besides those already mentioned, the excellent little monograph by Becker "*Die Roentgenstrahlen als Hilfsmittel für die Chemische Forschung*," Hirsch's "*Principles and Practice in Roentgen Therapy*," and the texts by de Broglie, Cermak, and Kaye. A large number of original papers, particularly the most recent contributions, have been consulted. Finally many experimental studies from my own laboratory, most of which have not been published, are included. The fact remains, of course, that in this rapidly growing science important advances have been made even during the preparation of the manuscript of this book.

I am deeply indebted, first of all, to Professor William Duane of Harvard University, pioneer and distinguished maker of light in the science of x-rays, whose inspirational guidance made

possible an enthusiastic acquaintance with this research tool; also to Professors W. K. Lewis, R. T. Haslam, and W. G. Whitman of the Massachusetts Institute of Technology, who as engineers had the vision of x-rays in industry, and the faith to install an x-ray laboratory and to provide the facilities for the task of writing this book; to my able assistant in authorship, Mr. Robert Landis Hershey; to my associates in x-ray research, particularly Dr. R. H. Aborn, Mr. E. W. Brugmann, and Dr. Marie Farnsworth; to my friend, Mr. J. P. Kelley, author of "Workmanship in Words," who has generously examined the manuscript with a critical eye on its English; and to my wife for her never-failing encouragement and for her assistance in the reading of manuscript and proof.

GEORGE L. CLARK.

CAMBRIDGE, MASSACHUSETTS,
November, 1926.

CONTENTS

| | |
|--|-------------|
| PREFACE TO THE THIRD EDITION | PAGE vii |
| PREFACE TO THE FIRST EDITION. | xi |

PART I GENERAL PHYSICS AND APPLICATIONS OF X-RADIATION

| | |
|--|-----|
| CHAPTER I | |
| BEFORE AND AFTER THE DISCOVERY BY ROENTGEN | 3 |
| CHAPTER II | |
| X-RAY TUBES. | 15 |
| CHAPTER III | |
| HIGH-TENSION EQUIPMENT | 44 |
| CHAPTER IV | |
| THE MEASUREMENT OF INTENSITY (DOSAGE). | 62 |
| CHAPTER V | |
| THE MEASUREMENT OF QUALITY (WAVE LENGTH). | 80 |
| CHAPTER VI | |
| X-RAY SPECTRA AND ATOMIC STRUCTURE. | 92 |
| CHAPTER VII | |
| CHEMICAL ANALYSIS FROM X-RAY SPECTRA. | 126 |
| CHAPTER VIII | |
| THE ABSORPTION AND SCATTERING OF X-RAYS. | 134 |
| CHAPTER IX | |
| RADIOGRAPHY. | 152 |
| CHAPTER X | |
| X-RAY PHOTOCHEMISTRY. | 185 |

CHAPTER XI

| | |
|--|-----|
| THE BIOLOGICAL EFFECTS OF X-RADIATION. | 198 |
|--|-----|

PART II

THE X-RAY ANALYSIS OF THE ULTIMATE
STRUCTURES OF MATERIALS

CHAPTER XII

| | |
|---|-----|
| CRYSTALLOGRAPHY AND X-RAY DIFFRACTION | 231 |
|---|-----|

CHAPTER XIII

| | |
|--|-----|
| THE EXPERIMENTAL X-RAY METHODS OF CRYSTAL ANALYSIS | 256 |
|--|-----|

CHAPTER XIV

| | |
|---|-----|
| THE INTERPRETATION OF DIFFRACTION PATTERNS IN TERMS OF ULTIMATE STRUCTURE. | 278 |
|---|-----|

CHAPTER XV

| | |
|--|-----|
| THE RESULTS OF CRYSTAL ANALYSIS: ELEMENTS AND INORGANIC COMPOUNDS | 324 |
|--|-----|

CHAPTER XVI

| | |
|---|-----|
| CRYSTAL CHEMISTRY: FUNDAMENTAL GENERALIZATIONS FROM EXPERIMENTAL DATA. | 337 |
|---|-----|

CHAPTER XVII

| | |
|---|-----|
| THE SILICATES. MINERALS, SOILS, CERAMICS, CEMENTS . | 375 |
|---|-----|

CHAPTER XVIII

| | |
|------------------|-----|
| ALLOYS | 390 |
|------------------|-----|

CHAPTER XIX

| | |
|--|-----|
| THE CRYSTALLINE AND MOLECULAR STRUCTURES OF ORGANIC COMPOUNDS | 415 |
|--|-----|

CHAPTER XX

| | |
|--|-----|
| THE STRUCTURE OF GLASSES, LIQUIDS, AND OTHER COL- LOIDAL AND AMORPHOUS MATERIALS. | 465 |
|--|-----|

CHAPTER XXI

| | |
|---|-----|
| THE INTERPRETATION OF DIFFRACTION PATTERNS IN TERMS OF GRAIN SIZE, ORIENTATION, INTERNAL STRAIN, AND MECHANICAL DEFORMATION | 489 |
|---|-----|

CONTENTS

xvii

PAGE

CHAPTER XXII

| | |
|--|-----|
| PRACTICAL APPLICATIONS OF X-RAY DIFFRACTION TO PROBLEMS OF THE METALLURGICAL INDUSTRY. | 554 |
|--|-----|

CHAPTER XXIII

| | |
|---|-----|
| POLYMERS—SYNTHETIC AND NATURAL MATERIALS WITH GIANT MOLECULES | 593 |
|---|-----|

| | |
|----------------|-----|
| INDEX. | 665 |
|----------------|-----|

PART I
GENERAL PHYSICS AND APPLICATIONS OF
X-RADIATION

CHAPTER I

BEFORE AND AFTER THE DISCOVERY BY ROENTGEN

The Experiment of Roentgen.—On Nov. 8, 1895, Wilhelm Konrad Roentgen, professor of physics at the University of Würzburg, Germany (Fig. 1), connected, as he had frequently done before, the terminals of a small induction coil with electrodes in an evacuated pear-shaped glass bulb. A similar apparatus might have been seen in laboratories of physics everywhere, for there was great interest in the phenomena of high-potential electrical discharges through vessels from which air had been pumped out as completely as possible. As far back as 1705 Hauksbee had observed flashes through evacuated spaces from electricity generated by friction. Abbé Nollet in 1753 had extended the observations with a series of bulbs. Morgan in 1785 had obtained a vacuum so high that no conduction occurred until a little gas was admitted to the tube. Faraday had discovered in 1825 a dark space in the luminous discharge between the electrodes if the residual gas pressure was low enough. In 1859 Plücker and in 1869 Hittorf had announced that in the process of electrical conduction through gases at very low pressures “cathode rays” move straight out

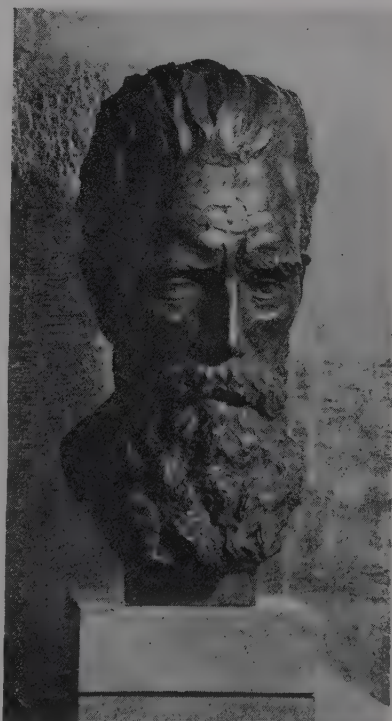


FIG. 1.—Bust of Roentgen at Lennep, his birthplace.

from the negative electrode, since they cast sharp shadows of any object placed between the cathode and the glass which the rays caused to fluoresce. Then, in a series of experiments over ten years, Sir William Crookes had greatly clarified the phenomena, particularly by his discovery that the rays were deflected by electric and magnetic fields and hence were probably negatively charged particles. In 1894 Lenard, the pupil of Hertz, succeeded in conducting the cathode rays through a thin metallic-foil window into the outer air. Such in brief was the state of affairs when Roentgen, among many others, undertook by further experiments to elucidate the nature of these cathode rays and the effects produced by them. Interested especially in the fluorescence produced when the rays impinged upon the glass walls of the tube, he covered the apparatus with black paper. In the darkened room the eyes of the experimenter beheld a brilliantly glowing screen of barium platinocyanide, placed some distance away from the Crookes tube. It was correctly deduced that an invisible radiation passing through the air from the tube was exciting the fluorescence of the screen. After six weeks of intensive research the comparatively unknown scientist modestly announced at the December meeting of the Würzburg Physico-Medical Society the discovery of a new kind of radiation, which penetrated and photographed through various objects and were designated x-rays. In less than a month Roentgen rays were being generated and studied in laboratories all over the world.¹

The claim of envious critics, calculated to discredit the modest and reticent Roentgen, that the discovery of x-rays was purely accidental cannot be supported. Actually it represented not only the scientific acumen of Prof. Roentgen, but also the culmination of more than two centuries of research by scores of great scientists, filling in the fundamental background of knowledge. Along various lines there had been developing independently experimental techniques and theories applied to high vacua, electricity and electromagnetic waves, discharges in vacuum, light and the science of optics, spectroscopy, ionization of gases, fluorescence of solids, photography, and other related physical and chemical phenomena. All these lines of develop-

¹ A dramatic account of the reception of the announcement and the amazingly rapid spread of the method, written in January, 1896, is given by H. J. W. Dam, *McClure's Mag.*, 6, 403 (1896).

ment converged and made possible the rational plan and the successful result in the Roentgen experiment. It is certain that x-rays had been generated many times before the momentous day in 1895. Sir William Crookes sought the cause of repeated and unaccountable fogging of his photographic plates stored near his cathode-ray tubes. In the prophetic words of Roentgen himself is a self-portrait:

If some phenomenon which has been shrouded in obscurity suddenly emerges into the light of knowledge, if the key to a long-sought mechanical combination has been found, if the missing link of a chain of thought is fortuitously supplied, this then gives to the discoverer the exultant feeling that comes with a victory of the mind, which alone can compensate him for all the struggle and effort, and which lifts him to a higher plane of existence.¹

The Significance of the Discovery of Roentgen Rays.—The importance of the discovery of x-rays, which has made the name of Roentgen immortal, cannot be estimated even after more than forty years. It came at a time when the greatest physicists honestly believed that the truths were all known and that the future of their science involved merely the addition of further decimal places in improved experimentation. Such complacency was completely shattered, for this gateway to the new physics opened the road directly to the discovery of radioactivity, natural and artificial, the inexhaustible field of nuclear physics and chemistry, the electron, the quantum theory in all its richness, cosmic rays, radio, and all the electromagnetic spectrum, not to mention the immeasurable direct services of x-ray science in medicine, biology, genetics, atomic physics, photochemistry, and structures of materials.

The Generation of X-rays.—The investigation of the source and the mechanism of production of the mysterious new rays immediately engaged the attention of Roentgen. It was soon demonstrated that the fluorescence of the glass walls of the cathode-ray tube was an incidental phenomenon and that the generation of x-rays was associated directly with the stoppage of cathode rays. Though Crookes's experiments seemed to indicate

¹ To Dr. Otto Glasser the world is indebted for his great biography "Wilhelm Konrad Roentgen" (English) published by C. C. Thomas, Springfield, Ill.; also German edition; also, "The Life of Wilhelm Konrad Roentgen as Revealed in His Letters," *Sci. Monthly*, **45**, 193 (1937).

that the rays consisted of negatively charged particles, it was not until 1897 Sir J. J. Thomson proved this to be the case and found in addition that each of the particles, or electrons, as they came to be known, had a mass about one eighteen-hundredth as great as that of the hydrogen atom.

The existence of electrons as the units of negative electricity has now been established as a fact by such classic researches as those of Thomson, Rutherford, and Millikan, the latter of whom by means of measurements with minute oil droplets determined the unit charge of the electron to be 4.770×10^{-10} electrostatic unit. Cathode rays, or streams of rapidly moving electrons, are always identical, regardless of the kind of gas or of the material of the cathode. This is but one of the evidences that electrons are a fundamental constituent of all matter and of atoms. They are spontaneously emitted by the radioactive disintegrations of heavy atoms and are called β -rays. They are liberated as photoelectrons under proper conditions when radiant energy—visible light, ultraviolet rays, x-rays, etc.—impinges upon matter. Glowing-hot wires produce thermionic emission of electrons; heated gases dissociate into electrons and residual ions; free electrons course through metallic conductors as a flow of electric current.

X-rays are emitted whenever matter is bombarded by cathode rays; in other words, the sudden stoppage of swiftly moving electrons by the atoms of matter is accompanied by the generation of x-rays. In addition to this process it will be shown that under certain conditions primary x-rays, upon being absorbed in matter, will themselves generate secondary x-rays. The essential parts of an x-ray generating apparatus therefore, are (1) a source of electrons proceeding from a cathode, (2) a target or anticathode or anode in the path of the cathode-ray stream, and (3) a means of applying a potential difference between the cathode and the target which will accelerate the electrons to the requisite velocity during passage across the intervening space.

X-rays, Light, and the Electromagnetic Spectrum.—The investigations of the discoverer and of other early experimenters demonstrated that there were certain striking similarities between these new rays and ordinary light. Both x-radiation and light moved in straight lines, passed through space without apparent transference or intervention of matter, affected a

photographic plate, excited fluorescence or phosphorescence in some substances, and ionized gases. Both were unaffected by electric or magnetic fields, indicating the absence of electric charges, and both exhibited polarization, or different properties in different directions at right angles to the line of propagation. Finally, convincing evidence was obtained, which has since been rigorously confirmed, that the velocities of the propagation of light and of x-rays were identical.

On the other hand, there were some respects in which x-rays and light seemed to differ. Roentgen and his contemporaries were unsuccessful in all their efforts to observe deflection of the new rays from mirrors, prisms, and lenses, to obtain diffraction by gratings, or to obtain double refraction and polarization in crystals. These phenomena in the case of light were, of course, well known. As a matter of fact, a quarter of a century passed before it was demonstrated that x-rays may be totally reflected at very small glancing angles from mirrors, refracted in prisms, and diffracted by finely ruled parallel lines on glass or speculum metal.

According to the classical theory, derived largely by Maxwell, light consists of waves of electromagnetic origin which are propagated in the ether. Maxwell conceived of an electric field whose intensity or direction might vary periodically so as to create waves. Since action at a distance between electric charges is not instantaneous, these waves can be produced by giving an electric charge a rapid oscillatory motion. Each of these electric waves must be accompanied by a magnetic wave propagated with the same velocity; the periodically variable electric and magnetic fields must be perpendicular to each other and to the direction of propagation—hence, transverse. But such a condition is actually found in light waves, which are, therefore, electromagnetic waves. As an experimental verification, Hertz, by using oscillating electric discharges, was able to produce waves similar to light, in that they could be reflected, refracted, diffracted, and polarized. Thus all radiation throughout the spectrum finds its origin in what may be termed the unrest of electric charges.

In 1912 Laue, reasoning from the electromagnetic-wave theory, predicted that x-rays would be diffracted by crystals, which serve as three-dimensional gratings, just as light is diffracted by

the finely ruled lines of an ordinary optical grating, which is essentially two-dimensional. The complete experimental verification of this prediction established beyond question the identical nature of x-rays and light. They are distinguished only by the fact that x-rays have a wide range of wave lengths shorter than those of light. Table I shows that the known x-ray range lies between 0.06 A.U., or even shorter, and 1019 A.U., thus overlapping the ranges of both γ -rays and ultraviolet rays. In the laboratory for crystal analysis an average wave length employed is 1 A.U., or a value about one six-thousandth the wave length of yellow light in the visible region. Not only are light and x-rays thus closely related, but also included in the electromagnetic spectrum are the γ -rays from radioactive disintegrations; possibly rays associated with the cosmic rays; the ultraviolet rays, which are just shorter than visible light; the infrared, or heat, rays; the long range of radio, or Hertzian, waves; and finally the very long electric waves such as are associated with alternating currents. All these waves, seemingly so different in properties and produced by such vastly different methods, are actually identical in every respect except length. All have the same velocity of propagation, namely, thirty billion centimeters per second.

The spectrum of electromagnetic waves is presented in Table I. The ranges in octaves and in angstrom units (one angstrom unit, A.U., = 10^{-8} cm., or one one-hundred-millionth of a centimeter)¹ and brief statements of the methods of generation and detection are included in this table.

The simple facts of the fundamental mutual similarity of electromagnetic waves and of the essential difference only in wave length suggest immediately the general practical properties and the uses that may be made of x-radiation of average wave length as compared with ordinary light. Since their wave lengths λ are so much shorter, or their frequencies ν greater ($\lambda = c/\nu$, where c is the velocity of light), x-rays may be expected to penetrate materials that are opaque to light and to be intimately related to a far finer subdivision of matter than is possible for light waves. Even under the ultramicroscope the examination of matter with the aid of visible light rays can reach only

¹ Another unit frequently used for x-rays is 1 X.U. = 10^{-3} A. U. = 10^{-11} cm.

TABLE I.—RANGE OF ELECTROMAGNETIC WAVES

| Type | Octaves | Wave-length range, A.U. (1 A.U. = 10^{-8} cm.) | Generation | Detection |
|---------------------|---------|---|--|---|
| γ -Rays..... | .. | 0.01-1.4 0.06-0.5 used in radiology | Emitted when atomic nuclei disintegrate (radioactivity) | As for x-rays but more penetrating |
| X-rays..... | 14 | 0.06-1019 | Emitted by sudden stoppage of fast moving electrons | a. Photography b. Phosphorescence c. Chemical action d. Ionization e. Photoelectric action f. Diffraction by crystals, etc. |
| Ultraviolet rays... | 5 | 136-3,900 | Radiated from very hot bodies and emitted by ionized gases | Same as x-rays a-e: reflected, refracted by finely ruled gratings |
| Visible rays..... | 1 | 3,900-7,700 Violet 3,900-4,220 Blue 4,220-4,920 Green 4,920-5,350 Yellow 5,350-5,860 Orange 5,860-6,470 Red 6,470-7,700 | Radiated from hot bodies and emitted by ionized gases | Sensation of light; same as ultraviolet rays |
| Infrared rays.... | 9 | 7,700- 4×10^6 | Heat radiations | Heating effects on thermocouples, bolometers, etc. Rise in temperature of receiving body. Photography (special plates). Reflected, refracted, diffracted by coarse gratings |
| Solar radiation.... | .. | Limiting wave lengths reaching earth 2,960-53,000 | | |
| Hertzian waves... | 28 | 1×10^6 to 3×10^{14} | | |
| Short Hertzian.... | 17 | 1×10^6 to 1×10^{11} | Spark-gap discharge oscillating triode valve, etc. | Cocherer. Spark across minute gaps in resonant receiving circuit. Reflected, refracted, diffracted |
| Radio..... | 11 | 1×10^{11} to 3×10^{14} | Same | Cocherer. Conversion to alternating current. Rectification with or without heterodyning and production of audible signals |
| Broadcasting band | .. | 2×10^{12} to 5.5×10^{12} | | Mechanical. Electrical. Magnetic. Thermal effects of alternating currents |
| Electric waves.... | .. | 3×10^{14} to 3.5×10^{16} | Coil rotating in magnetic field | |

a definite limit of size that is still far removed from that of the ultimate constituents. The ultraviolet microscope so successfully developed by Lucas¹ and by Barnard² discloses a fine structure that appears perfectly homogeneous under visible light rays, but here again a limit is reached. Beyond this, x-rays are able to take the investigator on to the ultimate molecules and atoms, even on to the universe within the atom, if he but interprets his information properly, the reason lying in the fact that in solid crystalline matter the spacings of the ultimate particles of mass (which may be ascertained from density, the molecular weight, and the mass of the hydrogen atom) are of the same order of magnitude as the wave length of the x-rays, namely, 10^{-8} cm.

In the consideration of radiation as continuous electromagnetic waves in the ether, the fact must not be dismissed that radiation also appears to be propagated in discontinuous bundles, or quanta, in accordance with the laws first enunciated by Planck more than a quarter century ago. In diffraction, refraction, and polarization and in phenomena involving interference, x-rays, together with all other related radiations, appear to act as waves, and λ has a real significance; in other phenomena, such as the appearance of sharp spectral lines, a definite short wave-length limit of the continuous spectrum, the shift in the wave length of x-rays scattered by electrons in atoms, and the photoelectric effect, the energy seems to be propagated and transferred in quanta defined by the values of $h\nu$, where h is the Planck action constant and ν the frequency of the rays. Such a corpuscle, or quantum, is called a *photon*.

Radiation, however, is not alone in displaying these dual properties. Electrons long considered to be definitely corpuscular were shown first by Davisson and Germer in 1927 and later by G. P. Thomson, Rupp, and others to possess definite wave properties in that they could be diffracted by crystals in very much the same way as x-rays. The electron-diffraction patterns for metal foils, for example, are formed of concentric rings just like the familiar Debye-Scherrer x-ray powder photographs, and

¹ An Introduction to Ultraviolet Metallography, *Am. Inst. Mining Met. Eng.*, Pamphlet 1576E (June, 1926), followed by several later publications.

² For the Beck-Barnard microscope and its use see Martin, *J. Roy. Soc. Arts*, 79, 887 (1931); Wyckoff and Ter Louw, *J. Expt. Med.*, 54, 449 (1931).

diffraction by single crystals is observed just as it is for x-rays. From the positions of the diffraction interference maxima and the lattice spacing of the crystal it is possible to deduce the wave length of the waves causing them; this is in agreement with the theoretical expression due to de Broglie, $\lambda = h/mv$, where h again is the Planck constant always associated with quanta, m the mass, and v the velocity of the electron. Hence, electrons behave as though guided by a train of waves. Another triumph was registered in 1930 when Dempster proved that hydrogen atoms are diffracted by crystals, so that even the combination of a proton and electron constituting the corpuscular atoms acts as though guided by a train of waves. The dual aspect of the ultimate building stones of the universe as waves and particles must, therefore, be very fundamental, although it is obviously impossible to construct a satisfactory model of electrons, radiation, or atoms. The mathematics of the new quantum and wave mechanics so wonderfully developed by de Broglie, Born, Heisenberg, Schrödinger, Dirac, and others is alone adequate to define the atom, and the fundamental units of matter—the electron, the positron, the mesotron (heavy electron), the neutron, the proton, the deuteron (nucleus of heavy hydrogen), and the α -particle.

The Properties of X-rays.—Some of the properties of x-rays have been mentioned already. For the purpose of a general summary of these and as an introduction to other properties which will be discussed in detail in later chapters, the following tabulation, essentially in the chronological order of discovery, will suffice.

X-rays, then, are

1. Invisible, and pass through space without transference of matter.
2. Propagated in straight lines.
3. Unaffected by electric or magnetic fields—hence, non-electrical in nature.
4. Reflected, diffracted, refracted, and polarized just as is light.
5. Propagated with a velocity of thirty billion centimeters per second, as is light.
6. Transverse electromagnetic vibrations.
7. Characterized by wide range of wave lengths (approximately 0.01 to 1000 A.U.).

8. Produced by the impact of cathode rays (and also positive ions) upon matter; probably generated on the interior of hot stars; produced during nuclear disintegrations by bombardment in the cyclotron.

9. Capable of blackening the photographic plate.

10. Capable of producing fluorescence and phosphorescence in some substances and of coloring some stones and minerals.

11. Able to ionize gases and to influence the electrical properties of liquids and solids.

12. Differentially absorbed by matter.

13. Able to liberate photoelectrons and recoil electrons.

14. Capable of acting photochemically.

15. Able to damage or kill living cells and to produce genetic mutations.

16. Emitted in a continuous spectrum, whose short wavelength limit is determined only by the voltage on the tube.

17. Emitted also with a line spectrum characteristic of the chemical elements in the anticathode.

18. Found to have absorption spectra characteristic of the chemical elements.

19. Diffracted by crystals acting as gratings in accordance with the fundamental equation $n\lambda = 2d \sin \theta$, to which a correction for refraction must be applied for very accurate work.

20. Diffracted by optical gratings and totally reflected at very small glancing angles.

21. Found to act in interference and related phenomena as waves but in other phenomena as discrete quanta of energy which may be scattered by single electrons.

X-rays Applied.—A radiation with as many distinctive characteristics obviously finds manifold applications in science, industry, and daily life. Some of these were immediately apparent to Roentgen. Before his death in 1923 he saw Roentgen rays being used throughout the world as an indispensable tool, but even then as compared with the science of today only the barest beginning had been made. To mention only a few examples at random, he did not live to see rays generated at one to three million volts as a common occurrence (he used 20,000 volts); amazing diagnostic shadowgraphs of all parts of the human body photographed in a thousandth of a second (the photograph of Frau Roentgen's hand showing bones and wedding

ring required an exposure of 30 min.); the construction of giant dams and bridges guided by searching x-ray test; x-ray apparatus as an indispensable equipment of art galleries; industry calling upon x-ray methods to solve the most difficult problems; the high quality of commodities, such as oranges, assured by routine

| Subject | Purpose or method | Property involved |
|---|--|--|
| 1. Spectroscopy | Identification of chemical element; atomic number; energy levels in atoms; quantum theory; atomic structure | Characteristic emission and absorption of rays; scattering |
| 2. Roentgenology (radiology) (medical): <i>a.</i> Radiography <i>b.</i> Fluoroscopy | Medical diagnosis (photographic) Diagnosis (visual, fluorescence) | Differential absorption (between bones and tissues, etc.) |
| 3. Roentgen therapy | Treatment of cancer, etc. | Lethal effect upon abnormal cells |
| 4. Industrial and art radiography | Testing of gross structures for homogeneity, soundness (castings, welds, etc.); examination of old paintings | Differential absorption |
| 5. Photochemistry | Chemical effects (photographic, oxidation, reduction, activation of H_2O , etc.) | Liberation of high-speed electrons, ionization, activation |
| 6. Radiobiology | Identification of cells and tissues | Specific sensitiveness of cells and tissues to radiation |
| 7. Radiogenetics | Production of mutations in sublethal doses | Effects on chromosomes and genes |
| 8. X-ray crystallography and crystal chemistry | Fine structures of materials | Diffraction of x-rays by crystals |

x-ray examination; a whole new science of the ultimate architectural plan of the solid state; new alloys, new textiles, and a host of other products derived from x-ray research; the analysis of the complex molecular structure of the tobacco mosaic virus, amino acids, and a long list of substances formed in living processes.

Any attempt to classify completely all the ramifications of Roentgen-ray science must fail. But, perhaps the principal applications may be summarized as shown in the table on page 13.

In the succeeding chapters of this book each of these items will be considered briefly as an integral part of the unified science of applied x-rays.

CHAPTER II

X-RAY TUBES

There are two general types of x-ray tube that fulfill the requirements for generation outlined in the previous chapter. In the first type, the so-called gas or ion tubes, the residual gas plays an important part; in the second or electron type the tubes are exhausted of gas to such an extent that no discharge takes place when a large difference of potential is applied.

X-ray tubes are also classified according to the use to which they are put, which in turn depends upon the penetrating quality of the rays and the applied voltage.

TABLE II.—CLASSIFICATION OF X-RAY TUBES

| Class | Type | Kilovolts |
|--|-------------------|--------------------|
| 1. Special high-voltage tubes..... | Electron | 800 to 3,000 |
| 2. Deep therapy..... | Electron | Average 160 to 400 |
| 3. Industrial radiography..... | Electron | 100 to 300 |
| 4. Diagnostic..... | { Electron Ion | Average 50 to 110 |
| 5. Diffraction..... | { Electron Ion | Average 25 to 50 |
| 6. Superficial therapy or Grenz ray..... | { Electron Ion | Average 10 |

Gas Tubes.—The gas tubes were the first to be developed for practical use. They still find wide application both for medical and for purely scientific purposes, but the electron tubes now in operation undoubtedly far outnumber the older type. In the gas tube the gas molecules are split up into electrons and residual ions when the voltage is applied. These positive ions are then hurled against the cathode by the electric field, so that electrons are set free in the bombardment. The cathode-ray stream thus generated bombards the positive electrode, or anticathode, and the x-rays are produced.

The cathode-ray tube used by Roentgen in the discovery of x-rays is diagrammatically represented in Fig. 2. A flat disk served as cathode, and the cathode rays impinged upon the opposite glass wall with the production of strong fluorescence, while the new rays passed through the glass. It is not surprising that it was thought that the source of the new rays resided in the fluorescence until Becquerel proved that this was not the case. The result of Becquerel's study was the discovery of radioactivity in 1896, only two months after Roentgen's discovery. Roentgen very soon constructed a tube with a special anticathode

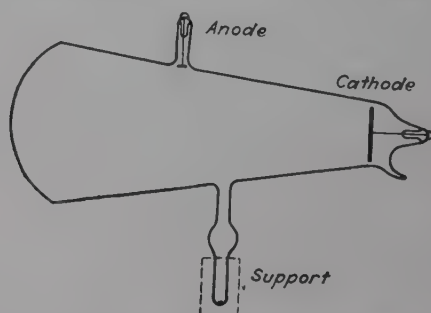


FIG. 2.—Diagram of cathode-ray tube used by Roentgen in the discovery of x-rays.

of platinum and a concave cathode for focusing the electron stream. Other tubes had both an anode and an anticathode bound together, with the idea that greater stability and less pitting of the anticathode would be attained. Some of Roentgen's tubes now at the Deutsches Museum in Munich are illustrated in Fig. 3.

At the present time, several manufacturers in the world still supply ion tubes of similar design, with sharp focus for medical diagnosis and for superficial therapy. Some water-cooled tubes may be operated at 25 ma. for harder rays and 40 to 50 ma. for softer. Others with special radiation cooling of both electrodes may be operated momentarily up to 150 ma. The fact remains, however, that for medical purposes the electron-type tube has displaced practically completely the ion tubes, largely because the former are free from complications inherent in the operation of the latter, such as the impossibility of varying independently of each other the intensity and quality of the x-rays.

The older varieties of the ion tube were provided with a device with which it was possible to add small amounts of fresh gas. The "hardness" of the x-ray tube (by which is meant the penetrating quality of the x-rays produced) is determined by the amount of the residual gas, since the lower the gas pressure, the higher the voltage required for production of x-rays. During

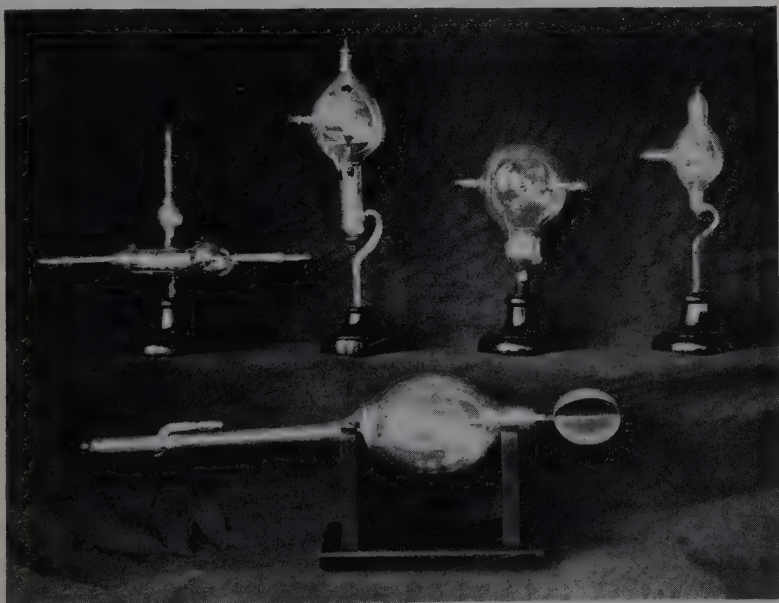


FIG. 3.—Some of Roentgen's early tubes, now in the Deutsches Museum at Munich.

operation the hardness of the tube increases as the amount of the available gas diminishes owing to adsorption on the glass walls and metal parts. Consequently, in order to maintain constancy, gas must be admitted by diffusion through thin metal or by heating or passing a spark through a small cylinder of some substance in a side tube.

Very recently, several modifications of the old gas-type tube have been made in Europe and America with such success that for many types of investigations of x-ray spectra and crystal structure these are competing favorably with the electron tubes. Seemann, Shearer, Hadding, Siegbahn, Müller, Wever, Becker, Wyckoff, Aminco-Ksanda, Baird, Hägg, and others have constructed tubes largely of metal, with interchangeable targets

(iron, copper, and molybdenum usually), thin-foil windows, water cooling, and permanent connections with vacuum pumps by means of which the gas pressure may be readily regulated,

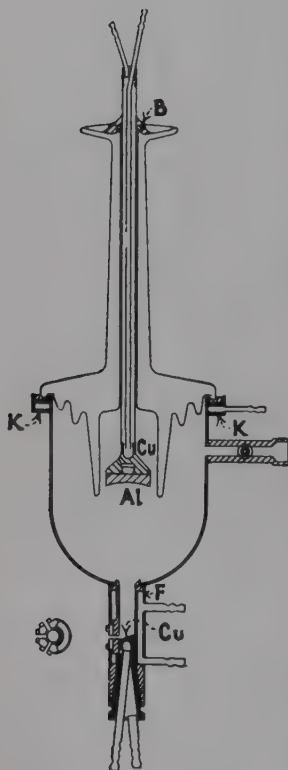


FIG. 4a.—Diagram of Hadling-Siegbahn gas-type x-ray tube used in crystal analysis.

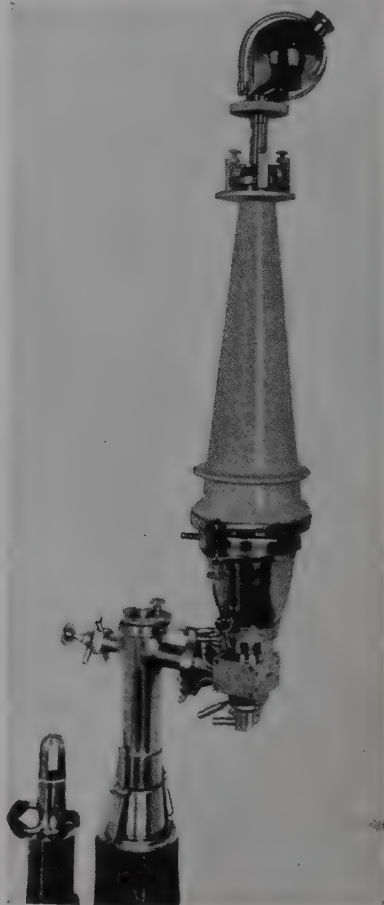


FIG. 4b.—Seemann gas-type tube.

thus eliminating special devices for controlling hardness. These tubes are very simple and rugged and may be operated with such large energy that the time of photographic exposures is greatly reduced from that normally required.¹

¹ For tubes of recent design, see Wyckoff and Lagsdin, *Rev. Sci. Inst.*, **7**,

Another advantage of great importance for precise spectroscopic and diffraction work is the purity of the spectrum, since it has been found easier to build a controllable gas tube than to prevent tungsten (from the hot-cathode filament) depositing on the target in one of the electron type.

Probably the most familiar of the gas-type tubes for diffraction is the so-called Hadding-Siegbahn metal tube. Figure 4*a* shows this tube diagrammatically, and Fig. 4*b* shows such a tube produced by the firm of Seemann. The body of the tube is entirely of metal, which permits self-protection for rays except as they pass through windows of thin foil. The entire metal part and the target are grounded and connected directly with the water mains for cooling. The cathode of aluminum, which is at high potential, is insulated through a porcelain cylinder. This cathode may be cooled with an insulated water or oil circulating system or simply by blowing compressed air through the cooling system. Tubes of this type, particularly for operation with copper targets when long wave lengths are required, have been in successful operation in the writer's laboratory for many years. These have interchangeable cathodes for operation, either as ion or as electron tube, and a whole series of interchangeable metal targets. Four sheets of metal are mounted on the four sides of a hollow copper rod with square cross section. By rotating the rod 90 deg. the various targets may thus be brought into alignment with the cathode. A needle valve is built in as an integral part of the tube. These tubes are ordinarily used with rectified high-tension current, but some are so designed and operated that they are self-rectifying just as electron tubes may be, the most familiar being the Shearer tube.¹

The newest commercially available gas-type tube, the Aminco-Ksanda,² is shown in a double assembly in Fig. 5. This unit has remarkable versatility inasmuch as the two tubes operating for the same high-tension transformer may have different target metals and may be adjusted independently at any angle. The

35 (1936); Ksanda, *ibid.*, **3**, 531 (1932); American Instrument Company, *Bulletin* 1045, Silver Spring, Md.; Bulletin of Baird Associates, Cambridge, Mass.; Hägg, *Rev. Sci. Inst.*, **5**, 117 (1934).

¹ Manufactured by A. Hilger, London.

² Manufactured by the American Instrument Company, Silver Springs, Md.

pumping and valve systems are enclosed in the supporting stand. A tube produced by the Baird Associates of Cambridge, Mass., is illustrated in assembly with its power unit in Fig. 6.

Some tubes of remarkably small size and simple construction have been devised and found to operate successfully at minimum wattage. One example is illustrated in Fig. 7.¹ This tube consists of a block of metal bored with a rounded hole, to serve

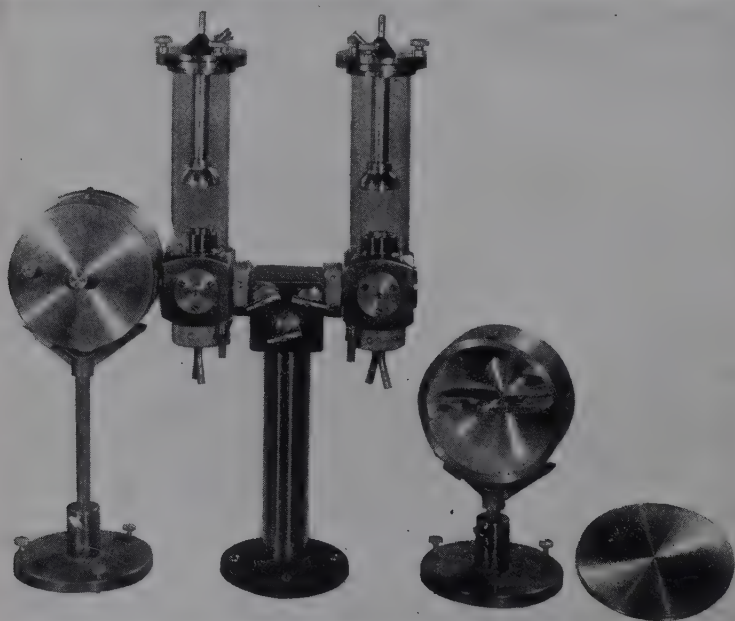


FIG. 5.—Aminco-Ksanda gas-type tube in double assembly with diffraction cameras.

as cathode. Across the mouth of this opening is sealed a plate of glass with a small circular opening upon which is mounted a thin piece of metal foil, which serves as the target through which x-rays issue. A pinhole and crystal may be mounted on this foil which is in direct contact with the focal spot. Negative potential is applied to the cathode block.

In the writer's laboratory an entire unit assembled at a cost under \$25, with a burned-out radio tube, type OHA, as the x-ray tube, produces a beam of surprising intensity. The

¹ Hess, *Z. Krist.*, **97**, 197 (1938).

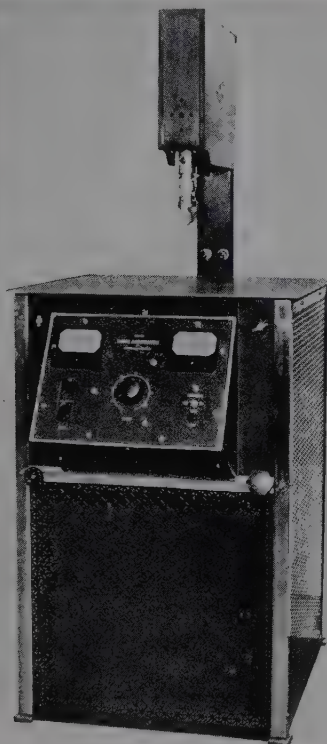
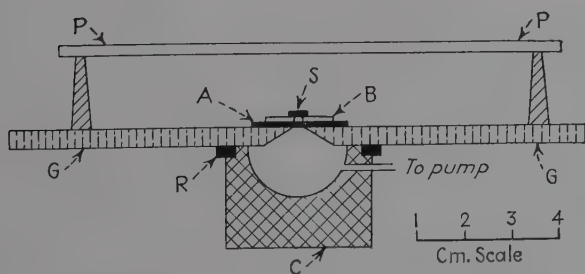


FIG. 6.—Baird gas-type tube in assembly with power unit.



P—Photographic plate
S—Sample
B—Pinhole
A—Anode foil

G—Glass plate
R—Rubber gasket
C—Cathode

FIG. 7.—Midget tube with rounded hole in metal block serving as cathode.

prongs of the radio tube are grounded, and the high tension is applied to a copper cap over the bulb, as shown in the circuit diagram in Fig. 8. The metal film "getter" in the tube apparently acts as target.¹

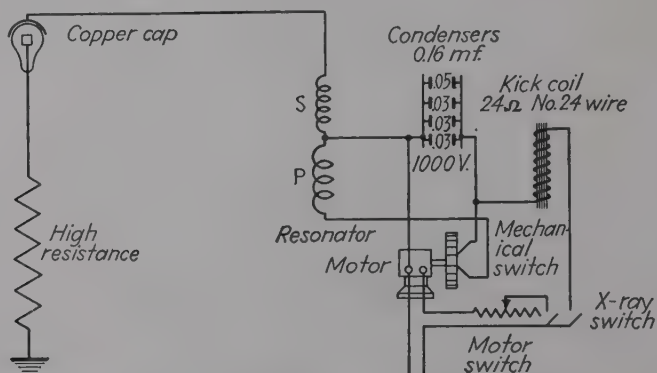


FIG. 8.—Burned-out radio tube serving as an x-ray tube and circuit. (Simons Clark, and Klein.)

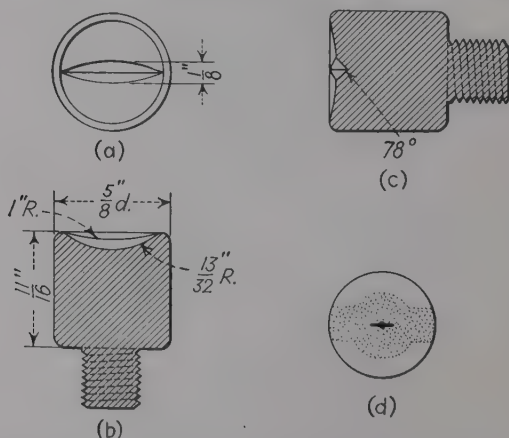


FIG. 9.—(a) Top view of a gas-type tube cathode yielding a linear focal spot. The line appears at right angles to the transverse cut. (b) and (c) Cross sections through this cathode tip. (d) A drawing from a used target showing the observed shape of the focal spot (in black). This spot is surrounded by a zone of discoloration (pebbled) which emits weak radiation. (Corey, Wyckoff, and Lagsdin.)

Numerous automatic- and needle-valve devices have been described for the automatic regulation of gas pressure (and thus of operation of the tube). In the great majority of cases,

¹ SIMONS, CLARK, and KLEIN, *Radiology*, **29**, 721 (1937).

however, the simplest expedient is preferred by the experienced worker with gas-type tubes. These are connected with the high-vacuum mercury or apiezon oil diffusion pumps and also with the fore-vacuum backing pump (Cencovac type). Regulation is effected with a simple pinch clamp on rubber-hose connections with the latter pump. Very often a tube may operate for hours untouched after the preliminary adjustment. The test, of course, is the production of x-rays steadily at a given voltage without a visible gas discharge.

Though all gas-type tubes are constructed on essentially the same principles, *i.e.*, replaceable water-cooled targets, glass-tubing body, and concave aluminum cathode, interesting variations in details have been introduced. One of these is the production of a line focus by means of a transverse cut on the cathode face, devised by Corey, Wyckoff, and Lagsdin¹ and illustrated in Fig. 9.

Electron Tubes. *The Coolidge Tube.*—In the electron-type tube it is necessary to have an independent source of electrons, since there is insufficient gas present to enable passage of the current. For an x-ray tube to operate with a pure electron discharge it is necessary to evacuate to the highest attainable vacuum, usually 0.01 bar or 0.0075μ of mercury. These electrons may be supplied by application of the Edison effect, *i.e.*, emission from a hot-wire cathode, or by oxides heated on the cathode, by illumination of the cathode by ultraviolet light, or by Lilienfeld's autoelectron-emission method. The first of these is the basis of the very familiar Coolidge tube which is now being manufactured on a large scale for research, therapy, medical diagnosis, industrial radiography, and diffraction analysis. The original Coolidge tube consisted of a glass bulb into which were sealed a solid metal target and a spiral of tungsten wire backed by a focusing shield of molybdenum as cathode. The emitting wire was 0.216 mm. in diameter, 33.4 mm. long, and wound in a flat spiral of $5\frac{1}{2}$ turns with a diameter of 3.5 mm. The spiral is heated to incandescence by a current of 3 to 5 amp. at 1.8 to 4.6 volts supplied in an independent circuit from storage batteries or step-down transformers. Under these conditions the wire has a temperature of 1890 to 2540° Abs. Electrons are liberated, and under a potential gradient between the terminals of the

¹ *Rev. Sci. Inst.*, **7**, 193 (1936).

x-ray tube they are drawn across to the target. The ordinary commercial Coolidge tubes are usually supplied with massive tungsten targets. In the "universal" type the target is not cooled and becomes white hot.

Thin plate targets enabling more rapid dissemination of heat are a more recent development (Fig. 10). These tubes are pumped

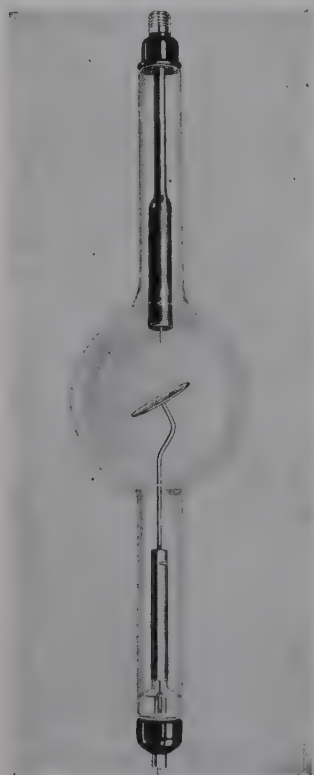


FIG. 10.—Deep-therapy tube of conventional design with thin plate target (Westinghouse).

to the proper vacuum at the factory by the very special technique involving pumping, baking, and operation under increasing voltages in order to remove the gas which is occluded in metal parts. Such tubes fail very often from development of gas during operation, and large currents begin to pass. Even if the operation is normal, however, there is a limit to the life. The glowing filament of the cathode vaporizes, and thus it becomes thinner and thinner until it is burned through. The time over which the resistance of the wire increases by 10 per cent may be designated the life, which on the average for the ordinary Coolidge tubes is about 2,000 hr. Danger of failure from puncturing these tubes at high voltages is lessened by immersing them in transformer oil.

One great advantage of the Coolidge tube is the independence of the current through the tube and the voltage. One may be altered without affecting the other, whereas in gas

tubes it is obvious that the number of the electrons and, hence, the current will increase with the voltage. The current in the electron type depends upon the number of electrons N , and this in turn depends upon the temperature of the hot-wire filament, by the Richardson relationship $N = CT^2e^{-d/T}$, where C and d are constants depending upon the metal (1.86×10^{11} and 4.95×10^4 , respectively, for tungsten), and T is the absolute temperature. On

account of the building up of a space charge, since the tube current does not increase so rapidly as does the number of electrons when the temperature of the filament is increased but the voltage held constant, a maximum or saturation current is reached at a point expressed by the equation deduced by Langmuir

$$i_{\max.} = \frac{\sqrt{2}}{4\pi} \sqrt{\frac{e}{m}} \frac{V^{\frac{3}{2}}}{x^2}.$$

Here e and m are the charge and the mass of the electron, V is the voltage, and x is the distance between electrodes. This relationship has enabled investigators to predict correct design for tubes.

Problems in Tube Design.—The steadily increasing demands for x-ray tubes to operate at higher and higher voltages in order to generate more penetrating radiation and at higher and higher currents in order to gain increased intensity call for the utmost care in the design of every detail. The first of these requirements involves essentially proper insulation of the two electrodes; the second involves adequate protection of the target from destruction. Coordinate with these problems of tube protection are those of protection of the operator against shock and against exposure to x-radiation, which may be solved by integral constructional details of tube design. Depending on the tube classification in terms of use, these problems appear in greater or lesser degree and in varying combination. The best methods of solution as a general case are summarized here.

1. *Insulation of Tube Electrodes and Electrical Stabilization.*—Obviously, the body of an x-ray tube—a bulb or cylinder of glass or porcelain—usually must serve not only as a rigid support but also as the insulating medium between two oppositely charged electrodes at high tension. It is not surprising, therefore, to find x-ray tubes varying in length from a few inches (dental radiographic tubes, oil-immersed) to 30 or 40 ft. (for operation at 1,000,000 volts or more).

Serious difficulties have been encountered in attempts to operate x-ray tubes of usual design at voltages very much higher than 220,000, not because power plants are not available, since 1,000,000 volts can easily be attained in commercial machines, but because of electrical phenomena within the tubes that prevent a satisfactory "life." In the first place the auto-electronic effect, or the release of electrons from metallic points or

sharp edges in the electric field, produces a discharge in the tube operated above a critical voltage. Momentary currents of several amperes may pass, followed by high-frequency electric oscillations which may result in ruin of the transformer and of the x-ray tube, especially if the discharge strikes the glass walls. In less severe cases the natural distribution of potential along the tube is affected, and gas is liberated from the glass walls in certain areas. This difficulty may be counteracted, so that higher potentials may be applied safely, by careful rounding of the cathode.

The second group of phenomena that introduces difficulties is the back diffusion of electrons from the anode to the inner glass

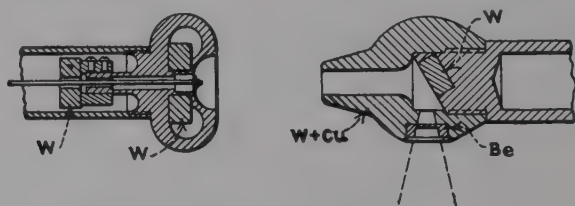


FIG. 11.—Design of electrodes in 400-kv. deep-therapy tube (Siemens-Pantix).

walls which become negatively charged. Next the outer glass wall becomes charged almost to the potential of the cathode, so that a high difference of potential is set up between the glass and the anode. A stream of ions will travel from the anode, through the glass, then through the air to the metal anode cap. It has been demonstrated that gaseous electrolytic products are liberated as a result of the passage through the glass of the current, even though smaller than 10^{-5} amp. The result again may be destructive discharge, depending on the potential and also the current. In order to avoid these effects so that a tube may operate with safety, the glass may be shielded from the secondary electrons.

A commercial Siemens-Pantix deep-therapy tube to operate at 400 kv. effective and 5 ma. embodies the rounded cathode and the shielded anode in a highly satisfactory manner.¹ The design of the electrodes is shown in Fig. 11, and the tube itself with protecting rings on the metallic caps is illustrated in Fig. 12. These rings involve the principle of a sphere-gap in which discharge takes place at higher potentials than between points (or

¹ MÜLLER and ZIMMER, *Fortschritte Gebiete Röntgenstrahlen*, **45**, 341 (1932).

small diameter caps) at the same distance. It is possible, therefore, to cut down the over-all length of the tube, particularly since the glass really serves as an insulator when the secondary electrons are screened off internally.

Aside from proper design of the electrodes the most important development in electrical stabilization of tubes is the use of a metal discharge chamber, with glass serving only to insulate the electrodes. The entire middle part of the familiar Philips Metalix tube, manufactured in Eindhoven, Netherlands, is a

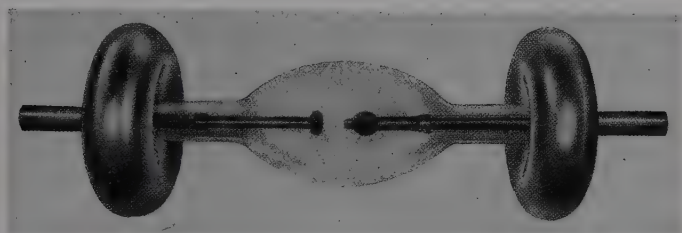


FIG. 12.—Siemens-Pantix 400-kv. deep-therapy tube with protective rings on caps.

chrome-iron cylinder, which is sealed vacuum tight and mechanically rigid to the glass of the electrode end sleeves. This metal center is grounded, which prevents destruction by interior discharges and also serves both as a shockproof and a ray-proof feature.

A photograph and a diagram of a Metalix tube are shown in Fig. 13. These tubes may be obtained in various sizes up to 240 kv. at 8 ma. with water cooling.

2. Special Tubes for Very High Voltages.—There are many points of interest in operating x-ray tubes at increasingly higher voltages. Since the effective wave length decreases as the voltage increases, the point might be reached where x-rays in the wave-length range of γ -rays might be generated with an output equivalent to thousands of grams of radium or with millions of times greater intensity than is observed for cosmic rays. The advantage in therapy and in biological action is obvious, even supposing that the *kind* of biological action might be anticipated as independent of wave length. The intensity of radiation in the voltage range of modern deep therapy with usual filtration increases with a high power (at least third) of the voltage. The gain in intensity with mounting voltage and constant current makes possible material reductions in time of

irradiation even with stronger filtration and increased distance from focal spot to patient, and a far higher percentage depth dose is attained. The physicist is also interested in the spectra

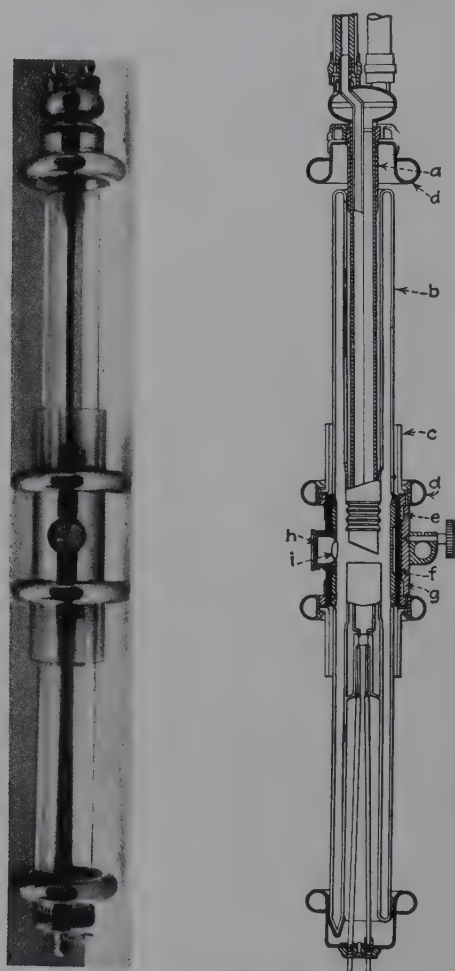


FIG. 13.—Photograph and diagram of construction of the Metalix tube, showing the central chrome-iron cylinder to which the glass anode and cathode arms are fused.

of radiation exerted at the highest attainable voltages and in the test of theories of atomic structure.

Throughout the world there are now several x-ray installations in hospitals and research laboratories in which the x-ray tube

is operating at 1,000,000 volts or higher and generating rays with wave lengths shorter than 0.01 A.U. These followed the pioneer tubes of Lauritsen¹ (600,000 volts, California Institute of Technology), Coolidge² (900,000 volts, Memorial Hospital of New York), Tuve and associates³ (2,000,000 volts, Carnegie Institution of Washington), and several others. Difficulties in elimination of cold cathode discharges, proper insulation, screening off of back-diffusion electrons, and maintenance of high vacua have been overcome to such an extent that sealed-off tubes to operate at 1,000,000 volts are commercially advertised and available. However, most of these supervoltage tubes are designed for continuous pumping; they are unisectional or multisectional (Fig. 14), glass- or porcelain-walled, and anode-grounded or mid-grounded and usually have a filament cathode. Thus, only the original Lauritsen tubes were unisectional, porcelain-walled, and anode-grounded. W. D. Coolidge first developed the multisectional construction, so that with intermediate electrodes between the cathode and anode the potential gradient could be better distributed. The million-volt tube at the Huntington Memorial Hospital in Boston, designed to operate with a direct-current Van de Graaff generator (see Chap. III) is of a cascade type made up of 15 porcelain sections about 10 in. in diameter, provided with diaphragms between



FIG. 14.—Three of the 10 sections of a 1,400,000-volt tube 23½ ft. long at National Bureau of Standards. (General Electric Co.)

¹ *Phys. Rev.*, **32**, 850 (1928); **36**, 988, 1680 (1930).

² *Am. J. Roentgenology*, **19**, 313 (1928); **24**, 605 (1930).

³ *Phys. Rev.*, **35**, 66, 1406 (1930).

sections, which serve to focus the electron stream in its passage from the upper end of the tube to the target and also to break up the total potential which must be insulated between the two ends of the tube. This cascade type of tube has been uniformly successful in resisting puncture and is now to be found in many hospitals that are giving uniform therapy treatment at 900 to 1,000 kv. at 3 ma. A tube of this type built for the U.S. National Bureau of Standards to operate at 1,400,000 volts and 10 ma. (140,000 volts over each of 10 sections) is shown in Fig. 14. Several recent papers on supervoltage tubes and technique are listed in the footnote.¹ The newest tube for operation with the amazing tuned resonance transformer, described in Chap. III and designed by General Electric, is illustrated in Fig. 15. This tube is built in 11 sections with grounded anode and operates at 1000 kv. and 3 ma. It is capable of producing radiation equivalent to that from \$9,000,000 worth of radium. Coordinate in interest with the design and operation of these supertubes is the comparative biological and therapeutic effects of rays generated at 1,000,000 and, say, 200,000 volts. The results of five years of experience, especially in cancer therapy, are considered in Chap. XI on The Biological Effects of X-radiation.

3. *Operation of Tubes at High Currents.* a. *The Focal Spot.*—The desire in every branch of x-ray science is the production of the most intense beam of radiation possible. For example, from the medical roentgenographic standpoint, any motion of the patient or areas under observation results in blurred details with consequent failure to obtain that definition which is vital to the most accurate and complete interpretation. The history of the development of x-ray tubes and accessories for diagnosis has

¹ COOLIDGE, DEMPSTER, and TAMS, High Voltage Cathode Ray and X-ray Tubes and Their Operation, *Physics*, **1**, 230 (1931).

CHARLTON, HOTALING, WESTENDORP, and DEMPSTER, An Oil-immersed X-ray Outfit for 500,000 Volts and an Oil-immersed Multi-section X-ray Tube, *Radiology*, **29**, 329 (1937).

DUMOND and YONTZ, The 30-kilowatt Continuous Input X-ray Equipment and High Constant Voltage Generating Plant of the Wattens Memorial Research Laboratory at the California Institute of Technology, *Rev. Sci. Inst.*, **8**, 291 (1937).

LEUCUTIA and CORRIGAN, Further Development in Supervoltage Therapy Apparatus, *Radiology*, **27**, 208 (1936).

LAURITSEN, The Development of High Voltage X-ray Tubes at the California Institute of Technology, *Radiology*, **31**, 354 (1938).

been one of an unremitting struggle to circumvent the effects of such motion. The trend has been definitely toward shorter and shorter exposures, demanding the employment of greater and greater electrical energies.

In an x-ray tube of conventional type, the electron stream is directed against a fixed area on the target called the focal spot, which is usually defined as a pitted or etched area on the target



FIG. 15.—Million-volt tube operating with new tuned resonance transformer at Memorial Hospital, New York. (*General Electric Co.*)

face. The size of this spot is determined by the method of focusing of the electrons, which in turn is defined by the size and shape of a shield around the filament and the position of the filament within this shield. Thus, a fine-focus or a broad-focus tube represents, respectively, a small or a large focal spot in which the energy is concentrated. Since sharply defined diagnostic radiographs require the finest focus possible,

the trend to shorter exposures and the need to retain fine focal spots have been in direct opposition to each other.

The *rating* of an x-ray tube is limited by the ability of the target or anode to dissipate the heat generated. The product of kv. p., (peak kilovolts), ma. (milliamperes), and time must be such that no portion of the area bombarded is brought too close to the melting point.

The necessity for cooling the target is explained by the following example: At 200 kv. and 3 ma. the kinetic energy of the electrons, which have a velocity of 220,000 km. per second as they strike the target, is transferred to the target at the rate of 150 cal. per second, or enough energy in 10 min. to raise 1 liter of water from 10°C. to boiling. Only about 2 per cent of this energy is transformed to x-radiation, and the remaining 98 per cent goes into heat.

b. Stationary-target Cooling.—The original Coolidge-tube design still retained in the "universal" type for operation at relatively small loads involved a massive "horse-hoof" target of tungsten, which could become white-hot because of the high melting point of the metal. Greater energy could be used by constructing the target as a large thin plate (Fig. 10) from which heat could be dissipated more readily. The next step was to add external air-cooling fins to

the anode connection, as shown in Fig. 16, or a reservoir containing oil or water. Still more efficient cooling is effected by a continuous stream of water conducted into a hollow target past the inner face of the target. If the anode is grounded, it may be connected directly with the city water mains and a continuous stream of 1 or more liters per minute used, depending on the heat evolution. If the anode is at high potential, an insulated pumping and radiator-cooling system keeps the liquid in circulation. Or if the voltage is



FIG. 16. —Air-cooled diagnostic tube (General Electric).

not too high, water from the mains may be circulated and the anode insulated from ground through a column of water in glass tubing 40 or 50 ft. in length. Several protective devices to shut off the electric current in case of failure of the cooling supply have been described and are highly desirable. Tubes with cooled targets through which currents of 200 ma. may be passed for 1 sec. or longer, or 400 ma. for 0.1 sec., are now fairly common.

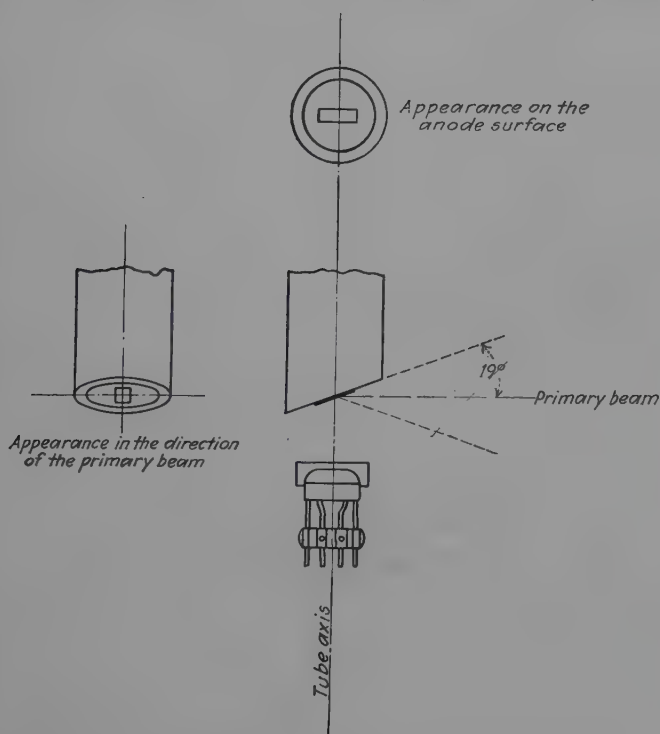


FIG. 17.—Diagram showing operation of a line-filament cathode.

Complete immersion of the entire tube in oil, one of the best methods of shockproofing, has the added advantage of rapid heat transfer from the anode, heavier loads being thus permitted.

c. The Line-focus Filament.—The desire to increase the load and intensity of x-radiation from such tubes in order to cut down exposure time to a minimum is opposed by the fact that greater energy input in a small focal spot results in melting and destruction of the target. Increase in size of the focal spot in all directions causes diagnostic photographs to lose sharpness. Hence

it is necessary to change the focus so that the cross section through the x-ray bundle at the focal spot is as small as possible. The line-focus filament of Goetze employed in the Philips tubes is a successful solution. A long cylindrical spiral of very small diameter produces a line focal spot on the target which by virtue of length can take up a very considerable amount of energy

TABLE III.—TYPICAL RATINGS OF DIAGNOSTIC TUBES FOR 1 SEC.

| Effective focal area | Full wave | | Half wave | | Self-rectified | |
|-------------------------|-----------|-----|-----------|-----|----------------|-----|
| | kv. p. | ma. | kv. p. | ma. | kv. p. | ma. |
| Stationary target: | | | | | | |
| 1.5 | 55 | 40 | 55 | 30 | 50 | 25 |
| | 73 | 30 | 65 | 25 | 63 | 20 |
| | 88 | 25 | 82 | 20 | 85 | 15 |
| | 110 | 20 | 110 | 15 | | |
| 3.7 | 55 | 125 | 48 | 100 | 50 | 75 |
| | 65 | 100 | 63 | 75 | 63 | 60 |
| | 85 | 75 | 80 | 60 | 75 | 50 |
| | 110 | 60 | 95 | 50 | | |
| 5.2 | 45 | 300 | 40 | 250 | 45 | 175 |
| | 55 | 250 | 50 | 200 | 52 | 150 |
| | 67 | 200 | 67 | 150 | 62 | 125 |
| | 90 | 150 | 100 | 100 | 78 | 100 |
| $\frac{1}{80}$ sec. | 72 | 500 | | | | |
| | 90 | 400 | | | | |
| | 104 | 350 | | | | |
| Rotating target: | | | | | | |
| 2.0 | 80 | 280 | | | | |
| $\frac{1}{80}$ sec. | 80 | 540 | | | | |
| 1.0 | 80 | 130 | | | | |
| $\frac{1}{80}$ sec. | 80 | 200 | | | | |

without damage to the target. The face of the target is inclined at an angle of 80 deg. to the tube axis, so that the line-focus spot in the principal direction of emergence of the x-rays appears shortened to a small point. The focal spot is actually about 2 mm. wide and 16 mm. long but from the front appears foreshortened to a spot 2 mm. square (Fig. 17).

General Electric XP tubes use a Benson-type cathode, 20-deg. anode, and a linear focal spot. Typical ratings for these tubes on the basis of air cooling and a constant time of 1 sec. are listed in Table III as illustrative of the safe performance of modern diagnostic tubes.

d. The Double-focus Tube.—In 1930 the first double-focus Coolidge tube was introduced, and it has proved very practical from the standpoint of economy of time and money. The smaller focal spot is at once available for fine definition in radiography and the large focal spot for techniques requiring greater amounts of x-ray energy. Thus, effectually there are two tubes in one, with a selector switch built into the cathode. A typical double-filament cathode is illustrated in Fig. 18. Because the electron bombardments from the two filaments are on separate areas of the target, longer tube life is further assured. The Machlett FCX tube has two filaments intended to be operated either singly or simultaneously in series so that the tube is applicable for both therapy (both filaments, double focus) and radiography (either filament, fine focus).



FIG. 18.—Double-filament line-focus cathode in General Electric XP tubes.

| Peak kilovolts | Milliamperes | Bias voltage | r per minute (50 cm.) |
|----------------|--------------|--------------|--------------------------|
| 221 | 15 | 0 | 46.5 |
| 220 | 15 | 300 | 49 |
| 219 | 15 | 525 | 50 |
| 219 | 15 | 750 | 52 |
| 218 | 15 | 1,500 | 53 |

e. The Grid-biased Tube.—The familiar principle of the grid bias in radio tubes has been successfully applied in Machlett x-ray tubes for operation in self-rectified units, so that they may give a radiation output closely approximating that of tubes operating on constant potential. The cathode has a grid-

bias lead insulated for 2,000 volts, although a potential of 1,000 to 1,500 volts is sufficient. This is best obtained from the voltage drop across a resistor in the tube circuit to charge a condenser of 3 mfd. capacity, the negative terminal of which is connected to the grid lead. The values shown in the table on page 35 have been reported for the bias effect on output (the quality, or effective wave length, is appreciably "harder").

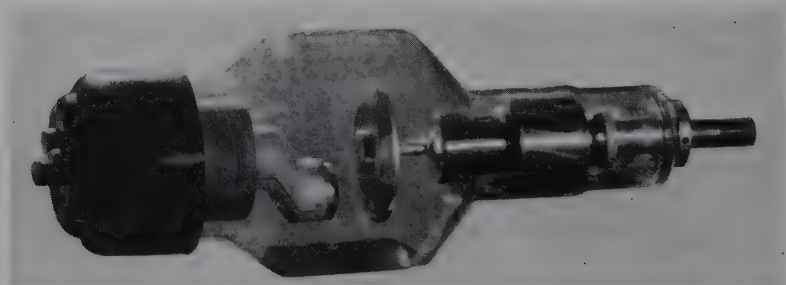
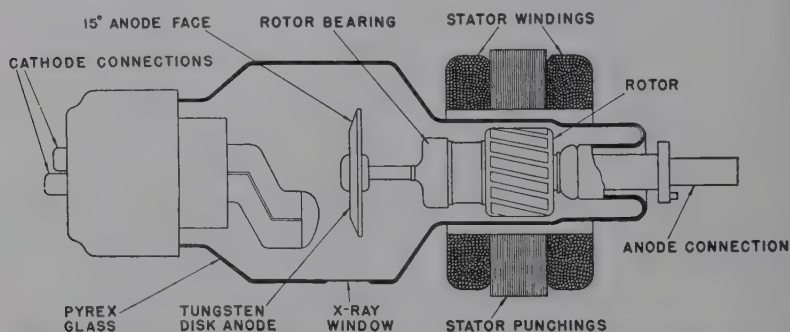


FIG. 19.—Diagram and photograph of rotating-target x-ray tube. (General Electric X-Ray Corporation.)

f. The Rotating Target.—The ultimate step in attaining a tube with minimum focal-spot area with maximum energy is obviously that of rotating the target at high speed so that relatively cool metal is brought continuously before the electron stream. This principle is used in highly successful tubes constructed by Philips, General Electric, Westinghouse, and others. A typical design is shown in Fig. 19. The anode is a disk of metal (tungsten for medical radiography) fastened to the end of a short shaft on the proximal end of which is the rotor of an induction motor, the assembly being mounted on ball bearings. Outside the glass wall of the tube and surrounding the circum-

ference of the rotor is the stator of the motor. When this is energized by 60-cycle current, electromagnetic induction causes the anode to rotate at about 3,000 r.p.m. The single- or double-filament cathode is arranged so that bombardment of the target takes place near the periphery. Thus, during operation the focal area becomes in effect a completely encircling ribbon with the effective, or projected, focal spot in the form of a small square, 1 or 2 mm. on a side. Actually for the 2-mm. spot the heat is distributed over an area $7\frac{1}{2}$ mm. wide and 190 mm. long. Such a tube obviously has a much higher rating, as illustrated in Table IV.

TABLE IV.—COMPARATIVE RATINGS, ROTATING- VS. STATIONARY-TARGET TUBES

| Time, sec. | Rotating | | Stationary | |
|----------------|-----------------------|------------|-------------------------|------------|
| | Effective focus 1 mm. | | Effective focus 3.8 mm. | |
| $\frac{1}{20}$ | 200 ma. 73 kv. p. | | 200 ma. 82 kv. p. | |
| $\frac{1}{10}$ | 200 ma. 68 kv. p. | | 200 ma. 70 kv. p. | |
| $\frac{1}{5}$ | 150 ma. 79 kv. p. | | 150 ma. 70 kv. p. | |
| 1 | 125 ma. 84 kv. p. | | 125 ma. 77 kv. p. | |
| | Effective focus 2 mm. | | Effective focus 1 mm. | |
| | Rotating | Stationary | Rotating | Stationary |
| $\frac{1}{20}$ | 530 ma. | 100 ma. | 200 ma. | 35 ma. |
| $\frac{1}{5}$ | 380 ma. | 70 ma. | 170 ma. | 25 ma. |
| 5 | 120 ma. | 50 ma. | 100 ma. | 20 ma. |

Table IV also shows that the rotating-target tube with 2.0-mm. focal spot operating at 80 kv. p. for 1 sec. has a rating of 280 ma., or the same as a stationary-target tube at 50 kv. p. (five-eighths as high) and a focal spot of 5.2 mm. (2.6 times larger).

Several rotating-target tubes have been constructed for research purposes and for very rapid examinations of structures of materials. Most of these involve mechanical rotations through suitable vacuum-tight joints. Mercury seals covered with a layer of apiezon oil to prevent access of mercury vapor are generally successful. A 50-kw. water-cooled tube with rotating target and leather-packed vacuum stuffing boxes is in satis-

factory use at the Davey-Faraday Laboratory of the Royal Institution.¹

In Fig. 20 is presented the photograph of a rotating-target tube designed, constructed, and used in the excellent laboratories of the French Air Ministry. With a copper target the continuous output rating is 60 kv. and 250 ma., or 600 ma. for 1 min. The

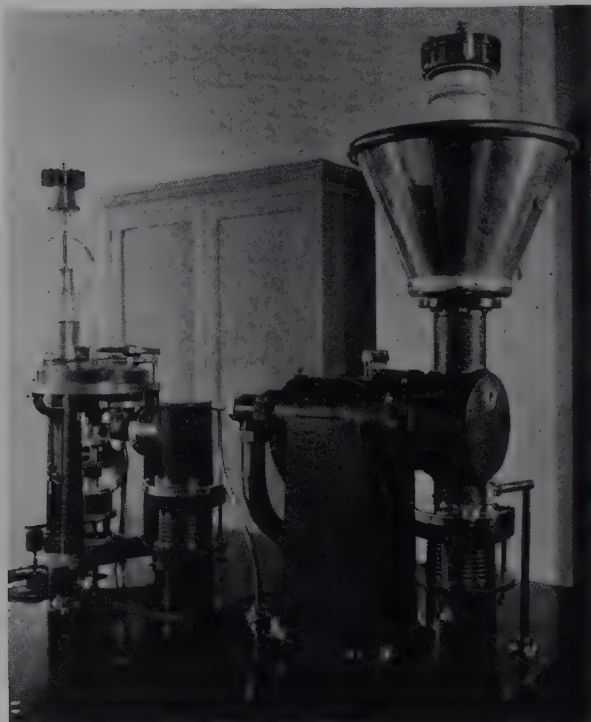


FIG. 20.—Rotating-target x-ray tube in laboratory of French Air Ministry, Paris.
(By permission.)

beam is so intense that in the presence of the writer diffraction patterns of copper wire were photographically registered in 1 sec., as compared with 1 hr. or more with the usual types of tube.

g. Condenser Discharge Tubes for Very High Intensities.—Even with all the devices mentioned in foregoing sections a limit is reached in the nondestructive operation of tubes to attain maximum intensity. There remain only practically instan-

¹ MÜLLER and CLAY, *J. Inst. Elec. Eng. (London)*, **84**, 261 (1939).

taneous discharges of relatively enormous energies. This precept has been incorporated in tubes designed by Kingdon and Tanis¹ at Schenectady for biological experiments at great intensities. The tube with a mercury-pool cathode cooled to 0°C. and a tungsten target is operated from a 0.025-mfd. condenser charged to 105 kv. and discharged through the tube. Each discharge of the condenser delivers 3.5 *r* (for the unit of intensity or dosage, see page 67) in 5×10^{-6} sec. at a distance of 11.5 cm. The condenser was discharged about once a second, so that the instantaneous x-ray emission reached $4.2 \times 10^7 r$ per minute, or an average of 200 *r* per minute as compared with

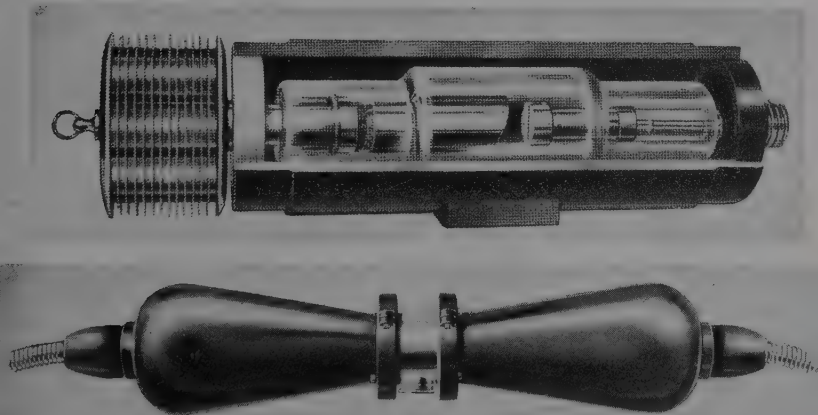


FIG. 21.—Types of shockproof x-ray tube casings: above, Machlett; below, Philips.

usual dosage of 3 to 4 *r* per minute for ordinary tubes. Immediately upon initiation of the discharge through such a tube, mercury vapor is produced by positive-ion bombardment of the mercury cathode. This vapor liberation takes place in the path of the discharge, when it is ionized, thus giving rise to further positive-ion bombardment of the cathode with the liberation of more electrons and the production of more vapor up to a limit that will not cause the voltage to fall off too rapidly.

h. Shock- and Ray-proofing.—The majority of x-ray tubes are built today with features of construction designed to protect patients and operators against danger of shock from high tension or of undue exposure to radiation. Protection against shock

¹ *Phys. Rev.*, **53**, 128 (1938); *Radiology*, **31**, 52 (1938).

involves an outer casing around the tube at ground potential with similarly protected leads (Fig. 21); better still, the tube is entirely immersed in oil inside the shockproof casing (Fig. 22); best of all, the tube is enclosed in the same grounded case and oil as the high-tension transformer coils and the rectifying valves (Fig. 23). Such devices also provide ray-proofing so that the desired beam of radiation is limited to certain openings. The

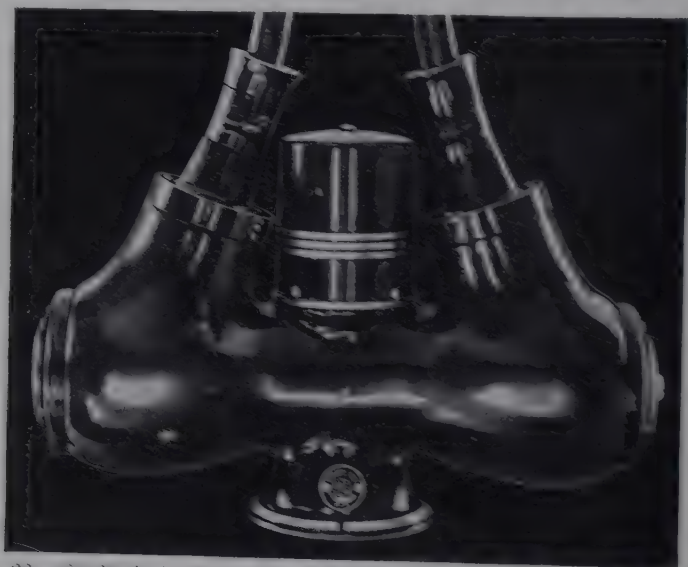


Fig. 22.—Oil-filled shockproof head for x-ray tube. (General Electric X-Ray Corporation.)

Metalix tube with chrome-iron center is self-shielding against radiation since x-rays emerge only through windows of Lindemann glass. Stem or scattered rays are stopped by a Pertinax housing around the glass parts of the tube, consisting of bakelite impregnated with lead oxide.

Diffraction Tubes for Fine-structure Examination of Materials.

In this great new branch of x-ray science the diffraction of rays by a suitable grating is used as a means of discovering the ultimate fine structures of crystals and materials of all kinds.

Though it was found that for determination of the gross structure of materials the medical deep therapy or diagnostic tubes could be used, special attributes are desirable in tubes for studies of fine structure:

Moderate voltages, 25 to 50 kv.

Largest possible tube currents so as to cut down exposure times.

Continuous operation, since diffraction photographs may require many hours or days.

Medium or fine focus.

Small dimensions so that distance from target to specimen may be a minimum.

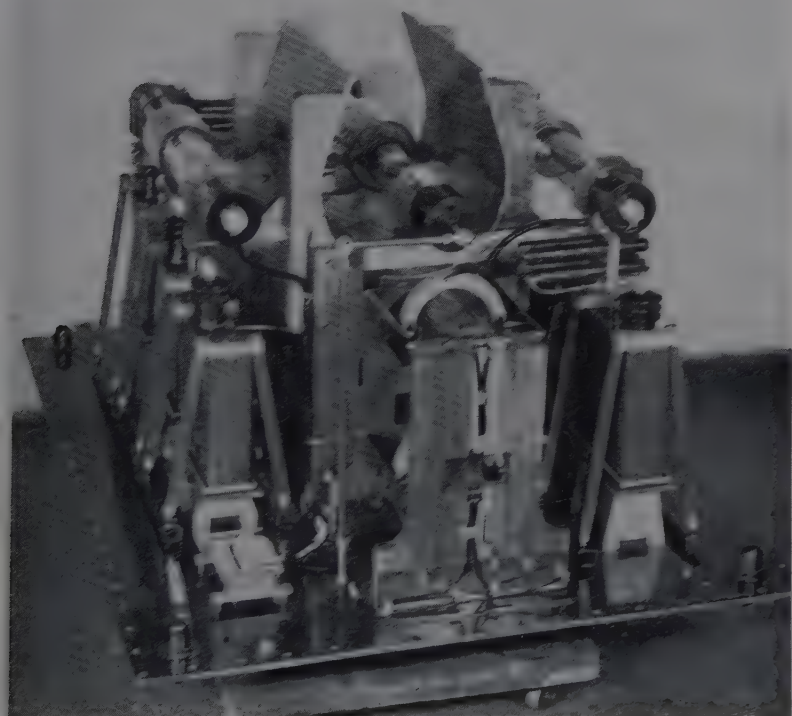


FIG. 28. - Complete x-ray and ray-proof unit with x-ray tube (top, center), enclosed in oil-filled case with transformer coils and rectifying valve tubes. (General Electric X-Ray Corporation.)

Minimum absorption of beam in desired directions.

Target usually not tungsten, but molybdenum, copper, iron, etc., and preferably easily interchangeable.

Multiple beams from the same target for routine examination of numerous specimens; hence flat target at right angles to cathode-ray beam from which rays at grazing angles may be defined radially.

Numerous modifications of the hot-cathode tube have been made, largely aimed at adapting it for use in x-ray diffraction work with crystals, where interchangeable targets, small dimensions in order to approach as closely as possible to samples and spectroscopic apparatus, and general flexibility and ruggedness are required.

The best features of the diagnostic tubes in which requirements are similar have been embodied by various manufacturers, particularly Philips, in diffraction tubes of the electron type. The most important of these are as follows:

1. Line-focus filaments for great intensity and sharp focus. In such a tube four diffraction photographs may be made simul-

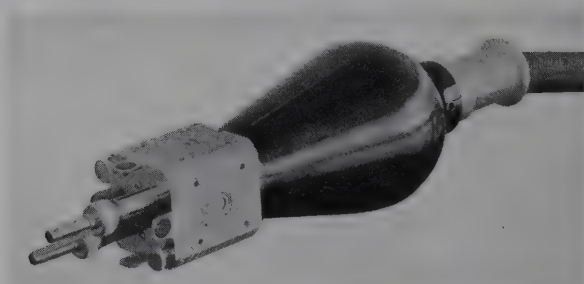


FIG. 24.—Newest Philips Metalix protected diffraction tube.

taneously with opposite beams from the line focal spot, two from the length (strong), and two from the breadth (weak), on a target at right angles to the cathode rays.

The diffraction tube of newest design with shock- and ray-proof outer casing with replaceable inserts is illustrated in Fig. 24. Four windows of *Lindemann glass* (containing boron, lithium, and beryllium instead of silicon, sodium, and calcium as in ordinary glass), through which the beam passes with little absorption, thus permit the study of four specimens simultaneously.

2. Demountable tubes. Besides the several varieties supplied by the manufacturers already pumped and permanently sealed off, demountable tubes are available. It is convenient to be able to interchange targets in the same tube for diffraction research and particularly for spectroscopic analysis in which the unknown substance must constitute the target and must be mounted or pasted on a suitable backing. This, of course, means

that the tubes must be pumped during operation. To one skilled in high-vacuum technique this does not present great difficulty, since equipment combining oil-backing pump, mercury-diffusion pumps in one or more stages, and liquid-air traps is well standardized.

Several tubes made largely of metal are in the market, and many have been designed and built in various laboratories. A photograph of the Ott-Selmayr tube in the writer's laboratory

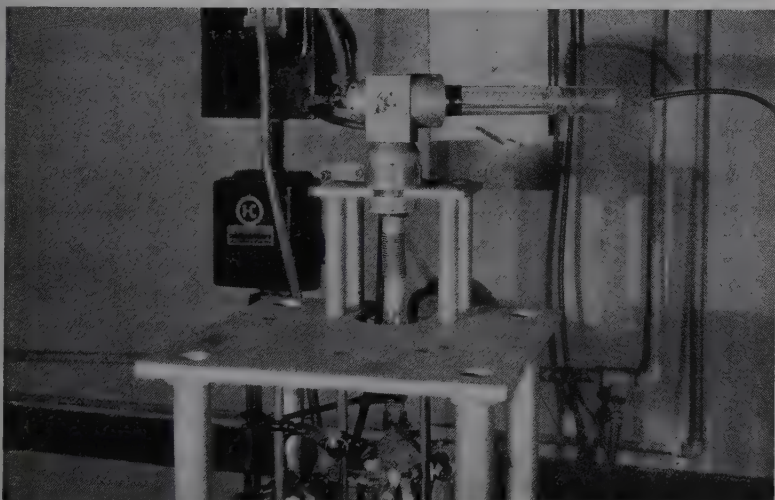


FIG. 25.—Ott-Selmayr demountable x-ray diffraction tube in University of Illinois laboratory.

is presented in Fig. 25. The body of the tube is essentially a heavy triangular block of metal into which the electrodes are fitted at an angle of 120 deg. The cathode arm is of glass, and the spiral or line-focus filaments are interchangeable. The targets of various metals are easily removable and interchangeable. The window of thin aluminum (or, better, beryllium) foil is only a few millimeters from the focal spot, and the specimen for structure analysis can thus be placed very close to the target. The result is a tube which provides radiation of extremely high intensity.¹ The rotating target is also utilized for currents of 150 ma. or more.

¹ For a description of this tube with improvements see Clark and Corrigan, *Ind. Eng. Chem.*, **23**, 815 (1931).

Diffraction apparatus is considered in detail in Chap. XIII.

CHAPTER III

HIGH-TENSION EQUIPMENT

Of the various methods of producing the difference of potential across an x-ray tube, the alternating-current high-tension transformer is now of greatest practical importance. Static induction machines and induction coils operating on direct current with interrupters were used widely for many years after the discovery



FIG. 26.—Storage battery, 100,000 volts, in Cruft Laboratory, Harvard University.

of x-rays. The latter are still to be found in some laboratories and hospitals, particularly where gas tubes operated at moderate voltages are used.

Singularly enough, the principle of the electrostatic generator, supposedly relegated to museums, has been resurrected in the sensational Van de Graaff generator, which has already contributed great impetus to installation of supervoltage x-ray

units as well as to the popular and fertile field of nuclear physics. Besides the transformer and the electrostatic generator, the storage battery, the radio-frequency generator as devised by Sloan and associates, and the remarkable new General Electric resonance transformer warrant consideration.

Storage Batteries.—The high-tension storage battery is, of course, the ideal source of power, since the voltage across the tube remains perfectly constant and no rectifying devices are required. Storage batteries have the disadvantages of being very expensive, difficult properly to insulate, and dangerous to the operator since very large currents may be instantaneously drawn from them, and of requiring constant attention. A 43,000-volt storage battery made from test tubes gave excellent results for more than twenty years at Harvard University. With it the precision researches on x-rays by Duane and his students, particularly the most accurate evaluation of the Planck constant h , were made possible.¹ A 100,000-volt plant (Fig. 26) with the cells in pint jars has much greater capacity and every possible improvement. This battery will operate a tube for two weeks before recharging is necessary.²

Transformers.—Most of the x-ray power units on the market are designed for therapeutic and diagnostic use at voltages up to 250 kv. These commercial machines are all similar in general operation but differ in details of design. They usually include:

A 60-cycle 110- or 220-volt alternating-current closed-core oil-immersed high-tension transformer.

A separate transformer for filament current up to 5 amp. at about 12 volts in the x-ray tube and in the rectifying valve.

An autotransformer or resistances for controlling input and thus secondary voltage.

A device for stabilizing and controlling the tube current.

A device for rectifying the alternating high-tension current, of either a mechanical or an electron-tube type.

The transformer comprises a magnetic core wound with primary and secondary windings. Alternating current supplied to the primary induces in the core a magnetic flux that cuts the

¹ *J. Optical Soc. Am.*, **5**, 213 (1921).

² A complete description of the installation is given in a paper by Armstrong and Stiffler, *J. Optical Soc. Am.*, **11**, 509 (1925).

secondary winding, thus generating in it an e.m.f. proportional to the number of turns. The fundamental equation involved for the induced e.m.f. (root mean square), on the assumption of sine wave form, is $E = \frac{2\pi f}{\sqrt{2}} \phi N \cdot 10^{-8}$ volt where ϕ is the total

magnetic flux lines through the core, N is the number of turns in the winding, and f is the frequency in cycles per second. The core is built up in laminar form from thin sheets of an alloy, usually silicon steel, with high magnetic permeability. Since a radial field between primary and secondary windings represents the most uniform electrical-stress distribution, circular coils are generally used in x-ray transformers. In practically all cases, core and windings are immersed in insulating oil.

The great majority of units operate on single-phase current though three-phase systems are growing in importance. Engineering problems include proper dimensions for desired loads, insulation within and between coils and of external terminals, cooling, tapping and grounding of the secondary, capacitance effects and screening, and combination with condensers for constant potential. Ordinarily the transformer is earthed at the center in the case that the x-ray tubes are operated with both ends at high potential, or at one end, especially when the anode of the tube is cooled by water from city mains. Complete details and specifications of transformer design are supplied by manufacturers or illustrated in suitable texts.¹

Rectifiers.—The x-ray tube is a device that can operate successfully only with a unidirectional electric current, *i.e.*, with the target serving as the anode and the filament as the cathode. However, an end of the secondary winding of the high-tension transformer is oscillatory between $+V$ and $-V$, so that each electrode in the x-ray tube connected with this secondary will be at negative potential half of the time and at positive potential the other half. In order to ensure that electrons will flow only from negative filament to positive target, the current must be rectified in the x-ray tube itself or by auxiliary mechanical or electron-tube rectifiers. In half-wave rectification, current flows only during the half time when the filament is negative and the target positive, the inverse wave being sup-

¹SARFIELD, "Electrical Engineering in Radiology," Instrument Publishing Company, 1936.

pressed. In full-wave rectification the total energy is utilized, the terminals of the secondary being connected alternately to opposite ends of the x-ray tube in synchronism with the alternations of the current.

Mechanical Type.—The mechanical full-wave rectifiers are crossarm arrangements revolving on the shaft of the alternating-current generator or driven by a synchronous motor. This rotating switch connects the terminals of the secondary alternately to opposite ends of the x-ray tube in synchronism with the alternations of the current. Only a portion of the top of these waves is applied to the x-ray tube, since the contacts are intermittent. The tube is, therefore, excited by pulses which are alike, as illustrated in Fig. 27. The mechanical rectifier has the advantage of ruggedness and adjustment so as to pick off any position of the voltage sine wave. It has the disadvantage of noise, moving parts, and electrical disturbances. Although many mechanically rectified units are still in operation and continue to give satisfac-

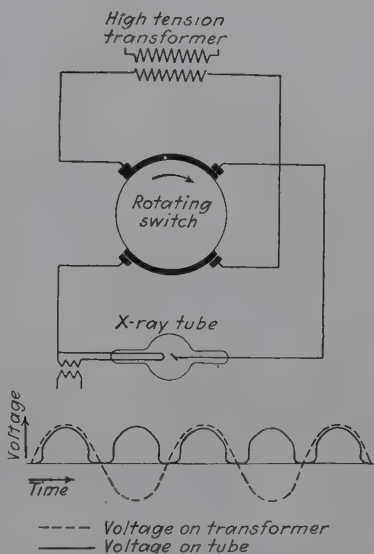


FIG. 27. —High-tension circuit and wave form with mechanical rectifier.

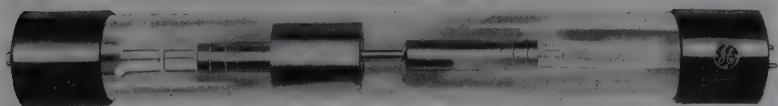


FIG. 28.—Electron valve-tube rectifier (Kenotron). (General Electric X-Ray Corporation.)

tory service, further consideration need not be given them in view of the overwhelming preference for the electron-tube valve, especially since these have become far less fragile than the early models.

Valve-tube Type.—This electron-tube rectifier is a vacuum tube operating on the same principle as the x-ray tube. In the

original Coolidge Kenotron, shown in modern form in Fig. 28, a tungsten-wire filament is at the center of a coaxial cylinder of sheet molybdenum. The filament is heated by a current from storage batteries or step-down transformers. Current passes

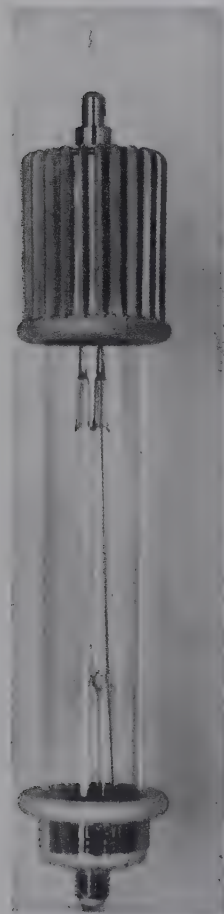


FIG. 29.—Philips Metalix valve tube.

through the valve, of course, in one direction only, since the hot wire is the only source of electrons. During the time of flow of current from hot cathode to anode, a difference of potential of only a few hundred volts at the most is required to overcome the space charge that develops around the filament owing to the emission of electrons. During the other half period when the cathode is positively and the anode negatively charged, the entire difference of potential on the x-ray tube is impressed on the valve tube, so that it must be constructed to withstand this. In another type the filament consists of three or more hairpin loops of wire, and the anode is a cup or disk. The filament heating current is 7.8 to 8.2 amp. at 12 to 14 volts, and such a tube passes a current of 300 to 400 ma. Glass tubes are made by all the prominent manufacturers. The Metalix valve tube (Fig. 29) has two metal cylinders which are fused on both sides of an insulating glass cylinder. The upper metal cylinder serves as anode with radiator-fin cooling. The heating voltage is 15 volts, and the emission at 8 amp. passes 600 ma. or at 8.5 amp. 1,100 ma.

To meet increasing demands for currents up to 1,000 ma. with small voltage drop the Metalix gas valve was designed (Fig. 30). It depends for its action on the rectifying properties of mercury vapor and consists of a number of small discharge tubes arranged end to end in a common envelope, the first in the series supporting the oxide filament cathode. In order to ensure uniform voltage drops across the successive stages, condensers are arranged in series around them, with each condenser in

parallel with a discharge stage. The heating energy for this valve is one-tenth of that required in the high-vacuum valve, and the tension drop is only about 50 volts. On account of these characteristics, the valve dimensions can be very small when it is immersed in the transformer oil.

The operating characteristics of the various types of valve are shown in Fig. 31.

One of the chief dangers of the valve tube is the generation of x-rays when operated beyond the saturation point defined by the equation

$$V = AI_s^{\frac{2}{3}} \left(1 + \frac{BI}{I_s - I} \right)$$

where V is the voltage, I is the current, I_s is the saturation current, and A and B are constants for particular valve and filament temperature (about $1000^\circ\text{C}.$). If the anode becomes hot, this is an indication that extensive power is being dissipated.

It is essential that the tubes should be constructed so as to withstand high voltages when the anode is at negative potential with respect to the filament.

Another high-voltage rectifier, which has come into recent use especially in Great Britain and is distinguished by both ruggedness and absence of moving parts, employs copper oxide film rectifier units connected in series and immersed in oil.

Circuits.—Numerous types of circuit involving transformers and valve-tube rectifiers with auxiliary equipment are employed for various x-ray purposes. Some of the more important are:

Self-rectifying Coolidge-type x-ray tube; half-wave rectification; for diffraction and other equipment up to 60 kv. where loss in power is not so important as simplicity and economy (Fig. 32).

Single-valve half-wave rectification; with or without condensers gives impulses; for use with gas- or ion-type tubes up to 80 kv. primarily (Fig. 33). A unit of this type is shown in Fig. 34.

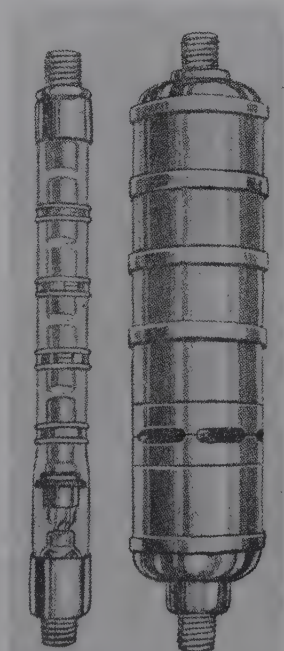


FIG. 30.—Gas-filled rectifying valve tube for high currents (Philips Metalix).

Full-wave Rectification. The Gratz Circuit.—This circuit employs four valves, as shown in Fig. 35. When q , one end of the secondary winding, is negative and p is positive, electrons will flow from q through valve 2, the x-ray tube, and then through valve 1 to p ; when p is negative, the electrons will flow through

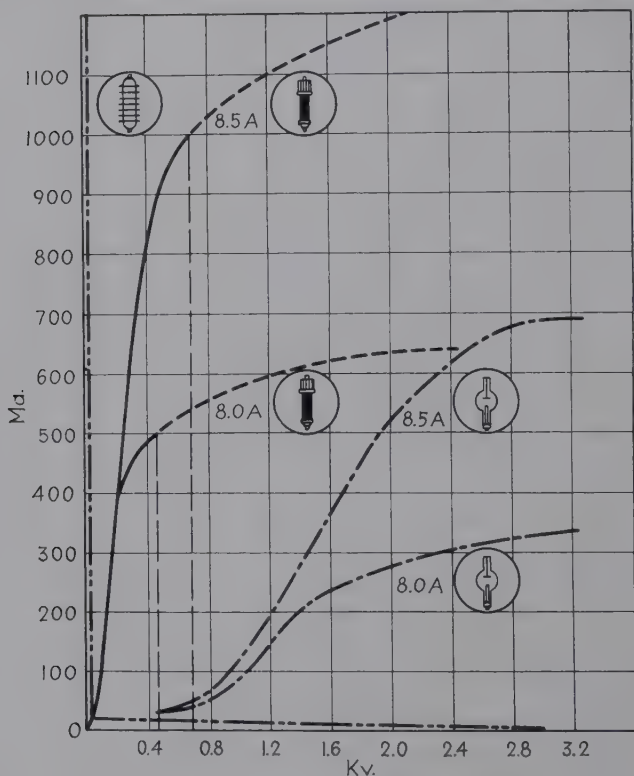


FIG. 31.—Comparative curves of current and voltage drop for various Philips valves.

valve 4, the x-ray tube, through valve 3 and then to q .^{*} Thus the continually changing transformer current reaches the x-ray tube so as to flow in one direction. This circuit has the disadvantage that two valves always must sustain the full transformer voltage.

^{*} It should be remembered that in electrical engineering practice the current is opposite in direction to the flow of electrons; thus when p is positive, the current is described as flowing from p , through valve 1, the x-ray tube, and valve 2 to q .

Other full-wave circuits are the potentiometer, in which the x-ray tube is excited at half the transformer voltage; and the Deman, which employs a valve, between one pole of the secondary and anode of the x-ray tube, and a condenser connected between the center of the transformer and the tube anode.

Voltage-multiplying Circuits.—(a) Villard circuit (Fig. 36). The transformer secondary is connected to the x-ray tube through two condensers, one at each pole. Across the x-ray

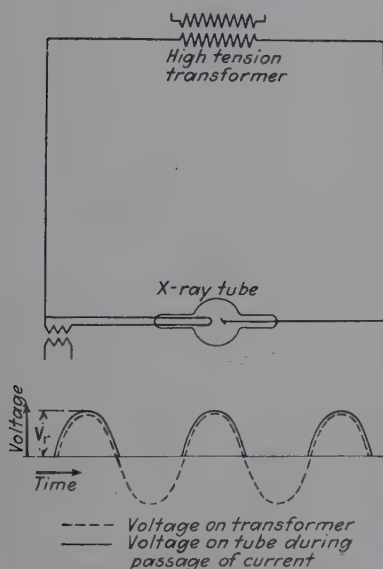


FIG. 32.—Circuit and wave form for self-rectifying x-ray tube (half-wave).

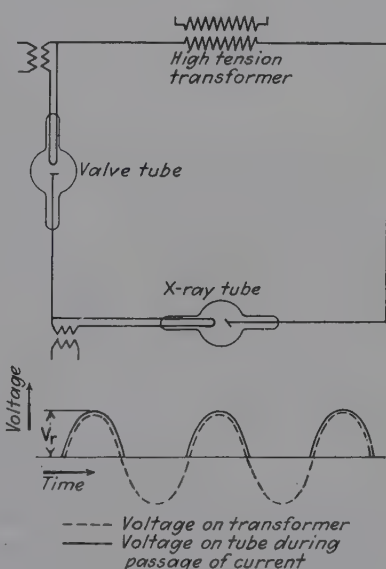


FIG. 33.—Circuit and wave form with one valve tube (half-wave).

tube in opposition is one valve. The sum of condenser voltages is alternately supplemented and reduced by transformer voltage so that the potential across the tube varies from $2V$ to 0. (b) The Witka circuit is similar except that it has two valves and two condensers so arranged as to treble the voltage. Each condenser is charged to the full voltage of the transformer during a half period. During the following half period, the valves are nonconducting and the condensers are thrown in series with the transformer to make the potential across the x-ray tube three times that of the transformer. (c) The Greinacher constant-potential circuit is the best known circuit that combines voltage multiplying with a constant potential (Fig. 37).

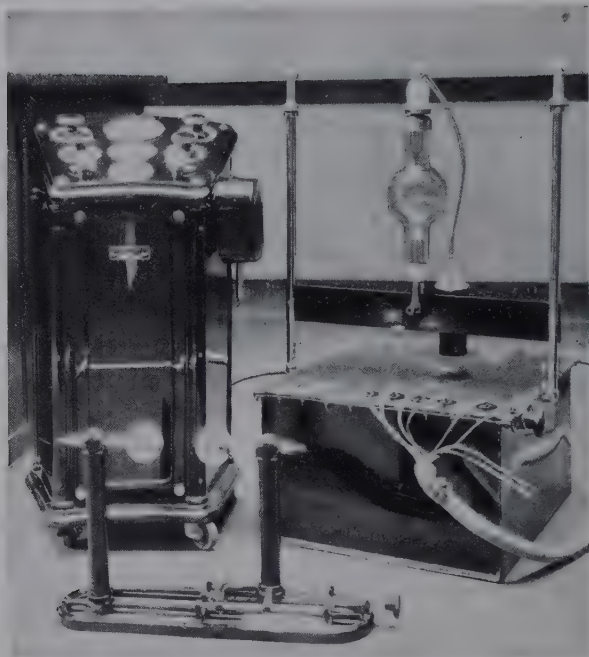


FIG. 34.—Power plant with single valve tube (circuit, Fig. 33). (*Standard X-Ray Company.*)

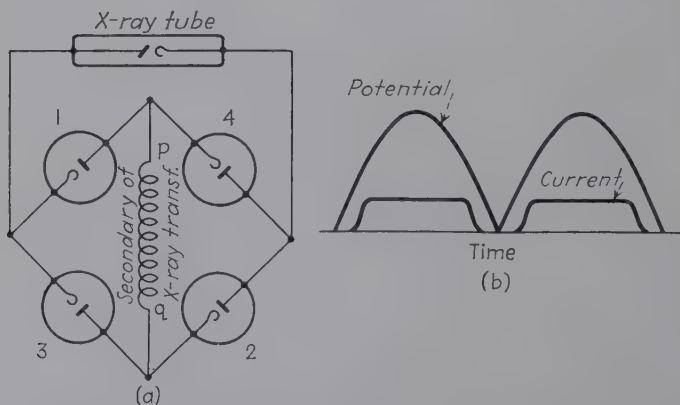


FIG. 35.—(a) Gratz circuit for four-valve whole-wave rectification. (b) Tube potential and current wave forms (approximate).

If two opposed valves are connected to the end of the transformer secondary whose potential is oscillating between $+V$ and

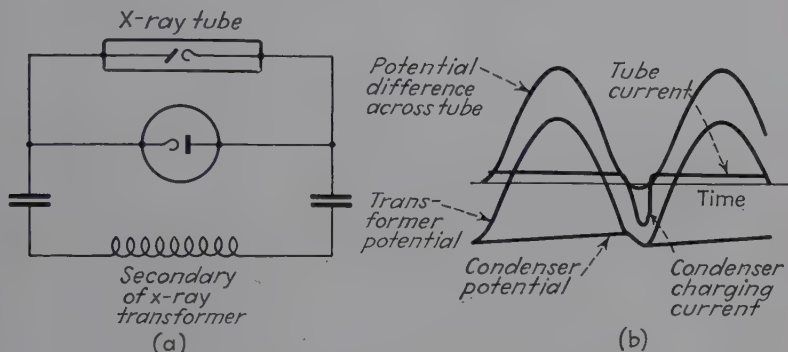


FIG. 36.—(a) Villard circuit connections. (b) Approximate wave forms.

$-V$, then the total difference of potential across the plates of the condenser and the terminals of the x-ray tube will be $+V -$

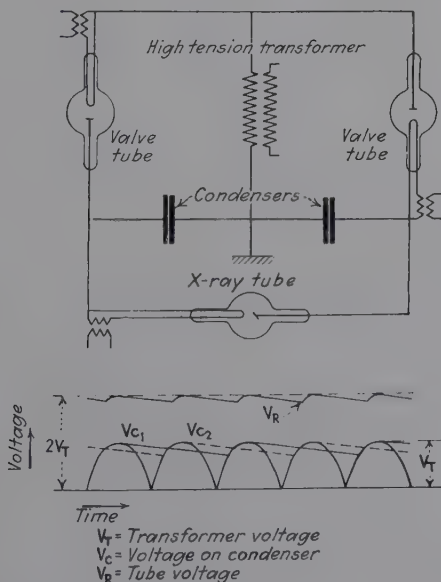


FIG. 37.—Greinacher constant-potential circuit with two valve tubes.

$(-V) = 2V$. The rectifiers must be able to withstand this voltage.

Voltage and current ripples are smoothed out to less than 1 per cent with 2 or 4 valves, a 500-cycle (or more) primary current, and condensers whose correct capacity depends upon the frequency. A highly satisfactory constant-potential direct-current (c.p.d.c.) installation due to Duane at the Huntington Memorial Hospital in Boston operates on 2,000 cycles with condensers of 0.0081 mf. capacity. With 60-cycle current no ordinary condenser capacity suffices to suppress the ripple, but a typical and usually unsymmetrical wave form is observed with an oscillograph. In any case this is subject to line fluctuations so that it is necessary to resort to separate generators.

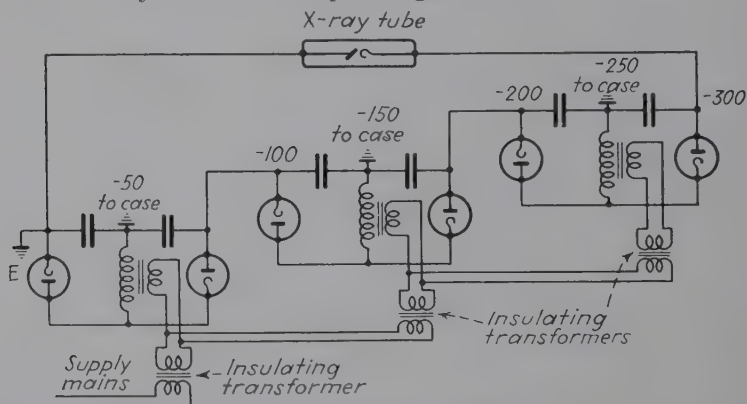


FIG. 38.—300-kv. cascade circuit using three 50-kv. transformers and three insulating transformers. One end of the system is earthed. (The figures indicate kilovoltages with respect to earth at various points.)

Cascade Circuits.—The Greinacher circuit is especially well adapted to the plan of cascading a number of similar units so as to obtain any desired supervoltage. Various combinations with mid-point or one end earthed have been described. Figure 38 shows a 300-kv. cascade circuit built up from three 50-kv. units. Most of the power plants operating American super-voltage installations of 1,000,000 volts are of this type. The Bouwers circuit of Philips manufacture is illustrated in Figs. 39, 40, and 41. It employs successive additions to a Villard circuit of valve and a common type of cylindrical condenser having concentric plates separated by layers of paper impregnated with bakelite.

The Van de Graaff Generator.—As previously indicated, the old principle of the electrostatic machine has reappeared in the

newest supervoltage installations as the Van de Graaff generator, which has proved so successful at the Massachusetts Institute of Technology, at the Huntington Memorial Hospital, Boston, Mass., and elsewhere. A system of moving belts conveys electric charge to collecting spherical terminals, which are 15 ft. in diameter. The belt material is electrical insulation paper, about 4 ft. in width. Charge as sprayed on the belt from a system of corona wires is removed from the ascending belt inside the terminal by a collector connected to an insulated upper frame. As the voltage of this frame increases owing to collector current, corona is produced at the upper spray wire and charge of opposite sign is deposited on the descending belt. A difference of potential between two generator terminals, one positive and one negative, may therefore reach 5 to 6 megavolts and provide a current of 2 ma. for the x-ray tube or any other type of accelerating tube.¹

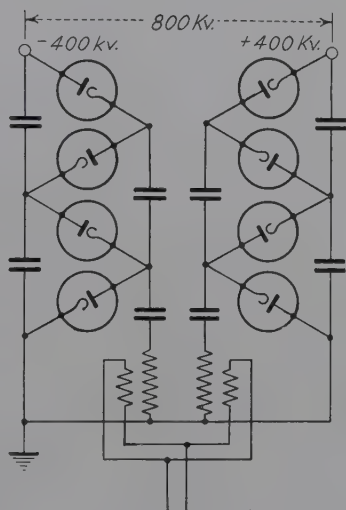


FIG. 39.—Bouwers voltage-multiplying circuit for 800 kv.p.

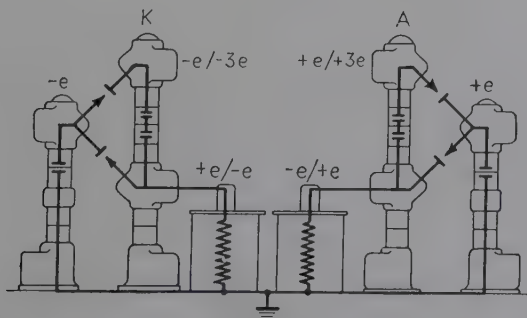


FIG. 40.—Diagram of Philips deep-therapy power unit with Bouwers circuit.

The Sloan Generator.—This most remarkable of all types is actually a high-tension transformer and x-ray tube combined within a steel case. The design as indicated in Fig. 42 is ideal for

¹ *Phys. Rev.*, **43**, 149 (1933); **49**, 761 (1936).

1,000,000 volts. Oscillating tubes more powerful than those of any short-wave radio station feed the apparatus at 6,000,000 cycles per second, self-rectifying. The entire transformer ($\frac{3}{4}$ turn primary and 14 turns secondary) hangs in the x-ray vacuum.¹

The General Electric Resonance Transformer (1,000,000 Volts, 3 ma.).—This transformer utilizes a new principle and

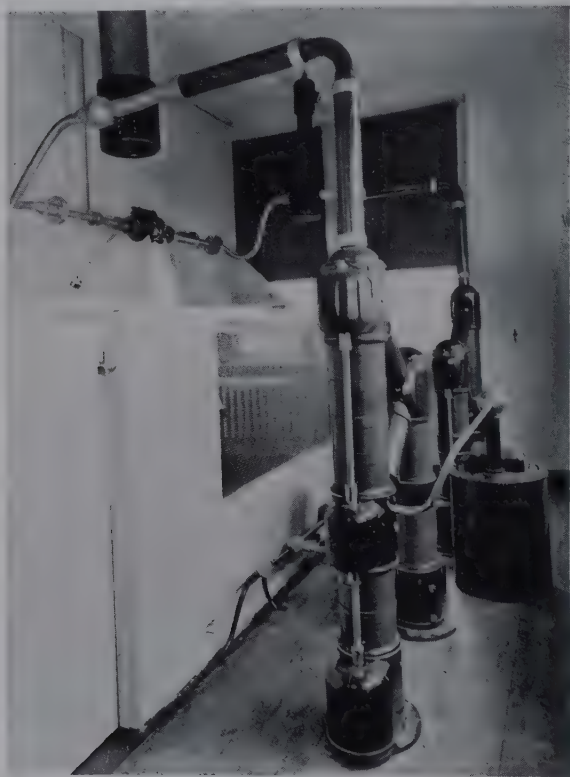


FIG. 41.—Hospital installation of unit in Fig. 40.

embodies a resonant system tuned to a frequency three times that of the supply; thus in the case of 60-cycle power service the transformer will operate at 180 cycles which frequency is obtained by means of a phase-reducing frequency-tripling transformer device connected to a three-phase power service. The transformer does not have a core through the coils, and the space usually occupied by the core is occupied by the x-ray tube.

¹ *Radiology*, **24**, 153, 298 (1935).

The only transformer iron used in the transformer is placed outside the coils and just inside the wall of the cylindrical steel tank. Because of the absence of iron in the transformer and also because a gas is used for insulation instead of the usual transformer oil, the construction is exceptionally light in weight in comparison with its capacity. One hundred pounds of gas (CH_2F_2) perform the insulating function of 6 tons of oil. The transformer is housed within a cylindrical steel tank approximately 4 ft. in diameter and 7 ft. in length with the extension chamber of the x-ray tube projecting from the bottom (Fig. 43).

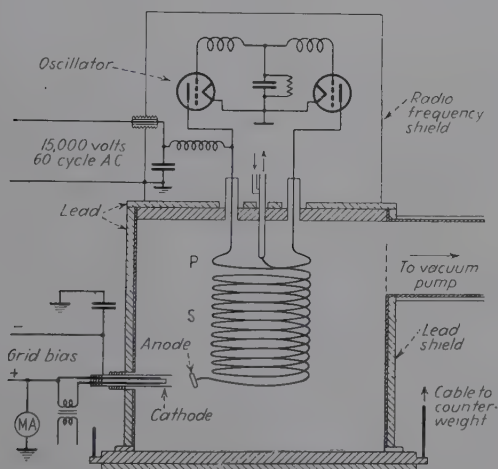


FIG. 42.—Sloan tube and generator for 1000 kv.; the entire transformer ($\frac{1}{2}$ turn primary and 14 turn secondary) hangs in the roentgen-ray vacuum and runs at 6,000,000 cycles per second, self-rectifying.

The method of controlling the power supplied to the high-voltage transformer is also new; the actual power service is three-phase which, through the tripling device already mentioned, is transformed into single-phase power with three times the frequency of that supplied. The output of the tripler is fed into an autotransformer designed for the triple frequency, and the output of the autotransformer is then supplied to the high-voltage transformer, through a saturated core reactor which has a motor-driven control device to provide proper control during the starting period.

The x-ray tube is a multisection tube (Fig. 15) and operates with the anode at ground potential. The tube is located at the

center of the tubehead, inside the secondary coils of the high-voltage transformer, and the anode and projects through the bottom of the tubehead. One of these units is in operation at the Memorial Hospital for the Treatment of Cancer and Allied Diseases, New York, N. Y.

Electrical Measurements.—Tube current is, of course, measured by the milliammeter, a moving-coil galvanometer with

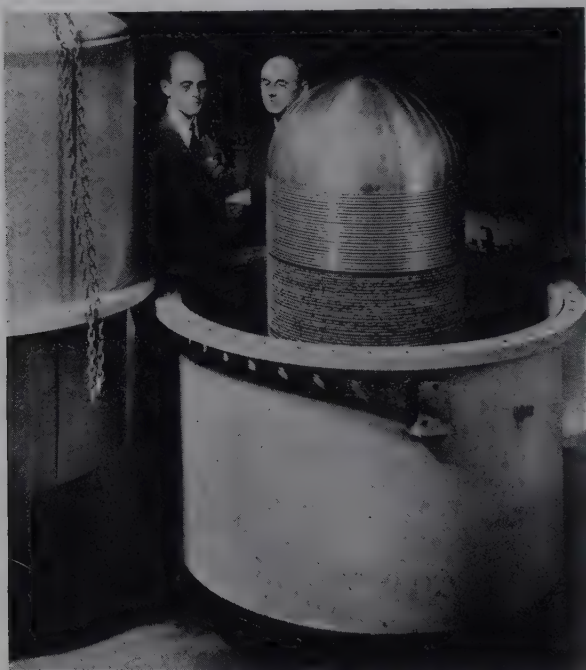


FIG. 43. —General Electric Resonance Transformer operating at 1,000,000 volts, 3 ma.

permanent magnetic field. Since dosage is often based on its reading, it is essential that it be a good instrument and well protected. It may be placed, properly screened against corona, in the high-tension circuit in any position except between the filament transformer and the tube, or it may be placed in the earthed part of the tube circuit and thus mounted in the control board.

The various methods of determining the peak or effective voltages applied to the x-ray tube are as follows:

1. Voltmeter reading of the transformer primary with known transformation ratio; a method accurate only with constant-potential apparatus.

2. Sphere-gap; the method most commonly used and the simplest, but giving only very approximate readings.

3. Electrostatic voltmeter; one type consists of large balls charged with high voltage and small balls on a bifilar suspension turning in the electrostatic field. This instrument requires calibration and is then very satisfactory, as a measure not only of the voltage but also of the constancy of the potential.

4. Measurement by ammeter of the current through a very high known resistance, 10,000,000 ohms, for example.

5. Spectrometric method; this consists in determining the shortest wave length in the spectrum of a beam of x-rays reflected from a crystal of known planar spacing, and substitution of this value in the very accurate quantum equation $V = hc/e\lambda$, where V is the voltage (peak), e , h , and c are constants (respectively, the charge of the electron, the Planck action constant, and the velocity of light, so that $hc/e = 12,350$), and λ is the short wave-length limit of the spectrum. This method is extremely accurate but, of course, requires special equipment and skilled technique.

6. Generating voltmeter, consisting of a simple armature rotating in an electrostatic field and a galvanometer for measuring the generated current.

7. Tapped condenser and oscillograph; the oscillograph strip is energized by currents in the plate circuit of a valve, the grid of which is connected to an appropriate tap from a capacitative voltage divider.

8. Condenser charging current; a condenser in series with a valve and ballistic milliammeter is connected across the x-ray tube whose voltage e is to be measured from $e = it/c$, where i is milliamperes, t is seconds, and c is microfarads, the known capacity of the condenser.

9. Tapped resistance method; voltage is directly measured by a voltmeter connected across a tap in a high resistance.

10. Secondary tapping, a direct voltage measurement by means of a tapping taken from a part of the transformer secondary winding near to earth, the number of turns being in a simple ratio to the total number.

Electrical Precautions.—Proper installation of x-ray equipment involves adequate protection for the operator both from the high-tension electrical power plant and leads and from the

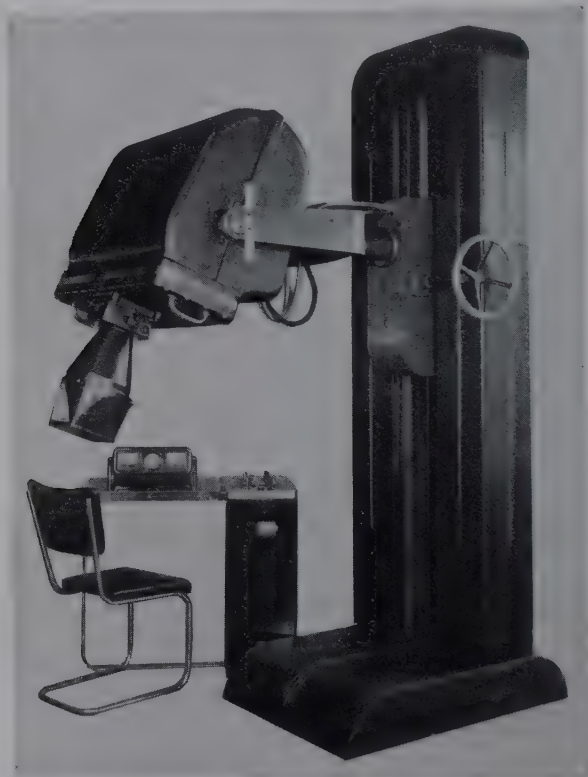


FIG. 44.—Shock- and ray-proof therapy unit with x-ray tube enclosed in adjustable head with transformer (Kelley-Koett).

x-rays themselves. The following are recommended electrical precautions:

1. Wooden, cork, or rubber floors or coverings.
2. High-tension leads concealed in an assembled unit with outside grounded; for exterior leads, preferably metal tubes or rods or tightly stretched insulated wire, suspended at a proper distance from floor and ceiling and screened from operator and patient.
3. Efficient earthing of all metal parts.
4. Safety switches, warning lights or signals, and fuses no heavier than absolutely necessary.

5. Magnetic circuit breakers to break contact with any unexpected surges.

6. Shockproof equipment. One of the best recent developments in commercial medical x-ray equipment has been in shockproof equipment. The x-ray tube is enclosed in the transformer

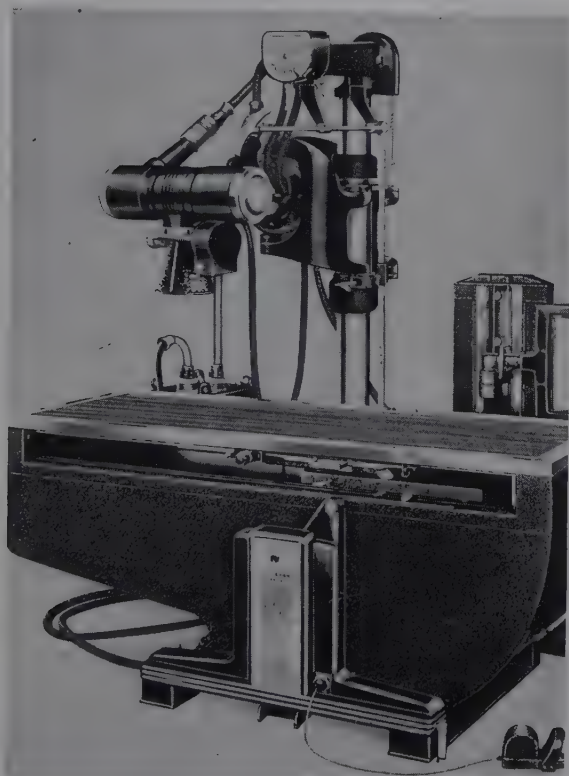


FIG. 45.—Complete diagnostic unit with protected tube, tube stand, transformers, and tilting table (Westinghouse).

itself with outer grounded and lead-covered cases. Such a unit, manufactured by the General Electric X-Ray Corporation, is pictured in Fig. 44. One of the newest complete medical units with the tube in a shock- and ray-proof casing of Westinghouse design is illustrated in Fig. 45. Suitable equipment for industrial radiography is illustrated in Chap. IX.

The protective measures to be used against the x-rays are considered in Chap. VIII.

CHAPTER IV

THE MEASUREMENT OF INTENSITY (DOSAGE)

A beam of x-rays is to be characterized by two factors: quantity (dosage or intensity); and quality (penetrating power or wave length). Certain physical, chemical, or biological effects of x-rays may be utilized for measurement of these defining factors. The measurement of intensity to be considered in this chapter can be accomplished by evaluating such x-ray properties as ionizing air and other gases, reducing silver bromide in a photographic emulsion to silver, exciting various chemical compounds to luminescence, and several others.

Heat Methods.—If a small beam of x-rays be allowed to impinge upon a metal block of such size that practically complete (97 per cent or more) absorption of the beam occurs, the net effect of the absorption will be an increase in the heat content of the block. That is to say that essentially all secondary rays, photoelectrons, etc., are absorbed in the block and their energy is converted into heat. This fact is the basis of present methods of determining accurately the total energy content of an x-ray beam. Such methods have been used to study the distribution of energy in the x-ray spectrum, the dependence of intensity upon the potential on the x-ray tube and upon the current through the tube, the relation between the energy input to the tube and the x-ray energy produced, the relation between energy, wave length, and ionization, and the relation between energy and photographic darkening.

The instruments employed generally consist of two elements, one heated by x-rays and one by electricity, which are balanced, by several different methods, against each other; the electric energy input is measured directly and, since the heat effects in the two elements are the same, is equal, after the instrumental corrections have been applied, to the x-ray energy input.

Terrill has used the method to determine the total energy of x-rays from a tungsten-target tube excited by constant potential direct current at 30 to 100 kv. The total output

of the tube was thus found to be from 0.00025 to 0.00192 times the input. Plotted against the square of the voltage these values give a straight line to 69.3 kv. where a change of slope occurs, probably due to the selective absorption of the target itself.

All these heat-measuring devices require the most careful construction and manipulation, the chances of experimental error being very great as the measured effects are usually very small; hence, they are not available for routine intensity measurements.

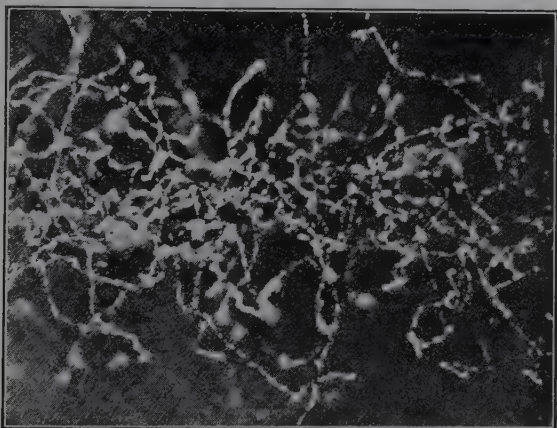


FIG. 46.—Tracks of β -rays liberated in gas by x-rays. (C. T. R. Wilson.)

Ionization.—When the x-rays pass through the gas, they liberate photoelectrons; they excite those characteristic radiations of the gas whose critical absorption frequencies are less than the frequency of the incident x-ray beam; they produce scattered radiation of the frequency of the incident beam; and they may produce recoil electrons and the accompanying secondary radiation (Compton effect).

Mechanism of Ionization.—The mechanism of ionization is now agreed to be as follows: The high-speed photoelectrons released by the x-ray beam have too much kinetic energy to be at once absorbed by adjacent molecules, and they consequently break down the molecules with which they come in contact into pairs of ions. The energy necessary for the production of one pair of ions in air, expressed as the number of volts necessary to impart to a single electron a kinetic energy equal to the energy in

question, is 33 volts. Thus they progressively dissipate their kinetic energy until it becomes so small that the electron is absorbed either by a molecule to form a negative ion or by a positive ion to cause neutralization. All this was excellently shown by the experiments of C. T. R. Wilson who, by condensing water on the ions at the moment of formation and simultaneously photographing them, was able to obtain actual photographic records of the paths of the photoelectrons. One of Wilson's photographs is reproduced in Fig. 46. Recoil or Compton electrons in addition to photoelectrons are excited by rays of shorter wave length; these electrons, though having little ionizing power, absorb much of the energy in the x-ray beam.

Ionization in Different Gases.—Table V, which lists values of relative ionization produced in various gases, shows that those which contain a heavy atom are most effective in producing large and easily measured ionization currents.

TABLE V.—RELATIVE IONIZATION PRODUCED IN VARIOUS GASES BY HETEROGENEOUS X-RAYS

| Gas or vapor | Density relative to air = 1 | Ionization relative to air = 1 | |
|-------------------------------------|-----------------------------------|-----------------------------------|-------------|
| | | Soft x-rays | Hard x-rays |
| Hydrogen, H_2 | 0.07 | 0.01 | 0.18 |
| Carbon dioxide, CO_2 | 1.53 | 1.57 | 1.49 |
| Ethyl chloride, C_2H_5Cl | 2.24 | 18.0 | 17.3 |
| Carbon tetrachloride, CCl_4 | 5.35 | 67 | 71 |
| Nickel carbonyl, $Ni(CO)_4$ | 5.90 | 89 | 97 |
| Ethyl bromide, C_2H_5Br | 3.78 | 72 | 118 |
| Methyl iodide, CH_3I | 4.96 | 145 | 125 |
| Mercury methyl, $Hg(CH_3)_2$ | 7.93 | 425 | |

Measurement of Ionization.—Ionization experiments are usually conducted so that the ionization is measured by the electric current passing through the ionized gas, under a definite potential difference. The gas is held in an ionization chamber between two electrodes which are connected to the source of electric potential. It is essential that this voltage should be high enough to produce a saturation current, that is, to draw all ions produced by the x-rays across to the electrodes. The condition of satura-

tion is recognized by the fact that further increase of the voltage applied to the chamber electrodes causes no further increase in the ionization current. It is also essential that the primary rays whose intensity is being measured shall not be permitted to strike directly on the walls or electrodes of the chamber, since otherwise secondary electrons with their own ionizing effect will be liberated.

Ionization Chambers.—Several types of ionization chamber have been designed for the determination of intensities, even in absolute units. The Duane ionization chamber, or iontoquantimeter, is one of especial merit. It consists simply of a series of aluminum sheets about 5 cm. long and 2 cm. broad held parallel to each other and 5 mm. apart by hard-rubber frames. Alternate sheets are connected, thus forming a small condenser with layers of air between the sheets. The condenser is joined in a simple electric circuit with a battery and sensitive galvanometer which is calibrated by means of a Weston standard cell and resistance. By comparison of the deflection produced by the known current with the deflection produced by the current from the ionization of air by the x-ray beam in the chamber of known volume, the intensity of the beam in r units may be calculated. Glasser at the Cleveland Clinic, Taylor at the Bureau of Standards, and others have designed large air ionization chambers for standardization purposes.

Friedrich introduced the use of an ionization chamber made of horn, the chemical elements in which are those found in the body, and containing only 1 cc. This has the advantage that intensities in absolute units may be read on a scale of the deflecting electroscope. Dauvillier has devised a spherical gas chamber containing xenon as the absorbing gas. Several other similar devices of bakelite, graphite, etc., are manufactured by equipment builders.

An unusually simple and efficient portable instrument is the Victoreen r -meter (Fig. 47), consisting of a small ionization chamber with condenser tube which may be connected with a string electrometer, the scale of which is calibrated in international units. The chamber is exposed for 1 min. to the rays and again inserted into the socket of the electrometer, and the scale read, the figure being r per minute. This instrument also serves readily in all kinds of absorption measurements including

the determination of effective wave length. Still another instrument, the Iometer, is a constancy meter, the function of which is to indicate continuously any variation from a previously established rate of r units per minute. The Integrator is a dosimeter of the integrating type designed to measure total treatment dose, for example, at skin surface, and to terminate automatically the treatment of shutting off the power to the

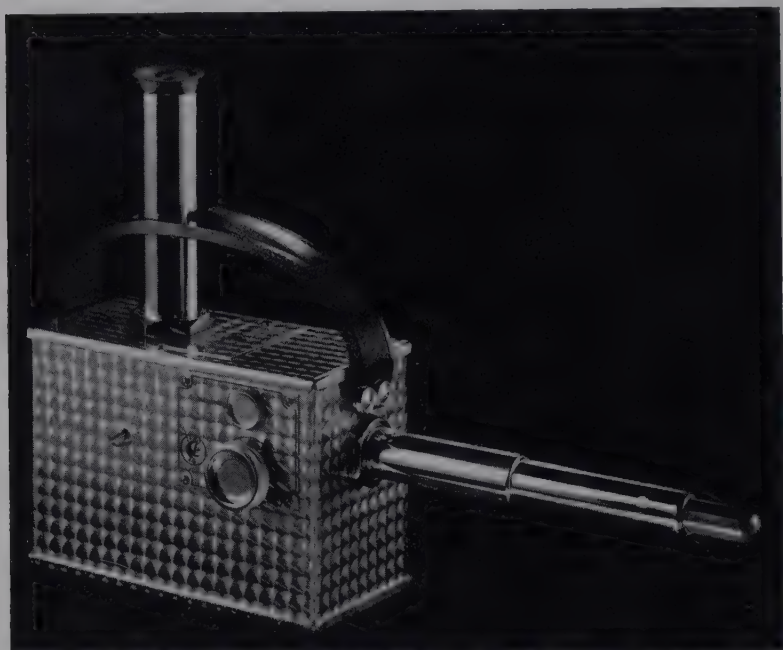


FIG. 47.—The Victoreen r -meter for measurement of intensity or dosage of x-rays.

x-ray machine. The Proteximeter is a small condenser with integral electrometer designed especially for measurement of very weak radiation as a means of protection of the worker against stray radiation.

Alternatively, by using a properly designed ionization chamber and by recording simply the ionization-chamber current as the index of intensity, the method becomes very valuable for many kinds of work, particularly in the analysis of crystal structure by the ionization spectrometer (see page 84), where only a relative measure of intensity is needed. The ionization chamber

should be large enough completely, or nearly completely, to absorb the rays; the electrodes must not be exposed to the incident rays; a gas of quite heavy molecular weight is most satisfactory, methyl iodide or ethyl bromide being often used.

There are several accepted ways of measuring the current through the ionization chamber. Some experimenters use an electroscope and time the fall of the leaf. Others use a quadrant or string electrometer. Recently it has been suggested that the current might be amplified by the use of three-element electron, or ordinary radio, tubes; and indeed such an arrangement has been developed by the Siemens and Halske Company in Germany in an instrument designed to measure dosage in x-ray therapy, usually in conjunction with the small thimble ionization chamber. This amplifies the current to such a magnitude that it may be measured by a microammeter. The General Electric Company has developed also a special amplifying tube for this purpose (see page 84).

The Unit of Dosage and Intensity.—The aim of practical dosage measurement, particularly for therapy, must consist in the selection of a radiation effect which can be measured and which changes with wave length in the same way as a given biological reaction, *e.g.*, skin erythema. Repeated experimentation has proved convincingly that a complete parallelism between skin erythema and air ionization exists independent of the quality of the radiation. Since the absorption coefficient depends not only on wave length but also on the density and on the atomic number of the elements constituting a material, it is to be expected that air consisting of the light elements oxygen and nitrogen should possess the same absorption properties as tissues consisting of organic compounds of carbon, nitrogen, and oxygen, or water. At the second International Congress of Radiology in 1928, therefore, the measurement of air ionization was accepted as the basis of international dosage measurement, and a definition was given of the unit of dosage, designated the roentgen unit, and written as “*r*,” as follows:

The *absolute unit of the x-ray dose*, one roentgen or *r*, is obtained from that x-ray energy which, when the secondary electrons are fully utilized and secondary radiation from the wall of the chamber is avoided, under standard conditions 0°C. and 760 mm. of mercury pressure, produces in 1 cc. of atmospheric air (0.001293

gram) such a degree of conductivity that the quantity of electricity measured at saturation current equals one electrostatic unit. The effective intensity, or dosage rate, of rays is expressed in r per minute or r per second.

Effect of Wave Length.—Except for heat methods involving complete absorption, the actual extent of various other effects of x-rays including ionization depends on radiation intensity and also on wave length, and on this account a different fraction of the

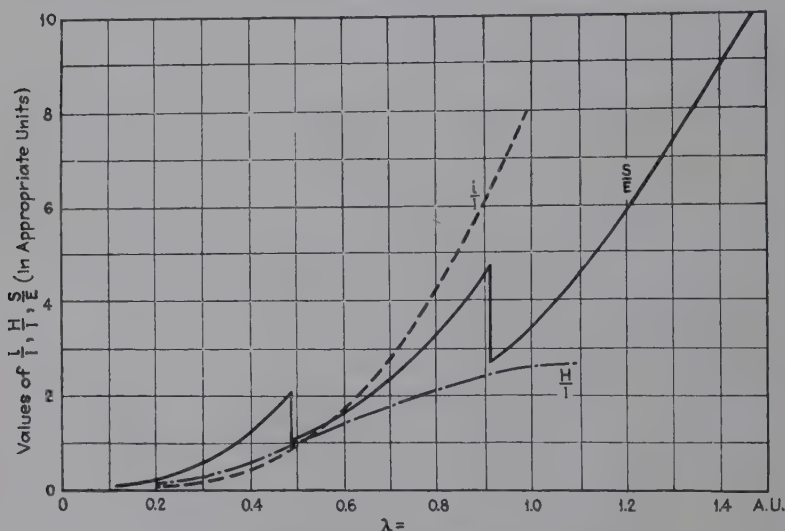


FIG. 48.—Effects of x-rays of different wave lengths.

$$\begin{aligned} i &= \text{ionization} \\ \bar{I} &= \frac{i}{\text{incident ray intensity}}; \\ H &= \text{fluorescent screen brightness}; \\ \bar{I} &= \frac{H}{\text{incident ray intensity}}; \\ S &= \text{photographic blackening}; \\ \bar{E} &= \frac{S}{\text{incident ray energy}}. \end{aligned}$$

initial radiation with varying intensity for different wave lengths is transformed in the irradiated medium into other energy forms. The action is independent of wave length only when the beam of given initial intensity, inclusive of secondary rays arising therefrom, is completely absorbed in the irradiated material. Hence the ionization current is a measure of the absorbed, not the incident, radiation intensity. The difference in the dependence of the sensitiveness of different methods of measurement upon the wave length is demonstrated in Fig. 48. If different homogeneous rays fall simultaneously with equal intensity upon

an air ionization chamber, a fluorescent screen, and a photographic plate, the brightness of the screen changes much less with wave length than the ionization current; the photographic sensitiveness changes with sudden jumps at 0.49 and 0.91 A.U. Since these wave lengths coincide with the discontinuities in absorption coefficients of silver and bromine, the two effective constituents of the photographic emulsion, the photographic action is closely connected with absorption. Hence the action of the rays changes with wave length in the same way as the intensity of the absorbed portion of the incident rays changes; exceptions occur in the rays of very short wave x-rays when the Compton effect (see Chap. VIII) is appreciable and in the case of the excitation of characteristic fluorescent rays of the irradiated material. The general rule holds for each known physical and chemical effect: The effect changes with wave length in the same way as the fraction of the incident radiation energy transformed into the energy of photoelectrons and Compton electrons. The values may be calculated for certain chemical compositions of a material from physical data (absorption coefficient, recoil coefficient, etc.), and Glocker has found excellent agreement between theory and experiment for ionization.

The Effect of X-rays on the Electrical Conductivity of Solids and Liquids.—Although there have been few experiments directly aimed at studying ionization in solids and liquids, it is certain that the increase in electrical conductivity of certain solid dielectrics such as sulfur, paraffin, hard rubber, and amber when exposed to x-radiation is exactly the same phenomenon as ionization of gases.

The conductivity of sulfur was found to increase rapidly to a constant and reproducible value if the raying was not continued over a period of more than about 2 min. In such cases, also, the conductivity fell to its original value almost immediately after the raying was discontinued. If, however, the dielectric was exposed to the rays for a somewhat longer period of time, the conductivity first rose, then gradually fell off, and did not drop immediately to its original value after cessation of the raying. It was found that the current through the sulfur was proportional to the voltage imposed and to the x-ray intensity. It may be concluded that those solids which are strong dielectrics undergo an ionization exactly similar to that of gases. Indeed,

it is probable that this phenomenon is of fundamental importance in every direct effect of radiation and that a more complete knowledge of it will lead to a better understanding of the many and diverse ways in which x-rays react upon matter.

The fact that saturation currents can be reached for amber, hard rubber, and paraffin makes these dielectrics more suitable for practical insulation in x-ray apparatus than sulfur, unless protection is provided against the x-radiation. Thus for thin insulator layers the conductivity of sulfur is appreciably higher than that of the others. In this connection it is interesting to notice that monoclinic sulfur is approximately three times as conductive as rhombic sulfur when irradiated with the same beam.

An effect somewhat similar to the one just discussed is the well-known change in the electrical resistance of selenium crystals when illuminated with ordinary light, ultraviolet rays, or x-rays. This phenomenon of resistance decrease, which must find its explanation ultimately in the peculiarities of the structure of the selenium crystal, has been explained upon the basis of several hypotheses, one of the most promising being that of resonance. By this theory the electrons in the crystal that have radiation frequencies in approximate correspondence with the frequency of the exciting radiation are temporarily loosened from their atomic bonds and become available for the transfer of electricity. In a practical way this phenomenon has found some application in estimating x-ray intensity. The method is only qualitative, and the cells must be checked frequently against a standard, since they change characteristics during usage.

The conductivity (C) of insulating liquids exposed to x-rays has been investigated a few times. A few typical results are as follows for

$$C = 10^{-4} \text{ ohm}^{-1} \text{ cm}^{-1}:$$

Carbon tetrachloride 8, carbon disulfide 20, amylene 14, benzene 4, liquid air 1.3, petroleum ether 15, vaseline oil 1.6.

The Excitation of Luminescence in Irradiated Substances.—The excitation of luminescence in many substances, when irradiated by x-rays, is a property that has played an important role in the history of the science. As a matter of fact, the fluorescence of neighboring objects led to Roentgen's discovery of the radiation.

The phenomenon depends upon the ability of substances to absorb the rays and transform the energy into radiation of longer wave lengths in the ultraviolet or visible regions.

Schuhknecht was the first to study the fluorescence of materials under x-rays, with the quartz spectrograph. Because of the excellence of his work, the results are presented in Table VI, showing the spectral regions and the wave lengths of the intensity maxima, in angstrom units.

Schuhknecht observed that the spectral distribution of the luminescence was profoundly influenced by minute amounts of impurities, as is well known for fluorescence under visible light.

TABLE VI.—WAVE LENGTHS OF FLUORESCENT LIGHT EXCITED BY X-RAYS

| | Region, A.U. | Position of maximum, A.U. |
|---------------------------------|-----------------|---------------------------------|
| Fluorspar..... | 3640–2400 | 2840 |
| Fluorspar and iron spar..... | 3900–2310 | 2800 |
| Scheelite (Ca tungstate)..... | 4800–3750 | 4330 |
| Zinc sulfide..... | 5090–4120 | 4500 |
| K platincyanoide..... | 4900–4120 | 4500 |
| Ba platincyanoide..... | 5090–4420 | 4800 |
| Ca platincyanoide..... | 5090–4550 | 4800 |
| U NH ₄ fluoride..... | 4400–3800 | 4100 |
| X-ray tube glass..... | 5090–3000 | 3750 |

Nichols and Merritt¹ found that the intensity distribution in a fluorescent band was independent of the exciting radiation, x-rays, ultraviolet light, or cathode rays. More recently Wick² has studied the fluorescence of uranium salts, and Newcomer³ that of about 500 chemical compounds (mostly organic). The latter found sodium bromide very strongly fluorescent in the ultraviolet and benzoic acid and naphthalene and their derivations in the yellow-green.

All workers with x-rays are probably familiar with the fact that when the radiation strikes the eyes there ensues a sensation of luminescence which may continue for several seconds after the

¹ *Phys. Rev.* (1), **21**, 247 (1905); **28**, 349 (1909).

² *Phys. Rev.* (2), **5**, 418 (1915).

³ *J. Am. Chem. Soc.*, **42**, 1997 (1920).

exciting source is removed. This latter phenomenon is an example of *phosphorescence*; with x-rays, phosphorescence, in general, is usually more pronounced than with light because of the deeper penetration of the former and hence of a greater volume effect. Gases and many solids are phosphorescent. Even powdered rock salt is easily visible in a darkened room for a half hour or more after its exposure to x-rays.

There are several practical uses of fluorescence under x-rays. The property may be used to differentiate between chemical substances, *e.g.*, diamond and a glass substitute. It may serve as the basis of developing invisible inks and identification marks.

For measuring intensity of x-rays by fluorescence methods, the fluorescence of a screen is compared with the fluorescence produced by a standard radiation. This is obviously a comparative method and is open to the objections that the fluorescing salt becomes "tired" under the action of the rays and that the screen may not be of uniform fluorescing power. The objections to using fluorescence methods to determine absolute intensity are that the relation between fluorescence and the x-ray intensity is unknown and that certain rays will excite a characteristic fluorescence.

The fluorescence of screens impregnated with such materials as zinc silicate is the basis of the very important application of visual radiography, or fluoroscopy, which will be described in Chap. IX.

Fluorescent Intensifying Screens.—A very practical use of the property of fluorescence is the intensifying screen, used with photographic films in x-ray radiographic and crystal diffraction applications in order to cut down the time of exposure, sometimes to one-twentieth of the usual value. For these screens, calcium or cadmium tungstate serves best because of its intense blue-violet fluorescence. The screens are usually placed behind the photographic plate or film, and the fluorescent portions add their action on the sensitive emulsion to the direct x-ray effects. Unless care is used, difficulties with the screens may arise, as follows:

1. If the calcium tungstate is not pure, the screen may have an appreciable hang-over, or phosphorescence. Several years ago some of the best commercial screens produced a distinct effect on a photographic plate for as long as three months

after their exposure to x-rays. Hence, this extraneous action of previously used screens may lead to misinterpretation of newly obtained x-ray photographs.

2. Unless the screen is very carefully prepared for uniform particle size and is placed in the closest proximity to the sensitive emulsion, it may reduce the definition of the photograph by broadening the image. This effect is observed easily, even when only the thickness of the glass of a photographic plate separates the emulsion and the luminescent image.

3. The intensity of fluorescence depends upon the wave lengths; although quantitative data on this point are lacking, de Broglie showed that a screen had no intensifying effect upon rays with

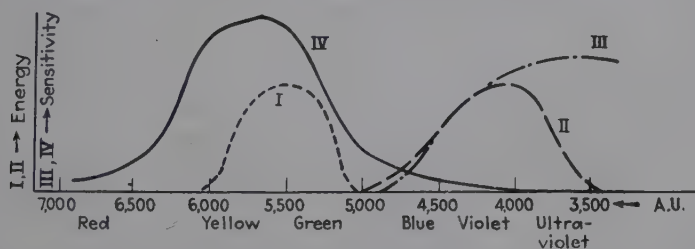


FIG. 49.—Curves showing spectral ranges of maximum sensitivity of the eye and photographic plate, to which should correspond, respectively, the fluorescent screen and the intensifying screen. I, fluorescent screen; II, calcium tungstate intensifying screen; III, silver bromide of photographic emulsion; IV, human eye.

wave lengths of 1.25 A.U. but displayed a gradual increase in effectiveness up to the critical absorption wave length of tungsten at about 0.179 A.U., at which point, corresponding to greater absorption, a sharp increase occurred for the shorter wave lengths. For this reason fluorescence cannot serve satisfactorily as a means of measuring x-ray intensities.

An interesting comparison is given in Fig. 49 of the spectral ranges of sensitivity of the eye, the fluoroscope screen (containing as the most important constituent zinc silicate), the silver bromide emulsion, and the calcium tungstate photographic intensifying screen. Very properly the first two and the last two show sensitivities over the same spectral range.

Biological Use of Fluorescence.—Finally, the newest and most remarkable application of fluorescence of substances irradiated by x-rays was that discovered by McDonald and associates in cancer researches in Philadelphia. Living cells comparatively

resistant to the direct action of x-rays were treated with solutions of organic compounds that fluoresce in the ultraviolet range when irradiated with x-rays. Under the action of these ultraviolet rays (2000 to 2500 A.U.) the cells were observed to become violently agitated and then killed in an astonishingly short interval of time as the result of specific photochemical action on the nucleus. Unquestionably favorable clinical results have been obtained by injecting sodium bromide solutions into tumors prior to x-ray therapy. This salt also fluoresces in the lethal range of the ultraviolet.

The Photographic Effect.—In their action on the photographic plate, x-rays seem similar to ordinary light, for there are no known plates sensitive to x-rays that are not also sensitive to the visible radiation. Examination of microscopic sections through the sensitive layer of exposed plates has shown, however, that x-rays, unlike light, produce an equal distribution of grains of reduced silver throughout the whole thickness of the layer. Consequently a greater blackening of the plate, when exposed to x-rays, can be obtained by increasing the thickness of the sensitive layer. Here, indeed, is found the chief difference between ordinary photographic films or plates and those manufactured for x-ray use; the latter are provided with a thicker sensitive layer and are usually “duplitized,” or coated on both sides with the sensitive silver bromide emulsion.

The laws of the blackening of photographic plates are more complex than might be expected. The frequency and intensity of the incident rays and the time of exposure are important factors. Rays of differing frequencies do not have an equal quantitative effect. Kulenkampff made calculations, based on intensity and ionization measurements, which appeared to show that equal blackening will result from equal energy absorption regardless of wave length. Furthermore, rays of frequencies higher than the critical absorption frequencies of bromine and silver are very highly absorbed and produce a large photographic effect, whereas rays of slightly lower frequency produce a relatively lower effect, though the incident intensities may be the same.

The portions of a developed plate or film that have been exposed to x-rays are darkened by the deposit of silver grains. This darkening is quantitatively described as the blackening S

where $S = \log (L_0/L)$, where in turn L_0 is the initial intensity of a beam of light, such as in a view box used to observe the film, and L is the intensity after the light has passed through the silver deposit; or sometimes as the density D where $D = \log (1/T)$ and T is the transparency. Thus a film density of 1.0 means that the blackening is such that only one-tenth of the incident light passes through; for $D = 2.0$, one one-hundredth is transmitted; etc. Actually S and D are identical since L_0/L may be defined as $1/T$. For the quantitative evaluation of the

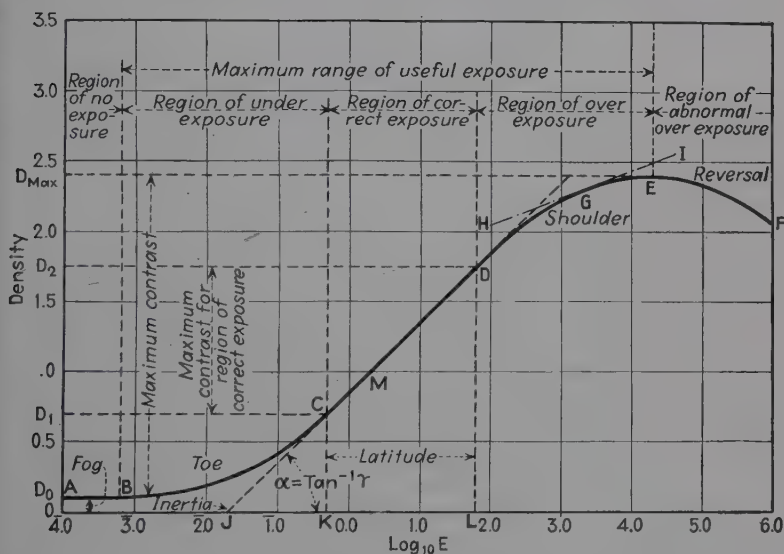


FIG. 50.—Photographic blackening curve. (*Photo Technique.*)

intensity of an x-ray beam the relation between intensities and densities must be established. This is best shown by plotting D (or S) against $\log E$ as in Fig. 50. In the case of constant intensity the log time of exposure may be plotted horizontally. At low intensities the curve rises very slowly, then more steeply as a straight line until it reaches a point of inflection where the slope decreases again. The straight-line steep portion of the curve defines the working region of the film, over which the x-ray image is faithfully rendered in terms of density, usually lying between 0.4 and 1.5 or an average of 0.7. The smallest difference in blackening of two adjacent areas that may be safely detected visually under the best conditions is 0.02. It is evident

that small intensity variations cannot be detected at the lower or upper ends of the curve. At the lower end, D or S are linearly related to intensity or time directly rather than to the logarithm.

Film emulsions are distinguished by speed, contrast, and latitude. Speed is a function of the length of the range of inertia at the left of the curve. Figure 51 shows how the use of double intensifying screens modifies the characteristic speed.

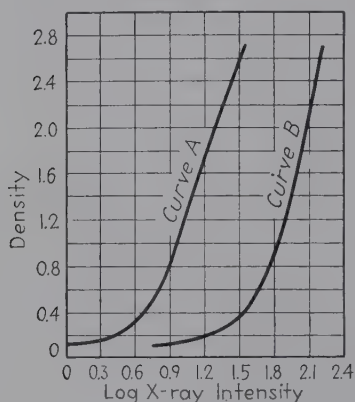


FIG. 51.—Characteristic curves for x-ray film. Curve A is taken with double intensifying screens and curve B without screens.

The contrast is measured by the slope of the characteristic working curve ($\gamma = \tan \alpha$). Thus a great contrast means a very steep slope, or a great difference in blackening for very slight differences in intensity of x-rays, and the working range of 0.4 to 1.5 is easily exceeded. This is sometimes a disadvantage especially in radiography, where an object of varying thickness is involved, and thus contrast must be sacrificed for a lower slope or latitude for a single exposure; or high contrast and detection

of very small differences or defects may be obtained by subjecting portions of different thicknesses to different exposure times.

The assumption is usually made that over the working range equal densities result from equal products of time \times intensity (Bunsen's reciprocity law). However, this assumption must be used with the greatest care, since intensifying screens and other factors introduce complications. The blackening curve of the visible light excited in intensifying screens is quite different from that of the direct action of the x-rays. Background corrections present one of the most serious and complex factors for very accurate quantitative measurement of intensity for dosage, spectroscopic, and diffraction analysis. The expression

$$\frac{I_1}{I_2} = \frac{S_1 - S_0}{S_2 - S_0}$$

(when S_0 is the background fogging) can be considered only as a working approximation simply because of the varying sensitivity

of different silver halide grains in the same emulsion. The photographic effect as a means of intensity measurement and as a photochemical reaction will be considered in specific applications in subsequent chapters.

The Microphotometer.—The microphotometer is an instrument that has become practically indispensable for any kind of x-ray photographic work. The general principle of its operation is as follows: A light of constant intensity passes through the film which is moved slowly and at constant speed. The light of varying intensity, depending upon the density of the photographic layer, then falls upon a delicate thermocouple (thermopile, photoelectric cell, etc.) which is connected with a galvanometer. The deflections of the mirror, which are a function of the thermoelectric current, the light intensity, and the photographic density, are then indicated by causing a reflected beam of light to register on sensitized paper on a slowly moving drum.

Spectral lines on the film are thus converted into peaks, and the completed curve gives a method of quantitative measurement.

The excellent new Leeds and Northrup instrument with Micromax recorder is illustrated in Fig. 52. The microphotometer is useful in the following types of investigation:

1. Accurate measurement of wave length and of relative intensities of spectral lines; indication of resolution of doublets; etc. The photometric curves measure position, fine structure, intensity from height of peak, and inherent breadth of lines.
2. Indispensable in quantitative chemical analysis, for which line intensities or height of absorption edges must be accurately compared with standards; indications of very faint foreign lines; etc.
3. Quantitative representation of radiographs.
4. Position and intensities of lines in diffraction photographs.
5. Indispensable in measurement of colloidal-particle size from widths of diffraction lines.

Chemical Dosimeters.—Certain photochemical reactions can be used as measures of x-ray intensity, for cases where a measurable change such as a precipitation or gas evolution is directly related to dosage and has been calibrated in terms of r units. One of the best examples is the reaction between mercuric chloride and ammonium oxalate to precipitate calomel, Hg_2Cl_2 (0.58 mg. as mercury per 840 r), and evolve carbon dioxide gas. The

decoloration of methylene blue and other reactions enumerated in Chap. X are also used specifically as dosimeters.

Biological Dosimeters.—The method of estimating dosage from skin reddening, or erythema, is familiar to all x-ray workers. This can never serve as an accurate method because of the widely

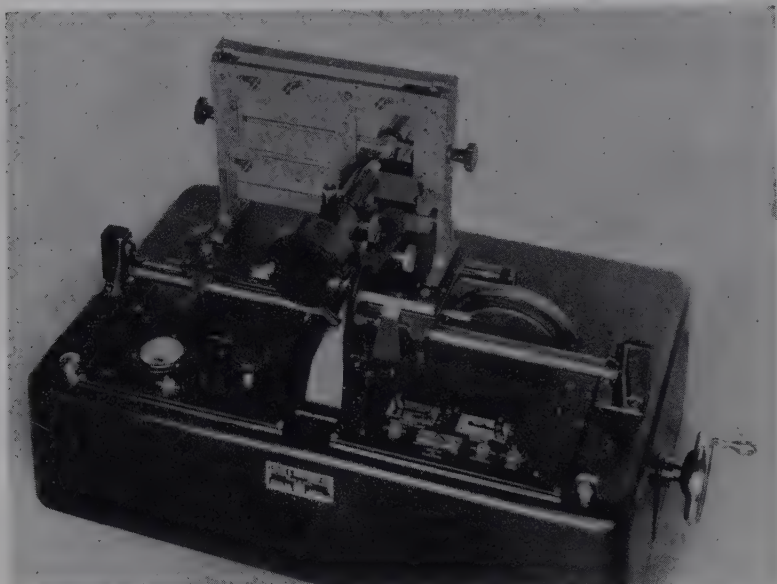


FIG. 52.—Leeds and Northrup microphotometer used with Micromax recorder (not shown).

varying sensitivity of the skin of different individuals to radiation. Glasser and Portmann¹ compiled data from 40 clinics on the number of r units for average erythema reaction in deep therapy. These varied from 500 to 1,250 r , or an average of 930. The threshold value of erythema is commonly taken to be 840 r .

A much more accurate "biological ionization chamber," as designated by Wood² are *Drosophila* (fruit fly) eggs. Invariably 50 per cent of the eggs are killed by 180 r and 90 per cent by 500 r . The points for the effect of radium fall directly on the curve experimentally determined for the percentage of eggs hatching as a function of r units (see Chap. XI).

¹ *Radiology*, **14**, 346 (1931).

² *Radiology*, **12**, 461 (1929).

The Efficiency of Production of High-voltage Radiation.—

As the voltage applied to an x-ray tube is raised, the efficiency of production of x-rays rapidly increases. In fact, if the amount of radiation is measured in terms of energy, for the same electric power passing through the tube, the x-ray emission is very nearly proportional to the voltage. For a tungsten-target tube operated at different potentials, the amount of x-rays per kilowatt of energy passing through the tube is approximately as follows:

TABLE VII.—X-RAY PRODUCTION

(Quantity of x-rays emitted by a tungsten-target tube per kilowatt of energy in cathode-ray beam¹)

| Operating potential, kilovolts | Power in total x-rays from focal spot, watts | Effective wave-length (unfiltered), angstrom units | Roentgens (r) per second at 1 meter from target (unfiltered) |
|--------------------------------|--|--|--|
| 50 | 2.5 | 0.56 | 1.2 |
| 70 | 3.5 | 0.40 | 0.62 |
| 100 | 5 | 0.28 | 0.34 |
| 200 | 10 | 0.14 | 0.39 |
| 500 | 25 | 0.056 | 1.1 |
| 1,000 | 48 | 0.028 | 2.1 |
| 2,000 | 95 | 0.014 | 4.0 |

¹ Compiled by A. H. Compton.

The feature of this table that is of greatest interest is the variation of the roentgens of x-ray intensity with the tube potential. It will be seen that the usual therapeutic range, of between 100 and 200 kv., is at just the minimum of efficiency. The physical reason for this is that for softer x-rays the fraction absorbed in air is greater, whereas for the harder x-rays a greater fraction of the energy is spent in producing the recoil electrons which are responsible for the ionization of air. It is because of this change in the absorption process that the emission as expressed in roentgens of ionization does not follow that expressed in watts of power. If, as is usually assumed, the biological effect is proportional to the ionization of air and hence to the roentgens, this table indicates that for potentials higher than 200 kv., the power input of the x-ray tube being kept constant, the biological effectiveness of the emitted radiation increases even more rapidly than the voltage.

CHAPTER V

THE MEASUREMENT OF QUALITY (WAVE LENGTH)

By x-ray quality is meant the constitution of the beam with regard to wave length. Ordinary white light is proved to be a mixture of many rays of visible light of different wave lengths and corresponding to pure colors, for the beam is spread into a spectrum from violet to red by refraction in a prism or by diffraction by the finely ruled lines of a grating. In analogous fashion the spectrum of a beam of x-rays whose constitution previous to analysis is unknown identifies the quality.

The following methods of measuring quality, "hardness," or wave lengths of an x-ray beam are classified according to the properties which are the same (refraction, diffraction) as those of the optical ranges of the electromagnetic spectrum, and also according to the properties which are different (power to penetrate matter opaque to light):

1. Diffraction by ruled gratings.
2. Diffraction by crystals.
3. Refraction in prisms.
4. Measurement of absorption by known materials.

By observations on absorption in screens of various elements of beams of x-rays generated at tube targets of known elements, many important facts of quality were discovered before wave lengths were actually evaluated: increasing absorbability of rays, the lower the voltage on the tube; the discovery by Barkla of the characteristic emission series for each element, *K* (most penetrating), *L*, *M*, etc.; increasing absorbability of the x-rays, the lower the atomic number of the target; the evaluation of hardness of a heterogeneous beam, in terms of "effective wave length" or the wave length of the monochromatic ray that is absorbed to the same extent as the beam of mixed rays of many wave lengths. However, though absorption coefficients do define penetrating power, they do not of themselves resolve and evaluate all the wave lengths in a beam, in the sense that spectroscopy implies. Furthermore, Chap. VIII is concerned

with absorption and scattering of x-rays, so that the subject can be dismissed from further immediate consideration.

X-ray Diffraction by Crystals.—Glass prisms or diffraction gratings consisting of finely ruled parallel lines on glass or metal can be used only under very special conditions for the spectra of x-rays, because these have wave lengths many times shorter than light. Crystals, however, are natural gratings in which parallel planes of regularly marshaled atoms are spaced from each other at distances that are of the same order of magnitude as x-ray wave lengths.

The analysis for quality is best made, therefore, with the crystal spectrometer originally designed by the Braggs. It is a device upon which crystals of known interplanar spacings are mounted and rotated; the quantities measured are the angles at which the various components of the beam are reflected by the crystal planes. Upon the photographic plate or plotted from ionization-current readings is the spectrum of the beam. The analysis is complete because the whole process is governed by a simple law $n\lambda = 2d \sin \theta$, where λ is a wave length, n is the order of the reflection, d is the known distance between the parallel planes in the crystal, and θ is the spectrometrically measured angle of incidence of the ray upon these planes (or 2θ , the angle of diffraction or reflection).

If crystals are built up of atoms and molecules marshaled in definite rows and in parallel planes with their mutual forces restraining them to relatively fixed positions in the rigid solid and if x-rays are scattered by atoms, then these crystals are potential three-dimensional diffraction gratings for x-rays. Such was the prediction in 1912 of Laue, after he had accepted the work of Schoenflies and Federov leading to the conception of space-groups and had calculated from the density, molecular weight, and weight of the hydrogen atom that the distances between regularly disposed particles of mass in crystals must be of the same order as the wave length of x-rays (10^{-8} cm.). Friedrich and Knipping verified the prediction, using a crystal of zinc blende. The original analysis by Laue was of considerable mathematical complexity, but the Braggs were able to reduce the interaction between x-rays and crystals to terms of great simplicity, by considering primary x-rays to be reflected by the face of a crystal. As a matter of fact, the mechanism

is far more complicated, since planes and atoms far below the "reflecting" surface are concerned and since the emergent "secondary" x-rays have been emitted as a consequence of electronic changes in the atoms across which the primary beam passes. Experiments have shown that the whole phenomenon appears to be simple reflection of the primary beam in accordance with the simple equation $n\lambda = 2d \sin \theta$. The simple relations among λ , d , and θ are at once seen from Fig. 53, which shows

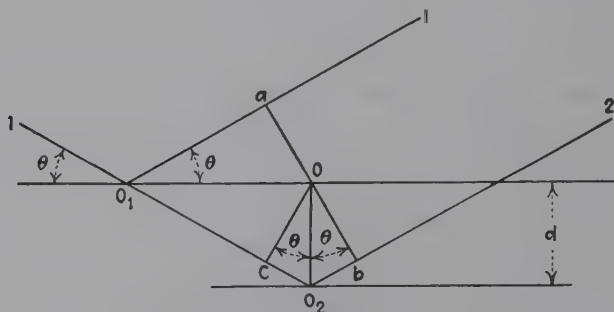


FIG. 53.—Derivation of Bragg law: $n\lambda = 2d \sin \theta$.

the incident beam I reflected at O_1 and O_2 . The line ab is perpendicular to the reflected rays O_1I and O_22 . The length of path O_1O_2b is greater than the length of the path O_1a by the length of the line cO_2b , the line Oc being perpendicular to O_1O_2 . The length of the line cO_2b is, obviously, $2d \sin \theta$. The condition that there should be a reflected beam is, therefore, that the reflected train O_22 shall be exactly one wave length or an integer multiple of wave lengths n behind the train O_1I or that

$$n\lambda = 2d \sin \theta.$$

This is the fundamental equation of x-ray spectroscopy and of the analysis of structure of crystalline materials. For ordinary purposes it may be considered as rigorous; slight departures from it, observed particularly at higher orders of reflection, are due entirely to refraction, for δ , in the expression for refractive index $\mu = 1 - \delta$, is not zero but of the order of 10^{-6} .

The crystals ordinarily used in spectrum analysis are rock salt, NaCl, in which the planes parallel to the cube-surface (100) planes are spaced 2.814 A.U. apart; or calcite with a spacing of 3.029 ± 0.001 A.U. Gypsum ($d = 7.579$), sugar ($d = 10.57$),

mica ($d = 9.93$), quartz ($d = 4.247$), and other crystals are also used. Of these, calcite is recommended as the primary standard. Siegbahn and his associates in the measurement of long wave lengths introduced the use of crystalline lauric ($d = 27.268$ A.U.), palmitic ($d = 35.49$ A.U.), and stearic ($d = 38.7$ A.U.) acids and lead melissate ($d = 87.5$ A.U.). The use of organic crystals has been practically discarded, however, in favor of the ruled gratings.

It is obvious that some other method of absolute wave-length measurement is needed to substantiate thoroughly the assumptions and calculations made with crystal gratings. The fundamental grating spacing of some one standard crystal (calcite) had to be calculated as a basis for wave-length measurements of x-rays which were then applied to the determination of the grating spacings of other crystals. For calcite, a rhombohedral crystal, the distance between face planes is

$$2d_{100} = \left[4 \frac{V_m}{\phi(\beta)} \right]^{\frac{1}{3}},$$

where V_m , the molecular volume, is $M/\rho N_0$ (M is the molecular weight; ρ is the density; N_0 is the Avogadro number, or number of molecules per mole); $\phi(\beta)$ is the volume of calcite rhombohedron with unit distance between these face planes $= (1 + \cos \beta)^2 / \sin \beta (1 + 2 \cos \beta) = 1.0962$, with $\beta = 101^\circ 55'$. The most uncertain quantities are ρ and N_0 ; repeated measurement has given $\rho = 2.7102$ as most reliable, and with the accepted value for $N_0 = 6.061 \times 10^{23}$ the grating constant comes out 3.029 ± 0.001 A.U.

The application of the Bragg law may be illustrated by the following examples:

At what angles may a ray of the wave length 0.440 A.U. be reflected from the cube face of a rock-salt crystal ($d = 2.814$ A.U.)?

$$\sin \Theta_1 = \frac{n\lambda}{2d} = \frac{1 \times 0.440}{5.628} = 0.0782, \quad \Theta_1 = 4^\circ 29.2',$$

$$\sin \Theta_2 = 2 \times 0.0782, \quad \Theta_2 = 8^\circ 59.75',$$

$$\sin \Theta_3 = 3 \times 0.0782, \quad \Theta_3 = 13^\circ 34',$$

$$\sin \Theta_4 = 4 \times 0.0782, \quad \Theta_4 = 18^\circ 13.5',$$

$$\sin \Theta_5 = 5 \times 0.0782, \quad \Theta_5 = 23^\circ 0.6', \text{ etc.}$$

What wave lengths in a beam containing the range 0.2 to 1.0 A.U. will be reflected when incident at 9° upon the cube face of a rock-salt crystal?

$$\begin{aligned} 1\lambda_1 &= 5.628 \sin 9^\circ = 0.8804, \\ 2\lambda_2 &= 5.628 \sin 9^\circ = 0.8804, & \lambda_2 &= 0.440, \\ 3\lambda_3 &= 5.628 \sin 9^\circ = 0.8804, & \lambda_3 &= 0.293, \\ 4\lambda_4 &= 5.628 \sin 9^\circ = 0.8804, & \lambda_4 &= 0.220. \end{aligned}$$

Hence the reflected beam contains four wave lengths, 0.880, 0.440, 0.293, and 0.220, which are related as $1:\frac{1}{2}:\frac{1}{3}:\frac{1}{4}$.

The ionization spectrometer consists essentially of a crystal table, which rotates about the axis of the spectrometer with reference to a fixed scale graduated in degrees and minutes; readings to seconds of arc may be made by means of a vernier or with microscopes with micrometer eyepieces. A separate movable arm carries the ionization chamber, whose angular position can be read on a second concentric scale. Two or more slits define the x-ray beam impinging on the crystal, and another slit is adjusted in front of the ionization chamber.

The ionization chamber is simply a container for a gas or vapor and two electrodes; reflected x-rays passing into the gas ionize it; with a sufficient difference of potential between the electrodes, a current results, which is measured by the speed of discharge of a gold-leaf electroscope or the deflection per second of a quadrant electrometer. In an experiment the ionization chamber is adjusted so as to receive the reflection from the crystal face. Then the crystal and ionization chamber are moved step by step (the latter at twice the rate of the former), and the ionization current is measured for each step. When the ionization current is plotted against the angle θ , or angular scale reading, a curve is obtained showing the characteristic peaks, which appear as spectral lines if a photographic plate is substituted for the ionization chamber.

The theory of ionization and the practical utilization of air ionization as a measure of x-ray dosage in tissues were considered in the preceding chapter.

The photograph of a precision-spectrometer equipment in the writer's laboratory is reproduced in Fig. 54. Upon the spectrometer, built (by the Société Genèvoise d'Instruments de Physique) with circular scales which may be read to 0.2 sec. of arc,

is mounted an ionization chamber of the original Duane design, consisting of a long glass tube, containing a cylindrical electrode connected with a battery and a central insulated-rod electrode running along the axis of the tube and connected with a pair of

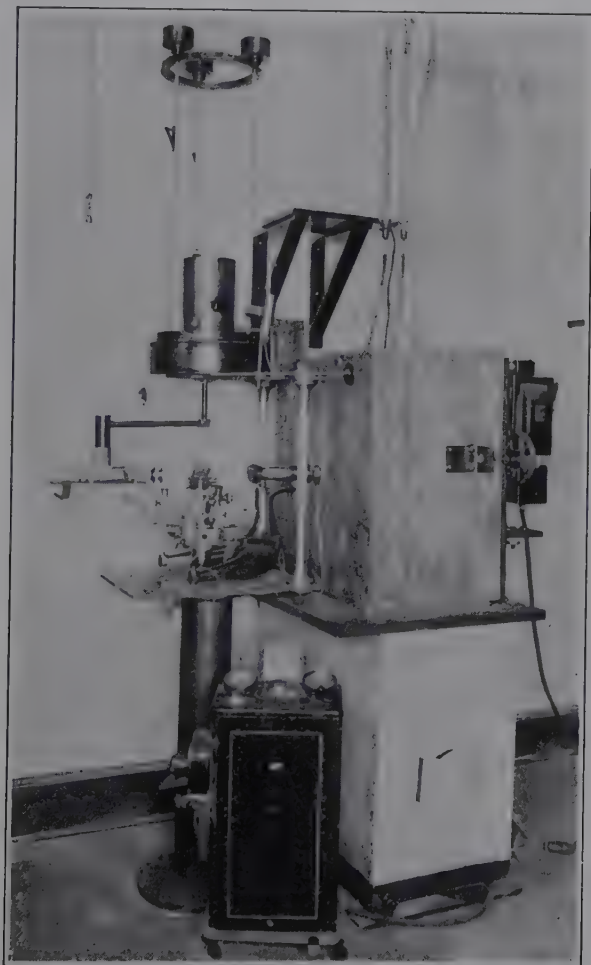


FIG. 54.—Ionization spectrometer with quadrant electrometer.

quadrants in an electrometer. The electrical connections of the system are shown diagrammatically in Fig. 55. The electrometer is of the Compton-Stryker type with sputtered quartz fiber suspension; it has proved eminently satisfactory. A source

of light is reflected by the mirror upon a large scale upon the side of the wall, so that extremely accurate readings of the speed of deflection are possible. The make-and-break switch consists of two fine longitudinal platinum wires, stretched on stirrups which are supported on quartz rods and make contact at right angles; from the standpoint of stray and induced e.m.fs. the arrangement is superior to any other. The quadrant or string electrometer

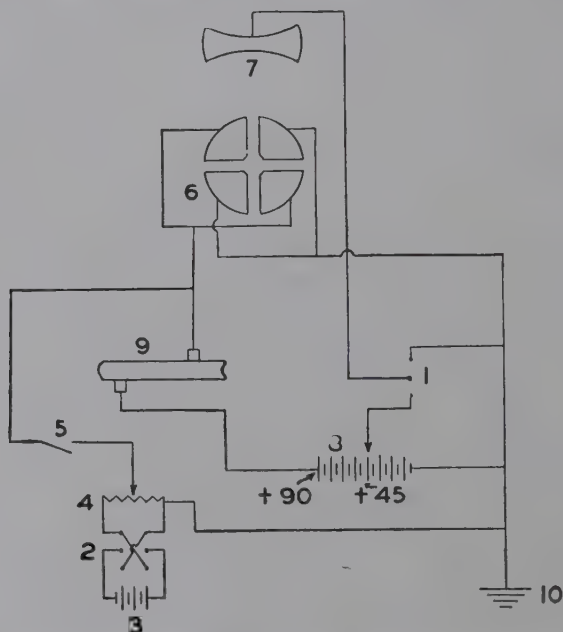


FIG. 55.—Potentiometric control of quadrant electrometer used to measure ionization currents.

1, single-pole, double-throw switch for charging needle; 2, reversing switch for potentiometer circuit; 3, 2-volt 20-amp.-hr. storage cell; 4, 400-ohm general radio potentiometer; 5, earthing key controlled by silk fishline for distance; 6, quadrant electrometer fixed quadrants; 7, movable needle of electrometer; 8, dry-cell radio "B" battery (90 to 150 volts); 9, ionization chamber; 10, earth.

may be used as null instruments, so that readings of potential are made by inducing such an opposite charge on the collecting system as to return the needle to the neutral position.

Numerous attempts have been made to displace the quadrant electrometer, string electrometer, or gold-leaf electroscope as measuring devices for ionization currents. Fonda and Collins¹ have described an amplifying system for ionization currents

¹ *J. Am. Chem. Soc.*, **53**, 113 (1931).

employing a new four-element vacuum tube characterized by a very high input resistance. The deflection of the galvanometer is taken directly as a measure of the relative intensities of the x-rays entering the chamber.

Many modifications of the Bragg spectrometric method have been made; chief among these are the remarkably precise instruments of Siegbahn, who has preferred the photographic method originally developed by de Broglie. Depending upon the range of wave lengths to be used, a somewhat different type of spectrometer has been devised by this master experimenter; the vacuum type for the spectroscopy of very soft x-rays, which are easily absorbed in air, is perhaps of the greatest interest and importance. These spectrographs are fully described in Siegbahn's book. A curved sheet of mica is often used as a focusing crystal grating on spectrometers, illustrating another type of variation.

The finest Bragg spectrometer in the world is the automatic instrument in the Crystallography Laboratory of the University of Cambridge, designed and built by Wooster and associates.¹

In six hours with this instrument, accurate intensity data are registered on photographic paper for 50 sets of planes in a crystal.

The Double Spectrometer.—A very useful modification of the spectrometer is that which employs two crystals, the first serving to select a ray of given wave length from the primary beam, by its setting at a given angle, and the second serving to analyze in detail this reflected beam for precision measurements of absolute glancing angles and for evidences of fine structure, width, etc. Or, of course, the second crystal may have an unknown structure for analysis by the strictly monochromatic beam from the first crystal. There are two arrangements for these crystals: type



FIG. 56.—Arrangement of crystals in double spectrometer; left 1, -1 ; right 1, 1. Dotted lines represent crystal faces; heavy lines below, planes parallel to the first crystals above.

¹ WOOSTER and MARTIN, *Proc. Roy. Soc. (London)*, **155**, 150 (1936).

I, in which the rays incident on crystal *A* and leaving from crystal *B* are on the same side of the ray between crystals, antiparallel, designated by the symbol 1,1; type II, in which the rays incident on crystal *A* and leaving from crystal *B* are on opposite sides of the ray between the crystals, designated by the symbol 1, -1. These are illustrated in Fig. 56. The theory, design, and use of the double spectrometer are fully treated by Compton and Allison.¹

A logical extension of this principle is a multicrystal spectrometer with still greater resolving power. Several of this type have been designed for special research purposes.

Refraction and Total Reflection of X-rays.—It will be remembered that Roentgen and his contemporaries in investigations of the nature of x-rays failed to find any experimental evidence of refraction because of the extremely small magnitude of the effect. The subsequent discovery of refraction and the measurement of indices of refraction represent the great improvement in experimental technique. Refraction is indicated and measured by three different effects:

1. Departures from the Bragg law. About 20 years ago it was discovered that wave lengths of a given line calculated from higher orders of reflection ($n = 3,4,5$) from a crystal face were smaller by several tenths of a per cent. Thus, the Bragg law in its simple form is only an approximation, and the discrepancies are to be ascribed to an index of refraction a little *less* than unity. Actually $n\lambda' = 2d \sin \theta'$, where λ' and θ' are, respectively, wave length and angle of incidence *in the crystal*, is accurate; but, for the wave length *in air* λ and the angle of incidence on the crystal face θ , the formula must be slightly corrected for refraction:

$$n\lambda = 2d \sin \theta \left(1 - \frac{1 - \mu}{\sin^2 \theta} \right)$$

where μ is the index of refraction of x-rays in the crystal. In general, μ differs from 1 by a quantity only of the magnitude of 10^{-6} , *i.e.*,

$$\delta = 1 - \mu = \frac{ne^2\lambda^2}{2\pi c^2} = 10^{-6}$$

where n is the number of electrons per unit volume.

¹ "X-rays in Theory and Experiment," D. Van Nostrand Company, Inc., New York, p. 709, 1935.

2. Measurement by a prism. By the use of a double spectrometer a monochromatic beam of rays from the first crystal K_1 falls on a second crystal K_2 , so that when this is exactly parallel to K_1 the beam is reflected into an ionization chamber. If a prism is now placed between K_1 and K_2 , the x-ray beam is deflected (in the opposite direction from that for light), so that K_2 must be moved to a new position in order to reflect the beam. The angular displacement Δ in position of the given line as reflected from K_1 onto K_2 is measured, and the value introduced into the equation $\mu = 1 + \sin \frac{\Delta}{2} \cot \frac{\Theta}{2}$.

3. Measurement by total reflection. Since the index of refraction of materials for x-rays is less than 1, a beam of x-rays incident upon a polished surface at very small grazing angles should be totally reflected. From optics, $\cos \Theta_R = \mu = 1 - \delta$; $\sin \Theta_R = \Theta_R = \sqrt{2\delta}$. Some values for the limiting grazing angle are as follows: glass 6 min. 10 sec. ($\lambda = 0.7078$), calcite 14 min. 25 sec. ($\lambda = 1.537$ A.U.). A. H. Compton first measured the values of δ by this method in 1922, by slowly turning a mirror through a small angle, over which the beam at grazing angle may be totally reflected.

Measurement of Wave Lengths by a Ruled Grating.—The discovery of total reflection of x-rays immediately opened the way

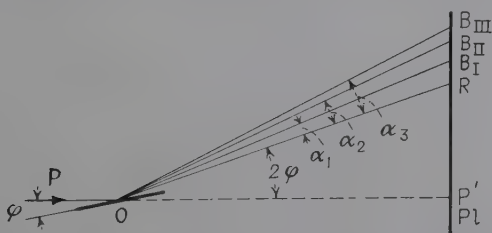


FIG. 57.—Diagram of grating spectrum. P , primary x-ray beam; O , ruled diffraction grating; Pl , photographic plate; R , totally reflected beam; B , diffracted rays.

for the use of a ruled grating to measure wave lengths, exactly as in the optical range, provided that the glancing angle of incidence of the beam on the grating is less than the critical angle of total reflection Θ_R . Compton and Doan in 1925 were the first to obtain such a spectrum with a grating of speculum metal with 50 lines per millimeter. Other gratings with 200 lines per

millimeter have given results of great precision. The general experimental arrangement is shown in Fig. 57. On the photographic plate, besides the primary intensity maximum and the totally reflected beam R , are lines for the diffracted ray in various orders B_1 , B_2 , B_3 , on both sides of R . The negative orders (below R) are so weak in intensity as to be negligible,

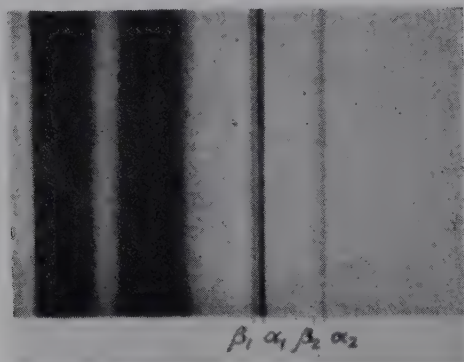


FIG. 58.—X-ray spectrum from ruled grating. K series of copper. (Thibaud.)

and only the positive orders are shown. Then the wave length is calculated from

$$n\lambda = d(\cos \theta - \cos (\theta + \alpha_n))$$

where d is the grating constant and n the order. On a photographic plate appear a central maximum for the primary beam, another for the total reflection, the distance between these being 2θ ; finally there is observed a diffraction spectrum of beam. In Fig. 58 is shown such a result for x-rays from a copper target. By means of such gratings Thibaud bridged the gap between the x-ray and ultraviolet regions and obtained in many cases the same wave length for a chemical element from the spectrum of a beam from an x-ray tube and from an ultraviolet spark spectrum. This region of long waves that are easily absorbed can be studied with the crystal spectrometer only in vacuum and with the greatest difficulty. There are still some discrepancies, however, between crystal and ruled-grating data. The latest precision comparative measurements have been made by Bearden with the following results:

| Spectral line | Crystal λ | Grating λ |
|---------------|-------------------|-------------------|
| CuK β | 1.38914 | 1.39225 |
| CuK α | 1.53838 | 1.54172 |
| CrK β | 2.08017 | 2.08478 |
| CrK α | 2.28590 | 2.29097 |

Thus, values from ruled gratings are consistently 0.2 to 0.3 per cent higher than those from crystal gratings for a reason which is not as yet altogether clear. The former are "absolute" in the sense that no physical constants are involved, whereas the latter depend upon a crystal spacing d . For a cubic crystal

$$d = \sqrt[3]{\frac{Me}{2\rho F}}$$

where M is the molecular weight, e the electron charge, ρ the density, and F the Faraday constant. Though ρ can be measured to an accuracy of 1 part in 10,000, it may not represent the true density for mosaic crystals, and hence d may be smaller than the true grating spacing, according to Zwicky.

CHAPTER VI

X-RAY SPECTRA AND ATOMIC STRUCTURE

The Continuous Spectrum.—Two kinds of x-radiation are known: (1) the general, “white,” or continuous spectrum x-radiation; (2) the characteristic x-radiation, which is composed of several monochromatic rays grouped in series, with wave lengths depending upon the atomic number of the emitting element. The continuous spectrum may be generated in a tube at sufficiently low potentials over certain ranges of wave lengths without characteristic lines under certain conditions, but the characteristic spectrum is always superposed upon a background of the general radiation. The outstanding property of the general radiation is that the smooth curve obtained by plotting intensity against wave-length or spectrometer reading has a sharp short wave-length limit (zero intensity), which does not depend upon the material of the target of the tube but upon the voltage applied to the tube, according to the fundamental Planck-Einstein quantum equation $Ve = h\nu_0 = hc/\lambda_0$, where V is the constant potential, e is the charge on the electron, h the Planck action constant,¹ c the velocity of light, ν_0 the maximum frequency, and λ_0 the minimum wave length occurring in the spectrum. This law was first applied to x-rays by Duane and Hunt in 1914, and it has been proved subsequently to be rigorously true, far more so than the other famous equation, $n\lambda = 2d \sin \theta$.

According to this equation,

$$\lambda_0 = \frac{hc}{eV_0} = \frac{6.556 \times 10^{-27} \times 3 \times 10^{10}}{1.59 \times 10^{-20} \times V_0} = \frac{12,350}{V_0},$$

where V_0 is in volts. Thus, at 300,000 volts, the highest ordinarily employed in deep therapy, the minimum wave length is 0.04 A.U.; a tube at 2,600,000 volts must generate rays with a minimum wave length of 0.005 A.U., in the extreme γ -ray region of the electromagnetic spectrum.

¹ h has the dimensions (L^2mT^{-1}) of a moment of momentum: (action) = (energy \times time).

It is obvious that precision researches on the general radiation spectrum should be a very exact method for evaluating the constant h ; λ_0 can be spectrometrically evaluated from $n\lambda_0 = 2d \sin \Theta$; V can be measured very accurately, particularly if the source of high potential is a storage battery, by reading the current after passage through carefully calibrated high resistances; and e is the well-known value of Millikan. The measurements in the laboratory of Prof. William Duane at Harvard¹ gave a value of 6.556×10^{-27} erg-sec. Several other investigators have obtained nearly the same value, which agrees well with evaluations by entirely different methods, such as the photoelectric effect.

Furthermore, the law of Duane and Hunt leads to the most accurate evaluation of peak voltage which is directly calculated from the sharp limit of a crystal spectrum:

$$V_0 = \frac{hc}{e\lambda_0} = \frac{12,350}{\frac{2d}{n} \sin \Theta_0},$$

where $2\Theta_0$ is the experimentally measured angle of the limit.

While the short wave length of the spectrum is entirely independent of the target element, the intensity is a function of the atomic number of the target element. The relationships are, however, quite complicated and remain still in doubt. The curves rise sharply to an intensity maximum, defined roughly by $\lambda = 1.3\lambda_0$, and then fall away more gradually.

The question of the mechanism of the production of the general radiation is one of the most difficult in x-ray science, and a completely satisfactory answer has not been given. If cathode rays are accelerated in an x-ray tube by the voltage V , the kinetic energy E_k will be $Ve = E_k$. If the electrons are stopped instantaneously at the target, the kinetic energy is transformed into the maximum possible radiation energy, or $E_k = V_0e = h\nu_0 = hc/\lambda_0$. If the stoppage of the electrons is stepwise as they penetrate the target, then the rays will have a variety of wave lengths longer than the limit. Though the quantum law governs the general radiation, the explanation of the actual emission process, which can indeed be made simply upon the basis of the electromagnetic or wave theory as a forced vibration of electrons

¹ *J. Optical Soc. Am.*, **5**, 213 (1921).

in bombarded atoms, is one of the great difficulties confronted by the modern theories of spectral emission by quantum processes.

The general radiation is of practical importance since it is employed in the Laue method of crystal analysis. In all applications at high voltages including radium therapy, radiography, etc., it comes prominently into play. The spectrum can be profoundly modified by filtration, inasmuch as rays of short wave lengths are absorbed far less than are those of the long wave length. The effect of filtration in the absence of characteristic effects is, then, to sharpen the curve and to shift the maximum to the shorter wave lengths, without in any way affecting the value of λ_0 . Filtration and the measurement of effective wave length of general radiation will be considered in Chap. VIII.

Characteristic Emission Spectra.—In addition to the continuous x-radiation, rays that have wave lengths characteristic of the anticathode elements are recognized. If the potential on the x-ray tube is sufficiently high, the spectrum of the emitted beam will show sharp lines (or peaks if the ionization current measured with an ionization spectrometer is plotted) superposed upon the continuous background. These same characteristic x-rays are emitted as fluorescent rays if a beam of primary x-rays with sufficiently short wave lengths falls upon an absorption screen containing the same element as the tube target. The characteristic emission lines appear in groups designated as the *K, L, M, N, O*, etc., series (beginning with the most penetrating or shortest wave-length group), following the nomenclature of Barkla who discovered the characteristic emission in the course of his absorption measurements.

Each of the series of *emission lines* contains several definite lines of different wave lengths. Probably the most remarkable characteristic of the x-ray range of the electromagnetic spectrum is the uniform simplicity of these spectra. The *K* series of all the elements except the lightest consists of four principal lines, the γ (also designated β_2 and actually a very close doublet), β (really a close doublet β_1 and β_3), and the doublet α_1 and α_2 , in the order of increasing wave lengths. The typical appearance of this spectrum is shown in Fig. 59. Practically, this is the most important series, since it is now used almost exclusively in crystal analysis. The more numerous *L* series lines, illustrated in Fig. 60, are in three groups γ , β , and α , corresponding to the

three *L* absorption discontinuities. About thirty have been identified. Because of the long wave lengths, measurements of the *M* and *N* series have been largely confined to the heaviest elements.

Characteristic Absorption Spectra.—There are also absorption discontinuities observed in x-ray spectra whenever a beam of

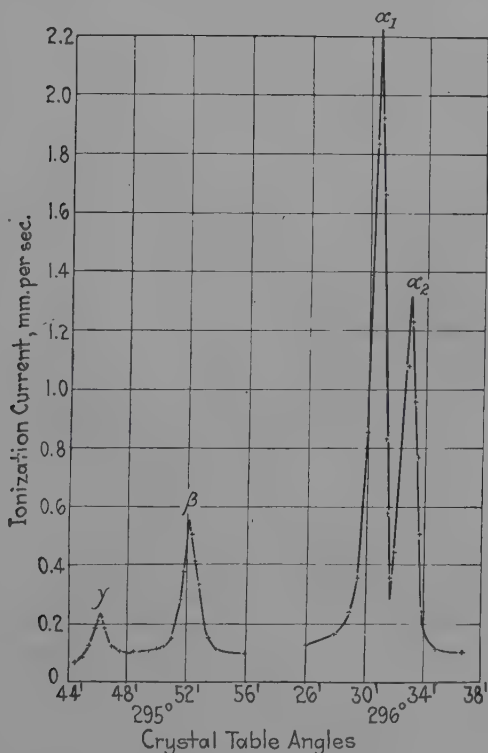


FIG. 59.—*K* series emission spectrum.

x-rays undergoing spectroscopic analysis passes through absorbing material; the wave lengths corresponding to these discontinuities, or edges, are also characteristic of each of the chemical elements. All rays with wave lengths shorter than that of a given discontinuity, or edge, will be absorbed by the element to a markedly greater extent than rays with wave lengths longer than this critical value. In other words, an absorbing screen that is relatively "opaque" to x-rays of a range of wave lengths

up to a characteristic value, is "transparent" to longer rays. Similarly, if a beam of x-rays is absorbed by a gas in which

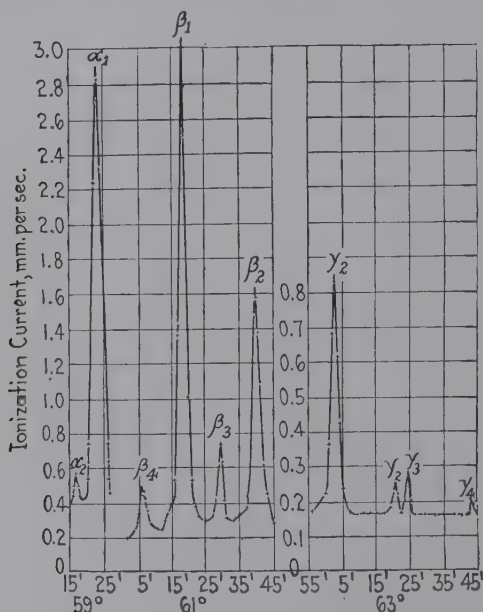


FIG. 60.—*L* series emission spectrum (tungsten).

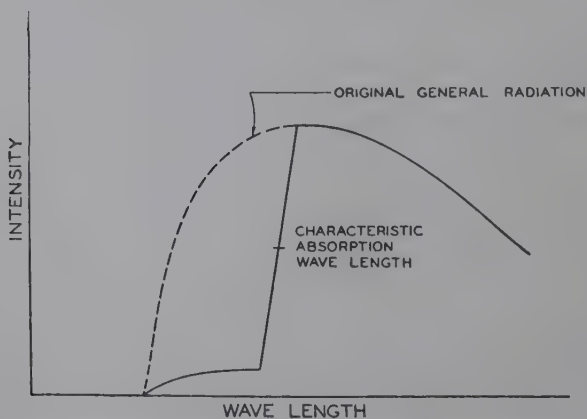


FIG. 61.—Characteristic *K* absorption edge plotted from ionization spectrometer data.

the ionization current is being measured, sharp discontinuities occur which correspond to wave lengths characteristic of the elements in the gas. A single absorption discontinuity is

associated with the K series, (Fig. 61) three with the L , five with the M , probably seven with the N , and five with the O . Absorption edges which are observed on all photographs correspond to the K discontinuities of silver and bromine; the intensities as compared with the ionization curves are, of course, reversed because the absorbed energy blackens the emulsion to the greatest extent.

The Relationship between Characteristic Emission and Absorption Discontinuities.—It is a singular fact that all the lines in the K series emission spectrum are excited simultaneously when the energy conditions permit. Thus the α doublet of the K series with definitely longer wave lengths cannot be made to appear without the γ and β lines, by adjusting the value of the voltage in the equation $Ve = hc/\lambda_{K\alpha}$. It is true that the spectrum obtained under such conditions will show the presence of rays with the same wave lengths as the $K\alpha$ lines, but this spectrum is due only to general radiation and is not characteristic of the chemical element on the target. Nor will the K series lines appear when $\lambda_{K\gamma}$, corresponding to the emission line of shortest wave length, is substituted in the energy equation. An examination of the value of the wave length corresponding to the K absorption discontinuity for a given element serving as an absorber discloses the fact that this value is slightly shorter than the wave length of the characteristic $K\gamma$ line emitted by this same element serving as a target. When the voltage on the x-ray tube is adjusted so that $Ve = hc/\lambda_{K\text{abs.}}$, then the entire emission series appears. It follows, also, that fluorescent x-rays can be emitted only when the primary x-ray beam contains rays with these critical wave lengths numerically the same as those which correspond to the absorption discontinuities, or shorter (*i.e.*, rays generated by a definite minimum voltage or higher). The energy represented by $hc/\lambda_{\text{abs.}}$ must be vitally related, therefore, to definite processes that are occurring in atoms when electrons in the cathode-ray stream strike them or x-rays pass over them. The L series can be generated in three groups, since there are three quantum wave lengths, or absorption discontinuities. Similarly there are $5M$, $7N$, $5O$, and $3P$ absorption edges (or energy levels) possible.

The effect of voltage on characteristic spectra differs markedly from that on the continuous spectrum. The latter is produced

at any voltage but the short wave-length limit moves to smaller values as the voltage is increased. An emission series appears only at a critical voltage, and the only effect of a further increase of voltage is to increase the intensity of all the lines without altering them in position or in relative intensities.

THE EXPERIMENTAL RESULTS OF THE MEASUREMENT OF WAVE LENGTHS¹

Characteristic Absorption.—The wave lengths of the *K* absorption limits have been measured for the elements with few exceptions from magnesium (12) to uranium (92); of the three *L* limits for those from rubidium (37) to uranium (92); of the five *M* limits for tungsten (74) to uranium (92). In each case

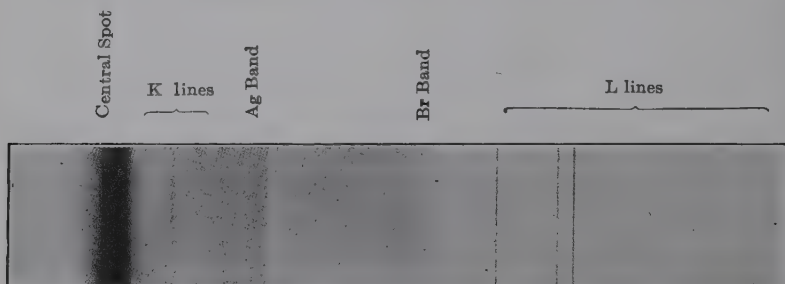


FIG. 62.—Spectrum from tungsten-target x-ray tube, showing the absorption edges of silver and bromine in photographic emulsion. (*de Broglie*.)

scattered data have been reported for elements of lower atomic number than those just mentioned. The characteristic absorption discontinuities were observed by Barkla in his absorption measurements with screens before the discovery of the use of crystals as diffraction gratings. De Broglie in his first spectral photographs discovered the sudden changes in the blackening of the photographic plate due to the characteristic absorptions of silver and bromine in the photographic emulsion (Fig. 62); in both cases the plate was blacker on the side nearer the zero direct-beam line, a phenomenon which accords with the definition of critical absorption wave length as the one such that the absorbing element absorbs x-rays of wave lengths shorter than the discontinuity to a greater extent than x-rays of longer wave lengths.

¹ For the detailed results of x-ray spectroscopy the reader is referred to "International Critical Tables," Vol. VI, pp. 36–44; Siegbahn, "Spektroskopie der Röntgenstrahlen," 2d ed., Berlin, 1931.

TABLE VIII.—CRITICAL ABSORPTION WAVE LENGTHS, *K* SERIES

| | | | |
|------------|--------|------------------|-----------------|
| 12 Mg.... | 9.5112 | 35 Br... 0.9182 | 56 Ba... 0.3308 |
| 13 Al..... | 7.9470 | 40 Zr... 0.6874 | 74 W... 0.17807 |
| 17 Cl..... | 4.3938 | 42 Mo... 0.61842 | 78 Pt... 0.1581 |
| 24 Cr..... | 2.0663 | 47 Ag... 0.4852 | 79 Au... 0.1534 |
| 26 Fe..... | 1.7405 | 53 I..... 0.3738 | 82 Pb... 0.1410 |
| 29 Cu..... | 1.3780 | | 92 U.... 0.1075 |

TABLE IX.—CRITICAL ABSORPTION WAVE LENGTHS, *L* SERIES

| Element | L_I (L_{11}) | L_{II} (L_{21}) | L_{III} (L_{22}) |
|------------|-----------------------|--------------------------|---------------------------|
| 47 Ag..... | 3.2474 | 3.5067 | 3.6908 |
| 53 I..... | 2.3839 | 2.5475 | 2.7139 |
| 56 Ba..... | 2.0620 | 2.1993 | 2.3568 |
| 74 W..... | 1.0205 | 1.0713 | 1.2116 |
| 78 Pt..... | 0.8921 | 0.9321 | 1.0709 |
| 82 Pb..... | 0.7806 | 0.8136 | 0.9500 |
| 92 U..... | 0.5687 | 0.5920 | 0.7216 |

The values in angstrom units of the *K* absorption limits for a few of the more commonly used elements are as shown in Table VIII.

Some values of the *L* absorption limits are given in Table IX.

M absorption limits for tungsten, bismuth, thorium, and uranium are given in Table X.

TABLE X.—CRITICAL ABSORPTION WAVE LENGTHS, *M* SERIES

| Element | (M_I) | (M_{II}) | (M_{III}) | (M_{IV}) | (M_V) |
|---------|-----------|--------------|---------------|--------------|-----------|
| W..... | 4.38 | 4.83 | 5.45 | 6.62 | 6.85 |
| Bi..... | 3.100 | 3.342 | 3.889 | 4.574 | 4.763 |
| Th..... | 2.388 | 2.571 | 3.058 | 3.552 | 3.721 |
| U..... | 2.228 | 2.385 | 2.873 | 3.326 | 3.491 |

Emission Spectra. *The K Series.*—In the wave-length region above 0.1 A.U. there have been experimentally measured four groups of emission lines, the *K*, *L*, *M*, and *N* series. For the heaviest atoms, *O* and *P* series lines are theoretically possible though these would lie in the ultraviolet range. Each group in general retains the same appearance from one element to the

next, with a given line simply displaced to a shorter wave length in passing from one element to a heavier. The K series, as first photographed by Moseley in 1914, seemed to consist of two lines, β and α , but these were later resolved into four lines γ (β_2 in I.C.T.), β , α_1 , and α_2 . The γ and β lines in experiments of great precision, are further resolved into doublets. The wave-length difference between α_1 and α_2 varies from 0.0044 A.U. for tin to 0.00484 A.U. for hafnium and the remaining heavy elements. The separation of the β doublet is about 0.00076 A.U. although there is a considerable variation; that of $\lambda_\beta - \lambda_\gamma$ varies from 0.00955 A.U. for tin to 0.0048 A.U. for the elements above tungsten.

The relative intensities of the K lines have been the subject of several investigations. Duane and Stenström found the following relative values for the K lines of tungsten:

| α_3 | α_2 | α_1 | β_1 | γ |
|------------|------------|------------|-----------|----------|
| 4 | 50 | 100 | 35 | 15 |

The ratio $\alpha_1/\alpha_2 = 2/1$ seems to be generally true for practically all the elements. Allison and Armstrong have obtained precision measurements for the following ratios: Mo- $K\beta$ /Mo- $K\alpha = 1/7.7$; Mo- $K\beta_1$ /Mo- $K\beta_3 = 2/1$ (the resolved doublet); Cu- $K\beta$ /Cu- $K\gamma = 42/1$; Cu- $K\alpha$ /Cu- $K\alpha_3\alpha_4 = 100/1$. The appearance of lines and the relative intensities are, of course, of utmost importance in their bearing upon the structure of atoms and the levels of energy within them.

TABLE XI.—CHARACTERISTIC EMISSION WAVE LENGTHS, K SERIES

| Element | $\gamma(\beta_2)$ | β_1 | β_3 | α_1 | α_2 |
|-------------|----------------------|-----------|-----------|------------|------------|
| 24 Cr..... | 2.0667(β_5) | 2.0806 | | 2.28503 | 2.28891 |
| 26 Fe..... | 1.74080(β_6) | 1.753013 | 1.75646 | 1.932076 | 1.936012 |
| 28 Ni. | 1.48561 | 1.49705 | | 1.65450 | 1.65835 |
| 29 Cu..... | 1.37824 | 1.38935 | | 1.53739 | 1.54123 |
| 42 Mo..... | 0.619698 | 0.630978 | 0.631543 | 0.707831 | 0.712105 |
| 45 Rh | 0.53396 | 0.54449 | 0.54509 | 0.61202 | 0.61637 |
| 47 Ag..... | 0.486030 | 0.496009 | 0.49665 | 0.55828 | 0.56267 |
| 74 W | 0.17899* | 0.18397 | 0.18477 | 0.20860 | 0.21341 |
| 78 Pt..... | 0.15887 | 0.16370 | | 0.18523 | 0.19004 |

* $\delta = 0.17803$, $\delta_2 = 0.17917$ (Duane, 1933).

The K emission wave lengths are now known with considerable accuracy for most of the elements between carbon (6) (λ for unresolved $K\alpha$ 44.79 A.U.) and uranium (92). In Table XI are the most probable values for the elements most commonly employed as targets in x-ray tubes.

For the lightest elements as many as 12 or more lines may appear in the K series instead of the usual 4 or 5. Wentzel first claimed that these lines are due to multiple ionization of the relatively simply constructed atoms and, therefore, are related to the ordinary lines (γ , β , α_1 , α_2) as the spark lines are to the arc lines in optical spectra. Thus an $\alpha_3\alpha_4$ line or doublet and other "nondiagram" lines appear in all elements below zinc, in addition to the regular $\alpha_1\alpha_2$ doublet. In the past 10 years great progress has been made on the interpretation of "satellite" or nondiagram lines by Richtmyer, Langer, and others as due to two-electron jumps in an atom.¹

It will be observed from the foregoing data that the wave length of the $K\gamma$ emission line is only a fraction of a per cent longer than that of the K absorption limit. It is a point of great interest whether there are any additional lines between $K\gamma$ and the limit. Larsson measured a $K\beta_4$ line for molybdenum at 0.61825 A.U. Duane in 1931 examined K series x-rays by means of a Bragg spectrometer, the Moseley photographic method being employed. The incident ray and that reflected by the crystal to the photographic plate through distances of 4,725 mm. passed through long metal tubes, exhausted of air in order to reduce the absorption. The $K\beta$ doublet lines of molybdenum ($\Delta\lambda = 0.00056$ A.U.), examined by photometric curves, were separated 0.88 mm. No third line lay in the immediate neighborhood of the β doublet. Between the γ line and the short wave-length limit of the series appeared a marked blackening that represented several lines close together. The new lines may be due to O electrons falling into the K level; but a better explanation is, perhaps, that the lines were produced by falls into the K level of conductivity electrons which may from time to time lie in outer atomic energy levels. Several photographs produced by long exposures showed a fainter single line, roughly halfway between the β and the γ lines. It did not correspond to a known x-ray line of any chemical element reflected in the first

¹ A complete account is found in Siegbahn, *op. cit.*, pp. 370-378.

or second order. Ross¹ has also found this line which he calls β_4 with an intensity of one one-thousandth that of $K\alpha$, another β_5 , and two groups of still fainter lines near γ and β lines.

The L Series.—The complexity of the L series, which has already been referred to, prevents its extensive use for practical purposes. It is interesting to note, however, that the new elements hafnium (72), rhenium (75), and illinium (61) were all discovered by means of analysis of their L emission lines. More than 20 lines in the α , β , and γ groups have been identified for uranium; this number decreases with decreasing atomic number, as is to be expected upon the basis of atomic models in which outer shells of electrons disappear. Measurements of the tungsten L series give the following values:

TABLE XII.—WAVE LENGTHS, TUNGSTEN L SERIES

| | | | | | |
|--------------------|----------------------|---------|-----------------------|----------------------|---------|
| γ_4 | $L_{11} - O_{22}$ | 1.02647 | β_7 | $L_{22} - N_{43,44}$ | 1.2208 |
| γ_9 | $L_{11} - N_{33}$ | 1.0439 | $\beta_{11,12}$ | | 1.2354 |
| γ_3 | $L_{11} - N_{22}$ | 1.05965 | β_2 | $L_{22} - N_{32,33}$ | 1.24191 |
| γ_2 | $L_{11} - N_{21}$ | 1.06584 | β_3 | $L_{11} - M_{22}$ | 1.26000 |
| γ_6 | $L_{21} - O_{32}$ | 1.0720 | β_1 | $L_{21} - M_{32}$ | 1.27917 |
| γ_8 | $L_{21} - O_{11}$ | 1.079 | β_6 | $L_{22} - N_{11}$ | 1.2871 |
| γ_1 | $L_{21} - N_{32}$ | 1.09553 | β_4 | $L_{11} - M_{21}$ | 1.29874 |
| γ_5 | $L_{21} - N_{11}$ | 1.1292 | β_{11} | $L_{11} - M_{11}$ | 1.3344 |
| β_9 | | 1.2021 | η | $L_{21} - M_{11}$ | 1.4177 |
| β_8 | $L_{11} - M_{33}$ | 1.2034 | α_1 | $L_{22} - M_{33}$ | 1.47348 |
| β_{10} | | 1.2094 | α_2 | $L_{22} - M_{32}$ | 1.48452 |
| β_5 | $L_{22} - O_{32,33}$ | 1.2125 | l | $L_{22} - M_{11}$ | 1.67505 |

The relative intensities of the lines $L\alpha_1/L\alpha_2$ are 10/1; the γ lines are in the order $\gamma_1:\gamma_2:\gamma_3:\gamma_4:\gamma_5:\gamma_6 = 100:14.0:22.3:7.0:3.0:2.3$; for the β lines $\beta_1:\beta_2:\beta_3:\beta_4:\beta_5:\beta_6:\beta_7:\beta_8:\beta_9:\beta_{10} = 100:49.3:15.0:7.7:0.47:2.0:0.4:0.68:0.60$.

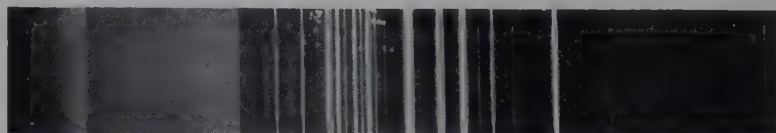


FIG. 63.—Spectrum for alloy of tungsten, osmium, tantalum, cobalt, nickel, and copper. (W. C. Pierce.)

The L series wave lengths are known more or less completely for all the elements from vanadium (23) to uranium (92). A

¹ *Phys. Rev.*, **39**, 536, 748 (1932).

typical spectrum for an alloy of tungsten, osmium, tantalum, cobalt, nickel, and copper is illustrated in Fig. 63.

With remarkable ingenuity in using, as diffraction gratings in their vacuum spectrograph, crystals of palmitic and stearic acid, Siegbahn and Thoraëus made measurements upon the very long wave length α and β lines in the L series spectra of zinc, copper, nickel, cobalt, and iron, the values ranging from 11.99 to 17.66 A.U. The longest L line recognized by I.C.T. is the $\alpha_{1,2}$ line of vanadium at 24.200 A.U. Practically all measurements are now being made with ruled gratings rather than with organic crystals.

The M and N Series.—The M series was discovered by Siegbahn in 1916, and later measurements with crystal gratings were made for the elements from uranium (92) to barium (56). In 1931 Lindberg using ruled gratings determined with great completeness and accuracy the wave length of the M series lines for elements from uranium (92) to cerium (58), with values ranging from 2.440 A.U. for the $M_{II}O_{IV}$ line of uranium to 14.030 for the $M_{VN_{VI}}$ or α_1 line of cerium. For tungsten the wave lengths of the strongest M emission lines are 6.076 (γ or $M_{III}N_V$), 6.743 (β or $M_{IV}N_{VI, VII}$), and 6.969 A.U. (α or $M_{VN_{VII}}$). Siegbahn and Magnusson¹ in 1934 extended the measurements down to bromine (35) with the ruled grating. Especially careful measurements have been made recently by Kiessig.² Figure 64 shows his grating spectrum for tin with 11 M lines together with L lines from copper in the backing of the target, K lines of oxygen, and the K absorption edge of carbon.

Hjalmar first photographed lines belonging to the N series of uranium, thorium, and bismuth. The line at 13.805 A.U. for thorium was the longest wave length spectroscopically measured prior to the studies of Siegbahn and Thoraëus using stearic acid crystals as gratings. Several other studies of the N series and some O lines have been reported in recent years.

The Measurement of Long Wave Lengths by Methods Other than X-ray Spectroscopy.—Many investigators have attempted to measure wave lengths of the soft x-rays, particularly for the very lightest elements, by locating the discontinuities in the slope of the curves representing the photoelectric current as a function

¹ *Z. Phys.*, **88**, 559 (1934).

² *Ibid.*, **109**, 671 (1938); **95**, 555 (1935).

of the exciting voltage. Essentially the method consists in allowing radiation from the target of a highly evacuated x-ray tube to fall on a plate within the tube, which is connected to an electrometer. The current is kept constant and the voltage varied in steps. The various potentials corresponding to dis-

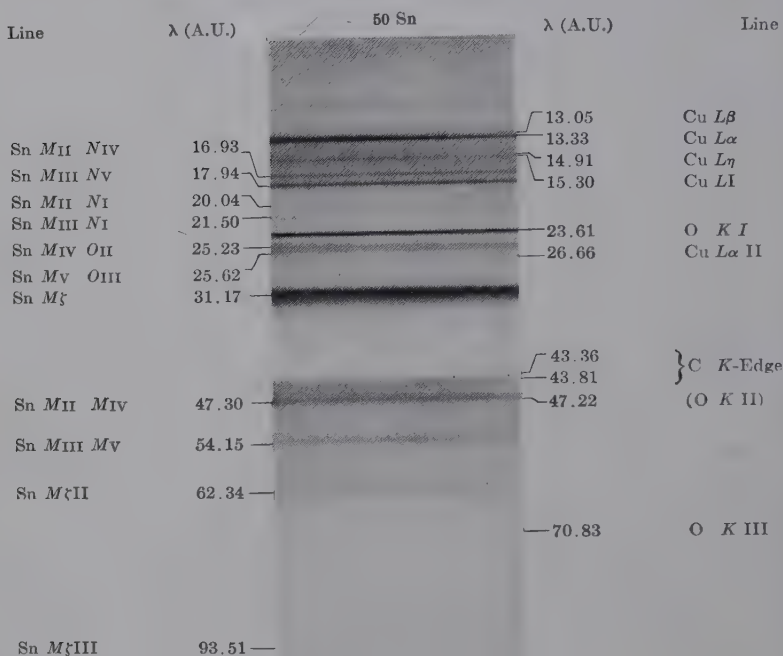


FIG. 64.—*M* spectrum of tin. (Reproduced directly from work of Kiessig.)

continuities in the curve are considered to be the limiting voltages for the *K* and *L* series. Important values in angstrom units so obtained are H-*K* 912, He-*K* 493, C-*K* 42.6 to 45.4, N-*K* 33.0 to 35.1, O-*K* 23.8 to 25.8, Na-*L* 35.3, Al-*L* 100, Al-*M* 326, etc.

In the range of very long wave lengths the same lines are obtained from an x-ray tube and from an ultraviolet vacuum spark. Grating results are as follows: O-*K* α 23.8, N-*K* α 31.8, C-*K* α 44.9, B-*K* α 68.0, Fe-*L* α 17.7, Fe-*L* η 19.6, Fe-*L* ι 20.1, Mo-*M* 65.0, 54.9, Ta-*N* 58.3, 61.4, W-*N* 56.0, 59.0, Pt-*N* 48.0,

51.0, Au-N 46.8, 49.4. These values have been a powerful aid in the establishment of energy levels.

The Effect of Valence and the Fine Structure of X-ray Spectral Lines and Absorption Edges.—Since characteristic x-ray absorption and emission are processes in which the innermost electrons

TABLE XIII.—PRINCIPAL AND SECONDARY ABSORPTION EDGES FOR CL AND S (Lindh)

| Absorber | K_1 | K_2 | Absorber | K_1 | K_2 |
|---------------------------|--------|--------|-----------------------------|--------|----------------------|
| Cl ₂ | 4.3938 | 4.3816 | S monoclinic.. | 5.0090 | 4.9946 |
| HCl..... | 4.3853 | | S rhombic..... | 5.0086 | 4.9938 |
| Chlorides ¹ .. | 4.3829 | 4.3600 | S crystal..... | 5.0088 | 4.9941 |
| Chlorates... | 4.3769 | 4.3574 | Sulfides..... | 5.0093 | Depends on metal ion |
| Perchlorates. | 4.3698 | 4.3478 | Sulfites..... | 4.9960 | 4.9881 |
| | | | SO ₂ | 5.0040 | 4.9964 |
| | | | Sulfates..... | 4.9879 | Depends on metal ion |
| | | | S ²⁺ (organic).. | 5.0068 | |
| | | | S ⁴⁺ (organic).. | 5.0019 | |
| | | | S ⁶⁺ (organic).. | 4.9939 | |

¹ The different edges for chloride, chlorate, and perchlorate enable an analysis for purity of any salt.

in the atom are concerned, it is reasonable to suppose that the external, or valence, electrons have little or no effect upon the wave lengths. For many years it was generally agreed that the characteristic wave lengths were entirely independent of the state of chemical combination of the element; thus sulfur or manganese as elements, or exhibiting various valences in compounds, were thought to give always the same critical absorption or emission wave-length values. Precision researches, largely in the Siegbahn laboratory, demonstrated that for lighter elements there are small but distinct variations in these values depending upon the state of the element in the absorbing screen or target of the x-ray tube.

As a single example, the values of the K absorption limit for iron compounds may be cited from the work of Lindsey and Voorhees¹ as shown in Table XIV.

Among several other reports Cairns and Ott² used such measurements to prove the existence of trivalent metal compounds.

¹ *Phil. Mag.*, **6**, 910 (1928).

² *J. Am. Chem. Soc.*, **56**, 1094 (1934).

Furthermore, a fine structure is found for the lines and absorption limits of certain elements. Lindh investigated both the emission lines and the absorption edges of chlorine, sulfur, phosphorus, and other elements. Results on wave lengths of the absorption

TABLE XIV

| Valence state | Absorber | $\Delta\lambda$, X.U., compared with pure iron |
|---------------|--|---|
| II | FeCO_3 | 1.4 |
| | $\text{FeSO}_4 \cdot (\text{NH}_4)_2\text{SO}_4 \cdot 6\text{H}_2\text{O}$ | 1.9 |
| II and III | Fe_3O_4 | 1.9 |
| | $\text{FeSO}_4 \cdot (\text{NH}_4)_2\text{SO}_4 \cdot 6\text{H}_2\text{O} + \text{FeCl}_3 \cdot 6\text{H}_2\text{O}$ | 1.8 |
| III | $\text{FeCl}_3 \cdot 6\text{H}_2\text{O}$ | 2.5 |
| | Fe_2O_3 | 2.5 |

edges of chlorine and sulfur are listed in Table XIII (K_1 and K_2 principal and secondary edges, respectively). These values have been verified and extended by Stelling and others. Complete data to 1931 are tabulated in the

second edition of Siegbahn, "Spektroskopie der Röntgenstrahlen," pages 278 to 306.

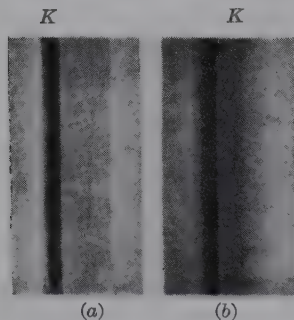


FIG. 65.— K absorption spectra showing (a) simple edge; (b) edge with secondary absorption. (Hanawalt.)

Monatomic vapors exhibit no secondary structure in absorption edges, whereas polyatomic vapors may, although there is usually additional structure observed for the same material in the solid state. This is shown in Fig. 65. The two crystalline forms of calcium carbonate, calcite, and aragonite, have markedly different absorption patterns, a fact

showing that the crystalline structure must have a primary influence in giving to the absorption edge a complex fine structure.

The "satellites" associated with emission lines have been mentioned. An example showing the fine structure of the $L\beta$ and $L\alpha$ lines of zinc and zinc oxide from the work of Gwinner is shown in Fig. 66.

Theories of the origin of these fine-structure features, and vice versa, and the use of these experimental data in deriving adequate atomic mechanisms are considered in a later paragraph in this chapter.

Methods of Obtaining Homogeneous Monochromatic X-rays.

The beam of x-rays produced by an ordinary x-ray tube is obviously heterogeneous and contains many wave lengths. The general radiation is a continuous band, and upon this is super-

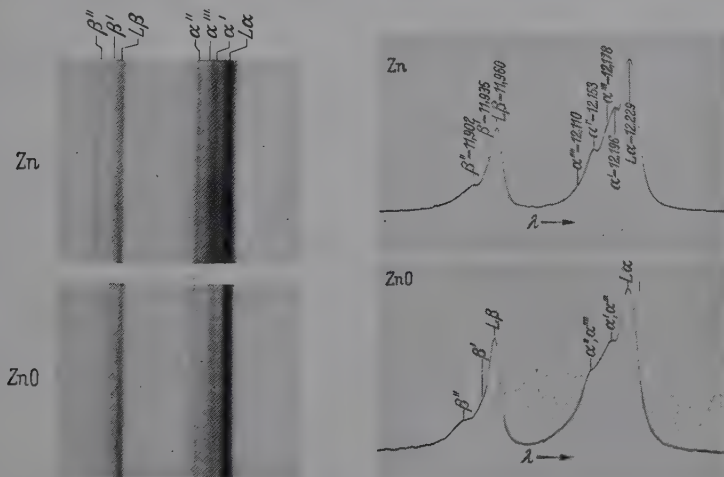


FIG. 66. — $L\beta$ and $L\alpha$ emission lines of zinc and zinc oxide showing satellites. (Gwinner.)

posed above certain voltages the characteristic spectral series. In many applications of x-rays it is highly desirable to have a homogeneous beam of known wave length. This is particularly true for the analysis of the fine structure of materials. Even at very high voltages for deep therapy, the effort is made to homogenize the beam by filtration through sheets of metal so that dosage can be reproduced.

There is only one method of assuring a monochromatic ray, and this is the use of the double spectrometer. At a given angular setting θ of a crystal grating with constant d , only those rays with a certain wave length λ can be reflected at the definite angle 2θ from the primary undeviated beam. Consequently the second spectrometer or other apparatus can be adjusted to receive the purely monochromatic beam.¹ Davis,

¹ Cf. COMPTON, *Rev. Sci. Inst.*, **2**, 365 (1931); ALLISON, *Phys. Rev.*, **41**, 1 (1932).

Compton, Allison, and others have made excellent use of the double spectrometer to measure wave lengths accurately, to study the natural widths of spectral lines, etc. For practical purposes the method has the disadvantage that a loss in energy occurs in every reflection or diffraction process, and the intensity of the radiation is thus diminished.

The second method of rendering a beam homogeneous is by the use of the characteristic absorption edges. Suppose that a molybdenum-target tube is excited at 30 kv.: the spectrum shows the K series lines superposed on the smooth general radiation curve. If, however, the first part of this band and the $K\gamma$ and $K\beta$ lines could be suppressed and the $K\alpha$ doublet left in essentially undiminished intensity, a useful "dichromatic" (since the doublet cannot be separated satisfactorily) beam would result. It is necessary only to discover an element whose K absorption-edge wave length lies between the $K\beta$ and $K\alpha$ wave lengths of molybdenum (*i.e.*, between 0.631 and 0.708 A.U.) and use this for a filtering screen. Table XV shows that zirconium has a K critical absorption wave length of 0.6874 A.U.; a thin screen interposed in the molybdenum-target beam will cut out practically completely radiation with wave lengths shorter than this value but will be nearly transparent to the most intense α doublet.

The following table presents some representative examples of selective absorption for obtaining homogeneous rays:

TABLE XV.—FILTERS FOR OBTAINING MONOCHROMATIC X-RAYS

| Target | Lowest approximate voltage for K series, kilovolts | λ for $K\alpha$ doublet | Filter | Thickness, millimeters | Grams per square centimeter |
|--------------|--|---------------------------------|-----------|------------------------|-----------------------------|
| Chromium.... | 6 | 2.287 | Vanadium | 0.0084 | 0.0048 |
| Iron..... | 7 | 1.935 | Manganese | 0.0075 | 0.0055 |
| Copper..... | 9 | 1.539 | Nickel | 0.0085 | 0.0076 |
| Molybdenum. | 20 | 0.710 | Zirconium | 0.037 | 0.024 |
| Silver..... | 25 | 0.560 | Palladium | 0.03 | 0.036 |

The third method of generating a nearly monochromatic ray is largely of theoretical interest only. Reasoning from the probable mechanism of the excitation of the continuous spectrum, Duane conceived the idea of bombarding a very thin stream of

mercury vapor and liquid with cathode rays so that there would be little chance for stepwise slowing up of the electrons. Under ideal conditions a single line for the short wave-length limit, instead of a continuous band, would be obtained. This ideal was very nearly realized by Duane in obtaining a very narrow sharp peak with a maximum only slightly longer than the λ , defined by $Ve = hc/\lambda_0$.

GENERALIZATIONS FROM X-RAY SPECTROSCOPIC DATA

The Moseley Law.—The brilliant young Englishman Moseley, who was called from his remarkable researches to lose his life in the Dardanelles in 1915, was the first to recognize the essential simplicity of the *K* emission series. He showed that the wave lengths of a given spectral line varied *continuously* step by step in proceeding from one atomic number to the next, and not *periodically* as is the case with so many atomic properties. Even in optical line spectra there are definite relationships

for chemically similar elements—doublets for the alkali metals, singlets and triplets for the alkaline earths—and spectra of increasing complexity in passing from left to right in the periodic table. The periodic properties such as these optical spectra, atomic volumes, etc., must find their origin in the outermost parts of the atoms; the nonperiodic properties such as the x-ray spectra must be ascribed to the interior. The original Moseley *K* series spectra for several neighboring elements beginning with arsenic (33) are reproduced in Fig. 67.

Moseley went further and showed that, if the square root of the reciprocal of the wave length (or of the frequency or of the wave number, which is the frequency divided by a funda-

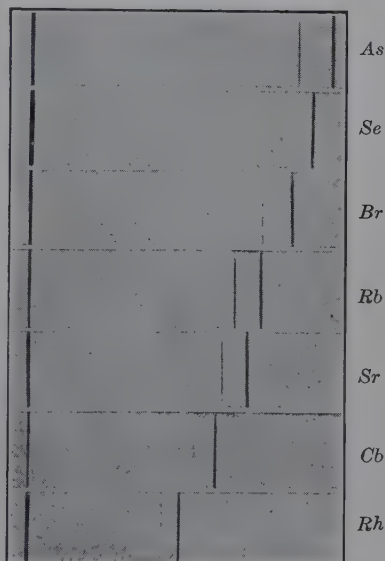


FIG. 67.—*K* series spectral lines as photographed by Moseley for several neighboring elements, illustrating the continuous wave-length progression and the Moseley law.

mental frequency constant R , the Rydberg constant) of a given x-ray line, $K\beta$, $K\alpha$, $L\alpha$, etc., were plotted against atomic number, a practically straight line resulted. Precision researches have demonstrated that the curves are very slightly concave upward. For a K line the curve is characterized by the equation $\sqrt{\nu/R} = \sqrt{\frac{3}{4}}(Z - 1)$, where Z is the atomic number, or $\nu = R(Z - 1)^2 \left(\frac{1}{1^2} - \frac{1}{2^2} \right)$, a form which is of great significance in its analogy to that expressing the frequencies of the ultraviolet Lyman spectral series of hydrogen. Similarly an L -series line frequency is given approximately by $\nu = R(Z - 7.4)^2 \left(\frac{1}{2^2} - \frac{1}{3^2} \right)$, which is analogous to the expression for the Balmer series for hydrogen.

A remarkable extension of the Moseley law has been made in the region of optical spectra by Millikan and Bowen in their experiments with stripped atoms. Working with elements in the second horizontal row in the periodic table, they have compared the spectra of sodium, magnesium⁺ (one electron removed), aluminum²⁺, silicon³⁺, phosphorus⁴⁺, sulfur⁵⁺, and chlorine⁶⁺, all of which, therefore, have exactly the same number of electrons and differ only in the mass and charge of the nucleus. The spectra are identical in appearance, and the square roots of the frequencies of a given line are a linear function of atomic number. Richtmyer has demonstrated also that Moseley relationships hold true for non-diagram or satellite lines. A Moseley diagram for M series lines is illustrated in Fig. 68.

Applications of the Moseley Law.—The simplicity of the relationship between spectral-line frequency and atomic number, which according to present conceptions represents the net positive charge on the nucleus, and also the number of non-nuclear electrons, suggests several valuable applications.

1. The law proves that a fundamental relationship exists among all elements from hydrogen to uranium; that these are all constructed of the same building units in definitely progressing complexity; and that if x-ray spectral lines are to be ascribed to the innermost electrons in atoms, as is indicated by the high frequencies and consequently large energy changes, these inner electrons must be essentially the same in number and disposition in all atoms, regardless of the number of electrons in the outer portions, or of the state of chemical combination of the element.

2. The law has been the fundamental basis upon which the discovery and identification of the recently discovered new elements have depended. Interpolation of the $\sqrt{\nu}$ —atomic-number

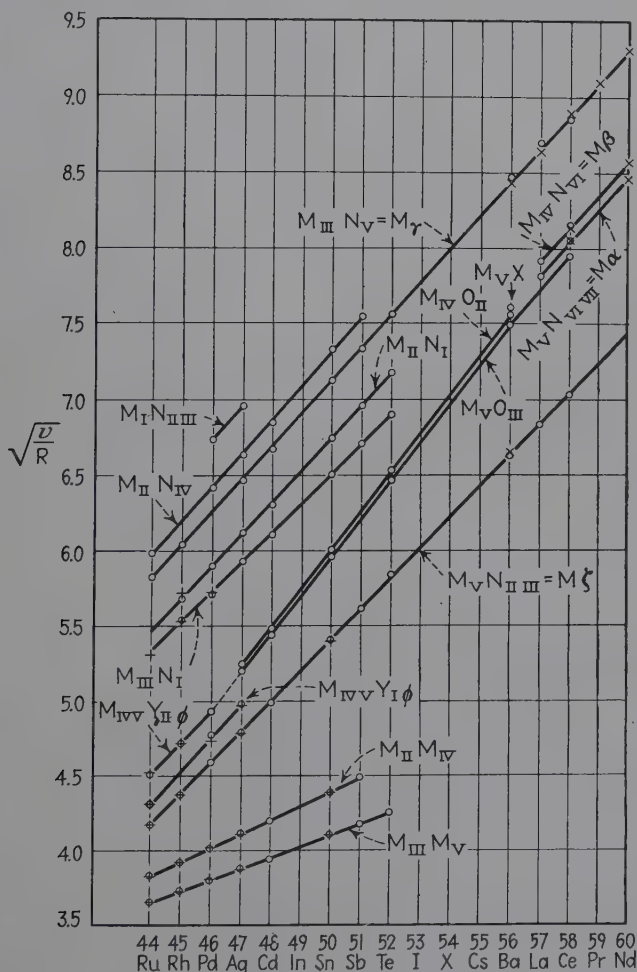


FIG. 68.—Moseley diagram for the *M* series of elements 44 (ruthenium) to 60 (neodymium).

curves, or calculation, gives the wave length that should be expected for a given *K* or *L* or *M* line in the spectrum of an unknown element. In every case the process of discovery has been the matching of experimental lines from the material used as

the target of an x-ray tube with the theoretical values. In this way Coster discovered hafnium (72), Tacke and Noddack discovered masurium (43) and rhenium (75), and Hopkins and his students in 1926 identified the rare earth illinium (61). In this last case the measured wave lengths of strong lines were 2.2781 and 2.0770 A.U., corresponding to the predicted values for the $L\alpha_1$ and $L\beta_1$ lines of the element 61, respectively, of 2.2777 and 2.0730 A.U. Elements formed by nuclear bombardment in the cyclotron and by artificial radioactive transformations are now being identified from the characteristic x-rays that are frequently emitted in these processes.

3. Qualitative and even quantitative analysis of any unknown substance are, of course, directly possible by analysis in similar fashion of the emission lines. Analytical applications of x-rays will be considered in Chap. VII.

The Combination Principle.—Though the Moseley law gives the relationship among elements of varying atomic number from the standpoint of any given x-ray spectral line, another principle observed from experimental data gives important information concerning the relationship between lines and absorption discontinuities in different series for the same element. Thus the frequency of the $K\beta$ line equals the sum of the frequencies of the $K\alpha$ and $L\alpha$ lines. The differences between the K critical absorption frequency and two of the L critical absorption frequencies equal, respectively, the frequencies of the $K\alpha$ emission lines; and the difference between the K absorption frequency and one of the M critical absorption frequencies is equal to the frequency of the $K\beta$ emission line; thus the differences between values of ν/R , where ν is the frequency and R the Rydberg constant, of the absorption discontinuities of tungsten are equal to ν/R values for emission lines, as follows:

$$K - L_{\text{III}} = 4.367 \rightarrow K\alpha_1 = 4.3682.$$

$$K - L_{\text{II}} = 4.268 \rightarrow K\alpha_2 = 4.2693.$$

In the same way the frequencies of L and M absorption discontinuities give the frequencies of certain L emission lines. Thus the combination principle, long known in optical spectra, applies simply to x-ray spectra. In addition, Sommerfeld, Siegbahn, and others have noted important relationships between doublets in x-ray spectra. As an example may be cited the following pairs of values of the wave numbers (ν/R) for tungsten:

| | | | | | |
|-------------------|--------------|-------------------|--------------|-------------------|--------------|
| $L\eta$ | 642.78 | $L\beta_1$ | 712.39 | $L\gamma_5$ | 831.81 |
| L_I | 544.03 | $L\alpha_2$ | 613.85 | $L\beta_6$ | 733.76 |
| | <u>98.75</u> | | <u>98.54</u> | | <u>98.05</u> |
| $L\gamma_6$ | 850.07 | $K\alpha_1$ | 4368.5 | | |
| $L\beta_3$ | 751.56 | $K\alpha_2$ | 4270.0 | | |
| | <u>98.51</u> | | <u>98.5</u> | | |

Here are at least six doublets with the same difference, which is simply that between two L absorption limits L_{II} 849.59 — L_{III} 750.88 = 98.71. The wave-length differences corresponding to these values for each of these doublets (regular or relativity) remain practically constant for all the elements. Another type of doublet (irregular or screening) is that observed by Hertz, where the difference in $\sqrt{\nu/R}$ values for pairs of critical absorption values (L_{II} and L_I) is constant from one element to the next. These two types of doublet occur alternately in the structure; thus L_{III} and L_{II} are relativity, L_{II} and L_I are screening, M_V and M_{IV} relativity, M_{IV} and M_{III} screening, and so on. Such facts as these indicate at once the possibility of definite levels of energy in atoms, the differences corresponding to the frequencies of emitted or absorbed radiation, and doublets to a doubling of energy levels.

The Facts of X-ray Spectra to Be Explained by a Theory of Atomic Structure.—Any comprehensive theory of atomic structure must be able to account for the following facts of x-ray spectroscopy:

1. Characteristic absorption wave lengths.
2. Sharp characteristic emission lines.
3. Grouping of spectral lines in series.
4. Critical excitation potentials for groups of lines.
5. Emission satellites and fine structure of absorption edges.
6. The Moseley law, continuous, nonperiodic progression in wave lengths.
7. The combination principle, regular and irregular doublets, and the relation between emission and absorption.

The Bohr Theory of Atomic Structure.—Before outlining very briefly the Bohr theory of atomic structure, by means of which a very useful mechanical model could be constructed and processes related to radiation clearly pictured, it must be frankly stated that the model is deficient and unable to meet the demands of the newest experimental physics. However, new quantum or wave

mechanics theory, in which the mechanical model of the atom is replaced by mathematical vector equations, has not advanced as yet to the stage where any very satisfactory geometrical model can be visualized in terms of the facts of x-ray spectra. Hence the Bohr theory of the planetary atom still is worthy of presentation and use as a qualitative tool, particularly as it utilizes fundamental quantum laws. Sir William Bragg advises that science must not be criticized for dropping one theory in favor of another, as a carpenter is not scolded for dropping his saw to use his chisel. In a word, science can neither believe wholly in the Bohr atom nor do without it.

In addition to some of the experimental facts of x-ray spectroscopy, there were in 1916 four other great factors, which were largely unrelated and even discrepant, to be taken into consideration by any theory. These were: the classical electromagnetic (wave) theory of radiation, the Planck quantum theory of radiation, the Rutherford nuclear atom, and the empirical (optical) spectroscopy of Balmer, Ritz, and Rydberg. The last factor refers to the relationships such as the following for the optical

series of hydrogen: Lyman series, $\nu_1 = \nu_0 \left(\frac{1}{1^2} - \frac{1}{n_1^2} \right)$, $n_1 = 2, 3, 4, \dots$; Balmer series, $\nu_2 = \nu_0 \left(\frac{1}{2^2} - \frac{1}{n_2^2} \right)$, $n_2 = 3, 4, 5, \dots$; Paschen series, $\nu_3 = \nu_0 \left(\frac{1}{3^2} - \frac{1}{n_3^2} \right)$, $n_3 = 4, 5, 6, \dots$; Bracken series, $\nu_4 = \nu_0 \left(\frac{1}{4^2} - \frac{1}{n_4^2} \right)$, $n_4 = 5, 6, 7, \dots$; etc., or in general $\nu = \nu_0 \left(\frac{1}{m^2} - \frac{1}{n^2} \right)$.

The fundamental assumptions of the original Bohr theory are as follows:

1. The atom consists of a positively charged, extremely minute nucleus, which accounts for practically all the mass, and of negative electrons as satellites. The number of these electrons is equal to the net number of positive charges on the nucleus, and this number is the atomic number. The table of elements is constructed by the addition of one net positive charge and one non-nuclear electron for each element, beginning with hydrogen with one positive charge on the nucleus and one electron.

2. The atom is a dynamic system, for the electrons are in rapid orbital motion.

3. Three laws govern this atom:

a. An acceleration law. In a simple atom like hydrogen, with the assumption that the mass of the nucleus M is infinitely great in comparison to the electron so that the nucleus remains in fixed position, the coulomb force of attraction between positive and negative charges is opposed by the centrifugal force required to keep the electrons revolving in a circle; in other words $e^2/a^2 = mv^2/a$, where e is the electric charge (+ or -), a the distance between two charges, m the mass of the electron, and v its velocity.

b. A momentum law. The angular momentum is governed by the equation $mva = nh/2\pi$, where n is an integer and h is a constant. In other words, the motion of the electron is very definitely restricted to orbits whose angular moment multiplied by 2π is equal to nh . The possible configurations under this quantum condition are called stationary states because no radiation is emitted while the atom remains in such a state.

c. A frequency law. While an electron is revolving in any definite orbit of definite energy W_1 , it is conceived to be non-radiating, for otherwise energy would be lost and the electron would be pulled gradually into the nucleus. Another orbit W_2 would correspond to a different energy level. It is only in the process of transition of an electron from one orbit to another that radiation may be emitted or absorbed; in other words, the energy difference $W_1 - W_2 = h\nu$, where ν is the frequency of the radiation and h the Planck action constant. Ordinarily an atom exists in the stationary state of lowest energy, but by absorption of radiation or some kinds of collisions it may be "excited" to a higher energy state. Radiation is emitted during the transition from a higher to lower state of energy.

A combination of these simple laws gives the equation

$$\nu = \frac{2\pi^2 e^4 m}{h^3} \left(\frac{1}{n^2} - \frac{1}{n'^2} \right), \text{ or } \nu = \nu_0 \left(\frac{1}{n^2} - \frac{1}{n'^2} \right),$$

where ν_0 is a fundamental constant frequency, the Rydberg constant already mentioned, and n and n' whole numbers; the equation expresses the frequencies of the spectral lines of hydro-

gen. There is thus immediate explanation for the empirical spectroscopic formulas of Balmer, Ritz, and Rydberg.

After the simple Bohr theory of hydrogen was announced, many corrections and additions were made. Briefly enumerated these were as follows:

1. Allowance for the mass of the nucleus (in ionized helium the mass 4 must be introduced).

2. Allowance for the revolution of the nucleus around the common center of gravity.

3. A relativity correction, taking into account the variation in mass with the velocity of electrons.

4. The introduction of elliptical orbits, in addition to Bohr's circular ones, to account for the fine structure of spectral lines. These orbits, in order to have energies which differ from those of the circular ones and thus to account for the complexity of apparently single lines, must undergo precession around the nucleus.

5. The most striking characteristic of the Bohr quantum theory of atomic structure was the frequent occurrence of integers and half integers; it was essentially a theory of numbers that are combined in all possible ways, and to this day this feature has been retained in the newer vector models of the atom. The types of elliptical orbit, upon which the electrons in the complicated atoms revolve, were characterized by quantum numbers n, k, j . The number n is related to the size of the orbit, k to its shape, and j to its position in the atoms relative to other electronic orbits. For convenience a particular orbit was referred to as n_{kj} . The larger the value of n , the more loosely is the electron bound to the atom. Thus the innermost electron "shell" consists of a single circular orbit 1_{11} , the second of two ellipses, 2_{11} (most eccentric) and 2_{21} , and a circle 2_{22} , and so on.

6. By combination of x-ray, spectroscopic, and chemical information the complete arrangement of electrons in various shells or orbits was derived for all the elements from hydrogen to uranium. As an example may be cited the structure for the rare gases of the atmosphere, which, except helium, always have eight outside electrons:

2. He $1_{11}(2)$.

10. Ne $1_{11}(2); 2_{11}(2); 2_{21}(2); 2_{22}(4)$.

18. A $1_{11}(2); 2_{11}(2); 2_{21}(2); 2_{22}(4); 3_{11}(2); 3_{21}(2); 3_{22}(4)$.

36. Kr $1_{11}(2)$; $2_{11}(2)$; $2_{21}(2)$; $2_{22}(4)$; $3_{11}(2)$; $3_{21}(2)$; $3_{22}(4)$; $3_{32}(4)$;
 $3_{33}(6)$; $4_{11}(3)$; $4_{21}(2)$; $4_{22}(4)$.
 54. Xe, same as Kr and in addition $4_{32}(4)$; $4_{33}(6)$; $5_{11}(2)$; $5_{21}(2)$;
 $5_{22}(4)$.
 86. Rn, same as Xe, and in addition $5_{32}(4)$; $5_{33}(6)$; $6_{11}(2)$; $6_{21}(2)$;
 $6_{22}(4)$.

This system explains many chemical and spectroscopic facts, the similarity in such homologous elements as Li, Na, K, Rb, and Cs, the chemical similarity of the triads Fe, Co, Ni; Ru, Rh, Pd; and Os, Ir, Pt; and the place of the 14 rare earths (57 to 71). Here the successive electrons are added in the 4_{43} and 4_{44} orbits, previously unoccupied, though electrons are being added in the fifth shell beginning with rubidium, atomic number 37.

LIMITATIONS OF THE BOHR THEORY AND THE DEVELOPMENT OF NEW ATOM MODELS

The Bohr theory, even with its additions, corrections, and empirical analogies, was not directly applicable to atoms containing more than one electron revolving around the nucleus, since there was no way to calculate the very appreciable effect of the presence of other electrons on the energy W corresponding to a particular orbit, or state. Furthermore, physicists became aware of the fact that they were not justified in their literal assignment to an imagined atomic architecture of the concepts of electrons revolving in privileged orbits, "jumps" from one orbit to another, and other geometrical pictures.

Language is incapable of describing processes occurring within atoms, for it was invented to express the experiences of daily life which consist of processes involving exceedingly large numbers of atoms. Furthermore, it is almost impossible to modify language so as to describe these atomic processes, since words can describe only things of which we can form mental pictures and this ability is a result of daily experience. Mathematics is not subject to this limitation.

Contradictions between theory (Bohr) and experiment led to the necessity of demanding that no concept which has not been experimentally verified should be involved in scientific formulations.

The principle of uncertainty was introduced to show among other things that the position and velocity of an electron (say, in an orbit) cannot be known simultaneously. Determinism is dropped out of the latest formulations of theoretical physics.

And yet these mechanical models or pictures with which the Bohr theory was associated are not easily discarded, for they help us to keep in mind the various states of the atoms. The picture may be defective and artificial, but the *energy associated with the various stationary states* is real. We speak of "orbit" and "energy corresponding to a given state" as synonymous terms, but only the latter has real physical significance. An energy-level diagram arising out of the Bohr solar system of orbits is an expression today of atomic "structure" and origin of spectral lines, free from artificial concepts of atomic architecture.

The new atom model departs from the older in the concept that the total angular momentum of the atom is the vector sum of the several components of momentum arising from the spin of the nucleus, the spin of the several electrons, and the orbital motion of the electrons around the nucleus (without any attempt to predict where they are or how they might look, for the recognition of the dual wave and particle behaviors of electrons as well as radiation precludes this). In the words of Richtmyer the vector model of the atom is built up out of these component parts, to each of which is assigned a quantum number; the numerical value of the latter may be conveniently thought of as the length of the vector which represents the angular momentum of that component part. The axes of the several angular momenta may point in various directions, subject to rules of quantization. Thus with each electron there is associated the following quantum numbers:

1. Total quantum number n , identical with the Bohr integers to designate the orbits $K = 1$, $L = 2$, $M = 3$, $N = 4$, $O = 5$, $P = 6$, and now referring to energy levels within the atom.

2. Orbital quantum number l , related to the Bohr azimuthal quantum number by $l = k - 1$, and having values from 0 to $n - 1$. In spectroscopic nomenclature an electron for which $l = 0$ ($k = 1$) is an *s* electron; $l = 1$, *p* electron; $l = 2$, *d* electron; $l = 3$, *f* electron; etc. Thus neon, for example, with a completed *L* shell of eight electrons has the electron configuration $1s^2 2s^2$ -

$2p_x^2 2p_y^2 2p_z^2$, or $1s^2 2s^2 2p^6$, the numerical prefixes 1 and 2 being the principal quantum number n , and the superscripts showing the number of electrons occupying the orbitals. This last word is used to refer to the wave function associated with the orbital motion of an electron. Uranium (92) has the designation

$$\overset{K}{1}s^2 \overset{L}{2}s^2 \overset{L}{2}p^6 \overset{M}{3}s^2 \overset{M}{3}p^6 \overset{M}{3}d^{10} \overset{N}{4}s^2 \overset{N}{4}p^6 \overset{N}{4}d^{10} \overset{N}{4}f^{14} \overset{O}{5}s^2 \overset{O}{5}p^6 \overset{O}{5}d^{10} \overset{P}{6}s^2 \overset{P}{6}p^6 \overset{Q}{6}d^4 \overset{Q}{7}s^2.$$

3. Spin quantum number $s = \frac{1}{2}$ always, expressing angular momentum due to spin of electron around its own axis. Thus the completed K shell consists of two electrons with opposed spin occupying the stable $1s$ orbital.

4. Total angular quantum number j , which, for example, for a one-electron system is the numerical value of the vector obtained by taking the vector sum of \mathbf{L} and \mathbf{S} (\mathbf{S} may be parallel or anti-parallel to \mathbf{L} , so that $j = l \pm \frac{1}{2}$). A closed shell contributes nothing to this number j , which is, therefore, determined by the electrons outside the closed shell.

5. In a strong magnetic field a magnetic spin quantum number m_s , and a magnetic orbital quantum number m_l .

These several vectors combine to make up the total angular momentum of the atom; thus \mathbf{S} is a resultant vector representing the total spin moment; \mathbf{L} the total orbital momentum; and \mathbf{J} from the combination of \mathbf{S} and \mathbf{L} the total angular momentum. Since \mathbf{S} , \mathbf{L} , and \mathbf{J} depend on the configuration of the electrons, they are characteristic of the energy states of the atom.

The Explanation of the Facts of X-ray Spectroscopy by the Atom Model.—It is now certain that the fundamental energy level (or orbit) of the x-ray K series is a one-quantum orbit ($n = 1$), that of the L series a two-quantum orbit ($n = 2$).

The existence of individual, widely separated spectral series leads directly to the fundamental conception that a number of electron groups are present in the atom which differ considerably from each other with respect to orbital energy and the distance between the electrons and the nucleus. Therefore, the K series arises from the transition of an electron from one of the outer groups (*e.g.*, the L , M , or N group) to the inner group (*e.g.*, the K group). The fine structure of the individual lines is due to the energy differences within a definite group; *e.g.*, the $K\alpha_1$ and $K\alpha_2$ lines are to be explained by transitions from two somewhat different L levels to the single K level. For the production of

$K\alpha_1$ the initial state of the atom is the K -ionized state (one electron from the innermost completed shell expelled), and the final state is an L_{III} -ionized state (one L_{III} electron missing by transition into the K shell). The atom itself undergoes the transition from the state K to the state L_{III} , in producing $K\alpha_1$.

The energies of the various orbits or shells or levels are designated by the $h\nu$ values of the experimentally measured critical limits, $1K$, $3L$, and $5M$, and presumably $7N$, $5O$, and $3P$. As a matter of fact, these are the energies required to lift an electron in its particular orbit out of the atom. For this reason, the various levels may be designated by reference to the letters K , L_I , M_I , etc., corresponding to a state of the atom in which an electron is missing from the corresponding subgroup. With the aid of Pauli's exclusion principle which states that no two electrons can have all quantum numbers the same, it has been possible to distribute the electrons in subshells and thus to build up the configuration of electrons in all the chemical elements. In the K shell the two electrons ($n = 1$, $l = 0$) differ only in that the spin axes are oppositely directed ($m_s = +\frac{1}{2}$ and $-\frac{1}{2}$). In the L shell the eight electrons are distributed as follows (m_j is the projection of the vector j in the direction of the magnetic field):

| n | l | j | m_j | Subgroup |
|-----|-----|---------------|--------------------------|-----------|
| 2 | 0 | $\frac{1}{2}$ | $-\frac{1}{2}$ } orbital | L_I |
| 2 | 0 | $\frac{1}{2}$ | $+\frac{1}{2}$ } $2s$ | |
| 2 | 1 | $\frac{1}{2}$ | $-\frac{1}{2}$ } orbital | L_{II} |
| 2 | 1 | $\frac{1}{2}$ | $+\frac{1}{2}$ } $2p_x$ | |
| 2 | 1 | $\frac{3}{2}$ | $-\frac{3}{2}$ } orbital | L_{III} |
| 2 | 1 | $\frac{3}{2}$ | $-\frac{1}{2}$ } $2p_y$ | |
| 2 | 1 | $\frac{3}{2}$ | $+\frac{1}{2}$ } orbital | L_{III} |
| 2 | 1 | $\frac{3}{2}$ | $+\frac{3}{2}$ } $2p_z$ | |

The theory, therefore, explains the facts of x-ray spectra as follows:

1. *Characteristic Absorption Limits.*—These are defined by the energy required in primary radiation quantum, or collision with

cathode rays, to lift electrons from a given energy level out of atom.

2 and 3. *Sharp Emission Lines in Series*.—When a K electron is removed, L electrons may fall into the vacancy producing $K\alpha_1$ and $K\alpha_2$ from two of the three L levels. The $K\beta$ doublet results from the transition of electrons from two of the five M levels, and $K\gamma$, an ordinarily unresolved doublet, from transition from two N levels. Thus the totality of such transfers in a large number of atoms gives rise to the entire K series. The relative intensities of the lines are governed by the relative probabilities of transfer from the various shells to the K shell. These probabilities depend partly on the number of electrons in each level. Thus the chance that an electron will drop from the L_{III} shell with four electrons should be twice that from the L_{II} shell with two electrons. Experimentally $K\alpha_1$ is twice as intense as $K\alpha_2$. If electrons in the L level are removed, the L series results by the transition from the higher M , N , etc., levels to the L level. With three L and five M levels, there are thus possible 15 lines from this one type. However, not all the lines so predicted appear. The spectra are governed by a *rule of selection* which states that the quantum number n must change, that l must change by one unit, and that j may change by one unit or remain unchanged, or in terms of vectors $\Delta\mathbf{L} = \pm 1$, $\Delta\mathbf{J} = 0$ or ± 1 . Recently a number of “forbidden” lines have been discovered, but they are very faint. Newly measured lines of very long wave length whose origins are transitions *within* the N shell ($\Delta n = 0$) have been reported. Energy-level diagrams have been constructed for all the atoms to show how spectral lines in x-ray and optical regions are related to these transitions. Optical spectral lines are produced, of course, by electronic changes between the orbits farthest removed from the center. The complete energy-level diagram is given in Fig. 69; each horizontal line represents a level characterized by an n_{lj} value, and the lines joining these levels represent electron transitions resulting in spectral lines. The diagram is a remarkably terse and complete expression of the origin of radiation and its relationship to atomic structure. It is independent of conceptions of orbits and the mechanism of electron jumps.

4. *Critical Excitation Potentials*.—The K series lines are not excited separately but appear together only when the kinetic

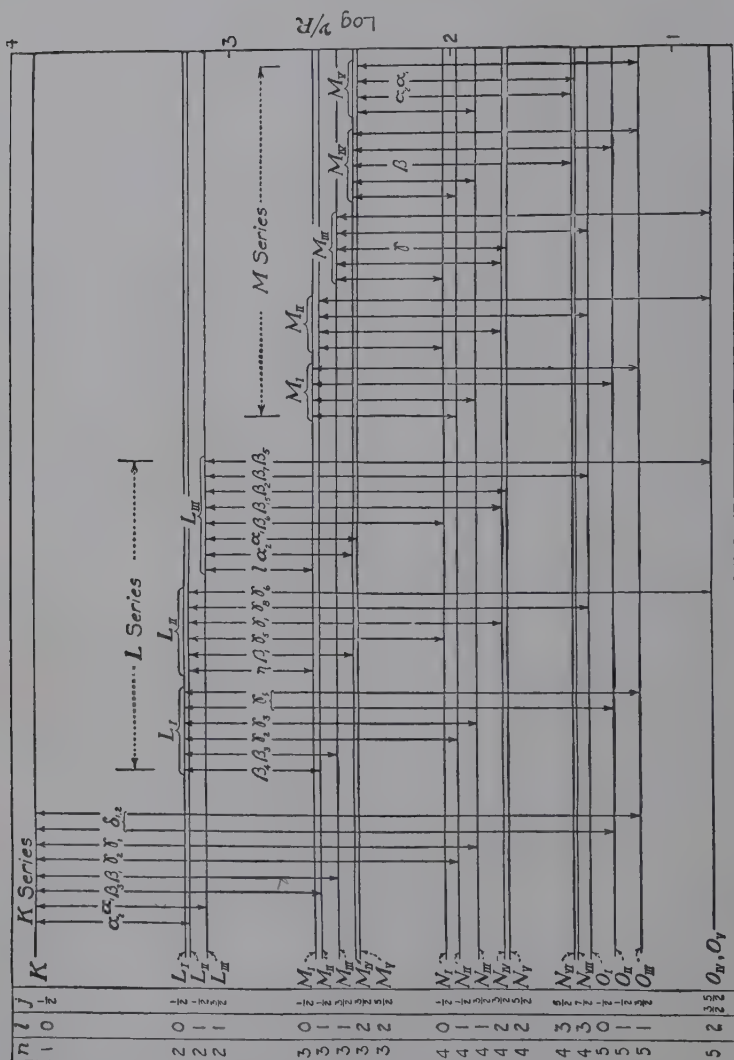


FIG. 69.—Complete energy-level diagram, showing the origin of x-ray spectral lines. (From Richtmyer, "Introduction to Modern Physics.")

energy of the bombarding electron stream in the x-ray tube is equal to or greater than the value given by the equation $E_k = Ve = h\nu_{K_{\text{abs.}}}$. Similarly K series secondary fluorescent x-rays are excited only by primary rays with energies equal to or greater than $h\nu_{K_{\text{abs.}}}$. Only under these conditions is it possible to impart sufficient energy to the K electron to remove it entirely from the atom (not to the L or M levels, for example). The vacancy is supplied then by an L , M , or N electron; the new vacancy is filled from a still more distant shell. The atom returns to a neutral state by a process which, in general, takes place as a series of steps; but jumping over several steps and even the direct return of an outer electron to the K level are not unusual.

5. *Emission Satellites and Fine Structure of Absorption Edges.*—No entirely adequate explanations of these effects have been given. The very weak satellite emission lines on the short-wave-length side of the principal lines, described in a preceding paragraph, do not correspond to lines forbidden by the selection rules or to any others. In general, elements Na 11 to Zn 30 show K satellites but no L or M satellites; Cu 29 to Sn 50 show L but no K or M satellites; Tb 65 to U 92 show M but no K or L satellites. Thus the K satellites are connected with a growing L shell, the L satellites with a growing M shell. Wentzel in 1921 presented the first theory for satellites as arising from single electron jumps in multiply ionized atoms. Thus $K\alpha_4$ corresponds to an initial state KK (two electrons missing in the K shell) and final state KL . Serious objections led to a modification in 1927 to the effect that multiple ionizations do not occur in the same level; thus $K\beta \sim K \rightarrow M$, $K\beta''' \sim KL \rightarrow LM$. The origin and mechanism of doubly ionized atoms form a major objection to these theories. In 1929 Richtmyer proposed a theory of a two-electron jump between multiply ionized states with but one emitted quantum of radiation; thus $h\nu_{\text{sat.}} = h\nu_i + h\nu_0$, with $h\nu_i$ the energy liberated when an electron drops into an inner shell, and $h\nu_0$ the energy liberated when a valence electron drops into an outer shell. This theory has many merits. In 1935 Coster and Kronig modified earlier theories with an Auger, or internal photoelectric, effect. For example, an atom originally in an L_I state will be left in a doubly ionized $L_{III}M$ state because a radiationless $L_I \rightarrow L_{III}$ transition takes place,

the energy being used to eject an M electron. The doubly ionized atom is then in a state to emit satellites, by the Wentzel theory. These radiationless transitions seem to be generally accepted, especially because the Auger effect is well established from measurements of β -ray spectra (Chap. VIII).

To explain the fine structure of absorption edges, the most comprehensive theory has been proposed by Kronig in 1931, based on wave mechanics. The absorbing crystal was considered as a periodic array of potential walls corresponding to the ions in the lattice. The ejected electron, resulting from the ionization of the K level, can enter only into certain energy bands resulting from the crystal lattice structure. The transition of an electron from a K level of an atom to the lowest of these energy bands accounts for the absorption edge. Absorption lines in the secondary structure of the edge correspond to energies an electron may possess after being ejected from the K shell. The values of these energies are given by $W_r = n^2 h^2 / 8ma^2$. Kronig suggested that the separation in the secondary structure should be inversely proportional to the square of the lattice constant of the crystal used as absorber. This was confirmed in certain cases, but other predictions from the theory have not been substantiated experimentally, especially in investigations by Lindsay and associates at the University of Michigan. Thus Kronig's theory is not in its present form capable of explaining completely the secondary structure of x-ray absorption edges of elements existing in crystals with polar binding.

6. *The Moseley law* is a consequence of the fact that the innermost levels in atoms, which take part in the production of x-rays, are all similarly constituted as regards number and disposition of the electrons. The stepwise change in wave length is simply a consequence of the increasing effect of the net positive charge of the nucleus on the inner electron shells in passing from one atomic number to the next higher.

7. *The combination principle* is a direct consequence of different energy levels with definite values. The same wave-number difference may be obtained by several combinations of the wave numbers of critical absorption limits and emission lines, when these are pictured as distinct jumps from lower to higher levels, or vice versa (Fig. 69). The principle thus affords several checks for numerical evaluation of the energy levels.

8. *The Chemical Bond and Molecular and Crystalline Structure.*

The significance of the vector model of the atom, orbitals, spins, and quantum numbers is by no means limited to purely theoretical characterization of individual atoms. For they determine the nature of the chemical bond between atoms which form molecules and crystals and thus the summation of physical and chemical properties of all matter. The covalent bond of elements, such as diamond, all organic compounds, and many inorganic compounds, is an electron pair with opposed spins. The formation of complexes such as $\text{Co}(\text{NH}_3)_6^{3+}$ involves orbitals not only of the valence shell but also of the next underlying shell. Resonance between covalent and ionic bonds and between single and double bonds is the consequence of electronic configuration which is assigned to atoms upon the basis of experimental x-ray data. These fundamental new principles in chemistry are considered in some detail in Chap. XVI on Crystal Chemistry: Fundamental Generalizations from Experimental Data.

CHAPTER VII

CHEMICAL ANALYSIS FROM X-RAY SPECTRA

Since definite x-ray wave lengths, both emission and absorption, are characteristic of the chemical elements, it follows that x-ray spectroscopy may find practical application in qualitative and quantitative analysis. The Moseley law, of course, is of splendid assistance, more particularly in the qualitative discovery of new elements in complex mixtures, since the wave lengths for these elements may be accurately predicted.

The five general procedures employed in analysis are as follows:

1. Measurement of primary spectral emission lines (*K* or *L* or *M* series) in which the unknown substance undergoing analysis is made the target of an x-ray tube.

2. Measurement of secondary fluorescent emission lines in which the unknown is so placed on some device *inside* the x-ray tube that it is screened from the cathode rays but directly irradiated by the primary x-ray beam.

3. The same except that the unknown is irradiated *outside* the x-ray tube; on this account the intensities are greatly decreased, and the time required for photographic registration of the spectrum is increased.

4. Measurement of wave lengths of characteristic absorption edges in which the unknown serves as an absorbing screen.

5. Use of a cathode-ray tube with thin windows for passage of rays, with bombardment of unknown outside and spectrographic analysis of x-rays generated.

Apparatus.—The essential apparatus for analysis comprises the x-ray tube and power plant and a crystal spectrograph. Special demountable tubes are required for methods 1 and 2. In the first case the sample must be pasted or fused on a cooled metal surface serving as anode. The tube so prepared is then pumped continuously. Any of the demountable electron or ion tubes described in Chap. II are used. For method 2 either a second target or some other special holder is required inside the

tube which must then be pumped. One of the best designs, due to Stintzing, is shown in Fig. 70. Both the vertical cone-shaped anode opposite the hot-filament cathode and the fluorescent-ray plate, horizontal left, are rotated. Another tube for method 2 which has been used with great success by Coster, Hevesy, and others is shown in Fig. 71.

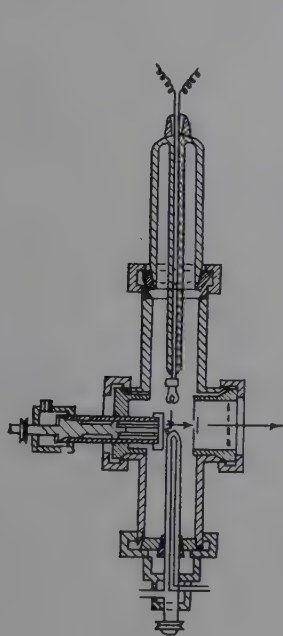


FIG. 70.

FIG. 70.—X-ray tube for chemical analysis by secondary fluorescent rays (Stintzing).

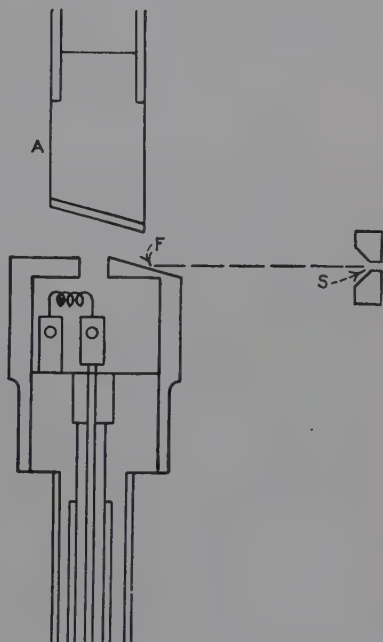


FIG. 71.

FIG. 71.—X-ray tube for chemical analysis by secondary fluorescent rays (Hevesy).

For methods 3 and 4 any standard x-ray tube with ordinary targets can be used, operated at requisite voltages for the excitation of the secondary radiation. Vacuum spectrographs are very largely used for analyses, particularly where minute amounts of substances are involved. Standard equipment such as that shown in Fig. 72 is available in which the high vacuum of the tube is separated from the moderate vacuum of the spectrograph by aluminum foil. A calcite crystal with cleavage face as reflecting plane is used as grating. Registration of the spectra is almost always photographic, although measurement of ionization

currents with the ionization-chamber spectrometer are easily possible without vacuum. The crystal is best oscillated over a small angle by means of a motor and heart-shaped cam.

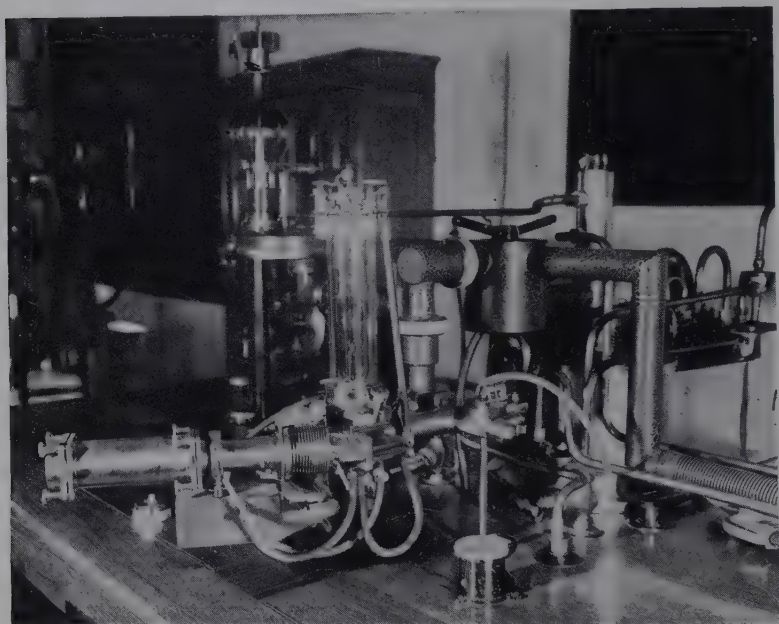


FIG. 72.—Seemann vacuum spectrograph and tube in the laboratory of the French Air Ministry, Paris. (*By permission.*)

ADVANTAGES OF X-RAY ANALYSIS

1. Over chemical methods.
 - a. Analysis of extremely minute amounts—triumph of discovery of elements 72, 43, 75, 61, and 87.
 - b. Analysis of rare earths, platinum metals, etc., where separations are difficult or impossible.
 - c. Material used in any available form without special preparation and independent of chemical combination and without loss; hence valuable for rare metals, gems, etc.
 - d. Greater safety, since no separation of elements is involved; hence much less work and great saving of time.
 - e. Permanent record on plates, largely independent of personal equation.
2. Over optical spectroscopy.
 - a. The great simplicity of x-ray spectra, particularly the *K* series emission, as compared with the great complexity of optical spectra (notably iron).

- b. Absolute independence of x-ray spectra (number of lines and relative intensities) from excitation conditions; optical spectra are affected by differences in arc and spark spectra, changes in capacity and induction of the current for ultraviolet causing disappearance or strengthening of lines, etc.
- c. Independence of x-ray spectra from chemical combination or valence, since only atoms and not molecules are involved; optical spectra are affected by kind of chemical combination, band spectra of molecules, presence of foreign substances, etc.

DISADVANTAGES

1. Cannot be used for analysis of lightest elements, since characteristic wave lengths are too long for measurement by usual crystal gratings; the practical limit is calcium ($Z = 20$).
2. Somewhat expensive and special equipment, much of it commercially available only in Europe.
3. Very special technique, including selection of proper voltage, etc., for accurate quantitative analysis.
4. Somewhat limited accuracy for quantitative work involving comparison of line intensities with standards. The line intensities are not proportional strictly to the weight proportions of elements in the preparation, for several reasons noted below. Intensities also depend on the particle size of the substance undergoing analysis, and minimum size is essential for true values.
5. Selective volatilization of constituents of mixture from focal spot of target for primary emission method, with erroneous results; this difficulty is partly alleviated by rotating the anode in order to present fresh surface or by using the fluorescent-spectra methods.
6. Great decrease in intensities and prolongation of time for fluorescent-spectra methods.
7. Serious difficulty for quantitative analysis in the effect of absorption edges on emission lines; if in a mixture one element has one characteristic absorption edge of longer wave length than the emission lines of other constituents of the mixture, these lines will be selectively absorbed. Such difficulties are avoided, when standardizing substances are used, by not mixing but by using a rotating target with the samples contiguous and excited to emission separately but, of course, registering on the same photographic plate. The effect of the absorption edges of silver and bromine in the plate must be taken into account also.
8. Line coincidence¹ which may occur and cause difficulties; avoided only by greater resolution of spectra and use of higher orders of reflection.
9. Appearance of foreign lines, such as mercury, from diffusion pump; tungsten from metal sputtered in target from hot cathode, fluorescent metal lines from slits, traces of material from previous experiments on surface of anode, etc.; these can be checked with blank runs of apparatus.
10. In certain mixtures characteristic rays of one element can be excited by the characteristic rays of another element and thus produce a strengthen-

¹ GLOCKER, "Materialprüfung mit Röntgenstrahlen," p. 119, Berlin, 1927.

ing of intensity of lines for the first. Günther, Stransky, and Wilcke observed that a mixture of chromium and copper in the ratio of 46:54 appeared to have the ratio 60:40 on account of characteristic rays of chromium excited by copper rays. Dilution with ground quartz produced true results.

11. Varying sensitivity of the photographic emulsion to different wave lengths; long-wave lines are blacker in proportion to intensity than shorter.

Qualitative Analysis.—For the case of qualitative analysis of materials most of the foregoing disadvantages of the x-ray method are unimportant and the method is straightforward for the analysis, particularly of rare earths and alloys of every kind (see Fig. 69, for example). The fluorescent method which has been hampered by low intensities and long exposure times is coming into almost universal use with the advent of high-power tubes producing very intense radiation.

Quantitative Chemical Analysis.—Methods of quantitative analysis using the emission spectrum have been described by Coster, Stintzing, Günther and Wilcke, Hevesy, Glocker, Goldschmidt, and others. In general these methods depend upon the comparison of the intensities of corresponding spectral lines of two neighboring elements in the periodic table, the assumption being made that the intensities of, say, the *K* lines of two such elements would be the same because of the similar electronic configurations, provided that the elements were present in the same amounts on the anticathode and provided also that the excess of the potential on the tube over the potential required to excite these lines was great compared with the difference between the characteristic excitation potentials of the two lines. (In the first approximation the intensity of a spectral line is proportional to the second power of the difference between the potential used and the characteristic potential.)

✓✓ The actual procedure in all these methods consists in determining, photographically, the emission spectrum of a mixture containing an unknown amount of the element for which the determination is being made and a known amount of the reference element. The intensities of the two corresponding lines of these two elements which have been chosen for comparison are then measured, and the elements are then, on the previous assumptions, present in amounts proportional to the intensities of their respective lines; or the amount of the reference material may be changed until the two intensities are equal, when their atomic amounts are also equal.

The differences in the methods mentioned are mainly differences in the technique of measuring the line intensities. Coster used a Siegbahn spectrograph and measured the relative line intensities with a Moll microphotometer. Günther and Wilcke used spectrograms made with very small times of exposure, the lines being hardly visible to the eye. By using a microscope of 800 magnification, they then directly counted the reduced silver grains in the film. The choice of the time of exposure is very delicate with this procedure, for too long a time causes agglomeration of the grains, which makes counting inaccurate and difficult. Stintzing mentions the use of a microphotometer and also suggests a simpler method. He proposes the use of several superimposed photographic plates to record the spectrogram, the intensities of the several lines being indicated by the number of films they penetrate.

Coster and Nishina, indeed, found the assumption of equal intensity of the lines for equal atomic concentration to be valid only under certain conditions. For instance, in analyzing zirconium ores for hafnium, tantalum was added as the reference element, and correct results were obtained if the tantalum was used as the dioxide. If, however, the pentoxide was used, the tantalum lines were $2\frac{1}{2}$ times as weak as the assumption would predict. Furthermore, the presence of only a small amount of lutecium oxide caused the dioxide to give results similar to those obtained with the pentoxide. These differences led Coster and Nishina to the adoption of an entirely empirical method in which any two lines near each other in the photographic plate may be used. Thus Hevesy and Jantzen used the $\text{Lu-L}\beta_1$ line and the $\text{Hf-L}\beta_2$ lines, which are 0.004 A.U. apart, in analyzing for hafnium. The method of Coster and Nishina has been used for the analysis of a large number of zirconium ores for their hafnium content. The determinations are said to have been made to 0.1 per cent with an accuracy of 10 per cent.

Because of the inherent difficulties of the emission-spectrum method, Glocker and Frohnmayer have developed a method which depends upon the relative intensities of the general radiation on each side of a characteristic absorption discontinuity of the element for which the analysis is being made. An ordinary Coolidge tube may be used; the sample may be in a number of different forms and may even be used without change if necessary. A photographic absorption spectrum is obtained in

the usual way, and the relative intensities are determined by a microphotometer; or an absorption spectrum may be determined by using an ionization chamber. The relation between the intensities and the amount of the element in the sample is given in general by the equation

$$\frac{I_2}{I_1} = e^{-cp},$$

where I_2 is the intensity of the radiation leaving the absorption screen on the short-wave-length side of the discontinuity, and I_1 is the intensity of the long-wave side; c is a coefficient that must be experimentally determined, and p is the amount of element present.

The following data include values of c and of the smallest mass m , in milligrams per square centimeter for the production of

TABLE XVI.—MINIMUM MASS OF ELEMENTS REQUIRED FOR ABSORPTION EDGE

| Element | c K edge | c L_I edge | m K edge | m L_I edge |
|------------|-----------------|-------------------|-----------------|-------------------|
| 42 Mo..... | 69 | .. | 0.7 | |
| 47 Ag..... | 45 | .. | 1.1 | |
| 50 Sn..... | 34 | .. | 1.5 | |
| 51 Sb..... | 31 | .. | 1.6 | |
| 56 Ba..... | 24 | .. | 2.1 | |
| 58 Ce..... | 22.5 | .. | 2.2 | |
| 74 W..... | 8 | .. | 6.0 | |
| 82 Pb..... | 5.7 | .. | 9.0 | |
| 90 Th..... | 3.2 | 50 | 16.0 | .0 |
| 92 U..... | | 45 | | 1.1 |

a true absorption edge (5 per cent intensity difference in two sides).

This method has been used by Glocker and Frohnmayer in the successful analysis of barium in glass, antimony in a silicate, salt mixtures of antimony, barium, and lanthenum, bismuth in alloys, etc. It cannot be used to advantage for elements below molybdenum.

Hevesy¹ has made a very careful study of the factors that determine the results by analysis with fluorescent secondary

¹ "Chemical Analysis by X-rays and Its Applications," McGraw-Hill Book Company, Inc., New York, 1932.

rays. Characteristic primary rays ordinarily give six or seven times more intense secondary rays than rays with a continuous spectrum. For greatest intensity a metal must be chosen for target whose characteristic rays are 0.15 to 0.20 A.U. shorter than the absorption bands of the elements undergoing analysis.

Especial attention also has been paid to the distorting effects upon emission-line intensity of absorption edges of a foreign element between comparison lines or lines of a foreign substance between the edges of the elements being compared, etc. The general conclusion is that the comparison element should be chosen so that the lines and absorption edges are as near as possible to those of the element being determined. The following table is an example of correct choice:

TABLE XVII.—COMPARISON ELEMENTS FOR QUANTITATIVE ANALYSIS

| Element analyzed | Line λ , A.U. | Edge λ | Comparison element | Line λ | Edge λ |
|------------------|-----------------------|----------------|--------------------|-------------------|----------------|
| Pt..... | $L\alpha_1$ 1.310 | 1.070 | Ta | $L\beta_3$ 1.303 | 1.058 |
| In..... | $L\alpha_1$ 3.764 | 3.313 | Cd | $L\beta_1$ 3.730 | 3.322 |
| Cd..... | $L\alpha_1$ 3.948 | 3.496 | Ag | $L\beta_1$ 3.927 | 3.505 |
| Mo..... | $L\alpha_1$ 5.394 | 4.914 | Cb | $L\beta_1$ 5.480 | 5.012 |
| Rb..... | $L\alpha_1$ 7.303 | 6.841 | Si | $K\alpha_1$ 7.109 | 6.731 |
| Ge..... | $K\beta_1$ 1.126 | 1.115 | Ta | $L\alpha_1$ 1.135 | 1.112 |
| Zn..... | $K\beta_1$ 1.293 | 1.281 | Hf | $L\beta_2$ 1.324 | 1.293 |
| Ni..... | $K\beta_1$ 1.497 | 1.489 | Er | $L\beta_2$ 1.511 | 1.480 |
| Ti..... | $K\beta_1$ 2.509 | 2.494 | Cs | $L\beta_2$ 2.506 | 2.466 |
| S..... | $K\beta_1$ 5.021 | 5.012 | Mo | $L\beta_2$ 4.909 | 4.909 |
| Al..... | $K\alpha_1$ 8.319 | 7.947 | Br | $L\alpha_1$ 8.108 | 8.357 |
| Mg..... | $K\beta_1$ 9.535 | 9.511 | As | $L\beta_1$ 9.394 | 9.300 |

Fortunately the distorting effect is appreciable only when there is a considerable amount of a foreign element present; in ordinary cases it may be neglected without seriously affecting the quantitative analysis. An important application of secondary-ray analysis is that of complex minerals down to 0.1 per cent of a constituent or even 0.001 mg. of any element. Another is in tests of preparations for purity, in which concentration of impurities of 1 part in 10,000 may be found. Eddy, Gaby, and Turner¹ were able to find 1 part of iron in 300,000 parts of zinc.

¹ *Proc. Roy. Soc. (London)*, **124**, 249 (1929); **127**, 20 (1930).

CHAPTER VIII

THE ABSORPTION AND SCATTERING OF X-RAYS

The fact that x-rays are absorbed in matter in accordance with definite laws is, of course, of very great practical importance. Differential absorption by heterogeneous matter of varying density is the fundamental basis of the entire science of radiography both in medical diagnosis and in the examination, for example, of metal castings for defects, inclusions, pipes, gas pockets, etc. The laws of absorption determine the protection that x-ray workers require against the harmful effects of the x-rays. Similarly, absorption must precede any effects of x-rays upon chemical action or biological functions.

X-ray science owes much to absorption measurements, since, properly interpreted, they give valuable information upon atomic structure. They were the sole method of investigating the quality of x-rays from the time of Roentgen's discovery down to 1913 when Laue and the Braggs introduced crystal analysis. By absorption measurements with screens of various materials Barkla discovered the absorption and emission of x-rays with wave lengths that are characteristic for each chemical element.

The Absorption Coefficients.—In traversing matter of all kinds, x-rays are absorbed in accordance with the usual exponential equation $I = I_0 e^{-\mu x}$, where I is the intensity after passage through homogeneous matter of thickness x , I_0 is the initial intensity, and μ is the absorption coefficient. One of the most useful applications of this formula is the expression of absorption properties in terms of the "half-value thickness" H , or that which diminishes the intensity of a parallel bundle of rays to one-half the initial value; thus $\frac{1}{2} = e^{-\mu H}$, $H = \log 2 / \mu = 0.69 / \mu$. When the intensity of a monochromatic beam of x-rays is plotted against the thickness of absorbing material (presupposing no characteristic absorption effects), a curve of the form illustrated in Fig. 73 is obtained. If values of $\log I$ are plotted against x , a linear relationship holds, as shown in Fig. 74, always provided that the beam is strictly homogeneous. The slope of the line

is an indication of quality, or wave length: the steeper the slope, the softer the ray.

Practically always, however, the absorption formula appears as

$I = I_0 e^{-\frac{\mu}{\rho} \rho x}$ where ρ is the density and μ/ρ , the mass-absorption coefficient, denotes the absorption by a screen of such thickness that it contains unit mass per square centimeter. Only in this way is it possible to compare rationally the absorption coefficients of different substances and the properties of the atoms

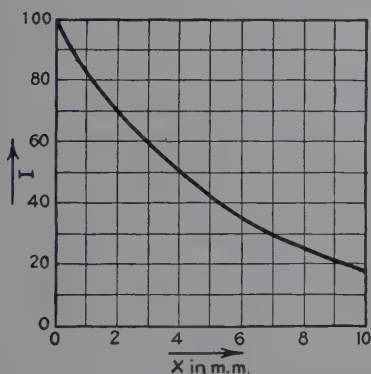


FIG. 73.—Intensity of x-rays plotted as a function of thickness (x) of an absorbing screen.

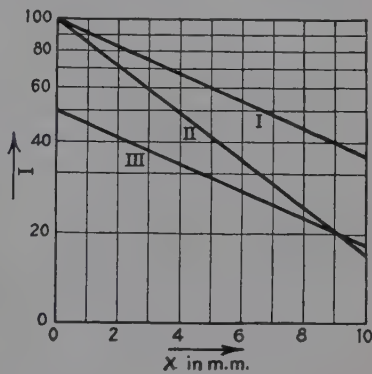


FIG. 74.—Semilogarithmic graph for absorption of x-rays; I and III represent beams with the same wave length but different initial intensities, while II has the same initial intensity as I but a longer wave length.

themselves. This μ/ρ is a simple function of atomic number whereas μ is not. The mass coefficient is independent of physical state, state of aggregation, and temperature and for chemical compounds is in the first approximation additive from the mass coefficients of the constituent elements. By multiplying μ/ρ by the absolute mass of an atom, which is the atomic weight A divided by the Avogadro number $N_0 = 6.063 \times 10^{23}$, the atomic-absorption coefficient is obtained. Since this refers to a screen that contains 1 atom per square centimeter, it leads to some interesting information concerning atomic structure.

It is now definitely established that μ/ρ is really the sum of two coefficients τ/ρ , the true, or fluorescent-ray mass-absorption coefficient, and σ/ρ , the mass-absorption coefficient due to scattering. The latter is usually much smaller in value than the coefficient for the absorption due to fluorescence. For light elements σ/ρ has

a practically constant value of 0.17 independent of the wave length for intermediate ranges. For heavier elements its experimental value changes in a complicated fashion. Some representative values for μ/ρ and σ/ρ are as follows:

TABLE XVIII.—MASS-ABSORPTION COEFFICIENTS
(Including very short wave lengths)

| Wave length, angstrom units | C | Al | Cu | Sn |
|-----------------------------------|-------|-------|-------|-------|
| 0.010 | 0.061 | 0.059 | 0.056 | 0.054 |
| 0.015 | 0.073 | 0.070 | 0.067 | 0.067 |
| 0.020 | 0.081 | 0.078 | 0.076 | 0.082 |
| 0.025 | 0.088 | 0.085 | 0.085 | 0.102 |
| 0.030 | 0.097 | 0.094 | 0.097 | 0.130 |
| 0.040 | 0.108 | 0.104 | 0.120 | 0.204 |
| 0.050 | 0.117 | 0.113 | 0.150 | 0.32 |
| 0.064 | 0.130 | 0.130 | 0.198 | 0.49 |
| 0.072 | 0.136 | 0.143 | 0.232 | 0.614 |
| 0.098 | 0.142 | 0.156 | 0.325 | 1.17 |
| 0.130 | 0.152 | 0.186 | 0.57 | 2.15 |
| 0.175 | 0.163 | 0.228 | 1.12 | 4.50 |
| 0.200 | 0.175 | 0.270 | 1.59 | 6.10 |
| 0.280 | 0.188 | 0.402 | 3.25 | 12.8 |
| 0.417 | 0.256 | 1.18 | 11.4 | 45.5 |
| 0.497 | 0.315 | 1.90 | 18.9 | 11.8 |
| 0.631 | 0.474 | 3.73 | 37.2 | 23.0 |
| 0.710 | 0.605 | 5.22 | 51.0 | 34.0 |

Barkla obtained the approximately constant value of 0.2 for σ/ρ in his pioneer experiments. When this value is equated with the J. J. Thomson theoretical value of scattering by electrons in accordance with the classical wave theory, the result comes out that the number of electrons per atom is half the atomic weight. Subsequent developments have proved that this deduction is only approximate.

The true, or fluorescent, coefficient may be written as a function of the cube of the wave length, *i.e.*, $K\lambda^3$. The atomic-fluorescent coefficient of absorption refers to a process of actual transformation of x-rays in the absorbing screen. It is a function of both the atomic number Z and the wave length; thus $\tau/\rho \cdot A/N = CZ^4\lambda^3$ (law of Bragg and Peirce). C for each element is constant only over certain ranges and then changes abruptly at wave

lengths that are characteristic of each element; the same is true of K in

$$\frac{\mu}{\rho} = \frac{\tau}{\rho} + \frac{\sigma}{\rho} = K\lambda^3 + \frac{\sigma}{\rho}.$$

The accepted values¹ of the constants for six metals in the equations for the mass-absorption coefficients above, K_K , and below, K_L , the first discontinuity (the characteristic K absorption) are given in Table XIX.

TABLE XIX.—VALUES OF CONSTANTS IN ABSORPTION EQUATION

| | Mo(42) | Ag(47) | Sn(50) | W(74) | Au(79) | Pb(82) |
|--------------------------|--------|--------|--------|-------|--------|--------|
| K_K | 375 | 545 | 595 | 1870 | 2230 | 2570 |
| K_L | 50 | 70 | 90 | 330 | 395 | 476 |
| K_K/K_L | 7.5 | 7.8 | 6.6 | 5.65 | 5.65 | 5.40 |
| $\tau_A(10^{-21})$ | 13.3 | 11.0 | 8.90 | 3.19 | 2.57 | 2.37 |

The formulas in Table XX for total mass-absorption values (μ/ρ) for several elements are useful.

TABLE XX

| Absorber | λ | μ/ρ |
|----------|------------------------------|-------------------------|
| Al..... | 0.1 to 0.4 | $14.45\lambda^3 + 0.15$ |
| Al..... | 0.4 to 0.7 | $14.30\lambda^3 + 0.16$ |
| Fe..... | 0.1 to 0.3 | $110\lambda^3 + 0.18$ |
| Co..... | 0.1 to 0.3 | $124\lambda^3 + 0.18$ |
| Ni..... | 0.1 to 0.3 | $145\lambda^3 + 0.20$ |
| Cu..... | 0.1 to 0.6 | $147\lambda^3 + 0.5$ |
| Mo..... | 0.1 to 0.35 | $450\lambda^3 + 0.4$ |
| Mn..... | $>\lambda_{K_{\text{abs.}}}$ | $51.5\lambda^3 + 1.0$ |
| Ag..... | 0.1 to 0.4 | $603\lambda^3 + 0.7$ |
| Ag..... | $>\lambda_{K_{\text{abs.}}}$ | $86\lambda^3 + 0.6$ |
| Pb..... | $>\lambda_{K_{\text{abs.}}}$ | $510\lambda^3 + 0.75$ |

Mechanism of Absorption.—When a beam of x-rays impinges upon matter, the radiation energy is partly transformed, as already indicated, and partly scattered. Figure 75 indicates the principal phenomena that have been identified, though others have some experimental proof.

¹ RICHTMYER, *Phys. Rev.*, **27**, 1 (1926).

Fluorescent Characteristic X-rays.—The energy of these secondary rays is accounted for in the term τ/ρ in the mass-absorption equation $\mu/\rho = \tau/\rho + \sigma/\rho$. Upon analysis with a spectrometer the rays are shown to be identical with those which would be emitted if the absorber element were used as an x-ray-

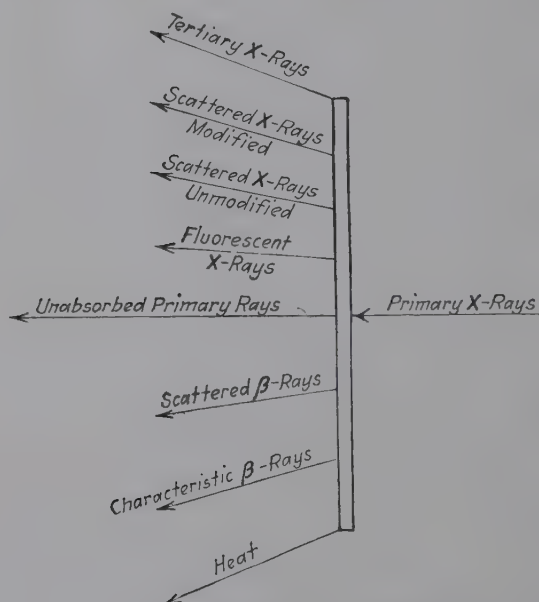


FIG. 75.—Phenomena occurring when x-rays impinge upon matter.

tube target, in that the line spectra in the K , L , M , etc., series are obtained with the same wave lengths. This presupposes that if the K series spectrum appears, the exciting primary beam must contain rays with a frequency equal to or greater than that which is characteristic of the K critical absorption limit of the absorber element. Fluorescent x-rays are unpolarized.

Primary x-ray quanta with an energy equal to or greater than $h\nu_{\text{absorber } K \text{ limit}}$ remove electrons from characteristic levels in the atom just as effectively as the cathode rays in an x-ray tube.

Scattered X-rays Unmodified.—These rays have the same wave lengths as the primary beam; for instance, if the primary beam contains the tungsten characteristic rays, then the spectrum of the scattered x-rays will show the tungsten lines; thus reflection from crystals is essentially a special case of scattering. If the

primary x-rays are transferred in energy quanta, the scattering is produced by atoms or groups of atoms that are too massive to be sensibly affected by the radiation quantum. These rays are polarized, usually completely; thus no reflection from a crystal occurs, when the primary rays are linearly polarized, if the direction of the reflected ray coincides with the electric vector of the incident ray.

Scattered X-rays Modified by the Compton Effect.—One of the great contributions in physics in recent years was the discovery by Compton and by Debye that the spectra of scattered rays, characteristic of the primary rays and not of the secondary radiators, show not only lines with the same wave length as those in the primary beam but also, on the long-wave-length side of these lines, other lines which indicate that in the process of scattering a distinct change has occurred. These modified lines were shown to be quantitatively explained upon the basis of a purely quantum phenomenon. A primary quantum of x-radiation energy $h\nu_0$ strikes an electron and imparts to it a certain amount of kinetic energy resulting in recoil. The radiation quantum is changed in its direction and proceeds with an energy $h\nu$, smaller by the amount involved in the recoil of the electron. Consequently the wave length will be longer.

From the law of conservation of energy

$$h\nu_0 = h\nu + mc^2 \left(\frac{1}{\sqrt{1 - \beta^2}} - 1 \right) \quad (1)$$

where the last term is the kinetic energy of the recoil electron with relativity correction ($\beta = v/c$, or ratio of velocity to that of light).

From the law of conservation of momentum

$$X \text{ component: } \frac{h\nu_0}{c} = \frac{h\nu}{c} \cos \phi + \frac{m\beta c}{\sqrt{1 - \beta^2}} \cos \Theta, \quad (2)$$

$$Y \text{ component: } 0 = \frac{h\nu}{c} \sin \phi + \frac{m\beta c}{\sqrt{1 - \beta^2}} \sin \Theta, \quad (3)$$

where ϕ is the angle between the incident and scattered rays and Θ is that between the incident ray and the direction of recoil of the electron. Combining the three equations above and converting frequency ν to wave length λ ,

$$\lambda = \lambda_0 + \frac{h}{mc}(1 - \cos \phi)$$

or

$$\delta\lambda = \lambda - \lambda_0 = \frac{h}{mc}(1 - \cos \phi) = \gamma \text{ vers } \phi.$$

Thus, at $\phi = 0$ deg. (direction of primary ray), $\delta\lambda = 0$; at 90 deg. $\delta\lambda = 0.0242$ A.U. (the numerical value of γ).

It is at once apparent that the Compton effect is independent of the atomic number of both the target and the scattering element and depends only upon the direction of the scattered beam with reference to the primary beam.

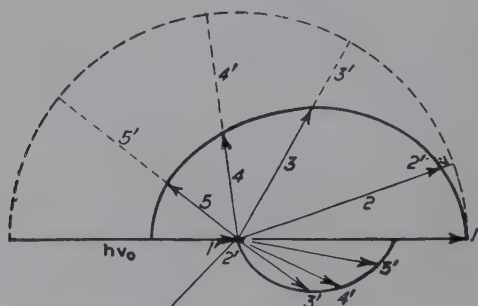


FIG. 76.—Diagram showing Compton effect.

The Compton effect is well illustrated in the diagram in Fig. 76. Here $h\nu_0$ is the primary quantum scattered by the electron e . The length of the arrow $h\nu_0$ measures the energy magnitude. According to classical, or unmodified, scattering, the scattered quanta will always have the same $h\nu_0$ value independent of the direction. This can be represented by the dotted semicircle with radii $h\nu_0$. Actually there is a wave-length change and this is represented for five directions 1, 2, 3, 4, 5, as full lines, the lengths $h\nu$ being smaller the greater the scattering angle, and the energy changes being the vector difference between the dotted and full portions of each radius. This energy change is accounted for in the kinetic energy of the recoil electrons represented by the arrows in the smaller curve; 1' is 0 because for the scattering angle 0 deg. no energy is available; 2', which is too small to show, corresponds to 2, 3' to 3, etc.

The ratio of the intensities of modified and unmodified rays in the Compton effect, however, varies with the atomic number

of the radiator element, from ∞ for lithium (all energy modified) to 5.48 for carbon, 1.91 for sulfur, 0.51 for iron, 0.21 for copper, and decreasing values for heavier elements to practically zero for lead. No such change in wave length has been observed in the reflection of x-rays by crystals or in the scattering of rays of light. As independent proof the tracks of the recoil electrons have been photographed by C. T. R. Wilson's cloud-expansion method.

The energy distribution

$$E_{\text{kinetic}} = h\nu_0 \frac{\alpha \text{ vers } \phi}{1 + \alpha \text{ vers } \phi} = h\nu_0 \frac{2\alpha \cos^2 \Theta}{(1 + \alpha)^2 - \alpha^2 \cos^2 \Theta}$$

$$\cot \frac{1}{2} \phi = -(1 + \alpha) \tan \Theta.$$

where $\alpha = \gamma/\lambda$, is verified experimentally.

It is interesting to calculate how much energy is involved in the recoil electrons for a practical case of irradiation of the human body from a tube at 200 kv. (average wave length 0.04 A.U.):

$$E_{\text{kinetic}} = h(\nu_0 - \nu).$$

If the average increase in wave length ($\phi = 90$ deg.) is 0.024 A.U.,

$E_k = h\left(\frac{c}{\lambda_0} - \frac{c}{\lambda_0 + 0.024}\right)$; expressing E in volts the recoil electrons have a velocity of about 50 kv. Thus $\frac{50}{200}$, or 25 per cent, of each quantum in the human body goes into the energy of recoil electrons. For rays generated at 200 kv., 2.5 per cent of the x-ray energy in each part of a tissue is transformed into the energy of photoelectrons. Of the fraction of primary energy that is scattered (12 per cent), 3 per cent (25 per cent of 12 per cent) goes into recoil-electron energy.

Absorption of High-voltage Radiation.¹—For the x-rays produced at less than 70 kv. the greater part of the energy absorbed in air or in body tissue is spent in producing photoelectrons. These particles in turn spend themselves in producing the ionization by which the rays are measured and which is responsible for the biological effects of the radiation. As the tube potential increases, the photoelectron production rapidly diminishes to a negligible value, and scattering of the x-rays becomes the most prominent phenomenon. This scattering process may best be thought of as a diffusion of the x-ray photons

¹ After A. H. Compton.

as they traverse the cloud of electrons of which the matter is composed. Most of the scattered energy reappears as x-rays going in every direction; an important part, however, appears as the energy of motion of the electrons with which the photons collide. These recoiling electrons take 10 to 40 per cent of the energy spent in the scattering process, for the range of wave lengths under consideration, and use their energy in ionization. The scattered photons form diffused x-rays of increased wave length which will probably escape from the region before they are again scattered or absorbed.

When the applied potential exceeds 1,000,000 volts, some of the highest energy x-rays may spend themselves in a new type of process, similar to the photoelectric effect, known as pair production. This process consists of the creation, by using the energy of an absorbed photon, of a positive electron (positron) and a negative electron (negatron). A part of the energy thus spent reappears as ionization by the resulting positive and negative electrons; the greater part, however, is used in forming another photon (or two photons), when the positive electron reunites with a negative electron. The photon thus produced is a very hard x-ray which will probably escape from the region before it is absorbed. Such a process may be viewed as the excitation of a kind of fluorescence. It is much more prominent with materials of high atomic number than with light atoms and for the range of potentials and absorbing materials with which we are now concerned may be neglected.

From the physical standpoint it is of interest to note that in order to understand the scattering of the x-rays, we find it necessary to suppose that the electrons which scatter them are tiny magnets as well as electric charges. This feature of the process, introduced theoretically by Klein and Nishina, has been amply verified by recent studies on the intensity and the polarization of the scattered rays.

The Klein-Nishina theoretical formula¹ has the form

$$I = I_0 \frac{e^4}{2m^2c^4} \cdot \frac{1 + \cos^2 \phi}{[1 + \alpha(1 - \cos \phi)^3]} \left\{ 1 + \frac{\alpha^2(1 - \cos \phi)^2}{(1 + \cos^2 \phi)[1 + \alpha(1 - \cos \phi)]} \right\}$$

¹ *Z. Physik*, **52**, 853 (1929).

where ϕ is the angle between primary and scattered radiation and $\alpha = h\nu/mc^2 = 22.2/\lambda$. From this formula, which is applicable down to γ -ray wave lengths, it is possible to calculate the number of scattered quanta and of recoil electrons, polarization, the total path of the electrons set free per unit energy absorption, etc.¹

Scattered and Characteristic β -rays.—X-rays that are impinging upon the surface of a secondary radiator eject photoelectrons. If the radiation is monochromatic (frequency ν), then the kinetic energy of some of the liberated (scattered) electrons will be $E_k = h\nu$, independent of the secondary radiator. The electrons are those so loosely bound in the atoms that the work required for their removal is negligible. In addition, however, other photoelectrons are ejected with kinetic energies that depend upon the particular kind of atom from which they are liberated; hence, their removal has involved a certain amount of work W . If a beam of these electrons is analyzed by causing them to bend in a magnetic field, then all electrons with the same value of $E_k = h\nu - W$ will register a sharp spectral line on a suitably disposed photographic plate. By means of these characteristic β -ray spectra, de Broglie showed that the energy necessary to eject an electron from an inner atomic shell, which is involved in the correction term W , is simply the quantity of energy representing the energy levels, K , L , M , N , etc., which is in turn measured by the frequency values of the critical absorption limits. These β -ray spectra, therefore, constitute another important method of measuring energy levels. In one photograph for photoelectrons ejected from a silver plate irradiated by the K -radiation of tungsten (and of course producing the secondary fluorescent silver K -radiation), de Broglie obtained six lines, corresponding to six different kinetic energies. He showed that these were:

- | | |
|---|-----------------------------------|
| (1) $h\nu_{AgK\alpha} - L_{Ag}$ (where L_{Ag} is the energy required to remove an L electron from the silver atoms, or $h\nu_{AgL_{abs.}}$). | |
| (2) $\begin{cases} h\nu_{AgK\alpha} - M_{Ag}; \\ h\nu_{AgK\beta} - L_{Ag}. \end{cases}$ | (4) $h\nu_{WK\alpha_2} - K_{Ag}.$ |
| | (5) $h\nu_{WK\alpha_1} - K_{Ag}.$ |
| (3) $h\nu_{AgK\beta} - M_{Ag}.$ | (6) $h\nu_{WK\beta} - K_{Ag}.$ |

¹ MAYNEORD, *Proc. Roy. Soc. (London)*, **146**, 867 (1934).

More recently Robinson and his associates have made notable contributions to the field of magnetic spectra of secondary electrons. By means of greatly improved experimental methods the values of energy levels have been determined for many of the chemical elements, including measurement of absorption limits in the range of long wave lengths in which the crystal-grating method is impracticable.¹ This new work has also included measurement of energy levels in multiply ionized atoms. Not only do the magnetic spectra yield energy values of secondary electrons that are ejected from inner levels by action of the primary x-rays; the secondary fluorescent x-rays generated in the radiator are also effective in liberating electrons. The process may be pictured as follows: a *K* electron is ejected through the agency of the primary x-rays, followed by the transition of an *L* electron, for example, to fill the vacancy. Normally a *Kα*-ray is emitted as a consequence of liberation of energy. However, this energy so released can be transformed in the atom into forms other than the quantum of radiation. For example, the transition $L \rightarrow K$ (i.e., from the state *K* with one electron missing, to the state *L*) may lead to the ejection of an *M* electron with a kinetic energy represented by the difference between the first energy ($L \rightarrow K$) and the work required to remove this *M* electron from the atom. This work is greater than that which normally corresponds to the *M* level, for an electron is missing from an inner level with the result that there is diminished screening of the positive nucleus. Therefore the work of separating an outer electron is equal to that required normally for the element of next higher atomic number. Such processes have been experimentally verified in Robinson's work.

Filtration.—The x-ray beams directly from a tube target are not of greatest usefulness as generated. The rays contain a large proportion of very soft components which are absorbed in the uppermost layers of any absorbing substance. For medical diagnosis and deep therapy they are obviously useless, particularly as they may cause harmful skin reactions because the absorption per unit volume for the soft rays is relatively so great. The necessity presents itself in medical and other uses of working

¹ For further detailed information see "International Critical Tables," Vol. VI, p. 2. The data of Robinson, together with all references, are given in Siegbahn, "Spektroskopie der Röntgenstrahlen," 2d ed., pp. 413–428.

with the most nearly homogeneous rays possible, *viz.*, those for which the relative ratios of components of various wave length do not change during penetration of the irradiated object.

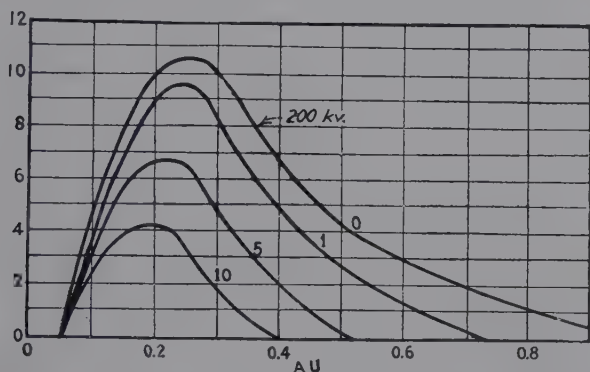


FIG. 77.—Curves showing effect of filtration of heterogeneous x-ray beam through 1, 5, and 10 mm. of aluminum.

The effect of filtration is illustrated by the following example: A mixture of rays consisting of 3 parts, soft, hard, and very hard constituents, with equal intensity, is filtered through 5 mm. of aluminum. For the very hard ray, $\mu = 0.405$, 80 per cent penetrates through, for the hard ray, $\mu = 1.08$, 60 per cent, and for the soft, $\mu = 6.75$, only 4 per cent. Thus, out of a continuous heterogeneous mixture actually generated, a beam less and less heterogeneous and with greater and greater average hardness (shorter wave length) results from greater filtration. Actual experimental results showing the effect of passage through 1, 5, and 10 mm. of aluminum are illustrated in Fig. 77. When the absorption results are plotted logarithmically as in Fig. 78, it is seen that the slope of the curve for small thicknesses changes continuously instead of being constant as is true for monochromatic rays (Fig. 74), showing that the quality of the beam

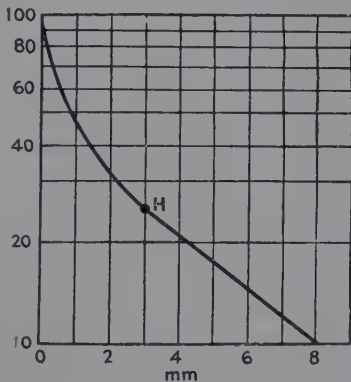


FIG. 78.—Semilogarithmic curve illustrating the homogenizing effect of filtering a beam of x-rays through copper foil. Compare with Fig. 74 for monochromatic rays.

is changing. Finally a point is reached where the curve becomes linear, and below this homogeneity point no further change in quality occurs. This does not mean that the beam is monochromatic or even homogeneous when filtered through other materials. A beam generated at 200 kv. and filtered through 1 mm. of copper behaves as though it were homogeneous when passed next through water or the human body, for the curve is linear; but the same filtered beam passed through more copper is by no means homogeneous. These different behaviors are, of course, determined by the relation between values of μ and σ . Hence filtration for the purposes of homogenizing is easily accomplished with a substance of higher atomic number than that of the object or body in which the rays are to remain homogeneous. In general medical practice copper is used as the homogenizing filter and aluminum as the test filter. If the radiation is homogeneous in aluminum, it will be so in the human body.

Measurement of Quality by Absorption Methods.—Since absorption depends so definitely upon the nature of the absorber or filter and upon the wave length of the ray, a practical measurement of the quality or hardness of an x-ray may be based upon it; for example, by comparing the absorption power of layers of aluminum to that of fixed thicknesses of silver, as judged by the fluorescent or photographic power of the emergent ray, a scale may be constructed and used without reference to wave lengths. Roentgen himself used such a device, and the Benoist penetrometer, consisting of a thin silver disk 0.11 mm. thick, surrounded by 12 numbered aluminum sectors from 1 to 12 mm. thick, is still widely used, particularly in the measurement of dosage in x-ray therapy.

In many cases an x-ray beam with a variety of wave lengths may be used, and the simple absorption equations cannot be used directly. Duane has suggested, however, the determination of the "effective" wave length, or the wave length of a monochromatic ray that has the same absorption under given conditions as the whole polychromatic beam. An experimental curve has been constructed, based upon the fact that the thickness of aluminum which has the same absorbing power as a given thickness of copper depends upon the wave length of the radiation; for soft or long-wave-length x-rays the thickness of aluminum must be large, and for hard x-rays small. Experimentally,

the percentage of the beam absorbed in 1 mm. of copper is first measured by the ionization produced in a gas or by the effect on a fluorescent screen or photographic plate; then the absorption in increasing thicknesses of aluminum is measured until it has the same value as for the copper. The wave length as a function of this equivalent thickness is read from a graph such

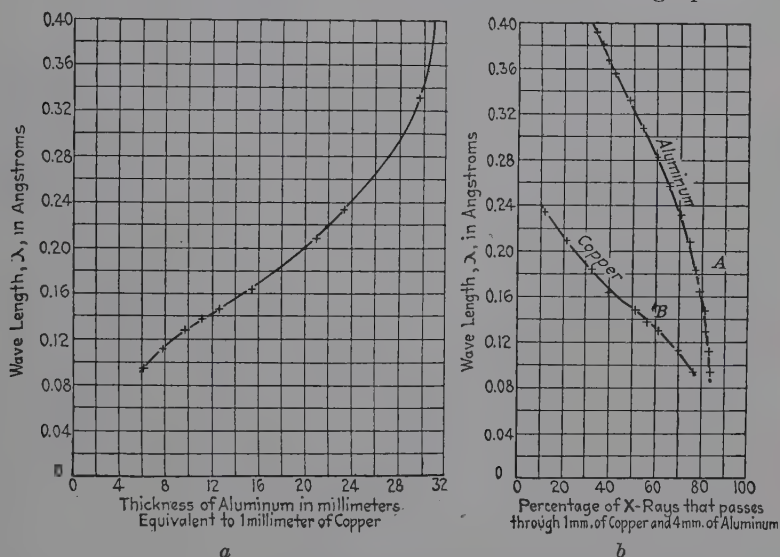


FIG. 79.—Methods of evaluating effective wave length of a heterogeneous beam of x-rays. (a) Curve showing the thickness of aluminum having the same absorbing power as 1 mm. of copper for a beam of heterogeneous x-rays; (b) curves showing the percentage absorption in 1 mm. of copper and in 4 mm. of aluminum as a function of wave length. (Duane.)

as is shown in Fig. 79a. Another method consists in the successive measurements of absorption in 1 mm. of copper and 4 mm. of aluminum. The wave length may then be read from the curves in Fig. 79b.

Protection from X-rays.—The definite laws that govern the absorption of x-rays also permit an exact determination of the thickness of protecting material that must be employed in all work with these rays in order to prevent dangerous physiological effects such as burns and anemia. Of the more readily available materials, lead is the best for protective purposes. Table XXI, from the work of Kaye and Owen, lists the thicknesses of lead in millimeters which are equivalent to 1 mm. of several protective materials in common use for x-rays generated by a Coolidge tube operated at 100,000 volts.

TABLE XXI.—PROTECTIVE POWERS OF MATERIALS RELATIVE TO LEAD

| | |
|-----------------------------|--------------|
| Lead glass..... | 0.12 to 0.20 |
| Lead rubber..... | 0.25 to 0.45 |
| Bricks and concrete..... | 0.01 |
| Woods..... | 0.001 |
| Barium sulfate plaster..... | 0.05 to 0.13 |
| Steel..... | 0.15 |

Adequate protection is a factor of vital importance that must be considered in the installation of x-ray equipment. Undue exposure to the radiation may lead to a lowering of the white-blood-corpusele count (leucopenia), to low blood pressure and anemia, as well as to the skin burns that were so fatal to the early workers. For those engaged in x-ray researches a dental film carried in the pocket for two weeks will give a quick index of excessive exposure; if it is then definitely fogged, protection should be increased. Blood-corpusele counts at intervals are advisable. Shortening the hours of work and increasing the amount of fresh air and recreation are effective in removing symptoms. A "tolerance dose" which the human body may withstand without ill effects has been determined as 1×10^{-5} r per second¹ for 200 working hours per month.²

TABLE XXII

X-rays Generated by Peak Voltage Minimum Equivalent Thickness of
Not in Excess of (Kilovolts): Lead, Millimeters

| | |
|-----|------|
| 75 | 1.0 |
| 100 | 1.5 |
| 125 | 2.0 |
| 150 | 2.5 |
| 175 | 3.0 |
| 200 | 4.0 |
| 225 | 5.0 |
| 300 | 9.0 |
| 400 | 15.0 |
| 500 | 22.0 |
| 600 | 34.0 |

An International Safety Committee under the auspices of the International Congress of Radiology has functioned for several years in standardizing requirements for adequate x-ray protection. As higher and higher voltages are being used in therapy, such standards become increasingly important. A new advisory

¹ The "r" unit of dosage is defined on p. 67.

² MUTSCHELLER, *Am. J. Roentgenology*, **13**, 65 (1925).

committee formed in the United States has prepared a unified and detailed set of safety recommendations (x-ray and high-tension protection, storage of inflammable film, etc.).¹

The minimum equivalent thicknesses of lead recommended as adequate for protection are listed in Table XXII.

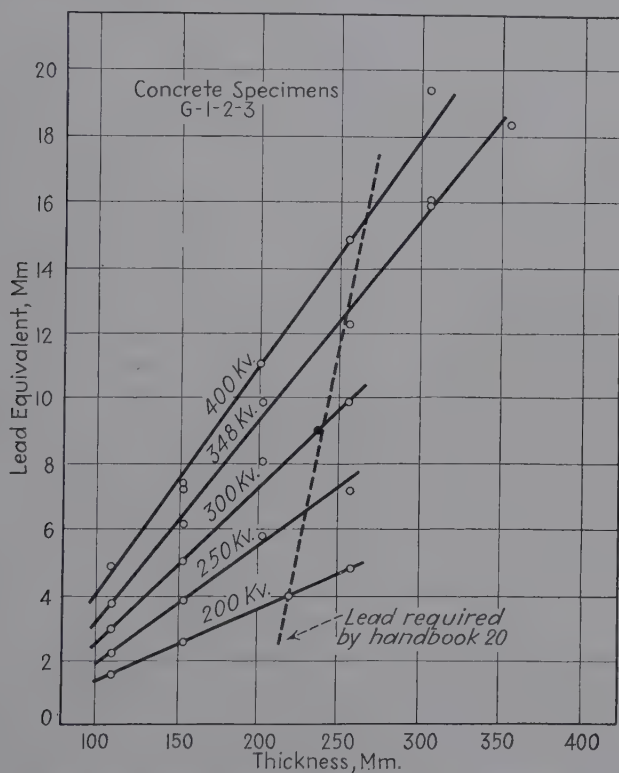


FIG. 80.—Curves for obtaining required thickness of concrete barrier of average density 2.35 grams per cubic centimeter. (National Bureau of Standards.)

In the x-ray laboratory at the University of Illinois which is devoted primarily to researches on ultimate structures of materials, the x-ray tubes are enclosed in lead-lined containers through which are adjusted the necessary slits and pinholes. Sheet lead $\frac{1}{8}$ in. thick gives a large factor of safety for a molybdenum-target tube operated at voltages up to 30,000 volts, and a thickness of $\frac{1}{4}$ in. suffices for tungsten-target tubes operated at voltages up to 150,000 volts. The new metal self-shielding

¹ National Bureau of Standards, *Handbook 20*.

x-ray tubes, which permit passage of rays only through very small windows, also simplify the matter of protection of the research worker. For radiographic examination of metals and in x-ray therapy, the rays from a tube cannot be so narrowly defined, and it is sometimes essential to line an entire room with sheet lead and to place the control instruments outside the room. Such equipment may be seen at the Watertown Arsenal and in the Physics Department of the Massachusetts Institute of Technology. New measurements at the National Bureau of Standards on concrete as a protective material are shown in Fig. 80. A barrier about 26.5 cm. thick is adequate at 400 kv., and 22 cm. at 200 kv.¹

Some Practical Applications of Absorption Measurements.—

Aside from the value of characteristic absorption edges in qualitative and quantitative analysis (Chap. VII) the simple exponential law $I = I_0 e^{-\mu x}$ is the basis from which valuable information may be obtained. Filtration, for the purpose of homogenizing beams for therapy, and the determination of quality and effective wave length have been considered already.

Other possibilities that have found interesting practical use are as follows:

1. Determination of the true thickness x of various specimens. As an example may be selected the classification of hides and finished leather. Because of the biological variable, constant quality and thickness are out of the question, and mechanical micrometric methods are ineffective. For such a classification the beam from an x-ray tube, which is operated so that wave length will be compatible with absorbing power of a specimen (soft rays for leather), is passed through a specimen, and the intensity I as well as the initial intensity I_0 is measured, best from the ionization current produced in a gas, which in turn is measured by the deflection of an electrometer or electroscope. The brightness of a fluorescent screen or darkening of a photographic plate could also be employed. With constant I_0 and μ for the given material it follows that the values of x from one sample to another may be ascertained with great accuracy. Other known examples are glass lenses, thin metal foils, paper, paint, and varnish films.

¹ SINGER, TAYLOR, and CHARLTON, *J. Research Nat. Bur. Standards*, **21**, 783 (1938).

2. Uniformity of gage. Variations in thickness in a sample of material are, of course, indicated by irregular results when the sample is moved around in the x-ray beam.

3. Composition of mixtures and solutions. In such cases quantitative analysis of the unknown composition of two or more substances mixed as powders or melted together, or dissolved, may be made if standard measurements of absorption as a function of known composition are available for comparison. Aborn and Brown¹ showed that the amount of lead tetraethyl in gasoline could be determined by measurement of the absorption of x-rays, generated under standard conditions, in a standard thickness of the solution and comparison with standard experimental curves showing absorption as a function of lead tetraethyl concentration. This method is, of course, best adapted for pairs of substances whose absorbing powers are widely different. Alloy composition, amount and uniformity of distribution of impregnating agents in wood, heavy metal content of glass, loading of silk fibers with tin dioxide, concentration of colloidal metal sols, and fillers in rubber are among the examples of this process.

4. Determination of porosity. The actual absorption measurements of a substance of certain apparent thickness depend, of course, on whether the substance possesses maximum density or whether the density is affected by a porosity, even microscopic, so that the absorbing power is smaller than the value predicted for the measured thickness. Charcoals, drying agents such as magnesium perchlorate, sodium silicates, and other substances have been studied in this way.

5. Detection of counterfeit coins; differentiation of true and imitation gems, such as diamonds, and of soft and lead glass; and other similar tests in which specimens may be compared side by side have depended upon the absorption laws for x-rays. The advantage is found in the extreme rapidity with which identification can be made, presupposing the availability of suitable apparatus.

6. Finally, the examination of all materials for gross interior structure, the discovering particularly of inhomogeneities and imperfections, depends upon the differential absorption of x-rays. This constitutes the familiar and extremely important and practical science of radiography to which the next chapter is devoted.

¹ *Ind. Eng. Chem.*, analytical ed., **1**, 26 (1929).

CHAPTER IX

RADIOGRAPHY

Although x-rays because of their short wave lengths are able to penetrate matter, still they are differently absorbed by different substances; that is to say, all materials are not equally transparent to x-rays. These facts are the basis of the science of radiography. Broadly defined, the experimental technique con-

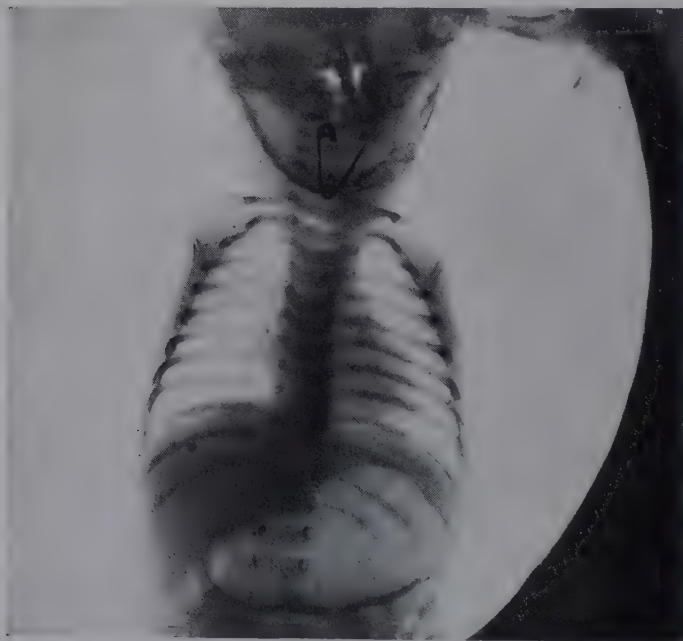


FIG. 81a.—Typical medical diagnostic radiograph for location of foreign bodies.

sists in passing a beam of x-rays through the object to be examined and, by means of a fluorescent screen or photographic plate, recording the varying intensities of the emergent beam and thus obtaining a shadow picture of the interior of the object. Probably the first practical uses of x-rays were of a radiographic

nature, and radiography today is a most useful tool to the medical and industrial diagnosticians.

MEDICAL DIAGNOSIS

In the discovery and location of internal defects of the human body, radiography has become indispensable. The use of x-rays to examine fractured bones preparatory to setting, to study conditions of the teeth as an index to subsequent treatment, and to



FIG. 81*b*.—Femur held to hip bone by nails (student in author's laboratory).

locate bullets, swallowed pins (Fig. 81*a* and *b*), etc., has become so routine that everyone is acquainted with it. Not so well-known, perhaps, are the uses of x-rays in the diagnosis of tumors (Fig. 82), of incipient tuberculosis of the lungs and joints, of diseases of the alimentary tract, of stones in the kidney and the gall bladder, of diseases of the liver and the pelvic organs, and of pregnancy (Fig. 83).

In the examination of the alimentary tract the use of barium sulfate or bismuth salts or emulsions and other similar agents, mixed with the food to produce opacity in the part to be examined,

has become a science in itself. Similarly, the injection of gases and iodized oil into affected parts enables these to be thrown into relief for diagnosis from radiographs. The application of such schemes is continually extending the field of x-rays in medical diagnosis, and wider and wider applications are certain to be found.



FIG. 82.—Radiograph showing bone tumor. (*Eastman Kodak Co.*)

An exceedingly interesting outgrowth of medical diagnosis has been the x-ray photography of mummies taken through wrappings. Some very interesting anatomical comparisons of ancient Egyptians with modern man have been made possible and the same evidences of disease and malnutrition in bone structures obtained as are common today. The Field Museum in Chicago has excellent complete x-ray photographs on display, including one in which the ancient embalmer had perpetrated a hoax entirely unsuspected from the exterior of the mummy by

connecting the head and the legs with a stick since the trunk of the body is entirely missing.

Still other applications are the fitting of shoes; identification of skeletons by radiographs of the skull which is as highly individualistic as finger prints; scientific studies of the diet as it affects bone and tooth structures of rats and test animals or



FIG. 83.—Radiographic diagnosis of pregnancy. (*Eastman Kodak Co.*)

produces rickets; and identification of cause of diseases in fish such as the knot-head carp in the Illinois River radiographed in the writer's laboratory.

It is obvious that a quantitative measurement of blackening of radiographic films by means of the microphotometer (page 77), or densitometer, may have important diagnostic and research significance. Very recently three new densitometers have been described for the following determinations: degree of mineralization of bone as a function of nutrition;¹ tuberculous

¹ MACK, *Science*, **89**, 467 (1939).

calcifications;¹ densities of bone and of muscle and other tissues in studies of child growth.² It is interesting to note that rickets may be detected in x-ray diffraction analysis of ultimate bone structure.

Diagnostic technique has gradually improved, particularly in the use of the finest possible focal spots for sharp radiographic definition, consistent with the highest possible intensities, so that times of photographic exposure may be reduced to the minimum as a safeguard against motion of the patient. The best modern technique, therefore, involves the use of the rotating-target tube described on page 36. The examples in Table XXIII serve to indicate present routine procedures, the voltages representing average values.

TABLE XXIII.—MODERN DIAGNOSTIC TECHNIQUE

| Part of the body | Kilovolts | Milli-amperes | Seconds | Distance, in. |
|-------------------------|-----------|---------------|----------------|---------------|
| Chest: | | | | |
| Posterior-anterior..... | 88 | 500 | | 72 |
| Lateral..... | 94 | 400 | | 60 |
| Gastrointestinal tract: | | | | |
| Stomach..... | 75 | 300 | $\frac{1}{4}$ | 30 (Bucky) |
| Colon..... | 75 | 300 | $\frac{1}{2}$ | 30 (Bucky) |
| Gall bladder..... | 75 | 300 | $\frac{1}{4}$ | 30 (Bucky) |
| Spine..... | 80 | 100 | 2 | 40 |
| Head..... | 70 | 100 | 2 | 25 (Bucky) |
| Extremities..... | 40 to 50 | 200 | $\frac{1}{20}$ | 40 |

The Bucky diaphragm is described in a later paragraph.

INDUSTRIAL DIAGNOSIS

Just as the inside of the opaque human body may be observed on the photographic film or fluorescent screen by virtue of the differential absorption of penetrating x-rays, and without damage, so also may any object be radiographed for the purpose of determining the gross structure and the presence of inhomogeneity or defect. The immeasurable importance of this information is evident in terms of the satisfactory behavior or failure of metal or other objects of practical utility and of the safety of human life that is so frequently involved.

¹ BLOCK *et al.*, *Am. J. Roentgenology and Radium Therapy*, **41**, 642 (1939).

² WEBBER, *Science*, **90**, 115 (1939).

General Principles and Technique of Radiography Applied to Industrial Materials.—1. The technique for preparing radiographic pictures is comparatively simple. A tungsten-target x-ray tube of the Coolidge or Metalix hot-filament type is ordinarily employed. The filament is heated to incandescence by a separate circuit, and this constitutes the cathode in the high-tension circuit, with the target as the anode. A closed-core oil-immersed high-tension transformer which may produce up to 400 kv. is almost invariably the modern equipment. The alternating high-tension current is rectified by mechanically rotating disks or by vacuum-tube valves. The targets may be water-cooled by an insulated circulating system and thus enable the passage of large currents through the tubes. Since radiographic exposures are usually of short duration, x-ray tubes of the universal type, in which the targets become hot, may be employed. The object that is to be radiographed is placed at some distance from the tube so that the rays proceeding from the focal spot on the target are essentially from a point source. Radiographs are merely shadow pictures produced by radiation traveling in straight lines from a point source.

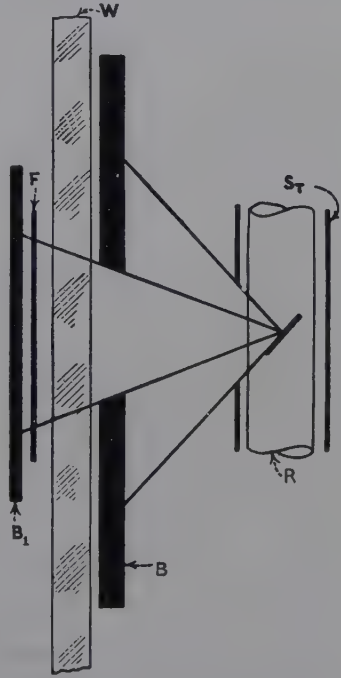


FIG. 84.—General arrangement for photographic radiography. *R*, x-ray tube; *S_T*, protecting cylinder; *B*, diaphragm; *W*, specimen; *F*, photographic plate; *B₁*, lead screen.

2. Registration of the radiograph is either photographic or visually observed on the fluorescent screen (calcium tungstate usually, or barium platinocyanide, zinc silicate, cadmium tungstate, etc.). The general arrangements for the two methods are shown in Fig. 84 for the photographic method and in Fig. 85 for visual observation. In the latter case a mirror is arranged so that the observer will not be in the direct path of the x-rays.

3. For each material and each thickness there is a certain optimum voltage for excitation of the x-ray tube: *e.g.*, 80 kv.

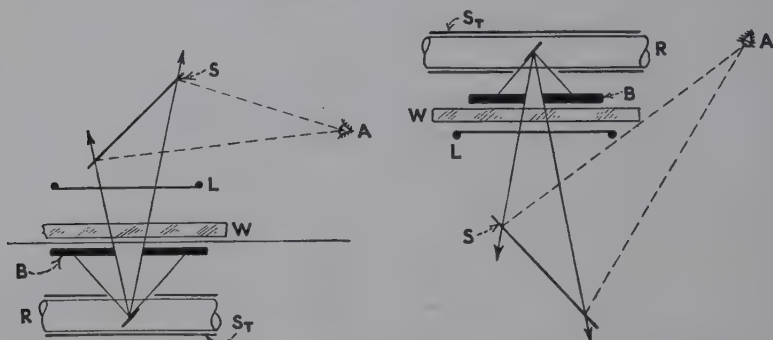


FIG. 85.—Two arrangements for x-ray fluorescence; *R*, x-ray tube; *S_T*, protecting cylinder; *B*, diaphragm; *W*, specimen; *L*, fluorescent screen; *S*, mirror for observation of fluorescent image without direct exposure to x-rays; *A*, eye.

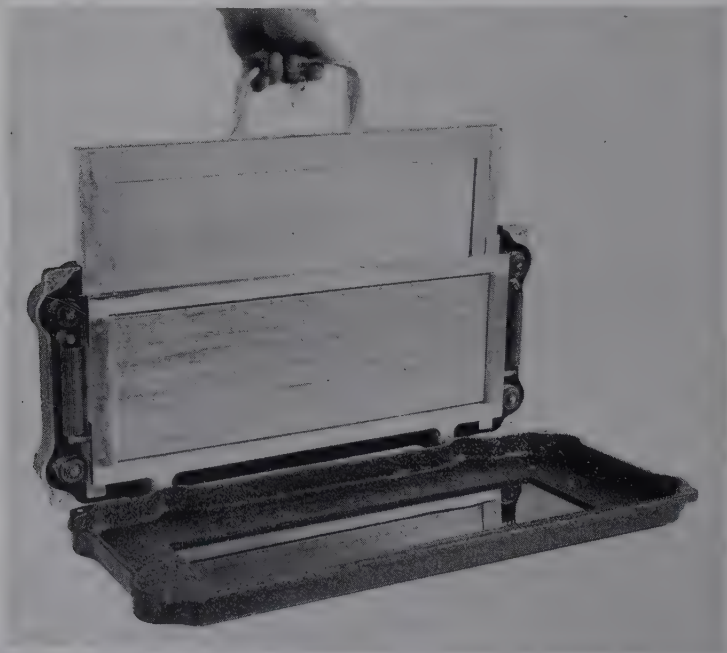


FIG. 86.—Bucky diaphragm or grid for industrial radiography. (*General Electric X-Ray Corporation.*)

for 4 cm. Al, 110 kv. for 10 cm. Al, 200 kv. for 6 cm. Fe, 230 kv.
for 6 cm. brass.

4. Secondary and scattered radiation plays a large part in the results obtained and, for the certain identification of small imperfections in an object on the plate, must be eliminated. A grid such as a Bucky diaphragm consisting of narrow strips of lead or other metal edgewise with free space between each strip is often placed between the object and the plate (Fig. 86). The

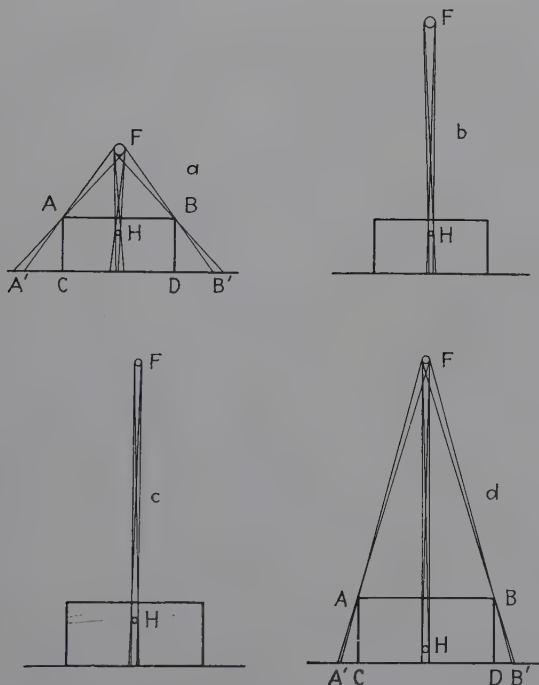


FIG. 87.—Effect of relative size and location of focal spot on definition in a radiograph. *ABCD* is specimen; *F*, focal spot; *H*, cavity in specimen.

primary rays pass straight through the gaps between these strips, while the secondary rays at various oblique angles from the specimen are entirely cut off. Such diaphragms must be moved slowly across the plate. Secondary rays also arise from the walls of the room and other objects, so that the film must be thoroughly protected by covering the back and edges with sheet lead.

5. Tubes with the sharpest possible focal spots are necessary for sharp definition and contrast on photographs at the bound-

aries of portions indicating different densities. This is seen very readily from the diagrams in Fig. 87.

6. Careful photographic technique must be employed in order to ensure distinction between the smallest differences in blackening of the plate. Experiment has indicated that the optimum blackening is $S = 0.7$ to 0.9 ($S = \log \frac{L_0}{L}$, the photo-

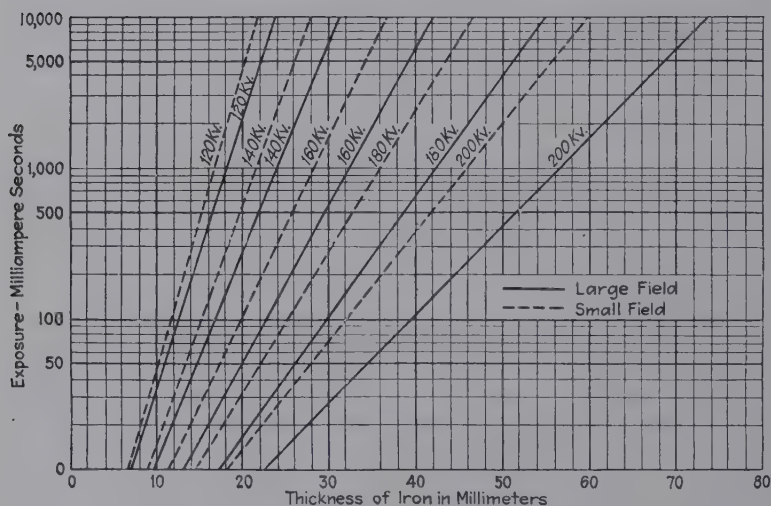


FIG. 88.—Exposure chart for radiography of iron or steel specimens.

metrically measured light intensities before and after passage through the photographic layer). The normal eye can detect with certainty a minimum blackening difference between adjacent areas of 0.02. The principles of photographic blackening are presented in Chap. IV.

7. The amount of exposure is defined by the product of the milliamperage through the x-ray tube and the time of exposure in seconds. Very complete and useful data have been obtained by Berthold¹ for iron, aluminum, copper, and brass. The chart for iron in thickness up to 80 mm. is reproduced in Fig. 88. This shows the log of milliampere seconds (m.a.s.) against thickness of iron in millimeters, for voltages from 120 to 200 kv. for both small field (less than 3 sq. cm.) and large field (50 to 100 sq. cm.), focal

¹ "Grundlagen der technischen Röntgendurchstrahlung," Leipzig, 1930.

distance 50 cm., two intensifying screens with Agfa films, absolute blackening 0.7.

8. For practical use of the fluorescent observation, at least a dose $5 \times 10^{-3}r$ per second¹ must fall upon the screen.

9. The practical limits of penetration and satisfactory radiographic examination of aluminum, iron, and copper are listed in Table XXIV for the following conditions: 200 kv. nonpulsating, 15 ma., 50 cm. focal distance, two intensifying screens, Agfa film, blackening $S = 0.7$, without screens for eliminating scattered radiation.

TABLE XXIV.—LIMITS OF THICKNESS IN MILLIMETERS FOR RADIOGRAPHIC EXAMINATION

| Element | Photographic, small field | | Photographic, large field | | Fluorescent screen, small field | Fluorescent screen, large field |
|------------------|------------------------------|---------|------------------------------|---------|---------------------------------------|---------------------------------------|
| | 10 min. | 60 min. | 10 min. | 60 min. | | |
| Aluminum | 240 | 280 | 355 | 415 | 120 | 175 |
| Iron | 59 | 70 | 73 | 86 | 30 | 40 |
| Copper | 39 | 46 | 46 | 56 | 20 | 25 |

10. The limit of recognition of inhomogeneities in a material of certain thickness is practically measured by the smallest sharply defined difference in thickness of this same material that can be recognized. Blowholes and gas pockets have little or no absorbing power, so that this definition accurately holds for such cases. This limiting difference in blackening of a film is of the order of 2.4 per cent.

Thus: $I_A = I_0 e^{-\mu x}$, for the sound specimen.

$I_B = I_0 e^{-\mu(x-D)}$, for a specimen containing an air pocket of thickness D .

Then, assuming negligible absorption for the defective area,

$$\frac{I_A}{I_B} = e^{\mu x}.$$

By means of such absorption calculations, taking into account scattering which serves to obscure the sharpness of delineation of defective areas, it is possible to calculate the limits of failure

¹ The r unit of x-ray quantity or intensity is considered on p. 67, in Chap. IV.

recognition and experimentally verify these data, such as are shown in Table XXV.

TABLE XXV.—REQUIREMENTS FOR RECOGNITION OF FAILURE RADIOGRAPHICALLY

| Kilo-volts | Material thickness, millimeters | | | Smallest thickness difference, millimeters | | | Per cent of irradiated material | | |
|------------|---------------------------------|----|------|--|------|-------|---------------------------------|------|------|
| | Al | Fe | Cu | Al | Fe | Cu | Al | Fe | Cu |
| 80 | 72 | .. | | 0.42 | | | 0.6 | | |
| 120 | 173 | 23 | 12.7 | 2.7 | 0.11 | 0.058 | 1.6 | 0.48 | 0.46 |
| 160 | 247 | 41 | 25 | 12 | 0.30 | 0.14 | 4.9 | 0.73 | 0.56 |
| 180 | 290 | 54 | 34 | 30 | 0.55 | 0.25 | 10 | 1.0 | 0.73 |
| 200 | 355 | 73 | 46 | | 1.20 | 0.49 | ... 1.6 | | 1.05 |

Conditions: Milliampere seconds 9000 (10 min. at 15 ma.), field < 100 sq. cm., 50 cm. focal distance, constant nonpulsating potential, blackening 0.7, no scattered ray screen, film with two intensifying screens.

For observation of inhomogeneities on the fluorescent screen, a difference in brightness of two adjacent areas of the shadow must be 15 per cent, and a blowhole or gas pocket in aluminum, iron, or copper must be 5 to 7 per cent of the total thickness of sound metal for certain conclusions.

11. Special technique is required for specimens of irregular shape in order that parts of the radiograph will not be over- or underexposed. Cylindrical bars or other specimens with circular parts should be placed in suitable holders of the same material so that the x-ray beam will pass through a constant thickness. Immersion in liquids, such as methylene iodide, having nearly the same opacity to x-rays as the piece to be examined removes this difficulty. Otherwise, sheet lead of varying thickness, lead shot, lead oxide paste, barium sulfate paste, and other absorbing materials can be used with irregularly shaped pieces and for the prevention of the undue fogging of the film by scattered radiation or halation from direct rays at the edges of the specimen.

12. Intensifying screens have played a most important part in bringing this branch of radiography to its present high state. The ordinary calcium tungstate screens are usually employed. It may be mentioned here that a metal screen may also be used, lead foil being sometimes employed. The intensifying factor of such screens is lower than that of calcium tungstate screens;

they have, nevertheless, some advantages over the tungstate screen. They absorb some of the secondary radiation from the underside of the piece being examined and, hence, reduce the fogging of the film; they produce finer grained and, hence, more sharply defined images and are, therefore, especially useful for the examination for fine cracks in the metal. For thick pieces, where a higher intensifying factor than a lead screen provides is necessary (*i.e.*, above 2 in.), the two kinds of screen may be used together with the lead one next to the film. Metal screens may find an increasing usefulness as higher powered tubes come to be used for thicker sections, because of their ability to reduce fogging. A combination of tin and lead is especially good since the tin will absorb the *K*-rays of lead and the characteristic rays of tin will be absorbed by the aluminum-foil cover of the film *cassette*.

13. Stereoscopic radiography for industrial diagnosis is often as valuable as it is in medical diagnosis. The depth and angular disposition of an inhomogeneity in any material may be ascertained with greater certainty than is possible with the ordinary technique. Two radiographs are made, in each of which the tube has been shifted about 1.25 in. on either side of the center of the object. The two films are then viewed in the stereoscope which fuses the two pictures into one with the appearance of three dimensions.

INDUSTRIAL RADIOGRAPHIC EQUIPMENT

With the rapid development of industrial radiography manufacturers found that 200- to 400-kv. medical equipment could be adapted readily for examination of the internal gross structure of materials ranging from steel 6 in. thick down to small fabricated objects, foods, fabrics, etc.

In Figs. 89 and 90 are illustrated typical installations for radiographic examination of welded pressure vessels. In the latter the x-ray tube and valve tubes are enclosed in the transformer case (see Fig. 23). Figure 91 shows a new mobile unit which may be used for a variety of purposes. Trucks and railway cars fully equipped with x-ray equipment are to be found in increasing numbers. A remarkably complete radiographic laboratory in a large truck is used by Prof. Schiebold of Leipzig for testing bridge structures on all the great, new German auto-

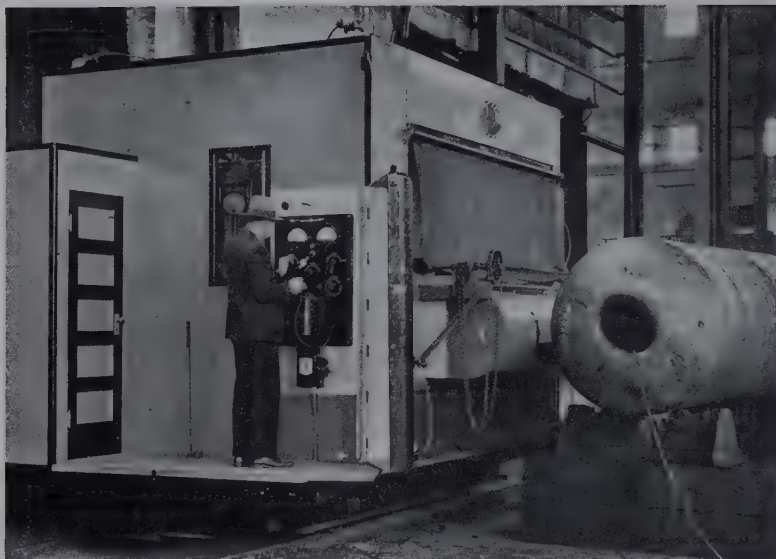


FIG. 89.—Exterior view of installation for radiographic examination of welded pressure vessels. (*Henry Vogt Machine Company, Louisville, Ky.*)

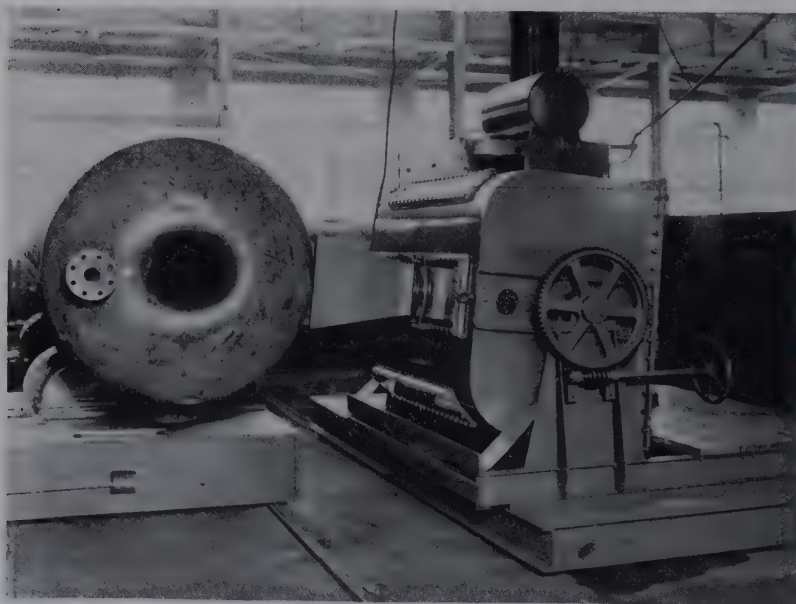


FIG. 90.—400-kv. oil-immersed industrial radiographic unit. (*General Electric X-Ray Corporation.*)

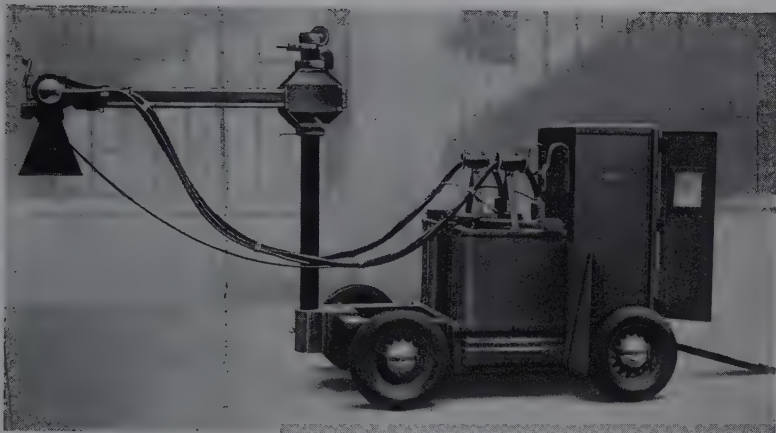


FIG. 91.—220-kv. industrial mobile radiographic unit. (*Westinghouse*).



FIG. 92a.—Routine radiographic inspection of airplane propellers. (*Industrial X-Ray, Seattle, Wash.*)

mobile highways. Figure 92a illustrates routine inspection of airplane propellers and Fig. 92b shows routine fluoroscopic testing with a very small x-ray unit through the thin foil covering of a wing during the construction of an airplane. Figure 93 shows a unit in operation inside one of the giant welded penstocks at Norris Dam. Three such units were in constant operation in testing every inch of 75 miles of welds at Boulder Dam. Finally

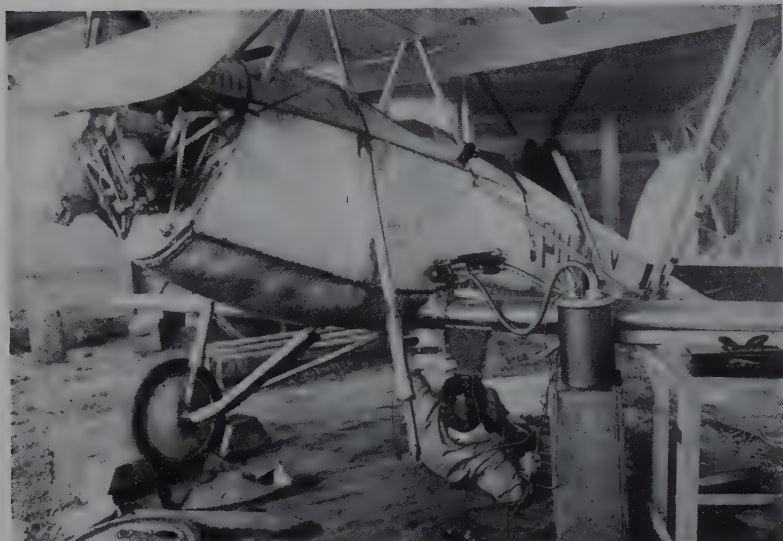


FIG. 92b.—Fluoroscopic examination of airplane wing. (*Philips Metalix Corporation.*)

in Figure 94 is illustrated a typical unit for continuous fluoroscopic inspection of such food products on the belt conveyer as oranges, packaged breakfast foods, boxed candy, canned goods, and cigarettes.

PRACTICAL APPLICATIONS OF RADIOGRAPHY

1. Metal Castings.—This is the most important application of x-ray radiographic diagnosis simply because of the wide use of castings and because of the uncertainty of gross structure with empirically developed foundry practice. The following defects may be radiographically detected on the interior of castings without in any way destroying or marring the specimens, although the diagnosis may be confirmed by “post-mortem” incisions:

Gas cavities.

Due to gases liberated from the hot metal.

Due to gases from the mold.

Sand inclusions.

Slag inclusions.

Pipe or shrinkage cavities.

Porosity.

Due to small gas cavities.

Due to small shrinkage cavities.

Cracks.

Metal segregations.



FIG. 93.—Radiographic unit inside welded penstock at Boulder Dam. (*General Electric X-Ray Corporation.*)

Figure 95 shows the interior gross structure of a steel casting 1.25 in. thick which is characterized by every type of defect noted above, particularly gas cavities, nonmetallic inclusions, and shrinkage cavities. The photographic reproduction is a negative,

and the spots of smaller absorbing power show up darker than the surrounding metal. Figure 96 shows typical gas cavities in cast

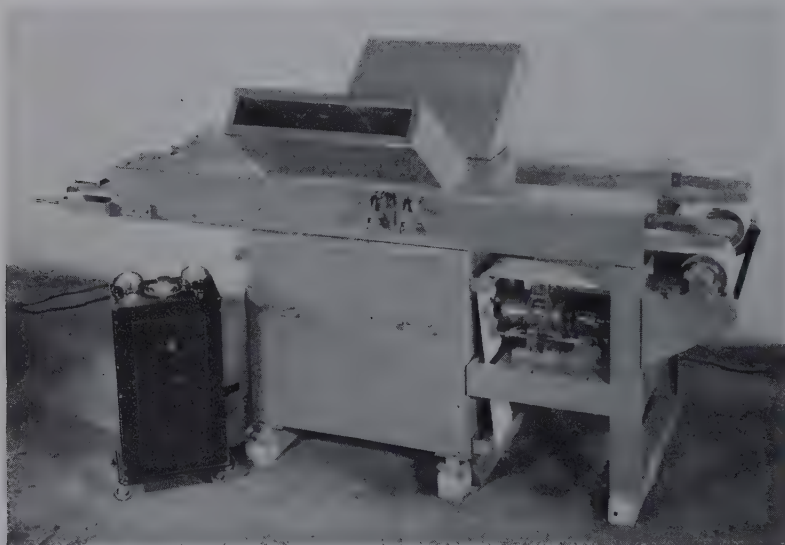


FIG. 94.—Fluoroscopic unit for continuous inspection of fruits. (*General Electric X-Ray Corporation.*)



FIG. 95.—Radiograph of steel casting, showing all types of internal defects.

steel 1 in. thick, and Fig. 97 demonstrates with remarkable clearness the presence of internal cracks entirely unsuspected in

cast steel 1.5 in. thick. These radiographs have been supplied through the generous cooperation of Dr. H. H. Lester of the Watertown Arsenal, a leading authority on metal radiography since the United States Army installed the first radiographic equipment for inspection of castings in 1922. The use of the radiographic technique in discovering defects in an aluminum-alloy sand casting, verified by sectioning the specimen, is illustrated in Fig. 98.

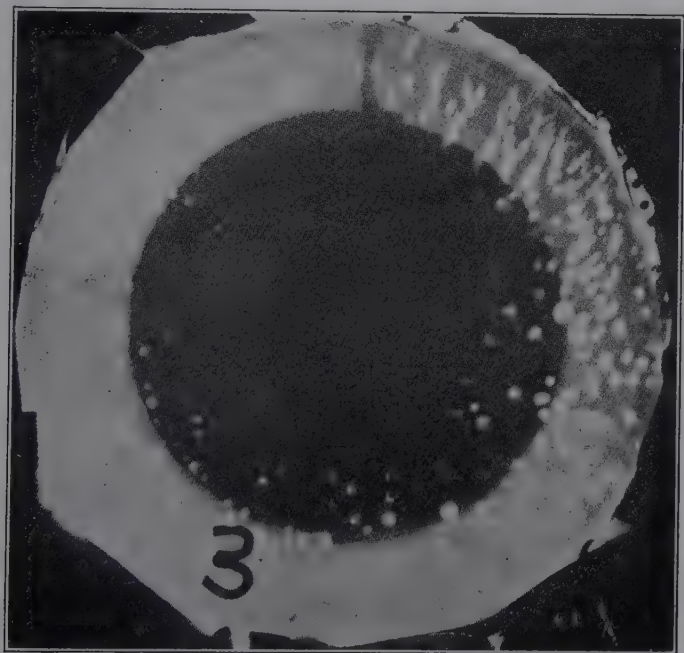


FIG. 96.—Radiograph of steel casting, showing blowholes.

The value of the x-ray method of inspection of castings to ensure soundness and safety in operation is readily apparent. The method may seem too expensive to utilize in the examination of every piece, but it may be employed to tremendous advantage in the derivation of a proper foundry technique and changes in the design of core and mold or in the process of gating. Many progressive foundries have adopted this practice, although the great majority still cling to the old empirical methods with the attendant uncertainty whether a casting will survive or fail. On the other hand, it is the part of wise economy often

to radiograph every unit of cast metal in an installation required to withstand high stresses or every piece that is intended for

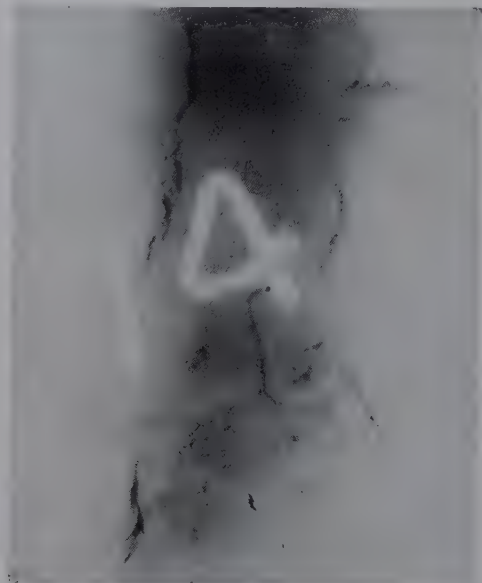


FIG. 97.—Radiograph of steel casting, showing internal cracks.

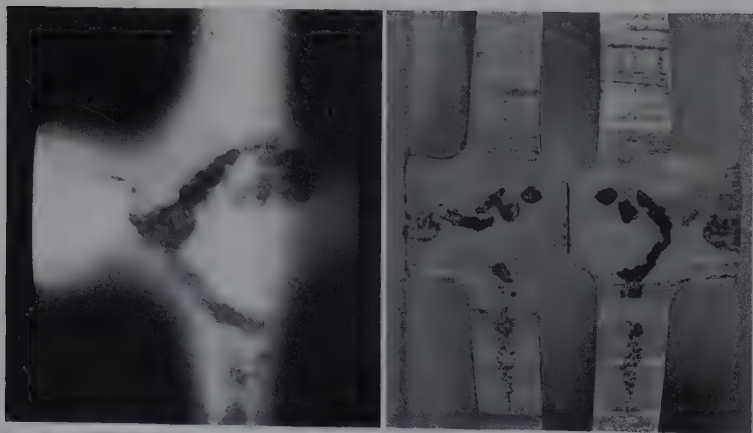


FIG. 98.— Defects in aluminum-alloy sand casting discovered by radiograph and verified in sectioned specimen. (*General Electric X-Ray Corporation.*)

expensive machining operations. An outstanding example in which extensive radiographic tests were used as specification for acceptance of parts is that of the high-pressure steam installation

in the Edgar power plant of the Boston Edison Company at Weymouth, Mass. The pipe and fittings for the 1,200-lb. steam line and the cast shell of a 3,000-kw. steam turbine were all examined, and many rejections were made upon the basis of the radiographs before acceptance. The justification lies in the fact that not a single failure or break of any kind has occurred since installation, even though the conditions represented are extreme. Examples of this type are being multiplied rapidly at the present time, and radiography must be considered an indispensable and thoroughly scientific testing and control method in the foundry industry. The Aluminum Company of America, for example, has considered as a sound and necessary investment the installation in all plants of radiographic equipment for the examination of aluminum and other light-alloy castings.

Similarly, the United States Army and Navy have been foremost in the world in the application of radiography as an indispensable test for soundness of materials.

The American Society for Testing Materials has an active committee continuously at work on radiographic specifications for foundry practice as the most generally practical method of nondestructive testing.¹

2. Welds.—Closely allied to the problem of testing metal castings for soundness is that of welds. Here again there is no positive assurance by the usual methods that a weld has been made perfectly. With the agency of x-rays the smallest defects, such as pipes or gas inclusions, are indicated directly, with the result that a vast improvement in the technique of welding has taken place in the space of a very few years. Welds are now made with certainty of safety where they would never have been attempted previously. In 1930 the United States Navy accepted



FIG. 99.—Radiograph of a defective weld.

¹ LESTER, *Bull. Am. Soc. Testing Materials*, October, 1938, p. 5, January, 1939, p. 13; "Symposium on Radiography and X-ray Diffraction Methods," p. 53, 1936.

welded steam boilers manufactured under radiographic control. In 1931 the American Society of Mechanical Engineers recognized in its boiler code radiographically tested welds for unfired pressure vessels. About 60 installations in this country are now in use for this purpose. Figure 99 shows the actual condition of a typical weld that appeared perfect on the outside. The radiography of welds in locomotive parts subjected to vibrations and stress is widely used, particularly in Germany. The writer recently advised the installation of an x-ray plant by a large manufacturer for the continuous inspection of welded rod to be used in the pumping of oil wells. Here is a case where rods hundreds of feet long depend entirely upon the strength of the weakest welded joint, for with a break the rod falls to the bottom of the well. Consequently, the manufacturer did not dare to market the product without the assurance of sound joints. Since the rodding was only about 1 in. in diameter, it was found possible to use visual inspection with a fluorescent screen as the welded pieces moved along on a belt. The inspector was protected from the radiation by observation of the screen by means of a series of mirrors arranged in baffle fashion through heavy lead glass.

Taxpayers may well be proud that every inch of welds in great public works projects such as Boulder Dam and Norris Dam has been radiographically tested and approved (Fig. 93) in the interest of enduring safety.

3. Automotive and Aircraft Parts.—It may be truthfully stated that the remarkable dependability of automobile and aircraft motors in races and endurance flights may be ascribed primarily to the assurance of soundness promoted by radiographic testing. This is particularly true for propellers, in which soundness is absolutely necessary. Not only internal defects but also *surface* cracks that have escaped attention are immediately detected. Pistons have been surprisingly prone to disclose serious though unsuspected defects. All parts of an airplane may be inspected with x-rays, from the cast cylinders to the spark plugs, the wing covering (Fig. 92), and the framework. And where the safety of life is so utterly dependent upon sound mechanism and faithful performance it would seem little short of criminal not to use this positive method of specification and selection.

4. Rolled and Drawn Metal.—Figure 100 is the radiograph of a rolled sheet of steel containing slag inclusions which have been fibered with the metal in the rolling process. The very poor quality of such a sheet is clearly demonstrated by entire failure in forming operations. Figure 101 shows how an aluminum rod is affected by extreme cold-drawing. The structure is such as to render the specimen worthless.

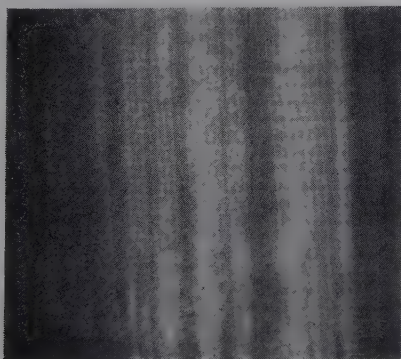


FIG. 100.—Radiograph of rolled sheet steel containing slag inclusions.

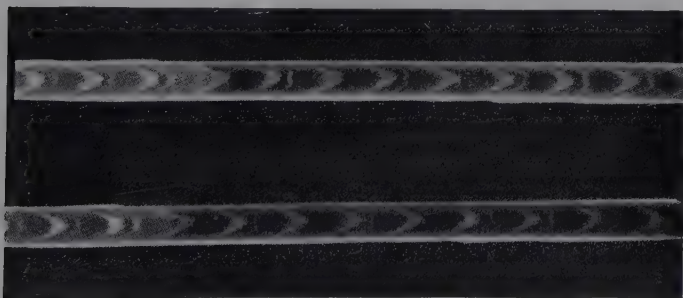


FIG. 101.—Radiograph of overdrawn aluminum rod.

5. Miscellaneous Applications of Metal Radiography.—Among many applications may be mentioned the inspection of insulated wires and cables and coated metals for breaks, of metal tubes and capillaries for clogging, of intricate assembled objects for proper adjustment of parts, of projectiles for proper location of caps and fuses as well as for complete filling by explosive, of gun barrels for rifling and defects, of molten metals inside furnaces for melting point and surface tension (Fig. 102), of ball bearings for soundness, of electric insulators for the presence of metallic

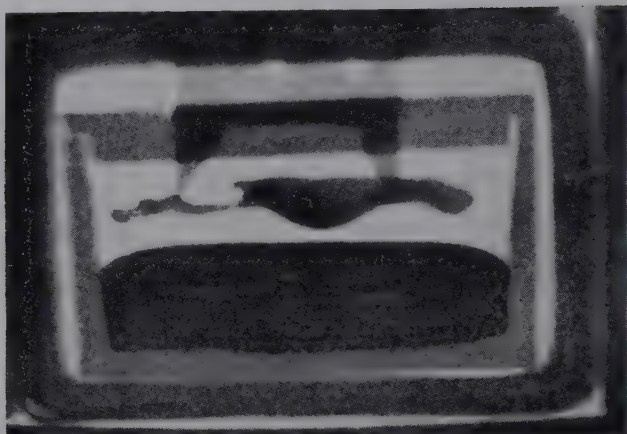


FIG. 102.—Radiograph through furnace, showing solid and liquid copper in equilibrium at the melting point.



FIG. 103.—Radiographs of coal lumps, showing nearly pure coal (lower right) contrasted with lumps containing mineral inclusions.

particles, of metal radio transmission tubes for proper position of grid and filament, of all sorts of sheets suspected of corrosion, and of steel Dewar flasks used for liquid air or oxygen, where corrosion may result in great decrease in wall thickness. This last test, in which microphotometric curves are made, is a standard procedure in the German railway shops.

Miscellaneous Practical Applications.—Besides those for innumerable metal products, numerous other practical applications

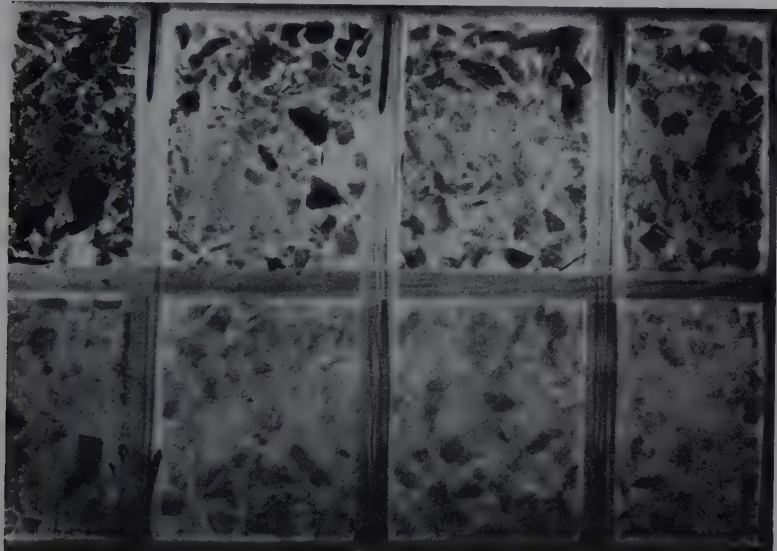


FIG. 104.—Radiograph showing steps in cleaning of coal by flotation. Upper left, maximum content of impurities; lower right, nearly pure coal.

of radiography have been made, and some of these are briefly enumerated:

- Arc electrodes for soundness.

- Coal for classification as to foreign mineral content (Fig. 103) and for control of cleaning by flotation (Fig. 104).

- Rubber tires for imperfect bonding to cords, presence of nails, or internal breaks.

- Reclaimed rubber for nails and other foreign bodies.

- Golf balls for centering of core.

- Complicated glass, hard rubber, and bakelite pieces of various kinds with internal seals, etc., for improper fabrication.

- Wood for cracks, wormholes, rot, knots, embedded nails, etc., as employed in aircraft frames, special lumber, telephone

poles, etc. By this means the aged wooden roof of the great cathedral at York, England, was found to be dangerously weakened by living larvae of the deathwatch beetle in a honeycomb of tunnels.

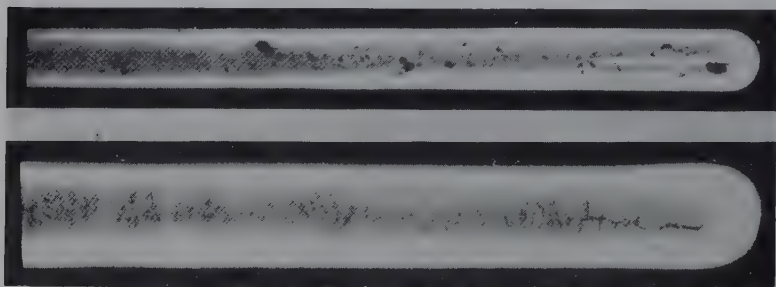


FIG. 105.—Radiographic detection of defects in porcelain tubes. (*Claud S. Gordon Company.*)

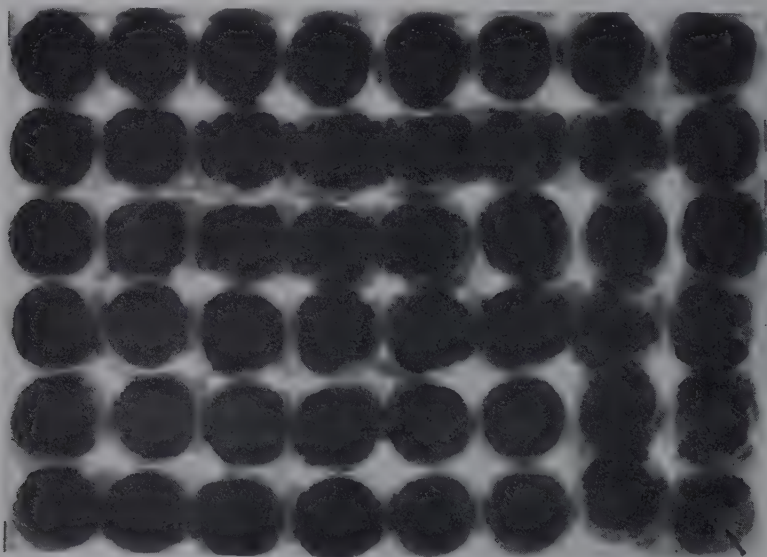


FIG. 106. —Radiographic detection of a tack in boxed candy. (*General Electric X-Ray Corporation.*)

Railway ties for compression or erosion under the plates (after soaking in mercuric chloride solution to increase x-ray absorption).

Shells and cartridges for improper filling.

Porcelain insulators, thermocouple tubes, spark plugs, etc., for internal cracks (Fig. 105), and mica for metal inclusions.

Location of pipes and wires in building walls.

Trunks with false bottoms for contraband goods, and suspicious packages for bombs, etc.

Routine fluoroscopic examination of food products of all kinds, tobacco, etc., in trays, packages, and cans and in bulk for the presence of foreign bodies (utilized especially by large candy manufacturers as an indispensable factor of safety) (Fig. 106).

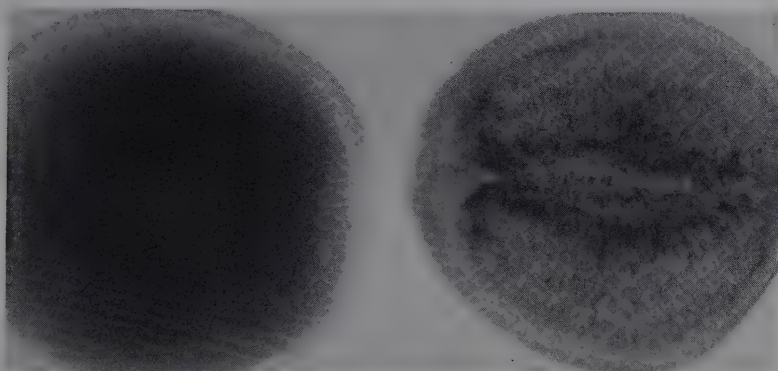


FIG. 107.—Radiographic classification of quality of oranges; left, juicy; right, crystallized or pithy. (*General Electric X-Ray Corporation.*)

Oranges for quality (juicy or pithy), fluoroscopically examined on belt conveyer shown in Fig. 94 and differentiated as shown in Fig. 107.

Counting of packaged materials such as cigarettes.

Identification of glass (used by National Physical Laboratory of England in testing clinical thermometers).

Measurement of plasticity of opaque materials such as tooth paste from the position of a steel ball sinking through the specimen.

Fabrics, cardboard, paper, and leather for texture, identification of fibers, and presence of fillers.

X-rays and Art.—One of the most striking applications of x-rays has been in the field of art. A well-established branch of radiography is now that of the examination of old paintings and art objects for evidences of retouching, work of more than one artist, and original paintings covered over with others, as well as to distinguish true masterpieces from copies. Important

court cases have been decided upon the base of the x-ray evidence. The old paint pigments consisted of inorganic substances which are heavily absorbing to x-rays as compared with modern organic dyes. Excellent x-ray laboratories are now to be found at the Fogg Art Museum of Harvard University, Metropolitan

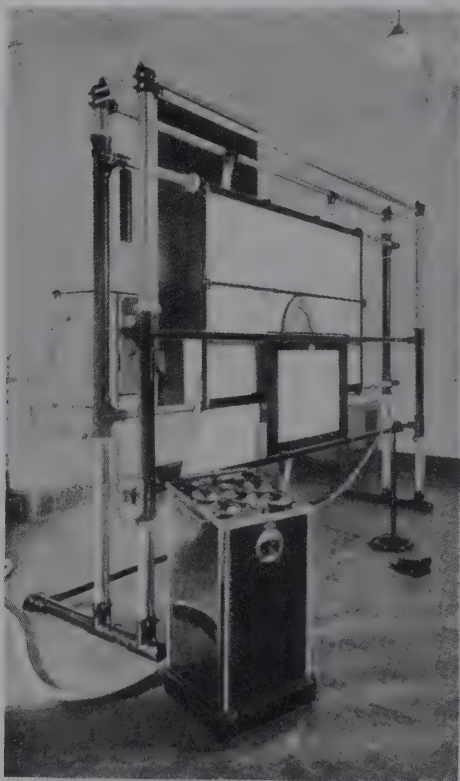


FIG. 108.—X-ray equipment in National Art Gallery, London, for radiographic examination of paintings. (*By permission.*)

Museum of New York, and the museums at Chicago, Philadelphia, Minneapolis, and elsewhere. An especially complete and efficient laboratory is that of the National Art Gallery of the British Museum in London. Figure 108 shows the upright casel for holding the picture both for fluoroscopic and photographic examination.¹ The average technique is 25 kv., 5 ma., for the former and 10 to 15 kv., 15 ma., for the latter. An

¹ RAWLINS, *Brit. J. Radiology*, **12**, 239 (1939).

example is reproduced in Fig. 109 from the paper by Dr. Alan Burroughs,¹ an outstanding authority on this subject. The x-ray photograph represents a portion of the painting "Mars and Venus" by Veronese. The painting shows the head of Venus

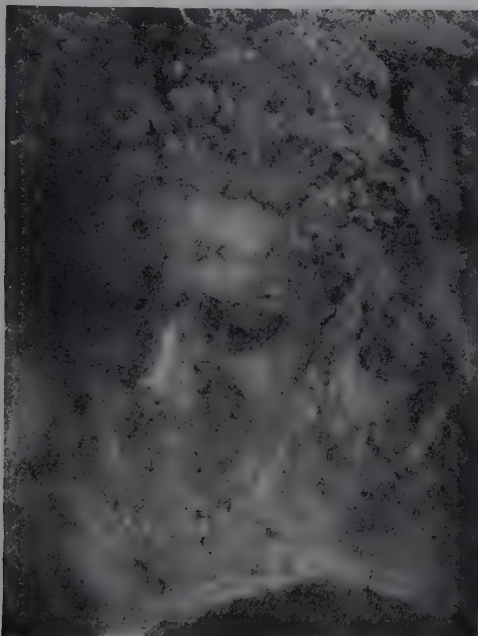


FIG. 109.—Typical result of application of radiography to old paintings. Detail from "Mars and Venus" by Veronese. The head at the right was painted out and disclosed only by x-rays. (Burroughs.)

upright, whereas the x-ray photograph shows two heads, the one more inclined to the right having been painted out, very probably by the master himself. Figure 110 shows a comparison of two Raphael madonnas. Experts at the National Gallery in London suspected that the "Madonna of the Tower," though pleasing and of good composition, did not compare in technique with the "Garvagh Madonna." The x-ray negatives fully confirmed this and led to the conclusion that, although the composition of the "Madonna of the Tower" may have been that of Raphael, the painting was probably done by students. Finally the decision to clean paintings by removal of layers of varnish often depends on details revealed by the radiograph. A good

¹ *Smithsonian Rept.*, 529 (1927).

example from the National Art Gallery in London is illustrated in Fig. 111.

Microradiography.—An entirely new application of radiography achieves great magnification of gross structure when there is available a photographic emulsion so fine that an enlargement of 100 times does not reveal the silver grains. This is the Lippmann emulsion originally available in Gevaert film. The micro-

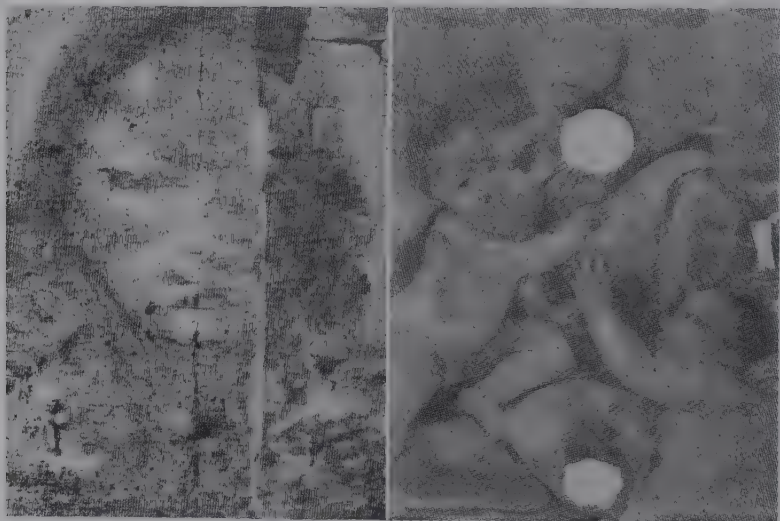


FIG. 110.—Radiographic identification of masterpieces from characteristic techniques of painters. Left, "Madonna of Tower," ascribed to Raphael; right "Garvagh Madonna," known to have been painted by Raphael. (Courtesy, F. I. G. Rawlins, National Art Gallery, London.)

method was first tried in the x-ray laboratory of the French Air Ministry in Paris, and it has been further developed in the writer's laboratory. The results of this method supplement those which may be obtained by microscopic examination of a polished and etched surface, say, of a metal or alloy specimen. A thin slice of metal for examination is placed between and in contact with a photographic film and a lead-foil screen with a hole of about the size of a lead pencil for defining the x-ray beam which passes through the specimen and registers as a small black dot on the film. This dot is then subjected to magnification of 100 to 200 under a microscope or projected on a screen. With the proper adjustment of wave length of the x-ray beam to the kind of

material in the specimen a clear delineation of grain boundaries and every type of inhomogeneity such as the minutest traces of segregation of one metal in another, the actual breakdown of alloy structure, or cracks appear on the photograph.

This microradiograph gives the actual structure through a layer of finite thickness rather than merely a polished surface.



FIG. 111.—Photograph of detail of St. John's arm in "Vision of St. Jerome" by Parmigiano, half cleaned after disclosure of masterly detail in radiograph. (Courtesy, National Art Gallery, London).

Specimens require no special polishing or preparation. Voltage on the x-ray tube is regulated so there will be the greatest possible difference in absorbing power, say, between copper and aluminum in an aluminum alloy. In such a case about 4,000 to 5,000 volts producing a range of soft rays is best. If the x-ray tube is constructed so that a high current up to 50 ma. will pass

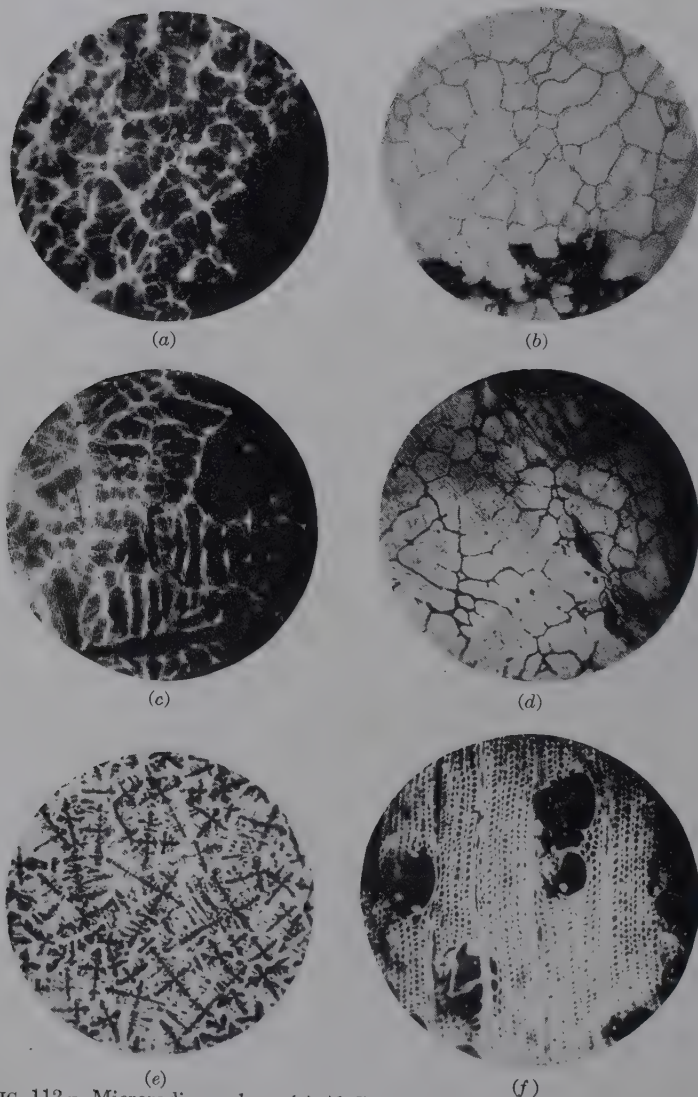


FIG. 112.—Microradiographs. (a) Al-Cu alloy; Cu, light; Al, dark; supposedly a homogeneous solid solution. (b) Corresponding photomicrograph; soda etch; Al, light, Cu, dark. (c) Al-Cu alloy used in airplane parts. (d) Corresponding photomicrograph. (e) Lead bronze. (f) Wood.

through it, the beam can still be made sufficiently intense so that the exposure is only a matter of 1 to 5 min. Another possibility is to filter an x-ray beam generated at higher voltages or reflect from a crystal to obtain a monochromatic ray of proper wave length. To illustrate the power of the method, examples are here given (Fig. 112 *a* to *d*) for copper-aluminum alloy of the small black dot as it is enlarged 100 times. This alloy was supposed to be a homogeneous solid solution of copper in aluminum. The



FIG. 113.—Radiograph with very soft x-rays of insect. (Sherwood.)

copper appears as the light areas corresponding to greater absorbing power, and the aluminum appears as the dark areas. In comparison the ordinary photomicrograph makes no such disclosure. The extension of this method to all sorts of alloys (lead bronze in Fig. 112*e*), to the determination of proper heat-treatment for ensuring homogeneity, and to all kinds of biological materials using very easily absorbed rays is obvious. The microradiograph of a slice of wood is shown in Fig. 112*f*.

Ordinary film may often be used with small biological specimens when an enlargement of 5 or 10 is sufficient. Figure 113 shows such a radiograph of an insect, made with grenz rays (x-rays generated at 4,000 volts with long wave lengths). A

logical extension, of course, is to motion pictures to show, for example, peristaltic wave in the intestines of insects.¹

Radiography by the Use of Gamma Rays.—The presentation of this subject would be incomplete without mention of the remarkable radiographic results obtained by Mehl and his associates with the γ -rays from radium emanation. Since the wave lengths of γ -rays are shorter than x-rays as generated under

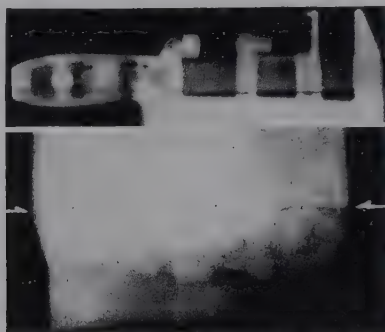


FIG. 114.—Radiographs of wrench and defective weld, with γ -rays.

practical conditions, it follows that they should penetrate thicker sections. Successful photographs were made through 10 in. or more of steel; only a small bulb of radium emanation at a certain distance from the specimen and a photographic film were utilized. Exposures of 10 or 12 hr. were necessary, but, of course, this is not a serious handicap, since no attention is required. The method is very promising for the examination of structures in position and because of the extreme simplicity and absence of all machinery. The γ -radiographs of a wrench and a weld are shown in Fig. 114. The United States Navy now uses 2.813 grams of radium in 11 units for the inspection of ship parts.²

¹ SHERWOOD, *J. Biol. Photographic Assoc.*, **5**, 138 (1937); *J. Soc. Motion Picture Eng.*, **28**, 614 (1937).

² For a full account of γ -ray radiography, cf. N. L. Mochel, "A.S.T.M. Symposium on Radiography and X-ray Diffraction Methods," p. 116, 1936.

CHAPTER X

X-RAY PHOTOCHEMISTRY

Threefold interest is attached to the subject of the chemical effects of x-rays:

1. Pure photochemistry, the mechanism and rate of reactions, the stability of chemical bonds, etc.

2. Light thrown on therapeutic effects by study of chemical changes.

3. Discovery of reactions that could be used as suitable dosimeters for quantity or intensity of radiation.

The casual observer could well believe that x-rays by virtue of their penetration and energy should have innumerable profound chemical effects, but as a matter of fact the examples of considerable chemical change are extraordinarily few in number. Systems that undergo change in ultraviolet light are apparently unaffected. The photographic effect, a few oxidation-reduction reactions, and some condensations and decompositions of organic compounds are almost unique among the large number of experiments already empirically tried. However, the hope remains that other chemical effects may be discovered which might serve the purpose even of a convenient dosimeter.

The Mechanism of Chemical Action.—It has already been indicated that absorption of radiation energy must precede any physical, chemical, or biological effects which may be observed. In pure absorption the energy of an x-ray quantum is transformed to that of electrons (photoelectrons) liberated from atoms, together with the net potential energy of the irradiated atom (ionization). In the latter case the atom remains in the ionized condition only a very short time (10^{-9} sec.); one of the electrons in the outer orbits falls into the vacancy created by the photoelectron. In so doing, the potential energy of the ionized atoms becomes the energy of secondary characteristic rays. The ionized atom by virtue of its changed condition can also enter into chemical reactions. Since secondary characteristic rays produced by return of the ionized atom to the normal state are softer than the primary rays, especially so in the human body on account of the light elements, they will be easily absorbed by one of two processes: The quantum of radiation may leave the mother atom and be absorbed by a neighboring atom, or it

may actually remain in the mother atom so that its energy is used for the liberation of a second electron (photoelectron of the second kind). This Auger effect or process of inner absorption can also be considered as a radiationless transition of an electron to a deeper orbit, in which the energy difference is imparted as kinetic energy to another electron.

The photoelectrons account for the second portion of the energy following absorption of a primary quantum (or x-ray photon). The variations in velocities as determined in β -ray spectra have already been considered, and it follows that the kinetic energy will have nearly the same value of the primary x-ray quantum for light elements or for outer electrons of heavier atoms, in which the work required to free the electron is small. The photoelectron is now free to liberate secondary electrons by impact with atoms, which, of course, have lower velocities, thus ionizing the atoms, or the impact may serve only to lift the electron to a higher energy level in the atom which becomes therefore excited, or activated.

Still another mechanism in the absorption of x-rays by atoms in molecules is the transformation into heat. An increase in energy of motion of atoms in molecules in position results in nothing more than local elevation in temperature. Of course, in an irradiated body the transformed x-ray energy is so small that a measurable increase in temperature is almost impossible to observe.

It is certain that in a biological or chemical medium the photoelectrons possess large initial velocity with a velocity distribution corresponding to the x-ray spectrum. The fate of the photoelectrons is widely varied, but in general it is the same as that observed for the impact of cathode rays on the anticathode of the x-ray tube. Between the first and last (heat) steps in the chain of transformations the widest variety of effects must be possible.

These high-speed electrons can bring into reactive form by impact other atoms and molecules that have been absolutely unaffected by the primary radiation quanta; in fact, the proportion of atoms and molecules activated by the photoelectrons may be very much larger. This mechanism differs from the chemical effects of ordinary light in which energy suffices only to excite atoms by lifting electrons to higher energy levels. X-rays also differ from ordinary light in that they may *have chemical action* because of scattering and recoil electrons and yet undergo no fluorescent absorption, a process unknown for light.

Besides the process of true absorption, the energy of a quantum of x-radiation can also be transformed into electron kinetic energy—that of the recoil electrons in the Compton effect. The velocity of these is considerably smaller than that of the photoelectrons and, of course, depends on the scattering angle. Their chemical and biological effects might be considered to be smaller than those incited by the photoelectrons at low and moderate voltages. However, at 200 kv. 2.5 per cent of the x-ray energy goes into photoelectrons and 3 per cent into recoil electrons. At higher voltages the latter figure becomes even more significant.

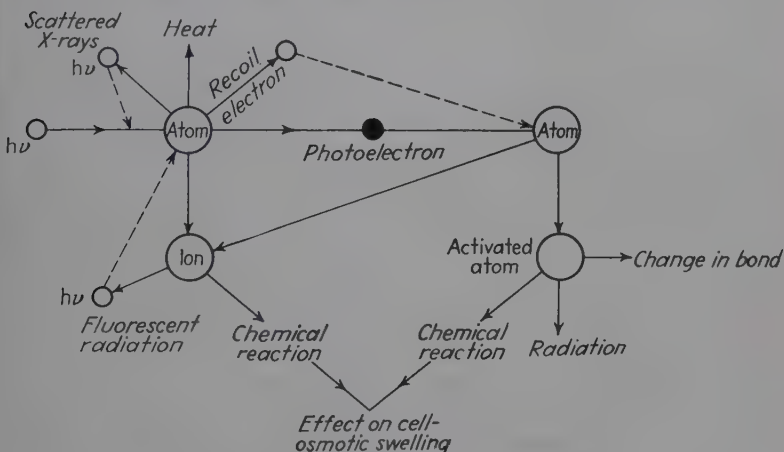


Fig. 115.—Mechanisms of chemical and biological effects of x-rays.

The above complex theory of chemical action, illustrated in Fig. 115, has been subjected by many workers to experimental test. Glocker and Risse¹ studied the decomposition of hydrogen peroxide and potassium persulfate in very dilute solutions. The amounts decomposed corresponded to the energy of the secondary electrons liberated in the system during passage of x-rays; 70,000 cal. (electrons in motion) are required to decompose 1 mole of H_2O_2 in $\frac{1}{600}$ normal solution, and 2.45 times as much for potassium persulfate. The dependence of chemical effect upon x-ray wave length is a question entirely of how much energy during passage of an x-ray beam of certain wave length through matter of certain composition is transformed into the energy of secondary electrons. Taking into account the complications of scattered and fluorescent rays that may form

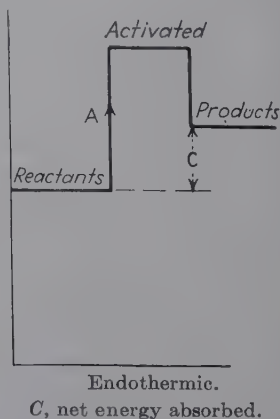
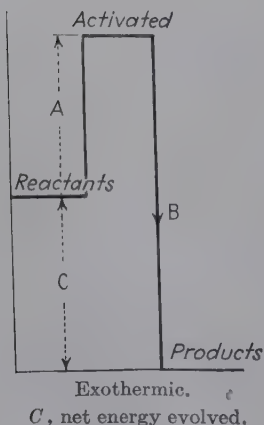
¹ *Z. Physik*, **48**, 845 (1928); *Z. physik. Chem. (A)*, **140**, 133 (1929).

secondary electrons, Glocker and Risse obtained verification of the theory a decade ago, and further substantiation has been obtained by other workers for other systems.

In general, the exact mechanism and kinetics of chemical reactions, though due to activation by electron impact, have been explained in only a very few instances. The photographic action is unusually simple, in that the silver and bromine ions are converted endothermically into neutral atoms through the energy of the secondary electrons. The evolution of hydrogen chloride from chloroform is an example of a reaction where far greater change is observed than can be accounted for by electron impact. It is, therefore, a chain reaction: a residual chloroform molecule disturbed by electron impact can react with an unchanged chloroform molecule, the product of this reaction with another unchanged chloroform molecule, and so on.

The principle of activation is the most important recent discovery in the elucidation of the photochemical results, especially in water solutions. In passing through water the photoelectron may come so close to an electron in a molecule that the repulsive force becomes sufficiently large to cause the orbit of this electron to become unstable. As a result the electron moves into an orbit, or energy level, different from that in the normal molecule. The characteristics of an activated molecule are instability and a high degree of chemical reactivity. It is generally accepted that a molecule, in order to pass from one state to another, must pass through an intermediate activated state for two cases:

TABLE XXVI



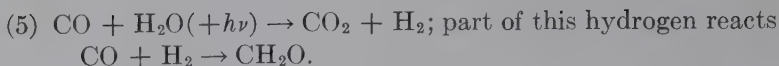
The energy of activation may involve (1) chemical change of the molecule involving initial activated bond; (2) emission as a quantum of light; (3) transmission of energy to another part of the molecule, activating another bond; (4) collision of the activated molecule with another molecule to which energy is transmitted.

Reactions of Water.—The great work of Fricke and associates has clarified the reactions of water and of very dilute aqueous solutions. A dosage of 1,000 *r* produces 2.8×10^{-6} gram-ion pair in 1,000 grams of water. With this are to be compared the numbers of activated water molecules.

- (1) $\text{H}_2\text{O} \rightarrow (\text{H}_2\text{O})'_{\text{act.}}$; 0.55 micromole per 1,000 cc. per 1,000 *r*.
- (2) $\text{H}_2\text{O} \rightarrow (\text{H}_2\text{O})''_{\text{act.}}$; 2.2 micromoles per 1,000 cc. per 1,000 *r*.
- (3) H_2O , pure, gas-free—unchanged.
- (4) For water with dissolved oxygen: $(\text{H}_2\text{O})'_{\text{act.}} + \frac{1}{2}\text{O}_2 = \text{H}_2\text{O}_2$; 1.1 micromoles per 1,000 cc. per 1,000 *r* or 0.55 micromole of oxygen molecules activated, independent of oxygen pressure but dependent on hydrogen-ion concentration.
- (5) $(\text{H}_2\text{O})'_{\text{act.}} + \text{H}_2\text{O}$ (presence of iodide ion, acid pH) = $\text{H}_2 + \text{H}_2\text{O}_2$; 0.55 micromole H_2 per 1,000 cc. per 1,000 *r*.
- (6) $(\text{H}_2\text{O})'_{\text{act.}} + \text{H}_2\text{O}$ (I^- , alkaline pH) = $\text{H}_2 + \frac{1}{2}\text{O}_2 + \text{H}_2\text{O}$.

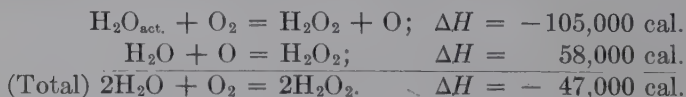
Examples of chemical transformation by irradiation of substances present in the water in such high dilution that their direct activation by the rays is negligible are as follows:

- (1) $\text{NO}_2^- + (\text{H}_2\text{O})'_{\text{act.}} \rightarrow \text{NO}_3^- + \text{H}_2$; 0.55 micromole per 1,000 cc. per 1,000 *r*.
- (2) $\text{AsO}_3^{3-} + (\text{H}_2\text{O})'_{\text{act.}} \rightarrow \text{AsO}_4^{3-} + \text{H}_2$; 0.55 micromole per 1,000 cc. per 1,000 *r*.
- (3) $\text{SeO}_3^{3-} + (\text{H}_2\text{O})'_{\text{act.}} \rightarrow \text{SeO}_4^{3-} + \text{H}_2$; 0.55 micromole per 1,000 cc. per 1,000 *r*.
- (4a) $2\text{FeSO}_4 + \text{H}_2\text{SO}_4 + (\text{H}_2\text{O})'_{\text{act.}} = \text{Fe}_2(\text{SO}_4)_3 + \text{H}_2 + \text{H}_2\text{O}$ (gas-free) depends on H^+ concentration. In the presence of oxygen, the same reaction occurs, except that hydrogen is oxidized to water in a secondary reaction, and in addition a reaction independent of pH is observed:
- (4b)
$$\left\{ \begin{array}{l} (\text{H}_2\text{O})''_{\text{act.}} + \text{O}_2 \rightarrow \text{H}_2\text{O} + \text{O}_{2\text{act.}} \\ 4\text{FeSO}_4 + 2\text{H}_2\text{SO}_4 + \text{O}_{2\text{act.}} \rightarrow 2\text{Fe}_2(\text{SO}_4)_3 + 2\text{H}_2\text{O}; 8.8 \end{array} \right.$$
 microequivalents per 1,000 cc. per 1,000 *r*.



Reactions Involving Hydrogen Peroxide.—It has been shown that hydrogen peroxide is formed when water containing dissolved oxygen is irradiated or by decomposition of water in the presence of iodide ion as catalyst at an acid pH. It is very important to determine whether or not reactions and radiation effects on living cells may be explained by the primary formation of hydrogen peroxide in solution, so that the net result is the same as though reagent H_2O_2 were added. X-rays not only cause its formation but also its decomposition: $\text{H}_2\text{O}_2 \rightleftharpoons \text{H}_2\text{O} + \frac{1}{2}\text{O}_2$. In contrast with most other reactions the amount decomposed per unit of dosage varies inversely as the square root of the x-ray intensity and increases with the square root of the H_2O_2 concentration. Only in some cases is it found that irradiation induces reactions that can be obtained also with H_2O_2 , if sufficient time is allowed for it to react. Thus solutions of $\text{K}_2\text{Cr}_2\text{O}_7$ at $\text{pH} < 1$ are reduced exactly the same as if the acid solution is irradiated and added to the dichromate. Solutions at pH 3 to 4 are unchanged; also, H_2O_2 added to a solution in this pH range has no effect, since H_2O_2 is decomposed by the dichromate whether formed by irradiation or added.

Table XXVII shows a comparison of energy relations of the reduction of ceric sulfate, potassium permanganate, and iodate, and the formation of H_2O_2 , as found by Clark and Coe.¹ Hydrogen peroxide is formed by the following mechanism:



Though H_2O_2 reduces ceric sulfate according to $2\text{Ce}^{4+} + \text{H}_2\text{O}_2 = 2\text{Ce}^{3+} + 2\text{H}^+ + \text{O}_2$, the actual reduction can be accounted for only in part by this mechanism and the remainder by the reaction $2\text{Ce}^{4+} + \text{H}_2\text{O}''_{\text{act.}} = 2\text{Ce}^{3+} + 2\text{H}^+ + \frac{1}{2}\text{O}_2$. Potassium iodate, reduced by x-rays, is completely unaffected by H_2O_2 , either added or formed by irradiation.

An important additional phenomenon is observed in these reductions, namely, the effects of addition agents. For example,

¹ *J. Chem. Phys.*, **5**, 97 (1937).

silver ion has a marked inhibitory and mercuric ion a positive catalytic effect upon ceric salt reductions. The former absorbs the activation energy from water before it is effective in producing a reaction, and the latter acts as an acceptor by intermediate reduction to mercurous ion and reoxidation by ceric ion.

TABLE XXVII

| Experimental and calculated quantities | Ce(SO ₄) ₂ reduced (0.1 <i>N</i> H ₂ SO ₄) | KMnO ₄ reduced (1.0 <i>N</i> H ₂ SO ₄) | KIO ₃ reduced (0.1 <i>N</i> H ₂ SO ₄) | H ₂ O ₂ formed (0.1 <i>N</i> H ₂ SO ₄) |
|--|---|---|--|--|
| "Equivalents" converted per <i>r</i> unit absorbed..... | 4.42×10^{12} | 7.45×10^{12} | 1.27×10^{12} | 2.30×10^{12} |
| <i>r</i> units absorbed per equivalent converted..... | 1.37×10^{11} | 0.81×10^{11} | 4.78×10^{11} | 2.63×10^{11} |
| Ions converted per ion pair..... | 2.0 | 3.7 | 0.62 | 1.1 |
| Calories of absorbed energy per equivalent reduced ¹ | 379,500 | 205,135 | 1,224,193 | 690,000 |
| Calories electronic energy for con- version of one equivalent ² | 344,000 | 204,000 | 1,095,000 | 602,000 |

NOTE.—"Equivalents" equal gram equivalents times 6.06×10^{23} .

¹ Calculated from ions per ion pair, electron volts per ion pair, and heat equivalence of electron volts.

² Calculated from total heat equivalence of *r* unit and total heat dissipated as electronic energy.

Energy Relationships. *Ceric Ions Reduced per *r* Unit.*—Values are obtained for amount of reduction of 0.0002*M* and 0.0004*M* ceric sulfate in 0.1 *N* H₂SO₄ by tungsten radiation (effective $\lambda = 0.60$) for varying periods of exposure. From the straight portion of the curve it can be seen that 41 min. were necessary for the reduction of 1.0 microequivalent weight or 6.06×10^{17} ceric ions. Since the incident intensity was 590 *r* per minute per square centimeter, $590 \cdot 11.94 = 7,050$ *r* per minute incident radiation on the total surface. Of this amount 47.5 per cent was absorbed by 0.1 *N* H₂SO₄; the absorption due to the small amount of Ce(SO₄)₂ present is negligible. From this it is calculated that 137,000 *r* units were absorbed in 41 min. Therefore, 6.06×10^{17} ions per 137,000 *r* units or 4.42×10^{12} ions per *r* unit absorbed were reduced; 1.37×10^{11} *r* units were necessary for complete reduction of 1 mole of ceric ions.

By definition 1 *r* unit corresponds to an ionization such that a current of 1 electrostatic unit flows in 1.0 cc. of air under saturation potential. The number of ion pairs in air is therefore

$$\frac{\text{Total energy}}{\text{Charge on electron}} = \frac{1}{4.770 \times 10^{-10}} = 2.1 \times 10^9 \text{ ion pairs per cubic centimeter in air and } 2.1 \times 10^9 \cdot 795^* = 1.7 \times 10^{12} \text{ ion pairs per cubic centimeters per } r \text{ unit incident radiation on the water surface.}$$
 These calculations are based on the assumption of a very thin layer of fluid so that the incident intensity is the same on all portions. Since this was not the case for the experimental conditions used, it is necessary to calculate the average incident intensity compared to that at the surface. Using the absorption equation $I = I_0 e^{-\mu x}$ and allowing I_0 to be 100 per cent, the area under the curve of intensity against depth of solution can be found as $\int_{0.84}^0 100 e^{-\mu x} dx$. Dividing this value by 0.84 gives an average for all portions of the solution of 73.3 per cent of the intensity incident upon the surface. There were, then, $590 r$ per minute $\cdot 0.733 \cdot 1.7 \times 10^{12} = 7.35 \times 10^{14}$ ion pairs per cubic centimeters per minute in the solution under the conditions used. But 1 microequivalent (6.06×10^{17} ions) of ceric ions was reduced for a 41 min. exposure in 10 cc.; this gives

$$\frac{6.06 \times 10^{17}}{7.35 \times 10^{14} \cdot 10 \cdot 41} = 2.01 \text{ ions reduced per ion pair.}$$

Energy of Reduction in Calories per Equivalent of Ceric Ions.—This calculation comes out directly from the ions reduced per ion pair (2.01), the energy in electron volts to produce an ion pair (33 volts), and the heat equivalence per mole of the electron volt (23,000). The result is 379,000 cal. per mole of ceric sulfate. By an entirely independent method based on the best data available on total heat equivalence of the r unit (148 ergs per r unit at the given wave length) and the proportion of total heat dissipated as electronic energy (0.71), the value 344,000 cal. is obtained as a very satisfactory check.

Decomposition of Organic Compounds.—The results of irradiating solutions of organic materials is of greatest significance. In all cases, hydrogen is produced and, for certain highly oxidized molecules, CO_2 .† The amounts decomposed increase with concentration, a fact indicating secondary reactions, but the

* The best value correlating the number of ion pairs in water and in air in terms of density difference.

† FRICKE, HART, and SMITH, *J. Chem. Phys.*, **6**, 229 (1938).

attachment of the oxygen molecule of the activated water molecule to the organic molecule is the primary reaction. Particularly interesting is formic acid:

- (1) $\text{HCOOH} = \text{H}_2 + \text{CO}_2$ (pH2-3) or $(\text{HCOOH})_{\text{act.}} + (\text{HCOOH}) = 2\text{H}_2 + 2\text{CO}_2$ ($3.2 \times 10^{-6}M$ per 1,000 cc. \times per 1,000 r of each).
- (2) $\text{HCOOH} = \frac{1}{2}(\text{COOH})_2 + \frac{1}{2}\text{H}_2$ (pH6).
- (3) $2\text{HCOOH} = \text{HCHO} + \text{CO}_2 + \text{H}_2\text{O}$ at high concentrations.
- (4) $(\text{COOH})_2$ (oxalic acid) $= 2\text{CO}_2 + \text{H}_2$.
- (5) $2\text{CH}_3\text{COOH}$ (acetic acid) $= (\text{CH}_2\text{COOH})_2$ (succinic acid) $+ \text{H}_2$.
- (6) Higher acids, no CO_2 , two-thirds as much H_2 .

In the presence of oxygen, no hydrogen is liberated, but there is an increase in hydrogen peroxide produced, as tested by reduction of dichromate.

- (7) Alcohols, aldehydes, urea, glycine, dextrose, and creatine give hydrogen.

The Preparation of Very Pure Water.—The decomposition with evolution of gases of organic compounds when present in the minutest traces suggests a method of testing and preparing the purest water. Fricke has found that when gas-free water from an ordinary tin still is irradiated there is generated as much as 10 or 20 micromoles of hydrogen and carbon dioxide per 1,000 cc., from organic impurities. After further purification by prolonged heating with acid dichromate, then basic permanganate, followed by distillation through a quartz tube at 900°C ., the water still yields 2 micromoles of H_2 and CO_2 . It is only by *prolonged irradiation with x-rays* that finally a product essentially free from organic impurities is obtained. The measurement of properties such as conductivity, of water of this highest degree of purity should yield interesting data.

Additional Important Reactions.—Besides the reactions of water, oxidation reductions, and decompositions of organic molecules already mentioned, some of the more important further reactions, some of which have possibilities as chemical dosimeters, are summarized in Table XXVIII.

X-rays and radium produce aggregation in positively charged suspensoids (precipitation of lyophobic and gelation of lyophilic),

TABLE XXVIII.—PARTIAL LIST OF THE CHEMICAL EFFECTS OF X-RAYS

| System | Reaction | Energy relations | Reference |
|---|---|--|--|
| Ferrous sulfate..... | Oxidized to ferric sulfate | 0.0027 mg. FeSO ₄ per cubic centimeter per 1,000 r. Independent of wave length between 0.204 and 0.765 A. U. | FRICKE and MORSE, <i>Phil. Mag.</i> , 7 , 129 (1929) |
| Oxyhemoglobin..... | Methemoglobin | Independent of wave length 50 per cent transformed by 56,000 r | FRICKE and PETERSON, <i>Am. J. Roentgenology and Radium Therapy</i> , 17 , 611 (1927) |
| Potassium dichromate..... | Reduced in 0.8 N H ₂ SO ₄ | 3.31×10^{-6} equivalent per 1,000 c.c. per 1,000 r independent of concentration and temperature; due to formation of activated H ₂ O ₂ ; very sensitive to organic impurities | FRICKE and BROWNSCOMBE, <i>J. Am. Chem. Soc.</i> , 55 , 2358 (1933) |
| Mercuric chloride and potassium oxalate | $2\text{HgCl}_2 + \text{C}_2\text{O}_4^{--} \rightarrow \text{Hg}_2\text{Cl}_2 + 2\text{Cl}^- + 2\text{CO}_2$ | 6×10^5 mole per ion pair | ROSEVEARE, <i>J. Am. Chem. Soc.</i> , 52 , 2612 (1930) |
| Mercuric chloride + ammonium oxalate (Eder's solution) | Hg ₂ Cl ₂ precipitated evolved | 0.58 mg. mercury per 840 r | WYCKOFF and BAKER, <i>Am. J. Roentgenology and Radium Therapy</i> , 22 , 551 (1929) |
| Sucrose..... | Solution inverted, crystals turned reddish brown | 6.5 per cent change in 2 per cent solution in 40 hr. | QUIMBY and DOWNES, <i>Radiology</i> , 14 , 468 (1930) |
| Amino acids..... | Cystine unchanged, tyrosine changed in phenol group | Proportional to dosage | REINHART and TUCKER, <i>Radiology</i> , 12 , 151 (1929) |
| α -Acetoxy mercuri- β -methoxy hydrocinnamic ethyl ester | Mercury liberated | 0.293 mg. mercury precipitated by 28,500 r | STENSTROM and LOHMANN, <i>J. Biol. Chem.</i> , 79 , 673 (1928) |
| | | | CLARK, PICKETT, and JOHNSON, <i>Radiology</i> , 15 , 245 (1930) |

| | | | |
|-------------------------|--|---|---|
| Aldehydes..... | Condense with ketones | Markedly catalyzed by x-rays | CLARK, PICKETT, and JOHN- SON, <i>loc. cit.</i> |
| Potassium iodide..... | Iodine liberated | Amount decomposed linear with dosage in absence of oxygen; larger unit in pres- ence of oxygen | CLARK, PICKETT, and JOHN- SON, <i>loc. cit.</i> |
| Potassium nitrate..... | Reduced to KNO_2 | Proportional to dosage 5.58×10^{11} molecules per r , 0.2 molecule per ion pair | CLARK, PICKETT, and JOHN- SON, <i>loc. cit.</i> |
| Methylene blue..... | Decolorized; change measured spectrophotometrically; best concentration 0.0016 mg. per cubic centimeter; acetone, etc., inhibit change | Change not proportional to dosage | STENSTROM and LOHMANN, <i>Radiology</i> , 16 , 332 (1931) |
| Aromatic colors..... | 127 examples studies; tetra- phenyl methane, alazarine, anthracine, indigo types promising | | CLARK, PICKETT, and JOHN- SON, <i>loc. cit.</i> |
| Thioglucose, etc..... | In presence of acceptor such as silver on a developed pho- tographic paper easily re- duced forming Ag_2S ; no reaction without x-rays | Very efficient; new light on biological effects | CLARK and FITCH, <i>Radiology</i> , 17 , 285 (1931) |
| Oil drops on water..... | Greatly increase diameter and spreading; oxidation and un- saturation | Increase with dosage, inde- pendent of wave length; greatest effect from oil first irradiated in test tube | CLARK and FITCH, <i>loc. cit.</i> |
| | | | Unpublished |
| | | | STENSTROM and VIGNERS, <i>J.</i> <i>Chem. Phys.</i> , 5 , 298 (1937); <i>Am. J. Roentgenology and</i> <i>Radium Therapy</i> , 40 , 427 (1938) |

TABLE XXVIII.—PARTIAL LIST OF THE CHEMICAL EFFECTS OF X-RAYS.—(Continued)

| System | Reaction | Energy relations | Reference |
|------------------------------|--|--|---|
| Catalysts..... | Activated in the presence of moisture (contact Pt for SO ₂ oxidation) | Activity decays with time, H ₂ O ₂ formation | CLARK, McGRATH, and JOHNSON, <i>Proc. Nat. Acad. Sci.</i> , 11 , 646 (1925) |
| Minerals, glass, etc..... | Colored by formation of colloidal aggregates | Positive ions neutralized by photoelectrons | BAYLEY, <i>Phys. Rev.</i> , 24 , 495 (1924) DAUVILLIER, <i>Compt. rend.</i> , 171 , 627 (1922) |
| Metastable solid states..... | Converted to stable forms (SO ₃ crystals) | Measured by x-ray patterns, vapor pressures, and melting points | SMITS and SCHOENMAKER, <i>J. Chem. Soc.</i> , 1926, pp. 1120, 1603. |

probably as the result of the discharge of charged particles by electrons freed in the ionization of the solvent; they disperse negatively charged suspensoids, making them more stable. Emulsoid colloids such as proteins are denatured whether they are positively or negatively charged, but only after prolonged irradiation. After denaturation, proteins flocculate if brought to the isoelectric point and are more easily precipitated by salts, alcohol, or heat. The decrease in solubility is most marked in albumins. Denaturation is accompanied or followed by an increase in viscosity and decrease in surface tension, most marked in globulins. The first step seems to be due to the ionization of water, followed possibly by formation of hydrogen peroxide which sometimes has similar effects on colloids. Crowther with his coworkers has been an outstanding leader in this field of investigation, which is fraught with great difficulty on account of extreme sensitiveness to impurities and other eccentricities of these colloids. Lately it has been demonstrated that a steadily increasing exposure to x-radiation produces alternate increases and decreases in the electrokinetic potential of certain colloid particles. The decrease in potential at the minima of the curve is sufficient to bring the colloid to its flocculation point. Gold sols were completely coagulated when exposed to doses of 4.9 to 5.5 *r*, partially at 5.8, and not at all from 6 up to about 13 *r*, when a new period of coagulation began. Similar observations on proteins have been made in the author's laboratory. Clark and Pickett found that the flocculation of clay slips as measured by viscosity changes is a direct function of the amount of organic protein matter present.

The irreversible denaturation and coagulation of cell proteins are obviously two of the most important factors in the lethal and other biological effects of radiation, with which the following chapter is concerned.

CHAPTER XI

THE BIOLOGICAL EFFECTS OF X-RADIATION

The value of x-rays as a research tool to the biologist in the field of genetics has been convincingly demonstrated in the past few years by the work of a very considerable number of investigators. Much less well known are the great possibilities of cell studies depending upon an increasingly quantitative evaluation of characteristic radiosensitiveness, which may well become the most powerful method of pathologic diagnosis. Uncertainty remains as to fundamental differences between normal and pathological tissues, and the mechanism involved in radiobiology and therapy of cancer cells. It has seemed desirable, therefore, to summarize briefly our present knowledge of the biological effects of x-radiation, under the following heads:

1. Bactericidal and general lethal effects.
2. Biological dosimeters.
3. Effects on the hereditary material.
4. Effects on embryos.
5. Effects on normal cells.
6. The radiosensitiveness of cells.
7. Recovery and the time factor.
8. X-ray effects on human tissues.
9. The stimulating effect of x-rays.
10. Photochemical experiments with a possible bearing on biological effects.
11. Mechanism of biological action.
12. Radiopathology.
13. Cancer.
14. A third x-ray application in medicine.

1. Bactericidal and General Lethal Effects of X-rays.—This is considered first since the first suggested possible biological application of the new rays, following announcement of their discovery by Roentgen in November, 1895, was directed to bactericidal properties. The rays were considered to be present in sunlight. Since the sun's rays were known to have bacteri-

cidal properties and were beneficial in treatment of diseases, especially tuberculosis, it was natural to turn to these rays as possibly possessing even more powerful physiological effects. On Jan. 29, 1896, T. Glover Lyon made definite suggestions in a letter to the London *Lancet*. But on Feb. 17, 1896, in another letter, he announced negative results on tuberculosis and diphtheria bacteria. This was the beginning of experiments on every type of organism in laboratories throughout the world, an account of which would occupy an entire volume. Some of the experiments were highly favorable, but the great majority were negative; positive bactericidal effects in one laboratory were entirely disproved in another. Thus began the great science of x-ray therapy under these highly unfavorable conditions. Though it became nearly universally agreed that bacterial cultures were nearly inert except to relatively enormous doses of radiation, the tremendous effect of rays on living tissue also became apparent. In 1902, Pusey and Caldwell stated in their book the following:

The fact that organisms in living tissues can be destroyed by exposure to x-rays, while the same organisms in inert cultures are uninfluenced by x-ray exposure, proves positively that it is not the influence of the x-ray *per se* that causes destruction, but that the tissues themselves doubtless under the conditions of activity excited by the x-rays play the important role in the germicidal process.

It would be profitless to enumerate the long series of experiments on bacterial cultures. The reputable results agree in showing logarithmic death rates for very large dosages, as exemplified in the results by the writer on *B. coli* and *Erythrobacillus prodigiosus*.

The irradiation was effected with a tungsten-target tube, using a potential of 65 kv. and a current of 4 ma. At certain time intervals, test tubes were removed and dilutions plated out to determine the total counts.

The following conclusions may be derived from these data:

1. X-rays act like sterilizing agents upon cultures of *B. coli* and *Erythrobacillus prodigiosus*, in that the curves are characteristic sterilization or death-rate curves, a fact showing that the total counts decrease logarithmically with time.

2. In this experiment *B. coli* did not show variation or mutation when it was treated with x-rays.

3. With increasing irradiation, *Erythrobacillus prodigiosus* showed a tendency toward lack of ability to produce its characteristic red pigment. By allowing the organism to grow on the plate for a period of five days, the greater portion of the colonies produced their pigment. If a transfer of a white colony is made to an agar slant, the characteristic pigment is produced in 12 hr.

Cultures of simple organisms have been used frequently to discover the effects of various x-ray wave lengths, generally indicating as in all other cases a biological effect independent of wave length under comparable conditions of energy absorption. Wyckoff found that rays kill *B. coli* and *B. aertryke* in linearly exponential fashion. He considers that death results by the absorption of a single x-ray quantum of energy. Since only 1 in 20 of the absorbed quanta kills, the sensitive-cell constituents, the destruction of which leads to cell death, must have a volume less than 0.06 of the bacterium itself. Closely related are experiments with yeast. Wyckoff and Luyet find that, unlike bacteria, yeasts can be injured, without being killed outright. Injury is followed by an extraordinarily large number of two-celled colonies, which on prolonged incubation ultimately die without further budding.

Of course, the final absolutely general effect of x-rays on living organisms is a lethal one.

2. Biological Dosimeters.—The quantity of radiation required for death is so definite for each particular type of cell that a lethal count serves as a quantitative dosimeter of the radiation. A few years ago, Wood showed that for *Drosophila* eggs 50 per cent are killed by 190 *r* and 90 per cent by 500 *r*.

The extended work by Packard has confirmed these values, and also the fact that these eggs give probably the best results of any biological material when used with a definite technique, such that generally average ages of the eggs are involved. For the radiosensitivity increases rapidly during early stages of nuclear division, attaining a maximum when the embryo shows the first sign of differentiation and falling abruptly thereafter. The 50 per cent survival dose for eggs 90 min. old is 163 *r*; for those 330 min., it is 1,044 *r*. Equal doses of x-rays generated at potentials from 12 to 700 kv. kill equal proportions of the eggs. This biological test object is also suitable for γ -ray dosage; Packard has found that the number of equivalent or biological roent-

gens per millicurie-hour is 5.00 r per millicurie-hour at 1 cm. distance and with a 0.5-mm. platinum filter.

The explanation of the fact that just half of a given number of eggs are killed by 190 r or that the survival curve in general is S-shaped either lies in the fact that eggs collected over a 2-hr. period have a distribution of ages and sensitiveness, giving on the average with a fixed routine this constant effect, or depends on the assumption of a differential portion in each cell, more sensitive than the rest, the destruction of which by one or more x-ray quanta will cause death. Therefore, the survival curve is determined by the size of the sensitive spot and the number of quanta required to kill it. This hypothesis requires that this spot shall be equally sensitive at all times, whereas the sensitiveness is known to change rapidly during mitosis. This method involves incubating the irradiated eggs and counting the survivors. Direct and immediate observation upon lethal effects of x-rays can be made on the hearts of the transparent *Daphnia magna*, which stop beating upon death. Other biological dosimeters that have been used are the familiar erythema reaction, the growth of seedlings, the hatching of *Ascaris*, grasshopper, and hens' eggs, and colony development of bacteria.

3. Effect of X-rays on Hereditary Material.—The experiments with bacteria have shown that the only observable biological effect is death, whereas in yeast it is indicated that reproductive processes may be greatly affected by irradiation energies far smaller than required for the death of the organism. This brings us to a brief discussion of x-rays in the science of genetics, already recognized by all biologists. In 1903, Albers-Schönberg discovered the sterilizing effect of x-rays. From that day to this, the controversy has raged as to what effect may have been suffered by those cells irradiated but not sterilized. The controversy has taken the principal direction of whether or not sterilization of human beings by x-rays is safe, or whether cells that have suffered changes in the hereditary material may not produce abnormal young when reproductive powers are reestablished. Muller, outstanding authority in the field, has the following to say about x-ray methods in the hands of the geneticist. Speaking of the gene he says:

It is evident that one chief method of attack in this new type of physiological analysis, a method which must be of high eventual impor-

tance to pathology, as well as to physiology and embryology, would be the alternation or the excision of individual genes, one at a time, out of these thousands of genes, followed by intensive embryological, physiological, and physicochemical study of the effects thereby produced on the organism. In other words, if we had the ability to change individual genes, we should have, in effect, a scalpel or an injecting needle of ultra-microscopic nicety, wherewith to conduct the most refined kind of vivisection or biochemical experiments on our experimental animals, not experiments in which gross parts are removed, injected, or otherwise changed, but experiments in which the finest, most fundamental elements of the body fabric are separately attacked. Changes in the genes, which have arisen spontaneously and are already at hand, can of course be used in such a study, but many of the most instructive types of these have already been largely weeded out by a process of natural dying off, in other words, natural selection, before we can find the individuals containing them, while many of those still existing lie scattered far apart and concealed. Moreover, in nature gene changes arise very rarely. Thus, the advantage which we would have if we were able to manufacture our own supply of them is evident. But apart from the action of radiation, no generally effective means of artificially producing such gene changes, or gene mutations, as they are called, has as yet been satisfactorily demonstrated, that is, demonstrated in such a way that most specialists in heredity are willing to agree that the case is proved. Hence, the question of the production of changes in the hereditary material by means of roentgen or radium rays becomes all the more urgent.

C. R. Bardeen, in 1906, first found that the ova of a toad fertilized by spermatozoa exposed to x-rays developed abnormally, and he concluded that the action of the rays must be on those unknown substances in the nucleus or the protoplasm most intimately associated with the nucleus which control the morphogenetic activities of the cell. Thus Bardeen was lacking only the concept of the chromosome. Most of the work between 1905 and 1925 has limited value largely because a great preponderance of new gene mutations probably escaped attention, since almost without exception these are recessive and cannot be detected until the third generation. Starting with the work of Koeneke, in 1905, on lilies, visible alterations on chromosomes of irradiated cells were recorded. Mohr, in 1919, reported that irradiation of locusts often caused a chromosome to enter the wrong cell (nondisjunction). It has remained for the work of Muller and associates, especially on *Drosophila*, to found a

technique and an entire science of radiogenetics. Briefly outlined, some of these facts are as follows:

1. There are two kinds of alterations in the structure of hereditary material: (a) intrachromosomal or change in linear arrangement of genes within the chromonema, which forms the basis of the chromosome, by simple loss, simple translocation, mutual translocation, inversion, deletion, and complex combinations of these; (b) a change in the composition of the genes themselves. Changes of both kinds can be produced in abundance in *Drosophila*, 150 or more times as abundant as in the controls. Over half of the sperm remaining capable of taking part in fertilization and development are genetically affected. Mutated genes and changed chromosomes are inherited in accordance with usual Mendelian and chromosomal properties.

2. Visible mutations extend to bodily form and size, colorations, conformation of individual organs, fertility, reaction to light and gravity; and heat tolerance. Morphologic changes are often obscure and secondary to physiological ones; at least 80 per cent are lethal and most of the rest detrimental. Changes are distinctly random; hence a very few may happen to be beneficial. For example, recent experiments by the General Electric Company on irradiation of bulbs of the lily *Lilium reginum* have led to a species that will not shed pollen; hence, discoloration of the flower and early wilting are prevented. Here a distinctly unfavorable mutation from the standpoint of propagation is very favorable commercially to the florist. The chromosome changes usually are more detrimental than gene mutations.

3. The mutations and changes are produced by x-rays in germ cells of all types, spermatozoa, whether irradiated in the testis or after reception by the female, spermatogonia, mature eggs, oöcytes, and oögonia. If an embryo is irradiated, the adult may show a patch of mutated tissue, in the midst of normal tissue, derived from a single embryonic cell. A great variety of plants and animals show results confirming those on *Drosophila*, including wasps and other insects, barley, tobacco, jimson weed, maize, wheat, cotton, primroses, snapdragons, petunias, mice, frogs, etc. Snell, in 1933, demonstrated that a quarter of the functional sperm of mice, after irradiation with only 400 r, carries chromosomal translocations to be detected

through inheritable infertility in the first and later generations; also, that over 50 per cent of embryos die *in utero* when one parent comes from an affected line, and that morphologic changes occur, such as misshaped spleens and dwarfism. The implications of such results in terms of human beings are greatly stressed by Muller.

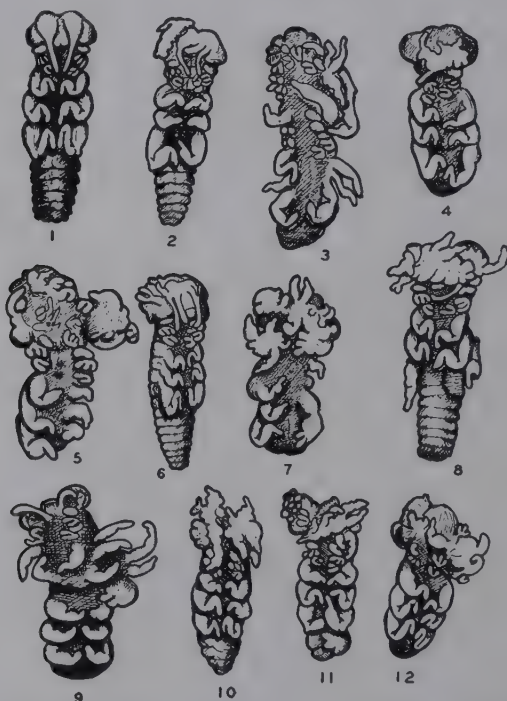


FIG. 116.—Abnormal embryos produced by irradiation of grasshopper eggs, compared with normal type (no. 1). (T. C. Evans.)

4. Chemical and molecular structural changes in reproductive cells still escape us and await the joint efforts of chemists, physicists, and biologists. It is certain that the gene, best seen in the giant chromosome of the salivary cell of *Drosophila*, is a proteinlike material, possibly each one being a giant single molecule, or group of molecules, or even a substituent group of the more complex chromosome. Further consideration will be given this subject in the discussion of protein structures in Chap. XXIII.

Calculations on the basis of the quantum theory have been derived for the effective volume of a single gene upon which x-rays must product their effect. For *Drosophila* the sex-chromosome volume has 0.00829 of its volume composed of vital dominant genes. Since there are 1,280 of these, the size of one of them would be 1.1×10^{-18} cc. In the cell there are 2,000 to 15,000 of these volumes.

4. Effects on Embryos.—Closely related to the effects on chromosomes and genes are those on the developing embryo. Here some of the most amazing evidence of the power of x-radiation is displayed. From a growing fund of experimental observations two examples are cited. T. C. Evans in his great work on all phases of the effects of x-radiation on grasshopper eggs¹ found that the frequency of appearance of abnormal embryos such as is illustrated in Fig. 116 is highest in the sixth and seventh days of development, which is a period of expansion and fundamental differentiation, with an optimum dosage of 200 to 400 *r*. This period corresponds to the gastrulation stage in many other organisms which has been found most susceptible to radiation. The anomalies are the result of injurious selective action of x-rays on more active cells, causing removal of inhibitory control over the development of cells of the head regions which have retained the potentiality of forming whole embryos. It is evident that embryonal rapidly dividing cells are extremely sensitive to radiations.

In a recent piece of work on the effects of x-rays on the developing chick,² dosages of 40 to 600 *r* and at egg ages ranging from 19 to 243 hr. were given. The following interesting results were noted:

1. In 45 per cent, there was no further development after irradiation.
2. In 24 per cent, chicks died in the shell at full development.
3. In 11.9 per cent, chicks died after developing $15 \pm$ days.
4. In 9 per cent, the legs of the chicks were paralyzed.
5. In 6 per cent, the legs and feet were deformed, ranging from distortion of toes to a total absence of one or both feet.
6. In 1.4 per cent, there was a hydrocephalic head deformity.

¹ *Physiol. Zoology*, **10**, 58 (1937).

² ESSENBERG, *Radiology* **25**, 739 (1935).

7. In 1 per cent, there were miscellaneous deformities (brain, beak, wing, etc.).

5. The Effects of X-rays on Normal Cells.—The very first step in a long series of events attendant upon irradiation of cells is a purely physical one—the collision of radiation quanta with electrons in the atoms and molecules of the chemical substances of a cell, and the release of these photoelectrons, leaving ionized atoms, or the raising of electrons to higher energy levels, leaving an activated atom or molecule. The ionized or activated atoms have properties no longer to be associated with the original unirradiated atom. The protoplasm and the protein molecules are of necessity changed and are usually broken down to other substances ordinarily simpler. These degradation products or molecular fragments must be as foreign to the cell in its normal structure and functions as though we had introduced materials from the outside by some microinoculation. Under these circumstances the morphology and physiology of the cell must change in such a way that at least the gross features can be recognized by the histologist and physiologist.

1. All changes follow a latent period after irradiation, which may be very short if our methods of detection are sufficiently sensitive for minute structural, chemical, and biological changes, but may be very long if we judge only by death or a gross phenomenon such as skin erythema. This latency is not yet explained, except that the radiation induces in the nucleus of the cell certain chemical changes which only gradually run their course and only at their completion set free irritative or destructive action.

2. It has long been known that exposure of young organisms to sufficiently large doses of short-wave-length radiation inhibits subsequent growth and development. That there is a marked effect upon normal cells is unquestioned. But the *possible seat of attack of the radiation* (and the high-speed photoelectrons liberated by it) is a far more difficult problem. Much research in the past few years has attempted to find the mechanism, but the answer is as yet incomplete. In studies with plants such as wheat and oat seedlings, Skoog and others proposed, in 1934, that inhibition of growth is attributable to the destruction of a growth-promoting substance, or plant hormone, auxin, which is produced in twice as great amount in light-grown seedlings

as compared with the dark-grown. Chesley has found this hypothesis supported experimentally in some but not in all respects. Considerably less is known about x-ray effects on growth-promoting hormones in animal or human tissues.

3. Translucent protoplasm first becomes turbid and then granular, indicating that the state of aggregation of protein molecules completely changes, because of disturbance in distribution of electric charges making for coagulation. The same effect may be produced *in vitro* by chemical effects and unfavorable mediums. Obviously, since irradiated cells are known to return to normal unless subjected to unbearable dosages, the process can be reversible. One theory due to Dessauer, and held by a number of radiologists, was coagulation by minute points of radiation heat generated in the tissue from the conversion of kinetic energy of the photoelectrons.

4. Many workers have demonstrated the shrinking and clumping of chromosomes, moving irregularly to daughter cells, some lagging behind and some entering the wrong cell. In more advanced stages the chromatin falls to pieces, and the pieces swell up and fill the cell body. After very heavy x-ray dosage the protoplasm is vacuolized and the mitochondria are fragmented; of course, death follows.

5. Often the marked swelling of irradiated nuclei and the ballooning of the cytoplasm are easily observed and must be interpreted as an increased capacity of these structures to absorb water through an altered cell membrane. Although this system is too complex for complete understanding and explanation, it is logical to believe that intracellular changes produce new electrolytes by decomposition of salts, proteins, and fats and that water is drawn in by simple osmosis.

6. The viscosity of protoplasm is increased following irradiation, although the first effect may be liquefaction.

7. The hydrogen-ion concentration is increased for the protoplasm. This effect may last for only a very short time in the case of the skin on up to hours and days, for example, in lymphoid tissue. The importance of this in therapy will become readily apparent when it is considered that in cancer the blood becomes decidedly more alkaline.

8. Cell respiration is decreased, according to a number of workers (Gottschalk and Nonnenbruch, Evans, Noller, Crabtree).

On the other hand, Chesley irradiated wheat seedlings and marine eggs with x- and γ -rays in such doses as markedly to impede growth as measured 24 hr. after treatment, and found that oxygen consumption per gram of growing tissue is not affected. In other words, growth is inhibited before respiratory rate changes. Developmental anomalies in the marine eggs appear before the respiratory rate is altered and do not depend upon respiratory impairment.

9. Some processes are accelerated such as the keratinization of epidermal cells.

10. Curtis, in work on such invertebrates as coelenterates, planarians, and annelids, Sheremetjava and Brunst, with axolotls, and Butler, with the vertebrate *Amblystoma*, have shown that the normal ability of these species to regenerate lost parts is completely destroyed when subjected to x-radiation. Hence, x-rays afford a method of studying experimentally the differentiation process in regeneration as compared with differentiation in normal embryonic development.

11. The rate of cell division is changed. It is a universal finding that cells which are in mitosis at the time of exposure to x-rays complete the division even with inordinately high dosages up to nearly 100,000 *r*, while other cells are prevented from undergoing mitosis. They lose motility and then may literally explode. After a while they may regain apparent normal behavior but occasionally after a few further divisions may die suddenly. In recent work in the writer's laboratory on salamander larvae, the depressing effect of x-rays on mitotic division was clearly demonstrated. A study of the neural tube of the larvae, given sublethal dosages of 400 and 800 *r*, reveals as the initial effect a disappearance of mitotic figures from the germinal cells of the ependymal layer; a period of pseudo-recovery, lasting 4 or 5 hr., during which mitotic activity reappears; a period of severe degenerative changes, occurring mainly among cells in the resting stage; and a period of remarkable regeneration which leads to evident recovery. Irradiation causes mitochondria to enspherulate at a dosage of 1,200 *r* given at a single exposure. The Golgi substance gives no specific reaction and is regarded most resistant. From this work the cell components in the order of their sensitiveness to irradiation are found to be as follows: nucleus, mitochondria, and Golgi substance.

12. Since it is believed that the whole action of radiation is due to the liberation of high-speed electrons whose energy, upon being stopped, produces destruction, the effects on cells are independent of wave length of the x-rays. But the biological effects in the bulk of *tissue* as a whole vary enormously with the wave length, as a result of back scatter, damage, or closing of the blood vessels, vasomotor changes, poisonous effects from decomposition products set free from dead or dying cells, etc.

6. The Radiosensitiveness of Cells.—This is the basis of one of the most important applications of radiation in biology, of identification of cells, of medical diagnosis, and of x-ray therapy. Prominent among a large group of experimenters who have demonstrated characteristic radiosensitiveness of cells is Dr. A. U. Desjardins, of the Mayo Clinic. The following classification is based upon his work. In 1904 Bértoni and Tribondeau announced the principle that young or immature cells are more radiosensitive than old or adult cells. This was the beginning of a vast number of observations on the effects of irradiation, ranging from the pregnant uterus to the single cell. To interpret the principle to the end that sensitiveness varies directly with the reproductive capacity of the cell, and inversely with the degree of differentiation, is perhaps not so satisfactory except in a general sense, since there are notable exceptions, as Packard has shown. Desjardins presents his own ideas in the following terms:

Indubitable as is the relation of the age of cells to radiosensitiveness, analysis of the experiments made to test the susceptibility of different organs and tissues brings out the even more important fact that each variety of cell in the body has a specific sensitiveness, or rather a specific range of sensitiveness, to radiation. This is not intended to imply that all cells of one kind, such as lymphocytes or squamous epithelial cells, react in precisely the same way to a given dose of rays. A certain measure of variation in reaction must necessarily occur, because different cells of the same kind are struck by the rays while in different stages of metabolism. (For example, dividing cells may be as much as eight times as sensitive to radiation as the same cell when in the resting phase.) Other still unknown factors also may play a part. However, if allowance be made for such variation, and if reaction time be taken as a criterion, the specific sensitiveness of each kind of cell looms up as the dominant single fact of radiology and deserves to be recognized as a law. And yet, if we may judge by present-day writings, the existence of such a law and of its medical and biologic implications is not at all

realized. For years much has been made of the dogma that pathologic cells are more radiosensitive than normal cells of the same kind, but, as Lazarus-Barlow and others have shown, the foundation on which this dogma rests is tenuous and insecure. The physiologic condition of cells undoubtedly has some influence on their sensitiveness, but such influence is small as compared with the specific natural susceptibility of each variety of cell. Although the factors responsible for such specificity have not yet been determined, the sensitiveness peculiar to each kind of cell appears to be related chiefly to the natural life cycle. Thus the lymphocytes, the metabolic cycle of which among human cells is the shortest, are also the most radiosensitive, and the nerve cells, the life cycle of which is the longest, are also the most resistant to irradiation. But to this question as to many others the final answer has not been given.

According to our present knowledge cells may be classified, according to their radiosensitiveness, in the following order:

TABLE XXIX.—RELATIVE SENSITIVITY OF A NORMAL TISSUE TO RADIATION OF MEDIUM HARDNESS (SKIN = 1.0)

| | |
|--------------------------------------|----------------------------|
| Leucocytes: | Blood vessels: |
| 2.5 Lymphocytes | 1.5 Endothelium (intima) |
| 2.4 Polynuclear | |
| Epithelial cells of salivary glands. | Dermal structures: |
| Germinal cells: | 1.4 Hair papillae |
| 2.3 Ovarian | 1.3 Sweat glands |
| 2.2 Testicular | 1.2 Sebaceous glands |
| Blood-forming organs: | 1.1 Mucous membrane |
| 2.1 Spleen | 1.0 Skin |
| 2.0 Lymphatic tissue | 0.9 Serous membrane |
| 1.9 Bone marrow | Viscera: |
| Endocrines: | 0.8 Intestine |
| 1.8 Thymus | 0.7 Liver, pancreas |
| 1.7 Thyroid | 0.6 Uterus, kidney |
| 1.6 Adrenal | Connective tissue: |
| | 0.5 Fibrous tissue |
| | 0.4 Muscle, fibrocartilage |
| | 0.3 Bone |
| | 0.2 Nerve tissue |
| | 0.1 Fat |

Destruction in a few minutes was first demonstrated in 1903 by Heineke, of cells in spleen, lymph nodes, lymphoid follicles of intestine and bone marrow. Another effect long known is that very light irradiation of the salivary glands on both sides of the face will cause almost complete suppression of the salivary secretion.

Although the difference in susceptibility between the most sensitive and the least sensitive varieties of cells is considerable, none of the cells is wholly invulnerable to radiation; all cells, whatever their variety, may be destroyed or injured if exposed to a sufficiently large dose of rays, especially if doses within the therapeutic range are disregarded.

7. Recovery and the Time Factor.—Closely connected with sensitiveness is the power of recovery, obviously a phenomenon of enormous importance in therapy. The protozoan paramecium can recover after x-ray dosages as high as 60,000 *r*. Numerous experiments have demonstrated that the best recovery is associated with the *low* reproductive and metabolic rate of the cells. Hence, susceptibility and recuperative powers are inversely proportional. It is not surprising that the intensity of the x-ray beam has a determining effect on the biological change. Weak dosages over a long time are decidedly less effective than intense radiation delivered in a short time. Holthusen found that, with intensities varying from 500 *r* per minute to 0.5 *r* per minute, erythema resulted with a total of 500 *r* for the maximum intensity; with a total of 1,200 *r* for a beam of 5 *r* per minute for 240 min.; and with a total of 2,000 *r* for an intensity of 0.5 *r* per minute. Thus a much larger total amount of radiation may actually be given underlying tissues by the fractional weak doses, without fear of skin injury or scarring, than with a single exposure to intense radiation. An injury slowly effected may be offset by definite repair processes. Packard calls attention to the analogy of a burning house. The most inflammable objects go first and then those that are more resistant. But when the house becomes a furnace of flame everything is consumed equally, regardless of whether some materials are slightly more resistant than others. So with intense doses, all tissues are injured, whereas with prolonged weak irradiation even small differences in susceptibility are revealed.

8. X-ray Effects on Human Tissues. *Action on the Skin.*—According to the dose applied, it is customary to recognize four degrees of skin reaction.

First degree: No visible inflammation, but epilation followed by tanning; lasts from two to four weeks and is followed by complete recovery.

Second degree: Moderate erythema with definite vascular dilation (hyperemia) and a sensation of increased temperature in

the treated area; epilation and pigmentation; duration from 6 to 12 weeks, with eventual recovery and disappearance of tanning.

Third degree: Erythema of reddish-blue color with vesiculation; epilation; loss of papillae and of sweat and sebaceous glands; pain; duration from 8 to 15 weeks; heals with epilated thin scar and often develops telangiectasis in an atrophic scar; danger of late reaction years after the injury.

Fourth degree: Deep reddish-blue erythema with vesiculation and necrosis of cutis, developing into an ulcer; extremely painful; prognosis as to complete recovery doubtful. In most cases, wide excision is the only remedy.

It is obvious, of course, that between these four degrees, there are all types of variation possible.

Numerous histological studies of the irradiated skin have been undertaken; they lead to the conclusion that the acute x-ray reaction of the skin is essentially a degeneration of the epithelium (germinative layer), combined with inflammatory processes (interstitial edema and leucocyte infiltration). There are also changes in the capillaries, namely, dilatation and later thickening of the walls. This picture is most characteristic in the base of a typical ulcer resulting from an x-ray burn. A similar result has been observed in a very recent histological study on frog skin.

According to the most modern viewpoint, "H" substance is liberated quite slowly from injured cells during a long period of time, causing the capillaries to dilate. Because of this gradual seepage of "H" substance, the dilation persists, and the power of contracting to the original state is lost as other cells grow and fill the stretched network forming the walls of the vessels. This action undoubtedly thickens the walls and makes them less permeable to the nutritive elements that are necessary for the growth of the tissue cells. Gradually some die while others acquire abnormal forms of growth. X-ray shock and increased nitrogen in the urine soon after irradiation might also be explained by the sudden release of "H" substance in more sensitive tissue.¹

Entirely different from this acute reaction are the findings in the skin of radiologists following the cumulative effect of numerous small doses or x-rays. Marked blood-vessel changes are absent. There is hyperemia, changes in the blood distribution, and hypertrophy of the epithelium (hyperkeratosis). Hair papillae and sweat and sebaceous glands have almost disappeared.

¹ Light, *Radiology*, **25**, 734 (1935).

Usually, there is edema in the corium accompanied by atrophy of the elastic elements. Microscopically, an acute ulcer can present the same changes and that, undoubtedly, explains the tendency of both to terminate in malignant degeneration (roentgen carcinoma).

Other Tissues.—The effects on other organs and tissues are those to be predicted from the general radiosensitiveness of the constituent cells, summarized as follows:

Circulating blood—resistant.

Bone-marrow-stem cells from which red cells arise—very sensitive.

Genital glands—very sensitive; 30 per cent of an erythema dose (600 *r*) effective in the testicle will produce temporary sterility; 50 per cent will produce permanent sterility; 28 and 34 per cent, respectively, effective in the ovaries will produce temporary and permanent sterilization; irradiation causes marked atrophy, especially of ovarian follicles.

Liver—resistant.

Lung—production of fibrosis.

Kidney—interstitial nephrosis with heavy doses.

Thyroid and goiter—resistant.

Thymus—very sensitive.

Pituitary and adrenals—fairly susceptible.

Intestinal mucosa—destroyed by large doses.

Nervous systems (spinal cord, brain)—large doses without symptoms.

Eye—insensitive except lens.

Bone—with not too intense doses, resistant, except marrow and epiphyseal junctures, where permanent shortening of limbs of young people may result from checking of growth by two or three doses of 540 *r*.

General Systemic Effect.—Following the application of a sufficiently high dose of x-rays to the human body, the organism responds, in a certain percentage of patients, with a syndrome of symptoms usually embraced under the term “x-ray sickness.” The clinical picture nearest to it is that of the well-known sea-sickness. Numerous investigations have been undertaken to find the cause of this systemic reaction, and several theories have been advanced to explain that x-ray sickness is, in all probability, due to the flooding of the organism with the products of cell destruction following the irradiation.

Other theories list as causes the lowering of sodium chloride content in blood serum (in many cases injection of 5 per cent salt solution has been effective); decrease in cholesterol content; increase in calcium and decrease in potassium; nitrogen increase

in blood; changes in protein; changes in blood sugar; increase in blood coagulability; change in sedimentation rate of red blood corpuscles; release of H substance from injured cells, etc. A highly important and interesting recent discovery is that injection of 1 cc. of liver extract is very effective in eliminating this effect. However, Wood points out that nausea occurs only when the abdomen is irradiated and that the sympathetic ganglia and adrenals must be responsible.

9. Stimulating Effect of Irradiation.—For years the legend that x-rays or radium, under certain conditions of dosage, may increase the growth and metabolism of cells has gained wide circulation. This notion has arisen from the attempt to apply to these agents the so-called Arndt-Schultz law, according to which small doses stimulate and large doses depress cellular metabolism. Based on pharmacologic grounds, this doctrine has not been generally accepted, even by pharmacologists. The attempt to apply it to the action of x-rays is unwarranted, for the experimental evidence on which it is based is extremely meager and apparently invalid. A measure of acceleration is a transient phase of reaction and is invariably followed by more or less pronounced inhibition of function and cellular degeneration. Another factor in the propagation of this notion of a stimulating action of the rays has been the regression of pathological lesions after exposure to small doses of x-rays. Such regression is best explained by the exceptional radiosensitiveness of certain varieties of cells. As the result of primary degeneration of certain cells a secondary and indirect stimulation may sometimes be observed. Such is the increase in connective tissue cells in certain tissues and organs after repeated irradiation; the connective tissue is laid down to replace other cells that the rays have caused to undergo degeneration. Any primary or direct acceleration of cellular metabolism must be regarded as an effort of the cell to counteract or compensate for the noxious influence of the rays; in other words, it is purely a defense reaction. Continued acceleration of metabolism cannot be induced by x-rays or radium, which always cause degenerative changes or have no effect whatever. Irradiation of certain tissues, such as the skin, repeated over a long period of time may cause hyperplasia of the epithelium, and this in turn may lead to malignant transformation. This is not stimulation in the sense

here employed, but the alteration of a normal to an aberrant function due to chronic irritation.

One phase of the problem of stimulation is found in the effect of x-rays on sensory processes. The experiments in the writer's laboratory on auditory effects in dogs are perhaps the most extensive of their kind. Animals were trained to a conditioned response, associating a standard sound with an electric shock through one paw, and the acuity of hearing was measured. Irradiation was made through the skull, with dosage up to 11,000 *r*. All animals showed a transient increase in *acuity* following a latent period of 11 days of 5.5 decibels, continuing over a period of 12 to 36 days. Even though the animal showed deleterious effects from the x-rays, such as loss of hair, skin burns, anemia, and extreme restlessness, the acuity of hearing increased. When the animal is irradiated over parts of the body entirely removed from the brain and auditory mechanism in order to ascertain whether the effect is a direct or indirect systemic one, no such increase in acuity is observed. Latest experimental data indicate the possibility that the pituitary gland is involved.

10. Photochemical Experiments with a Possible Bearing on Biological Effects.—As indicated in the preceding chapter, a considerable number of experiments on the photochemical effects of x-rays on simple systems have been attempted in the effort to throw some light on observed biological effects. However, there are very few chemical reactions in which the measurable change on irradiation is comparable with changes in the normal or abnormal cell. Of direct significance biologically are the following:

1. Formation of hydrogen peroxide when water containing dissolved oxygen is irradiated.
2. Decomposition of water (comprising 70 per cent of cells) only in the presence of a catalyst such as iodide ion.
3. Precipitation of proteins produced by irradiation of serum or albumin *in vitro*; denaturation.
4. Change of phenol group of tyrosine in aqueous solution.
5. Deactivation of solutions of various ferments.
6. Oxidation of oxyhemoglobin to methemoglobin.
7. Decomposition of very dilute solution of organic compounds in the absence of oxygen, as measured by hydrogen, carbon

dioxide, and oxygen evolution, must be the result of reaction with activated water molecules rather than a direct effect of the radiation or the formation of hydrogen peroxide. The primary reaction is evidently the attachment of the oxygen of the activated water molecule to the organic molecule, with liberation of hydrogen.

The conclusion is that biological changes produced by x-rays may result from the partial transformation of a great number of different substances present in the cell, and very difficult to ascertain. However, the whole change observed in a mixture of substances, each of which would change if irradiated separately, may be in only one substance even in very low concentration. When a complex molecule is irradiated, the change may be in one sensitive bond only. When such a molecule with a physiological function is irradiated, the very first change in the molecule may and often does destroy its potency.

8. Much has been made of the possibilities of secondary radiation from heavy metal atoms in biological systems, without conclusive results.

11. Mechanism of Biological Action of Radiation.—The complex mechanisms of the photochemical effects of x-rays have been outlined in the preceding chapter, and some of the reactions pertinent to effects on cells and tissues have just been enumerated. It remains to consider the effects characteristic of a cell structure, the most important of which is the swelling. From a consideration of colloidal systems it is evident that swelling is caused by a difference in ion concentrations across a semipermeable cell boundary. Dilution of cell cytoplasms may easily result in damage and then death. Failla¹ of the Memorial Hospital, New York, N. Y., has given the most likely theory based upon known experimental observations for the swelling process. The x-ray photon liberates in the irradiated area photoelectrons and Compton electrons, which in their passage produce "radio ions," atoms, molecules, or aggregates which have gained or lost electrons. Ordinarily there are rapid recombination and disappearance of the effect in contrast with the constant equilibrium between electrolytic ions and undissociated molecules. However, in proteins the *radio* ionization may easily induce chemical changes which produce new mole-

¹ "The Cancer Problem," p. 202, Science Press, 1937.

cules by rearrangement or fragmentation. These in turn may be capable of *electrolytic* ionization. Some of these new ions and molecules may not be able to pass through a cell wall, with the result that ionic concentration within the cell increases persistently. This would be sufficient to set up an osmotic system in which water must pass from the environment through the wall and thus cause dilution and swelling. But the tendency is still further aided by the removal of ions outside the cell by the constant renewal of streaming fluid which conveys nutrition to the cell and waste products away from it. A still further assisting factor is the possibility of weakening of the cell membrane by the superposed bombardment of electrons in localized areas. Once swelling and dilution have been initiated as a result of excessive ion concentration within the cell, this may continue because of interference with normal biological processes. Furthermore, as already indicated, new chemical substances within the cells may be as incompatible to normal existence as though toxins were introduced by microinjections; or coagulated colloidal particles would induce fluid intake by the cell in the attempt to dissolve them. Such effects are enhanced in the smaller, more sensitive, nucleus, which normally is protected by the outer parts of the cell but to which the radiation penetrates easily. Upon the basis of the theory a distinctly cellular tissue should be, and in general is, more radiosensitive than connective and similar tissues. Time is required for uniform diffusion of ionized substances throughout the cell from the initially concentrated tubular areas along the electron tracks. A biologically active cell, such as one in the process of dividing, will aid this diffusion, thus accelerating the establishment of a differential ionic concentration and swelling, and therefore is more radiosensitive. Recovery is explained by the fact that some of the electrolytic ions produced within the cell by radiation are small enough to diffuse out of the membranes, thus decreasing the deleterious effect. In cells that divide rapidly the excess in ion concentration is halved at each division and soon becomes harmless. According to this theory it should be expected that tissues into which *excess water* has been injected should show a greater response to irradiation by osmotic swelling than ordinary untreated controls. This has been verified experimentally and clinically in 1939 by Failla and associates.

12. Radiopathology.—X-ray therapy is indicated when it is desirable to produce the following effects:

1. *Inhibition of the growth or function of glands and cells.* Differentiated cells such as those composing glands and hair follicles, physiologically active cells, young cells, cells about to divide, lymphoid tissue, and tissue of embryonic type are all markedly radiosensitive. Skin diseases characterized by hyperactivity of the glands, hyperthyroidism, diseases that may be cured by checking ovulation, leukemia, and many other conditions are successfully treated by irradiation.

2. *Solution of hyperplastic connective tissue* such as uterine fibroid (microscopic examination reveals atrophy of myomatous cells) and hyaline sclerosis of the connective tissue with dilatation of blood vessels.

3. *Reduction of lichenification*, by inhibition of overgrowth of epidermal cells, and destruction of fungi.

4. *Anodyne effect.* The relief of itching has been very frequently accomplished. The relief of pain, except when due to a lesion that can be cured by irradiation, is less certain, though many writers have reported an analgesic effect upon neuralgic pain.

5. *Reduction of inflammation.* There is a favorable experience in the treatment of carbuncles, pneumonia in certain stages, erysipelas, etc. The rate and mode of reaction of inflammatory lesions indicate that the rays act chiefly by destroying the infiltrating lymphocytes, the exceptional sensitiveness of which has already been pointed out. Evidently these cells contain protective substances that enable them to neutralize bacterial or other toxic products, which give rise to the inflammation. When the cells are destroyed by irradiation, these protective substances are liberated and become immediately available for defensive purposes.

6. *Gas gangrene infections.* Unquestionably x-ray treatments are a definite aid to recovery, either because hydrogen peroxide, fatal to anaerobic organisms, is formed in body fluids or because, as previously indicated, a substance resistant to toxins is released.

7. *Miscellaneous pathological conditions.* At one time or another x-rays have been used in the treatment of almost every conceivable ailment—tuberculous meningitis, arthritis, poliomyelitis, whooping cough, hay fever, angina, pituitary and adrenal disturbances, vasomotor disturbances, hyperinsulinism,

hyperthyroidism, goiter, leukemia, etc., in addition to tumors of all varieties.

8. *Destruction of benign and malignant tumors.*

13. Cancer.—There is no greater challenge, and no greater achievement, in x-ray science than the treatment and cure, in a great number of cases, of cancer, or, specifically, carcinomas and sarcomas.

1. *Statistics of the Cancer Problem.*—During the present year 150,000 people, the great majority above 50 years in age, will die of cancer in the United States, a mortality second only to that caused by heart diseases. Women will be in the majority for ages under 55, and men for ages over 55. Of cancers in men, 57 per cent will be in the digestive tract, 7 per cent in the mouth, and 3 per cent on the skin; 40 per cent of the women will die of cancers of the digestive tract, 30 per cent of cancers of the genital organs, and 15 per cent of cancers of the breast. But on the other side of this extraordinarily dark picture is the fact that tens of thousands of cancer patients will be cured by x-rays, γ -rays, surgery, or a combination; others diagnosed too late will have pain and suffering alleviated and life prolonged by the agency of radiation—in spite of the fact that cancer remains one of the great enigmas of medical science.

2. *What Is Cancer?*—The general term “cancer,” originally assigned in ancient times from an imagined resemblance to the claws of a crab, is applied to an abnormally organized tissue which usually grows at a greater rate and to a much greater extent than the normal tissue from which it develops. More specifically, carcinoma refers to a malignant epithelial tumor, and sarcoma to such a growth derived from a nonepithelial tissue of mesodermal embryonic origin (connective lymphoid, cartilage, bone tissue, etc.). C. C. Little has advocated instead of the word “cancer” the phrase “hypernomic histoplasia,” meaning “tissue formation outside the law” of orderly ontogenetic processes or of growth control. Cancerous growth is initiated whenever other types of growth (normal, regenerative, or inflammatory) are intensified and continued over relatively long periods of time. In abnormal growth, cells undergoing proliferation never exceed a certain intensity and are always under control. Some types of abnormal growth are self-limiting or are terminated by eliminating stimuli such as bacteria. But in cancerous growths there is an increase in normal proliferative energy that

is continuous and unending, without regard for the physiological needs of the tissue in which they have arisen or for its physiological boundaries.

Cancer cells never again assume the behavior and reactions of normal cells; they easily invade neighboring tissues and lymph or blood vessels, because of failure of the normal mutual interactions of adjoining cells, causing metastases, or new tumors of exactly the same kind of cells. They may remain structurally immature since there is no time for full differentiation and hence may usually be distinguished microscopically from corresponding normal cells; they may be transplanted easily and made to grow in successive generations indefinitely, thus making possible the great researches on cancer, especially in mice and fowls, by Maude Slye and countless others. Cancer cells possess an unusual capacity of establishing connection with a regional blood supply. By interfering with various organ functions, by their degeneration products, by causing hemorrhage, and by undergoing secondary infection the cancerous growths cause anemia, emaciation, loss of strength; and finally death.

3. *Chemical Behavior of Cancer Cells.*—Besides the morphological differences just noted, it has been demonstrated that the cancer cell is distinguished from the normal cell in the following respects:

a. In tumor tissue, for every 13 sugar molecules attacked, 12 are split into lactic acid and 1 is oxidized, whereas in normal tissue the ratio is 1:1. Hence nutrition of the cancer cell is derived from a fermentation process.

b. In cancer, blood plasma pH is 7.47, or 8.7 per cent more alkaline than normal.

c. Blood glucose is high.

d. Calcium is low.

e. Potassium is high.

f. The glycolysis activator in cancer tissue is known to be pyruvic acid.

g. Carrel has shown that malignant types of cell digest fibrin and feed upon substances or tissues that are not utilized to the same extent by normal cells.

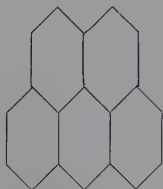
h. Cancer tissue does not utilize hexose phosphates or glycogen added to the suspending medium, whereas most types of normal tissue do.

i. In 1939 Kögel and Erxleben¹ of Utrecht showed that the proteins of malignant tissues are partially racemized. Normal tissues yield on short acid hydrolysis *l*-glutamic acid with normal optical rotation, while the products isolated from tumors have as high as 50 per cent of the *d*-glutamic acid.

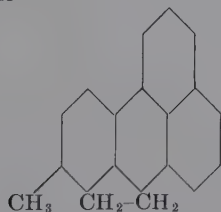
4. *The Cause of Cancer*.—The fundamental cause of cancer is an intracellular change that becomes self-perpetuating.

The cancerous change may be initiated according to Morton by any irritating or stimulating agent of the following three main groups and by combinations of 1, 2, and 3.

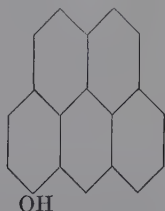
1. Physical.
 - a. Traumatic (injury).
 - b. Thermic.
 - c. Actinic—ultraviolet, x-rays, radium.
2. Chemical.
 - a. Stasis (arrest of blood current in capillaries).
 - b. Pure carcinogenic chemicals: 1, 2 benzantracene derivations of which benzpyrene



isolated as the active agent in coal tar and methylcholanthrene



are good examples, whereas, for example, the compound



¹ *Nature*, **144**, 71 (1939).

is entirely noncarcinogenic, showing the great importance of substituent groups in the molecule. Most of these active agents are closely related chemically to bile acids, sterols, and hormones.

c. Coal tars.

d. Internal secretions—estrogens, hormones.

3. Biological.

a. Bacteria.

b. Viruses.

c. Helminths (intestinal worms).

Every potentially growing cell can be made to undergo neoplastic change by long continued and unremitting action of the inciting agent (except viruses). After a certain summation of action on the cell, the change proceeds inexorably regardless of whether or not the inciting factor is withdrawn. Next to the chemical stimulants, greatest interest is developing in the effects of hormones.

Experimentally, development of breast carcinoma in mice can be prevented by ovariectomy which eliminates the hormone oestrin. That the latter is responsible for such cancers is proved by injecting it into normal animals, whereupon it acts by inducing rhythmic growth process in the mammary tissue.

The question of the factor of heredity in cancer has been one of the most bitterly controversial because of its obvious incalculable importance. It is certain that some factor is transmitted from generation to generation in certain families and strains of mice. Breast cancer never occurs in certain strains whereas in others every female mouse becomes cancerous if it reaches a certain age. A single recessive gene cannot be responsible for the hereditary transmission since the hereditary tendency of the mother to acquire cancer is more important in determining its development in the offspring than the hereditary constitution of the father. Thus cancer is due to cooperation of various kinds of stimulating factors and certain specific substances acting together with hereditary constitutional factors. In mice these factors have been variable and known but in man unknown. The greatest difficulty in the search for stimuli and agents responsible for cancer in man is due to the conditioning influence of susceptibility and resistance which must be multiple factors in inheritance. Cancer as such is not handed down in heredity. It is the result of interplay between constitution and environment. Inherited susceptibility to cancer may

never appear if the individual is protected from adverse environmental stimulating factors; inherited resistance can be broken down by repeated application of strongly inciting factors, such as x-rays or occupational hazards.

A possible complication is the fact that in certain tumors of fowls it is possible to separate from the tumor a substance free from living cells which on injection into another individual of the same or related species gives rise to a new tumor. Furthermore Peyton Rous has shown that the virus which causes skin papilloma in cottontail rabbits transmits the disease. Hence viruses may act as growth stimulators, which may be present in the tissues in a nonpathogenic condition and become pathogenic for the cells when these have been sufficiently altered by the action of a carcinogenic agent (such as oestrin in breast cancer in mice).

To summarize, there are at present two conceptions possible of the origin of cancer. (1) If normal tissue cells receive an amount of stimulation exceeding a certain limit that permits the normal cycle of metabolic and proliferative processes to take place, an irreversible cancerous equilibrium is obtained, in which the cells assume all the characteristics that distinguish this pathological state. Further, under the influence of these stimuli, with the cooperation of hereditary factors, a growth substance is formed newly, or in a quantity larger than normal, and is propagated indefinitely within the cells by means of a process, resembling autocatalysis, responsible for continued cancerous growth. (2) The cancerous transformation is due to the cooperation between two conditions. In the first phase stimuli of various kinds that induce growth processes must be active, followed by a second phase in which viruses having a specific affinity for certain tissues enter the stimulated cells and cause, from then on, their continued propagation. It is possible that in some cancers the first of these two mechanisms is involved, and in others the second. Since it has been demonstrated that the viruses are complex proteins (see Chap. XXIII) rather than living organisms, they may resemble the autocatalysts of the first alternative, and thus essential differences between the two conceptions disappear.

5. *Cancer Therapy*.—All sorts of procedure have been suggested for treating cancer other than surgery, x-rays, radium, or neutrons, but as yet no chemical (including snake venom),

hormonal, biological, or dietetic method has proved of the least value in the control of this disease.

In the problem of x-ray cure of cancer, two important phases must be recognized: (1) destruction of the localized growth, together with detoxication and elimination of cell debris, and (2) repair at the site of the destroyed neoplasm by normal tissue and compensation for the damage created in the organism by the tumor, its toxins, and x-rays. Ewing upon the basis of long experience lists four factors in the process of cure: (1) destruction of tumor cells; (2) destruction of normal epithelium; (3) regeneration of normal epithelium; (4) adaptation by epithelium. Normal epithelium acquires a resistance to the rays by a process of adaptation and is able to regenerate under a dosage that originally destroyed the preexisting epithelium. The tumor cells, subjected to the same dosage, do not exhibit this power of adaptation and regeneration but perish.

Modern therapeutic technique involves not only the radiosensitiveness of tumors but also the relationship of the normal matrix. Tumors proceeding from radioresistant matrix tissues are likewise radioresistant in a state of complete differentiation. Osteosarcomas, fibrosarcomas, and adenocarcinomas showing little sensitiveness imitate the structure of the matrix tissue and in all such cases, even including growths in relatively atypical manner, have the same radiobiological quality as their matrix tissue. What in practice divides radiosensitive from radioresistant tumors is not the amount of radiation required for destruction of the tumor but whether or not this amount is permissible from the standpoint of its effects on other tissues that are necessarily included in the irradiation. The radiosensitiveness of malignant tumors is not in all cases greater than that of their matrices; otherwise there would be no malignant tumor that could not be made to disappear under irradiation, and cancer would be a completely curable disease. Complete disappearance of the tumor can be achieved with certainty only when the matrix tissue can be destroyed. However, some tumors have an entirely different structure from their matrices, such as round-cell sarcomas. These are composed of cells not found in mature connective tissue and possess a radiosensitiveness that makes possible their disappearance. Spindle-cell

sarcoma, on the other hand, does not differ in sensitiveness from its matrix, but in most cases therapy must involve an injury to the irradiated matrix, the reaction of which is a criterion of the reaction of tumor tissue.

This gives us a new principle of dosage, based not on the destruction of the tumor, but on disappearance of normal tissue of the matrix; the radiobiology of the normal tissue becomes the basis of radiotherapy of malignant tumors.

Questions naturally arising in connection with x-ray therapeutic technique are concerned with the dosage required to kill tumor cells: whether the irradiation should be massive, *i.e.*, given at one time, or fractionally divided; whether the effect is a function of wave length; and whether 1,000,000-volt x-rays have great advantages over 200,000-volt x-rays and radium. The answers upon the basis of present available knowledge are as follows:

a. The dosage required to kill tumor cells varies with different tumors but averages, with back scatter eliminated, 2,500 to 3,500 *r* (five to seven times the erythema dose) (Wood).

b. For the great majority of cases the fractional method of treatment usually identified as the Coutard method seems greatly to be preferred by the majority of roentgenologists. This involves frequent doses of relatively small proportions (50 to 250 *r* per day), well below an erythema effect, and protraction until a large total dose has been administered. Certainly this type of treatment is best for palliation of advanced malignant disease. However, many prominent authorities still believe that the single massive dose is essential to prevent recuperative powers of the cancer cell from repairing the destructive effects of x-rays, in spite of possible irreparable damage to normal tissue. The skin effect with the massive dose is avoided by irradiation through multiple ports instead of restriction to one area.

c. The lethal point for cancer cells is independent of wave length for the same number of *r* units administered.

d. There are now several million-volt x-ray installations in cancer hospitals, and there is available the experience of more than five years. Advantages of the million-volt technique are deeper penetration and less damage to the skin because there is less back scatter and less radiation sickness. But the popular

conception that higher voltage means better treatment is not generally correct. The results, though hopeful, do not as yet show that this form of therapy can replace the procedure with the usual 200-kv. unit, and they are not more startling. The number of patients who have died in the period of use indicates clearly that no appreciable advance has been made by increasing the voltage. The wave lengths at supervoltages are comparable with those of γ -rays, but radium therapy has not been and will not be replaced simply because radium is the most effective agent for intracavity treatment, eliminating the necessity of reaching a tumor only after passage through the skin and underlying normal tissues. It has been well said that a knife never cured a patient, but a surgeon with a knife has cured many. Similarly, an x-ray machine can never control cancer, but a skilled radiologist using an x-ray machine has accomplished much in that direction. Skill with a 200-kv. irradiation is infinitely more promising than mere increased voltages. Skill with a million volts may yet surpass all present expectations.

14. A Third X-ray Application in Medicine.—The great value of the microscope in diagnosis is self-apparent. And yet it is clear that many problems of cell structure and behavior are beyond the power of any microscope to solve. For this reason other methods such as specific radiosensitiveness have been welcomed. A few years ago the x-ray diffraction method of structure research was extended to the actual structure of normal and pathological tissues, which can now be studied exactly as crystals of metals, or cellulose, or fibrous proteins can be studied. With this "supermicroscopic" penetration down to molecules of the complex substances of cells, a fundamental molecular change from normal to abnormal was demonstrated with comparable specimens. Hence, though only the slightest beginning has been made, another great application of x-rays has been opened to biology and medicine. It is singular that x-rays will produce subtle changes in tissues and that we can use x-rays, now in a different sense, to find out what change has been wrought by the original irradiation. Beyond a doubt, in some great clinic with every intellectual and experimental facility, this new method of fine-structure analysis can be made to answer many of the unanswered questions of radiobiology and by improved diagnosis lessen the scourge of cancer on the earth.

BIBLIOGRAPHY

Besides hundreds of original papers, reference may be made to the following books:

"Biological Effects of Radiation," edited by Duggar *et al.*, under the auspices of the Committee on Radiation, National Research Council, 2 vols., McGraw-Hill Book Company, Inc., New York, 1936.

"Some Fundamental Aspects of the Cancer Problems," A.A.A.S. Symposium, Science Press, New York, 1937.

"Theoretical Principles of Roentgen Therapy," edited by Pohle, Lea and Febiger, Philadelphia, 1938.

"The Science of Radiology," American Congress of Radiology, C. C. Thomas, Springfield, Ill., 1933.

Yearbook of Radiology, Yearbook Publishers, Chicago, 1933, 1934, 1935, 1936, 1937, 1938, 1939.

"Symposia on Quantitative Biology," Vol. II, III, Biological Laboratory, Cold Spring Harbor, N. Y. 1934, 1935.

"Fundamental Cancer Research," Report of Committee Appointed by the Surgeon General, *U. S. Public Health Reports*, 53, 2121 (1939).

PART II

THE X-RAY ANALYSIS OF THE ULTIMATE STRUCTURES OF MATERIALS



CHAPTER XII

CRYSTALLOGRAPHY AND X-RAY DIFFRACTION

The Solid State of Matter.—Knowledge of the crystalline state of matter was decidedly limited prior to the discovery by Laue and the Braggs that x-rays could be applied to the analysis of the internal structure of crystals. The great and relatively aged science of crystallography had been built up to the conclusion, from careful observations with microscopes and optical goniometers, that apparently almost all true solids were really crystals, either single entities with pairs of parallel bounding surfaces disposed in definite geometric fashion at angles which could be measured, or aggregates of these single crystals. Though regularity of exterior appearance indicated some kind of regular internal arrangement of unit building material, whatever that might be, yet, without experimental methods of investigation and without adequate conceptions of atomic and molecular structure and the forces holding atoms and molecules together, physicists and chemists were unable to find points of useful contact with the essentially applied geometric science of crystallography. Concerning the gaseous and liquid states of matter, much more was known in the sense that their behavior could be explained by simple hypotheses. They are characterized by disordered arrangement of atoms or molecules which are relatively free to move, even in liquids. Since all directions are alike, it is possible to calculate with considerable accuracy the behavior of gases and liquids in very practical phenomena. Chemists have worked very largely with gases and liquids because the freedom of motion of the molecules has permitted reactions more readily. But in solids great complications arise because the atoms and molecules are bound together tightly by their mutual forces. It is evident that the exercise of these forces should tend to produce regularity of arrangement. X-ray analysis has shown that such a regularity does exist in practically every solid substance.

The great practical importance of scientific knowledge of the ultimate structure of solids, which are crystals in the natural state, is self-evident, when consideration is given to the definition of desired physical and chemical properties. The strength of steel girders, the corrosion of aluminum alloys, the wearing properties of casehardened steel, the plasticity of lime, the dielectric capacity of materials, the lubricating properties of long-chain paraffins or of graphite, the stretching of rubber, the covering power of pigments, and innumerable other practical phenomena of everyday life—all depend upon ultimate crystalline structure. Bragg has shown clearly that as a matter of fact the only properties of solid bodies which are not directly and obviously related to crystal structure are those, few in number, which depend upon atomic characteristics alone, such as weight. With few exceptions every aspect of the behavior of a solid substance depends on the *mode of arrangement* of its atoms and molecules.

A clear distinction must be made relative to the ultimate crystalline structure of materials. Sir William Bragg speaks in the following inimitably clear fashion of the three types of assemblage:

The simplest is that of the single atom as in helium in the gaseous state, in which the behavior of every atom is on the whole the same as the behavior of any other. The next is that of the molecules, the smallest portion of a liquid or a gas which has all the properties of the whole; and lastly, the crystal unit, the smallest portion of a crystal (really the simplest form of a solid substance) which has all the properties of the crystal. There are atoms of silicon and oxygen; there is a molecule of silicon dioxide, and a crystal unit of quartz containing three molecules of silicon dioxide. The separate atoms of silicon and oxygen are not silicon dioxide, of course, in the same way the molecule of silicon dioxide is not quartz; the crystal unit consisting of three molecules arranged in a particular way *is* quartz.

The new chemistry of the solid state derived from direct structural analysis is decidedly unconventional and almost shocking to some chemists. The conception of the molecule has come to play far too great a part in chemistry, for, though the molecule is a very real entity in the gaseous state, this is by no means necessarily so in the solids. Here it is the exception rather than the rule for the molecule to have a discrete existence.

In its turn this picture of the sanctity of the molecule has created a quite false impression of the importance of classical laws of chemistry. The laws of constancy of composition and of simple proportions now appear as trivial and insignificant consequences of geometrical requirements rather than as profound and fundamental expressions of the laws of nature. The conception of valence, too, so successful in organic chemistry has been widely and sometimes blindly applied in fields altogether outside its scope, until, on chemical grounds alone, it has become clear that certain classes of compounds refuse resolutely to conform to accepted chemical principles. This is notably the case with intermetallic systems, but we shall find that it is also true of other types of compound, including many that have been revealed and could only have been revealed by x-ray methods. Therefore, this new chemistry presents a challenge of remarkable interest which we shall try to indicate in briefest and simplest fashion in this and succeeding chapters.

The first aim of the x-ray analysis of crystals is to determine the arrangement of the atoms in the crystal unit and to account for the properties of the crystal in terms of that arrangement. The interference of x-rays in gases and liquids has made possible more recently fine-structure determination even for these states. The simple Bragg law $n\lambda = 2d \sin \theta$, derived on page 82, governs the process of analysis of ultimate fine structure of materials.

Fundamentals of Crystallography.—In Chaps. I to XI attention has been given primarily to the fundamental properties of x-rays which are to be used subsequently simply as a tool in the analysis of fine structure of matter. The crystal grating of known constant by which it is possible to analyze x-radiation and measure wave lengths has been taken more or less for granted. It is now appropriate to take the radiation for granted and to inquire into the reasons for the satisfactory action of crystals as gratings and for the fact that the analysis of x-ray spectra from each crystal leads directly to the interpretation of how a particular crystal is built from ultimate atomic units.

Entirely apart from x-ray data a systematic science of crystallography has been developed which serves as the basis for rational interpretation of x-ray data. The steps in the development of this information may be summarized briefly as follows:

1. *The Indices of Crystal Faces and Planes.*—The important properties of a crystal visible to the eye are the planar bounding

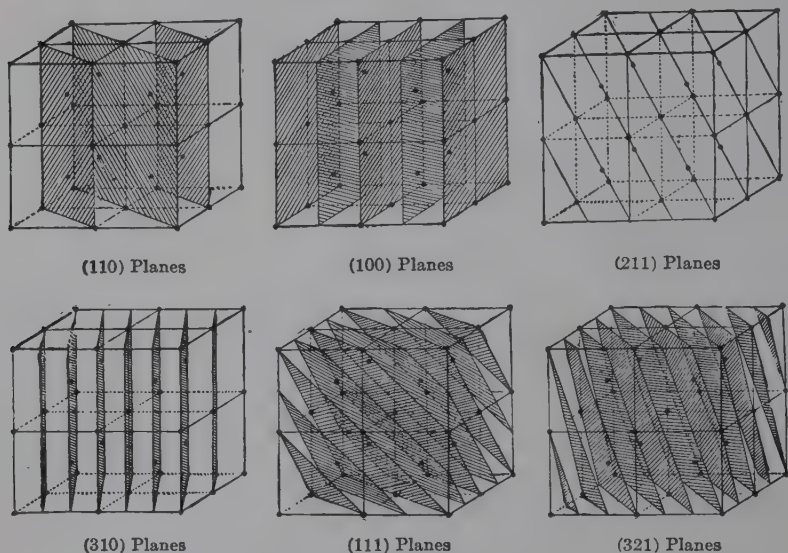


FIG. 117.—Typical sets of parallel planes in a cubic lattice.

faces and the symmetry. The first logical step is to measure the *angles* between faces with the goniometer. In order to express then the positions in space of these planes relative to each other, it is essential to derive a system of co-ordinates. The planes may then be indexed in terms of their intercepts upon the axes of a system of coordinates; upon each axis a unit distance is chosen, and then the distances from the origin of the given plane along the three axes is measured; the reciprocals of these intercepts are then the indices of the plane. Thus a plane intersecting the *X* axis at unit distance from the origin and parallel to the *Y* and *Z* axes has the intercepts 1, ∞ , ∞ and the indices 1, 0, 0, usually written (100) (Fig. 117). Other cubic faces have the indices (010) and (001), and the planes that bisect diagonally

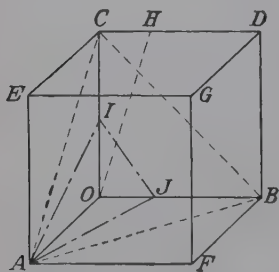


FIG. 118.—Directions and planes in cubic lattice: direction *OA*, [100]; direction *OD*, [011]; direction *OG*, [111]; direction *OH*, [013]; plane *AEGF*, (100); plane *ABC*, (110); plane *AIJ*, (132).

1, 0, 0, usually written (100) (Fig. 117). Other cubic faces have the indices (010) and (001), and the planes that bisect diagonally

the cube faces are (110), (101), and (011). Also there are the similar planes with negative indices where the intercepts are in other octants. A single specific plane or crystal face is usually designated with parenthesis, thus (100), a family of

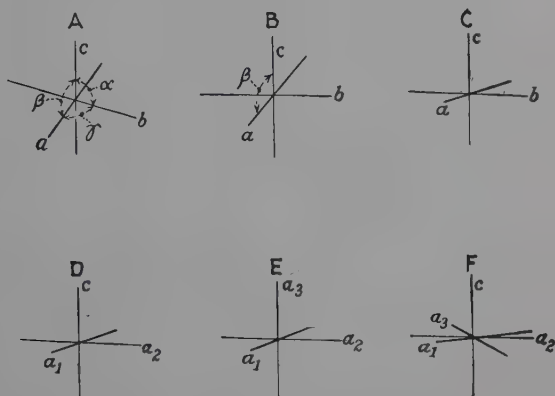


FIG. 119.—The coordinate axes of crystal systems. (A) Triclinic, $a \neq b \neq c$, $\alpha \neq \beta \neq \gamma \neq 90^\circ$. (B) Monoclinic, $a \neq b \neq c$, $\alpha = \gamma = 90^\circ$, $\beta \neq 90^\circ$. (C) Orthorhombic, $a \neq b \neq c$, $\alpha = \beta = \gamma = 90^\circ$. (D) Tetragonal, $a = b \neq c$, $\alpha = \beta = \gamma = 90^\circ$. (E) Cubic, $a = b = c$, $\alpha = \beta = \gamma = 90^\circ$. (F) Hexagonal, $a = b \neq c$, $\alpha = \beta = 90^\circ$, $\gamma = 120^\circ$.

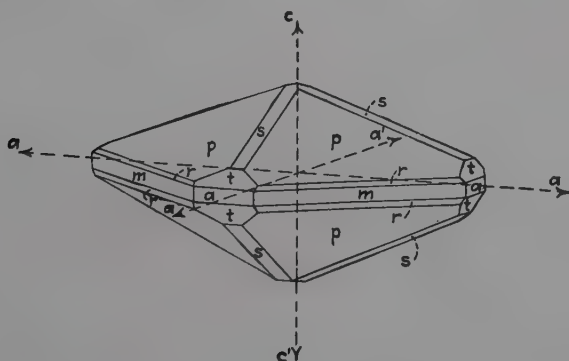


FIG. 120.—Diagram of faces of a single crystal of white tin, after Schiebold. See text for method of indexing face planes.

parallel planes $\langle 100 \rangle$ or 100, and a direction or normal to a set of parallel planes [100] (Fig. 118); if the faces of a crystal are completely developed, then the form is designated {100} to include the six cubic faces, etc. A crystal in the cubic system may have the form {100}, cubic shape, or {111}, an octahedron. In Fig. 117 are shown six of the various sets of planes into which

a cube may be imagined to be sliced up. Planes in general are designated by the indices hkl .

2. *Crystal Systems*.—Now an immense amount of experimentation has proved that all angle measurements and indexing of plane faces are accounted for by six systems of coordinates (Fig. 119). In other words, there are six crystal systems: triclinic, monoclinic, orthorhombic, tetragonal, hexagonal (rhombohedral classed under hexagonal), and cubic. As an example of these relationships whereby a crystal is characterized, the case of tetragonal tin (Schiebold) is represented in Fig. 120. The outer form of a single crystal is represented on tetragonal axes, a, a, c , $\alpha = \beta = \gamma = 90^\circ$. The most characteristic faces are designated p , the indices being (111) , $(1\bar{1}1)$, $(\bar{1}\bar{1}1)$, $(\bar{1}11)$, $(11\bar{1})$, $(1\bar{1}\bar{1})$, $(\bar{1}\bar{1}\bar{1})$, or the form $\{111\}$. The other faces can also be symbolically represented, so that the crystal habit is completely described as follows:

$$\begin{aligned}
 p &= \{a, a, c\} = \{111\}; r = \left\{\frac{a}{3}, \frac{a}{3}, c\right\} = \{331\}; \\
 m &= \{a:a:\infty c\} = \{110\}; \\
 s &= \{a, \infty a, c\} = \{101\}; t = \left\{\frac{a}{3}, \infty a, c\right\} = \{301\}; \\
 a &= \{a:\infty a:c\} = \{100\}.
 \end{aligned}$$

From the angle between the faces $s:a = 68^\circ 54'$, the axial ratio can be calculated to be $a:c = 1:0.3857$.

Another important property is illustrated by this figure, namely, that several faces intersect in parallel edges—*stats*, *prmrp*, etc. The aggregation of all faces or planes that intersect with parallel edges is called a *zone* and the common edge direction a *zone axis*. It follows that every possible crystal face must belong to at least two crystallographic zones.

3. *Space Lattices*.—As a further result of the experience of two hundred years it is now definitely assured that the indices of all the plane faces of crystals are always small whole numbers (*i.e.*, 100, 321, 568, etc.)—the law of rational indices. The crystallographer is guided by external form of the crystal in selecting three nonparallel faces of the crystal whose intersections give the directions of crystal axes OA, OB, OC . A fourth plane may be chosen as standard and called (111) since it intercepts all three axes at distances proportional to a, b, c . Then faces of the

crystal are parallel to planes making intercepts a/h , b/k , c/l on the axes where h , k , l are small integers. Thus we think of the axes OA , OB , OC divided up into h , k , and l equal parts, respectively, the indices of the set of planes being (hkl) . The crystallographer measures simply the ratio $a:b:c$, with b usually given the value unity, whereas x-ray methods measure the actual lengths of the unit translations. In most cases these are proportional to the axial ratios of the goniometer measurement. If this is true, then only a definite *lattice* in three dimensions formed by the intersection of three sets of parallel planes can explain the rational intersections on axes. These lattices are, of course, considered to be built on the above-mentioned systems of coordinates, and there are 14 of these spatial patterns geometrically possible (Fig. 121).

There is only one true space-lattice for each crystal pattern, but the choice of axes, the ways of drawing row lines and net standard planes, or unit cells formed by joining points in the lattice so that space is divided into a series of parallel-sided equal volumes, is arbitrary. The best guide is that the indices of the commonest faces shall be as simple as possible and that the largest number of points (atoms) shall lie in them. The lower the indices of a set of lattice planes the more thickly populated are they with points and the greater is the interplanar spacing ($d_{100} > d_{110} > d_{321}$ etc.). Similarly along any line or *direction* the lower the indices, the larger the number of points through which it passes and the shorter the identity period.

4. *The Unit Cell*.—The unit cell is defined as the smallest possible subdivision which has the properties of the visible macrocrystal and which, by the repetition or translation of itself in all directions, builds the crystal. There are many ways in which a cell can be drawn in a unique space-lattice; but usually the edges a , b , c or unit translations are parallel with the respective crystallographic axes, and the smallest of the several possibilities is chosen.

The necessity of a unit cell such as that defined above arises from observations made upon the geometrical regularity of crystals. A "primitive cell" postulated long before the discovery of x-rays contained the essentials of the foregoing definition.

Since the unit cell builds the crystal through repetition, it is necessary that every possible interplanar spacing of the crystal

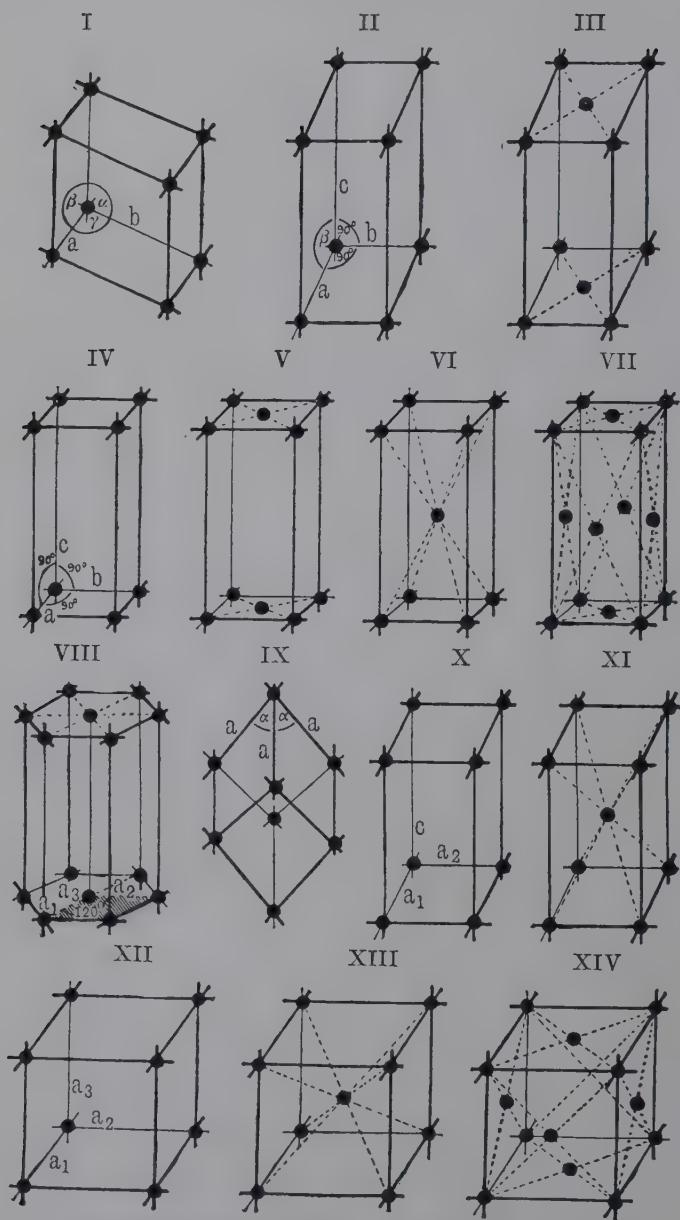


FIG. 121.—Space-lattices: I, triclinic; II, simple monoclinic; III, end face-centered monoclinic; IV, simple rhombic; V, end face-centered rhombic; VI, face-centered rhombic; VII, face-centered tetragonal; VIII, hexagonal; IX, body-centered tetragonal; X, simple tetragonal; XI, body-centered cubic; XII, simple cubic; XIII, body-centered cubic; XIV, face-centered cubic.

can be described in terms of one unit cell. This is true since each interplanar spacing must be repeated along a given direction in the crystal if it is to be detected by x-ray methods, and the only manner in which such a condition may be satisfied is that the interplanar spacing represent a rational fraction of the repeating unit in the direction considered. For if the interplanar spacing represented some irrational fraction of the unit-cell dimension and was repeated throughout the crystal, the arrangement of atomic planes in the adjacent unit cell could not be exactly the same as that in the first, and we have a contradiction of the given definitions. The geometric unit cell itself is pictured such that by starting from any point in the structure, by going a distance equal and parallel to any cell edge, or by any combinations of such movements we arrive at a point where the whole surrounding structure has the same form and orientation as at the point from which we started. But the spacings between planes with which x-rays are concerned need not refer only to the perpendicular distance between opposite faces, edges, or corners of the unit cell.

Thus, every effective interplanar spacing must represent some fraction of the effective dimension of the unit cell in the direction considered, *i.e.*, if the effective, or repeating, dimension of the unit cell in one direction may be designated d , possible x-ray interferences may occur only for those positions with an interplanar spacing d/n where n is an integer. The expression d/n suggests the use of analogous fractions already mentioned which indicate the intercepts of the plane, a_0/h , b_0/k and c_0/l where a_0 , b_0 , and c_0 are the edge lengths of the unit cell and h , k , and l are integers, representing the number of parts into which each edge is divided.

By doubling the values of h , k , and l we double the number of equal divisions along each edge of the unit cell; thus we have a given interplanar spacing of interest, and the condition is exactly the same as though we had considered the second order of the original plane. This permits us to simplify our x-ray investigations by completely disregarding n , the quantity for order in the Bragg formula, and using suitable hkl values to designate all reflections (the hkl corresponds to a plane that would produce a given reflection on a pattern whether such a plane actually exists in the physical sense or not). Thus an x-ray interference

may be identified as related to 200 planes as if these had real existence whereas actually the reflection is the second order from the 100 planes.

5. *Symmetry and Point-groups.*—To the systematic classification into six crystal systems, the experimentally founded law of

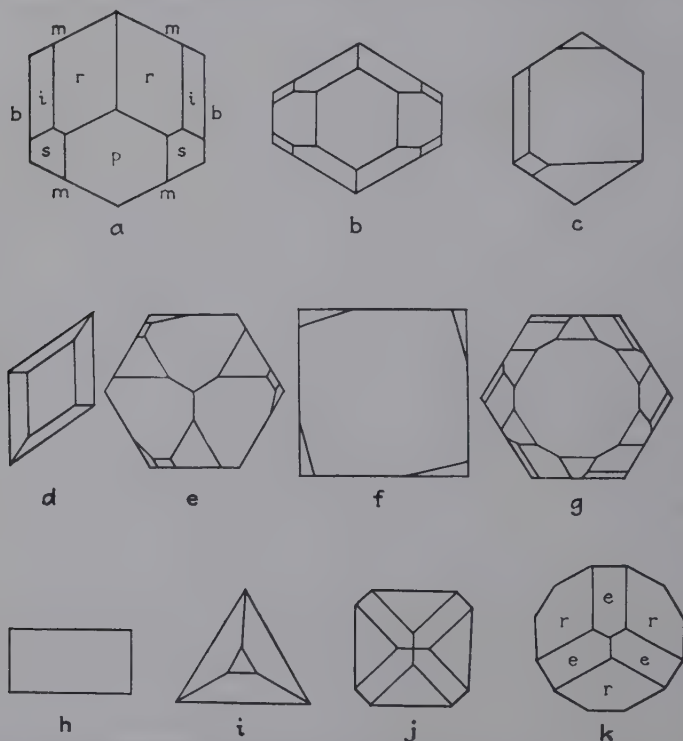


FIG. 122.—Ornamental figures illustrating crystal symmetry: *a*, plane of symmetry, hornblende; *b*, two planes of symmetry, aragonite; *c*, ornament with a plane of symmetry; *d*, twofold axis of symmetry, gypsum; *e*, threefold axis of symmetry, quartz; *f*, fourfold axis of symmetry, wulfenite; *g*, sixfold axis of symmetry, apatite; *h*, ornament with mirror and rhythmic symmetry; *i*, planes of symmetry and threefold axis, tourmaline; *j*, planes of symmetry and fourfold axis, tinstone; *k*, planes of symmetry with threefold rhythmic symmetry calcite. (After Schiebold.)

rational indices, and the consequent hypothesis of space lattices may be added other types of information affording an approach to the subject of symmetry. Some of these are velocity of solution of different crystal faces, etch figures, birefringence, optical activity, piezo- and pyroelectric properties. In general, it might be expected that two crystals which gave identical

measurements of angles between faces indicating identical disposition of planes should also have identical properties. It soon becomes evident, however, that the formal classification of crystals thus made has not been extended far enough. Mark¹ points out that angle measurements class both barium antimonyl tartrate and calcium molybdate as tetragonal, but this in no sense explains why one has optical activity and the other has not. Account, therefore, must be taken of different symmetries.

The symmetry of an object is an expression of the fact that the object has equal properties in different directions. Two positions of a crystal, in which the equivalent directions may be brought into coincidence, say, by a simple rotation around an axis, are not distinguishable by any physical-chemical means. Now the following symmetry operations may be performed to bring equivalent points in space into coincidence:

a. Axes of symmetry (cyclic operation). Points in crystals may have one-, two-, three-, four-, or sixfold axes by which is meant coincidence of equivalent points by rotation of 360 (every point has this identity operation), 180, 120, 90, or 60 deg. The fact that there is no five- or sevenfold axis is further indication of a space-lattice structure.

b. Plane of symmetry (mirror operation), in which points on one side of a plane are mirror images of points on the other.

c. Center of symmetry or a combined rotation and reflection across a plane perpendicular to the axis.

These symmetry elements are well illustrated by the ornamental figures selected by Schiebold, shown in Fig. 122. The symmetry planes, axes, and center for the highest form of cubic symmetry are illustrated in Fig. 123. These elements are:

1. Fourfold axes [100].
2. Threefold axes [111].
3. Twofold axes [110].

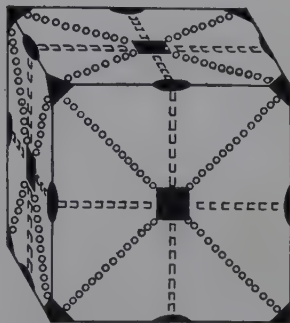


FIG. 123.—Symmetry elements in a cubic crystal; squares, fourfold axes; triangles, threefold; ellipses, twofold.

¹ *Z. Metallkunde*, **20**, 342 (1928).

4. Reflection planes [100].
5. Reflection planes [110].
6. Center of inversion.

When now these symmetry operations are combined in every possible way, using the six systems of coordinates, it develops that there are 32 point-groups which define 32 crystal classes in terms of symmetry. A combination of goniometric and physical measurements makes it possible to classify crystals as to system and as to the finer subdivision of class or point-group. But it is to be observed that this is still a macroclassification, and the idea of the lattice, except as an explanatory hypothesis, or of the ultimate units from which crystals are built does not enter in. For by definition all the symmetry elements of each point-group are associated with a single central point and translation is impossible.

6. *Space-groups*.—The final step in the further refining of classification of crystals was taken as a result of the work of Schoenflies in 1890, with the three-dimensional lattice theory and the idea of atoms at the points of the lattice as a basis. In other words, by combining the 32 classes of symmetry around a point with translation in three directions to other equivalent points, arranged according to a definite spatial pattern (the lattice), at a distance of the order of 10^{-8} cm. or atomic dimensions apart, other symmetry operations involving this translation become evident, namely, two-, three-, four-, and sixfold *screw* axes of symmetry, involving rotations about and translations along an axis, and glide planes of symmetry in which a figure is brought into coincidence by reflection in a plane combined with translation of a definite length and direction in the plane. These were called by Schoenflies "microscopic symmetry elements." When these are included in the process of placing each of the 32 point-groups at the points of the 14 lattices, the result is a total of 230 combinations, or *space-groups*.

It must be remembered that if the space-group has a screw axis the point-group has a corresponding rotation axis. The *macroscopic* properties of the crystal cannot distinguish between screw or rotation. Similarly reflection and glide planes both correspond to the reflection planes of the point-group. The translation that accompanies the rotation or reflection is immaterial to the symmetry of the crystal considered as a single unit.

Thus a space-group is an extended network of reflection planes, glide planes, rotation axes, screw axes, axes of rotating inversion, and symmetry centers, based on a space lattice. Its operations are self-consistent in that each operation or translation brings all the others into self-coincidence. Copper and diamond both have the same holohedral cubic point-group; but they represent 2 of 10 entirely different space-groups. Whereas copper has the symmetry elements for the cube in Fig. 123, diamond has four-fold *screw* axes and *glide* planes, as illustrated in Fig. 124.

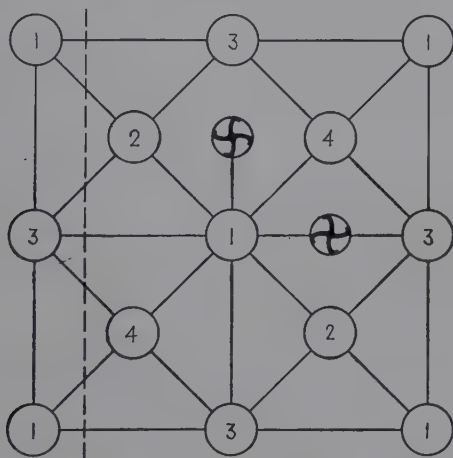


FIG. 124.—Glide planes and screw axes of the diamond structure. Atoms marked (1) are on the lower face of the cubic unit cell and repeat again in the upper face. If the cube edge is denoted by a , atoms marked (2), (3), and (4) are at heights $a/4$, $a/2$, $3a/4$, respectively.

It is obvious that the classification of a crystal by its space-group is unique. X-ray diffraction analysis alone has made possible this last refinement in classification and has verified the geometrical theory of space-groups. Conversely the theory of space-groups is an indispensable tool to the x-ray analyst. For each space-group is distinguished by certain definite x-ray diffraction criteria, which are discovered in the course of interpretation of patterns, as will be illustrated in the next chapter.

7. Space-group Notation.—The 230 space-groups have been designated for many years by the symbols proposed by Schoenflies. A symbol was assigned to each point-group, such as C_{2h} for monoclinic holohedral, O_h for cubic holohedral, etc. The space-groups in each class are designated by indices, such as

C_{2h}^1 , C_{2h}^2 , etc. Subsequently, Wyckoff proposed an improved notation. A far more rational system has been suggested recently by Hermann and Mauguin, and this has been adopted internationally now by all x-ray workers and is employed in the standard "Internationale Tabellen zur Bestimmung von Kristallstrukturen" (1935). The symbolism of the Hermann-Mauguin method is built upon two principles: (1) a symbol for the translation group (which involves such translations of a fundamental group as are necessary to build the crystal lattice) and (2) one to three symbols for the elements of symmetry that lie along special directions in the crystal system of interest.

a. Translation Groups.—The translation group furnishes a picture of the method in which groups are distributed throughout space to give the three-dimensional lattice necessary for the description of the crystal. Such translations simply consist of taking some point in the unit cell (identified by its symmetry) and arranging like points throughout space to give the crystal. Such arrangements of points may be considered to designate a number of unit cells.

These translation groups are represented by capital letters; each precedes the section used to describe it.

P—denotes the simply primitive translation group, *i.e.*, such a group as can be represented with the aid of a cell that is as nearly rectangular as possible. A *P* cell has the property that all elements of symmetry of the same kind belonging to one axial direction have gliding components equal to each other.

C—the *c*-face-centered cell. The point $\frac{1}{2} \frac{1}{2} 0$ is equivalent to the corner point of the cell, 0 0 0. This symbol serves to denote the hexagonal translation group also, since the group can be referred to a rectangular cell with its base face-centered, and the axial ratio $a:b = 1:(3)^{\frac{1}{2}}$ (orthorhombic cell).

A—*a*-face-centered cell, analogous to *C*.

B—*b*-face-centered cell, analogous to *C*.

H—hexagonal cell similar to *C*, but having the inverse axial ratio.

I—body-centered cell. The mid-point $\frac{1}{2} \frac{1}{2} \frac{1}{2}$ is equivalent to the corner 0 0 0.

F—A lattice with all faces face-centered (the smallest rectangular cell is already quadruply primitive). Here $0 \frac{1}{2} \frac{1}{2}$, $\frac{1}{2} 0 \frac{1}{2}$, and $\frac{1}{2} \frac{1}{2} 0$ are equivalent to 0 0 0.

R—the rhombohedral cell, which can be based upon a rectangular one only by using the axial ratio given above. In this case $\frac{1}{2} \frac{1}{2} 0$, $0 \frac{2}{3} \frac{2}{3}$, $\frac{1}{2} \frac{2}{3} \frac{1}{3}$, $\frac{1}{2} \frac{1}{6} \frac{2}{3}$ are equivalent to 0 0 0. This cell is a sextuply primitive one.

After the lattice has been described by the first symbol of the symmetry expression, one to three other symbols are given for

the elements of symmetry which lie along special directions in the crystal system. The special directions are:

Monoclinic system. The orthoaxis (b direction).

Orthorhombic system. The directions of the three mutually perpendicular axes.

Tetragonal system. The "principal axis" (c direction), the secondary axis (a direction) perpendicular to this, and the tertiary axis which is also perpendicular to the principal axis and cuts the secondary axis at 45 deg.

Trigonal and hexagonal systems. The principal axis (c) and secondary and tertiary axes as above, which here form an angle of 30 deg.

The elements of symmetry, with their designations, and the commonly used symbols (both for symmetry terms and for graphical designation) are listed in Table XXX and Figs. 125 and 126, with examples of each.

b. Pure Rotation Axes.—Axes of symmetry usually operate in such a way that after a rotation of $2\pi/p$ (where $p = 2, 3, 4$, or 6) the crystal comes into a congruent position.

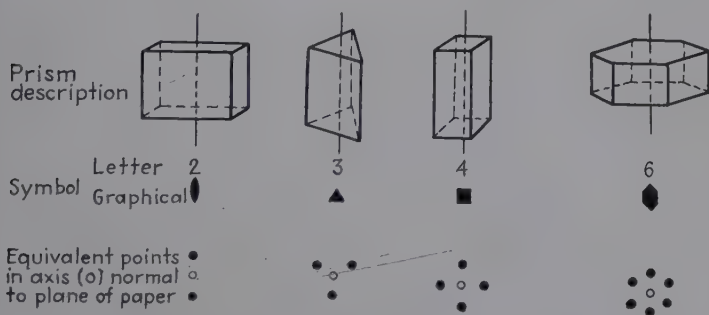


FIG. 125.—Prism description, symbol, and equivalent points defining rotation axes.

The symbols for these pure rotation axes are numbers that denote their multiplicity, 2-, 3-, 4-, or 6-fold axes of rotation. The number 1 is used to indicate that the direction represented includes no element of symmetry. In Fig. 125 is shown first a prism with an axis vertical, the axis being designated below. Below this graphical definition is shown the symmetry of the axis in a plane normal to the axis. In this case the plane is the plane of the paper, and we are looking down the axis of symmetry.

With the pure rotation axis, the equivalent points are all included in a common plane, which stands normal to the rotation

axis. This suggests consideration of the rotation axis where the points are at different elevations above a reference plane.

c. Screw Axes.—The screw axis is designated p_q ; p denotes a p -fold axis of rotation associated with a translation in such a manner that for each rotation of $2\pi/p$ there is a displacement of

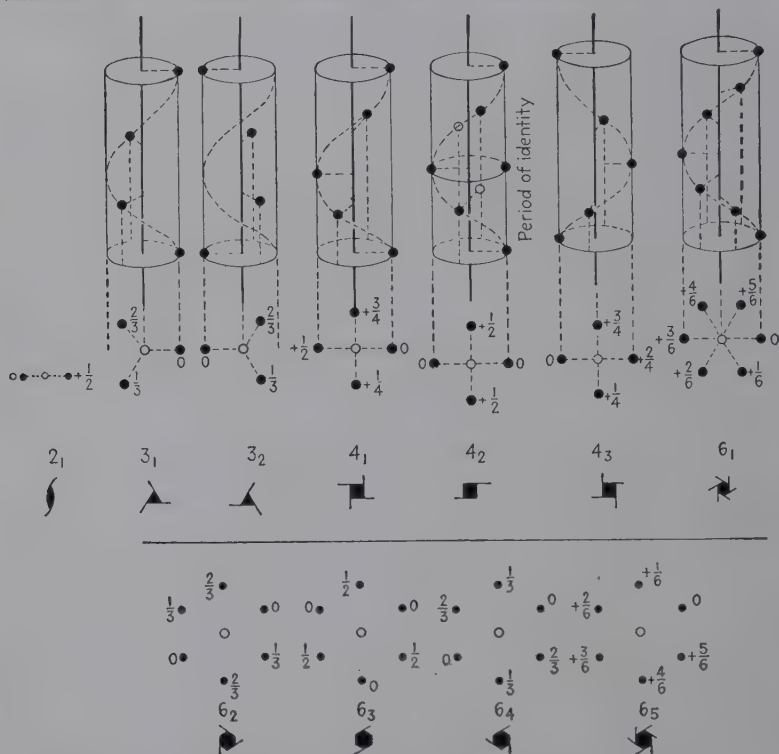


FIG. 126.—Description, symbols, and equivalent points for screw axes.

q/p of the shortest translation parallel to the axis. The following screw axes exist:

$$2_1, 3_1, 3_2, 4_1, 4_2, 4_3, 6_1, 6_2, 6_3, 6_4, 6_5.$$

These are illustrated in Fig. 126. In those figures where the axis is designated by (O) , it stands normal to the plane of the paper, and fractions indicate the distance of the point above the paper.

Two axes having the same principal number and the sum of whose indices is equal to the principal number stand to each other in an enantiomorphic relation (see Fig. 126). Only the axes 2_1 , 4_2 , and 6_3 are enantiomorphic with themselves and

fundamentally they represent a rotation of 180, 90, or 60 deg., respectively, combined with a displacement of half the shortest translation parallel to the axis. The axis 4_2 is a 2-fold axis; the axis 6_3 is a 3-fold axis, as pure rotation axes; the screw character of these axes can only be recognized when the full multiplicity is examined.

d. Rotary Inversions.—These are termed symmetry elements of the second kind. They operate in such a way that after a rotation through $2\pi/p$ the edges, corners, and faces must be inverted through the origin to bring them into congruence with the original position of the crystal.

They may be regarded as a combination of rotation and reflection at a center of symmetry. If the axis of rotation involved has an odd multiplicity, it is found on continued repetition of the elementary operations that the multiplicity of the axis of rotary inversion is double that of the rotation axis and contains this rotation axis and a center of symmetry as subgroups (ultimate elements). If the multiplicity of the rotation axis is even, that of the corresponding rotary inversion axis has the same value. If the multiplicity is divisible by 4, the axis of rotary inversion is a symmetry element incapable of further reduction.

The axis of rotary inversion is denoted by a stroke above the symbol of the corresponding rotation axis. Thus we have:

$\bar{1}$ —the center of symmetry (2-fold element of symmetry).

$\bar{2}$ —a 2-fold axis of rotary inversion; equivalent to a reflection plane. A reflection plane is given another symbol, however, on account of numerous possibilities of glide components (see next paragraph).

$\bar{3}$ —a 3-fold axis with center of symmetry (6-fold element of symmetry).

$\bar{4}$ —a 4-fold rotation-reflection axis; a 4-fold irreducible element of symmetry.

$\bar{6}$ —a 3-fold rotation axis with perpendicular reflection plane (6-fold element of symmetry).

e. Reflection Planes.—When a plane of symmetry is present, every corner, edge, and face has a corresponding corner, edge, or face bearing a mirror-image relation to it, the mirror coinciding with the plane of symmetry.

m (mirror)—signifies the simple reflection plane.

a, *b*, or *c*—a glide reflection plane with a glide of $\frac{1}{2}a$, $\frac{1}{2}b$, or $\frac{1}{2}c$ is simply given the corresponding symbol.

n—a glide plane with a glide of $\frac{1}{2}(b + c)$, $\frac{1}{2}(a + b)$, etc., is called *n* because by connecting a point to all its equivalent neighbors (into which it is transformed by this operation) a net is formed.

d -glide reflection planes with a glide of $\frac{1}{4}(b+c)$, etc. Called d because of the diagonally arranged construction leading in this case to diagonally arranged chains, just as in the case of a , b , or c it leads to chains running parallel to the direction of the axis. A d plane involves equivalence of the mid-point and corner of the parallelogram built up of the two elementary translations parallel to the reflection plane; d planes can, therefore, exist only parallel to centered faces.

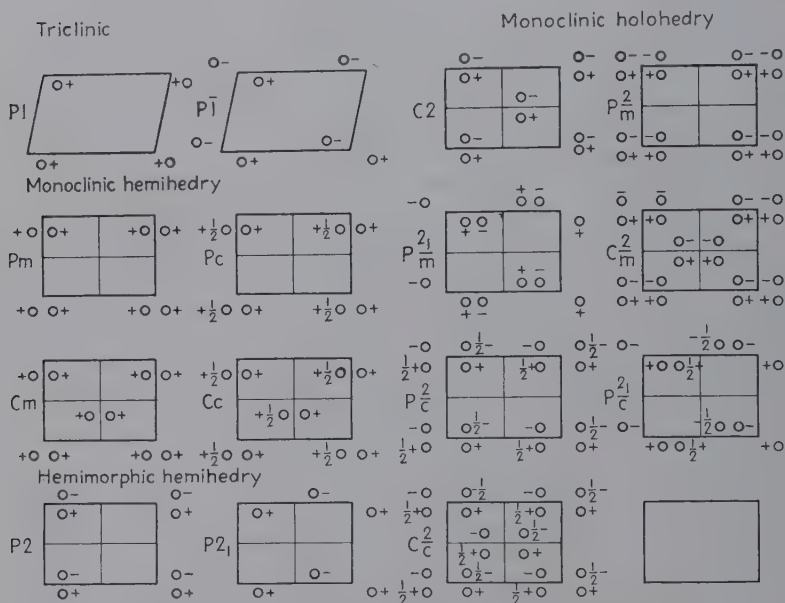


FIG. 127.—Projections illustrating symmetry characteristics of triclinic and monoclinic space-groups.

In the symbol for rhombic holohedry the three 2-fold axes follow directly from the reflection planes, *e.g.*, the 2-fold axis in the x direction from the two reflection planes perpendicular to the y and z directions, etc. The whole crystal class and likewise all space-groups isomorphous with it can be characterized merely by the reflection planes; as symbol mmm is sufficient. In the tetragonal and hexagonal holohedry a specification of the nature of the principal axes (rotation or screw axis) can be omitted, since this follows directly from the glide components of the generating reflection planes.¹

¹ A more thorough treatment may be found in *Z. Krist.*, **68**, 257; **69**, 226 (1928).

The crystal class isomorphous with any space-group is obtained by omitting the translation symbol and replacing all screw axes by the corresponding rotation axes, and all glide reflection planes by m planes.

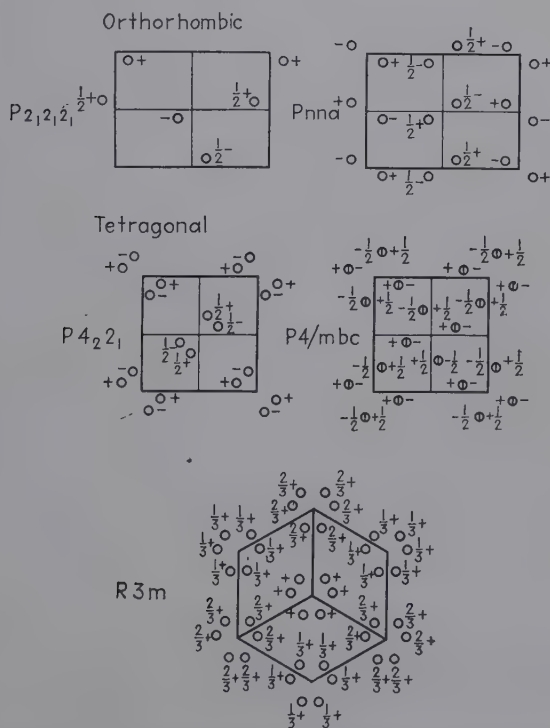


FIG. 128.—Selected examples of orthorhombic, tetragonal, and hexagonal space-groups.

The symbols are written in the following order:

- (1) Translation groups.
- (2) Symbols for special directions.

In Figs. 127 and 128 are presented examples of several of the different space-groups (all triclinic and monoclinic are included, with representatives of other important types of combination of symmetry groups).

Steps in the X-ray Analysis of Crystal Structures.—Regardless of the experimental method of analysis (considered in the next chapter), the information vouchsafed by interference patterns of crystals is essentially the same. This is the determination

TABLE XXX.—SPACE-GROUPS

| | |
|--|--|
| C_1 —triclinic hemihedry. 1 | D_2 —orthorhombic enantiomorphic hemihedry. 222 |
| 1. $P1$ | 1. $P222$ |
| C_3 —triclinic holohedry. $\bar{1}$ | 2. $P222_1$ |
| 1. $P\bar{1}$ | 3. $P2_12_12$ |
| C_s —monoclinic hemihedry. m | 4. $P2_12_12_1$ |
| 1. Pm | 5. $C222_1$ |
| 2. Pc | 6. $C222$ |
| 3. Cm | 7. $F222$ |
| 4. Cc | 8. $I222$ |
| C_2 —monoclinic hemimorphic hemihedry. 2 | 9. $I2_12_12_1$ |
| 1. $P2$ | D_{2h} —orthorhombic holohedry. mmm |
| 2. $P2_1$ | 1. $Pmmm$ |
| 3. $C2$ | 2. $Pnnn$ |
| C_{2h} —monoclinic holohedry. $2/m$ | 3. $Pccm$ |
| 1. $P2/m$ | 4. $Pban$ |
| 2. $P2_1/m$ | 5. $Pmma$ |
| 3. $C2/m$ | 6. $Pnna$ |
| 4. $P2/c$ | 7. $Pmna$ |
| 5. $P2_1/c$ | 8. $Pcca$ |
| 6. $C2/c$ | 9. $Pbam$ |
| C_{2v} —orthorhombic hemimorphic hemihedry. mm | 10. $Pccn$ |
| 1. Pmm | 11. $Pbcm$ |
| 2. Pmc | 12. $Pnnm$ |
| 3. Pcc | 13. $Pmmn$ |
| 4. Pma | 14. $Pbcn$ |
| 5. Pca | 15. $Pbca$ |
| 6. Pnc | 16. $Pnma$ |
| 7. Pmn | 17. $Cmcm$ |
| 8. Pba | 18. $Cmca$ |
| 9. Pna | 19. $Cmmm$ |
| 10. Pnn | 20. $Cccm$ |
| 11. Cmm | 21. $Cmma$ |
| 12. Cmc | 22. $Ccca$ |
| 13. Ccc | 23. $Fmmm$ |
| 14. Amm | 24. $Fddd$ |
| 15. Abm | 25. $Immm$ |
| 16. Ama | 26. $Ibam$ |
| 17. Aba | 27. $Ibca$ |
| 18. Fmm | 28. $Imma$ |
| 19. Fdd | S_4 —tetragonal tetartohedry, second kind. $\bar{4}$ |
| 20. Imm | 1. $P\bar{4}$ |
| 21. Iba | 2. $I\bar{4}$ |
| 22. Ima | |

TABLE XXX.—SPACE-GROUPS.—(Continued)

| | | |
|--|--|--|
| C_4 —tetragonal tetartohedry. 4 | | 6. $P4_22_1$ ($C4_22_1$) |
| 1. $P4$ ($C4$) | | 7. $P4_32$ ($C4_322$) |
| 2. $P4_1$ ($C4_1$) | | 8. $P4_32_1$ ($C4_322_1$) |
| 3. $P4_2$ ($C4_2$) | | 9. $I42$ ($F42$) |
| 4. $P4_3$ ($C4_3$) | | 10. $I4_12$ ($F4_12$) |
| 5. $I4$ | | D_{4h} —tetragonal holohedry. |
| 6. $I4_1$ | | 4/ mmm |
| C_{4h} —tetragonal paramorphic hemi- | | 1. $P4/mmm$ |
| hedry. 4/ m | | 2. $P4/mcc$ |
| 1. $P4/m$ 4. $P4_2/n$ | | 3. $P4/nbm$ |
| 2. $P4_2/m$ 5. $I4/m$ | | 4. $P4/nnc$ ($C4/acn$) |
| 3. $P4/n$ 6. $I4_1/a$ | | 5. $P4/mbm$ ($C4/mmb$) |
| $D_{2d}(V_d)$ —tetragonal hemihedry, | | 6. $P4/mnc$ ($C4/mcn$) |
| second kind. $\bar{4}2m$ | | 7. $P4/nmm$ ($C4/amm$) |
| 1. $P\bar{4}2m$ ($C\bar{4}m2$) | | 8. $P4/ncc$ ($C4/acc$) |
| 2. $P\bar{4}2c$ ($C\bar{4}c2$) | | 9. $P4/mmc$ ($C4/mcm$) |
| 3. $P\bar{4}2_1m$ ($C\bar{4}m2_1$) | | 10. $P4/mcm$ ($C4/mmc$) |
| 4. $P\bar{4}2_1c$ ($C\bar{4}c2_1$) | | 11. $P4/nbc$ ($C4/acb$) |
| 5. $C\bar{4}2m$ ($P\bar{4}m2$) | | 12. $P4/nnm$ ($C4/amn$) |
| 6. $C\bar{4}2c$ ($P\bar{4}c2$) | | 13. $P4/mbc$ ($C4/mcb$) |
| 7. $C\bar{4}2b$ ($P\bar{4}b2$) | | 14. $P4/mnm$ ($C4/mnm$) |
| 8. $C\bar{4}2n$ ($P\bar{4}n2$) | | 15. $P4/nmc$ ($C4/acm$) |
| 9. $F\bar{4}2m$ ($I\bar{4}m2$) | | 16. $P4/ncm$ ($C4/amc$) |
| 10. $F\bar{4}2c$ ($I\bar{4}c2$) | | 17. $I4/mmm$ ($F4/mmm$) |
| 11. $I\bar{4}2m$ ($F\bar{4}m2$) | | 18. $I4/mcm$ ($F4/mmc$) |
| 12. $I\bar{4}2d$ ($F\bar{4}d2$) | | 19. $I4/amd$ ($F4/ddm$) |
| C_{4v} —tetragonal hemimorphic hemi- | | 20. $I4/acd$ ($F4/ddc$) |
| hedry. 4 mm | | C_3 —rhombohedral tetartohedry. 3 |
| 1. $P4mm$ | | 1. $C3$ 3. $C3_2$ |
| 2. $P4bm$ | | 2. $C3_1$ 4. $R3$ |
| 3. $P4cm$ | | C_{3i} —hexagonal tetartohedry, sec- |
| 4. $P4nm$ | | ond kind. $\bar{3}$ |
| 5. $P4cc$ | | 1. $C\bar{3}$ |
| 6. $P4nc$ ($C4cn$) | | 2. $R\bar{3}$ |
| 7. $P4mc$ ($C4cm$) | | C_{3v} —rhombohedral hemimorphic |
| 8. $P4bc$ ($C4cb$) | | hemihedry. 3 m |
| 9. $I4mm$ ($F4mm$) | | 1. $C3m$ ($H31m$) |
| 10. $I4cm$ ($F4mc$) | | 2. $H3m$ ($H3m1$) ($C31m$) |
| 11. $I4md$ ($F4dm$) | | 3. $C3c$ ($C3c1$) ($H31c$) |
| 12. $I4cd$ ($F4dc$) | | 4. $H3c$ ($H3c1$) ($C31c$) |
| D_4 —tetragonal enantiomorphic | | 5. $R3m$ |
| hemihedry. 42 | | 6. $R3c$ |
| 1. $P42$ | | D_3 —rhombohedral enantiomorphic |
| 2. $P42_1$ | | hemihedry. 32 |
| 3. $P4_12$ | | 1. $H32$ ($H321$) ($C312$) |
| 4. $P4_12_1$ ($C4_122_1$) | | 2. $C32$ ($C321$) ($H312$) |
| 5. $P4_22$ ($C4_222$) | | 3. $H3_12$ ($H3_121$) ($C3_112$) |

TABLE XXX.—SPACE-GROUPS.—(Continued)

| | |
|---|---|
| 4. $C_{31}2$ ($C_{31}21$) ($H_{31}12$) | 1. $C6/mmm$ ($H6/mmm$) |
| 5. $H_{32}2$ ($H_{32}21$) ($C_{32}12$) | 2. $C6/mcc$ ($H6/mcc$) |
| 6. $C_{32}2$ ($C_{32}21$) ($H_{32}12$) | 3. $C6/mcm$ ($H6/mmc$) |
| 7. $R32$ | 4. $C6/mmc$ ($H6/mcm$) |
| D_{3d} —rhombohedral holohedry. $\bar{3}m$ | T —cubic tetartohedry. 23 |
| 1. $H\bar{3}m$ ($H\bar{3}m1$) ($C\bar{3}1m$) | 1. $P23$ |
| 2. $H\bar{3}c$ ($H\bar{3}c1$) ($C\bar{3}1c$) | 2. $F23$ |
| 3. $C\bar{3}m$ ($C\bar{3}m1$) ($H\bar{3}1m$) | 3. $I23$ |
| 4. $C\bar{3}c$ ($C\bar{3}c1$) ($H\bar{3}1c$) | 4. $P2_13$ |
| 5. $R\bar{3}m$ | 5. $I2_13$ |
| 6. $R\bar{3}c$ | T_h —cubic paramorphic hemihedry. $m\bar{3}$ |
| C_{3h} —trigonal paramorphic hemihedry. $\bar{6}$ | 1. $Pm\bar{3}$ |
| 1. $C\bar{6}$ ($H\bar{6}$) | 2. $Pn\bar{3}$ |
| C_6 —hexagonal tetartohedry. 6 | 3. $Fm\bar{3}$ |
| 1. $C6$ ($H6$) | 4. $Fd\bar{3}$ |
| 2. $C6_1$ ($H6_1$) | 5. $Im\bar{3}$ |
| 3. $C6_5$ ($H6_5$) | 6. $Pa\bar{3}$ |
| 4. $C6_2$ ($H6_2$) | 7. $Ia\bar{3}$ |
| 5. $C6_4$ ($H6_4$) | T_d —cubic hemimorphic hemihedry. $\bar{4}3m$ |
| 6. $C6_3$ ($H6_3$) | 1. $P\bar{4}3m$ |
| C_{6h} —hexagonal paramorphic hemihedry. $6/m$ | 2. $F\bar{4}3m$ |
| 1. $C6/m$ ($H6/m$) | 3. $I\bar{4}3m$ |
| 2. $C6_3/m$ ($H6_3/m$) | 4. $P\bar{4}3n$ |
| D_{3h} —trigonal holohedry. $\bar{6}m2$ | 5. $F\bar{4}3c$ |
| 1. $C\bar{6}m2$ ($H\bar{6}2m$) | 6. $I\bar{4}3d$ |
| 2. $C\bar{6}c2$ ($H\bar{6}2c$) (given as $c2$ in "International Critical Tables") | O —cubic enantiomorphic hemihedry. 43 |
| 3. $H\bar{6}m2$ ($C\bar{6}2m$) | 1. $P43$ |
| 4. $H\bar{6}c2$ ($C\bar{6}2c$) | 2. $P4_23$ |
| C_{6v} —hexagonal hemimorphic hemihedry. $6mm$ | 3. $F43$ |
| 1. $C6mm$ ($H6mm$) | 4. $F4_13$ |
| 2. $C6cc$ ($H6cc$) | 5. $I43$ |
| 3. $C6cm$ ($H6mc$) | 6. $P4_33$ |
| 4. $C6mc$ ($H6cm$) | 7. $P4_13$ |
| D_6 —hexagonal enantiomorphic hemihedry. 62 | 8. $I4_13$ |
| 1. $C62$ ($H62$) | O_h —cubic holohedry. $m\bar{3}m$ |
| 2. $C6_12$ ($H6_12$) | 1. $Pm\bar{3}m$ |
| 3. $C6_52$ ($H6_52$) | 2. $Pn\bar{3}n$ |
| 4. $C6_22$ ($H6_22$) | 3. $Pm\bar{3}n$ |
| 5. $C6_42$ ($H6_42$) | 4. $Pn\bar{3}m$ |
| 6. $C6_32$ ($H6_32$) | 5. $Fm\bar{3}m$ |
| D_{6h} —hexagonal holohedry. $6/mmm$ | 6. $Fm\bar{3}c$ |
| | 7. $Fd\bar{3}m$ |
| | 8. $Fd\bar{3}c$ |
| | 9. $Im\bar{3}m$ |
| | 10. $Ia\bar{3}d$ |

of a series of values of d for different sets of planes by use of the Bragg equation. Now, if a crystal is really a lattice, it follows that planes of three sets in the principal directions will enclose a small unit cell—the smallest possible subdivision which has the properties of the visible macrocrystal and which by repetition or translation of itself in all directions actually builds the crystal. It is the size of this fundamental architectural unit that may be determined directly from the experimental values of d_1 , d_2 , and d_3 —the respective edge lengths of the small parallelepiped. This presupposes some previous information about the crystallographic system, whether the axes are at right angles or not or are of equal length or not. As previously indicated, this may easily be obtained by goniometer measurements of angles between faces. But if optical data are not available, the angles between the axes and axial ratios may be measured by reflection of x-rays from a crystal mounted on a goniometer head just as readily as by the optical method. Assuming this to be the process employed, the steps in analysis are as follows:

1. Goniometric determination of crystallographic system.
2. Determination of dimensions and volume of unit cell.
3. Determination of the number of atoms or molecules in each unit cell. This involves a measurement of the density of the crystal and the use of the volume of the unit cell in the following formula:

$$n = \frac{\rho V}{Mm},$$

where n is the number of atoms (of an element) or molecules per unit cell; ρ is the density; V is the volume of the unit cell (d^3 for a cubic crystal, or, in general,

$$V = abc\sqrt{\sin^2 \alpha + \sin^2 \beta + \sin^2 \gamma - 2(1 - \cos \alpha \cos \beta \cos \gamma)},$$

where a , b , and c are edge lengths, and α , β , and γ the angles enclosed by the edges); M is the atomic or molecular weight; and m is the absolute weight of the hydrogen atom (1.663×10^{-24} gram).

4. Identification of interference maxima with the indices of planes.

5. Application of the theory of space-groups. Each of these space-groups is characterized by certain diffraction criteria, to

be considered in Chap. XIV, such as the apparent halving of spacings due to nonappearance of odd-order ($n = 1, 3, 5$, etc.) interferences. Screw axes and glide planes can be detected.

6. Determination of the symmetry of the molecule from the space-group of the crystal, the number of entirely unsymmetrical molecules theoretically required, and the number of molecules per unit cell actually found.

7. An analysis of the structure factor from intensity measurements, defining the positions within the unit cell of the diffracting centers, and even of the symmetry and positions of atoms in molecules if these are the lattice units. This is the most difficult, least direct, and yet the most interesting stage in crystal analysis. Briefly put, the process consists in assuming certain values for parameters and upon the basis of known laws of scattering and interference in calculating from these the theoretical intensity of reflections from a set of planes. These results are compared with observed intensities, and the process of trial and error is continued until there is an agreement. Bernal has likened the process to the solution of a crossword puzzle. The cell and space-group provide the square and pattern, the atoms the letters, and the intensities the clues. A more elegant method is the use of Fourier equations for the calculation of the distribution of electrons and thus unique atomic positions in unit cells.

8. A coordination and test of the completed structure with other known physical and chemical properties, such as atomic or ionic radii, optical activity, and polarization.

Types of Information Obtainable from X-ray Diffraction Data.—From the foregoing development of the subject it might be concluded that the lattice-type and unit-cell dimensions of crystals, together with the consequent explanation of certain properties, are the only facts to be gained from x-ray diffraction data. Suppose that we know that a whole series of samples of metal has exactly the same lattice structure, characteristic of iron or copper, etc. Is there any further differentiation possible upon the basis of x-ray diffraction patterns?

The dependence of x-ray interferences upon the condition as well as the kind of lattice makes it possible to detect very minute changes in atomic position or in lattice constituents. Consequently a fund of purely scientific and technological information

is obtained from this fine-structure method which is almost universal in its scope.

Following is a tabulation of the principal types of information, each of which will receive discussion:

1. Crystalline or noncrystalline.
2. Crystallographic system, unit-cell dimensions, space-group, parameters of atoms or molecules.
3. Deduction of crystal unit (atom, ion, molecule), of size of unit, of type of binding, and of general properties of solid to be expected.
4. Chemical identity, chemical and crystallographic changes and stability.
5. Allotropic modifications.
6. Type and mechanism of alloy formation.
7. Single crystal or aggregate.
8. Crystallographic orientation of single crystal or of grains in aggregate.
9. Random or fibered aggregate and relative degree of preferred orientation in intermediate stages.
10. Grain size in an aggregate (particularly in colloidal range).
11. Internal strain or distortion.
12. Extent of deformation and mechanism of fabrication in rolling, drawing, etc.
13. Analysis of effect of heat-treatment, grain growth, control and mechanism of recrystallization, and the establishment of scientifically correct annealing technique.
14. Differentiation between surface and interior structure, and film structure.
15. Atomic distribution in liquids and glasses.
16. The nature of substances with very high molecular weights.

CHAPTER XIII

THE EXPERIMENTAL X-RAY METHODS OF CRYSTAL ANALYSIS

The several methods of analysis of crystal structure by x-rays involve the following essential differences: single crystals or powders; monochromatic or polychromatic x-rays; photographic or ionization-current registration; and reflection or diffraction from a single set of parallel planes or from many different sets simultaneously. It is evident, therefore, that the information obtained will differ somewhat, depending upon the combination of these variables. The proper selection of the method for the material under investigation and for the type of information wanted is of utmost importance. To this end the five more important methods have been compared and contrasted in tabular form (Table XXXI) under the heads: kind of x-ray, beam definition, specimen (single crystal or powder), mounting, method of registration, pattern, interpretation, chief uses, modifications. Representative photographs or ionization-current curves obtained by each method are shown in this and other chapters.

Special Notes on Apparatus. 1. *The Laue Method.*—The experimental equipment here is relatively so simple, as shown in Fig. 129, that little additional explanation is required. Typical Laue patterns are illustrated in Figs. 130 and 131. The design and construction of the pinhole for defining the beam are most important. With a single orifice, of course, a pinhole image of the target is obtained by the pinhole camera effect. The longer the collimator, which is simply a pinhole in a solid block or two apertures in metal plates separated by a fixed distance, the more nearly parallel is the x-ray beam. The diameter of the pinhole is of importance from the standpoint of detail in the diffraction pattern. The interferences become sharper the smaller the diameter.

On the other hand, the time of exposure increases with increase in length or decrease in diameter. For average purposes a size of 0.025 in. is satisfactory, although a range from 0.005 to

0.060 in. for various specimens is desirable. Voltages are usually not higher than 60,000 volts, since higher values merely compli-

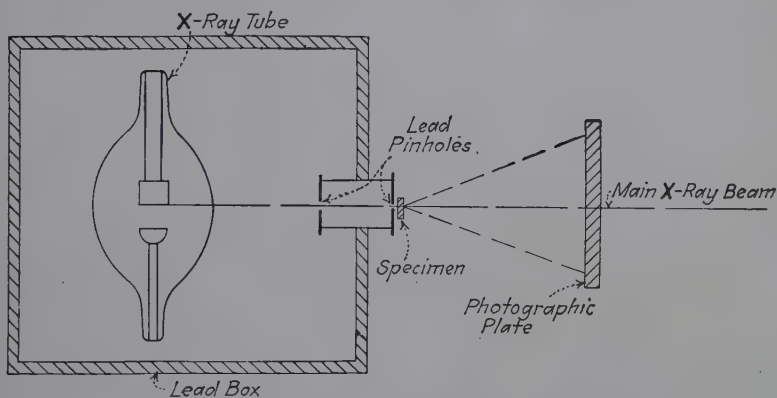


FIG. 129.—Diagram of the Laue and monochromatic pinhole x-ray methods.



FIG. 130.—Symmetrical Laue pattern of an iron crystal.

cate the range of wave lengths which in this method are unknown except in so far as there is a short wave-length limit corresponding

TABLE XXXI.—EXPERIMENTAL DIFFRACTION METHODS

| Method | Laue | Bragg | Rotating crystal (Schiebold-Polanyi) goniometer | Powder (Hull-Debye-Scherrer) | Monochromatic pinhole (fiber) |
|---|---|---|--|--|--|
| X-ray beam..... Beam definition..... | Polychromatic Pinhole (Fig. 129 with- out filter) | Monochromatic Slit | Monochromatic Pinhole usually; also wedge with knife-edge on crystal face | Monochromatic Hull, slit; Debye- Scherrer pinhole | Monochromatic Pinhole (Fig. 129 with filter) |
| Specimen..... | Single crystal | Single crystal or film of oriented molecules | Single crystal | Powder or random ag- gregate | Any—fibers particularly |
| Mounting..... | Fixed according to def- inite crystal direction | Oscillation; reflection from face or transmis- sion; successive settings of angle in ionization spectrometer | Rotated or oscillated over fixed angle around principal axis; mount- ing on goniometer head for proper orientation | Fixed, in small tubes, threads, wires, ribbons, etc. | Fixed with fiber axis ori- ented, over pinhole and beam transmitted per- pendicular |
| Usual registration..... | Flat photographic film | Flat or cylindrical film; ionization chamber | Flat or cylindrical film with crystal at center | Narrow film bent in arc with specimen at center | Flat film, perpendicular to beam |
| Pattern..... | Symmetrical spots each from different set of planes and particular value of d , λ , Θ | Line spectrum from sin- gle set of planes | Diffraction spots lying on layer lines, parallel horizontal with cylin- drical film, and hyper- bolas with flat film | Line spectrum, each line corresponding to differ- ent sets of planes | For random aggregate, concentric rings or dia- gram 360° in azimuth; for fibers, layer-line pat- tern like rotating single crystal |
| Interpretation..... | Calculation of spacings according to spots. Assignment of indices with assistance of stere- ographic or gnomonic projections. Estima- tion of relative intensi- ties | Calculation of spacings for set of planes involv- ed in particular orienta- tion ($n\lambda = 2d \sin \Theta$) and thence from three experiments size of unit crystal cell. Determi- nation of missing or- ders, etc., in aiding to- ward structure factor | Measurement of identity period from layer lines by $I = n\lambda/\sin \mu_n$ and exact size of unit cell. Straightforward in- dexing of diffraction spots on layer line. Comparison with space- group criteria | Calculation of spacings for lines. In simpler cases assignment of in- dices from $\sin^2 \Theta$ data, and unit-cell dimen- sions. Measurement of line breadths for par- ticle size | Same as for powders. Identity period along fiber axis from $I =$ $n\lambda/\sin \mu_n$. Orienta- tion of planes in all fiber particles from po- sitions of interference maxima on Debye- Scherrer rings |

TABLE XXXI.—EXPERIMENTAL DIFFRACTION METHODS.—(Continued)

| Method | Laue | Bragg | Rotating crystal (Schiebold-Polanyi) goniometer | Powder (Hull-Debye-Scherrer) | Monochromatic pinhole (fiber) |
|--------------------|--|---|---|--|--|
| Chief uses..... | Symmetry, indices, and intensities for assignment of space-group. Practical determination of orientation as of large grains with respect to surface of sheet | Occasionally used to determine or check lattice spacing; for all films of long-chain carbon compounds | Commonly used for determining uniquely crystal structure and constitution where single crystals are available | Used in the great majority of cases (single crystals unavailable) for crystalline structure, allotropy, qualitative and quantitative analysis, purity, grain size from line breadths, etc. | Same for powders or random aggregates. Determination of actual state of any specimen, such as degree of fiber-ing and internal strain, and of the effect of any process such as working or heat-treatment; thus for the control of industrial processes and as a method of specification |
| Modifications..... | Unsymmetrical patterns | | Special goniometers (Weissenberg, Schiebold-Sauter etc.) described in text | Bohlin-Westgren method has slit, flat sample, and film on same circumference permitting focus and rapid exposure by reducing absorption of rays in specimen to a minimum | Cylindrical film with axis perpendicular to beam or coaxial with beam. Reflection from surface at fixed angle, back reflection |

to each voltage, so that in the interpretation of the patterns all lower values of λ can be at once eliminated.

The average length of exposure with ordinary equipment for a Laue photograph of a single crystal without heavily absorbing elements is 30 min. to 1 hr. The new high-powered tubes described on page 42 allow a reduction of time to a matter of seconds or minutes. A flat *cassette* or film holder is shown in Fig. 132.

2. *The Bragg Method (Spectrometry).*—Since the Bragg method of crystal analysis involves direct angular measurements of θ ,



FIG. 131.—Laue pattern of rock salt.

the use of monochromatic radiation, and reflection from a single set of planes, the significance of the results is readily understood in terms of the preceding development. By successive resettings of the crystal so that the planar distances for various sets of planes that have a common zone axis are ascertained, it is usually possible to arrive at something like a complete structure; the difficulty arises in the tedious repetition of measurements and the accurate orientation of the crystal specimen on

the spectrometer. This method is described in some detail in Chap. V. In 1922 Clark and Duane in a series of investigations found evidence of the reflection by crystals of x-rays with wave lengths characteristic of the elements in the crystal, generated as fluorescent radiation by irradiation with polychromatic rays above critical voltages. This effect was used in the preliminary studies of crystal structures not previously known. A considerable opposition was expressed by other workers, and because of low intensities the method was not extended. The validity of the phenomenon itself, and of the interpretation, has been completely established in authoritative work by Laue¹ and by Hassel.²

3. *The Rotation Method.*—The most powerful method of crystal analysis is undoubtedly the rotation method which is known

¹ *Ann. Physik*, **23**, 705 (1935).

² *Avhandl. Norske Videnskaps-Akad. Oslo*, I, No. 2 (1937).

in several modifications. Ordinarily the single crystal is mounted and rotated around a principal axis. Three such photographs around the principal axes make possible almost complete information. In the usual method a stationary film is used, either flat at a fixed distance from the crystal or preferably bent on the circumference of a circle with the crystal at the center. A satisfactory design of rotation camera or spectrograph is shown

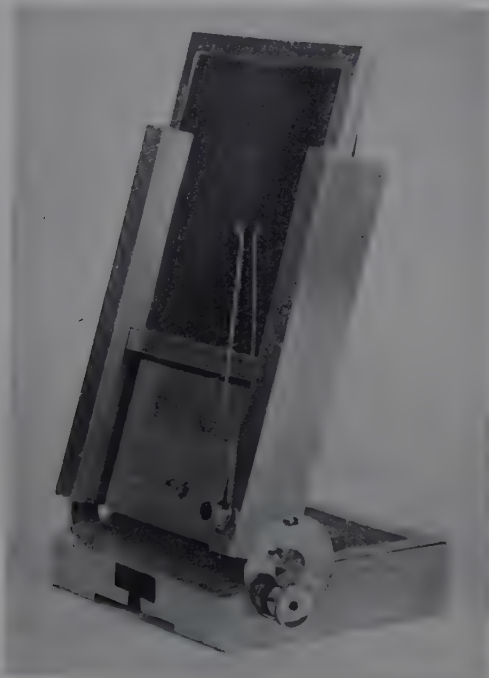


FIG. 132.—Flat cassette for Laue patterns, for use on Hayes multiple diffraction unit.

in Fig. 133 either for special units or for commercial multiple apparatus. Frequently it is desirable to mount the crystals on a goniometer head by means of which the angles between axes may be measured. If, for example, a rational layer-line pattern for the rotation method is obtained for one orientation of an orthorhombic crystal, another will be obtained when the crystal is shifted 90 deg. and again rotated, and still another after it is shifted 90 deg. in the third direction. In all cases a complete spectral diagram for all possible reflections from a given crystal-

line zone (the rotation axis) is obtained, such as appears in Fig. 134.

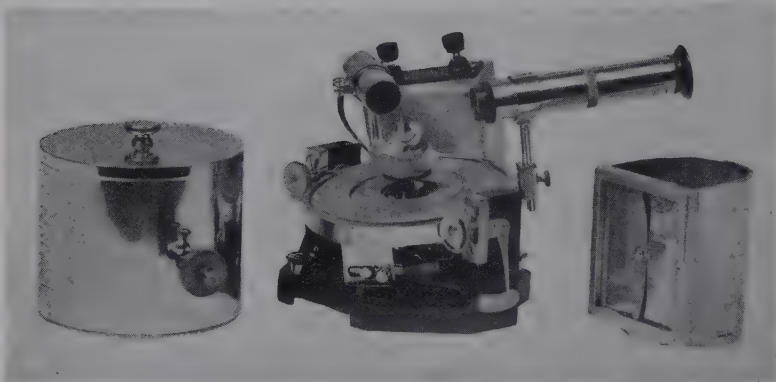


FIG. 133.—Camera with interchangeable parts for rotation method; left, cylindrical film holder; center, camera base, rotating mechanism, goniometer mount, and telescope for alignment of crystal; right, flat film holder. (Built by J. B. Hayes.)

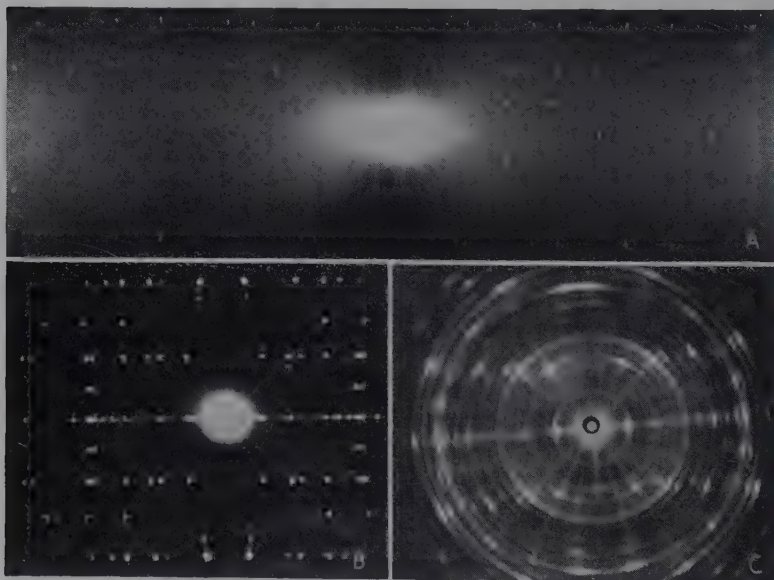


FIG. 134.—Typical rotation patterns: (A) CsNO_3 ; (B) $\text{Na}_3\text{PO}_4 \cdot 12\text{H}_2\text{O}$; (C) $\text{Na}_3\text{PO}_4 \cdot 16\text{H}_2\text{O}$ after losing water.

A complete diagram for rotation around 360 deg. is, of course, the summation of a series of diagrams which may be prepared by

oscillating the crystal over fixed angles, 1 to 20 deg., 20 to 40 deg., etc., by means of a heart-shaped cam. This interpretation of a complex rotation pattern is often greatly simplified by these oscillation diagrams.

Aside from the arrangement of the photographic film and the method of mechanically rotating or oscillating the crystal, the principal variable in the simple method is the method of beam definition. Here as in the Bragg spectrometer the most common equipment is a pair of slits for rendering the rays parallel. These

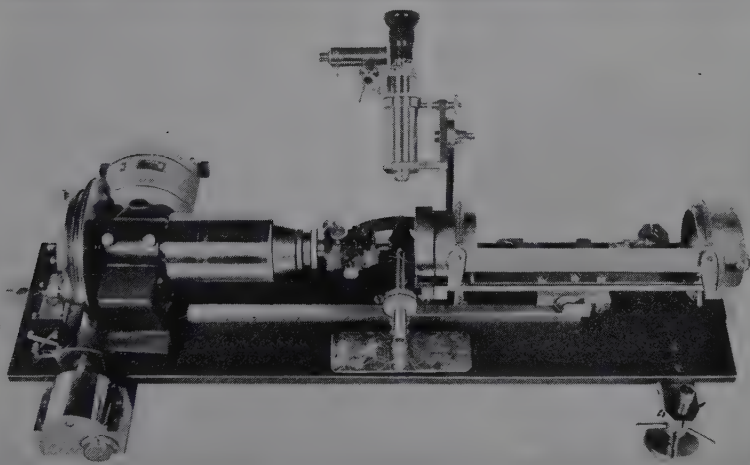


FIG. 135.—Weissenberg-Seemann goniometer.

are made of lead, lead alloy, gold, or even brass for softer rays. For only very small crystals the slits may be so short as actually to be pinholes, as is the case of the rotation camera pictured in Fig. 133. The smaller the slit width or pinhole diameter, the sharper are the interferences.

For increasing accuracy and sensitiveness special modifications of the rotation method are employed as follows:

- a. Displacement of the film parallel to the direction of the axis of rotation of the crystal (Weissenberg goniometer).
- b. Displacement of the plate or film parallel to the X axis (Dausar).
- c. Displacement of the film parallel to the direction of the primary beams (Kratky).

d. Rotation of the photographic plate or film around the Z axis (Seemann, Mark, and Wigner).

e. Rotation of the film around the Y axis (primary beam) (Schiebold-Sauter goniometer).

f. Displacement of two photographic plates in directions parallel and perpendicular to the axis of rotation.

Of these the Weissenberg and the Schiebold-Sauter methods are most generally employed, largely because of the simplicity of

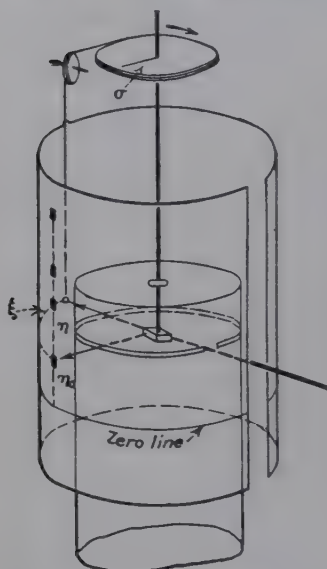


FIG. 136.—Principle of operation of the Weissenberg goniometer.

interpretation and because of the availability of excellent commercial instruments. The purpose of both is to resolve or sweep out a single layer line in a rotation pattern consisting often of many very close or overlapping interference spots. Figure 135 shows a Weissenberg goniometer as designed by Bohm and built by Seemann. The cylindrical film, coaxial with the rotating crystal fragment, is gradually displaced during the exposure in the direction parallel to the axis. The principle of the apparatus is shown diagrammatically in Fig. 136, and in Fig. 137 is reproduced a diffraction pattern; the line spectrum above is that obtained by the ordinary rotation method. In the

Weissenberg diagram the spectra of

the various surfaces of the zone of rotation are not superimposed but are arranged in hyperbolas which allow relatively simple assignment of indices. When several lattice planes are equivalent, such as (110) , $(\bar{1}\bar{1}0)$, $(\bar{1}10)$, $(1\bar{1}0)$ in a rhombic crystal, and have the same lattice spacing d and the same diffraction angle 2θ , they will all register on a stationary film the same interference point, whereas in this modification with moving film each set of planes will register its own interference lying on a vertical line.

The Schiebold-Sauter camera such as is pictured in Fig. 138 has a number of advantages over the more complicated Weissenberg camera, especially in interpretation. It consists essentially

of a rotating crystal, arranged with a shield so that only the interferences from one layer line may be recorded on a flat circular film, which is rotated at the same rate as is the crystal. With this arrangement, the angular distance separating two interferences of the same interplanar spacing is equal to the angular distance through which the crystal must be turned in order to pass from the position for reflecting the first set of planes to the

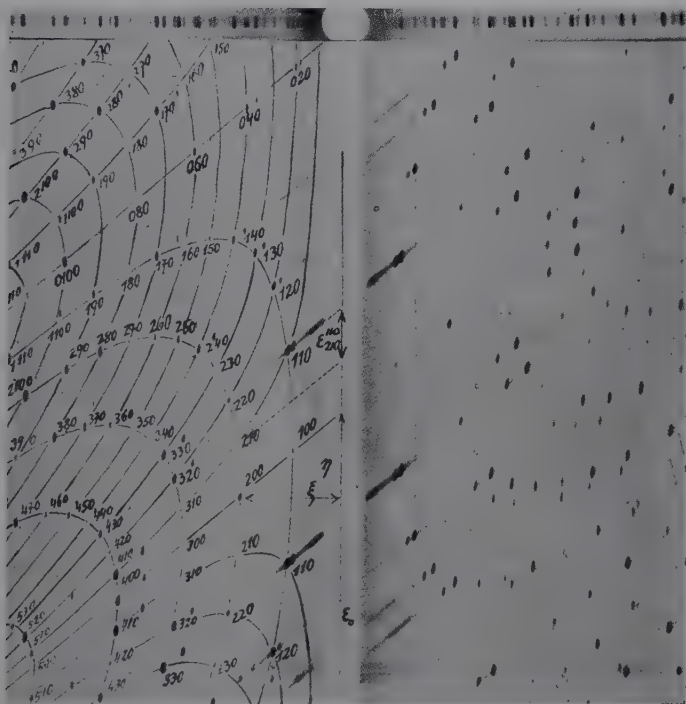


FIG. 137.—Typical Weissenberg diagram compared with ordinary rotation pattern above.

position for reflecting the second set. In the writer's laboratory such a camera has been employed where synchronous motors, such as are used in electric clocks, are used for rotating the crystal and the film. This makes the camera suitable for the study of layer lines higher than the equatorial layer line. The equatorial layer line is ordinarily employed, since this will furnish the data necessary for determination of the unit-cell dimensions and shape. Since reflection occurs from a crystal face when the crystal is tilted at θ deg. to the incident x-ray beam, the interferences are

recorded when the crystal is turned θ deg. beyond the point at which the set of reflecting planes are normal to the x-ray beam. For calculations it is necessary that we consider the angular distances separating the *normals* of the different sets of planes, so that in most cases it is necessary to subtract (or add, as the case may be) θ deg. from the angular position of each interference on the film. If this is done, the curved lines formed by inter-

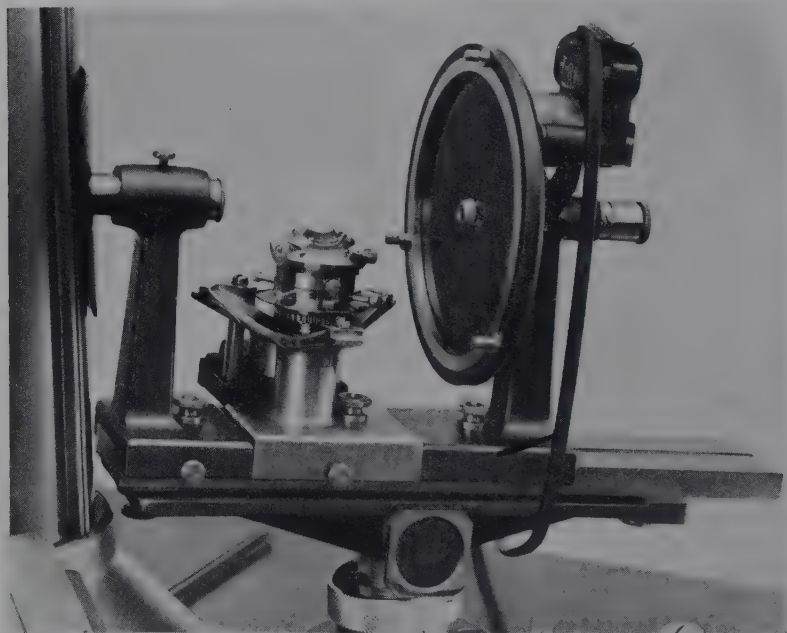


FIG. 138.—Schiebold-Sauter goniometer (General Electric X-Ray Corporation): left, defining pinholes; center, goniometer head and rotating mechanism; right, holder for circular flat film, rotated around horizontal axis.

ferences of various orders from the same set of planes will be straightened, and the interpretation will be greatly simplified.

By bending the film, or by proper selection of the angle of the rotating film with respect to the primary x-ray beam and the axis of crystal rotation (Clark-Gross modification of Schiebold-Sauter technique), the corrections may be made directly on the film, so that the patterns obtained, such as those in Fig. 139, are characterized by linear arrangements of interferences which are easily interpreted.

The Diffraction of X-rays by Powders.—Thus far the consideration of the reflection or diffraction of x-rays by crystals has been on the assumption of essentially single crystals. On account of the fact that so many interesting chemical substances, including practically all metals, cannot be obtained in the form of

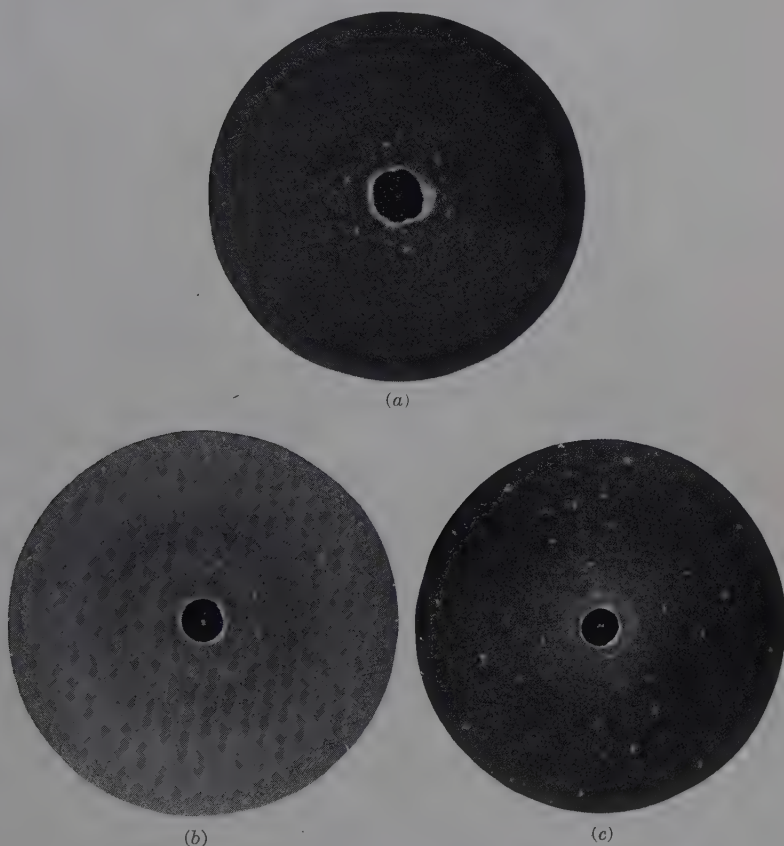


FIG. 139.—Goniometer patterns (Clark-Gross modification of Schiebold-Sauter method): (a) orthophenanthroline (equator); (b) Pb_3O_4 (equator); (c) Pb_3O_4 (first layer line).

sufficiently large single crystals, one of the great contributions to x-ray science has been the discovery, independently by Debye and Scherrer in Europe and by Hull in America, that fine powders, or crystalline aggregates of all kinds, may be analyzed for ultimate crystalline structure in a most satisfactory way. The diffraction depends upon the fact that in a fine powder the grains

are arranged in an entirely chaotic manner. There should be enough particles in this array, turned at just the right angle to the incident primary beam of monochromatic x-rays, to allow strong reflection from one set of parallel planes; other particles turned at another angle will produce reflection from another set of planes (the same set in many particles cooperating). Thus a beam passing through a powder specimen will fall upon a per-

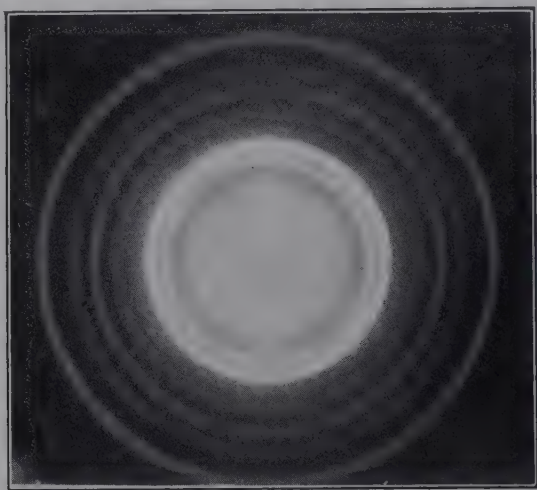


FIG. 140.—Monochromatic pinhole diagram of steel ribbon showing continuous rings.



FIG. 141.—Powder diffraction pattern for metallic lead made with cylindrical camera.

pendicular flat photographic film as a series of concentric rings (Fig. 140), each uniformly intense throughout and corresponding to one set of planes of spacing d . A horizontal section cut through this diagram has, therefore, the appearance of a line spectrum (Fig. 141). This same result may be obtained by bending a narrow film in a *cassette* on the circumference of a circle, at the center of which is the specimen. In the so-called Debye-Scherrer camera the film is bent around 360 deg., and the beam, defined by

pinholes, passes through a hole in the film; in other modifications where larger dispersion is desired, the film may occupy only a quadrant or semicircle.

The sample may have one of various forms, the essential point being random orientation of grains; powders of 200 mesh or smaller size may be placed in fine capillary tubes of glass or celluloid, pasted by collodion on ribbons or threads, or pressed

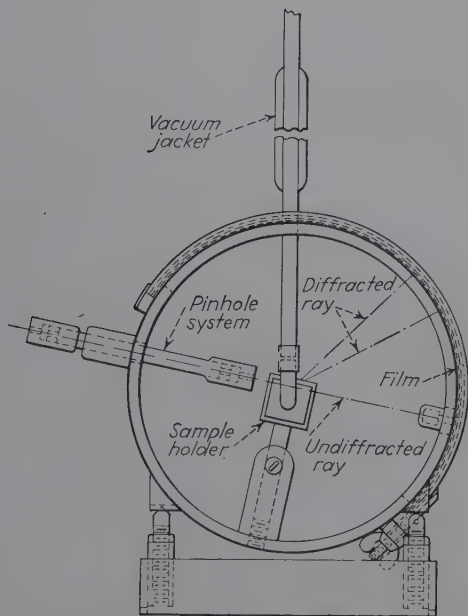


FIG. 142.—Cylindrical powder diffraction camera of type in general use at the University of Illinois, in this case arranged for maintaining the specimen at a low temperature.

into slabs. Metals may be used in the form of fine wires or as small beveled plates with the beam grazing the blunt knife-edge at a small angle and passing through a sharp edge. Wedge-shaped samples even of powders formed in small cradle holders are almost exclusively used in the writer's laboratory. A camera arranged for work at very low temperatures is illustrated in Fig. 142.

For powders of heavily absorbing substances such as lead it is desirable to use a noncrystalline diluent such as gum tragacanth or powdered starch. A complete table of proper proportions

has been worked out by Davey. The volume of the diluting material with 1 volume of a chemical element varies from 1 for elements 10 to 26, 3 for 18 to 28, 5 for 29 to 44, 6 for 36 to 46, 7 for 47 to 53, 8 for 54 to 57, and 9 to 10 on up to 92.

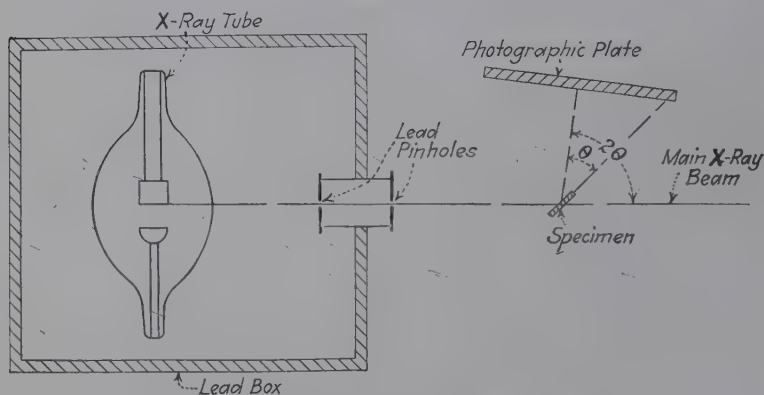


FIG. 143.—Diagram of surface reflection method.

On account of the complexity of the spectrum it is desirable that the beam of x-rays should be as nearly monochromatic as possible. With molybdenum rays the zirconium filter eliminates all but the $K\alpha$ doublet, and a nickel filter serves for copper, etc. (see page 108).



FIG. 144.—Experimental arrangement for back-reflection method.

The accurate measurement of the crystal-powder spectrum lines is, of course, of great importance in analyses of unknown mixtures. Where semicircular *cassettes* or cylindrical cameras are used, the undeflected beam strikes the center of the film and

diffraction lines are registered on both sides of this zero position. Uncertainties as to this are eliminated by measuring from one line to the corresponding line on the opposite end of the film. If, however, the zero position is at one end of the film as in the case of quadrant *cassettes*, greater resolution is possible but it



FIG. 145a.—Back-reflection pattern from a specimen of metallic lead.

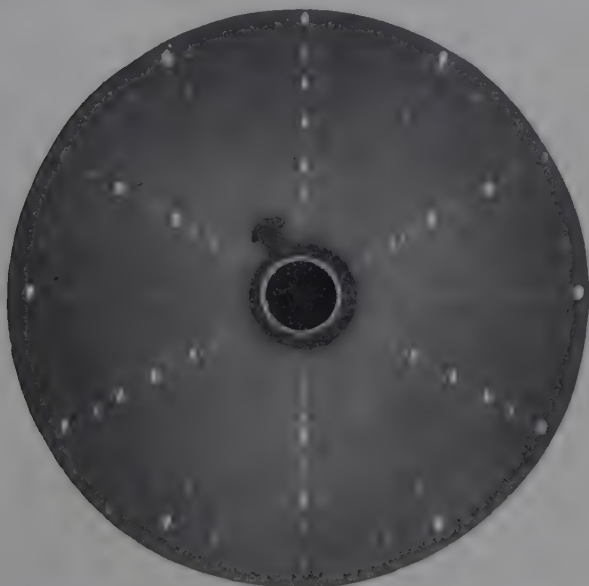


FIG. 145b.—Back reflection Laue pattern for quartz plate used in radio transmission circuit (normal to 0001).

is often necessary to run a calibrating spectrum for known pure crystal powders such as sodium chloride on the same film, either mixed with the unknown or placed in half of the small capillary tube. Since the spacings for each of these lines are accurately known and, hence, the necessary displacement on the film, the zero position may be accurately determined as well as all evidences of film shrinkage and inaccurate alignment of the specimen.

Reflection Methods.—Reflection from the surface of samples too thick for penetration by x-rays can be used, as illustrated in Fig. 143.

In practically all cases, x-ray diffraction patterns are made by transmission through the specimens. But in industrial practice it is frequently desired to know the ultimate crystalline condition

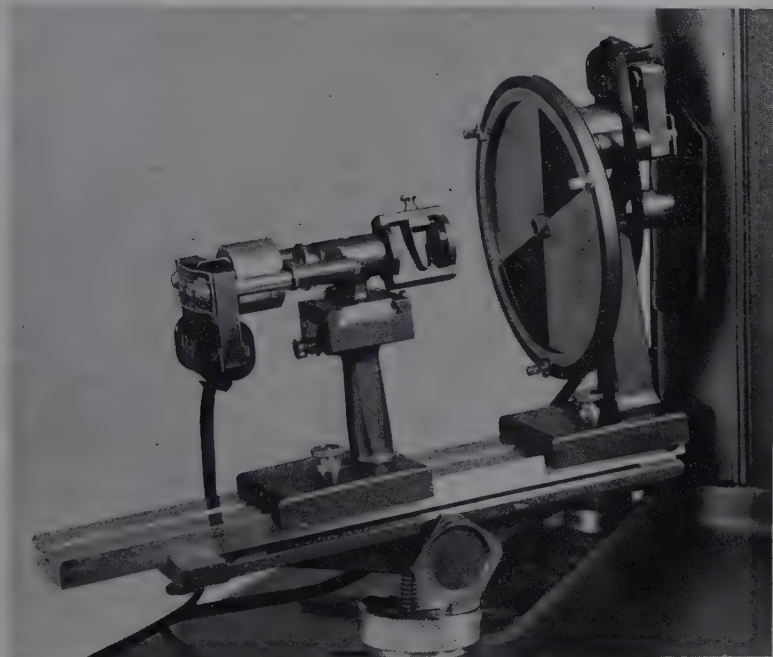


FIG. 147.—Back-reflection camera for measurements of high precision; a sector screen in front of the film makes it possible to photograph patterns of two specimens on the same film, and thus to compare line positions. (*General Electric X-Ray Corporation.*)

of a finished product or of a large specimen that cannot be cut up. For example, in steel rails, in aluminum-alloy airplane propellers, and in very large steel structures such as oil stills where sound structure and freedom from strain are so essential for safety at high temperatures and pressures, such an examination of a finished unit before installation would be invaluable.

One method would, of course, consist in making hollow borings, with subsequent welding of the holes. However, nearly twenty years ago the writer deemed it advisable to try and develop a

method in which the x-ray beam might be reflected from the surface. Utilizing the usual equipment, it is necessary to reflect straight back from the surface of very large specimens as shown in Fig. 144. In this case, therefore, the photographic film is mounted *around* the pinhole and registers the patterns of rays

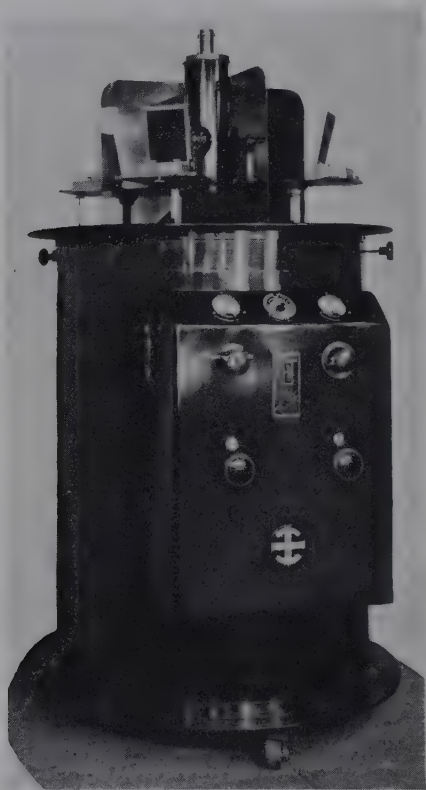


FIG. 148.—Hayes multiple diffraction unit, of which five are in constant use at the University of Illinois. The transformer is enclosed in the grounded large cylindrical case, with the control panel integral with the door; the x-ray tube is adjusted upright in the upper small cylinder.

diffracted directly back from the surface. A typical pattern from a specimen of metallic lead is shown in Fig. 145a. The concentric pairs of rings seem at first sight to be very familiar until it is noticed that the less intense line is inside the stronger line of each pair. If these pairs represent resolution of the $K\alpha$ doublet of copper, then in ordinary powder diffraction films, of course,

the stronger $K\alpha_1$ line comes inside the weaker $K\alpha_2$. This apparent reversal is, of course, readily explained by a consideration of Fig. 146. The photographic plate is at ACB . If a cylindrical film, as in the Debye-Scherrer method, were placed coaxial with the specimen, the primary beam passing through the specimen would strike the film at the top of the circle and the

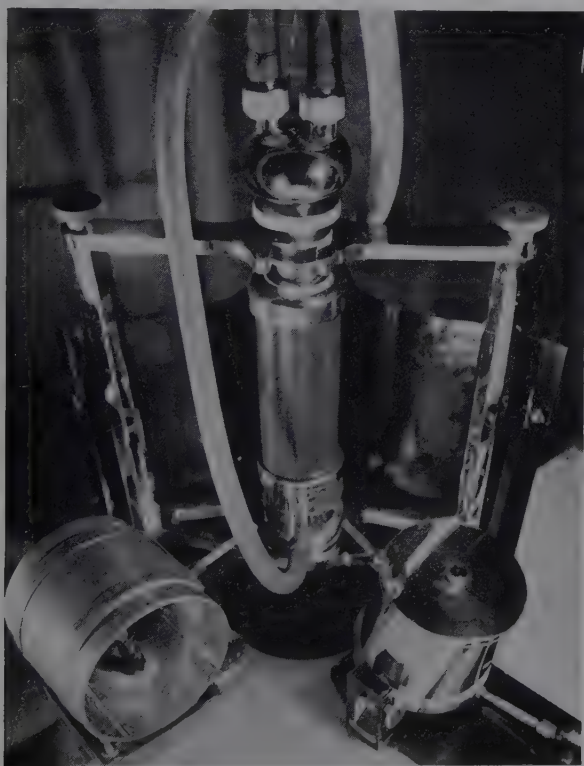


FIG. 149. —Arrangement of cameras for four windows of Philips Metalix diffraction tube in multiple unit.

diffraction lines would appear as shown. The pattern in Fig. 145a is, therefore, to be read from the *outside in* toward the center, rather than from the center, as would be the case if the film were placed on the opposite side of the circle. These diffraction circles correspond, therefore, to lines appearing at the very end of usual spectra and hence to planes of relatively high indices.

The method has the disadvantage, of course, that long exposure is required to develop sufficient intensity for these diffraction

effects from sparsely populated but closely spaced planes. However, large specimens of Armco iron with grains large enough to produce a spotted pattern by direct transmission also gave back-reflection patterns with large spots. On account of the large resolutions of the $K\alpha$ doublet the method is useful for evaluating spacings very accurately and for following small

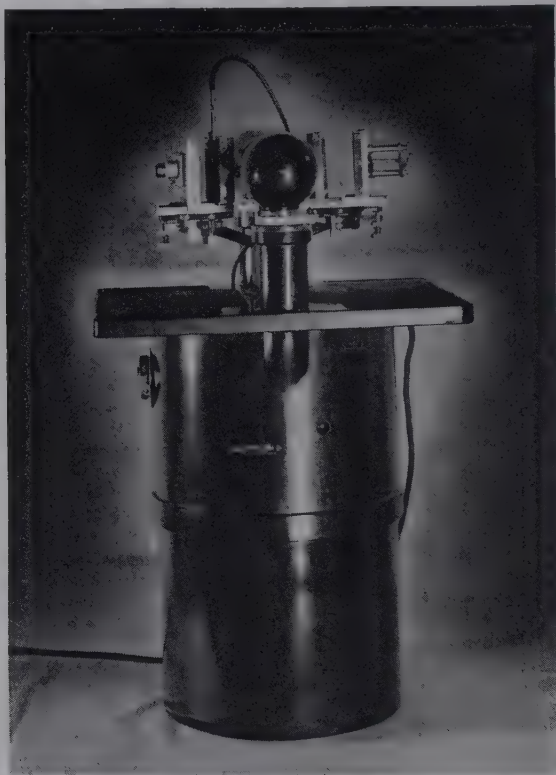


FIG. 150.—Small Philips Metalix diffraction unit with two cameras in position.

changes due to solid solution and to deformations as in fatigue. The grinding and orientation of quartz plate oscillators used in radio transmission circuits may be tested with great accuracy from back-reflection Laue patterns (Fig. 145b). A back-reflection camera of high precision is illustrated in Fig. 147.

Multiple Apparatus.—The most useful apparatus for industrial and chemical applications is the multiple diffraction unit. This

consists of a transformer operating usually at 30,000 volts with an enclosed filament transformer, an operating switchboard with filament current stabilizer, a water-cooled self-rectifying tube (usually Philips Metalix), a pinhole system which permits four simultaneous exposures radially around the vertical tube at a grazing angle of 15 deg. upon the target, and the various *cassettes*

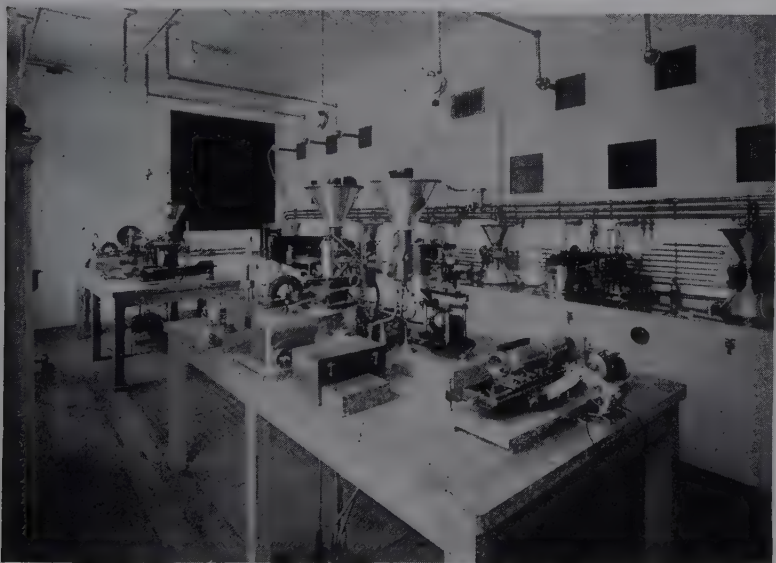


FIG. 151.—Part of x-ray diffraction laboratory of the French Air Ministry, Paris.
(By permission.)

and cameras mounted in fixed positions on slides. The Hayes unit designed and used in the University of Illinois X-ray Laboratory is pictured in Fig. 148. The arrangement around a Philips Metalix tube of cameras in a multiple-diffraction unit is shown in Fig. 149.

A new Philips Metalix crystal analysis unit weighing only 54 lb. is shown in Fig. 150. The Metalix tube and two Debye-Scherrer cameras are shown in position. Part of the splendid x-ray diffraction laboratory of the French Air Ministry in Paris is pictured in Fig. 151.

CHAPTER XIV

THE INTERPRETATION OF DIFFRACTION PATTERNS IN TERMS OF ULTIMATE STRUCTURE

Steps in the Derivation of Structure from the Diffraction Pattern.—Having photographed the diffraction patterns of a crystal under structural investigation by one or more of the methods outlined in Chap. XIII, the experimenter is confronted with the problem of measuring and extracting every possible bit of information from the patterns that may lead to the final proof of structure. The steps in the analysis have been enumerated in Chap. XII. It is now necessary to examine in detail the available tools that the analyst has at hand as he begins the interpretation of the pattern of lines or spots registered on the film before him as the result of the diffraction of x-rays by the ordered array of atoms or molecules or ions in the crystal.

1. First of all, he has made use of observations of the outer form of his crystal, recognizing that single crystal data will almost invariably be required for a complete analysis, in order to orient the specimen properly in his x-ray camera or goniometer. Optical examination has classified the crystal as triclinic, monoclinic, hexagonal, orthorhombic, tetragonal, or cubic, and the crystallographic axes have been located so that symmetrical Laue patterns and rational clear-cut rotation patterns are registered. Or by trial and failure he has changed his crystal orientation until such patterns are obtained.

2. He may know from symmetry observations deduced from crystal habit, angles, etc., to which class or point-group the crystal belongs. He has available certain auxiliary diagnostic tests for symmetry, such as pyro- and piezoelectric effects, which may be useful as preliminary information leading to proper space-group identification or which may be introduced in cases of uncertainty.

3. He has Bragg's law, $n\lambda = 2d \sin \theta$, by means of which he may proceed to calculate the interplanar spacings d_{hkl} for each

interference on his pattern. On a flat film perpendicular to the primary x-ray beam he measures the distance from the center of the undiffracted beam to the diffraction interference. This distance a , divided by the known fixed distance from specimen to film, b , gives the tangent of the diffraction angle 2θ , from which θ , $\sin \theta$, and d are readily determined. On a film exposed in a cylindrical camera $a = R \sin 2\theta$ where R is the radius of the camera, or θ in degrees $= \frac{1}{2} \frac{360}{2\pi R} = \frac{90a}{\pi R}$, with a and R measured in millimeters.

4. The dimensions of the unit cell are deduced fairly easily, especially if the analyst has a rotation pattern around each of the three axes (two for tetragonal, one for cubic, etc.). For, independent of other data, a measurement of the layer-lines displacement gives these fundamental spacings. The analyst also knows that the boundary planes of the unit cell almost certainly have very low indices and maximum spacings and produce maximum diffraction intensities because these planes are most thickly populated with atoms.

5. The analyst knows that he can test his preliminary decision on the size of the unit cell from the pycnometrically measured density of the crystal. For the number of atoms or molecules per unit cell is necessarily a whole number, in order to preserve the identity of the cell and of the chemical formula. This does not mean that the value of n must come out, for example, exactly 4.0, for a value such as 3.94 is evidence of this. The x-ray density is an ideal limiting value, which does not take into account cracks and imperfections that influence the pycnometer value. This true limiting density can be calculated by substituting the integral value of n back in the formula $\rho = nMm/V$.

6. There are available the formulas for calculating all planar spacings in all directions through the unit cell; for example,

$$d_{hkl} = \frac{a_0}{\sqrt{h^2 + k^2 + l^2}}$$

in the cubic system. These formulas give the values for all planes and hence of the maximum possible number of diffraction interferences that may ever be expected. They are not concerned with interferences that may be missing. In any case, however, all the observed interferences for a given crystal system must be interrelated by means of the appropriate equation.

7. The analyst before applying the theory of space-groups must identify each interference with the corresponding planar indices. In simple cases the method of the preceding section is adequate: *i.e.*, by trial and failure bringing a whole series of values of d_{hkl} into correspondence. In more complex cases the experimenter has at his command various methods of projection of interferences on networks—stereographic and gnomonic for Laue patterns, nets for rotation and goniometric methods. He has available the very fruitful concept of the reciprocal lattice, in which points represent ordinary lattice planes, and thus simplifies difficult calculations. In fact, he may find it possible to produce an *actual pattern that is itself a direct representation of the reciprocal lattice* and hence immediately interpreted.

8. Now the theory of space-groups may be applied, for all the interferences have been listed in terms of the planar indices. By inspection the experimenter notes certain regularities in the interferences that are and are not present, and hence the *extinctions* are noted, as the clues to the selection of the proper space-group that uniquely defines the crystal. These criteria are conveniently listed in tables by Astbury and Yardley, Wyckoff, and in the International Tables. The well-trained experimenter could calculate for himself these criteria, of course, from the principles of interference that determine intensities. Whether the atomic units occupy general positions in the unit cell (maximum number without affecting symmetry) or special positions may be deduced from the available data, and hence the coordinates of scattering points will be useful in further intensity calculations.

9. The analyst begins the last stage of his interpretation with the fundamental formulas relating intensities of interferences with structure factors. Tables of atomic structure factors that lead to the crystal structure factor now are available. He knows how to calculate intensities from a logical assumed structure, which are to be compared with experimental values. Better still he uses these experimental F values as coefficients in a Fourier series to calculate electron densities throughout the unit cell and thus to find the unique parameters that define the position of every atom even in a molecule. He recognizes that his enormous task is greatly simplified if the crystal has a center of symmetry. He uses the mathematical aids—calculating

machines, printed strips of numbers, etc.—to shorten the task of summation. From this analysis come the size, shape, and disposition of molecules, the length of bonds, the existence of hydrogen bonds, and all the information that finally explains just why the crystal and its component atoms and molecules act as they do in physical and chemical phenomena.

10. Finally, with this rigorous analysis completed correctly, all auxiliary tests—packing radii, physical and chemical properties—are found to be in accord with an architectural plan in which atoms and molecules in spatial arrangement have inscribed their own signatures which have been deciphered.

It is obvious that an exhaustive treatment of the details of the extended process of complete interpretation just outlined would run far beyond the bounds of this book. In the paragraphs that follow, the attempt is made to explain as simply as possible some of the aids to interpretation.

Interplanar Spacing Formulas.—With the concept of the planes already developed it is not difficult to develop general formulas for the interplanar spacings in a given unit cell. At this point we shall discuss only the cubic, tetragonal, and orthorhombic cells, *i.e.*, those with their coordinate axes at right angles.

If line d is normal to a plane, and the reference plane is assumed to pass through the origin, length d represents the interplanar spacing. Since d is normal to the plane, we may write

$$d = a_0 \frac{\cos \alpha}{h} = b_0 \frac{\cos \beta}{k} = c_0 \frac{\cos \gamma}{l}.$$

But if α , β , and γ are the direction cosines of the normal to the plane, we may write

$$\cos^2 \alpha + \cos^2 \beta + \cos^2 \gamma = 1;$$

substituting, we find

$$d^2 \left(\frac{h^2}{a_0^2} + \frac{k^2}{b_0^2} + \frac{l^2}{c_0^2} \right) = 1,$$

or

$$d = \frac{1}{\left(\frac{h^2}{a_0^2} + \frac{k^2}{b_0^2} + \frac{l^2}{c_0^2} \right)^{\frac{1}{2}}}.$$

This formula may be written in a form more generally useful as

$$\sin \Theta = \frac{\lambda}{2} \left(\frac{h^2}{a_0^2} + \frac{k^2}{b_0^2} + \frac{l^2}{c_0^2} \right)^{\frac{1}{2}}.$$

Of course, in the tetragonal system, $a_0 = b_0$; in the cubic system $a_0 = b_0 = c_0$.

Thus for a cubic crystal

$$n\lambda = \frac{2a_0}{\sqrt{h^2 + k^2 + l^2}} \sin \Theta,$$

where a_0 is the lattice constant or length of the unit-cube edge and h, k, l are the indices of any planes. Hence

$$d_{hkl} = \frac{a_0}{\sqrt{h^2 + k^2 + l^2}}.$$

If an unknown crystal is cubic, all the diffraction interferences must be related in this way; the usual method is therefore to correlate calculations with experimental values. In the same way equations may be derived for all other simple lattices. In general

$$n\lambda = 2d_{hkl} \sin \Theta_n = \frac{2a_0}{\sqrt{F(hkl; abc; \alpha\beta\gamma)}} \sin \Theta_n,$$

where abc are unit lengths in three dimensions, and $\alpha\beta\gamma$ are axial angles. Table XXXII lists the formulas for d_{hkl} in convenient form.

From the mathematical expressions, $n\lambda$ may be calculated by substituting the values of d_{hkl} in $n\lambda = 2d \sin \Theta$. For the cubic system therefore

$$n\lambda = \frac{2a_0}{\sqrt{h^2 + k^2 + l^2}} \sin \Theta_n.$$

Squaring,

$$n^2\lambda^2 = \frac{4a_0^2}{h^2 + k^2 + l^2} \sin^2 \Theta_n,$$

$$\sin^2 \Theta_n = \left(\frac{n^2\lambda^2}{4a_0^2} \right) (h^2 + k^2 + l^2).$$

All the possible values of $\sin^2 \Theta_n$ may then be calculated when the cube-edge length a_0 and the wave length are known, assigning all values of hkl . These values are then compared with the experimental $\sin^2 \Theta$ values for the interferences appearing on the pat-

TABLE XXXII.—CALCULATION OF INTERPLANAR SPACINGS, d_{hkl}

| System | $a:b:c$ | α, β, γ | d_{hkl} |
|-------------------|---------|---|---|
| Cubic..... | 1:1:1 | $\alpha = \beta = \gamma = 90^\circ$ | $\frac{a_0}{\sqrt{h^2 + k^2 + l^2}}$ |
| Tetragonal..... | 1:1:c | $\alpha = \beta = \gamma = 90^\circ$ | $\frac{a_0}{\sqrt{h^2 + k^2 + (l/c)^2}}$ |
| Orthorhombic..... | a:1:c | $\alpha = \beta = \gamma = 90^\circ$ | $\frac{b_0}{\sqrt{(h/a)^2 + k^2 + (l/c)^2}}$ |
| Hexagonal..... | 1:1:c | $\alpha = \beta = 90^\circ, \gamma = 120^\circ$ | $\frac{a_0}{\sqrt{\frac{4}{3}(h^2 + hk + k^2) + (l/c)^2}}$ |
| Rhombohedral..... | 1:1:1 | $\alpha = \beta = \gamma \neq 90^\circ$ | $\frac{a_0 \sqrt{1 + 2 \cos^3 \alpha - 3 \cos^2 \alpha}}{\sqrt{(h^2 + k^2 + l^2) \sin^2 \alpha + 2(hk + hl + kl) (\cos^2 \alpha - \cos \alpha)}}$ |
| Monoclinic..... | a:1:c | $\alpha = \gamma = 90^\circ, \beta \neq 90^\circ$ | $\frac{b_0}{\sqrt{\frac{(h/a)^2 + (l/c)^2 - \frac{2hl}{ac} \cos \beta}{\sin^2 \beta} + k^2}}$ |
| Triclinic..... | a:1:c | $\alpha \neq \beta \neq \gamma \neq 90^\circ$ | $\frac{1}{\sqrt{\frac{h/a}{k} \frac{h/a}{l/c} \cos \gamma \cos \alpha \cos \beta + \frac{1}{l/c} \cos \gamma \cos \alpha \cos \beta + \frac{1}{k} \cos \gamma \cos \alpha \cos \beta + \frac{1}{l/c} \cos \gamma \cos \alpha \cos \beta + \frac{1}{k} \cos \gamma \cos \alpha \cos \beta + \frac{1}{l/c} \cos \gamma \cos \alpha \cos \beta}}}$ |

tern, and the crystallographic system is thus established. The interferences may be those on different photographs for difficult zones or all on the same film as in the powder method.

It is clear that with decreasing symmetry the number of possible interference maxima increases. The derivation of the quadratic form from the x-ray data therefore becomes difficult except in the cases of highest symmetry. In a cubic lattice it is possible to have 48 planes of the same form (hkl) where h , k , and l are all different, with the same spacing, and hence cooperating to produce only a single interference maximum, whereas in the triclinic lattice there are 24 different spacings and hence 24 reflection lines or spots corresponding to these hkl planes. Theoretically possible maxima may overlap and thus render derivation of the quadratic form and the crystal system practically impossible.

DETERMINATION OF SPACE-GROUP FROM X-RAY EXTINCTIONS

I. Translation groups or space lattices.

P—no regular extinctions associated with the primitive lattice.

A, *B*, *C*—with the face-centered lattices of this type:

A face-centered: $k + l = 2n$ for every reflection hkl .

B face-centered: $h + l = 2n$ for every reflection hkl .

C face-centered: $h + k = 2n$ for every reflection hkl .

F—face-centered lattices; hkl all odd or all even.

$$\left. \begin{array}{l} h + k = 2n. \\ h + l = 2n. \\ k + l = 2n. \end{array} \right\} \text{if reflection } hkl \text{ is to occur.}$$

I—body-centered lattice.

$$h + k + l = 2n \text{ for reflection } hkl \text{ to occur.}$$

II. Microsymmetry elements.

1. Screw axis: screw axis p_q in x direction; $h00$ may appear only when $h = pn/q$ (integer). Similarly in direction y and direction z in case the screw axis lies parallel to one of their directions.

2. Glide planes:

a. Glide plane normal to x axis with glide b . $0kl$ can only appear when $k = 2n$.

(Index of normal to glide plane must be 0; direction of gliding has spacings halved.)

b. The n glide plane. Assume the n glide plane takes place normal to direction x [glide = $\frac{1}{2}(b + c)$].

$0kl$ appears only when $k + l = 2n$.

(Index of normal to glide plane 0.)

c. The d glide plane. Assume a d glide plane normal to the a direction [glide = $\frac{1}{4}(b + c)$].

$0kl$ appears only when $k + l = 4n$.

The lattice restrictions may tend to cover up those due to symmetry elements, *i.e.*, with A lattice $k + l = 2n$, whether the interference is hkl or $0kl$; but an n glide plane normal to direction x requires the $0kl$ to reflect only when $k + l = 2n$ —therefore, in this case the existence of the glide plane cannot be demonstrated.

EXAMPLE.— $\text{BaCl}_2 \cdot 2\text{H}_2\text{O}$ is monoclinic; $\beta = 91^\circ 5'$; $a_0 = 6.69$ A.U., $b_0 = 10.86$ A.U., $c_0 = 7.15$ A.U.; and $n = 4$. Some of the observed interferences are listed below:¹

| $h00$ | $h0l$ | $0k0$ | $hk0$ | $0kl$ | $00l$ | hkl |
|-------|-------|-------|-------|-------|-------|-------|
| 200 | 101 | 020 | 110 | 011 | 002 | 111 |
| 400 | 202 | 040 | 120 | 021 | 004 | 211 |
| 600 | 103 | 060 | 210 | 012 | 006 | 131 |
| ... | 301 | 080 | 130 | 031 | ... | 122 |
| ... | 402 | ... | 220 | 022 | ... | 221 |
| ... | 105 | ... | 140 | 032 | ... | 113 |
| ... | ... | ... | 310 | 041 | ... | 311 |
| ... | ... | ... | 150 | 013 | ... | 321 |

I. *The Space-lattice.*—In the monoclinic system only C and P are possible, and since cases may be observed in which $h + l =$ odd integer ($k \neq 0$) the lattice may be described as primitive.

II. *The Symmetry Elements.*—Only four regularities may be found; $h00$ (h even), $0k0$ (k even), $00l$ (l even), and $h0l$ ($h + l$ even). Since the last regularity includes the first two, we may write

$h0l$ appears when $h + l =$ even integer.

$0k0$ appears when $k =$ even integer.

This requires that the crystal class have both an axis and a plane of symmetry; *i.e.*, 2_1 is necessary for the second restriction, and the first can be described only with an n glide plane normal to the twofold axis.

Therefore, we may designate the space-group

$$P2_1/n$$

The equivalent points may be expressed analytically as

$$xyz; \bar{x}\bar{y}\bar{z}; \frac{1}{2} + x, \frac{1}{2} - y, \frac{1}{2} + z; \frac{1}{2} - x, \frac{1}{2} + y; \frac{1}{2} - z.$$

Since four molecules of $\text{BaCl}_2 \cdot 2\text{H}_2\text{O}$ are present per cell, no special

¹ NARAY-SZABO and SASVARI, *Z. Krist.*, 97, 235 (1937).

positions can be occupied. Since the intensity contribution of the barium may be considered as predominant, its position may be roughly fixed by a consideration of the following intensities:

| Interference | Intensity observed | | |
|--------------|--------------------|--------|-----|
| | | | |
| 200 | 10 | 020 | 12 |
| 400 | 0.5 | 040 | 0.5 |
| 600 | 0.5 | 060 | 8 |
| 002 | 8 | 080 | 0.5 |
| 004 | 6 | 0,10,0 | 3 |
| 006 | 4 | 0,12,0 | 2 |

Other important intensities are 202(10), 012(10), 170(12), 103(10), 131(10).

The Interpretation of Laue Photographs.—The growing usefulness of this historically first method for obtaining information, even as to the probable space-group characteristics of a crystal, makes desirable some further comment upon interpretation, although detailed discussion is to be found in the several technical treatises on crystal analysis. A single Laue photograph taken alone yields only a limited amount of information. It appears as a series of spots (Fig. 130) whose loci are symmetrically disposed ellipses, passing through the central direct-beam image if the primary beam has passed through the crystal parallel to a principal axis. The galaxy of spots is an indication of the ability of the many families of planes, each at a certain angle θ with respect to the primary x-ray beam, to pick out, from the assortment of rays of different wave lengths, the particular one for reflection according to $n\lambda = 2d \sin \theta$. The symmetry is a proof of the orderly arrangement within the crystal, suggested by the external crystalline form. Thus, if the beam passes parallel to a cubic axis, with fourfold symmetry, the pattern has a fourfold symmetry.

The 32 point-groups may be divided into 11 groups by the symmetries displayed by Laue patterns. These patterns are such that all crystals seem to have a center of symmetry, and for this reason unique identification cannot be made. In the following tabulation the point-group symbols are those listed in Table XXX, page 250.

reflected spot appears on the plate at R . A line from S through Q , where the ray cuts the sphere, meets the plate at R' , the projection of R . This spot will be on a circle with the projections of the other spots originating from planes with a common zone axis.

A stereographic projection of potassium chloride is shown in Fig. 153. The Laue pattern of this simple cubic crystal is characterized by spots with perfectly regular distribution of intensities, at every intersection of circles. The Laue pattern for sodium chloride, on the other hand, differs in that the spots which

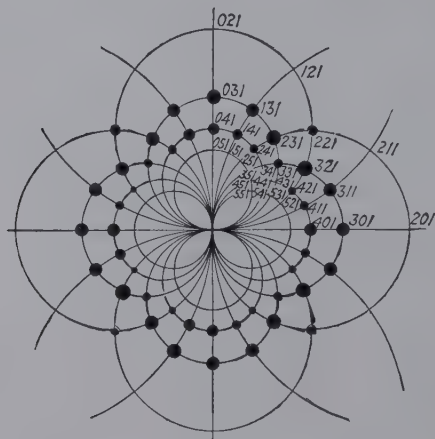


FIG. 153.—Stereographic projection of Laue pattern of KCl.

for KCl have odd and even indices (*e.g.*, 341) are absent. Thus the face-centered cubic lattice for which the structure factor predicts this very fact may be assigned as the underlying arrangement of the heavier chlorine atoms in rock salt.

The gnomonic projection is even more valuable for the complicated types of Laue patterns. The essential process involved is shown in Fig. 154; R is the Laue spot and OQ the zone axis of the plane which is perpendicular to the plane of the paper. The perpendicular to this plane strikes the plane of projection and

$$P'S = P'O \cos \theta \text{ and } PR = PO \tan 2\theta,$$

where $P'S$ is the distance of the gnomonic projection from the center, $P'O$ is the radius of projection, PR is the distance of the Laue spot from the center, and PO is the radius of the Laue film (*i.e.*, distance from specimen to film). $P'O$ and PO may be

Wyckoff has used, with great success, unsymmetrical Laue photographs, obtained by inclining one of the crystal axes to the beam. In Fig. 155 is shown the gnomonic projection for such a photograph of a potassium iodide crystal.

Laue patterns sometimes display abnormal effects which may have a highly significant bearing upon the condition or texture of the crystal: "asterism" streaks on bending or distorting the

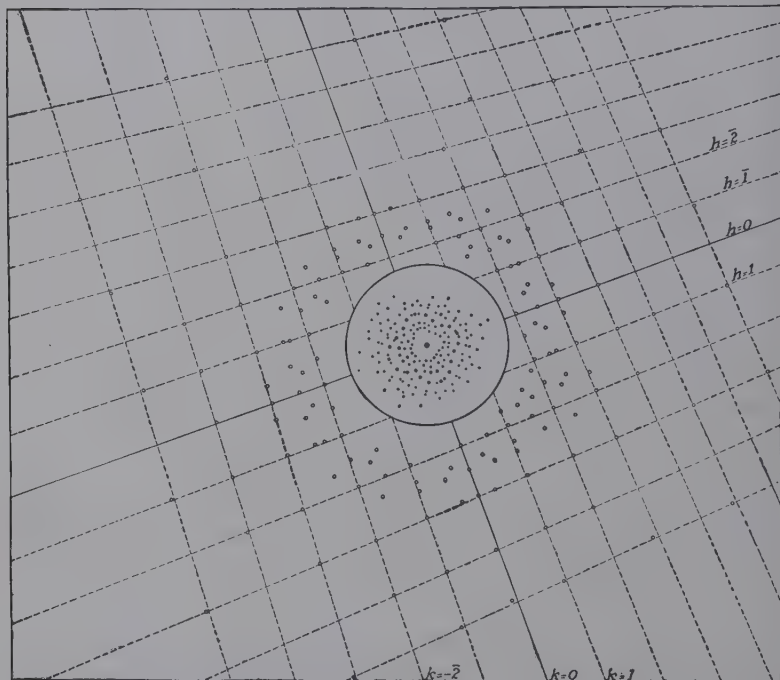


FIG. 155.—Gnomonic projection of an unsymmetrical Laue pattern of KI.

specimen (Chap. XXI); changes in the lattice during age-hardening of alloy single crystals (Chap. XVIII); and faint diffuse extra spots which become increasingly intense as the temperature is raised. These spots were found by Clark and Duane for crystals of KI, etc., in 1922, but this work was criticized by other experimenters. Now, however, Preston convincingly proves the real existence of this effect as due to thermal vibrations of the lattice which break the crystal up into groups, consisting, for a face-centered cubic lattice, of an atom

and its 12 neighbors (dodecahedral coordination).¹ Typical patterns are reproduced in Fig. 156.

The dimensions of the unit cell may sometimes be estimated from Laue data, and, of course, for cubic crystals the value of $n\lambda$ for each spot is given by $\sin \Theta$ and a_0 and hkl from the equation

$$n\lambda = \frac{2a_0}{\sqrt{h^2 + k^2 + l^2}} \sin \Theta_n.$$

The fact that general radiation is employed, however, is always a complication. At moderate voltages, 50,000 kv., the maximum intensity in the spectrum is at 0.48 A.U., the characteristic absorption wave length of the silver in the photographic emulsion. If the voltage is known, $\lambda_{\min.}$ is, of course, at once established and this at once limits the possibilities of interpretation of Laue spots and eliminates some of the alternative possible unit crystal cells.

Intensity data from Laue patterns are not accurately determined but simply classed relatively by visual comparison on the photographic negative.

Numerous complications are involved, as explained earlier, and in addition there is absorption in the crystal. However, the Laue data even though only approximate are sometimes very important, since by this method alone are reflections from planes of high indices and complicated structure registered. The greatest usefulness of the method therefore lies in conjunction with other methods with which quantitative information can be easily obtained.

The Interpretation of Rotation Patterns.—When a single crystal is rotated around one of its principal crystallographic axes in the path of an x-ray beam defined by pinholes or slits, a very characteristic pattern is registered on the photographic



FIG. 156.—Laue pattern of penterythritol, showing extraneous "Preston" spots (four strong and four weak diffuse spots) from effect of temperature on lattice.

¹ *Proc. Roy. Soc. (London)*, **172**, 116 (1939).

film. It is called a layer-line diagram because the interference maxima all lie on horizontal layers or lines. If a flat film is used, these lines are hyperbolas above and below a straight equatorial line. On a cylindrical film bent on the circumference of a circle at the center of which is the crystal the layer lines are straight lines parallel to the equator. A representative photograph is shown in Fig. 157. It follows that all the interference maxima lying on these layer lines are produced by planes with the same zone axis, namely, the common crystallographic and rotation axis. The spectrum is therefore "complete." The familiar Bragg spectra are, of course, produced by only one

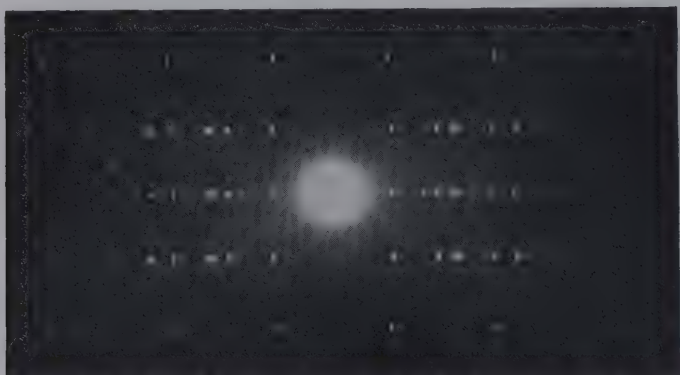


FIG. 157.—Rotation pattern of a crystal of orthophenanthroline.

set of planes, the experimental arrangement of slits and crystal being such that other planes cannot register. The lines or spots lying on the equator of the oscillation or rotation pattern therefore are really the "Bragg principal spectrum."

As explained in the preceding chapter, the angles between principal axes may be determined in many cases by reorienting the crystal on its goniometer head until sharp layer-line diagrams are obtained. With three such rotation patterns corresponding to the three principal axes, the dimensions of the unit crystal cell may be directly deduced. These patterns have the great advantage that one lattice spacing, namely, that for the atomic planes along the rotation axis, may be measured independently of any assumption as to crystal system or planar indices. It is necessary only to measure the distances $e_1, e_2 \dots e_n$ of the vertices of the hyperbolas on the tangent film (or the straight

layer lines on a film that had been bent on a cylinder coaxial with the specimen) from the central zero point of the main beam. The distance from specimen to film, a , being known, the diffraction angles $\mu_1, \mu_2 \dots \mu_n$ (Fig. 158a) may be calculated, since the tangents are e_n/a . The identity period or spacing along the rotation axis is then simply calculated from

$$I = n\lambda/\sin \mu_n,$$

where n is the number of the layer line (1, 2, 3, etc.). Then identically the same value is obtained from all the layer lines.

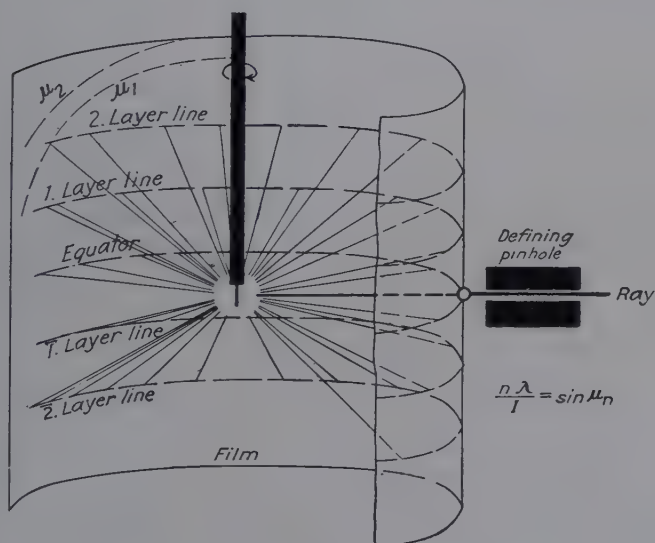


FIG. 158a.—Diagram of the rotation method.

Three such values of I for each of the principal axes give the size of the unit cell.

The process of assigning indices to the interference maxima lying on the layer line is usually straightforward. Thus on the equatorial line the index h_3 in $h_1h_2h_3$ is zero; in other words all indices must be h_1h_20 ; h_3 must be 1 on the first horizontal layer line, 2 on the second, etc. These maxima lie not only on horizontal layer lines but also on vertical loci which are zone curves (Fig. 158b). Schiebold calculated these two types of layer lines (*Schichtlinien*) of the *I* and *II* kind. Thus if the first maximum on the equator is due to 100 planes, then the spot on the first

layer line lying on the common vertical zone curve is 101; if the second spot on the equator is 110, the spot above or below it on the first layer line and the second zone curve is 111. It is at once evident that oscillation photographs taken over a fixed angle are much simpler to interpret than a composite pattern made for a complete rotation around 360 deg.

Besides giving direct information concerning the crystallographic system and the dimensions and shape of the unit cell together with the number of atoms or molecules per unit cell.

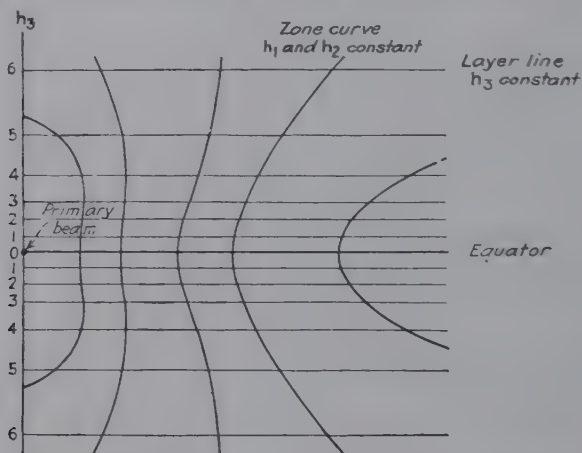


FIG. 158b.—Diagram of two types of layer lines on rotation patterns.

these spectrum photographs permit space-group assignment. When the interference maxima have been identified with the planar indices, the presence or absence of possible reflections can at once be noted and the criteria for a specific space-group set up.

The matter of interpretation may become very complex for the monoclinic and triclinic systems unless a more powerful aid is sought. This is found in the concept of the reciprocal lattice introduced by Ewald.

The Reciprocal Lattice.—The reciprocal lattice is a three-dimensional network of points throughout the space surrounding the unit cell. Each point in the reciprocal lattice is separated from the origin of the lattice by a distance inversely proportional to the interplanar spacing of the planes that it represents, and its direction from the origin is exactly the same as the direction

of the normal to the planes. To show the relationship more clearly a two-dimensional reciprocal lattice plane for a monoclinic crystal is shown in Fig. 159, with its position in respect to one of the monoclinic unit cells. There is a point in the reciprocal lattice for every possible reflection. The line connecting the origin and the reciprocal lattice point is a vector and can be considered by the usual methods applicable to vectors. As

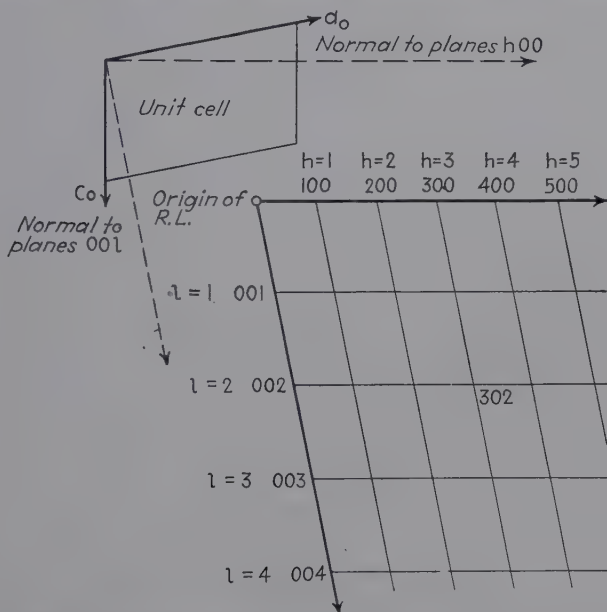


FIG. 159.—Two-dimensional reciprocal lattice in reference to monoclinic unit crystal cell.

can be noted from the diagram of the monoclinic lattice, the indices of the reciprocal lattice point are exactly the same as the Miller indices defining the original interplanar distances, and this is, of course, due to the fact that the Miller indices are reciprocal quantities.

The importance of this concept may be shown by considering a set of planes undergoing the Bragg reflection. If an arbitrary distance K is selected along the incident beam and transferred to the reflected beam, we may construct an isosceles triangle with a height ρ (see Fig. 160) along the normal to the planes. An analysis of the figure shows that

$$\rho' = K \sin \Theta \quad (1)$$

where K is the distance selected along the incident beam, and Θ is one-half of the diffraction angle. If we use the Bragg relation to eliminate the $\sin \Theta$, the following equation, which serves to define the reciprocal lattice, is obtained:

$$\rho'd = K\frac{\lambda}{2} = K' \text{ (for a given } \lambda\text{)}. \quad (2)$$

It is convenient to let the arbitrary constant equal $2/\lambda$, whence $\rho'd = 1$.

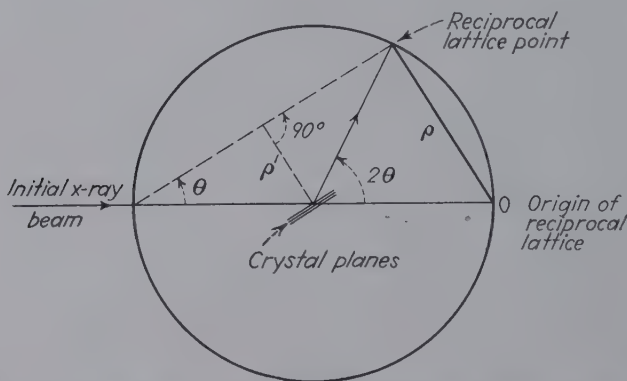


FIG. 160.—Construction of the reciprocal lattice and sphere of diffraction.

Equation (2) shows that ρ' varies inversely as d (the wave-length being considered constant), so that ρ' can be considered as the distance from a point in the reciprocal lattice to its origin. (Since ρ' was constructed normal to the planes diffracting and passes through the origin, it fulfills the conditions for the reciprocal lattice.)

So diffraction can occur, for any interplanar spacing, when the reciprocal lattice point (defined here by the intersection of ρ' and of the base of the triangle) intersects the locus of all such possible points, *i.e.*, upon our diagram a small circle (not shown) or in three-dimensional space a sphere. Such a sphere is usually termed the "sphere of diffraction." The dimension of the sphere of diffraction is, of course, dependent upon the constant chosen in converting the unit cell to a reciprocal lattice, or conversely we may say that the constant employed in converting the reciprocal lattice to a unit cell is determined by the size of the sphere of diffraction employed.

The reciprocal-lattice intersections with the sphere, however, furnish, when projected from the pole of the sphere to a cylindrical or spherical surface, a pattern which although distorted is still similar to the original reciprocal lattice. Calculations are simplified with this method since all that is necessary is to correct the distortion from the x-ray pattern made and determine directly the reciprocal-lattice dimensions (this, of course, also determines the h , k , and l for each interference). After the reciprocal lattice is known, the unit vectors may be converted readily with the formulas given below, to give the dimensions (and, in some cases, the angles) of the unit cell.

The unit vectors along the coordinate axes of the reciprocal lattice are, of course, related to the (100), (010), and (001) *interplanar spacings* by formulas of the type

$$b_r^* d_{010} = K'. \quad (3)$$

The equations necessary to transform *any* unit cell into the reciprocal lattice involve vectors (since a lattice point represents not only a magnitude $K \sin \Theta$ but also a direction). It should be noted that operation of the equations carried out on a reciprocal-lattice unit will rederive the unit cell, since these quantities are reciprocal. The most general case is, of course, the triclinic crystal. The volume of a triclinic solid, bounded by parallel planes, is given by

$$V = abc(1 + 2 \cos \alpha \cos \beta \cos \gamma - \cos^2 \alpha - \cos^2 \beta - \cos^2 \gamma)^{\frac{1}{2}}.$$

The distance between parallel planes making up a triclinic figure may be expressed

$$d_a = \frac{V}{bc \sin \alpha}, \quad d_b = \frac{V}{ac \sin \beta}, \quad d_c = \frac{V}{ab \sin \gamma},$$

where d_a is the normal distance between the set of planes separated in the figure by the edge designated a_0 . Angular transformation to or from the reciprocal lattice:

$$\begin{aligned} \cos \alpha_r^* &= \frac{(\cos \beta \cos \gamma - \cos \alpha)}{\sin \beta \sin \gamma}, \\ \cos \beta_r^* &= \frac{(\cos \alpha \cos \gamma - \cos \beta)}{\sin \alpha \sin \gamma}, \\ \cos \gamma_r^* &= \frac{(\cos \alpha \cos \beta - \cos \gamma)}{\sin \alpha \sin \beta}. \end{aligned}$$

If all angles in the unit cell are 90 deg., the corresponding angles in the reciprocal lattice cell will be 90 deg., and in the monoclinic system the relations give 90 deg. angles for all but one, where $\cos \beta_r^* = -\cos \beta$.

Transformation formulas for reciprocal lattices or unit cells are as follows:

If $K\lambda/2 = K' = \rho'd$,

$$a_r^* = \frac{K'bc \sin \alpha}{V},$$

$$b_r^* = \frac{K'ac \sin \beta}{V},$$

$$c_r^* = \frac{K'ab \sin \gamma}{V}.$$

The reciprocal lattice is especially well adapted for analysis of the patterns made from rotating crystals. Although its importance with the ordinary rotation pattern cannot be neglected, its most effective use is with patterns made upon x-ray goniometers. For this purpose, it is somewhat more convenient to reconstruct the geometrical figure in Fig. 160 by incorporating it in the sphere of diffraction itself. Consideration of the diagram will show that if the sphere of diffraction is drawn with the diffraction planes as the center and the reciprocal lattice (magnified by a value of 2) rotated about one end of a diameter of the sphere of reflection, the direction of the diffracted radiation is determined by the reciprocal lattice point without additional geometrical construction.

In this diagram ρ is the basis of the new reciprocal lattice, and R is taken as the *radius* of the sphere of diffraction. We may note briefly the following relations:

$$\rho' = R \sin \Theta, \rho = 2R \sin \Theta, \rho d = R\lambda.$$

If we imagine a spherical film, with a diffracting crystal at the center, each point at which a reciprocal lattice point cuts the sphere will represent a possible interference recorded on the film. A line drawn from the center of the sphere (the sample) through such a point must represent the direction of the diffracted x-ray beam.

For circular cameras the picture must be modified a trifle, since in this case the film does not coincide with the sphere except as the circumference of a circle. The sphere may be used, how-

ever, to indicate the direction of the diffracted x-ray beams for purposes of construction.

The Reciprocal Lattice in the Interpretation of Rotation Patterns.—It has been shown that a single crystal may be regarded as a reciprocal lattice in space. When we study rotating crystals, we can simply consider the reciprocal lattice as rotating, and we have a quasi-geometrical picture, then, of the reflecting process as it occurs. This picture is the basis of all single-crystal techniques employed at the present time, with the exception of some Laue-pattern methods.

Layer Lines.—If the reciprocal lattice is rotated in such a manner that a set of planes is rotated about a common normal, we find layers of reciprocal-lattice points intercepting the rotating axis at equal intervals. As the crystal (or lattice) rotates, these planes of points will remain at a constant height above the equatorial plane and so must intersect the sphere of reflection at a certain height. The circle formed by this intersection will contain all possible positions in which the points lying in the specific reciprocal-lattice plane considered may intersect the sphere.

From the preceding section it is obvious that all interferences would fall upon the circle defined by the intersection of the plane and the sphere as designated above if a spherical film were used to record the pattern. Spherical films, however, are not feasible, so that it is necessary to consider the commonly used circular camera. The direction of the interferences for any specific layer of the lattice can be defined by two angles, one corresponding to elevation and the other to a rotation from the direction of the incident beam. The elevation remains constant for any given lattice plane and, therefore, a circular film will exhibit all interferences from a given plane of the reciprocal lattice on an imaginary straight horizontal line, at a fixed distance above the equator of the pattern. (The equator is that straight line which contains the undiffracted x-ray beam effects in its center.) The height of this set of interferences above the equatorial layer line must evidently fix the identity unit (or distance) between the layers of the reciprocal lattice along the axis that was used for rotation. The height of a layer line may, of course, be measured from any interference occurring on the layer line of interest, and usually the measurement is made to the symmetri-

cal interference in the layer line on the opposite side of the equator, for greater accuracy.

For a specific case let us assume a crystal rotating in such a manner that the planes rotating about their normal are the hk planes; *i.e.*, the normal (in case the crystal is orthogonal) corresponds to the direction 001; and the identity period along this axis will be in the reciprocal lattice c_r^* . Let μ_n be the angle measured from the equator to the n th layer line, and, of course, the normal distance separating the planes will then be nc_r^* . From the reciprocal-lattice sphere-of-reflection diagram we can see that

$$\rho = \frac{nc_r^*}{\cos \mu},$$

$$\rho = 2R \sin \mu,$$

or, equating the two expressions,

$$nc_r^* = R \sin 2\mu.$$

Of course, c_r^* corresponds to the reciprocal-lattice distance describing the 001 dimension of the unit cell (d_{001}) so that since

$$\rho d = R\lambda, \quad c_r^* d_{001} = R\lambda,$$

and

$$d_{001} = \frac{nR\lambda}{R \sin 2\mu},$$

$$d_{001} = (\text{orthogonal}) \ c_0 = \frac{\lambda n}{\sin 2\mu}.$$

Of course, any set of planes may be used, not only those normal to 001. Each of the three principal dimensions of the unit cell may be determined and such other interplanar spacings as are of importance.

Analysis of Rotation Patterns.—The preceding section has indicated the use of the reciprocal lattice in permitting the visualization of many data at the same time. The results of such a procedure are quite correct in terms of the Bragg law.

To visualize the pattern better, though, let us approximate our general geometrical picture. We shall assume that the sphere of diffraction has infinite radius and thus becomes, rather than a sphere, a plane of diffraction (see Fig. 159).

If the reciprocal lattice is now rotated in this plane each point of the lattice as it passes through the plane may be

considered to leave a mark; the plane with its marks would then correspond to a rotation pattern. If the reciprocal lattice is orthorhombic, with rotation about c , we shall find a definite regularity in this arrangement of marks. Our pattern will tend to resemble Fig. 161. To express this in words, we shall

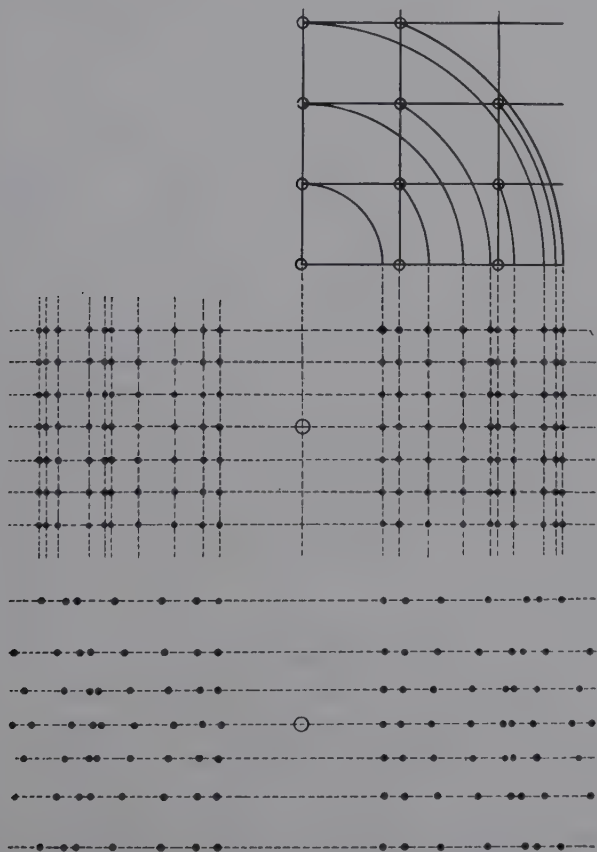


FIG. 161.—The rotation pattern (below) in relation to the construction of the reciprocal lattice.

have lines of spots formed vertically as well as those formed horizontally. A horizontal line of spots, as we know, contains interferences in which l has the same value; these vertical lines (which are somewhat distorted on the actual pattern because of the sphere) are “row lines” or “secondary layer lines,” and all spots on such a line will have the same hk

value. That is, hkl must be directly above $hk0$ in the reciprocal lattice (with the orientation we are considering). It is always possible that another interference than the $hk0$ considered might be in such a position as to appear in the same row line, but such coincidences are rare except in the monoclinic and triclinic systems.

In many cases rotation patterns may be interpreted visually, by examining some of the various factors of the approximate picture discussed above.

X-ray Goniometer Patterns.—Diffraction patterns of rotating crystals, made so that the angle of the crystal at the moment of diffraction is recorded, furnish valuable information in the determination of unit cells, especially in dealing with the oblique systems. Such instruments may be generally termed "x-ray goniometers." Perhaps the most widely known is the Weissenberg goniometer, in which the film is moved behind a shield as the crystal rotates, in such a manner as to add a new coordinate to the recorded diffraction spots. The coordinate system obtained with this instrument is rather complex, and for this reason other types of camera are coming into more general use.

The Schiebold-Sauter camera consists essentially of a rotating pillar (bearing the oriented crystal) before a shield which permits the reflections of but one layer line to be recorded on the film behind the shield. This film is arranged to rotate perpendicularly to the undiffracted x-ray beam at exactly the same rate as the crystal is rotated. The interferences obtained lie at the intersections of a distorted reciprocal lattice, and usually the indices may be determined by examination.

The usual arrangement of reflections is on double spirals which cut the central primary-beam spot. Each curve is the geometrical locus of the reflections of different orders from the same lattice planes. The distance r of a reflection from the central spot is $r = A \tan 2\theta$, where A is the distance of the crystal axes of rotation to the center of the rotating films. The azimuthal angle ϕ of the diagram in polar coordinates is equal to the rotation angle of the crystal. The angles ϕ_1 , ϕ_2 , etc., of interferences are proportional to θ_1 , θ_2 , and the radial distances V_1 , V_2 , etc., are proportional to $\tan \theta_1$, etc. In Fig. 162a is shown a pattern of urea rotated around the c axis, and in

Fig. 162b the indexed network, representing a distorted reciprocal lattice made directly from the pattern. The shaded area represents the unit cell. The interference D_1 is, therefore, 220 , D'_1 , $2\bar{2}0$, etc. Thus the edge lengths of the elementary cell for the a and b directions are directly evaluated, and the c



FIG. 162a.—Schiebold-Sauter goniometer pattern for urea crystal, rotated around c axis. (Glocker.)

dimension is derived from the layer-line displacements on the ordinary rotation pattern. The angle that the two edges of the cell make with each other is equal to the angle of intersection of the two curves $n00$ and $0n0$ in the primary spot; for urea this is a right angle. The principal value of the Schiebold-Sauter diagram consists in the immediate disclosure of which planes are reflecting and which are not.

The most recent development gives the undistorted reciprocal-lattice image itself. Essentially the method consists in placing the film in the exact position of a plane of points (normal to the axis of rotation) in the reciprocal lattice. The film and

lattice are then rotated together through a sphere of diffraction. If the interferences of other layer lines are screened off, the only x-ray beams striking the film pass at the same time through a reciprocal-lattice intersection in the plane of the film. Effectively, this transfers the position of the lattice intersection defining the specific interference to the film, and the final result is a scale diagram of the intersections of the reciprocal-lattice net that correspond to the permitted hkl values.

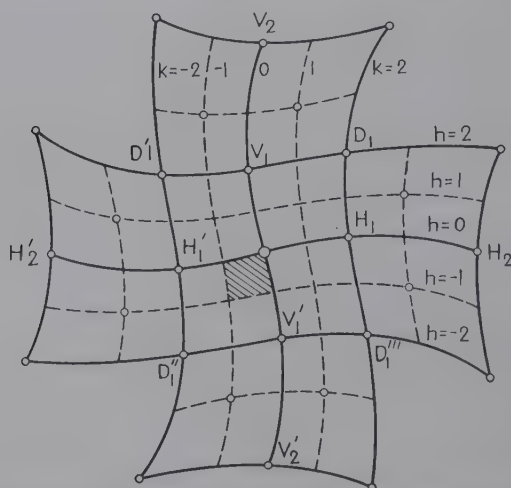


FIG. 162b.—Projection and indexing of pattern in Fig. 162a, showing distorted reciprocal lattice.

The dimensions of the equipment fix the constants, so that the dimensions on the film are related to those of the unit cell by

$$\rho'd = K' = K' \text{ (equipment).}$$

If the x-ray beam is perpendicular to the rotating crystal, then a specific K' value may be used for all layer lines. However, if the x-ray beam is placed at an angle to the rotating crystal, for the purpose of obtaining the reciprocal-lattice diagram of the equatorial or low layer line, this constant will change. The constant will also be different if a different wave-length radiation is employed. The patterns shown in Fig. 139 were made in this manner at the angle of 30 deg. so that each is a completely undistorted representation of a reciprocal-lattice plane.

The Interpretation of Powder Spectra.—In this method there is simultaneous registration of all sets of planes due to the random distribution of fine grains. If the crystal system and unit-cell dimensions are known from independent measurements with single crystals, the assignment of indices is not difficult, since $d_{hkl} = \frac{a_0}{\sqrt{F(hkl; abc; \alpha\beta\gamma)}}$, or for the cubic system $d_{hkl} = \frac{a_0}{\sqrt{h^2 + k^2 + l^2}}$. Under the discussion of determination of space-groups from the absence or extinction of certain reflections,

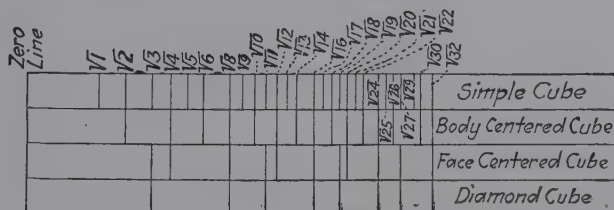


FIG. 163.—The relations between powder spectra for various cubic crystals.

a differentiation was found for simple, body-centered, and face-centered cubic lattices depending upon nonappearance of reflections for certain planes. The structure factor clearly indicates that if all possible values of hkl appear the crystal is simple cubic; for the body-centered lattice the sum of hkl indices must be even and 110, 200, 211, 220, 310, 222, 321, 400, etc., will appear; and for the face-centered cubic lattice the indices must be all odd or all even as in 111, 200, 311, 222, 400, etc. The powder spectra are illustrated in a diagram in Fig. 163. It will be noticed that even for the cubic system lines related to $\sqrt{7}$, $\sqrt{15}$, $\sqrt{23}$, $\sqrt{28}$, $\sqrt{31}$, etc., are absent, since in $\sqrt{h^2 + k^2 + l^2}$ no sum of squares of integers will give these numbers. If values of a_0 , etc., are unknown, trial and failure methods may be successfully used. Thus for a cubic crystal

$$d_{hkl} = \frac{a_0}{\sqrt{h^2 + k^2 + l^2}} = \frac{n\lambda}{2 \sin \Theta_n},$$

$$\frac{4a_0^2 \sin^2 \Theta_n}{\lambda^2} = (h^2 + k^2 + l^2)n^2.$$

Any two powder spectra lines must have $\sin^2 \Theta_n$ values which will be in the ratio of whole numbers, since $(h^2 + k^2 + l^2)n^2$ is

TABLE XXXIII.—POSITIONS OF POWDER DIFFRACTION INTERFERENCES FOR CUBIC, TETRAGONAL, AND HEXAGONAL CRYSTALS

| | | | |
|------------|------------------------|------------------------|---|
| Cubic | I. Cubic lattice | $a = 4.0 \text{ A.U.}$ | $\sin^2 \theta = \frac{\lambda^2}{4a^2}(h^2 + k^2 + l^2).$ |
| Tetragonal | II. Tetragonal lattice | $a = 4.0 \text{ A.U.}$ | $\sin^2 \theta = \frac{\lambda^2}{4a^2} \left(h^2 + k^2 + l^2 \frac{a^2}{c^2} \right)$ |
| Hexagonal | III. Hexagonal lattice | $a = 4.0 \text{ A.U.}$ | $\sin^2 \theta = \frac{\lambda^2}{4a^2} \left[\frac{4}{3}(h^2 + k^2 + kh) + l^2 \frac{a^2}{c^2} \right]$ |

$$\frac{\lambda^2}{4a^2} = 0.037$$

$$\lambda = 1.539 \text{ A.U.}$$

| I | | | | II | | | | III | | | |
|-----|-----|-----|-------------------|-----------------|-----|-----|-----|-------------------|-----------------------|--|-----------------|
| h | k | l | $h^2 + k^2 + l^2$ | $\sin^2 \theta$ | h | k | l | $h^2 + k^2 + l^2$ | $\frac{l^2 a^2}{c^2}$ | $\frac{4}{3}(h^2 + k^2 + l^2 + \frac{a^2}{c^2})$ | $\sin^2 \theta$ |
| 0 | 0 | 1 | 1 | 0.037 | 1 | 0 | 0 | 1 | 0.376 | 0.376 | 0.014 |
| 0 | 1 | 1 | 2 | 0.074 | 1 | 1 | 0 | 2 | 0 | 1.33 | 0.049 |
| 0 | 1 | 1 | 3 | 0.111 | 0 | 0 | 1 | 1 | 0 | 0 | 0.055 |
| 0 | 1 | 2 | 5 | 0.148 | 0 | 1 | 1 | 2 | 0.37 | 1.7 | 0.063 |
| 0 | 1 | 2 | 6 | 0.185 | 2 | 0 | 0 | 4 | 1.5 | 2.83 | 0.104 |
| 0 | 1 | 2 | 8 | 0.222 | 1 | 1 | 1 | 3 | 0 | 3.37 | 0.125 |
| 0 | 2 | 2 | 9 | 0.296 | 1 | 2 | 0 | 5 | 0 | 4 | 0.148 |
| 0 | 2 | 2 | 9 | 0.333 | 1 | 2 | 1 | 6 | 0.37 | 4.37 | 0.162 |
| 0 | 0 | 3 | 9 | 0.370 | 2 | 0 | 1 | 5 | 0 | 4.70 | 0.174 |
| 0 | 1 | 3 | 10 | 0.407 | 2 | 2 | 0 | 8 | 0 | 5.33 | 0.198 |
| 2 | 2 | 2 | 12 | 0.444 | 0 | 0 | 2 | 8 | 1.5 | 5.5 | 0.204 |
| 0 | 2 | 3 | 13 | 0.481 | 3 | 0 | 0 | 9 | 0.37 | 5.7 | 0.211 |
| 2 | 1 | 3 | 14 | 0.518 | 1 | 3 | 0 | 10 | 6 | 6 | 0.223 |
| 0 | 0 | 4 | 16 | 0.592 | 2 | 2 | 1 | 9 | 1.5 | 6.83 | 0.253 |
| 0 | 0 | 4 | 16 | 0.592 | 2 | 2 | 1 | 10 | 6 | 7.33 | 0.272 |
| 0 | 0 | 4 | 16 | 0.592 | 2 | 2 | 1 | 10 | 6 | 7.33 | 0.273 |
| 0 | 0 | 4 | 16 | 0.592 | 2 | 2 | 1 | 10 | 6 | 7.33 | 0.273 |
| 0 | 0 | 4 | 16 | 0.592 | 2 | 2 | 1 | 10 | 6 | 7.33 | 0.273 |
| 0 | 0 | 4 | 16 | 0.592 | 2 | 2 | 1 | 10 | 6 | 7.33 | 0.273 |
| 0 | 0 | 4 | 16 | 0.592 | 2 | 2 | 1 | 10 | 6 | 7.33 | 0.273 |
| 0 | 0 | 4 | 16 | 0.592 | 2 | 2 | 1 | 10 | 6 | 7.33 | 0.273 |
| 0 | 0 | 4 | 16 | 0.592 | 2 | 2 | 1 | 10 | 6 | 7.33 | 0.273 |
| 0 | 0 | 4 | 16 | 0.592 | 2 | 2 | 1 | 10 | 6 | 7.33 | 0.273 |
| 0 | 0 | 4 | 16 | 0.592 | 2 | 2 | 1 | 10 | 6 | 7.33 | 0.273 |
| 0 | 0 | 4 | 16 | 0.592 | 2 | 2 | 1 | 10 | 6 | 7.33 | 0.273 |
| 0 | 0 | 4 | 16 | 0.592 | 2 | 2 | 1 | 10 | 6 | 7.33 | 0.273 |
| 0 | 0 | 4 | 16 | 0.592 | 2 | 2 | 1 | 10 | 6 | 7.33 | 0.273 |
| 0 | 0 | 4 | 16 | 0.592 | 2 | 2 | 1 | 10 | 6 | 7.33 | 0.273 |
| 0 | 0 | 4 | 16 | 0.592 | 2 | 2 | 1 | 10 | 6 | 7.33 | 0.273 |
| 0 | 0 | 4 | 16 | 0.592 | 2 | 2 | 1 | 10 | 6 | 7.33 | 0.273 |
| 0 | 0 | 4 | 16 | 0.592 | 2 | 2 | 1 | 10 | 6 | 7.33 | 0.273 |
| 0 | 0 | 4 | 16 | 0.592 | 2 | 2 | 1 | 10 | 6 | 7.33 | 0.273 |
| 0 | 0 | 4 | 16 | 0.592 | 2 | 2 | 1 | 10 | 6 | 7.33 | 0.273 |
| 0 | 0 | 4 | 16 | 0.592 | 2 | 2 | 1 | 10 | 6 | 7.33 | 0.273 |
| 0 | 0 | 4 | 16 | 0.592 | 2 | 2 | 1 | 10 | 6 | 7.33 | 0.273 |
| 0 | 0 | 4 | 16 | 0.592 | 2 | 2 | 1 | 10 | 6 | 7.33 | 0.273 |
| 0 | 0 | 4 | 16 | 0.592 | 2 | 2 | 1 | 10 | 6 | 7.33 | 0.273 |
| 0 | 0 | 4 | 16 | 0.592 | 2 | 2 | 1 | 10 | 6 | 7.33 | 0.273 |
| 0 | 0 | 4 | 16 | 0.592 | 2 | 2 | 1 | 10 | 6 | 7.33 | 0.273 |
| 0 | 0 | 4 | 16 | 0.592 | 2 | 2 | 1 | 10 | 6 | 7.33 | 0.273 |
| 0 | 0 | 4 | 16 | 0.592 | 2 | 2 | 1 | 10 | 6 | 7.33 | 0.273 |
| 0 | 0 | 4 | 16 | 0.592 | 2 | 2 | 1 | 10 | 6 | 7.33 | 0.273 |
| 0 | 0 | 4 | 16 | 0.592 | 2 | 2 | 1 | 10 | 6 | 7.33 | 0.273 |
| 0 | 0 | 4 | 16 | 0.592 | 2 | 2 | 1 | 10 | 6 | 7.33 | 0.273 |
| 0 | 0 | 4 | 16 | 0.592 | 2 | 2 | 1 | 10 | 6 | 7.33 | 0.273 |
| 0 | 0 | 4 | 16 | 0.592 | 2 | 2 | 1 | 10 | 6 | 7.33 | 0.273 |
| 0 | 0 | 4 | 16 | 0.592 | 2 | 2 | 1 | 10 | 6 | 7.33 | 0.273 |
| 0 | 0 | 4 | 16 | 0.592 | 2 | 2 | 1 | 10 | 6 | 7.33 | 0.273 |
| 0 | 0 | 4 | 16 | 0.592 | 2 | 2 | 1 | 10 | 6 | 7.33 | 0.273 |
| 0 | 0 | 4 | 16 | 0.592 | 2 | 2 | 1 | 10 | 6 | 7.33 | 0.273 |
| 0 | 0 | 4 | 16 | 0.592 | 2 | 2 | 1 | 10 | 6 | 7.33 | 0.273 |
| 0 | 0 | 4 | 16 | 0.592 | 2 | 2 | 1 | 10 | 6 | 7.33 | 0.273 |
| 0 | 0 | 4 | 16 | 0.592 | 2 | 2 | 1 | 10 | 6 | 7.33 | 0.273 |
| 0 | 0 | 4 | 16 | 0.592 | 2 | 2 | 1 | 10 | 6 | 7.33 | 0.273 |
| 0 | 0 | 4 | 16 | 0.592 | 2 | 2 | 1 | 10 | 6 | 7.33 | 0.273 |
| 0 | 0 | 4 | 16 | 0.592 | 2 | 2 | 1 | 10 | 6 | 7.33 | 0.273 |
| 0 | 0 | 4 | 16 | 0.592 | 2 | 2 | 1 | 10 | 6 | 7.33 | 0.273 |
| 0 | 0 | 4 | 16 | 0.592 | 2 | 2 | 1 | 10 | 6 | 7.33 | 0.273 |
| 0 | 0 | 4 | 16 | 0.592 | 2 | 2 | 1 | 10 | 6 | 7.33 | 0.273 |
| 0 | 0 | 4 | 16 | 0.592 | 2 | 2 | 1 | 10 | 6 | 7.33 | 0.273 |
| 0 | 0 | 4 | 16 | 0.592 | 2 | 2 | 1 | 10 | 6 | 7.33 | 0.273 |
| 0 | 0 | 4 | 16 | 0.592 | 2 | 2 | 1 | 10 | 6 | 7.33 | 0.273 |
| 0 | 0 | 4 | 16 | 0.592 | 2 | 2 | 1 | 10 | 6 | 7.33 | 0.273 |
| 0 | 0 | 4 | 16 | 0.592 | 2 | 2 | 1 | 10 | 6 | 7.33 | 0.273 |
| 0 | 0 | 4 | 16 | 0.592 | 2 | 2 | 1 | 10 | 6 | 7.33 | 0.273 |
| 0 | 0 | 4 | 16 | 0.592 | 2 | 2 | 1 | 10 | 6 | 7.33 | 0.273 |
| 0 | 0 | 4 | 16 | 0.592 | 2 | 2 | 1 | 10 | 6 | 7.33 | 0.273 |
| 0 | 0 | 4 | 16 | 0.592 | 2 | 2 | 1 | 10 | 6 | 7.33 | 0.273 |
| 0 | 0 | 4 | 16 | 0.592 | 2 | 2 | 1 | 10 | 6 | 7.33 | 0.273 |
| 0 | 0 | 4 | 16 | 0.592 | 2 | 2 | 1 | 10 | 6 | 7.33 | 0.273 |
| 0 | 0 | 4 | 16 | 0.592 | 2 | 2 | 1 | 10 | 6 | 7.33 | 0.273 |
| 0 | 0 | 4 | 16 | 0.592 | 2 | 2 | 1 | 10 | 6 | 7.33 | 0.273 |
| 0 | 0 | 4 | 16 | 0.592 | 2 | 2 | 1 | 10 | 6 | 7.33 | 0.273 |
| 0 | 0 | 4 | 16 | 0.592 | 2 | 2 | 1 | 10 | 6 | 7.33 | 0.273 |
| 0 | 0 | 4 | 16 | 0.592 | 2 | 2 | 1 | 10 | 6 | 7.33 | 0.273 |
| 0 | 0 | 4 | 16 | 0.592 | 2 | 2 | 1 | 10 | 6 | 7.33 | 0.273 |
| 0 | 0 | 4 | 16 | 0.592 | 2 | 2 | 1 | 10 | 6 | 7.33 | 0.273 |
| 0 | 0 | 4 | 16 | 0.592 | 2 | 2 | 1 | 10 | 6 | 7.33 | 0.273 |
| 0 | 0 | 4 | 16 | 0.592 | 2 | 2 | 1 | 10 | 6 | 7.33 | 0.273 |
| 0 | 0 | 4 | 16 | 0.592 | 2 | 2 | 1 | 10 | 6 | 7.33 | 0.273 |
| 0 | 0 | 4 | 16 | 0.592 | 2 | 2 | 1 | 10 | 6 | 7.33 | 0.273 |
| 0 | 0 | 4 | 16 | 0.592 | 2 | 2 | 1 | 10 | 6 | 7.33 | 0.273 |
| 0 | 0 | 4 | 16 | 0.592 | 2 | 2 | 1 | 10 | 6 | 7.33 | 0.273 |
| 0 | 0 | 4 | 1 | | | | | | | | |

always an integer and q_0 and λ are constant. Thus a slide rule by virtue of its principle of construction can be used to demonstrate cubic structure. For other systems the ratio will not be that of whole numbers. In Table XXXIII are given typical calculations for cubic, tetragonal, and hexagonal lattices. In systems of symmetry lower than cubic (in which only the cube-edge length need be known) the calculations from quadratic equations listed in Table XXXII may become increasingly difficult, particularly when the crystal system is unknown. Numerous criteria have been set forth, but most useful probably is the graphic method of Hull and Davey for the hexagonal, rhombohedral, tetragonal, and (partially) the orthorhombic systems. For each system the logarithms of the spacing d calculated for each set of planes are plotted against axial ratios. The experimental data are plotted to the same logarithmic scale and then moved over the graph until a match is found, system and axial ratios as well as planar indices for each interference being thus identified.

The measurements taken from an x-ray pattern may be expressed in one of two useful forms: (a) as the $\sin \Theta$ values and (b) as the interplanar spacing (d) values. We shall consider the $\sin \Theta$ values. Generally for an orthorhombic crystal

$$\sin \Theta = \frac{\lambda}{2} \left(\frac{h^2}{a_0^2} + \frac{k^2}{b_0^2} + \frac{l^2}{c_0^2} \right)^{\frac{1}{2}}.$$

For simplification we shall designate $a_r^* = 1/a_0$, $b_r^* = 1/b_0$, and $c_r^* = 1/c_0$. Let $1/R = \lambda/2$. Then we may write the equation above in a form reminiscent of the reciprocal lattice,

$$R \sin \Theta = [(ha_r^*)^2 + (kb_r^*)^2 + (lc_r^*)^2]^{\frac{1}{2}}.$$

Let us first consider all those reflections which may be described by the indices $hk0$. For this simplified case, we may write

$$R^2 \sin^2 \Theta = (ha_r^*)^2 + (kb_r^*)^2.$$

This is simply the description of the hypotenuse of a right triangle equal to $R \sin \Theta$ with the sides equal to ha_r^* and kb_r^* .

If we draw two sets of parallel lines (see Fig. 164) perpendicular to one another, with all the lines in one set separated by the distance a_r^* and all those of the other separated by b_r^* , we may choose one intersection as origin. A line drawn from

this origin to any other intersection must correspond to the hypotenuse of such a right triangle, and such a line can be drawn for every possible hk combination. So circles of radius $R \sin \theta$ may be drawn to correspond to the observed pattern, and in the two-dimensional case every circle must pass through some intersection that fixes an h and a k value of the Miller indices.

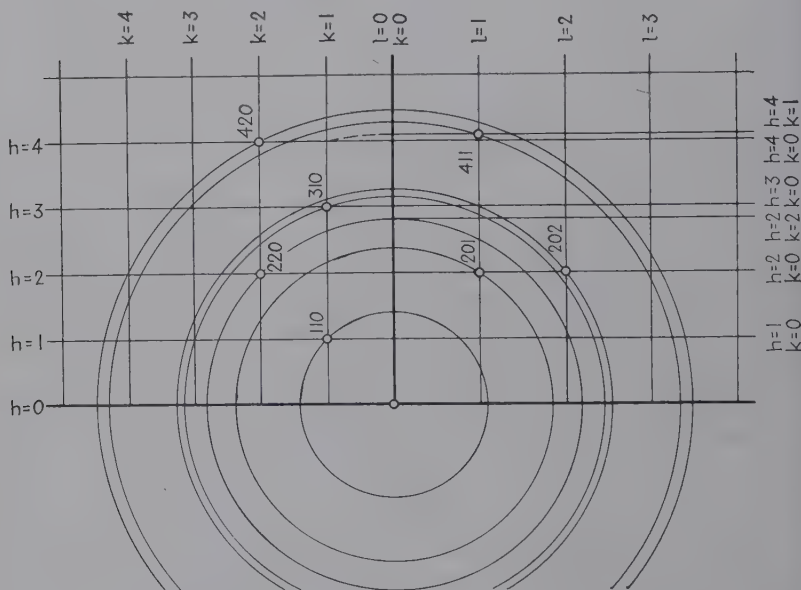


FIG. 164.—Reciprocal lattice construction of powder pattern of Pb_3O_4 .

In the general case we are dealing with a three-dimensional network rather than a two-dimensional one. One three-dimensional graph could be used exactly in the manner indicated by the treatment of the special case; but since we cannot easily treat with a three-dimensional figure, we find it more convenient to replace the three-dimensional graph by two graphs of two dimensions. One of these graphs may be considered as the special case above.

We can construct a second graph with one set of parallel lines spaced at lc_r^* , the other set spaced at distances designated by the $\sin \theta$ values as determined from the first graph, *i.e.*, h and k values of 10, 11, 01, 20, 21, etc. In Fig. 164 the two graphs, for convenience, are chosen in such a manner that they

have the same origin. Consider some intersection on graph 2 due to the line 1 and that designated hk ($\sin \theta$ determined by hk). The line from the origin to the intersection in question may be designated ρ . From the theorem of Pythagoras we may write

$$\rho^2 = (lc_r^*)^2 + (R \sin \theta_{hkl})^2;$$

but from the conditions of the first graph

$$(R \sin \theta_{hkl})^2 = (ha_r^*)^2 + (kb_r^*)^2,$$

so that

$$\begin{aligned}\rho &= [(lc_r^*)^2 + (ha_r^*)^2 + (kb_r^*)^2]^{\frac{1}{2}} \\ &= R \sin \theta_{hkl}.\end{aligned}$$

This provides a picture of the $\sin \theta$ values for cases in which h, k, l all have integral values other than zero; and, of course, reflections such as $h0l$, $0kl$, etc., may also be described since we have in our composite set of parallel lines those described by $h = 0$, $k = k$, and by $h = h$, $k = 0$.

With assumed unit cells, synthetic patterns may be determined rapidly by this method. The reverse process, however, is not so clear. It is, in brief, to construct the various sets of parallel lines so that intersections are provided to account for every interference observed on the patterns in question.

The Practical Use of the Powder Diffraction Pattern; the Crystal "Fingerprint."—The following facts are obvious in the interpretation of these line crystal spectra:

1. Only definite lines in a definite pattern correspond to a pure crystalline substance in the same sense as a "fingerprint." A thousand substances are listed in the so-called Dow tables of standard patterns. The identification of any pattern with that of a known pure chemical compound immediately constitutes a unique chemical analysis of an unknown crystalline substance that has produced the pattern. Typical patterns for a number of lead compounds are illustrated in Fig. 165. Hanawalt has devised a logical system of classification and a code system based on two or three strong lines, by means of which reference to standard patterns may be made rapidly.¹

2. Foreign lines indicate the presence of other crystalline substances as impurities; each entity produces its own spectrum

¹ *Ind. Eng. Chem., Anal. Ed.*, **10**, 457 (1938). See also DAVEY, *J. Applied Phys.*, December, 1939.

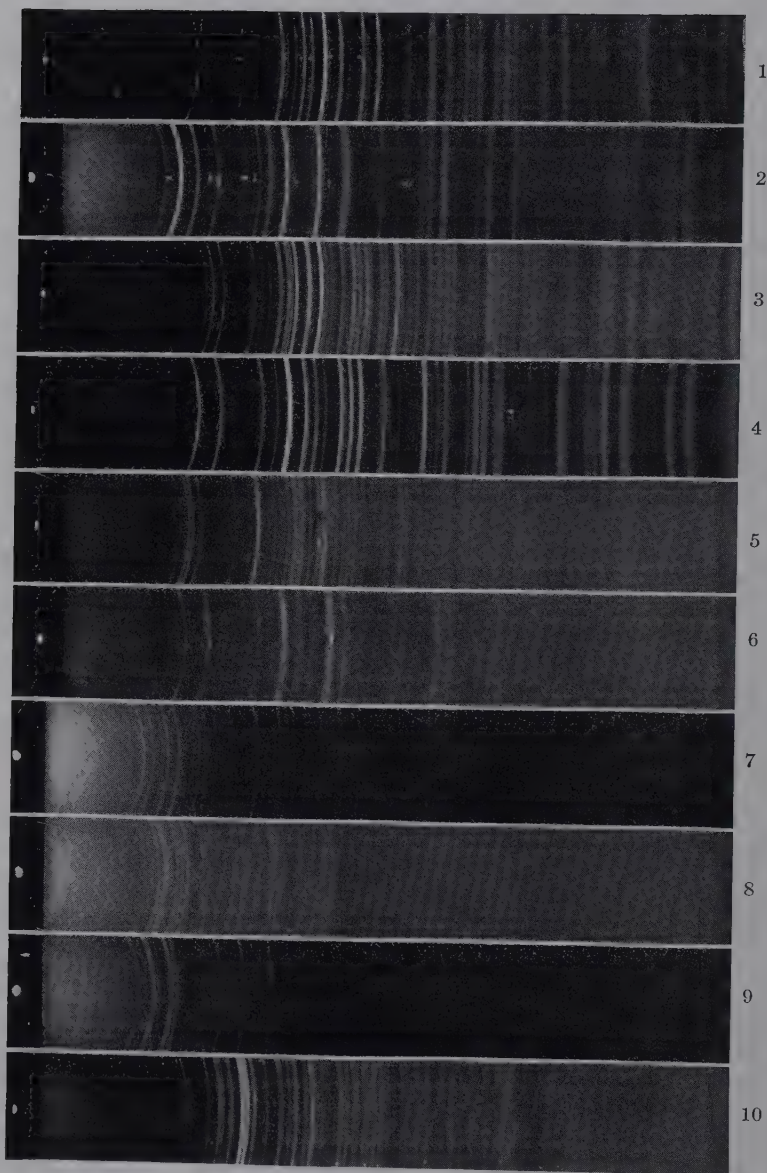


FIG. 165.—Powder patterns for lead compounds.

- | | |
|----------------------------|--------------------------------------|
| 1. PbO (orthorhombic) | 6. Pb_5O_8 |
| 2. PbO (tetragonal) | 7. $4\text{PbO} \cdot \text{PbSO}_4$ |
| 3. Pb_3O_4 | 8. $3\text{PbO} \cdot \text{PbSO}_4$ |
| 4. PbO_2 | 9. $2\text{PbO} \cdot \text{PbSO}_4$ |
| 5. Pb_2O_3 | 10. PbSO_4 |

if present in sufficient quantity (above 0.2 to 1 per cent usually), and the comparison of intensities is a method of quantitative analysis.

3. Solid solution is indicated by no change in the pattern of lines of a pure constituent, but in a shift in position of the lines, toward smaller angles (nearer the zero main beam) if the lattice is expanded by the addition of foreign atoms, or to larger angles if contracted. In many cases the lattice spacing is linearly related to atomic percentage of constituents of a solid solution alloy, as will be illustrated later.

4. The powder method may be made very accurate in evaluating the lattice constant of a pure substance and from this the ideal density of the material. The value for tungsten so obtained has been of utmost value in vacuum-tube applications where tungsten filaments are employed.

5. The widths of the diffraction lines serve as a means of determining grain size in the specimen as will be demonstrated in a later section.

6. Any departure of the powder or aggregate from purely random arrangement that results in continuous diffraction circles or lines of uniform intensity is manifested by the patterns. Thus if the grains are too large to permit the probability of random arrangement, the lines become spotted and dashed owing to reflection from individual grains (Fig. 166). In general, the grain diameter must be smaller than 10^{-3} cm. to prevent this. Most metals with grains that will pass through a 200-mesh sieve will give uniform lines. Again, if the grains are sufficiently small but are oriented in some preferred direction, as by some deforming force, some lines may become shortened or may disappear or assume localized intensity maxima. This process of fibering will be now considered.

The Fiber Pattern.—Figure 167 taken by the monochromatic pinhole method is reproduced as an example of the structure

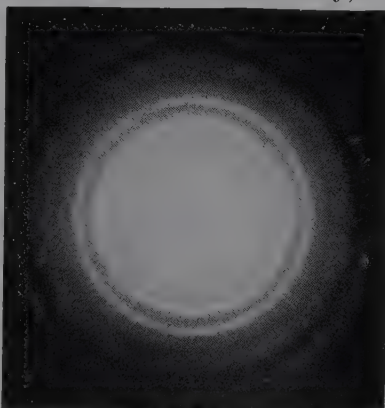


FIG. 166.—Pinhole pattern illustrating effect of large grain size (black diamond or carbonado used in mining drills).

of a natural fiber, asbestos. This mineral is not a single crystal, since otherwise it would give a Laue pattern of symmetrical spots. But neither is it constituted of grains in random arrange-

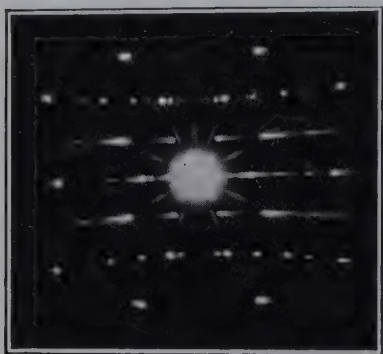


FIG. 167.—Monochromatic pinhole diagram of chrysotile (asbestos) showing almost perfect fiber structure. The smearing of spots along the layer lines is a significant indication of distortion.

ment, since this would mean a pattern of concentric uniformly intense rings. It may be seen, however, that circles may still be drawn through the diffraction maxima, although the more prominent loci are hyperbolas. These would be parallel straight horizontal lines (as in Fig. 157) if a cylindrical film had been used instead of a flat one. In this mineral, therefore, the grains are oriented in a common direction with respect to the fiber axis. The pattern is

typical of a fibered aggregate. Similarly many natural materials—cotton, stretched rubber, silk, hair, tendon, etc.—produce fiber patterns. It should be noted that the pattern obtained

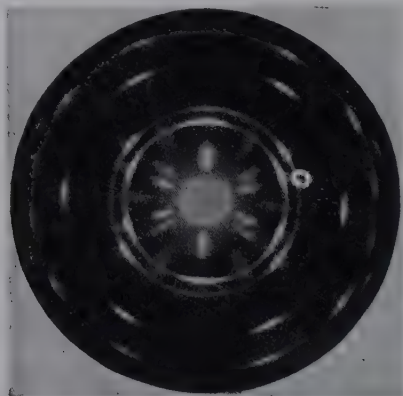


FIG. 168.—Fiber diffraction pattern for cold-drawn aluminum wire.

by rotating a crystal around a principal axis is a layer-line diagram exactly like that produced by a fiber without rotation. With a fiber, of course, only one such result is obtainable, whereas with a single crystal three patterns corresponding to

rotations around the three principal axes are possible. Now a fine-grained aggregate may be made fibered by rolling or drawing in one direction, as shown by Fig. 168 for cold-drawn aluminum wire. The desirability of a pattern 360 deg. in azimuth is at once apparent if the degree of fibering is to be estimated and if the actual location of the symmetrically placed maxima is to be used in the determination of the mechanism of deformation by mechanical work, as explained in Chapter XXI. A fiber diagram has a great advantage over an ordinary powder pattern, and this is that a measurement of a lattice spacing, namely, the atomic plane periodicities along the fiber axis, may be made independently of any assumption as to crystal system or planar indices. It is necessary only to measure the distances $e_1, e_2, e_3 \dots e_n$ of the vertices of the hyperbolas (or of the straight layer lines on a film that has been bent on a cylinder coaxial with the specimen) from the central zero point of the main beam. If we know the distance from specimen to film, a , the diffraction angle $\mu_1, \mu_2 \dots \mu_n$ may be calculated, since the tangents are e_n/a . The identity period, or spacing along the fiber axis, is then simply calculated from $I = n\lambda/\sin \mu_n$, where n is the number of the layer line (1, 2, 3, etc.). Thus identically the same value is obtained from all the layer lines. For the other lattice spacings it is necessary, of course, to interpret the pattern exactly as in the powder method since the Debye-Scherrer circles may still be evident. The degree of perfection of preferred orientation is, of course, indicated at once by the patterns, since there may be a continuous transition between the concentric circles for a random aggregate and the sharp horizontal layer lines for perfect fibering. The interpretation of fiber patterns in terms of the preferred orientation of planes and the texture of materials is considered in Chap. XXI.

The Laws That Determine the Intensities of X-ray Interferences.—On page 281 there were listed certain effects in the geometrical arrangement of crystallographic planes that result in the nonappearance of expected x-ray interferences, *i.e.*, interferences that have zero intensity. Other factors in the structure may contribute to a maximum intensity from cooperating planes or for a whole range of possible values between a maximum and zero. A proper measurement and interpretation of intensities thus lead to the final and most powerful step in

complete analysis of the structure. The intensity of a given interference from a given set of parallel planes depends upon a number of factors which will be briefly enumerated.

1. *The Atomic Structure Factor f_0 .*—First of all, scattering and intensity must basically depend on the kind of atom or the number of electrons in it. The atomic structure factor is defined as the ratio of the amplitude of waves scattered by the atom to that of a free classically scattering electron. If the atom were essentially a point, then $f_0 = Z$, the atomic number, or number of external electrons. However, the atom has a diameter comparable in size with the wave lengths. Hence the secondary waves from the different electrons in space have phase differences so that in certain directions there is strengthening and in others weakening of radiation. It is found that f_0 is a function of $\sin \Theta/\lambda$, or, completely expressed,

$$f_0 = \int_0^\infty \frac{U(r) \sin (4\pi r \sin \Theta/\lambda)}{4\pi r \sin \Theta/\lambda} dr \quad (1)$$

where $U(r)$ is the density of electrons between r and $r + dr$. For small values of Θ

$$f_0 = \int_0^\infty U(r) dr = Z. \quad (2)$$

Values of f_0 are now known with considerable accuracy from the work of Hartree, Pauling-Sherman, and Thomas-Fermi and are listed in the International Crystal Structure Tables. Particularly

TABLE XXXIV.—ATOMIC STRUCTURE FACTORS

| $\sin \Theta/\lambda$ | 0.0 | 0.1 | 0.2 | 0.3 | 0.4 | 0.5 | 0.6 | 0.7 | 0.8 | 0.9 | 1.0 | 1.1 | 1.2 | 1.3 |
|-----------------------|-----|------|------|------|------|------|------|------|------|------|------|-----|-----|-----|
| Cesium..... | 55 | 50.7 | 43.8 | 37.6 | 32.4 | 28.7 | 25.8 | 23.2 | 20.8 | 18.8 | 17.0 | | | |
| Diamond..... | 6 | 5.35 | 4.25 | 2.85 | 2.1 | 1.75 | 1.6 | | | | | | | |
| Graphite..... | 6 | 5.2 | 3.0 | 1.95 | 1.3 | 0.8 | 0.5 | | | | | | | |
| Oxygen..... | 8 | 8.0 | 5.8 | 3.7 | 2.5 | 1.7 | 1.1 | 0.7 | 0.5 | 0.4 | 0.3 | | | |
| Fluorine..... | 9 | 8.6 | 6.6 | 4.8 | 3.3 | 2.4 | 1.7 | 1.2 | 0.9 | 0.6 | 0.5 | 0.4 | | |
| Sodium..... | 11 | 9.5 | 8.0 | 6.4 | 4.8 | 3.6 | 2.6 | 2.0 | 1.5 | 1.2 | 0.9 | 0.7 | 0.6 | |
| Magnesium..... | 12 | 10.4 | 8.5 | 7.0 | 5.5 | 4.2 | 3.2 | 2.5 | 1.9 | 1.5 | 1.2 | 1.0 | 0.8 | |
| Aluminum..... | 13 | 10.6 | 9.0 | 7.5 | 6.1 | 4.9 | 3.9 | 3.0 | 2.4 | 1.9 | 1.5 | 1.2 | 1.1 | 1.0 |
| Silicon..... | 14 | 11.2 | 9.6 | 8.0 | 6.6 | 5.5 | 4.4 | 3.6 | 2.9 | 2.4 | 1.9 | 1.6 | 1.4 | 1.3 |
| Chlorine..... | 17 | 15.2 | 11.6 | 9.2 | 7.6 | 6.4 | 5.3 | 4.4 | 3.7 | 3.0 | 2.5 | 2.1 | 1.7 | 1.5 |
| Potassium..... | 19 | 16.9 | 13.0 | 10.5 | 8.6 | 7.2 | 6.0 | 5.1 | 4.3 | 3.7 | 3.1 | 2.6 | 2.2 | 2.0 |
| Calcium..... | 20 | 17.6 | 13.8 | 11.1 | 9.1 | 7.6 | 6.4 | 5.5 | 4.6 | 4.0 | 3.4 | 2.9 | 2.6 | 2.3 |
| Iron..... | 26 | 22.6 | 18.0 | 14.9 | 12.5 | 10.7 | 9.3 | 8.2 | 7.2 | 6.3 | 5.6 | 4.9 | 4.3 | 3.7 |

important are the values for cesium (55) inasmuch as f_0 for elements of higher atomic number can be calculated by multiplying f_0 for cesium by $Z/55$. In Table XXXIV values are listed for cesium, diamond, and graphite (important for organic compounds) and for a number of elements involved in structure analysis of silicates.

All these values correspond to atoms at rest at absolute zero; hence for ordinary temperatures at which intensities are appreciably weakened, a correction deduced by Debye and Waller must be used, namely,

$$f = f_0 e^{-M} \quad (3)$$

where $M = \frac{6h^2}{mk\Theta} \left(\frac{\sin \Theta}{\lambda} \right)^2 \left(\frac{\phi(X)}{X} + \frac{1}{4} \right)$, where k is the Boltzmann constant, Θ is the characteristic temperature (Debye) calculated from specific heat, $X = \Theta/T$, and $\phi(X)/X = \pi^2 T^2 / 6\Theta^2$.

2. *The Crystal Structure Factor F .*—The scattering intensity of a lattice unit cell, which contains only a single atom, is expressed by $f_0^2 e^{-2M}$. If more atoms are present in the cell, as is the actual case, then the phase differences of scattered waves from different atoms must be taken into consideration. The crystal structure factor F thus involves the coordinates of atoms in the cell. Thus

$$F_0 = \sum f_0 e^{2\pi i \left(\frac{hx}{a} + \frac{ky}{b} + \frac{lz}{c} \right)}, \quad (4)$$

$$F = F_0 e^{-M} = F_0 e^{-B \left(\frac{\sin \Theta}{\lambda} \right)^2} = \sum f_0 e^{-M} e^{2\pi i \left(\frac{hx}{a} + \frac{ky}{b} + \frac{lz}{c} \right)}. \quad (5)$$

Here, i is the indeterminate, and the coordinates of a given point xyz are expressed as fractional parts of the axial lengths a, b, c . F_0 is a complex quantity, so that the absolute value $|F_0|^2$ to which intensity is proportional is expressed as follows:

$$|F_0(hkl)|^2 = \left[\sum \sum f_0 \cos 2\pi \left(\frac{hx}{a} + \frac{ky}{b} + \frac{lz}{c} \right) \right]^2 + \left[\sum \sum f_0 \sin 2\pi \left(\frac{hx}{a} + \frac{ky}{b} + \frac{lz}{c} \right) \right]^2, \quad (6)$$

$$|F_0(hkl)| = \sqrt{(\sum f_0 A)^2 + (\sum f_0 B)^2} = \sqrt{A'^2 + B'^2} \quad (7)$$

thus $|F_0(hkl)| = A' + iB'$.

$A = \sum \cos 2\pi \left(\frac{hx}{a} + \frac{ky}{b} + \frac{lz}{c} \right)$ and $B = \sum \sin 2\pi \left(\frac{hx}{a} + \frac{ky}{b} + \frac{lz}{c} \right)$ are characteristic of each space-group, since they depend entirely on the equivalent points in the unit cell. Values of A and B have been calculated for each space-group by Lonsdale in the "Structure Factor Tables." For crystals with a center of symmetry the B or sine term becomes zero, and calculations are greatly simplified.

3. *Simple Examples of Structure-factor Calculation (Debye-Waller Temperature Correction Included).* a. *Body-centered Cubic* (Fig. 169).

Equivalent point coordinates: $000, \frac{1}{2} \frac{1}{2} \frac{1}{2}$.

$$F = [e^{2\pi ni 0} + e^{\frac{2\pi ni(h+k+l)}{2}}]f = [1 + e^{\pi ni(h+k+l)}]f.$$

$$F = (1 + 1)f = 2f, \quad h + k + l \text{ even.}$$

$$F = 1 - 1 = 0, \quad h + k + l \text{ odd.}$$

b. *Face-centered Cubic* (Fig. 170a).

Equivalent point coordinates: $000, \frac{1}{2} \frac{1}{2} 0, \frac{1}{2} 0 \frac{1}{2}, 0 \frac{1}{2} \frac{1}{2}$.

$$F = [1 + e^{\pi ni(h+k)} + e^{\pi ni(h+l)} + e^{\pi ni(k+l)}]f.$$

$$F = 4f, \quad h, k, l, \text{ all odd or all even.}$$

$$F = 0, \quad h, k, l \text{ mixed.}$$

c. *Hexagonal Close-packed* (Fig. 170b).

Equivalent point coordinates: $000, \frac{1}{3} \frac{2}{3} \frac{1}{2}$.

$$F = [1 + e^{\frac{\pi i}{3}(2h+4k+3l)}]f = [1 + e^{\pi il} e^{\frac{\pi i}{3}(2h+4k)}]f.$$

$$F = 0, \quad l \text{ uneven,}$$

$$h + 2k = 3n.$$

$$F = \sqrt{3}f, \quad l \text{ uneven,}$$

$$h + 2k = 3n + 1 \text{ or } 3n + 2.$$

$$F = 2f, \quad l \text{ even,}$$

$$h + 2k = 3n.$$

$$F = f, \quad l \text{ even,}$$

$$h + 2k = 3n + 1 \text{ or } 3n + 2.$$

d. *ZnS.*

Coordinates: Zn— $000, 0 \frac{1}{2} \frac{1}{2}, \frac{1}{2} 0 \frac{1}{2}, \frac{1}{2} \frac{1}{2} 0$.

S— $\frac{1}{4} \frac{1}{4} \frac{1}{4}, \frac{1}{4} \frac{3}{4} \frac{3}{4}, \frac{3}{4} \frac{1}{4} \frac{3}{4}, \frac{3}{4} \frac{3}{4} \frac{1}{4}$.

$$F = f_{zn}[1 + e^{\pi i(h+k)} + e^{\pi i(k+l)} + e^{\pi i(h+l)}] + f_s[e^{\frac{\pi i}{2}(h+k+l)} + e^{\frac{\pi i}{2}(h+3k+3l)} + e^{\frac{\pi i}{2}(3h+3k+l)} + e^{\frac{\pi i}{2}(3h+k+3l)}] = [f_{zn} + f_s e^{\frac{\pi i}{2}(h+k+l)}][1 + e^{\pi i(h+k)} + e^{\pi i(k+l)} + e^{\pi i(h+l)}].$$

| | |
|--|-----------------------|
| $F = 0,$ | hkl mixed. |
| $F = 4(f_{zn} - f_s),$ | hkl unmixed, |
| | $h + k + l = 4n + 2.$ |
| $F = 4(f_{zn} + f_s),$ | hkl unmixed, |
| | $h + k + l = 4n.$ |
| $F = 4(f_{zn} + if_s) \text{ or } 4\sqrt{f_{zn}^2 + f_s^2},$ | hkl unmixed, |
| | $h + k + l = 4n + l.$ |

e. Monoclinic Space-group P_{21}/c .

Symmetry elements: Dyad axes parallel to b axis.

Glide planes $a/2$ parallel to 010 .

Coordinates: $xyz; \bar{x}\bar{y}\bar{z}; x, \frac{1}{2} - y, \frac{1}{2} + z; \bar{x}, \frac{1}{2} + y, \frac{1}{2} - z.$

$$A = 4 \cos 2\pi\left(hx + lz + \frac{k+l}{4}\right) \cos 2\pi\left(ky - \frac{k+l}{4}\right).$$

$$B = 0.$$

| | | |
|-------|-----------------------|------------------|
| $h00$ | $A = 4 \cos 2\pi hx,$ | h even or odd. |
|-------|-----------------------|------------------|

| | | |
|-------|-----------------------|-----------|
| $0k0$ | $A = 4 \cos 2\pi ky,$ | k even. |
|-------|-----------------------|-----------|

| | | |
|--|----------|----------|
| | $A = 0,$ | k odd. |
|--|----------|----------|

| | | |
|-------|-----------------------|-----------|
| $00l$ | $A = 4 \cos 2\pi lz,$ | l even. |
|-------|-----------------------|-----------|

| | | |
|--|----------|----------|
| | $A = 0,$ | l odd. |
|--|----------|----------|

| | | |
|-------|------------------------------------|---------------|
| $0kl$ | $A = 4 \cos 2\pi ky \cos 2\pi lz,$ | $k + l$ even. |
|-------|------------------------------------|---------------|

| | | |
|--|-------------------------------------|--------------|
| | $A = -4 \sin 2\pi ky \sin 2\pi lz,$ | $k + l$ odd. |
|--|-------------------------------------|--------------|

| | | |
|-------|-----------------------------|-----------|
| $h0l$ | $A = 4 \cos 2\pi(hx + lz),$ | l even. |
|-------|-----------------------------|-----------|

| | | |
|--|----------|----------|
| | $A = 0,$ | l odd. |
|--|----------|----------|

| | | |
|-------|------------------------------------|-----------|
| $hk0$ | $A = 4 \cos 2\pi hx \cos 2\pi ky,$ | k even. |
|-------|------------------------------------|-----------|

| | | |
|--|-------------------------------------|----------|
| | $A = -4 \sin 2\pi hx \sin 2\pi ky,$ | k odd. |
|--|-------------------------------------|----------|

4. *Intensity and the Structure Factor.*—This relation is one of considerable difficulty, for the state of perfection of the crystal specimens plays an important part. The theory was originally developed by Darwin and Ewald.

The x-ray reflection from a crystal does not occur sharply but takes place over a small angular range on either side of θ defined by the Bragg law. The integrated intensity is experimentally measured by $E\omega/I_0$ where E is the total energy received

by the photographic film or ionization chamber, while the crystal is turned through the reflecting position with angular velocity ω , and I_0 is the incident beam energy per second per square centimeter at the crystal. For a crystal of small volume δV

$$\frac{E\omega}{I_0} = \left[N \frac{e^2}{mc^2} F(hkl) \right]^2 \lambda^3 \frac{1 + \cos^2 2\theta}{2 \sin \theta} \delta V.$$

Here N is the number of unit cells per unit volume, or the reciprocal of the volume V of the unit cell; e^2/mc^2 comes from $\bar{A} = Ae^2/mc^2$, classical electromagnetic equation for amplitude \bar{A} of rays, primary amplitude A , scattered by an electron; and $1 + \cos^2 2\theta$ is the polarization factor for unpolarized rays. This equation applies only to ideally imperfect crystals with mosaic structure or to powders. For perfect crystals with reflection over a very small angle

$$\frac{E\omega}{I} = \frac{8}{3\pi} N \frac{e^2}{mc^2} F(hkl) \lambda^2 \frac{1 + |\cos 2\theta|}{2 \sin 2\theta},$$

with F only in the first power.

Nearly all crystals lie somewhere between the perfect and the ideal mosaic structure, but nearer to the latter. A number of formulas have been deduced taking into account the type of specimen and absorption of radiation and are listed in the International Crystal Structure Tables, page 562. For example, to a powder pattern taken with a cylindrical film is assigned the formula

$$\frac{I_l}{I_0} = \frac{l}{16\pi r} \left(\frac{Ne}{mc^2} F(hkl) \right)^2 \lambda^3 H V \frac{1 + \cos^2 2\theta}{\sin 2\theta \sin \theta},$$

where l is the height of a section of a Debye-Scherrer ring of radius r , as it intercepts the cylindrical film; H is the number of planes $\{hkl\}$ producing interferences that coincide [48 cubic, 16 tetragonal, 8 orthorhombic for (hkl)]; and V is the volume irradiated. In all these cases, F includes the Debye-Waller temperature corrections.

The principal corrections to be made for actual crystals are for two kinds of extinction. The formula for the mosaic crystals implies the condition that the number of planes in a mosaic block m_p multiplied by the relative amplitude of reflection from a single plane must be very small: for NaCl m_p must be less

than 500, or a size of 1400 A.U. for the 200 reflection. Actual crystals have mosaic blocks that are too coarse to satisfy the condition. In other words, they approach to an ideal perfect crystal. This is serious only for strong reflections, where F is large and $\sin \Theta/\lambda$ small. Nothing can be done to correct for this primary extinction because there is no way to measure mosaic-block size. Secondary extinction occurs even in good mosaic specimens, so that upper planes in each block shield the lower part from the radiation with the result that the effective absorption coefficient of the crystal is increased when set at the reflecting angle. Corrections can be made in the intensity formula, but the extinction is largely avoided by working with fine powders. Experience has shown that in the exceedingly important complete structure determinations of organic crystals the uncorrected formulas above can be used safely with small single crystals which have small absorbing power and ordinarily produce no very strong reflections because of unsymmetrically arranged atoms.

5. *The Procedure in Crystal Structure Analysis.*¹—The usual procedure in analysis is to determine experimentally the values of $F(hkl)$ for as many planes as possible especially for planes in the principal zones. The kinds and numbers of atoms or ions in the unit cell being known, all the peculiarities of intensity distribution are next used in order to decide approximately the most probable distribution of scattering material in the cell, *i.e.*, the most probable values of xyz for each kind of atom or ion. At this stage it may be necessary to use other available crystallographic physical or chemical information about the substance (for example, optical and magnetic properties, cleavage planes, presence or absence of pyro- or piezoelectric effects, presence of long-chain or ring-shaped molecules, etc.); or in particularly favorable cases it may be possible to ignore all such outside information in the first place and to use it only as a final check on the structure obtained from x-ray results alone. The approximate values of xyz so obtained when substituted in Eq. (6) should give values of $F(hkl)$ not far from the observed values for all the observed reflections. Experimental observation alone cannot determine the phase angle $\alpha(hkl)$; but if this can be estimated with sufficient accuracy from the approximate

¹ As described by Lonsdale, "Structure Factor Tables," London, 1938.

structure, then a Fourier analysis in two or three dimensions can be carried out (note that this is a step of refinement rather than a primary operation) and the distribution of electron density in the unit cell can be determined accurately and uniquely. If on comparison of the Fourier analysis it is found that the approximate structure was not sufficiently exact, it may be necessary to repeat the analysis using as an approximate structure the result of the previous analysis and thus arriving at the true structure by a series of successive approximations.

6. *Expression of Electron Density by Fourier Series.*—It is clear that though the process is a difficult one the magnitude of the structure factor $F(hkl)$ can usually be determined from the experimental measurements of intensity. The relation between $F(hkl)$ and the density of the scattering medium $\rho(xyz)$ is written

$$F(hkl) = \frac{V}{abc} \int_0^a \int_0^b \int_0^c \rho(xyz) e^{2\pi i \left(\frac{hx}{a} + \frac{ky}{b} + \frac{lz}{c} \right)} dx dy dz.$$

It is important to note that $F(hkl)$ for any given plane is a complex quantity, characterized by an amplitude and a phase constant. It is obvious that the experimental measurements of intensity, though defining the amplitude of the structure factors $F(hkl)$, can give no information regarding these relative phase relationships. The different reflections are measured at different times with the crystal in different positions, so that information regarding phase relationships is necessarily lost in making the experiment. This ambiguity represents the fundamental difficulty in x-ray analysis. Although we assume no symmetry in the density distribution, the nature of the crystal requires the structure to be essentially periodic over a range defined by a , b , c of the unit cell. Hence $\rho(xyz)$, the electron density at any point, can be represented by a Fourier series

$$\rho(xyz) = \sum_{-\infty}^{+\infty} \sum_{-\infty}^{+\infty} \sum_{-\infty}^{+\infty} \frac{F(hkl)}{V} e^{-2\pi i \left(\frac{kx}{a} + \frac{ky}{b} + \frac{lz}{c} \right)},$$

where $F(hkl)/V$ values are the coefficients of the terms. The zero term $F(000) = \frac{V}{abc} \int_0^a \int_0^b \int_0^c \rho(xyz) dx dy dz = Z$, the total number of electrons in the unit cell.

In accordance with Friedel's law, $|F(hkl)| = |F(\bar{h}\bar{k}\bar{l})|$; then

$$\rho(xyz) = \sum \sum \sum \left| \frac{F(hkl)}{V} \right| \cos \left[2\pi \frac{hx}{a} + 2\pi \frac{ky}{b} + 2\pi \frac{lz}{c} - \alpha(hkl) \right]$$

where $\alpha(hkl)$ is the phase constant and is the angle $\tan^{-1} \frac{B}{A}$, where B and A are the quantities defined in Eq. (7).

Therefore, if the electron density distribution in a crystal lattice is analyzed into a series of harmonic terms corresponding to various possible crystal planes, then the coefficients of these terms are given by the absolute values of the structure factors for the corresponding plane divided by the volume of the unit cell. The resultant wave scattered by the unit cell is compounded from the contributions of all the electrons in the cell. There is an infinite series of such resultant waves corresponding to all possible crystal planes, and these waves can themselves be compounded by means of a Fourier series to give an expression of the electron distribution in the unit cell.

The method is most readily applied to those structures which contain a center of symmetry, an element that fortunately occurs quite frequently in crystals. When this symmetry is present in the unit cell as a whole, it must apply to each of the component waves that define the structure. Hence, if we had the origin of coordinates (xyz) at the center of symmetry, then either a peak or a trough of each of these components must coincide with the origin. The phase angle $\alpha(hkl)$, which measures the displacement of the peak of the wave from the origin, must in this case be limited to the value 0 or π , and these two cases can be covered by making the signs of the coefficients $F(hkl)/V$ either positive or negative. For a center of symmetry

$$\rho(xyz) = \sum \sum \sum \pm \frac{F(hkl)}{V} \cos 2\pi \left(\frac{hx}{a} + \frac{ky}{b} + \frac{lz}{c} \right).$$

Most frequently the two-dimensional series for all reflections ($hk0$) from one zone in the crystal is used, and the density per unit area A in any projection of the structure is given by the series

$$\rho(xy) = \sum \sum \pm \frac{F(hk0)}{A} \cos 2\pi \left(\frac{hx}{a} + \frac{ky}{b} \right).$$

The electron density contour map of molecular structure which will be illus-

trated for organic molecules in Chap. XIX is the result of such an analysis. The simple one-dimensional series gives the density per unit length d arranged in sheets parallel to any given plane, and the successive orders of reflections from that plane ($h00$) give the coefficients in the series

$$\rho(x) = \sum \pm \frac{F(h00)}{d} \cos 2\pi \frac{hx}{a}.$$

Within the range of experimental limitations the larger the number of terms included in the Fourier series the more perfect will the representation become. Such a process may become extremely laborious. Robertson cites the case of two projections of the double series for phthalocyanine. A total of 281 different terms were used in the series which had to be evaluated at 1,800 different points over half the molecule in each case. Thus the total number of terms necessary to evaluate and add for these two projections is well over 500,000. Devices for shortening calculations are obviously called for.

The double-series equation may be written

$$\rho(xy) = \Sigma(\Sigma K \cos h\theta_1) \cos k\theta_2 - \Sigma(\Sigma K \sin h\theta_1) \sin k\theta_2,$$

where K is the coefficients, and $\theta_1 = 2\pi x/a$, $\theta_2 = 2\pi y/b$. The summations in parentheses are carried out first and become the coefficients for the final summation $\rho(xy) = \Sigma A \cos k\theta_2 - \Sigma B \sin k\theta_2$. The method of Beevers and Lipson, which is the most familiar, involves 4,000 strips of cardboard upon which are printed all two-figure coefficients, positive and negative, for sines and cosines of angles at intervals of 6 deg. and all values of the index h from 0 to 20. The synthesis reduces to selecting sets of cards and adding up successive columns of figures.

Patterson-Harker Fourier Synthesis.—The uncertainties involved in the phase angle for the usual Fourier analysis led Patterson¹ to develop a valuable new direct method of analysis which has proved invaluable in the field of organic structures. The quantity $A(u)$ represents the weighted average distribution of density about a point X , or

$$A(u) = \frac{1}{a} \int_0^a \rho(x) \rho(x+u) dx,$$

¹ *Z. Krist.*, **90**, 517 (1935).

where $\rho(x + u)$ is the distribution about x as a function of the parameter u , weighted by the amount of scattering matter between x and $x + dx$. Expanded by a Fourier series

$$A(u) = \frac{1}{d^2} \sum F^2(h00) e^{2\pi i \frac{hu}{a}}$$

for the one-dimensional case. Thus $A(u)$ depends upon F^2 instead of F and is independent of signs or phase constants. In three dimensions

$$A(uvw) = \frac{1}{V} \int_0^a \int_0^b \int_0^c \rho(xyz) \rho(x + u, y + v, z + w) dx dy dz = \\ \frac{1}{V^2} \sum \sum \sum F^2(hkl) e^{2\pi i \left(\frac{hu}{a} + \frac{kv}{b} + \frac{lw}{c} \right)}.$$

$A(uvw)$ will be large only when there are high values in $\rho(xyz)$ both at xyz and $x + u, y + v, z + w$. A peak in the function $A(uvw)$ at u, v, w corresponds to an *interatomic distance* in the crystal. The only difficulty involved sometimes is an ambiguity as to which pairs of atoms are involved. Harker's¹ extensions have included simplifications by including symmetry properties of the crystal. For example, for a crystal with a plane of symmetry and equivalent atoms at xyz and $x\bar{y}z$ the vector components are $0\ 2y\ 0$. The maximum in $A(uvw)$ lies on the b axis and the series becomes only one-dimensional with the far simpler calculations

$$A(0v0) = \sum_{k=-\infty}^{\infty} \left[\sum_{h=-\infty}^{\infty} \sum_{l=-\infty}^{\infty} F^2(hkl) \right] \cos 2\pi \frac{kv}{b}.$$

It is with such powerful aids that the x-ray crystal analyst now works and is able to achieve the remarkable success in the results that are to be outlined briefly in the succeeding chapters.

¹ *J. Chem. Physics*, **4**, 381 (1936).

CHAPTER XV

THE RESULTS OF CRYSTAL ANALYSIS: ELEMENTS AND INORGANIC COMPOUNDS

The Chemical Elements.—By the methods of x-ray analysis outlined in the preceding chapter nearly 80 of the known chemical elements have been assigned definite lattice structures in the solid state. At least 20 of these crystallize in two or more different polymorphic modifications. Seventeen types of structure have been definitely established, designated A1 to A17 by Ewald and Hermann in the four volumes of the "Strukturbe-

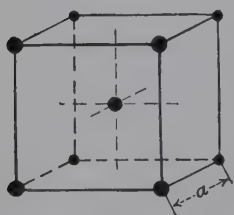


FIG. 169.—Body-centered cubic lattice (tungsten type).

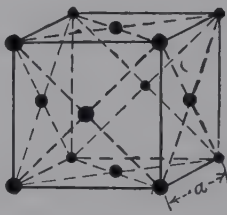


FIG. 170a.—The close-packed crystal structures, face-centered cubic (copper type).

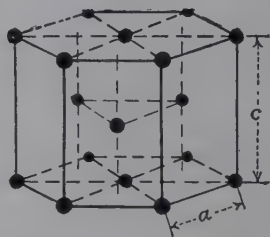


FIG. 170b.—The close-packed crystal structures, hexagonal close-packed (zinc type).

richt," and a few others (X_1 to X_{10}) have been only partially analyzed. These types are listed and defined in Tables XXXVa and XXXVb; Table XXXVI presents in detail the most recent and reliable data for the elements alphabetically arranged.¹

Pure metals are, of course, chemical elements; every metal except a few of the rarest in nature may be classified now according to the pattern by which its atoms form crystals and according to the numerical values which define the unit crystal cell.

Fortunately for practical purposes most of the metals are grouped in only three structures, face-centered cubic (A1) (Fig. 170a), hexagonal close-packed (A3) (Fig. 170b), and body-centered cubic (A2) (Fig. 169). The first two represent the alternative

¹ Taken mostly from the paper by Neuberger, *Z. Krist.*, **93**, 1 (1936).

TABLE XXXVa.—LATTICE TYPES OF THE ELEMENTS

| Type symbol (Ewald-Hermann) | Type element | Space-lattice | Space-group | Z = atoms per unit cell | Elements and modifications | Distinctive feature |
|-----------------------------|--------------------------------|-----------------------------------|--------------|-------------------------|--|---|
| A1 | Copper | Face-centered cubic (f.c.c.) | $Fm\bar{3}m$ | 4 | Ag, Al, A, Au, α -Ca, β -Ce, β -Co, Cu, γ -Fe, Ir, Kr, β -La, Ne, β -Ni, Pb, Pd, Pt, β -Rh, Sr, Th, β -Ti, Xe | C.N. 12 |
| A2 | Tungsten (β) | Body-centered cubic (b.c.c.) | $Im\bar{3}m$ | 2 | Ba, Cb(Nb), α -Cr, Cs, α -Fe, K, Li, Mo, Na, Rb, Ta, β -Ti, β -U, V, β -W, β -Zr | C.N. 8 |
| A3 | Magnesium | Hexagonal close-packed (h.c.p.) | $C6/mmc$ | 2 | α -Be, Cd, α -Ce, α -Co, α -Ni, β -Cr, α -Er, γ -Ca, Hf, α -La, Mg, α -Nd, Os, α -Pr, Re, α -Ru, α -Ti, α -Tl, Y, Zn, α -Zr | C.N. 12 |
| A4 | Diamond (carbon) | Two interpenetrating f.c.c. | $Fd\bar{3}m$ | 8 | C(diamond), Ge, Si, α -Sn(gray) | C.N. 4 |
| A5 | β -Tin (white) | Double b.c. tetragonal | $I4/amd$ | 4 | β -Sn(white) | Flattened A4 |
| A6 | Indium | F.c. tetragonal | $I4/mmm$ | 2 | Indium, γ -Mn | Deformed simple cubic |
| A7 | Arsenic | B.c. rhombohedral | $R\bar{3}m$ | 2 | As, Bi, Sb | |
| A8 | γ -Selenium (hexagonal) | Hexagonal (deformed simple cubic) | $C3_12$ | 3 | Se, Te | |
| A9 | Graphite (carbon) | Hexagonal | $C6/mmc$ | 4 | Graphite(C) | Planar rings of 6C |
| A10 | Mercury | Rhombohedral | $R\bar{3}m$ | 4 | Hg | C.N. 6 |
| A11 | Gallium | Rhombic | $Cmca$ | 8 | Ga | 6 (5 in one layer) |
| A12 | α -Manganese | B.c.c. complex | $I\bar{4}3m$ | 58 | α -Mn, γ -Cr | Mg ₃ Al ₂ , isomorphous |
| A13 | β -Manganese | Cubic | $P4_3$ | 20 | β -Mn | Molecular lattice |
| A14 | Iodine | Rhombic | $Cema$ | 8 | I ₂ , Br ₂ | C.N. 14 instead of 12 |
| A15 | α -Tungsten | Cubic | $Pm\bar{3}n$ | 8 | α -W | Puckered S ₈ rings |
| A16 | α -Sulfur | Rhombic | $Fddd$ | 128 | α -S | Double layers |
| A17 | Phosphorus | F.c. rhombic | $Bmab$ | 8 | P (black) | Molecular lattice of Cl ₂ |
| A18 | Chlorine | Tetragonal | $P4/nem$ | 16 | Cl ₂ | Distorted A ₁₀ |
| A19 | Polonium | Monoclinic | C_2 | 12 | Po | |

TABLE XXXVb

| Type symbol | Type element | Space-lattice |
|-----------------|---|---------------|
| X ₁ | β -Beryllium | Hexagonal |
| X ₂ | Boron* | Hexagonal |
| X ₃ | Hydrogen (para-), β -nitrogen | Hexagonal |
| X ₄ | α -Nitrogen, γ -oxygen (8O ₂) | Cubic |
| X ₅ | α -Oxygen (2O ₂) | B.c. rhombic |
| X ₆ | β -Oxygen (6O ₂) | Rhombohedral |
| X ₇ | Phosphorus (white) (4P ₄) | Cubic |
| X ₈ | α -Rhodium | Cubic |
| X ₉ | α -, β -Selenium (monoclinic), S(fibers) | Monoclinic |
| X ₁₀ | α -Uranium | Monoclinic |

* "Crystallized" boron always contains some Al and may be the intermetallic compound AlB₁₂ rather than a solid solution approximating pure B. A "diamondlike" and two "graphitelike" modifications have been analyzed [Noray-Szabo, *Z. Krist.*, **94**, 367 (1937); Halla and Weil, *ibid.*, **101**, 435 (1939)].

methods of packing spheres in closest array. A layer is formed such that each atom is in contact with six neighbors at the corners of a regular hexagon. The next layer is placed on this so that each sphere is in contact with three spheres in the layer below. The

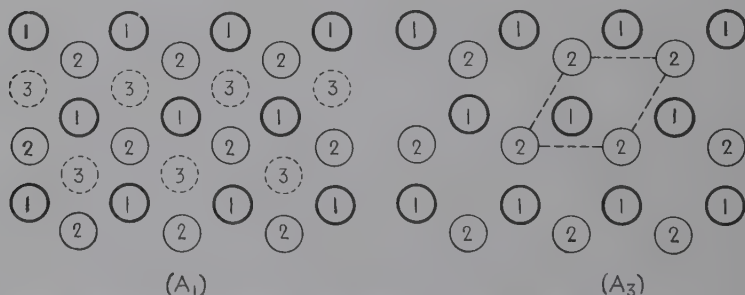


FIG. 170c.—The close packing of spheres: (A₁) cubic close packing; (A₃) hexagonal close packing. In (A₃) the hexagonal unit cell is outlined. The numbers correspond to the successive layers of the structures. In both arrangements each sphere is surrounded by 12 equidistant neighbors.

difference between A₁ and A₃ is to be found in the placing of the third layer. For A₃ the third layer is exactly over the first layer so that the sequence of all layers is 1 2 1 2 1 2; for cubic A₁, the third layer differs from 1 or 2, thus producing the sequence 1 2 3 1 2 3 . . . as illustrated in Fig. 170c. But in both A₁ and A₃, each atom has 12 equidistant neighbors or in other words a

TABLE XXXVI.—LATTICE CONSTANTS FOR ELEMENTS (1939)

| Element | Sym- bol | Atomic number | Lattice type | Edge length <i>a</i> ; <i>a</i> , <i>c</i> ; <i>a</i> , <i>b</i> , <i>c</i> | Density (x-ray) |
|----------------------|-------------|------------------|------------------------|--|--------------------|
| Aluminum..... | Al | 13 | A1 | 4.0414 | 2.694 |
| Antimony..... | Sb | 51 | A7 | 4.4976, $\omega = 57^\circ 6.5'$ | 6.686 |
| Argon..... | A | 18 | A1 | 5.42 | 1.654 |
| Arsenic..... | As | 33 | A7 | 4.135, $\omega = 54^\circ 7.5'$ | 5.71 |
| Barium..... | Ba | 56 | A2 | 5.015 | 3.590 |
| Beryllium..... | Be | 4 | α A3 | 2.2680, 3.5942 | 1.857 |
| | | | β X ₁ | 7.1, 10.8 | 1.89 |
| Bismuth..... | Bi | 83 | A7 | 4.7356, $\omega = 57^\circ 16'$ | 9.785 |
| Boron..... | B | 5 | X ₂ | | |
| Bromine..... | Br | 35 | A14 | 4.48, 6.67, 8.72 | |
| Cadmium..... | Cd | 48 | A3 | 2.9731, 5.607 | 8.634 |
| Calcium..... | Ca | 20 | α A1 | 5.56 | 1.537 |
| | | | γ A3 | 3.94, 6.46 | 1.52 |
| Carbon..... | C | 6 | Diamond A4 | 3.5606 | 3.508 |
| | | | Graphite A9 | 2.46, 6.78 | 2.227 |
| Cerium..... | Ce | 58 | α A3 | 3.65, 5.91 | 6.775 |
| | | | β A1 | 5.143 | 6.792 |
| Cesium..... | Cs | 55 | A2 | 6.05 | 1.977 |
| Chlorine..... | Cl | 17 | A18 | 8.56, 6.12 | |
| Chromium..... | Cr | 24 | α A2 | 2.8786 | 7.188 |
| | | | β A3 | 2.717, 4.418 | 6.07 |
| | | | γ A12 | 8.717 | 7.507 |
| Cobalt..... | Co | 27 | α A3 | 2.507, 4.072 | 8.766 |
| | | | β A1 | 3.545 | 8.72 |
| Columbium..... | Cb | 41 | A2 | 3.294 | 8.567 |
| Copper..... | Cu | 29 | A1 | 3.6080 | 8.923 |
| Dysprosium..... | Dy | 66 | | | |
| Erbium..... | Er | 68 | A3 | 3.74, 6.09 | 7.49 |
| Europium..... | Eu | 63 | | | |
| Fluorine..... | F | 9 | | | |
| Gadolinium..... | Gd | 64 | | | |
| Gallium..... | Ga | 31 | A11 | 4.506, 4.506, 7.642 | 5.925 |
| Germanium..... | Ge | 32 | A4 | 5.647 | 5.316 |
| Gold..... | Au | 79 | A1 | 4.0700 | 19.28 |
| Hafnium..... | Hf | 72 | A3 | 3.200, 5.077 | 13.08 |
| Helium..... | He | 2 | | | |
| Holmium..... | Ho | 67 | | | |
| Hydrogen (para)..... | H | 1 | X ₃ | 3.75, 6.12 | 0.089 |
| Illinium..... | Il | 61 | | | |
| Indium..... | In | 49 | A6 | 4.585, 4.941 | 7.28 |
| Iodine..... | I | 53 | A14 | 4.791, 7.248, 9.771 | 4.933 |
| Iridium..... | Ir | 77 | A1 | 3.8312 | 22.64 |
| Iron..... | Fe | 26 | α A2 | 2.8610 | 7.861 |
| | | | β A1 | 3.564 | 8.13 |
| Krypton..... | Kr | 36 | A1 | 5.684 (82°K.) | 3.005 |
| Lanthanum..... | La | 57 | α A3 | 3.754, 6.063 | 6.188 |
| | | | β A1 | 5.296 | 6.165 |
| Lead..... | Pb | 82 | A1 | 4.9389 | 11.341 |
| Lithium..... | Li | 3 | A2 | 3.51 | 0.53 |
| Lutecium..... | Lu | 71 | | | |
| Magnesium..... | Mg | 12 | A3 | 3.2022, 5.1991 | 1.7365 |

TABLE XXXVI.—LATTICE CONSTANTS FOR ELEMENTS (1939).—(Continued)

| Element | Sym- bol | Atomic number | Lattice type | Edge length <i>a</i> ; <i>a</i> , <i>c</i> ; <i>a</i> , <i>b</i> , <i>c</i> | Density (x-ray) |
|------------------|-------------|------------------|--|---|-------------------------------|
| Manganese..... | Mn | 25 | α A12 β A13 γ A6 | 8.894 6.300 " " " 526 | 7.464 7.24 7.21 |
| Masurium..... | Ma | 43 | | | |
| Mercury..... | Hg | 80 | A10 | $\approx 70^\circ 31.7'$ | 14.24 |
| Molybdenum.... | Mo | 42 | A2 | | 10.22 |
| Neodymium..... | Nd | 60 | A3 | 5.87, 5.880 | 6.984 |
| Neon..... | Ne | 10 | A1 | 52(5°K.) | 1.44 |
| Nickel..... | Ni | 28 | α A3 β A1 | 2.49, 4.08 3.5170 | 8.8 8.895 |
| Nitrogen..... | N | 7 | α X ₄ β X ₃ | 5.66 4.034, 6.587 | 1.02 0.995 |
| Osmium..... | Os | 76 | A3 | 2.730, 4.310 | 22.69 |
| Oxygen..... | O | 8 | α X ₅ β X ₆ γ X ₄ | 5.50, 3.82, 3.44 (21°K.) 6.19 ω = 99.1° (35°K.) 6.83 (48°K.) | 1.46 1.394 1.32 |
| Palladium..... | Pd | 46 | A1 | 3.8817 | 12.028 |
| Phosphorus..... | P | 15 | White X ₇ Black A17 Red, violet, unknown | 7.17 3.31, 4.38, 10.50 | 2.22 2.686 |
| Platinum..... | Pt | 78 | A1 | 3.9158 | 21.438 |
| Polonium..... | Po | 84 | A19 | 7.42, 4.29, 14.10 | |
| Potassium..... | K | 19 | A2 | 5.333 | 0.850 |
| Praseodymium... | Pr | 59 | A3 | 3.657, 5.924 | 6.77 |
| Protoactinium... | Pa | 91 | | | |
| Radium..... | Ra | 88 | | | |
| Radon..... | Rn | 86 | | | |
| Rhenium..... | Re | 75 | A3 | 2.7553, 4.4493 | 20.996 |
| Rhodium..... | Rh | 45 | α X ₃ β A1 | 9.21 3.7956 | 10.42 12.418 |
| Rubidium..... | Rb | 37 | A2 | 5.62 | 1.587 |
| Ruthenium..... | Ru | 44 | α A3 β , γ , δ reported | 2.699, 4.274 | 12.436 |
| Samarium..... | Sm | 62 | | | |
| Scandium..... | Sc | 21 | | | |
| Selenium..... | Se | 34 | γ hexagonal A8 α monoclinic X ₂ β monoclinic X ₉ | 4.337, 4.944 8.99, 8.97, 11.52 12.74, 8.04, 9.25 | 4.845 4.48 4.40 |
| Silicon..... | Si | 14 | A4 | 5.418 | 2.326 |
| Silver..... | Ag | 47 | A1 | 4.0778 | 10.489 |
| Sodium..... | Na | 11 | A2 | 4.30 | 0.954 |
| Strontium..... | Sr | 38 | A1 | 6.075 | 2.577 |
| Sulfur..... | S | 16 | α A16 β X ₉ | 10.40, 12.92, 24.55 2.64, 9.26, 13.3 β = 79° 15' | 2.04 2.00 |
| Tantalum..... | Ta | 73 | A2 | 3.296 | 16.79 |
| Tellurium..... | Te | 52 | A8 | 4.445, 5.912 | 6.23 |
| Terbium..... | Tb | 65 | | | |
| Thallium..... | Tl | 81 | α A3 β A1 | 3.450, 5.520 4.841 | 11.842 11.878 |

TABLE XXXVI.—LATTICE CONSTANTS FOR ELEMENTS (1939).—(Continued)

| Element | Sym- bol | Atomic number | Lattice type | Edge length <i>a</i> ; <i>a</i> , <i>c</i> ; <i>a</i> , <i>b</i> , <i>c</i> | Density (x-ray) |
|----------------|-------------|------------------|--|--|--------------------|
| Thorium..... | Th | 90 | A1 | 5.077 | 11.695 |
| Thulium..... | Tm | 69 | | | |
| Tin..... | Sn | 50 | Gray α A4 nite β A5 | 6.46 5.8194, 3.1753 | 5.806 7.278 |
| Titanium..... | Ti | 22 | α A3 β A2 | 2.953, 4.729 3.32 | 4.42 |
| Tungsten..... | W | 74 | α A15 β A2 | 5.038 3.1583 | 18.97 19.255 |
| Uranium..... | U | 92 | α X ₁₀ β A2 | 2.83, 4.89, 3.31 β = 64° 18' 3.43 | 19.05 19.45 |
| Vanadium..... | V | 23 | A2 | 3.034 | 6.015 |
| Xenon..... | Xe | 54 | A1 | 6.24(88°K.) | 3.56 |
| Ytterbium..... | Yb | 70 | | | |
| Yttrium..... | Y | 39 | A3 | 3.663, 5.814 | 4.34 |
| Zinc..... | Zn | 30 | A3 | 2.6590, 4.9368 | 7.123 |
| Zirconium..... | Zr | 40 | α A3 β A2 | 3.223, 5.123 3.61 | 6.525 6.39 |

coordination number (C.N.) of 12. For both the volume of space occupied by each sphere is $5.66a$, where a is the radius. The axial ratio c/a for hexagonal close packing of spheres must be $2\sqrt{2}/\sqrt{3} = 1.633$; of 21 elements crystallizing in this manner, 19 have this value within 4 per cent. But there is an important difference which is clearly reflected in the properties of metals belonging to each type of structure. In A3, there is only one direction normal to which atoms are arrayed in individually close-packed sheets, whereas in A1 such sheets are disposed in four directions normal to four cube diagonals. Several metals crystallize in both ways as polymorphic forms stable over different temperature ranges. The type A2 body-centered cubic is characterized by a coordination number of 8 and a less tightly packed structure. The simple cubic lattice representing still looser packing is not represented by any element but requires ions of opposite charge for its stabilization.

Among the true metals there are only a few departures from these simple structures. Some cases of complex structures are actually not anomalous; β -manganese with 20 atoms per unit cell has a structure intermediate between body-centered and face-centered structures. Similarly one of the modifications of tungsten (A15) has two kinds of atoms, one with 12 neighbors

at 2.816 and the other with 2 neighbors at 2.519, 4 at 2.816, and 8 at 3.025 A.U., again a transition between face-centered cubic and body-centered cubic.

The B subgroup metals Zn, Cd, Hg, Al, Ga, In, Tl, Si, Ge, Sn, Pb, As, Sb, Bi, Se, Te as a class are far more complicated. Al, Tl, and Pb actually are close-packed but still possess some properties of both true and B subgroup metals.

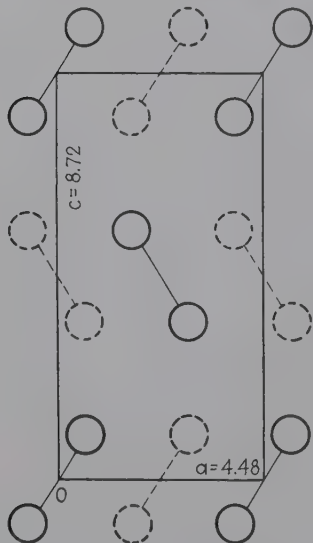


FIG. 171—Structure of crystalline bromine projected upon the 010 plane. Full circles represent atoms in the plane of the paper, broken circles represent atoms above and below the plane of the paper by $b/2$. The Br_2 molecules are indicated by the connecting lines. (Vonnegut and Warren.)

There is a veritable mine of information in the assembled data of crystal structures of the elements. Only a few of the generalizations can be considered here; for example, the crystallized rare gases of the atmosphere in Group 0 are face-centered cubic; the alkali metals and barium are body-centered cubic; Group 2 metals are hexagonal close-packed except strontium, with a transition at calcium which is dimorphic, and mercury; Group 5 and 6 metals are body-centered cubic; Group 8 triad metals, copper, silver, and gold, are close-packed as face-centered cubic or hexagonal. The periodic table might be divided into four classes of element. The nonmetallic elements in classes I and II present a number of interesting problems. The crystals of the rare gases exist only at very low temperatures, and hence the

forces holding the atoms in ordered array in a three-dimensional lattice must be exceedingly weak. An examination of the models for crystalline iodine, bromine, and chlorine shows that the molecules I_2 , Br_2 , and Cl_2 retain a very definite identity in the lattice (Fig. 171). Thus each atom has one close twin neighbor as written electronically $\text{:}\ddot{\text{I}}\text{:}\ddot{\text{I}}\text{:}$; or a completed electron shell 8 minus 7, the number of electrons in the outer shells of these halogen atoms, equals 1, the number of neighbors, or the coordination number. This suggests an $8 - n$ rule, which may

be tested now for other elements. Selenium crystallizes as a series of endless spiral chains (Fig. 172) by actual analysis; here $8 - 6 = 2$ neighbors or a chain $-\ddot{\text{Se}}:\ddot{\text{Se}}:\ddot{\text{Se}}:\ddot{\text{Se}}:-$ with each

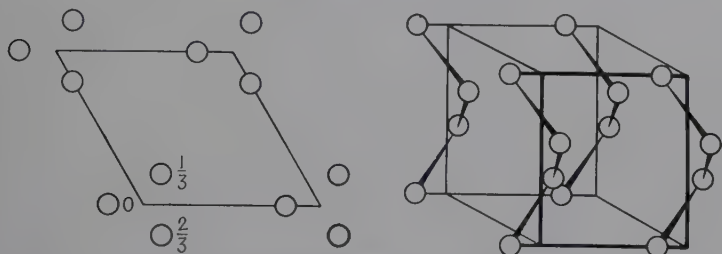


FIG. 172.—Plan and perspective diagram of the hexagonal unit cell of the structure of selenium and tellurium. The spiral chains extend indefinitely through the crystal in the vertical direction.

selenium atom showing an electron pair on either side with other atoms.

Arsenic for which $8 - 5 = 3$ would be expected to crystallize in sheets, with each atom having 3 neighbors; and so it does. Carbon ($8 - 4 = 4$) should have each atom tetrahedrally surrounded by 4 other carbon atoms. This is precisely the structure of diamond (Fig. 173). So far the $8 - n$ rule has not failed, for these cases of homopolar combinations. But when we try to apply the principle to a Group 2 element such as calcium or zinc, we should expect a coordination number $8 - 2 = 6$, whereas actually it is 12 for face-centered cubic or hexagonal close-packed. This discrepancy

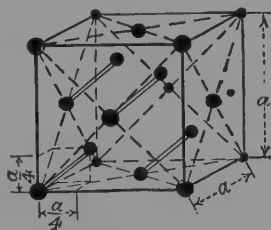


FIG. 173.—The unit crystal cell of diamond (type A_4).

in the fact that there are not enough electrons to account for the large number of equidistant lattice neighbors seems to reside, therefore, in what may be termed the property of being a metal, one of the states that will be considered later. Zinc and cadmium, though metallic in nature, still seem to retain some of the character of Group 4, 5, and 6 elements. These are hexagonal but with an axial ratio $c/a = 1.856$ and 1.886 , respectively, instead of 1.633 for the closest packing of spheres in the hexagonal close-packed arrangement. Thus of the 12 neighbors of each atom, 6 are closer than the remaining 6 (2.660 and 2.907 A.U. for zinc, 2.973 and 3.287 A.U. for cadmium);

the closest 6, therefore, represent an example of the $8 - n$ rule (homopolar bonds), and the other 6 are linked by metallic bonds. Mercury has a similar coordination in its rhombohedral lattice of 6 at 2.999 and 6 at 3.463 A.U. Questions naturally arise as to why an element crystallizes as it does, what are the relationships between structure and properties, and what can be done about predicting the structures of other elements or the behavior in alloys and compounds. The answers to these and many more are the province of the young and incomplete science of crystal chemistry, which has grown directly from the experimental x-ray determinations.

| Type | Formula | Classes |
|------|--|---------|
| B | AX | 33 |
| C | A ₂ X, AX ₂ | 46 |
| D | A _m X _n | 46 |
| E | A _m X _n Y _p (no radicals) | 25 |
| F | A _m (BX) _n and A _m (BX ₂) _n radicals | 14 |
| G | A _m (BX ₃) _n | 21 |
| H | A _m (BX ₄) _n | 46 |
| I | A _m (BX ₆) _n | 16 |
| K | Compounds with complex radicals | 11 |
| S | Silicates | 46 |

Inorganic Compounds.—Several hundred inorganic compounds have now been subjected to crystal-structure examination and more or less complete analysis by x-rays. These data are readily available for reference in the International Critical Tables (Vol. I), Wyckoff's "The Structure of Crystals" (second edition and supplement), and especially in the monumental "Strukturbericht" (four volumes through 1936) of Ewald and Hermann which appeared serially in the *Zeitschrift für Kristallographie*. Hence, only the general types and relationships need be considered here. Ewald and Hermann's type classification has been adopted as a standard, and so this method is followed in this volume. The list does not include hundreds of compounds which have been subjected to crystal analysis but for which results are still incomplete owing to extreme structure complexity, such as some of the natural silicates, or to very complex or poorly defined chemical formulas.

TABLE XXXVII.—RÉSUMÉ OF CRYSTAL STRUCTURES OF INORGANIC COMPOUNDS
(Binary compounds AX)

| Type | Typical compound | Lattice | Space-group | Number of mols, Z | Cell dimensions | Remarks; other examples |
|------|-----------------------|---------------|--------------|---------------------|--|--|
| B1 | NaCl | Simple cubic | $Fm\bar{3}m$ | 4 | 5.628 | (Li, Na, K, Rb) (F, Cl, Br, I); CsF, β -CsCl; NH_4 (Cl, Br, I); Ag(F, Cl, Br); (Mg, Ca, Sr, Ba, Cd, Mn, Fe, Co, Ni)O; (Mg, Ca, Sr, Ba, Pb, Mn)S; β (Na, K, Rb)SH; (Mg, Ca, Sr, Ba, Pb, Mn)Se; (Ca, Sr, Ba, Sb, Pb)Te; (Sc, Ti, Zr, V, Nb)N; (Ti, Zr, V, Nb, Ta)C; LiH; LiD |
| B2 | CsCl | B.c.c. | $Pm\bar{3}m$ | 1 | 4.110 | (α -Rb, Cs, NH_4 , Tl) (Cl, Br, I); CsSH; TiSb, TiBi, CuZn, AgZn, AuZn, CuPd, AlNi, CsBe, MgAu, MgHg |
| B3 | ZnS (zinc blende) | Diamond cubic | $F\bar{4}3m$ | 4 | 5.42 | Cu(F, Cl, Br, I); AgI, (Be, Zn, Cd, Hg) (S, Se, Te); AlP, GaP, AlAs, GaAs, AlSb, GaSb, InSb, SnSb, CSi |
| B4 | ZnS (wurtzite) | Hexagonal | $C6mc$ | 2 | $\begin{cases} a = 3.84 \\ c = 6.28 \end{cases}$ | NH_4 F, BeO, ZnO, ZnS, CdS, MgTe, CdSe, AlN, AgI |
| B5 | Carborundum III | Hexagonal | $C6mc$ | 4 | $\begin{cases} a = 3.095 \\ c = 10.09 \end{cases}$ | |
| B6 | Carborundum II | Hexagonal | $C6mc$ | 6 | $\begin{cases} a = 3.095 \\ c = 15.17 \end{cases}$ | |
| B7 | Carborundum I | Hexagonal | $R\bar{3}m$ | 15 | $\begin{cases} a = 3.095 \\ c = 37.95 \end{cases}$ | |
| B8 | Nickel arsenide, NiAs | Hexagonal | $C6/mmc$ | 2 | $\begin{cases} a = 3.61 \\ c = 5.03 \end{cases}$ | (Fe, Co, Ni)S; (Fe, Co, Ni)Se; (Co, Ni)Te; NiAs, (Cr, Mn, Fe, Co, Ni)Sb |
| B9 | Cinnabar, HgS | Hexagonal | $C3_2$ | 6 | $\begin{cases} a = 4.14 \\ c = 9.49 \end{cases}$ | Layer, but deformed B1 |
| B10 | PH ₄ I | Tetragonal | $P4/nmm$ | 2 | $\begin{cases} a = 6.34 \\ c = 4.62 \end{cases}$ | NH_4 SH |
| B11 | PbO (red) | Tetragonal | $P4/nmm$ | 2 | $\begin{cases} a = 3.98 \\ c = 5.01 \end{cases}$ | (Pb, Sn, Pd)O |

TABLE XXXVII.—RÉSUMÉ OF CRYSTAL STRUCTURES OF INORGANIC COMPOUNDS.—(Continued)

| Type | Typical compound | Lattice | Space-group | Number of mols, Z | Cell dimensions | Remarks; other examples |
|------|-------------------------------|--------------|-------------|-------------------|---|---|
| B12 | BN | Hexagonal | $C6/mmc$ | 4 | $\begin{cases} a = 2.51 \\ c = 6.69 \end{cases}$ | Same as A9 |
| B13 | Millerite, NiS | Rhombohedral | $R3m$ | 3 | 5.65 | Chains |
| B14 | FeAs | Orthorhombic | $Pmcn$ | 4 | $\begin{cases} a = 3.67 \\ b = 6.02 \\ c = 5.43 \end{cases}$ | Similar to B8 |
| B15 | FeB | Orthorhombic | $Pbnm$ | 4 | $\begin{cases} a = 4.053 \\ b = 5.495 \\ c = 2.946 \end{cases}$ | Coordination lattice 4 Fe tetrahedrally around 1B |
| B16 | GeS | Rhombic | $Pbnm$ | 4 | $\begin{cases} a = 4.29 \\ b = 10.42 \\ c = 3.64 \end{cases}$ | Deformed B1 |
| B17 | PtS, cooperite | Tetragonal | $P4/mmc$ | 2 | $\begin{cases} a = 3.47 \\ c = 6.10 \end{cases}$ | Similar to B3 Pt, fc. S in tetrahedral holes |
| B18 | CuS, co- vellite | Hexagonal | $C6/mmc$ | 6 | $\begin{cases} a = 3.80 \\ c = 16.4 \end{cases}$ | CuI, CuII, SI, and (SII) ₂ groups |
| B19 | AuCd | Orthorhombic | $Pmcm$ | 2 | $\begin{cases} a = 3.144 \\ b = 4.851 \\ c = 4.745 \end{cases}$ | Transition between B2 and A3 C.N. 14 |
| B20 | FeSi | Cubic | $P2_13$ | 4 | 4.467 | 7-coordination |
| B21 | CO | Cubic | $P2_13$ | 4 | 5.63 | CO molecules |
| B22 | KSH | Rhombohedral | $R\bar{3}m$ | 1 | 4.374 | $\alpha(\text{Na, K, Rb})\text{SH}$ |
| B23 | $\alpha\text{-AgI}$ | Cubic | | 2 | 5.034 | Ag^+ ions at random; disorder |
| B24 | TlF | Rhombic | $Fmmm$ | 4 | $\begin{cases} a = 5.180 \\ b = 5.495 \\ c = 6.080 \end{cases}$ | Deformed B1, layer |
| B25 | $\gamma\text{-NH}_4\text{Br}$ | Tetragonal | $P4/nmm$ | 2 | $\begin{cases} a = 6.007 \\ c = 4.035 \end{cases}$ | Rotating NH_4^+ |
| B26 | CuO (Tenor- ite) | Monoclinic | $C2/c$ | 4 | $\begin{cases} a = 4.653 \\ b = 3.410 \\ c = 5.108 \\ \beta = 99^\circ 24' \end{cases}$ | CN4 |
| B27 | FeB | Rhombic | $Pbnm$ | 4 | $\begin{cases} a = 4.053 \\ b = 5.495 \\ c = 2.946 \end{cases}$ | B in three-sided prism in zigzag chains parallel to c (B15) |
| B28 | FeSi | Cubic | $P2_13$ | 4 | 4.438 | Cf. B20 (Fe, Co, Mn, Cr, Ni)Si |
| B29 | SnS | Rhombic | $Pmcn$ | 4 | $\begin{cases} a = 3.98 \\ b = 4.33 \\ c = 11.18 \end{cases}$ | Deformed B1, CN6; also PbSnS_2 |
| B30 | MgZn | Hexagonal | $C6/mmc$ | 48 | $\begin{cases} a = 10.66 \\ c = 17.16 \end{cases}$ | Like C14 (MgZn_3) |
| B31 | MnP | Rhombic | $Pbnm$ | 4 | $\begin{cases} a = 5.905 \\ b = 5.249 \\ c = 3.167 \end{cases}$ | Layers—Mg-Zn-Mg Closely similar to B8 P in zigzag chains |

TABLE XXXVII.—RÉSUMÉ OF CRYSTAL STRUCTURES OF INORGANIC COMPOUNDS.—(Continued)

| Type | Typical compound | Lattice | Space-group | Number of mols, Z | Cell dimensions | Remarks; other examples |
|------|------------------|---------|-------------|---------------------|---|---|
| B32 | NaTl | Cubic | | 8 | 7.742 | Na and Tl both A4 interpenetrating $\frac{1}{2} \frac{1}{2} \frac{1}{2}$. Also, LiZn, LiCd, LiGa, LiIn, NaIn, LiAl |
| B33 | TlI | Rhombic | <i>Amma</i> | 4 | $\begin{cases} a = 5.24 \\ b = 4.57 \\ c = 12.92 \end{cases}$ | Layer |

A general impression to be gained from a tabulation of x-ray crystal analyses is that the field of inorganic chemistry is a hopelessly complex one from the structural standpoint. Thus for the various classes of compounds there are the definitely classified types shown in the table on page 332, to which must be added numerous highly characteristic structures for individual compounds reported since 1936 by workers throughout the world.

Thus over 300 crystal types, not counting organic compounds, have been established in the Ewald-Hermann classification, with the possibility of many more as further crystal analyses are reported. Space limitations prevent the presentation of a complete tabulation, but in Table XXXVII are listed the data for the 33 types of simple binary AX compounds to illustrate the general method. At first sight the fact alone that there are at least 33 ways in which compounds whose molecules consist of only two atoms may crystallize is discouraging evidence of the extraordinary complexity in nature's building plans. But there is difficulty only so long as strict adherence to traditional concepts of chemistry incorrectly applied to the solid state is maintained. The new and still incomplete science of crystal chemistry has arisen as one of the most fascinating fields in science directly from experimental x-ray diffraction determinations of structure. It has demanded a profound reorientation of accepted principles of chemistry. Instead of chaos a remarkable orderliness is indicated as crystal-structure plans are laid down in obedience to geometric laws far more fundamental even than the concepts

of chemical valences and rigid stoichiometric proportions. And the 33 types of AX compounds are accounted for, not as a complication, but as a simplification. Several succeeding chapters deal with the crystal chemistry of elements and inorganic compounds, minerals and silicates, alloys, organic compounds, and natural materials.

CHAPTER XVI

CRYSTAL CHEMISTRY: FUNDAMENTAL GENERALIZATIONS FROM EXPERIMENTAL DATA

The complexities that confront the crystal analyst when he attempts to generalize on the modes of crystal construction have been amply demonstrated by the data of the preceding chapter. In spite of the immensity of the field, however, a brilliant chapter in science is being written by the Braggs, Fajans, Pauling, Bernal, Goldschmidt and others. From their work it is possible to advance a theory of why crystals are built as they are, which not only explains at least the simpler types of structure already known semiquantitatively but allows even the prediction of new structures and properties. The concepts of the new wave mechanics have assisted materially in these developments, and great further progress may be expected of this infant branch of chemistry. The fundamental unit to be considered in these structural inquiries is, of course, the atom, which may be now pictured roughly (see page 117) as a nucleus surrounded by shells of diffuse negative electricity, which is denser the nearer the nucleus. On the older theory each shell is thought of as composed of a set of Bohr orbits. Thus the atom has a size, and since it certainly is not rigid it must have a certain degree of compressibility and deformability. It has been amply demonstrated many times that the chemical and crystallographic properties of atoms depend on the size and particularly on the condition of the outer shell of electrons. Each ion or atom in a compound must be considered as forming a lattice of its own, the interpenetration of the various lattices resulting in the structure of the compound. Since very satisfactory books on crystal chemistry¹ are now available, only a

¹ STILLWELL, "Crystal Chemistry," McGraw-Hill Book Company, Inc., New York, 1938.

EVANS, "An Introduction to Crystal Chemistry," University Press, Cambridge, London, 1939.

PAULING, "Nature of the Chemical Bond," Cornell University Press, Ithaca, N. Y., 1939.

TABLE XXXVIII.—CLASSIFICATION OF CRYSTALS

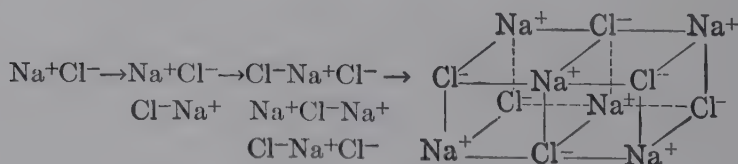
| Crystal type | Crystal units | Type of binding | Characteristic properties | | | | Typical crystals |
|----------------------|---|--|---|---|---|--|--|
| | | | Optical | Electrical | Thermal | Mechanical | |
| Ionic..... | Simple and complex ions | Electrical attraction between ions of opposite signs (e/r^2) balanced by repulsion of negative outer shells ($\frac{-e}{r_0}$) | Transparent; absorption in visible color if present is due to atoms | Moderate insulators in high fields; conduct by transfer of ions | Fairly high melting point; ionization occurs in liquid and vapor | Hardness increasing with higher ionization. Tendency to fracture by cleavage | NaCl CaF ₂ CaCO ₃ K ₂ SO ₄ (NH ₄) ₂ PtCl ₆ |
| | | | In short infrared due to complex ions In long infrared due to crystal lattice Refractivity due to positive ions | When polarization is slight they dissolve with ionization in ionizing solvents (water); when stronger are insoluble | Very high melting points, glasses formed on cooling of melt | Very hard with tendency to cleave or fracture conchoidally | Olivine, Mg ₂ SiO ₄ Cyanite, Al ₂ SiO ₅ Garnet, R ₁ R ₂ R ₃ Si ₃ O ₁₂ Spinel, Al ₂ MgO ₄ Corundum, Al ₂ O ₃ |
| Homopolar (covalent) | Atoms of the fourth group and groups on either side of it | Homopolar bonds throughout or strongly polarized ionic binding | Transparent with high refractivity or opaque metalloid | Diamond is a perfect insulator. The others conduct metalloidally. Very insoluble | Very high melting points with tendency to vaporize except in more metalloid | Very hard. Hardness less for metalloid types | Diamond, C Zinc Blende, ZnS Wurtzite, ZnS Carborundum, CSI |

| Molecular van der Waals | Inert gas atoms. Non-polar and polar molecules | Van der Waal's forces or residual electric fields between molecular poles | Transparent optical properties due to molecules and similar to gas and liquid phases As homopolar | Insulators except when very polar; soluble in non-ionizing (molecular) solvents except when polar Various, similar to both molecular and homopolar | Melting point very low with neutral atoms, rises with heavier molecules and polar molecules | Very soft, hardness increasing with polarity of molecules. Deformation plastic | Argon, A CO ₂ Ice H ₂ O Paraffins, C _n H _{2n+2} Calomel, Hg ₂ Cl ₂ |
|-------------------------|--|---|--|---|---|--|--|
| Layer..... | Strongly polarizing and easily polarized ions | In layers. Homopolar or polarized ionic. Between layers molecular | | | | Cleaving readily in layers which are soft and flexible | Graphite, C CdI ₂ |
| Metallic..... | Positive ions and electron gas | Electrical attraction between positive ions and electron gas | Opaque (due to free electrons) with selective reflection in infrared | Conductors, conductivity inversely proportional to number of free electrons. Soluble in acids where H ⁺ ions absorb free electrons | Moderate to very high melting points. Long liquid interval | Moderate hardness increased by alloying. Elastic but yield by glide plane slipping when overstressed | Copper, iron Iron, sodium Zinc |
| Metalloidal..... | Metal atoms and atoms of the sulfur and arsenic type | Mixture of homopolar ionic and metallic binding | Opaque metallic or transparent with high refractivity and color | Medium to bad conductors. Soluble only with decomposition | Tendency to vaporize or decompose at high temperatures | Moderately hard to soft. Properties a mixture of those of other types | Nickel arsenide, NiAs Fahlertz, R ^{II} ₂ SbS ₃ Pyrites, FeS ₂ |

few of the simpler and most fundamental generalizations need be considered here.

Types of Crystal in Terms of Bonding Forces.—A careful survey of all crystal-structure data leads to the conclusion that all crystalline substances may be classed under four principal types according to the types of combination of atoms into molecules and solid crystals: ionic or heteropolar, homopolar or covalent (sharing of electron pairs), molecular, and metallic. A structure characterized by a single kind of principal bond is called *homodesmic* and one with mixed types is called *heterodesmic*, in which case the weakest binding force determines the crystalline character. This does not mean that the division lines are clear-cut, for many substances may be thought of as in the transition zone between two or more types. Bernal has therefore added three of the most important intermediate classes: silicates, layer lattices, and metalloids. The fundamental classification and properties have been assembled by Bernal¹ as shown in Table XXXVIII.

Ionic or Heteropolar Combination.—There remains little doubt that in a large number of crystals the atoms are really ions in the familiar chemical sense and that they are held together in space with requisite rigidity by electrostatic forces of attraction between positively and negatively charged particles, inversely as the square of the distance. When the outer electron shells of positive and negative ions are in close proximity, however, a repulsion sets in inversely at about the ninth power of the distance between them. Thus in a crystal like rock salt a condition is easily reached like



and so on, till the whole single crystal is thus constructed. Thus sodium chloride diffracts x-rays in a way that leads to the assignment of a structure in which each sodium ion is not bound to a single chlorine ion as in the simple chemical molecule (vapor

¹ "Encyclopaedia Britannica," 14th ed., Vol. 23, p. 857.

state) but exerts its attraction on six equidistant chlorine neighbors, and each chlorine ion is surrounded by six sodium ions. Stated otherwise, each ion has a *coordination number* of 6. Thus each ion tends to surround itself with as many oppositely charged ions as possible. In the electrically neutral crystal there are not pairs of sodium and chlorine atoms or ions, but simply an equal number of oppositely charged ions. In a sense, the chemical molecule seems to be lost sight of, and proper formulas would seem to be Na_6Cl and NaCl_6 . However, an analogy cited by Sir William Bragg serves to clarify the situation. Several couples of men and women go in to dinner and are seated at a circular table. Each man now has a lady on either side (or coordination number 2), and the identity of the original couple is obscured though by no means destroyed on account of the seating arrangement.

It follows that the structure of an ionic crystal is determined very largely by the purely geometric concept that each ion is surrounded by the largest possible number of oppositely charged neighbors, consistent with the requirement that electrical neutrality be maintained for the crystal as a whole. NaCl and CsCl are closely related and would be expected to crystallize alike. However, they crystallize differently, simply because the question of geometric size enters. Six chlorine ions are octahedrally arranged around each sodium ion; but eight chlorine ions are cubically arranged around each cesium ion because there is room for them.

Application of Ionic Crystal Chemistry Laws to Prediction of Properties.—Goldschmidt has shown that the hardness and related cohesive properties of ionic crystals depend directly upon the electrostatic forces between ions. The hardness of crystals increases with decreasing distance between the ion centers, the charge being kept constant; and the hardness increases with increasing ionic charge when the distance is kept constant; for example:

| Property | BeO | MgO | CaO | SrO | BaO | NaF | MgO | ScN | TiC |
|-------------------|------|------|------|------|------|------|------|------|------|
| Distance A-X..... | 1.65 | 2.10 | 2.40 | 2.57 | 2.77 | 2.13 | 2.10 | 2.23 | 2.23 |
| Hardness..... | 9.0 | 6.5 | 4.5 | 3.5 | 3.3 | 3.2 | 6.5 | 7-8 | 8-9 |

Partial correlations have been made between ionic structure and optical properties¹ (see page 369 in this chapter), compressibility, expansion coefficients, elastic constants, cohesion, melting point, and solubility.

Thus in a series of related salts the melting point decreases, and the coefficient of expansion increases with increasing inter-atomic distance:

| Property | NaF | NaCl | NaBr | NaI | NaF | KF | RbF | CsF |
|--|------|------|------|------|------|------|------|------|
| Distance..... | 2.31 | 2.79 | 2.94 | 3.18 | 2.31 | 2.66 | 2.82 | 2.98 |
| Melting point..... | 988 | 801 | 740 | 660 | 988 | 846 | 775 | 684 |
| Coefficient of expansion, $\alpha \times 10^3$ | 39 | 40 | 43 | 48 | | | | |

Classification of Ionic Crystals.—Suppose that n anions are coordinated around a central cation of charge z . The electrostatic valence of the bond between the cation and each anion is, therefore, z/n . Similarly the sum of bonds reaching an anion must equal its negative charge. This simple principle, which may be extended to the case of several cations bound to one anion, leads to the fundamental classification proposed by Evans, Bernal, and others as follows:

1. *Isodesmic*: Bond $A-X < z/2$; no discrete groups in structure. Example: NaCl, where Na^+-Cl^- bond = $\frac{1}{6}$.

a. Simple. Single cation, A_mX_n .

b. Multiple. Example: Spinel $MgAl_2O_4$.

2. *Anisodesmic*: Bond $A-X > z/2$; discrete groups or radicals in structure. Example: Nitrates in which N^{5+} is coordinated with $3O^{2-}$; hence, $N-O = \frac{5}{3}$ and NO_3^- radical appears in lattice.

a. Anhydrous.

b. Hydrus.

3. *Mesodesmic*: Bond $A-X = z/2$. Example: All silicates where Si^{4+} is coordinated with $4O^{2-}$; hence, $Si-O = \frac{4}{4} = 1$ = strength of all other bonds reaching O ions.

4. *Hydrogen compounds*: Acids, etc., distinguished from salts because of vanishingly small size of H^+ , twofold coordination, and strong polarization (the hydrogen bond).

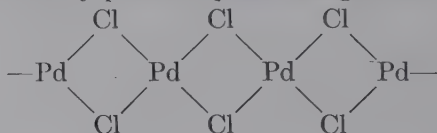
¹ See, for example, WOOSTER, Relation between Double Refraction and Crystal Structure, *Z. Krist.*, **80**, 495 (1931).

Covalent or Homopolar Combination.—In terms of modern theories of valence this means that atoms are held together by sharing electrons, usually in pairs called covalences. The stable diatomic molecules such as H_2 , O_2 , N_2 , etc., and H_2O , CO_2 are built up in this fashion in order to complete the various quantum electron shells. In organic molecules the carbon atoms form long chains by homopolar bonds. The best example is in diamond where each carbon atom is sharing electron pairs with four others, so that this linking is extended indefinitely in all directions to the limits of the crystal itself which thus may be considered a single solid molecule. The word "adamantine" has been ascribed to this class by Bernal.

The covalent bond is distinguished from the ionic bond in many ways. The latter is essentially undirected, hence spherically distributed, since it is distributed by coordination over as many neighbors of opposite charge as can be packed around a central ion, whereas the number of homopolar bonds by which a given atom can be linked to others is limited. This is the essence of the $8 - n$ rule, discussed in the preceding chapter. Homopolar compounds differ also from ionic in that they are nonconductors in the molten state. They are insoluble in water, but so also are many ionic compounds. The optical properties differ because the character of the binding is such that electrons are linked not in atomic orbitals of individual ions, but in diatomic orbitals embracing two neighboring atoms, though varying widely in tightness in such a series as diamond to tin. On this account, the optical absorption of solutions of ionic compounds is essentially the same as that of the solid, whereas in the homopolar compounds a great change results from disappearance of the diatomic orbitals.

It is now generally recognized that, given two electrons with opposed spins, an atom can form an electron pair or covalent bond for each stable orbital (the wave function associated with the orbital motion of an electron). Hydrogen with only one stable orbital can form only one covalent bond; carbon with four electrons in the L shell can and does form four covalent bonds. A molecule is the more stable the greater the number of electron-pair bonds; thus $:N::N:$ is more stable than $:N:\dot{N}:$, and the former is probably the predominating structure of the nitrogen molecule. The energy of a covalent bond has been

shown to be largely the energy of resonance of two electrons between two atoms. Such bonds may be directed in space where the p orbitals (s is spherical) are involved, since it was found by Slater that these tend to be at right angles to each other. Hence the measurement of *bond angles* has been one of the important contributions of crystal analysis. For a large number of substances these have been found to be between 90 and 110 deg. (water, H-O-H 105 deg., H-S-H 92 deg., etc.), the discrepancy being accounted for either by steric effects or by a partial ionic character of the bond. Quantum mechanical treatment of orbitals and related magnetic measurements have accounted remarkably well for double and triple bonds; tetrahedral bonds; octahedral bonds in $[\text{Co}(\text{NH}_3)_6]^{3+}$, $(\text{PdCl}_6)^{2-}$, etc.; square bonds as in $[\text{Ni}(\text{CN})_4]^{2-}$, $(\text{PdCl}_4)^{2-}$, and PdCl_2 , which polymerizes into a chain of nearly perfect square configuration



and the configuration of such polyhalide ions as $(\text{ICl}_4)^-$, which actually has two unshared electron pairs of the iodine atoms octahedrally arranged above and below the plane of the square.

It is perhaps strange that the homopolar bond is characteristic of the ZnS structure (also AgI, AlP, etc.) which is like that of diamond except that adjacent atoms are of opposite kind (four sulfur atoms around each zinc, and vice versa). It is sufficient that the total number of valence electrons is just four times the total number of atoms, and it is for this reason that the homopolar bond is practically invariably associated with tetrahedral coordination.

The single- and triple-electron homopolar bonds are predicted by quantum theory, as is also their rarity. These bonds can exist between atoms A and B, respectively, if $\text{A}^\cdot + \text{B}$, and $\text{A} + \cdot\text{B}$, and $\text{A}^\cdot + \cdot\text{B}$, and $\text{A}^\cdot + :\text{B}$ have essentially the same energy. The compound B_2H_6 has two single-electron bonds between B and H, resonating over the six hydrogen atoms and increasing thereby the stability of the molecule. Magnetic measurements on crystals referred to elsewhere as a valuable aid in crystal-structure analysis are of especial significance for the homopolar bond. Paired electrons with opposing spins

contribute nothing to the magnetic moment of a molecule or complex ion, so that observed moments determine at once the number of unpaired electrons present.

Polarization and Ionic-covalent Bonds.—Many inorganic compounds display properties that are characteristic of both ionic and covalent bonds. Modern quantum mechanics provides for resonance of a system between structures I and II, for example, so that over a period of time a bond may represent a mixture of two types. Polarization is really another way of expressing this possibility. For example, if a small highly charged positive ion is combined with a larger diffuse negative ion like S^{2-} , this would be not only activated but actually distorted, since the negative shell would be pulled toward the cation and the nucleus repelled. Formally the covalent bond may be represented $A:X$, with the electron pair centered between the atoms; the ionic bond A^+X^- , with both electrons on one atom; the ionic-covalent or state of polarization $A:X$, with the electron pair nearer one atom than the other. Or HCl resonating between ionic and covalent, for example, may be represented as $(H^+Cl^-, H:\ddot{Cl}:)$, or combined $H-Cl$. For a series of ions with the same charge, the smaller the ionic radius, the greater the polarizing effect of the ion and the higher the ionization potential. Of the alkali metals Li^+ has the greatest polarizing effect and the greatest tendency to form a covalent bond. For two ions of the same size, one with 18 electrons in the outer shell exhibits a greater polarizing effect and has a higher ionization potential than an ion with an 8-electron shell. For example, Ca^{2+} (radius 0.98 A.U.) and Cd^{2+} (0.99 A.U.) have the same ionic radii, but Ca^{2+} has an 8- and Cd^{2+} an 18-electron shell. The latter is more strongly polarizing, is more likely to form a covalent bond, and, as a matter of fact, gives rise to layer lattices. The larger the negative ion, the more easily may it be polarized and the lower is its electron affinity. Thus, of the halogens, the iodide ion is most easily polarized and most likely to form a covalent bond. In Table XXXIX are correlated polarizabilities, polarizing power, and sizes of a number of ions. The importance of this whole matter lies in the fact that compounds with purely ionic bonds may be expected to obey a series of generalizations and have essentially constant radii and properties in agreement with predictions, while discrepancies are to be ascribed to this

admixture of bond types. Thus the distance between the nuclei of two atoms A and X joined by a covalent bond will generally be smaller than the distance between the nuclei of the ions of the same elements. In fact, X atoms may be drawn in so closely around A that the coordination number may be decreased. The compounds CaO, CaS, CaSe, and CaTe all crystallize like NaCl (C.N. 6); but CdS, CdSe, and CdTe crystallize like ZnS (C.N. 4) though Ca^{2+} and Cd^{2+} have the same size. ZnS is a typical case of mixed ionic and covalent bond. Pauling calculates that the salts of alkali and alkaline earth metals are more than 50 per cent ionic except Li—I, Li—C, Li—S; Be—F 79 per cent, Be—O 63 per cent, Be—Cl 44 per cent; Be—Br 35 per cent; Be—I 22 per cent; B—F 63 per cent, B—O 44 per cent, B—Cl 22 per cent; C—F 44 per cent (highest ionic); Si—F 70 per cent, Si—Cl 30 per cent, Si—O (silicates) 50 per cent; Ag—F 70 per cent, Ag—Cl 30 per cent, Ag—Br 23 per cent, Ag—I 11 per cent.

TABLE XXXIX

| | | | | | | | |
|---|---|---|-----------------|----|-----------------|------------------|------------------|
| Decreasing polarizability Increasing polarizing power Decreasing radius | ↑ | O^{2-} | F^{-} | Ne | Na^{+} | Mg^{2+} | Al^{3+} |
| | | S^{2-} | Cl^{-} | A | K^{+} | Ca^{2+} | Sc^{3+} |
| | | Se^{2-} | Br^{-} | Xe | Rb^{+} | Sr^{2+} | Y^{3+} |
| | | Te^{2-} | I^{-} | Kr | Cs^{+} | Ba^{2+} | La^{3+} |
| | | → | | | | | |
| | | Decreasing polarizability Increasing polarizing power Decreasing radius | | | | | |

Resonance and Covalent Mixed Single and Double Bonds.—

Attention already has been directed to one type of mixed bond, the covalent-ionic, representing resonance between the two types of structure. Another type of resonance is involved in some covalent single bonds that seem to possess some double-bond character. This is of special significance in C—C linkages, making possible the exact equivalence of the six carbon atoms in the benzene ring; these cases will be discussed in Chap. XIX. Attention here may be directed to fluorides and chlorides of silicon, phosphorus, sulfur, germanium, arsenic, tin, and antimony, for the interatomic distances such as Si—Cl are all shorter (2.00 A.U.) than the sum of the covalent radii in a single covalent

bond (2.16 A.U.). It has been demonstrated amply that the bond resonates between the two bond types Si—Cl and Si=Cl (the dash representing covalent bonds with partial ionic character). The same is true of the tetrahedral ions SiO_4^{4-} , PO_4^{3-} , SO_4^{2-} , and ClO_4^{-*} and in a variety of other acid ions.

| | Si-O | P-O | S-O | Cl-O |
|-----------------|------|------|------|------|
| Observed..... | 1.60 | 1.55 | 1.51 | 1.48 |
| Radius sum..... | 1.83 | 1.76 | 1.70 | 1.65 |

Finally some of the difficult questions that arise in connection with covalent complexes of the transition elements, *e.g.*, cobalt-ammines, $[\text{Fe}(\text{CN})_6]^{4-}$, $\text{Ni}(\text{CO})_4$, are explained by the fact that these atoms can form multiple covalent bonds with electron-accepting groups by making use of electrons and orbitals of the *shell within the valence shell*.

The Metallic Bond.—Metallic combination, which is considered in detail in Chap. XVIII, occurs when atoms tend to lose electrons easily. Typical metal structures have been described in the preceding chapter. The best simple picture of metallic structure is that of a lattice of positive ions held together by an electron gas in which no particular electron belongs exclusively to a particular metal atom.

This arrangement confers neither spatial nor numerical limitations on the metallic bond; hence, as expected, high coordination numbers are the general rule. The metallic bond resembles the ionic in this respect, but differs in that it is exerted not between two entirely different ions of opposite charge, but between identical atoms in metallic elements or chemically similar atoms in alloys, without being called upon to satisfy electrical neutrality. In this respect, there is a much closer resemblance to the covalent bond, with added freedom of motion, giving a flexibility that alone is adequate to explain why laws of constant composition and simple proportions arising for ionic compounds through the demands of electrical neutrality need not and do not apply to alloy systems. In a sequence, diamond, carborundum (CSi), silicon, germanium, gray tin, all are tetrahedral, and the typical metallic properties first appearing in carborundum increase

* PAULING, *op. cit.*, p. 222.

rapidly toward tin. The ease of deformation of metals (malleability and ductility) is a structural characteristic arising from the undirected nature of metallic bonds, as a result of which the crystal may glide on atomic planes, in contrast with the generally brittle character of ionic and homopolar combinations. A further consequence is that a metal can form bonds after deformation of an original structure with considerable ease and thus "heal" itself.

The Hydrogen Bond.—One of the most important modern concepts in chemistry is the hydrogen bond, or bridge, between two atoms. It plays an important role in an ever-increasing list of known compounds from water up to the most complex proteins. First mentioned in 1912 its importance was first pointed out by Latimer and Rodebush in 1920. It is characterized as a link between two electronegative atoms only, the strength of the bond increasing with the electronegativity of the two bonded atoms in the order chlorine, nitrogen, oxygen, and, strongest, fluorine. The hydrogen bond will be illustrated for organic compounds in Chap. XIX, but note may be taken here of direct crystal structure evidence in $(\text{NH}_4)_2\text{F}$, which differs from all other ammonium halides in that each nitrogen atom is surrounded tetrahedrally by four fluorine atoms with which it forms hydrogen bonds. The striking physical properties, melting point, boiling point, dielectric constant, etc., of H_2O , HF , and NH_3 in solid, liquid, and even gas (polymerized HF molecules) are now explained by this bonding. In NH_4HF_2 around each nitrogen ion are four fluorine ions at a distance 3.07 A.U. and four are drawn in to 2.76 A.U. by $\text{N—H} \dots \text{F}$ bonds. The same is true of NH_4N_3 . Boric acid contains layers of $\text{B}(\text{OH})_3$ molecules held together by hydrogen bonds. Each oxygen forms two hydrogen bonds coplanar with and holding together the BO_3 groups. A classical example is KH_2PO_4 which has received much attention because the $\text{O—H} \dots \text{O}$ distance of 2.54 A.U. is the shortest known. This crystal is built from H^+ ions, PO_4 groups and irregular KO_8 groups, so that each O^{2-} ion belongs to one PO_4 and two KO_8 groups, with a bond strength of $\frac{5}{4} + 2 \times \frac{1}{8} = \frac{3}{2}$. Since two positive charges are required to saturate each O^{2-} , it is satisfied by a bond of strength $\frac{1}{2}$ to H^+ . Finally several minerals, notably diaspore, $\text{AlO}(\text{OH})$, and lepidocrocite, $\text{FeO}(\text{OH})$, have their unique crystalline structures determined by $\text{O—H} \dots \text{O}$ bonds. The concept, so well proved

from crystal structures even though the actual positions of hydrogen atoms cannot be ascertained from x-ray data because of negligible scattering power, has the great support of the infrared absorption spectrum. In the course of investigations on structures of high polymers in the writer's laboratory, these spectra have been used to indicate the presence or absence of hydrogen bonds and thus to help place the hydrogen atoms in logical positions. The subject is clearly presented by Pauling in "The Nature of the Chemical Bond."

Van der Waals Bond, or Molecular Combination.—Organic compounds form the great class of crystals whose pattern units are the whole molecules in which, in turn, the atoms are linked together by pairs of electrons held in common. While in the ionic lattice the identity of the single molecule of potassium chloride, for example, is somewhat obscured (though by no means destroyed) by the division of the bonding forces of one atom among six neighbors, in the molecular lattices the molecule of the chemists' formula and of the gaseous phase is built essentially unchanged into the solid structure. The van der Waals bond is quite similar in some respects to the metallic bond in that it may link an indefinite number of neighbors and is spatially undirected. By virtue of the residual stray fields of the electrically neutral molecules, it is possible for one molecule to lie up against another and form the regularly built-up solid. Thus there are two molecules of naphthalene in the unit crystal cell. Because the stray forces holding the molecules in their fixed position cannot compare in intensity with the strong polar or nonpolar bondings between atoms, the substance easily melts or throws off single whole molecules in the process of sublimation. This type of combination will be considered in detail in Chap. XIX on the structure of organic crystals. In the case of electrically neutral inert gas atoms, which crystallize with the only homodesmic molecular bonds, the residual attraction is effective only at very close distances and consequently except at lowest temperature the substance remains a gas. Molecular lattices are also to be found among inorganic compounds, notably solid HCl , SnI_4 ,* and the cubic forms† of arsenious and antimonious

* DICKINSON, *J. Am. Chem. Soc.*, **45**, 958 (1923).

† BOZORTH, *ibid.*, **45**, 1621-1629 (1923).

oxides. These are heterodesmic since the bonds *within* the molecules are homopolar, etc.

Coordination and Radius Ratios.—The various types of lattices enumerated in Chap. XV for inorganic compounds are distinguishable by their coordination numbers as originally defined chemically by Werner, or the number of neighbors possessed by each ion; thus the following simple coordination types for the compounds AX and AX_2 may be recognized:

- AX : 1: single molecules and molecular lattices.
 2: double molecules, molecular chains.
 3: BN type.
 4: diamond type lattices of zinc blende and zinc oxide.
 6: NaCl and NiAs types.
 8: CsCl type.
- AX_2 . 2 and 1: single molecules and molecular lattices.
 4 and 2: α - and β -quartz, cristobalite, tridymite, cuprite.
 6 and 3: anatase, rutile, brookite, layer lattice CdI_2 .
 8 and 4: fluorite.

Each of these types is characterized by a definite energy stability, which may be deduced theoretically and the constants evaluated from the compressibility and related data.

Goldschmidt has shown from simple geometry that, in order to arrange a number of spheres X so that they will touch around a central sphere A , the following ratios must hold:

| Number spheres X | Arrangement | Limiting R_A/R_X |
|-----------------------|----------------------|-----------------------|
| 2 | Opposite | |
| 3 | Equilateral triangle | 0.15 |
| 4 | Tetrahedral corners | 0.22 |
| 4 | Square corners | 0.41 |
| 6 | Octahedral corners | 0.41 |
| 8 | Cube corners | 0.73 |

Such simple relationships which determine possible arrangements in space for given ratios of radii hold true in remarkable fashion for the packing of ions in crystals.

The way in which atomic diameter influences structure can be seen from the simplest ionic structure of the type AX , with

equal numbers of ions of opposite signs. The simplest of these is the structure of rock salt, where sodium and chlorine ions occupy alternate corners of a cubic lattice. The coordination number is 6:6; *i.e.*, each sodium ion has six chlorine neighbors, and vice versa. Actually, the chlorine ions are so large compared to the sodium that they form an octahedron which encloses it almost completely. Simple geometry shows that this can only be the case if R_A (radius of positive ion): R_X (radius of negative ion) = 0.73. This relation holds for all halides of the alkaline metals with the exception of the chloride, bromide, and iodide of cesium where the ratios R_A/R_X are 0.91, 0.84, and 0.75, respectively. Now these last three are the only alkaline halides that belong not to the sodium chloride type but to the cesium chloride type. Here the coordination number is 8:8, and there is, so to speak, more room for the larger cesium ion inside the cube of chlorine ions. Where $R_A:R_X$ is very small, the factor of polarization comes in, and the structure ceases to be ionic and becomes covalent or molecular.

Types of structures for AX compounds, therefore, may be represented by the following:

| Compound | Bond type | R_A/R_X | C.N. |
|--------------|-------------------|-----------|------|
| CsCl..... | Ionic | >0.73 | 8 |
| NaCl..... | Ionic | 0.41–0.73 | 6 |
| NiAs..... | Covalent metallic | 0.41–0.73 | 6 |
| ZnS–ZnO..... | Covalent | 0.22–0.41 | 4 |
| BN..... | Covalent (layer) | 0.15–0.22 | 3 |
| HCl..... | Molecular | <0.22 | |
| etc..... | | | |

The following monatomic ions are found in ionic AX compounds:

Cations: Li^+ , Na^+ , K^+ , Rb^+ , Cs^+ , Ag^+ , Tl^+ , $(\text{NH}_4)^+$

Be^{2+} , Mg^{2+} , Ca^{2+} , Sr^{2+} , Ba^{2+} , Ti^{2+} , Pb^{2+} , Mn^{2+} , Fe^{2+} , Co^{2+} , Ni^{2+}

Ti^{3+} , Zr^{3+} , V^{3+} , Cb^{3+} , Ta^{3+} , Cr^{3+}

Ti^{4+} , Zr^{4+} , V^{4+} , Cb^{4+} , Ta^{4+}

Anions: H^- , F^- , Cl^- , Br^- , I^- , $(\text{OH})^-$, $(\text{CN})^-$, $(\text{NO}_3)^-$

O^{2-} , S^{2-} , Se^{2-} , $(\text{CO}_3)^{2-}$, $(\text{SO}_4)^{2-}$

N^{3-} , P^{3-}

C^{4-}

Complex ions in parentheses are included because they are intrinsically spherical or may act so by free rotation at elevated temperatures.

If we pass to the next series AX_2 , a similar situation occurs. Where $R_A:R_X$ is greater than 0.73, the structure is of the fluorite type (see Fig. 174). Here the coordination number is 8:4, the calcium ions being surrounded by a cube of eight fluorine ions just as the cesium is by the chlorines. A number of compounds

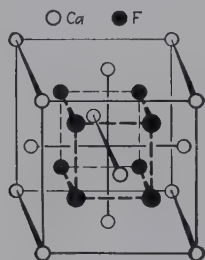


FIG. 174.—Crystal unit cell for fluorite (CaF_2).

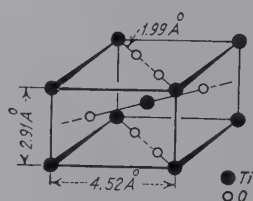


FIG. 175.—Crystal unit cell for rutile (TiO_2).

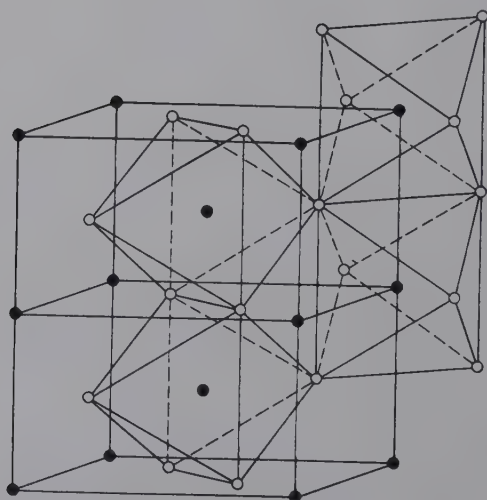
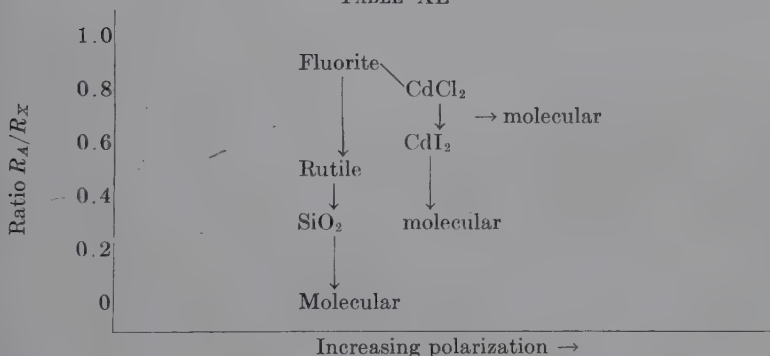


FIG. 176.—The structure of PbO_2 , showing the coordinating octahedra of anions round the cations.

belong to this type, which includes the fluorides of the alkaline earths and the dioxides of zirconium, thorium, praseodymium,

cerium, and uranium. If $R_A:R_X$ lies between 0.73 and 0.41, a structure is formed analogous to rock salt. This is the rutile structure (see Fig. 175). Here the coordination number 6:3 cannot be satisfied in the cubic system, and the octahedron of oxygen ions is placed on its side in a tetragonal structure. The two other forms of TiO_2 , anatase and brookite, are also built with the same coordination but with the octahedra distorted and differently placed. A large number of substances belong to the rutile structure: the fluorides of Mg, Mn, Co, Fe, Ni, Zn and the dioxides of Mn, V, Ti, Ru, Ir, Os, Mo, W, Cb, Sn, Pb, and Te. The coordination structure of PbO_2 is drawn in Fig. 176.

TABLE XL



When $R_A:R_X$ lies between 0.41 and 0.22, the coordination number is 4:2, which is approaching a homopolar structure. This is the case for the different forms of silica (SiO_2), cristobalite, tridymite, and quartz. Though apparently different, these structures have the essential point in common that they are built from silicon ions completely surrounded by four oxygens in a tetrahedron. Each oxygen is shared between two tetrahedra and the different forms of structure are merely due to different arrangements of these tetrahedra. Thus the polymorphism of silica is not due to any change in the molecule. The tetrahedral coordination does not determine whether the bonds are ionic or covalent. An ionic structure would allow the oxygen bonds to assume any angles, while covalent bonds should be limited to 90 or 109.5 deg.; β -tridymite with an angle of 180 deg. is ionic, and α -quartz probably covalent.

The general structural types of AX_2 compounds are as follows:

1. A and X are individual units in ionic or atomic lattices; examples, CaF_2 , TiO_2 , CdI_2 , MoS_2 , $CdCl_2$ (all different).
2. A and X_2 or A and XY are units; examples, CaC_2 , FeS_2 (pyrites), KCN.
3. AX_2 molecules are units in the lattice; examples, CO_2 , N_2O , etc.

AX_3 compounds are classified in the same manner, with the following examples:

1. AlF_3 , AsI_3 .
2. NaN_3 , KN_3 , $CsCl_2I$, $NaHF_2$, KHF_2 .
3. NH_3 .

Table XL shows the influences of radius ratio and polarization (increasing homopolar character) in determining the structures in AX_2 compounds.

Layer Lattices.—The most important influence, next to the size of the ions, in determining how a compound shall crystallize is the phenomenon of polarization, which includes all alterations that particles show under the influence of electric forces. Polarization resolves itself into resonance between ionic and covalent bonds. The simplest case is the formation of a dipole under the influence of an electric field. The negative iodide ion is a typical polarizable ion. Cadmium iodide, by analogy with related compounds and the transition $CdF_2 \rightarrow CdI_2$ and by consideration of the ratio of ionic radii $R_{Cd^{2+}}/R_{I^-}$, would be expected to have a rutile structure, but instead it forms a distinctive type of its own. The coordination arrangement is such that any cadmium ion is surrounded symmetrically by six iodine ions rhombohedrally, but each iodine ion is in contact with three cadmium ions *on one side*, an ideal condition for polarization. The structure is built up in layers with the sequence iodide ion-cadmium ion-iodide ion layers being repeated. In each layer there is really a giant ionic molecule as large as the extension of the layer, whereas the layers are held together by secondary forces, which accounts for the very prominent cleavage. Of course, graphite is a prominent example among the elements. The transitions $TiO_2 \rightarrow TiS_2$ and $SnO_2 \rightarrow SnS_2$ also result in changes to layer lattices. Layer lattices in minerals are illustrated in the next chapter.

The Sizes of Atoms and Ions.—In Table XLI are listed the latest values for (1) the radii of atoms in covalent compounds

for single, double, and triple bonds and for the special cases of tetrahedral and octahedral coordination; (2) metallic radii calculated from the crystal structures of the metallic elements for coordination members of both 12 (closest packing, face-centered cubic, or hexagonal close-packed) and 8 (body-centered cubic), these being similar to but not identical with covalent radii; (3) ionic radii for valence states corresponding to periodic table positions; and (4) van der Waals, or nonbonded, radii, or the radial distance of nearest approach of adjacent molecules in a lattice held by van der Waals forces.

1. *Covalent Radii*.—Since the values of equilibrium distance between atoms A and B connected by a covalent bond, single, double, or triple, are very nearly the same, radii, as reliably determined from x-ray data on crystals, and band spectra and electron diffraction by gas molecules can be deduced and be used in any molecule involving the bond. In diamond the C—C distance is 1.54 A.U., and in a great variety of organic compounds the same value is obtained; hence the radius 0.77 A.U. may be assigned to carbon. In compounds with the linkage C—O the value is 1.43 A.U., so that 0.66 is obtained for the covalent radius of oxygen by simple subtraction of 0.77 from 1.43.

In acetylene the triple-bond distance $C\equiv C$ is 1.204, $C\equiv N$ in HCN is 1.154, and $N\equiv N$ in N_2 is 1.094. Thus for the first row of atoms the single-bond radii are to be multiplied by 0.78 for triple bonds and 0.87 for double bonds. In second-row atoms these factors are, respectively, 0.85 and 0.91.

Concordant radii for tetrahedral arrangement as in diamond sphalerite or wurtzite structures are derived for C, Si, Ge, Sn, SiC, AlN, AlP, AlAs, AlSb, GaP, GaAs, GaSb, InSb, ZnO, ZnS, ZnSe, ZnTe, CdS, CdSe, CdTe, HgS, HgSe, HgTe, CuCl, CuBr, CuI, AgI, MgTe, BeS, BeSe, and BeTe, all being at least predominantly covalent.

For octahedral arrangements, examples are: pyrites, FeS_2 [with six sulfur atoms around each iron atom, and $Fe-S=2.27$ A.U.; hence $2.27 - 1.04$ (tetrahedral S) = 1.23 A.U. for the octahedral covalent radius of bivalent iron, Fe^{II}]; CoS_2 , $CoSe_2$, $NiAsS$, $AuSb_2$, (Ru, Pt, Pd, Os) (sulfides, etc.), FeP_2 , $FeAs_2$, $FeSb_2$; and also complex ions such as $[PtCl_6]^{2-}$, $[SnCl_6]^{2-}$, $[PbBr_6]^{2-}$, $[SeBr_6]^{2-}$, etc.

TABLE XLII.—RADII OF ATOMS AND IONS (A.U.)

| Element | Covalent ¹ | | | Metallic (atomic) | | Ionic | van der Waals |
|---------------------|--------------------------|---------------------|---------------------|-------------------|--------|-------------------|---|
| | Single | Double | Triple | C.N. 12 | C.N. 8 | | |
| | | | | | | | |
| 1. Hydrogen..... | 0.30 | | | | | | 1.2 {CH ₃ 2.0 aromatic 1.85 |
| 2. Helium..... | | | | | | | |
| 3. Lithium..... | | | | | | | |
| 4. Beryllium..... | 1.06 ^t | | | 1.58 | 1.52 | 0.60 ⁺ | |
| 5. Boron..... | 0.88 | | | 1.12 | 1.07 | 0.31 ⁺ | |
| 6. Carbon..... | 0.77 | 0.76 | 0.68 | | | 0.20 ⁺ | |
| 7. Nitrogen..... | 0.70 | 0.67 | 0.60 | | | 0.15 ⁺ | 2.60 ⁺ |
| 8. Oxygen..... | 0.66 | 0.61 | 0.55 | | | 0.11 ⁺ | 1.71 ⁺ |
| 9. Fluorine..... | 0.64 | 0.57 | 0.51 | | | 0.09 ⁺ | 1.40 ⁺ |
| 10. Neon..... | | 0.55 | | | | 0.07 ⁺ | 1.36 ⁺ |
| 11. Sodium..... | | | | | | | |
| 12. Magnesium..... | 1.40 ^t | | | 1.92 | 1.86 | 0.95 ⁺ | |
| 13. Aluminum..... | 1.26 ^t | | | 1.60 | 1.55 | 0.63 ⁺ | |
| 14. Silicon..... | 1.17 | | | 1.43 | 1.39 | 0.50 ⁺ | |
| 15. Phosphorus..... | 1.10 | 1.07 | 1.00 | | | 0.41 ⁺ | 2.71 ⁺ |
| 16. Sulfur..... | 1.04 | 1.00 | 0.93 | | | 0.34 ⁺ | 2.12 ⁺ |
| 17. Chlorine..... | 0.99 | 0.95 | 0.88 | | | 0.29 ⁺ | 1.84 ⁺ |
| 18. Argon..... | | 0.90 | | | | 0.26 ⁺ | 1.81 ⁺ |
| 19. Potassium..... | | | | | | | |
| 20. Calcium..... | | | | 2.38 | 2.31 | 1.83 ⁺ | |
| 21. Scandium..... | | | | 1.97 | 1.91 | 0.99 ⁺ | |
| 22. Titanium..... | 1.36 ^o | | | 1.66 | 1.60 | 0.81 ⁺ | |
| 23. Vanadium..... | | | | 1.47 | 1.42 | 0.68 ⁺ | 0.69 ⁺ |
| 24. Chromium..... | | | | 1.36 | 1.31 | 0.59 ⁺ | 0.66 ⁺ |
| 25. Manganese..... | | | | 1.30 | 1.26 | 0.52 ⁺ | 0.64 ⁺ |
| 26. Iron..... | | | | 1.27 | 1.24 | 0.46 ⁺ | 0.80 ⁺ |
| 27. Cobalt..... | 1.56 (MnS ₂) | 1.20 ^{IV} | | 1.26 | 1.23 | 0.75 ⁺ | 0.62 ⁺ |
| 28. Nickel..... | 1.23 ^{oII} | 1.32 ^{II} | | 1.25 | 1.22 | 0.72 ⁺ | |
| 29. Copper..... | 1.22 ^{oIII} | 1.30 ^{III} | 1.39 ^{III} | 1.25 | 1.22 | 0.70 ⁺ | |
| 30. Zinc..... | 1.21 ^{oIV} | | | 1.28 | 1.24 | 0.96 ⁺ | |
| 31. Gallium..... | 1.35 ^t | | | 1.37 | 1.32 | 0.74 ⁺ | |
| 32. Germanium..... | 1.31 ^t | | | 1.53 | 1.48 | 0.62 ⁺ | |
| 33. Arsenic..... | 1.26 ^t | | | | | 0.53 ⁺ | 2.72 ⁺ |
| 34. Selenium..... | 1.22 | 1.12 | 1.18 | | | 0.47 ⁺ | 2.22 ⁺ |
| | 1.21 | 1.11 | 1.14 ^t | | | 0.42 ⁺ | 1.98 ⁺ |
| | 1.17 | 1.08 | 1.40 ^o | | | | |
| | | 1.05 | 1.11 ^t | | | 0.39 ⁺ | 1.95 ⁺ |
| 35. Bromine..... | 1.14 | | 1.52 ^o | | | | 2.00 |

| | | | | | |
|-------------------------|-------|-------|-------|-------|-------------------|
| 36. Krypton..... | | | 2.53 | 2.43 | 1.48 ⁺ |
| 37. Rubidium..... | | | 2.15 | 2.07 | 1.13 ⁺ |
| 38. Strontium..... | | | 1.82 | 1.76 | 0.93 ⁺ |
| 39. Yttrium..... | | | 1.60 | 1.54 | 0.80 ⁺ |
| 40. Zirconium..... | | | 1.47 | 1.43 | 0.70 ⁺ |
| 41. Columbium..... | | | 1.39 | 1.36 | 0.62 ⁺ |
| 42. Molybdenum..... | | | 1.35 | 1.32 | |
| 43. Mesurium..... | | | 1.34 | 1.31 | |
| 44. Ruthenium..... | | | 1.34 | 1.31 | |
| 45. Rhodium..... | | | 1.37 | 1.34 | |
| 46. Palladium..... | | | 1.44 | 1.40 | |
| 47. Silver..... | | | 1.54 | 1.49 | 1.26 ⁺ |
| 48. Cadmium..... | | | 1.67 | 1.62 | 0.97 ⁺ |
| 49. Indium..... | | | | | 0.81 ⁺ |
| 50. Tin..... | | | | | 0.71 ⁺ |
| 51. Antimony..... | 1.30 | 1.45° | | | 2.94 ⁺ |
| 52. Tellurium..... | 1.31 | 1.36° | | | 0.62 ⁺ |
| 53. Iodine..... | 1.37 | 1.32° | | | 2.45 ⁺ |
| 54. Xenon..... | 1.24 | 1.28° | | | 0.56 ⁺ |
| 55. Cesium..... | | | | | 2.21 ⁺ |
| 56. Barium..... | | | 2.72 | 2.62 | 0.50 ⁺ |
| 57. Lanthanum..... | | | 2.24 | 2.17 | 2.16 ⁺ |
| 58. Cerium..... | | | 1.86 | 1.80 | |
| 59-71. Rare earths..... | | | 1.86 | 1.80 | |
| 72. Hafnium..... | | | 1.62 | 1.57 | |
| 73. Tantalum..... | | | 1.49 | 1.44 | |
| 74. Tungsten..... | | | 1.41 | 1.37 | |
| 75. Rhenium..... | | | 1.37 | 1.33 | |
| 76. Osmium..... | | | 1.35 | 1.31 | |
| 77. Iridium..... | | | 1.36 | 1.32 | |
| 78. Platinum..... | | | 1.39 | 1.35 | |
| 79. Gold..... | 1.40° | | 1.46 | 1.42 | |
| 80. Mercury..... | | | 1.57 | 1.52 | 1.37 ⁺ |
| 81. Thallium..... | | | 1.71 | 1.66 | 1.10 ⁺ |
| 82. Lead..... | 1.50° | | | | 0.95 ⁺ |
| 83. Bismuth..... | | | | | 0.84 ⁺ |
| 88. Radium..... | | | | | 0.74 ⁺ |
| 90. Thorium..... | | | 1.79 | | 1.82 ⁺ |
| 92. Uranium..... | | | | 1.48 | 1.02 ⁺ |
| | | | ... | | 0.97 ⁺ |

¹ Numbers followed by superscript symbols refer, not to single, double, or triple bonds, but to octahedral covalent radii, *o*, or tetrahedral covalent radii, *t*, at valence states represented by roman numerals. Radii without superscripts generally represent values for molecules in which atoms form covalent bonds to a number determined by position in periodic table.

2. *Atomic Radii*.—The atomic radii present no particular difficulty in calculation but show the following interesting features:

a. A small and systematic decrease in radius with decreasing coordination as follows:

| C.N. | Radius |
|------|--------|
| 12 | 1.00 |
| 8 | 0.97 |
| 6 | 0.96 |
| 4 | 0.88 |

b. A metal atom very often has a different state of coordination in an alloy from that which it has in the pure element. Thus the radius of germanium with 12-fold coordination may be deduced from the hexagonal close-packed copper-germanium alloy, whereas no such coordination may be found for the element.

c. There is no wide variation in values of radii, since the expected increase in size of the electron shells in heavier atoms is compensated by greater nuclear charge. In each period the alkali metal has by far the largest radius.

d. A noticeable decrease in radius occurs for the elements immediately following lanthanum so that the radii of the elements of the third long period are about the same as those of the second long-period elements. This has been called the *lanthanide contraction* and leads to the close similarity between zirconium and hafnium and between columbium and tantalum.

3. *Ionic Radii*.—Numerous methods have been employed to calculate the radii of ions, but the most widely accepted values today are those of Goldschmidt, empirically determined from crystal-structure data and from Wasastjerna's values (optical) $F^- = 1.33$ and $O^{2-} = 1.32$ A.U.; and of Pauling, calculated from quantum mechanics considerations starting from experimental interionic distances in NaF, KCl, RbBr, CsI, and Li_2O . Zachariasen made calculations similar to those of Goldschmidt but corrected the radii for the effects of coordination. The agreement in values is remarkably good. The Pauling values are listed in the table.

It may be seen at once that the positive ion of an element is always smaller and the negative ion always larger than the neutral atom of the same element and that the size of the positive ions in the same periodic group increases with atomic number,

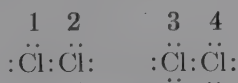
whereas it decreases in the same periodic series with increasing charge which tends to tighten the structure. In negative ions the increased size due to repulsion of the extra electrons is balanced by the greater electric field, so that doubly charged negative ions are no larger, and are sometimes smaller, than singly charged ions. The tightening effect of increased charges is shown by comparing K^+Cl^- and $Ca^{2+}S^{2-}$; although all four ions have 18 electrons, the interatomic spacing for KCl is 3.14 A.U. and for CaS 2.84 A.U. In general, the factors that affect the size of an atom or ion are: (1) type of bond; (2) coordination number; (3) valence of coordinated ions; (4) radius ratio of central ion and coordinated ions. The influence of coordination on distance in ionic crystals is illustrated in the following table:

| Transition in lattice type | Change in C.N. | Decrease in distance, per cent |
|---|-------------------------|--------------------------------|
| CsCl \rightarrow NaCl..... | 8 \rightarrow 6 | 3 |
| NaCl \rightarrow ZnS..... | 6 \rightarrow 4 | 5.8 |
| CaF ₂ \rightarrow TiO ₂ (rutile)..... | 8, 4 \rightarrow 6, 3 | 3 |
| Metal \rightarrow metal..... | 12 \rightarrow 8 | 3 |

Thus, the fewer the neighbors around an ion the shorter the interionic distance. Similarly the radius of a cation is larger when its neighbors are univalent than when they are divalent.

Correction tables for these effects have been published by Zachariasen and Pauling.¹

4. *Van der Waals Radii*.—The van der Waals, or nonbonded, radius is illustrated by the distance 2-3 between adjacent chlorine molecules in the crystal



This radius should be larger than the covalent bond between atoms 1 and 2 because there are two electron pairs between atoms instead of one; it should be about the same as ionic chlorine since the bonded atom presents the same outer appearance away from the bond as the ion. The two values are,

¹ ZACHARIASEN, Z. *Krist*, **80**, 137 (1931); PAULING, *J. Am. Chem. Soc.*, **50**, 1036 (1928).

respectively, 1.80 and 1.81 A.U. In general, the van der Waals radius may be calculated by adding 0.80 A.U. to the corresponding covalent radius.

Isomorphism, Morphotropism, Polymorphism.—Goldschmidt's great contributions have been the result of his experimental method of substituting one ion for another in compounds and observing what change in structure occurred. It is clear that comparability in size of ions of analogous formulas and polarizabilities is the most important attribute contributing to isomorphism. This accounts for unsuspected cases of isomorphism such as lead and strontium, and magnesium and cobalt or nickel, and salts of NaNO_3 and CaCO_3 , and for lack of isomorphism among salts far more nearly related chemically, such as salts of magnesium and calcium and even of sodium and potassium. In general, one atom or ion may be replaced by another or solid solution may occur without destroying the crystalline arrangement when the ionic distances do not differ by more than 10 per cent.¹ This is also the degree of disarrangement thermally possible before a crystalline arrangement of planes is destroyed by melting; thus the isomorphic and thermal tolerances are the same. When by chemical substitution the limit of homogeneous deformation is surpassed, a new atomic arrangement in space takes place; such a process Goldschmidt calls morphotropism. This occurs in the series of dioxides when the ratio R_A/R_X reaches 0.7 and in numerous other series of compounds in which stepwise substitutions are made to points where sudden changes in properties occur. Polymorphism, the phenomenon in which the same substance under different thermodynamic conditions may have different crystal structures, is simply a case of morphotropism brought about not by substitution but by thermodynamic alteration (temperature, pressure, directed force, etc.) so that the substance is no longer isomorphous with itself. These are but a few simple examples of the rational explanations of crystal chemistry based on x-ray crystal-structure data.

Goldschmidt has gone even further and used a model principally employing substitution of ions of the same size and shown that TiO_2 is like MgF_2 , ThO_2 like CaF_2 , SrTiO_3 like KMgF_3 ,

¹ However, ability to form solid solutions or mixed crystals is not always a safe criterion of isomorphism; AgBr (NaCl structure) and AgI (ZnS structure) form mixed crystals, as do CaF_2 and YF_3 .

BaSO_4 like RbBF_4 , Zn_2SiO_4 like Li_2BaF_4 . Thus the properties of a very difficultly prepared salt may be anticipated by the study of a substituted model more easily available.

Mixed Oxides (Multiple Isodesmotic Structures).—Growing importance is being attached to the structures of ionic compounds in which a single anion is combined with two or more cations, or *vice versa*. By far the most important are the compounds $\text{A}_m\text{B}_n\text{O}_x$, in which oxygen ions are coordinated with two cations, particularly in perovskite, ABO_3 , and spinel, AB_2O_4 . Figure 177 shows the unit perovskite cell in which the larger A cations are at the corners, coordinated with 12 oxygen ions, and a B ion is at the center coordinated with 6 oxygen ions. Thus each oxygen ion is linked to four A and two B cations. The following compounds have this structure: NaCbo_3 , KCbo_3 , KIO_3 , RbIO_3 , CaTiO_3 (perovskite), SrTiO_3 , CaZrO_3 , CuSnO_3 , YAlO_3 , LaAlO_3 , LaGaO_3 , $(\text{KMgF}_3, \text{KZnF}_3)$. It is evident that the

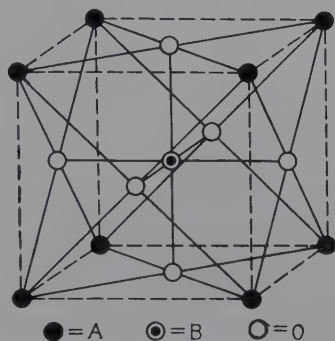


FIG. 177.—The structure of perovskite, ABO_3 .

valences of the cations A and B are of no significance, so long as they have a combined valence of +6 to impart electrical neutrality; so there are combinations above of $1 + 5$, $2 + 4$, and $3 + 3$ in the oxides. It is especially significant that in KIO_3 and RbIO_3 , the iodate ion with I^{5+} does not exist as an entity as is true in chlorates. Sodium bronze, NaWO_3 , also has the perovskite structure, which it retains even though the composition varies to a deficiency in sodium atoms. In this case there must be *vacancies* in the lattice, and one W^{5+} must change to a W^{6+} for every missing Na^+ , these being distributed absolutely at random in order to retain the cubic crystal. This is the first example of a fascinating field of lattice defects and disorder in the solid state which will be further considered.

Spinel, AB_2O_4 , show similar interesting phenomena. The unit cell with 8 molecules has 32 oxygen ions, 4 tetrahedrally coordinated with each A and 6 octahedrally with each B. Usually A is divalent (Mn^{2+} , Fe^{2+} , Co^{2+} , Ni^{2+} , Zn^{2+} , Mg^{2+} , etc.) and B trivalent (Al^{3+} , Cr^{3+} , Fe^{3+} , Ga^{3+} , etc.); but all that is

essential is that the valences of $A + 2B$ shall be 8. The following curious facts have been established: (1) Besides the normal type of spinel above described, there is another described as "variate atom equipoint." In $MgGa_2O_4$, half the Ga^{3+} ions occupy the four-fold coordinated positions, and the other half plus the Mg^{2+} ions are distributed at random over the six-fold positions—in other words, $B(AB)O_4$. (2) In $ZnAl_2O_4$, etc. the smaller ion (Al^{3+}) has the higher coordination. (3) $LiAl_5O_8$ has a spinel structure, derived from $Mg_2Al_2O_8$ by replacing $2Mg^{2+}$ with $(Li^+ + Al^{3+})$. (4) S_4 , F_4 , and $(CN)_4$ may replace O_4 in several compounds; the valence sums of $A + B$ are 4 instead of 8 for the F^- and CN^- [$BeLi_2F_4$, $ZnK_2(CN)_4$]. (5) Fe_2O_3 and Al_2O_3 form unlimited solid solutions with spinels for the reason that their structures are closely compatible—32 oxygen atoms and $21\frac{1}{3}$ cations distributed over 24 positions, leaving $2\frac{2}{3}$ cation positions vacant per unit cell.

Disorder in the Solid State; Defect Structures.—The observations on perovskite and spinel structure types have introduced a revolutionary and fascinating new concept in the chemistry of the solid state—that of disorder or defect in solid crystalline structures, first proposed by Strock in 1936. The following types are possible:

1. Complete lattice. Two or more chemically different atoms occupy crystallographically equivalent sites. Called by Hassel "internal mixed crystal." Examples: variate equipoint spinel; intermetallic systems (see Chap. XVIII); $(NH_4)_3MoO_3F_3$ (Pauling), in which O^{2-} and F^- occupy one set of equivalent positions; $Li_2Fe_2O_4$ and Li_2TiO_3 , in which Li and Fe or Ti are just as randomly distributed as Cl^- and Br^- in a solid solution of $KCl + KBr$ and form solid solutions with each other and with MgO because of the close similarity of radii of Li^+ , Mg^{2+} , Fe^{3+} , Ti^{4+} ; $CdBr_2$, which is partly $CdCl_2$ and partly CdI_2 layer-lattice structure.

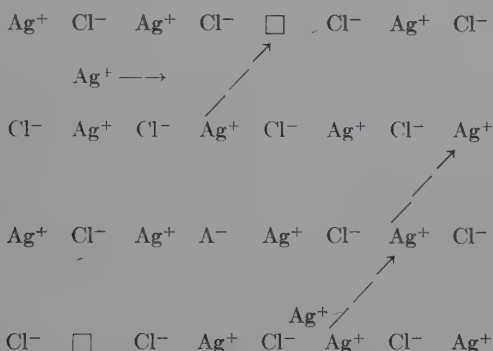
2. Incomplete lattice. One or more sets of crystallographically equivalent positions only partially occupied, leaving vacant spaces in the lattice. Examples: sodium bronze, $NaWO_3$ (missing Na^+); $\gamma-Al_2O_3$ ($2\frac{2}{3}$ missing Al^{3+}); pyrrhotite, FeS_{1+} (missing Fe^{2+}); $\alpha-AgI$ stable above 146° , body-centered cubic iodine lattice stable up to 555° , with silver atoms *at random* wandering as fluid through structure, whereas in β - and $\gamma-AgI$ silver atoms

are fixed. Lead peroxide in the positive plate of the storage battery always has a deficiency in oxygen, but retains its structure down to $\text{PbO}_{1.66}$.

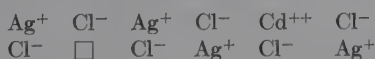
3. Combination of (1) and (2). Solid solution of $\gamma\text{-Al}_2\text{O}_3$ in spinel; Ag_2HgI_4 (Ketelaar) with ZnS structure, in which 2Ag^+ and Hg^{2+} ions are distributed at random over four positions.

Electrical Conductivity of Solids and Defect Structure.¹—

In many solid ionic compounds electrical conductivity is caused by the movement of ions. Disorder in AgCl is represented by Frenkel as follows:



In such a case only the cations are in disorder; some Ag^+ ions are at interstitial positions, having left their original places in the lattice, and conductivity is the result of movement of the cations. This has been confirmed by Wagner (Darmstadt) who showed that CdCl_2 will go into solid solution in AgCl up to 10 per cent, greatly increasing the electrical conductivity. For in CdCl_2 the ratio of cations to anions is 1:2 instead of 2:2 for AgCl, so that there is one cation too few for every Cd^{2+} ion and a vacant position when CdCl_2 substitutes for AgCl:



Koch and Wagner have determined for AgCl at 350° the following values: an electrical conductivity of $7.57 \times 10^{-3} \text{ ohm}^{-1} \text{ cm}^{-1}$, a mobility of the vacant positions in the Ag^+ lattice having a velocity (in centimeters per second) for 1 volt per centimeter of 6.6×10^{-4} ; and the fraction of Ag^+ ions in interstitial positions equal to the vacant positions in the Ag^+ lattice 1.5×10^{-3} .

¹ See C. WAGNER, "Chemical Reactions Involving Solids," Faraday Society discussion, April, 1938.

α -AgI represents extreme disorder of Ag^+ ions in an iodine lattice so that the ionic conductivity of solid and molten AgI are nearly the same ($1 \text{ ohm}^{-1} \text{ cm.}^{-1}$). Schottky disorder is exemplified by KCl in which both anions and cations contribute to electrical conductivity. In NaCl there are perhaps 10^{14} vacant lattice points of either sign per cubic centimeter.

In most oxides and sulfides electrical conductivity is caused by deviations from strict stoichiometric composition. ZnO conducts at 600° because oxygen has been lost, an excess of metal

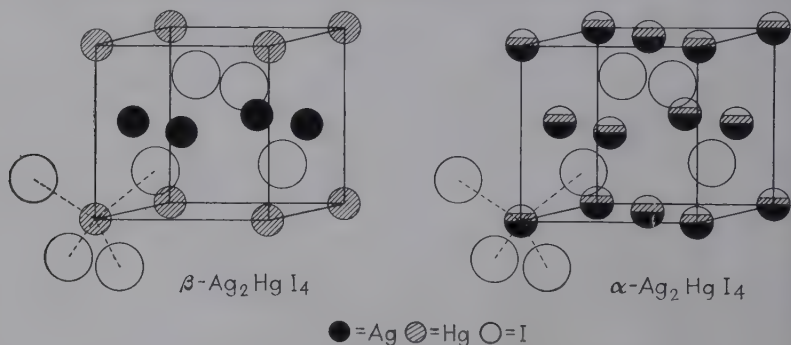
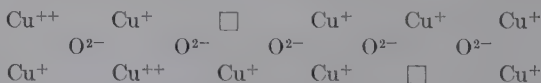


FIG. 178.—Crystal structure of β - and α - Ag_2HgI_4 .

atoms being left as cations and free electrons. Conductivity at this temperature decreases with increasing oxygen pressure because the excess of zinc ions and electrons is reduced. Exactly the opposite is true of Cu_2O , for excess oxygen tends to remove electrons from Cu^+ to form Cu^{2+} , with increase in conductivity by electron exchange between Cu^+ and Cu^{2+} .



Empty cation spaces in FeO, FeS, and FeSe have been proved by x-ray analysis (Jette and Foote, Hägg).

The remarkable case of α - Ag_2HgI_4 is considered above. Figure 178 shows the unit cells of the β form, in which silver and mercury atoms are in fixed positions, and the α form, where silver and mercury ions statistically fill three out of four equivalent positions. Between 40 and 50° a transformation (β to α) sets in with relatively enormous increase in conductivity as a result of disorder in which Hg^{2+} ions transfer 6 per cent and Ag^+ ions 94 per cent of the current.

A solid theoretical background from wave mechanics for conductivity and energy levels in real and ideal crystals has been provided by Mott, Slater, Pohl, De Boer, and others.

These disorder phenomena are extended to the explanation of chemical reactions of solids.

Wagner and associates have shown that oxidation or rusting of metal surfaces proceeds as a result of varying ratio of metal to oxygen, and by actual diffusion of cations and electrons from the *metallic phase toward the oxygen phase*. At an iron surface the ratio of Fe:O = 1:1, whereas at the oxide-gas boundary there may be as high as a 10 per cent deficit of iron, with the result that iron tarnishes more rapidly than other metals.

Anion Radicals in Solids; Anisodesmic Structures.—Whenever a cation B usually of relatively high charge and small size is coordinated with ions with bond strength $z/n > \frac{1}{2}$, a discrete complex group or radical exists in the crystal which is bound together by forces so much stronger than those binding it to the rest of the structure that it may persist even in solution. The shape and size of this radical are the determining factors, though details of structures may vary depending on the relative dispositions of the cations A.

The structures of some of the common complex anions are classified in Table XLII.

TABLE XLII.—ANION SHAPES

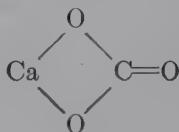
| Type | Arrangement | Examples |
|-----------------|------------------------------|---|
| XY | Linear | CN ⁻ , O ₂ ⁻ , O ₂ ²⁻ , N ₂ ⁻ |
| XYZ | Linear | N ₃ ⁻ , CNO ⁻ , CNS ⁻ , Cl ₃ ⁻ , ClCl ⁻ |
| | Bent | ClO ₂ ⁻ , NO ₂ ⁻ (132°) |
| BX ₃ | { Plane equilateral triangle | CO ₃ ²⁻ , NO ₃ ⁻ |
| | { Regular trigonal pyramid | PO ₃ ³⁻ , SO ₃ ²⁻ , ClO ₃ ⁻ |
| | { Regular tetrahedron | PO ₄ ³⁻ , SO ₄ ²⁻ , ClO ₄ ⁻ , CrO ₄ ²⁻ , MnO ₄ ⁻ , SeO ₄ ²⁻ , BF ₄ ²⁻ |
| BX ₄ | { Distorted tetrahedron | MoO ₄ ²⁻ , WO ₄ ²⁻ , ReO ₄ ²⁻ , IO ₄ ⁻ |
| | { Plane square | Ni(CN) ₄ ²⁻ , PdCl ₄ ²⁻ , PtCl ₄ ²⁻ |
| BX ₆ | Regular octahedron | SiF ₆ ²⁻ , TiCl ₆ ²⁻ , SiCl ₆ ²⁻ , ZrCl ₆ ²⁻ , SnCl ₆ ²⁻ , PtCl ₆ ²⁻ , PbCl ₆ ²⁻ |

Special Notes on Structures.—1. Peroxides and dioxides. BaO₂ and SrO₂ are easily distinguished from MnO₂, PbO₂, etc., with two separate O²⁻ ions, by the existence of the O₂²⁻ ion,

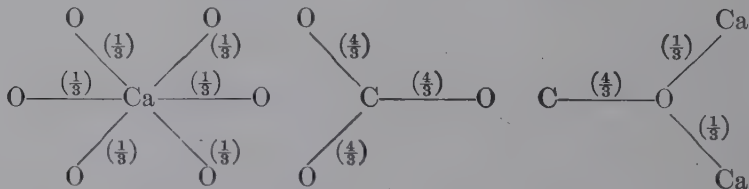
consisting of 2 O atoms strongly bound by a single homopolar bond $(\text{O}—\text{O})^{2-}$. The normal valence of Ba^{2+} and Sr^{2+} is maintained. In KO_2 the ion O_2^- represents resonance between the neutral oxygen molecule $(\text{O}=\text{O})^0$ and the ion $(\text{O}—\text{O})^{2-}$.

2. Calcite and aragonite. Rhombohedral calcite is derived from a cubic NaCl structure, Ca^{2+} for Na^+ and CO_3^{2-} for Cl^- , by compression along a triad axis. The CO_3^{2-} groups are planes parallel to each other and normal to the triad axis. Coordination: each Ca^{2+} by irregular octahedron of 6 O^{2-} , each O^{2-} by 2 Ca^{2+} and C^{4+} . Structure for carbonates and nitrates with radius of A less than 1.1. CaCO_3 dimorphous because Ca^{2+} radius at critical value. Aragonite derived from NiAs structure, with CO_3 groups still planar and parallel. Coordination: each Ca^{2+} by 9 O^{2-} , each O^{2-} by 3 Ca^{2+} and C^{4+} . For radius above 1.45 A.U. structure changes to RbNO_3 .

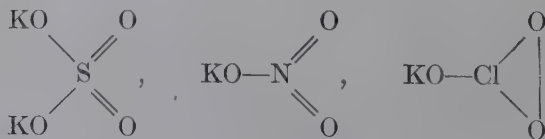
Here again the chemical molecule is completely lost. A structural formula for CaCO_3 such as



has no meaning and furthermore is erroneous since it distinguishes one oxygen atom from the other, whereas all three are structurally equivalent and linked both to calcium and carbon ions. The following formula alone is possible, though it fails to represent correct geometrical disposition of the bonds:



Similarly



bear no relation whatever to the crystal structures of potassium sulfate, nitrate, and chlorate.

3. Polynuclear anions—the sulfur acids. Zachariasen has shown some remarkable relationships in the series of $S_mO_n^{2-}$ groups that explain chemical behavior: SO_4^{2-} is tetrahedral; $S_2O_6^{2-}$, dithionate, is formed by removing one oxygen atom from each of two sulfate tetrahedra and joining the two sulfurs

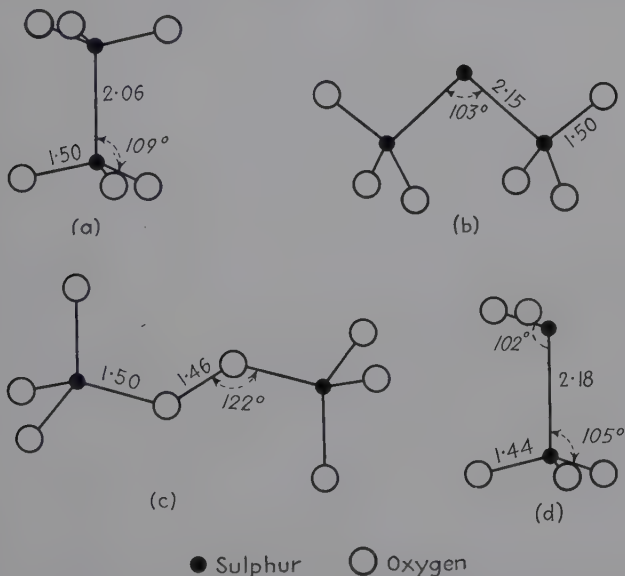
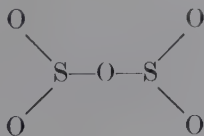


FIG. 179.—Structures of polynuclear complex sulfur acid ions. (a) Dithionate ion, $S_2O_6^{2-}$; (b) trithionate ion, $S_3O_6^{2-}$; (c) persulfate ion, $S_2O_8^{2-}$; (d) pyrosulfate ion, $S_2O_5^{2-}$.

as in Fig. 179; $S_2O_5^{2-}$, pyrosulfate, is formed by removing one oxygen from $S_2O_6^{2-}$, the structure

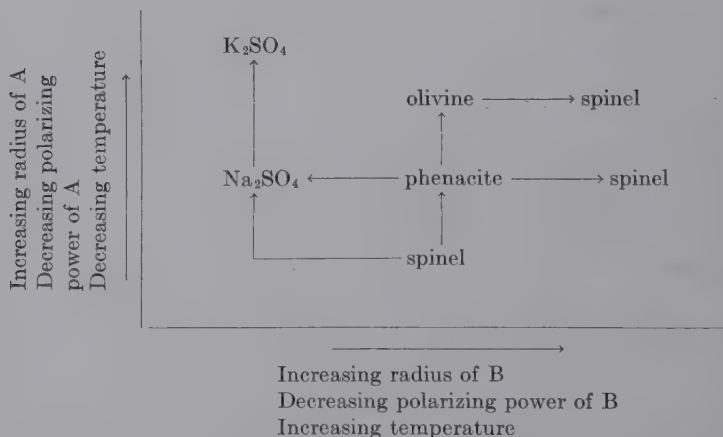


usually accepted being thus eliminated. $S_2O_2^{2-}$, $S_2O_3^{2-}$, and $S_2O_4^{2-}$ are formed from the same basic structure; SO_3^{2-} is represented by one of the single pyramids in Fig. 179a; SO_2^{2-} by the top of Fig. 179d; and S_2 of pyrites by stripping the dithionate

ion (Fig. 179a) of all oxygen atoms, $S_2O_8^{2-}$; persulfate, shown in Fig. 179 is made from 2 SO_4 tetrahedra joined by an O—O bond; and $S_3O_6^{2-}$, trithionate, consists of two tetrahedra sharing a common third sulfur atom, which has replaced a shared oxygen in a hypothetical S_2O_7 group.

4. Morphotropy of A_2BX_4 . These compounds show a remarkable range from anisodesmic structures retaining the BX_4 radical, through mesodesmic olivine and phenacite (silicate) types (see next chapter), to the isodesmic spinels. The determining factors are the sizes and polarizing powers of the cations A and B as shown in Table XLIII.

TABLE XLIII



5. Rotation in the solid state. It would be expected that highly symmetrical groups such as tetrahedral BX_4 and octahedral BX_6 should act like spheres and result in comparatively simple structures. Such is indeed the case. It is very difficult to account for the simplicity of some structures with non-symmetrical anions such as CN^- ($NaCN$ is like $NaCl$), C_2^{2-} , O_2^{2-} , CO_3^{2-} , NO_3^- , ClO_3^- , and ClO_4^- . In 1930 Pauling proposed the concept of free rotation in the solid state to account for anomalous entropy of solid hydrogen, and this has now been widely applied to many other cases of apparently inconsistent crystal structures. Free rotation is most common with symmetrically shaped molecules of small moment of inertia, in loosely bound structures, at high temperatures. The transition

to the state of free rotation extends over a finite temperature range. Unsymmetrical molecules may have rotations around different axes excited successively at different temperatures, accompanied by structural change and anomalies in physical properties. Alkyl ammonium halides, at first thought to have linear carbon chains with C—C spacing of 1.25 A.U., entirely contrary to the usual tetrahedral zigzag chain with C—C spacings 1.54, now are believed to have the carbon chains rotating around their lengths so that the 1.25 spacing is simply the projec-

TABLE XLIV

| Shape and arrangement of groups | Optical properties | Conclusion | Examples |
|---|-----------------------|--|--|
| 1. Roughly spherical | Isotropic | | Quartz Felspars Sulfates |
| 2. Rod-shaped: | | | |
| <i>a.</i> All parallel to 1 direction | Large + birefringence | Molecules parallel to direction of greatest refractive index | Selenium Paraffins |
| <i>b.</i> All parallel to plane but not to each other | Large - birefringence | Plane of molecules parallel to direction of least refractive index | $C_{18}H_{37}NH_3Cl$ |
| <i>c.</i> Inclined in all directions | Isotropic | Not 2 <i>a</i> or 2 <i>b</i> | CO_2 |
| 3. Flat: | | | |
| <i>a.</i> Planes parallel | Large - birefringence | Planes of molecules normal to direction of least refractive index | Layer micas, calcite, 1-,3-,5-tri-phenyl benzene |
| <i>b.</i> Planes parallel to line but not to each other | Large + birefringence | Normal to direction of greatest refractive index | Urea Benzene |
| <i>c.</i> Planes inclined in all directions | Isotropic | Not 3 <i>a</i> or 3 <i>b</i> | Resorcinol |

tion on the axis of the chain of the inclined 1.54 A.U. bonds. The NH_4^+ ion rotates in its cubic halides but not in NH_4F (wurtzite structure). The most remarkable case is NH_4NO_3 in which both ions may or may not rotate, six modifications being

the result. In the cubic form only, stable above 125° (Hendricks, Posnjak, and Kracek), both ions are rotating and behave as spheres (NH_4^+ , 1.46 A.U., and NO_3^- , 2.35 A.U.). In the other forms with more complex crystal structures, some or all of the rotational degrees of freedom of one or both ions are inhibited.

6. Optical properties. From consideration of polarized-light vectors and ion dipoles it is not difficult to see that the optical properties of crystals should reflect the form and arrangement of complex anion groups. Table XLIV from Wooster's "Crystal Physics" summarizes these interesting and important data, first proposed for calcite by W. L. Bragg.

7. Hydrate and ammine structures. Neutral molecules of H_2O and NH_3 may be bound in ionic structures, quite contrary to usual rules, because of their small size and electric polarity.

The large dipole moment of water is due to a tetrahedral distribution of charge over the surface of the spherical molecule (Bernal, Fowler), with two corners positive and two corners negative regions. Thus water must be packed into crystals so that the charged areas are directed toward ions of opposite sign, or two molecules of water are linked to each other by having opposite charges turned together. This requirement limits and complicates hydration of solid salts, as well as the structure of ice. This has the same structure as the silicon ions in β -tridymite, SiO_2 , with each molecule coordinated by four neighbors at the corners of a tetrahedron, so disposed that regions of opposite charge are adjacent.

Types of Hydrate.—1. Coordinated water. Functions to surround cations with neutral shell, increase radius, and thus coordinate larger number of anions [Al^{3+} , 0.57; $\text{Al}(\text{H}_2\text{O})_6^{3+}$, 3.3 A.U.]; x-ray patterns entirely different from that of anhydrous salt, for water molecules play an essential part in determining stability of lattice as a whole and cannot be removed without complete breakdown of structure.

The complete structure analyses of hydrates such as $\text{NiSO}_4 \cdot 7\text{H}_2\text{O}$, $\text{CuSO}_4 \cdot 5\text{H}_2\text{O}$, etc. (Beevers and associates), represent an outstanding achievement, since they involve the correct bonding of H_2O molecules with their tetrahedral disposition of charges. The bond structure of the familiar blue vitriol, $\text{CuSO}_4 \cdot 5\text{H}_2\text{O}$, is shown in Fig. 180. Each Cu^{2+} ion is coordinated with four H_2O molecules and two O^{2-} ions from the SO_4 groups.

The fifth H₂O molecule, long known on chemical grounds to be different from the other four, is coordinated only by other H₂O molecules and O²⁻ ions.

Many compounds $A^{2+}B^{4+}X_6^{-}$ (such as $NiSnCl_6 \cdot 6H_2O$) are isomorphous and have comparatively simple structures of octahedra of $A(H_2O)_6^{2+}$ and BX_6^{2-} .

2. Hydrates of mixed type. In alums $A^+B^{3+}(SO_4)_2 \cdot 12H_2O$, Lipson and Beevers showed that each cation is surrounded by six H_2O but quite differently in detail. In $KAl(SO_4)_2 \cdot 12H_2O$,

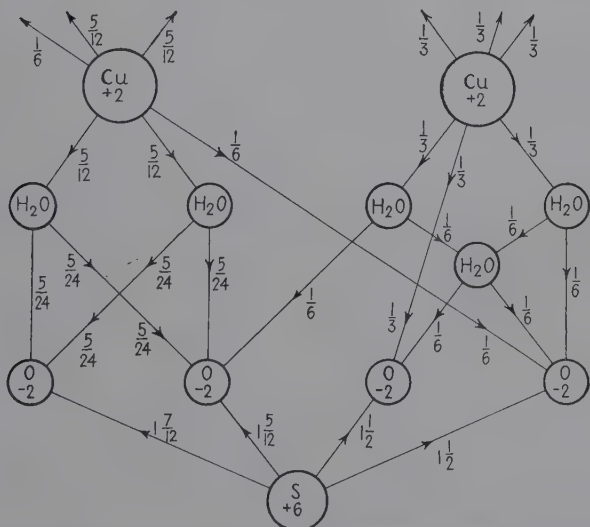


FIG. 180.—The electrostatic valence bond structure of copper sulphate pentahydrate, $\text{CuSO}_4 \cdot 5\text{H}_2\text{O}$.

each of the six H_2O around Al^{3+} is closely bound to Al^{3+} and has two external contacts. Each of the six around K^+ contacts two O^{2-} ions of SO_4 groups and one H_2O of the $\text{Al}(\text{H}_2\text{O})_6$ group, this outer contact being more important than the high coordination expected for K^+ . X-ray analysis alone has revealed that there are three different cubic structures among alums, depending on the arrangement of the groups: $\text{A}(\text{H}_2\text{O})_6^+$, $\text{B}(\text{H}_2\text{O})_6^{3+}$, and SO_4^{2-} .

3. Structural water. H_2O molecules occupy interstices in lattice; in many cases they may be expelled from lattice without breakdown of structure; x-ray pattern same or very similar to that of anhydrous salt.

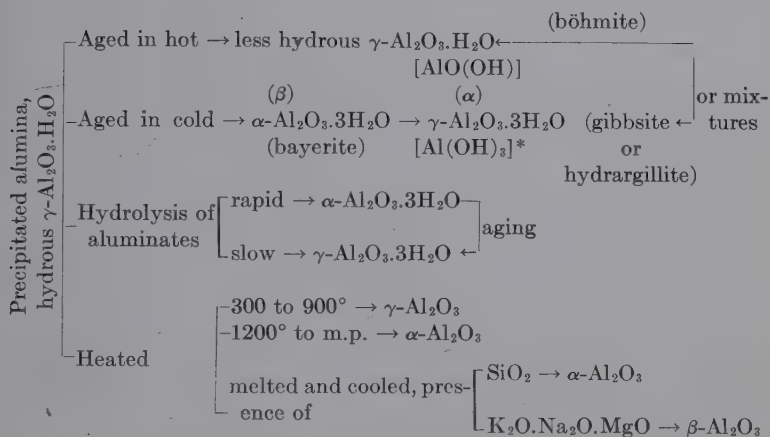
The role of water in zeolites (water softeners) and various silicate minerals will be noted in the next chapter. In some of these, the three-dimensional crystal framework of SiO_4 is so rigid that water may be bound or expelled, all in accordance with the dipole properties without affecting the crystal structure. In other minerals the H_2O plays a more important role in holding layers together. A similar case is found in gypsum, $\text{CaSO}_4 \cdot 2\text{H}_2\text{O}$, analyzed by Wooster. This is a layer lattice in which sheets of Ca^{2+} and SO_4^{2-} ions are arranged so that each cation is surrounded by six O^{2-} ions and two H_2O molecules. Each H_2O molecule is linked to one Ca^{2+} ion, to one O^{2-} ion in its own sheet, and to one O^{2-} ion in a neighboring sheet, this last bond holding the sheets together and yet accounting for the perfect cleavage and high thermal expansion across this weak bond.

4. Colloidal hydrous oxides, oxide hydrates, and hydroxides. A subject of considerable difficulty, which has commanded attention for more than a century in analytical chemistry and in industry such as the manufacture of paint pigments, is the composition and structure of the gelatinous precipitates, thrown down from salt solutions above some critical pH value and generally termed "hydrous oxides" and exemplified by gels of ferric, aluminum, chromic, titanium, zirconium, and silicon oxides. The implication of the term is that gel water is held by the oxide by means of adsorption and capillary forces. Sometimes water is chemically bound in stoichiometric ratio, and the result is a hydrous hydrate or hydroxide. The latter indicates indubitable evidence of the presence of OH^- ions, but the two terms are used interchangeably.

In years past very complex polymerized structures have been postulated for these hydrous systems. But careful phase rule structures, and especially the method of x-ray diffraction analysis, have greatly clarified the whole field and revealed comparative simplicity of constitution.¹ Typical x-ray results are illustrated by the following diagram for hydrous alumina² from the work of Weiser and Milligan:

¹ For an excellent review by leading authorities, see Weiser and Milligan, *Chem. Rev.*, **25**, 1 (1939).

² There is a great confusion in the literature in nomenclature; for example, böhmite is referred to as $\gamma\text{-Al}_2\text{O}_3 \cdot \text{H}_2\text{O}$, $\alpha\text{-Al}_2\text{O}_3 \cdot \text{H}_2\text{O}$, and $\text{AlO}(\text{OH})$; gibbsite as hydrargillite, $\gamma\text{-Al}_2\text{O}_3 \cdot 3\text{H}_2\text{O}$, $\alpha\text{-Al}_2\text{O}_3 \cdot 3\text{H}_2\text{O}$, and $\text{Al}(\text{OH})_3$, etc.



Thus the whole hydrous alumina system shows the existence *only* of $\gamma\text{-Al}_2\text{O}_3\cdot 3\text{H}_2\text{O}$, $\alpha\text{-Al}_2\text{O}_3\cdot 3\text{H}_2\text{O}$, and $\gamma\text{-Al}_2\text{O}_3\cdot\text{H}_2\text{O}$ instead of series of very complex compounds. Diaspore, $\alpha\text{-Al}_2\text{O}_3\cdot\text{H}_2\text{O}$ or HAlO_2 (hydrogen-bonded), does not appear in this artificial system. It dehydrates to corundum, $\alpha\text{-Al}_2\text{O}_3$; gibbsite, $\text{Al}(\text{OH})_3$, dehydrates to böhmite, and this in turn to $\gamma\text{-Al}_2\text{O}_3$, spinel-like in structure.

The gel of gallia is hydrous Ga_2O_3 which goes over into hydrous $\text{Ga}_2\text{O}_3\cdot\text{H}_2\text{O}$. The trihydrate is known also.

The gel of scandia is hydrous $\text{Sc}_2\text{O}_3\cdot\text{H}_2\text{O}$, only, disproving many complex formulas in the literature.

All precipitated stannic oxides, including so-called ortho- and metastannic acids give identical patterns among themselves and with anhydrous SnO_2 (allowing, of course, for much broader lines for the colloidal preparations). The gel precipitates from stannous salts as hydrous $\text{SnO}\cdot 0.5\text{H}_2\text{O}$, which dehydrates spontaneously at room temperature to $\alpha\text{-SnO}$.

There is a single hydrous oxide of TiO_2 , ZrO_2 , and ThO_2 , and α and β modifications do not exist, as in the case of SnO_2 . TiO_2 gels are interesting in that one formed from hydrolysis of titanium chloride or nitrate has the rutile structure, whereas one from the sulfate corresponds to anatase.

* Megaw, *Z. Krist.*, **87**, 185 (1934), shows that in this layer lattice Al^{3+} ions lie between 6OH^- in two-thirds of the possible positions. Hence $\text{Al}(\text{OH})_3$ may be the preferable formula.

The brown gel precipitated at room temperatures from ferric salt solutions is hydrous $\alpha\text{-Fe}_2\text{O}_3$, instead of the usually designated $\text{Fe}(\text{OH})_3$. Aging serves merely to improve the crystalline character of the precipitate, which at first appears to be amorphous. There is no evidence from x-ray analysis of at least 10 different hydrates that have been reported. The compound $\alpha\text{-Fe}_2\text{O}_3 \cdot \text{H}_2\text{O}$, or HFeO_2 , analogous to diaspore, HAlO_2 , with oxygens structurally equivalent, found in nature as göthite, is produced by slow hydrolysis of most ferric salts and goes over into $\alpha\text{-Fe}_2\text{O}_3$; $\beta\text{-Fe}_2\text{O}_3 \cdot \text{H}_2\text{O}$ discovered by Weiser and Milligan is formed from ferric chloride; $\gamma\text{-Fe}_2\text{O}_3 \cdot \text{H}_2\text{O}$, or $\text{FeO}(\text{OH})$, analogous to böhmite, with two types of oxygen, is found in nature as lepidocrocite (hydrogen-bond structure). Göthite dehydrates to hematite, $\alpha\text{-Fe}_2\text{O}_3$, and lepidocrocite to $\gamma\text{-Fe}_2\text{O}_3$, spinel-like and strongly magnetic.

Finally the hydrous oxide sols produce x-ray patterns of water and simple oxide or oxide hydrate as above noted for the gels. Basic salts containing chloride have no real existence, for in these sols the chloride is merely adsorbed in amounts depending on the size and physical character of the primary particles.

Complex Coordination Compounds; the Cobaltamines, Etc.—Coordination of NH_3 molecules around the cation as in $\text{Co}(\text{NH}_3)_6\text{Cl}_3$ is very similar usually to that of H_2O molecules in hydrates, in that the cation is enlarged so that it may coordinate a larger number of anions and produce actually simpler lattice structures than anhydrous compounds. Thus $\text{Co}(\text{NH}_3)_6\text{I}_2$ crystallizes like cubic CaF_2 while CoI_2 has a layer lattice because of the polarizing effect of Co^{2+} ions on I^- . Sometimes H_2O and NH_3 molecules are interchangeable as in isomorphous $\text{Co}(\text{NH}_3)_4(\text{H}_2\text{O})_2\text{Co}(\text{CN})_6$, $\text{Co}(\text{NH}_3)_5(\text{H}_2\text{O})\text{Co}(\text{CN})_6$, and $\text{Co}(\text{NH}_3)_6\text{Co}(\text{CN})_6$; in other cases such as $\text{Al}(\text{H}_2\text{O})_6\text{Cl}_3$ and $\text{Al}(\text{NH}_3)_6\text{Cl}_3$ there is a marked difference in structures.

Finally, the newly determined structure of PCl_5 may be cited as unique evidence of the validity and universality of the concepts of crystal chemistry. In independent and concordant work at Illinois, Oxford, and Cambridge, reported in March, 1940, x-ray data prove that crystalline PCl_5 is built up from $(\text{PCl}_4)^+$ tetrahedra and $(\text{PCl}_6)^-$ octahedra. Thus is answered one of the long-standing questions in chemistry.

CHAPTER XVII

THE SILICATES. MINERALS, SOILS, CERAMICS, CEMENTS

On page 342 of the preceding chapter ionic crystals were classified as isodesmic, anisodesmic, mesodesmic, and hydrogen-bonded. Silicates as a class were designated mesodesmic because $z/n = \frac{4}{4} = 1$ where z is the charge of the cation Si^{4+} and n the number of anions O^{2-} ; thus the bond reaching each oxygen from silicon has exactly the same strength as the sum of all other bonds reaching that oxygen in order to produce electrical neutrality. The silicate structures, therefore, are intermediate between the isodesmic class, in which no discrete units persist in the lattice, and the anisodesmic, in which discrete tightly bound groups of atoms or radicals do exist. It would thus be expected that chains, sheets, and frameworks would be formed as an intermediate state of combination. Such, of course, is the case in silicates.

It is perhaps not surprising that chemistry in the past has avoided, whenever possible, consideration of the natural silicate minerals (as it also tried to overlook most alloys) because of the very complex formulas, apparently often in entire disagreement with the traditional principles of chemical valence and, because of variability of composition, with laws of definite proportion. There were no clarifying principles of classification beyond those of the optical mineralogist; chemical analysis merely confused the issue. It is to the credit of x-ray crystal-structure analysts that they brought their methods to bear upon this chaos fearlessly and without prejudice. It was necessary to drop the traditional principles of chemistry and to violate the rigorous concept of the chemical molecules in the solid state. Out of these efforts to interpret structures came principles so simple and straightforward that the silicates even of the most complex type are now as well known and completely classified as any group of crystals. Nature takes the same simple building blocks and puts them together in a variety of ways, corner to corner, edge to edge, face to face, to form all the silicate minerals. Thus

their chemical formulas, if they mean anything, are the logical consequence of architectural geometry, rather than a violation of laws of chemical valence.

An authoritative work, "The Atomic Structure of Minerals" by W. L. Bragg, has presented recently the classification and detailed structures of minerals including the silicates. Consequently only a few of the important generalizations will be considered here. Prof. Bragg gave the first clue to these complex structures several years ago in the idea of close packing of oxygen ions as the largest units present. Since that time the principles of coordination of anions at the corners of polyhedra around cations, discussed in the preceding chapter, have developed into a comprehensive representation of structures.

The Pauling Rules.—In 1929 Pauling formulated five rules of coordination applicable to all ionic crystal structures but particularly helpful in the interpretation of the complex silicates.

1. A coordinated polyhedron of anions is formed around each cation, the cation-anion distance being determined by the radius sum and the coordination number of the cation by the radius ratio (the first law of crystal chemistry, Goldschmidt, 1926). In silicates the fundamental unit is the tetrahedral arrangement of 4O^{2-} around each Si^{4+} .

2. In a stable coordination structure the total strength of the valence bonds that reach an anion from all the neighboring cations is equal to the charge of the anion (electrostatic valence principle). In perovskite, CaTiO_3 , previously considered, each Ca^{2+} is coordinated by 12 O^{2-} and each Ti^{4+} by 6 O^{2-} , so that the electrostatic valence strengths of $\text{Ca}-\text{O}$ and $\text{Ti}-\text{O}$ are $\frac{2}{12} = \frac{1}{6}$ and $\frac{4}{6} = \frac{2}{3}$; each O^{2-} ion is bound to 4 Ca^{2+} and 2 Ti^{4+} , since $\frac{4}{6} + \frac{4}{3} = 2$ which satisfies the valence of oxygen.

3. The existence of edges, and particularly of faces, common to two anion polyhedra in a coordinated structure decreases its stability; this effect is large for cations with high valence and small coordination number and is especially large when the radius ratio approaches the lower limit of stability of the polyhedron. Thus SiO_4 tetrahedra almost invariably share only corners, TiO_6 octahedra may have common edges, and AlO_6 octahedra common faces.

4. In a crystal containing different cations those of high valence and small coordination number tend not to share polyhedron elements with each other.

5. The number of essentially different kinds of constituent in a crystal tends to be small (principle of parsimony).

Additional Complications in Silicates.—Besides the foregoing rules the following features of silicate structure account for some of the apparent complexities:

1. Isomorphous replacement of cations by others of same charge but similar size, or of several cations by others of different valence but same aggregate charge (already noted for mixed oxides, perovskite, and spinel types, page 361).

2. Isomorphous substitutions of anions O^{2-} , OH^- , F^- , wholly or statistically.

3. Stable mixed structures, with parts of crystal of one type and remainder of another.

4. The peculiar role of Al^{3+} , arising from the fact that the $Al:O$ radius ratio 0.43 is nearly the critical value 0.414 for transition from sixfold to fourfold coordination: thus Al may appear in the same structure in both capacities or, when fourfold coordinated, may substitute for Si^{4+} , necessitating a corresponding substitution of Ca^{2+} for Na^+ , Al^{3+} for Mg^{2+} , Fe^{3+} for Fe^{2+} , etc., to maintain neutrality.

5. The appearance of O^{2-} and OH^- as water of hydration or uncoordinated with Si^{4+} , giving false indication of composition and structure; thus cyanite, Al_2SiO_5 , has one O^{2-} uncoordinated with Si^{4+} , and the formula is OAl_2SiO_4 , an orthosilicate.

Classification of Silicates.—The SiO_4 tetrahedra and the sharing of corners determine the general composition and classification of silicates, which are tabulated in Table XLV.

Zeolites and Ultramarines.—The zeolite minerals call for special attention on account of their unique constitution, structure, properties, and uses, for example, in permutite water softening. Essential facts established by x-ray analysis may be summarized as follows:

1. Open framework structure with large open channels, and with ideal $O:Si$ ratio 2:1.

2. Contain water which in many cases may be driven off by heat without destroying structure (see preceding chapter on hydrates) and reversibly replaced.

3. Water may be substituted by NH_3 , alcohol, Hg , I_2 , etc.

4. Cations may be substituted reversibly without affecting structure: (a) Two by two others of similar sizes and same total charge, such as $K^+ + Si^{4+} \rightleftharpoons Ba^{2+} + Al^{3+}$; $Na^+ + Si^{4+} \rightleftharpoons Ca^{2+}$

+ Al^{3+} . (b) Change in number of cations, such as $\text{Ba}^{2+} \rightleftharpoons 2\text{K}^+$, $\text{Ca}^{2+} \rightleftharpoons 2\text{Na}^+$, $\text{Na}^+ + 2\text{Ca}^{2+} \rightleftharpoons 3\text{Na}^+ + \text{Ca}^{2+}$ as in water softeners in which Ca^{2+} is removed from hard water by replacing Na^+ and the zeolite regenerated by NaCl .

TABLE XLV.—THE SILICATES

| Structural arrangement | Oxygen-silicon ratio | Examples |
|---|----------------------|---|
| 1. Independent SiO_4 tetrahedra bound in structure by cations | 4:1 | Orthosilicates—olivine, Mg_2SiO_4 ; cyanite, Al_2SiO_5 , really OAl_2SiO_4 ; topaz, $(\text{F}, \text{OH})_2\text{Al}_2\text{SiO}_4$; euclase, $(\text{OH})\text{BeAlSiO}_4$; chondrodite (mixed lattice), $\text{Mg}(\text{F}, \text{OH})_{2.7}\text{Mg}_2\text{SiO}_4$; phenacite, Be_2SiO_4 , complex rhombohedral because both Be and Si tetrahedrally coordinated |
| 2. Pair of tetrahedra sharing one O atom | 7:2 | Thorveitite, $\text{Sc}_2\text{Si}_2\text{O}_7$; hemimorphite, $(\text{OH})_2\text{Zn}_4\text{Si}_2\text{O}_7 \cdot \text{H}_2\text{O}$ (formerly $\text{H}_2\text{Zn}_2\text{SiO}_5$); vesuvianite (both SiO_4 and Si_2O_7), $(\text{OH})_4\text{Ca}_{10}\text{Al}_4(\text{Mg}, \text{Fe})_2[(\text{Si}_2\text{O}_7)_2 \cdot (\text{SiO}_4)_5]$ |
| 3. Closed rings of tetrahedra each sharing two O atoms | 3:1 | Three-membered ring, benitoite, $\text{BaTiSi}_3\text{O}_9$; six-membered, beryl, $\text{Be}_3\text{Al}_2\text{Si}_6\text{O}_{18}$ (Fig. 181), with marked open-channel structure |
| 4. Infinite chains of tetrahedra each sharing two O atoms | 3:1 | Pyroxenes—diopside, $\text{CaMg}(\text{SiO}_3)_2$ (Fig. 182) |
| 5. Infinite double chains of tetrahedra sharing alternately two and three O atoms | 11:4 | Amphiboles—tremolite, $(\text{OH}, \text{F})_2\text{Ca}_2\text{Mg}_5\text{Si}_8\text{O}_{22}$ (formerly $\text{Ca}_2\text{Mg}_5\text{Si}_8\text{O}_{24}$); fibrous, cleavage parallel to chains (Fig. 182) characterized by extensive isomorphous substitutions, including Al^{3+} for Si^{4+} ; general formula $(\text{O}, \text{OH}, \text{F})_2(\text{Ca}, \text{Na})_2(\text{Na}, \text{K})_{0-1}(\text{Mg}, \text{Fe}^{2+})(\text{Mg}, \text{Fe}^{2+}, \text{Al}, \text{Fe}^{3+})_4[(\text{Al}, \text{Si})_2\text{Si}_6\text{O}_{22}]$ |
| 6. Infinite sheets of tetrahedra each sharing three O atoms | 5:2 | 1. Talc, $(\text{OH})_3\text{Mg}_3\text{Si}_4\text{O}_{10}$ 2. Micas—muscovite, $(\text{OH})_2\text{KAl}_2(\text{Si}_3\text{Al})\text{O}_{10}$ 3. Margarite, $\text{CaAl}_2(\text{Si}_2\text{Al}_2)\text{O}_{10}$ [note K in (2) and Ca in (3)] made possible by substitution of one Al^{3+} for one Si^{4+} and two Al^{3+} for two Si^{4+} 4. Phlogopite, $(\text{OH})_2\text{KMg}_3(\text{Si}_3\text{Al})\text{O}_{10}$ |
| 7. Infinite framework of tetrahedra each sharing all four O atoms | 2:1 | All forms of SiO_2 . Felspars—orthoclase, $\text{K}(\text{Si}_3\text{Al})\text{O}_8$ (Si^{4+} must be replaced by Al^{3+} to give negative charge to balance cations); albite, $\text{Na}(\text{Si}_3\text{Al})\text{O}_8$; anorthite, $\text{Ca}(\text{Si}_2\text{Al}_2)\text{O}_8$, zeolites, sodalite, ultramarine |

5. Defect structure (page 362); in analcite, $\text{NaAlSi}_2\text{O}_6 \cdot \text{H}_2\text{O}$ 16Na^+ ions in the unit cell occupy 24 equivalent positions, hence

are in a decidedly "fluid" condition; chabazite, $(\text{Ca}, \text{Na}_2)(\text{Al}_2\text{Si}_4\text{O}_{12}) \cdot 6\text{H}_2\text{O}$ has sixfold rings of tetrahedra.

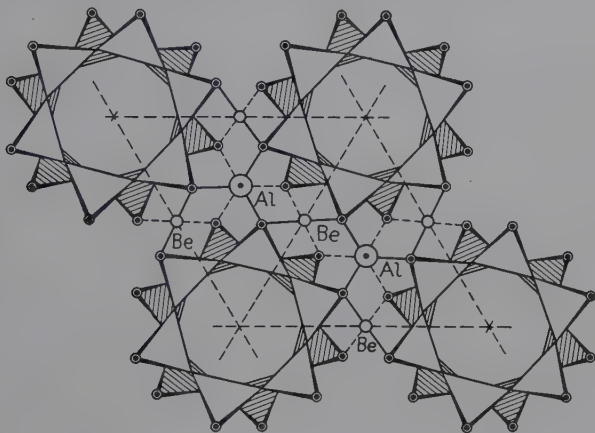


FIG. 181.—The structure of beryl, $\text{Be}_3\text{Al}_2\text{Si}_6\text{O}_{18}$.

6. The structures may display fibrous or lamellar properties, though still retaining the ratio $\text{O}:(\text{Si}, \text{Al})$ 2:1. Natrolite, $\text{Na}_2(\text{Al}_2\text{Si}_3\text{O}_{20}) \cdot 2\text{H}_2\text{O}$, is fibrous, and heulandite, $\text{Ca}(\text{Al}_2\text{Si}_7\text{O}_{18}) \cdot 6\text{H}_2\text{O}$, lamellar.

7. Closely related are framework structures that do not contain water, including ultramarine, the first framework silicate to be established, by Jaeger, in 1927. Two representative minerals are sodalite, $\text{Na}_8(\text{Al}_6\text{Si}_6\text{O}_{24}) \cdot \text{Cl}_2$, and noseilite, $\text{Na}_8(\text{Al}_6\text{Si}_6\text{O}_{24}) \cdot \text{SO}_4$, which may be converted one into the other by heating in fused Na_2SO_4 or NaCl , respectively. The natural compound that gives its blue color to lapis lazuli and artificial ultramarines is the result of replacement of Cl and SO_4 in the above compounds by sulfur, which in

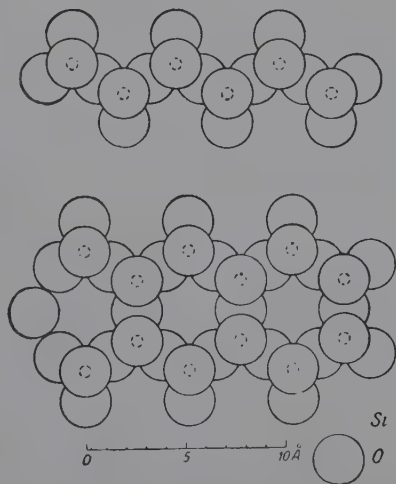
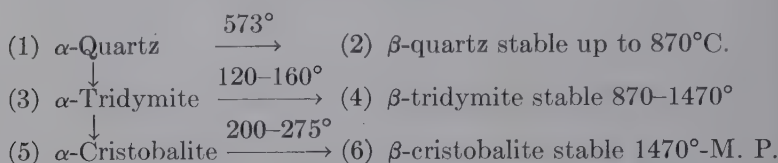


FIG. 182.—Silicon-oxygen chains in pyroxene (diopside), above; and double chains in amphibole, below. Mica is built from a further extension of these chains into a sheet.

varying amounts is responsible for a wide range of colors. Industrial ultramarines are classified according to the ratios of Al:Si, 1:1 and 1:1.5. Base exchange is possible, but it is likely that the ions tend to remain more nearly in fixed positions than in analcite.

The Forms of Silica.—Silica, SiO_2 , exists in six different crystalline forms, although all are frameworks of tetrahedra each sharing all four oxygen atoms. The modifications are:



In each case the low- to high-temperature transformation takes place quickly and reversibly, while the transformations quartz to tridymite to cristobalite are so sluggish that tridymite and cristobalite are found in minerals and remain indefinitely in their metastable states; their α to β inversions are studied actually at temperatures where they are metastable forms.

Quartz, tridymite, and cristobalite are distinguished by completely different plans of linking of tetrahedra. The high- and low-temperature modifications of each involve no change in plan of linking but merely a displacement and rotation of tetrahedra that alter symmetry, from the higher type in β to a lower in α forms (see Fig. 183 for alteration in quartz).

| Form | Structure | Space-group | Z | Cell dimensions |
|-----------------------------|------------|-----------------------------|----|--|
| α -Quartz..... | Trigonal | $C3_12$ | 3 | $\begin{cases} a = 4.903 \\ c = 5.393 \end{cases}$ |
| β -Quartz..... | Hexagonal | $C6_22$ | 3 | $\begin{cases} a = 4.989 \\ c = 5.446 \end{cases}$ |
| α -Tridymite..... | Rhombic | ? (complex) | 64 | $\begin{cases} a = 9.88 \\ b = 17.1 \\ c = 16.3 \end{cases}$ |
| β -Tridymite..... | Hexagonal | $C\bar{6}2c$ or $C6/mmc$ | 4 | $\begin{cases} a = 5.03 \\ c = 8.22 \end{cases}$ |
| α -Cristobalite..... | Tetragonal | $D4_22_1$ | 4 | $\begin{cases} a = 4.96 \\ c = 6.92 \end{cases}$ |
| β -Cristobalite..... | Cubic | $Fd\bar{3}m$ or $P2_13$ | 8 | 7.12 |

The structure of β -cristobalite proposed by Wyckoff is the only case of a linear arrangement of $-\text{Si}-\text{O}-\text{Si}-$ consistent with a purely ionic bond; for all other forms the angle of the bond is less than 180° , so that there is a tendency toward the spatially directed bonds of homopolar type. Barth assigns a lower symmetry however to β -cristobalite, and it is possible that in it also the bonds are inclined while cubic symmetry is attained through rotation of the oxygen atom.

The identification of these various modifications forms one of the principal applications of diffraction analysis to ceramic materials, gems, industrial dusts, soils, devitrified glass, etc.

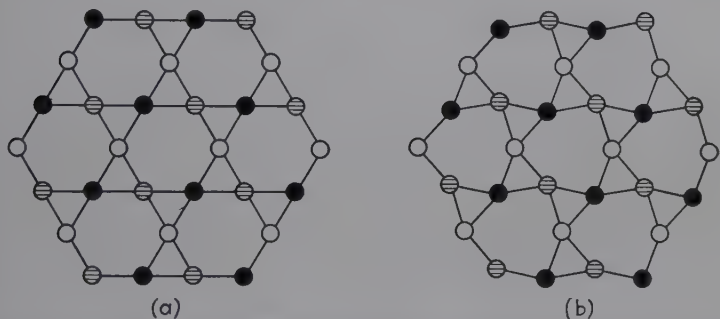


FIG. 183.—The relation between (a) β -quartz and (b) α -quartz. Silicon atoms only are shown.

Industrial Dusts and the Diagnosis of Silicosis.—The identification and quantitative determination of the crystalline constituents of mine and industrial dusts and the correlation of these with the appearance of silicosis in the lungs are among the useful and unique applications of x-ray diffraction analysis. The mineralogical composition, or state of chemical combination, of a dust has vastly greater pathological significance than the elementary composition deduced by chemical or spectroscopic analysis. The failure of the usual and generally dependable petrographic immersion microscope to distinguish between free quartz and some silicate minerals in the dusts of some Canadian gold mines led to the development by Clark and Reynolds¹ of a quantitative x-ray diffraction procedure, utilizing the familiar "internal-standard" technique. A pure crystalline powder, known not to be present in the dust being examined, is added to

¹ *Univ. Toronto Studies*, geol. ser., **38**, 13 (1935); *Ind. Eng. Chem., Anal. Ed.*, **8**, 36 (1936).

the unknown in a definite ratio and the diffraction pattern registered. The ratio of the density of a line sought to that of a near-by line of the added standard is determined photometrically. The ratio thus obtained is proportional to the line intensity of the substance sought, which in turn is proportional to the amount of the substance in the mixture. By reference to a curve that is prepared empirically from mixtures of known composition, the percentage of the constituent sought is obtainable at once. Figure 184 shows the pattern for a typical dust sample compared with a standard pattern for ordinary quartz. This method, of course, is applicable to the determination of any selected mineral constituent. The next step was to attempt to identify the particular variety of silica or silicate responsible for silicosis. Through cooperation with the Municipal Tuberculosis Sani-

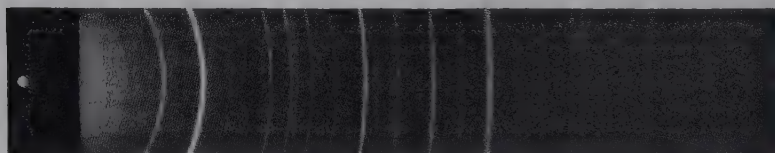


FIG. 184.—Powder diffraction pattern for quartz as standard for dust analysis.

tarium of Chicago, it was possible to make an x-ray analysis of lung tissue from 31 cases of known or suspected silicosis (among miners, stonecutters, cement workers, etc.) with the usually attendant tuberculosis.¹ In all definite cases of silicosis, crystalline quartz was identified varying in amount from a threshold value of 0.2 per cent (about 0.09 per cent silica can be found in an infant's lungs) up to nearly 2.5 per cent. The lungs of some persons showed high contents of silicon by chemical analysis; but wherever the crystal lines corresponded to a compound other than quartz, there was no silicotic condition. This analysis must be made after death, but the method can be made to apply to body fluids, particularly sputum, for diagnosis. Best of all is the protection of workers against industrial dusts shown to contain crystalline quartz. Powdered aluminum in amounts of only 1 per cent is the most effective combative agent against quartz. X-ray and electron diffraction analysis have proved that an extremely thin film (less than 250 A.U.) of a hydrous alumina hydrate gel forms on the surface of silica particles which prevents

¹ SWEANY, KLAAS, and CLARK, *Radiology*, **31**, 399 (1938).

them from dissolving in the lung tissues and thus prevents toxic effects. The hydrous material dries to $\alpha\text{-Al}_2\text{O}_3\cdot\text{H}_2\text{O}$, böhmite.¹

Clay and Soil Minerals.—The classification and constitution of the clay minerals present a problem, at once of the greatest importance and of great difficulty, upon which only a beginning has been made. It is certain that the essential structure must be

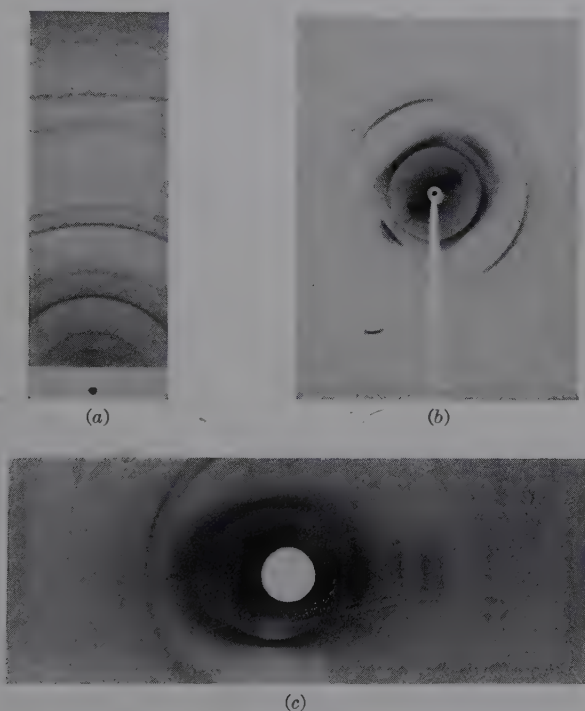


FIG. 185.—Patterns for clay: (a) powder; (b) flake formed on surface of evaporated suspension; (c) oscillation (Bragg) pattern of flake.

a layer silicate; that base exchange must be possible; that water and nutrient solutions must be held in unique fashion; that individual crystals are extremely small ordinarily, which in itself limits the x-ray method largely to the powder method and renders almost impossible the derivation of complete structures depending upon single crystals. However, the tendency of wet clay particles to orient with their cleavage faces parallel to a surface makes it possible to employ oriented flakes for obtaining a fiber pattern.

¹ GERMER and STORKS, *Ind. Eng. Chem., Anal. Ed.*, **11**, 583 (1939).

This is the basis of the development of the new commercial sheet material from clay called "Alsifilm" (E. A. Hauser). In Fig. 185 is shown the powder pattern and the fiber pattern of a flake of clay composed of kaolinite and mica. Here the short arcs represent successive orders of basal reflections (001) which are most significant in the identification of clay minerals. Oscillation Bragg patterns record many more orders. These clay minerals therefore are micaceous in structure, consisting of thin hexagonal flakes with perfect cleavage, built up from the linked tetrahedral SiO_4 groups referred to in Table XLV.

The clay minerals are classified as follows:

1. Kaolin type. Kaolinite, nacrite, dickite, $2\text{H}_2\text{O} \cdot \text{Al}_2\text{O}_3 \cdot 2\text{SiO}_2$; single sheets, $\text{O}_3 \cdot \text{Si}_2 \cdot \text{O}_2\text{OH} \cdot \text{Al}_2(\text{OH})_3$, polar with one side consisting of bases of SiO_4 tetrahedra, the other of OH^- and metal ions in six-coordination, with the polar OH^- groups in contact with the basal oxygen atoms of tetrahedra of the next sheet; composition rather exact; crystals very small and imperfect.

2. Montmorillonite (beidellite)¹ type (bentonite, fuller's earth), $(\text{OH})_2(3\text{Mg} \cdot 2\text{Fe} \cdot 2\text{Al})\text{Si}_4\text{O}_{10} \cdot n\text{H}_2\text{O}$. Bradley, Grim, and Clark² have demonstrated that 0, 1, 2, 3, or 4 layers of H_2O molecules may be introduced in swelling to form discrete hydrates (possibly 0, 4, 8, 12, $16\text{H}_2\text{O}$ molecules) with periodicity values along the c axis of 9.6, 12.4, 15.4, 18.4, and 21.4 A.U. (Fig. 186). As d_{001} increases with hydration, it becomes difficult to understand what forces hold the layers together at all. Above the highest hydrate it may be assumed that layers are comparatively free, and it is under this condition that exchange bases have access to the mineral and assume the role of binding it together as water content decreases. Giesecking³ has shown convincingly for bentonite that large substituted ammonium ions, NH_3R^+ , NH_2R_2^+ , NHR_3^+ , NR_4^+ , and methylene blue replace H^+ , Na^+ , or Ca^{2+} with great increase in the 001 or c spacing and hence that cation substitution takes place in this variable spacing rather than within a layer by breaking of bonds. Montmorillonite must be defective in metal

¹ These two names are used interchangeably since the same patterns are obtained for both minerals. However, "beidellite" refers to the limiting aluminum mineral; "nontronite" to the limiting ferrie composition, and "montmorillonite" to the magnesium-bearing mineral.

² *Z. Krist.*, **97**, 216 (1937).

³ *Soil Science*, **47**, 1 (1939).

cations (usually Mg^{2+}), giving a net negative charge on the oxygens; in the water layers are found the compensating H^+ , Na^+ , or Ca^{2+} ions.



FIG. 186. Patterns for montmorillonite with increasing water content (0 to $16H_2O$ hydrates).

All these minerals including the micas resemble each other in the definiteness of hexagonal network structure of linked SiO_4 tetrahedra in the plane of the sheets ($a = 5.1$ to 5.3 , $b = 9.0$ to 9.3 A.U.) and in the variation of ways in which sheets are piled

on each other and of the spacing along the c axis; all are pseudo-hexagonal but actually monoclinic, with β nearly 90 deg.

3. Micas. Muscovite, a typical mica, has the composition $(\text{OH})_2\text{KAl}_2(\text{Si}_3\text{Al})\text{O}_{10}$. Like montmorillonite it has sheets of SiO_4 tetrahedra arranged in pairs with their vertices and bases alternately together (Fig. 187). These vertices are strongly cross-linked by Al^{3+} each of which is octahedrally coordinated by four O^{2-} belonging to the sheets and two OH . The bases of the tetrahedra are linked through K^+ ions coordinated by 12 O^{2-} neighbors, but

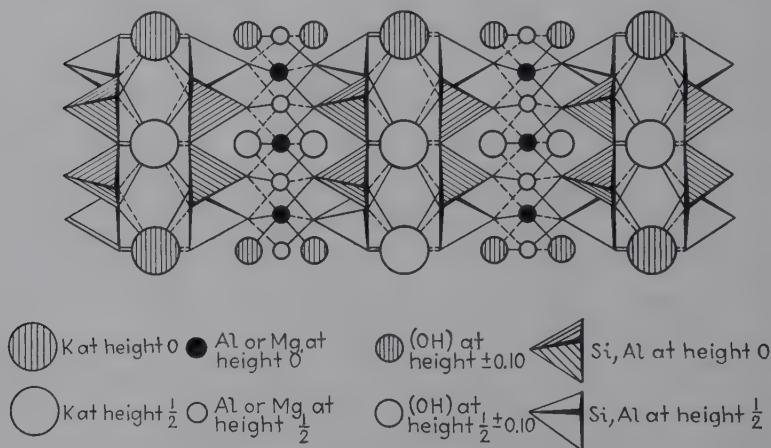


FIG. 187.—The structure of muscovite mica, $(\text{OH})_2\text{KAl}_2(\text{Si}_3\text{Al})\text{O}_{10}$. The sheets are seen edge on.

only in so far as Si^{4+} is replaced by Al^{3+} are these O^{2-} ions actively bound by electrostatic valences. As Si^{4+} increases relative to Al^{3+} , K^+ ions which serve to “tack” layers together decrease. Many Midwest clays have constituents of this type down to the limiting case of talc $(\text{OH})_2\text{Mg}_3(\text{Si}_4\text{O}_{10})$, or pyrophyllite with no K^+ ions and with layers held solely by the van der Waals forces. Chlorites have intermediate Mg-Al hydroxide layers, and vermiculites have intermediate H_2O layers. Other constituents in shales are only imperfectly known.

Analysis of Soil Profiles.—An example of soil analysis is afforded by studies of fractions of genetic soil profiles, especially 1–2 μ particles.¹ Quartz, mica, calcite, beidellite, kaolinite, montmorillonite, muscovite, etc., can all be identified by charac-

¹ CLARK, RIECKEN, and REYNOLDS, *Z. Krist.*, **96**, 273 (1937).

teristic spacings, although many spacings are common to several of the sheet minerals. These results lead to definite conclusions as to origin of soils at different profile levels, and these to valuable contributions to geology and agronomy.

Cement.¹—The characteristic feature of cement compounds is ability to react with water and harden. These compounds are formed at high temperatures and seem to involve the active and unstable coordination by Ca^{2+} of oxygens already claimed by SiO_4 coordination in close-packed structure. These anhydrous compounds undergo polymorphic transformations on account of instability or split hydrolytically on contact with water and are changed into stable lime silicate, lime aluminate, or hydrates with “inactive” calcium ions. The following cement compounds have been identified almost solely by x-ray methods in spite of great difficulties in obtaining crystals:

(1) $3\text{CaO} \cdot \text{Al}_2\text{O}_3$. Cubic, $a_0 = 15.22$, 24 mols per unit cell, related to perovskite, network of AlO_4 , AlO_6 , and CaO_6 groups (Ca^{2+} in an open basket of O^{2-} ions) with embedded “inactive” Ca^{2+} ; reactivity due to CaO_6 and large holes.

(2) $8\text{CaO} \cdot \text{Na}_2\text{O} \cdot 3\text{Al}_2\text{O}_3$. Obtained by substituting Na_2O for CaO in compound above, with resulting distortion.

(3) $12\text{CaO} \cdot 7\text{Al}_2\text{O}_3$ (formerly $5\text{CaO} \cdot 3\text{Al}_2\text{O}_3$) } constituents of hydraulic

(4) $\text{CaO} \cdot 2\text{Al}_2\text{O}_3$ (formerly $3\text{CaO} \cdot 5\text{Al}_2\text{O}_3$) } cements.

(5) $2\text{CaO} \cdot \text{Al}_2\text{O}_3 \cdot \text{SiO}_2$. Does not react with water; SiO_4 , AlO_4 tetrahedra held together in eight-coordination by inactive Ca^{2+} ion.

(6) $4\text{CaO} \cdot \text{Al}_2\text{O}_3 \cdot \text{Fe}_2\text{O}_3$. Reactive because of FeO_4 tetrahedra and CaO_6 “baskets” open toward cavities.

(7) $3\text{CaO} \cdot \text{SiO}_2$ (most important cement compound). Since $\text{Si}:\text{O} = 1:5$, some oxygen ions are coordinated with Ca^{2+} alone, which is active as a coordination center of 6 O^{2-} .

(8) $2\text{CaO} \cdot \text{SiO}_2$. Exists in three forms, α and β (active), γ (inactive), because of complete difference in Ca^{2+} coordination.

The recognized hydrates after reaction and setting with water, upon which x-ray work is still fragmentary, are:

(1) $\text{Ca}(\text{OH})_2$.

(2) $\text{Al}_2\text{O}_3 \cdot 3\text{H}_2\text{O}$. Probably $\text{Al}(\text{OH})_6$ octahedra.

(3) AlOOH . Diaspore.

(4) $3\text{CaO} \cdot \text{Al}_2\text{O}_3 \cdot 6\text{H}_2\text{O}$. Cubic, $a_0 = 15.56$.

(5) $4\text{CaO} \cdot \text{Al}_2\text{O}_3 \cdot 12\text{H}_2\text{O}$.

¹ For the most recent account, see “Symposium on the Chemistry of Cements,” Stockholm, 1938.

(6) $3\text{CaO} \cdot \text{Al}_2\text{O}_3 \cdot 8\text{H}_2\text{O}$, and possibly seven or eight other hydrates all resembling each other. According to Brandenberger formed from mixed layers of $\text{Ca}(\text{OH})_2$ and hydrous alumina with water.

(7) $2\text{CaO} \cdot \text{SiO}_2 \cdot 4\text{H}_2\text{O}$. The principal cement "glue."

(8) $2\text{CaO} \cdot \text{SiO}_2 \cdot \text{H}_2\text{O}$. Four different hydrates of this composition have been described.

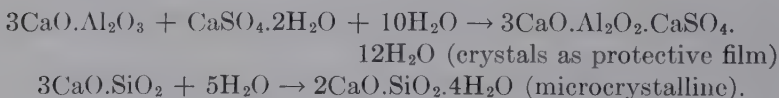
(9) $3\text{CaO} \cdot 2\text{SiO}_2 \cdot x\text{H}_2\text{O}$. The most important crystalline hardening agent in Portland cement.

(10) $2\text{CaO} \cdot \text{Al}_2\text{O}_3 \cdot \text{SiO}_2 \cdot x\text{H}_2\text{O}$. Lime water plus dehydrated kaolin, or tricalcium silicate and tricalcium aluminate precipitated in water.

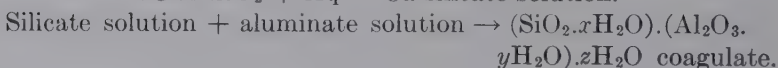
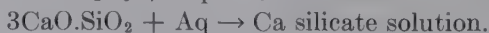
(11) $3\text{CaO} \cdot \text{Fe}_2\text{O}_3 \cdot 6\text{H}_2\text{O}$. Corresponds to (4) above.

(12) $3\text{CaO} \cdot \text{Al}_2\text{O}_3 \cdot \text{CaSO}_4 \cdot 12\text{H}_2\text{O}$. Precipitated when gypsum is added as a retarder to setting; as a film protects grains of compounds from hydration.

Thus, upon the basis of x-ray research, normal set may be represented by



Quick set is represented by:



The low strength at quick set is due to the mechanical properties of this gel.

Thus a retarder is a compound that decreases solubility of aluminates and forms a semipermeable membrane around cement grains.

An accelerator like CaCl_2 hastens solution of the silicates by decreasing pH and increasing Ca^{2+} concentration, without dissolving aluminates. Complexes with CaCl_2 have been identified by x-rays.

A destroyer is a compound that dissolves aluminates (sugar, borax, humus) and causes quick set or that precipitates insoluble and impermeable film around grains (phosphates, fluorides).

Basic blast-furnace slag reacts like Portland cement if the solubility of aluminates is reduced by a retarder and the reaction of silicates quickened by an accelerator.

Glasses.—Glasses form one of the most important groups in silicate chemistry, not only because they are so considerable an

industrial product, but also because they are present frequently in minerals and cements. Since a glass is a state of solid matter, rather than a chemical composition, and since it is not crystalline but still may be studied by x-ray diffraction methods, with suitably modified methods of structural interpretation, the subject will receive special consideration in conjunction with liquids in Chap. XX.

CHAPTER XVIII

ALLOYS

The Metallic State.—In Chap. XV the crystalline structures of pure metals have been summarized; and in Chap. XVI have been considered the characteristic features of the metallic bond that give to some chemical elements those peculiar properties of opacity, conductivity, etc., which distinguish the metallic state. Again reviewed these features are as follows:

1. All theories are variations on the theory of a structure of a lattice of positive ions in an electron gas, or of electrons free to conduct electric current through the lattice.

2. The bond is associated with high coordination number (up to 12 in metals and 16 in alloys) and is spatially undirected, in some respects resembling features of both ionic and covalent bonds.

3. The metallic state may be attained at sufficiently high temperatures and pressures, as in the interior of stars, so that all elements and compounds may become metals in the sense of conduction by electron transport.

4. The average concentration of valence electrons is far more important than atomic number or atomic weight.

5. The bond is equally efficacious in the liquid state.

6. Its force varies inversely as some high power of internuclear distance, as shown by extreme weakness in the alkali metals with low melting points and large atomic volumes, in contrast with the opposite properties of the platinum-group metals; in equilibrium with this force of attraction is a force of repulsion that is an atomic property as shown by the constancy of atomic volume in alloy formation.

7. Characteristic mechanical properties arise from the ease with which a metal is deformed by gliding and the bond is reestablished or healed, particularly for simple structures.

8. According to wave mechanics the whole assemblage of electrons no longer occupies a continuous range of energies but

is divided into a series of discrete so-called "Brillouin zones" of permitted and forbidden energy values. A free electron does not necessarily give rise to conductivity; for if one zone is completely filled with electrons and the next one above it empty, it is impossible for electrons to receive a small increment of energy, since this would bring them within a forbidden range and the solid is an insulator. Only if a zone is incompletely filled or overlaps a higher zone can conduction occur. Intricate broadening and overlapping of zones is a characteristic of metals and arises from the profound influence that the formation of the lattice exercises on the electronic orbits of the individual atoms. For a full exposition of this theory of the metallic state, and indeed of the zone theory of the solid state in general, reference should be made to papers by Bloch, Wigner and Seitz, Johnson, Slater, Mott, Jones, and others, well summarized in Evans's "Crystal Chemistry," page 74.

9. One of the chief difficulties of dealing with the metallic state is the fact that there are so many degrees of what may be termed metallic properties. It is impossible to find, for example, where metallic combination leaves off and homopolar begins. This difficulty leads to the classification of metals on the basis of crystal structures into true metals (alkali and alkaline earth, Be, Mg, Cu, Ag, Au, and transition elements) and B subgroup metals (Zn, Cd, Hg, Al, Ga, In, Tl, Si, Ge, Sn, Pb, As, Sb, Bi, Se, Te). In general the latter are distinguished by: (1) more complex structures and lack of closest packing; (2) obedience to the $8 - n$ rule; (3) hard and brittle properties and anisotropic thermal expansion and compressibility; (4) possession of structural diamagnetism, thus revealing partially homopolar binding, which disappears on melting; (5) anomalous positions of Al, Tl, and Pb which confer on them properties of both true and B subgroup (or half) metals; (6) greatly different behavior in alloy formation.

The Classification of Binary Intermetallic Systems.—We begin the discussion of the crystal chemistry of alloys with a summary in Table XLVI of general structure types that have been deduced from the x-ray diffraction analyses of hundreds of binary intermetallic systems. Specimens are prepared from melts of the metals; or alloys are made by electrodeposition under suitable conditions from solution.

TABLE XLVI.—CLASSIFICATION OF ALLOYS (EVANS)

| True metals | | | B subgroup metals | |
|-------------------|--|---|--|--|
| | | | B1 Groups 2, 3, 4 | B2 Groups 4, 5, 6 |
| True metals | Transition metals, Cu, Ag, Au T | 1. Wide range of solid solu- tion Superlat- tices | 2. Electron com- pounds | 4. NiAs, FeS ₂ , MoS ₂ , and CdI ₂ structures |
| | A group metals (alkali, alkaline earth metals, Be, Mg) A | | 3. CsCl and NaTl structures | 5. Ionic, NaCl, and CaF ₂ struc- tures |
| B subgroup metals | B1 Groups 2, 3, 4 | 2, 3 | 6. Solid solution if chemically similar and of comparable size | 7. Zinc blende and wurtzite (homopolar) structures |
| | B2 Groups 4, 5, 6 | 4, 5 | 7 | 8. NaCl structure |

1. *Alloys Formed by a Continuous Series of Solid Solutions (Substitutional).*—In such alloys the atoms of one kind of metal that is being alloyed with another replace at random the atoms of the latter at the lattice points.



FIG. 188.—Powder diffraction patterns illustrating solid solution; upper, α -brass, 80 per cent copper, 20 per cent zinc; lower, pure copper.

Microscopic evidence: Only one kind of crystal appears in any specimen ranging from one pure component to the other.

Thermal evidence: Smooth continuous curve in phase diagram between pure components.

X-ray evidence: Only one type of diffraction pattern throughout, the only variation being a change in the lattice parameter.

Figure 188 shows how the diffraction lines for a pure metal are shifted for a solid solution.

Requirements: Only two metals that have the same lattice structure (*i.e.*, both face-centered cubic, for example) can form a continuous series of solid solutions. All pairs of metals with common lattice structure do not form continuous series (*e.g.*, aluminum-gold). Two metals may be miscible in all proportions if the atoms are small, highly charged, and of similar electronic configuration and differing in size by not more than 10 or 12 per cent.

Additivity relations: Vegard's law of additivity states that in a binary system forming a continuous series of solid solutions the lattice parameters are linearly related to atomic percentage of one of the components. In other words, upon a straight line joining the numerical values of the edge lengths of the unit-crystal cells of the two pure metals lie all the lattice values for all possible solid solutions of the two metals.

General properties: The electrical and mechanical properties of these solid-solution alloys vary more or less as expected with the lattice constant. All compositions retain metallic properties; the solid solution is usually harder than the pure solvent metal; the conductivity decreases as one metal is dissolved in another but is less dependent upon temperature than that of a pure metal (constantan, an alloy of copper and nickel containing small amounts of iron and manganese, is especially valuable for resistance measurements on this account). Quite characteristic also are the differential vaporization of one metal from the other, the lattice constant changing in the purely solid phase with change in composition, and the behavior in corrosive media. For example, Graf and Glocker¹ in a remarkably clear-cut x-ray study analyzed gold-copper crystals after etching with oxidizing agents. The resulting specimens produced the interferences for pure gold in a surface layer oriented exactly like the original alloy layer. Thus with the removal of the less noble copper atoms from the mixed crystal lattice the remaining gold atoms had sufficient mobility to group themselves together into a pure-gold crystal layer with entirely different lattice spacing from the underlying unattacked alloy. In some cases a small fraction of copper atoms completely surrounded and protected by gold

¹ *Metallwirtschaft*, **11**, 77 (1932).

atoms remains in the layers, as is readily ascertained from the diffraction patterns.

Examples investigated by x-rays are: gold-copper, gold-silver, gold-palladium, nickel-copper, cobalt-nickel, nickel-palladium, platinum-palladium, potassium-rubidium, strontium-calcium, etc.

2. *Substitutional Solid Solution over Limited Ranges.*—It follows, of course, that other systems which do not form a continuous series of solid solutions will show substitutional mixed crystals over limited ranges of B in A and A in B. In cases where atomic sizes differ by more than 15 per cent, two metals may be immiscible.

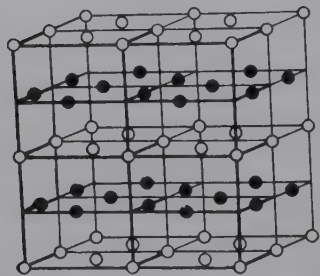


FIG. 189.—The structure of the ordered phase CuAu.

3. *Superstructures.*—The solid solutions involving random substitution just considered are typical ordinarily of specimens at high temperatures or quenched. A good example is the copper-gold system. When, however, such a specimen is very carefully annealed, a new phenomenon enters; the two kinds of

atom tend to occupy definite geometrical positions, instead of a random distribution. At a composition corresponding exactly to AuCu, the segregation is complete, as shown in Fig. 189. There are now gold atoms at the corners of each cell and in the top and bottom face centers and copper at the centers of the side faces, or vice versa; and the layers and difference in radii of the two atoms result in a departure from cubic symmetry (tetragonal $c/a = 0.932$). Again as more copper is added to this, statistical distribution begins; but, at the composition AuCu_3 , again there is regular arrangement with gold atoms at the corners and copper at the face centers. Further addition of copper atoms replace gold atoms one at a time until the face-centered lattice of pure copper remains. Structures for AuCu and AuCu_3 in the ordered state, in which the pattern of all positions is that of the initial random solution but over which the two kinds of atom are distributed in a regular way, are *superlattices*. Such a condition was predicted in 1919 by Tammann from corrosion experiments. It is recognized on diffraction patterns through

the appearance of new lines, a redistribution of intensities, splitting of single lines (cubic to tetragonal), etc. The list of examples is surprisingly large, not only for alloy systems of true metals, but for more complex cases such as Fe-Al, where the two metals have different initial structures. In the quenched alloys Fe_3Al is random, but FeAl by the operation of probabilities already has CsCl structure, whereas in the annealed alloys Fe_3Al becomes ordered.

These cases of order-disorder transformations were the first to be recognized and led to the extended general application of defect structures considered on page 362. W. L. Bragg in 1933 showed that the development of superlattices was the natural consequence of the tendency of solute atoms to be as widely separated as possible. The presence of a foreign atom in a lattice of solvent atoms must introduce local strains, and the most stable structure, obtained under the equilibrium conditions of annealing, will have these strains as widely distributed as possible. This will be the ordered structure, since in disorder two solute atoms may statistically come into juxtaposition. It is clear that at low concentrations the probability of such a condition will be small, and hence the structure remains disordered; or if solute and solvent atoms are very nearly alike in size as in silver-gold, the strain will be inconsequential and the disordered solid solutions will prevail over all ranges. It is also true that every possible condition may be found between the limits of order and complete disorder, each as a function of an exact temperature of heat-treatment. The Bragg-Williams theory considers a state of thermal equilibrium in which the atoms seek to assume the ordered structure of lowest potential energy whereas thermal agitation seeks to promote a state of disorder. Thus the actual degree of order (estimated from intensities of new "forbidden" x-ray lines) will be determined by temperature and by a parameter of the system representing the difference in energy between ordered and disordered states. Thus there is a critical temperature above which every trace of order disappears and at which it is expected properties, such as specific heat, should display sharp changes. The theory involves also the rate of attainment of equilibrium which may be very slow—and, indeed, a metastable disordered state preserved by quenching. The actual behavior of any system, therefore, is determined by the relation of

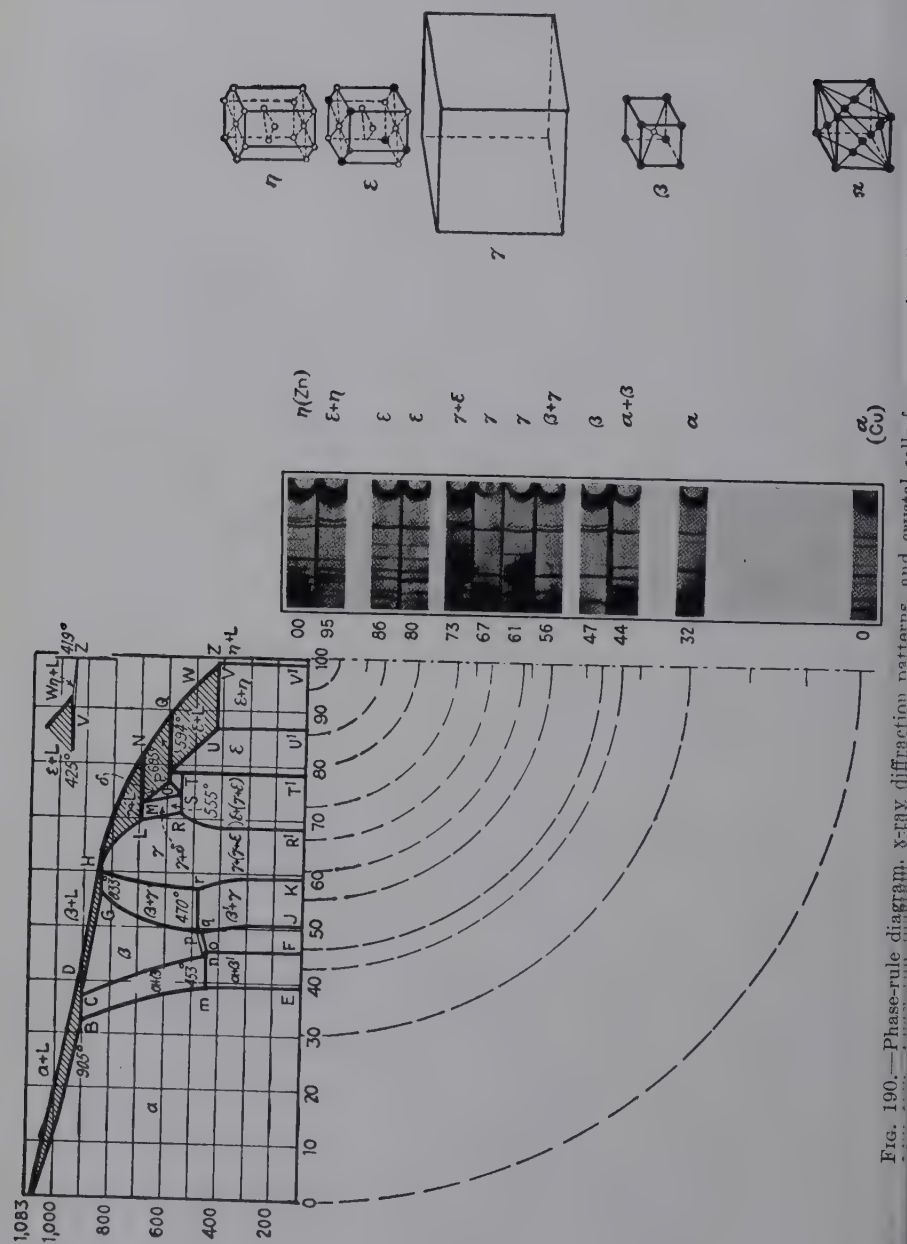


Fig. 190.—Phase-rule diagram, X-ray diffraction patterns and crystal structures for the Zn-Cu system.

the critical temperature T_c to an annealing temperature T_a and a quenching temperature T_q .

4. *Alloys, T-B₁; Intermetallic Compounds.*—These may be represented by the familiar system Cu-Zn, or brass (Fig. 190); starting with pure copper and adding zinc in increasing amounts up to pure zinc, the following phases are identified:

α —pure copper, face-centered copper ($a_0 = 3.61$ A.U.) and solid solution of zinc in this lattice; 38% Zn, $a = 3.68$ A.U.

β , (β')—CuZn, body-centered cubic; 46–48% Zn, $a = 2.945$ A.U.

γ —Cu₅Zn₈, cubic, 52 atoms per unit cell; 61% Zn, $a = 8.85$ A.U.

ϵ —CuZn₃, hexagonal; 80% Zn, $a = 2.745$, $c = 4.294$; 86% Zn, $a = 2.761$, $c = 4.286$.

η —solid solution of copper in zinc to pure Zn, hexagonal; 96% Zn, $a = 2.67$, $c = 4.92$; 100% Zn, $a = 2.66$, $c = 4.94$.

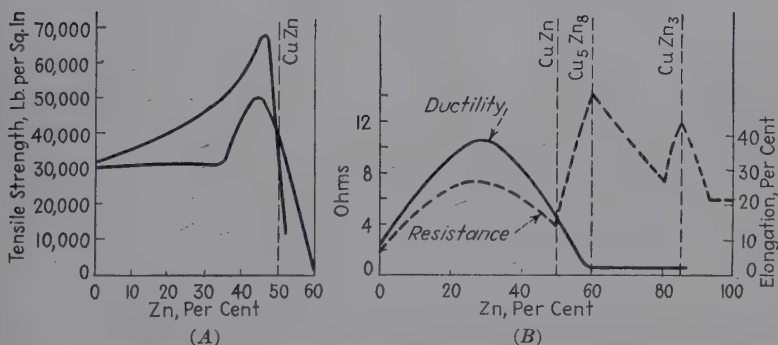


FIG. 191.—Physical properties of brass (A) tensile strength; (B) ductility and electrical resistance. (Stillwell, "Crystal Chemistry.")

The beginning and end phases of binary systems naturally depend upon the particular metals involved; but more important are the remarkable generalizations that apply to the intermediate β , γ , and ϵ phases. Mechanical and electrical properties of brasses are graphically shown in Fig. 191 as functions of the phase compositions. Thus tensile strength reaches a maximum at β , then falls off greatly for γ and ϵ ; electrical resistance reaches maxima at γ and ϵ , showing presence of homopolar as contrasted with metallic bonds; ductility has minima at γ and ϵ .

a. β Phase.—In 1926 W. Hume-Rothery suggested that the β phases of the systems Cu-Zn, Cu-Al, and Cu-Sn are analogous in structure. As their compositions correspond approximately to the formulas CuZn, Cu₃Al, and Cu₅Sn, he also put forward the hypothesis that their structural similarities might be due to

the fact that in each case the ratio of valence electrons to atoms is 3:2. X-ray investigations have confirmed the assumption that these phases have the same type of structure. In each case the atoms occupy the points of a body-centered cubic lattice. In the β copper-tin phase the copper and tin atoms seem to be distributed at random over the lattice points; but in the β copper-zinc and β copper-aluminum phases the different kinds of atom are oriented in networks of their own, thus forming superstructures. Phases of this structure have been found in several binary alloys of the transition-group metals copper, silver, and gold, with other metals of the B subgroups in the second and third vertical rows of the periodic table; and, in fact, they all occur at concentrations making the ratio of valence electrons to atoms 3:2. Examples; CuBe, AgMg, CuZn, AgZn, AuZn, MnZn₃, CuCd, AgCd, AuCd, Cu₃Al, Cu₅Sn, MnAl, FeAl, CoAl, NiAl, and Cu₃Ga. The number of valence electrons assigned to each metal is as follows: Cu, Ag, Au = 1; Be, Mg, Zn, Cd = 2; Al, Ga = 3; Sn = 4; Mn, Fe, Co, Ni = 0 (see under γ Phase below).

b. β' Phase.—In some cases when in an alloy the ratio of valence electrons to atoms is 3:2 and a phase having body-centered cubic lattice might thus have been expected, the atoms are found to be grouped instead in the same way as in β -manganese. Just as this material differs from its neighboring elements in respect to crystal structure and actually seems to act like an alloy of itself, these intermetallic phases for some reason form exceptions to the general rule. A phase of this kind designated β' is found in the silver-aluminum system (Fig. 192). Its range of homogeneity is so narrow that it may be denoted by a mere line in the equilibrium diagram. Its composition corresponds to Ag₃Al from which it is evident that the ratio of valence electrons to atoms is 3:2. In β -manganese there are two groups of equivalent positions with 12 and 8 atoms, respectively. In Ag₃Al, also, with 20 atoms per unit cell the 15 silver atoms are more than adequate for the 12 equivalent positions so that some must occupy positions equivalent to aluminum. In other words, the silver and aluminum atoms are distributed at random and approximately uniformly over the two groups of structurally equivalent positions. Other good examples are Au₃Al, Cu₅Si, and CoZn₃.

c. γ Phase.—In many cases a γ phase of complicated cubic structure has been found in alloy systems of the T and B₁ metals, having usually 52, but in some cases $8 \times 52 = 416$ atoms, in

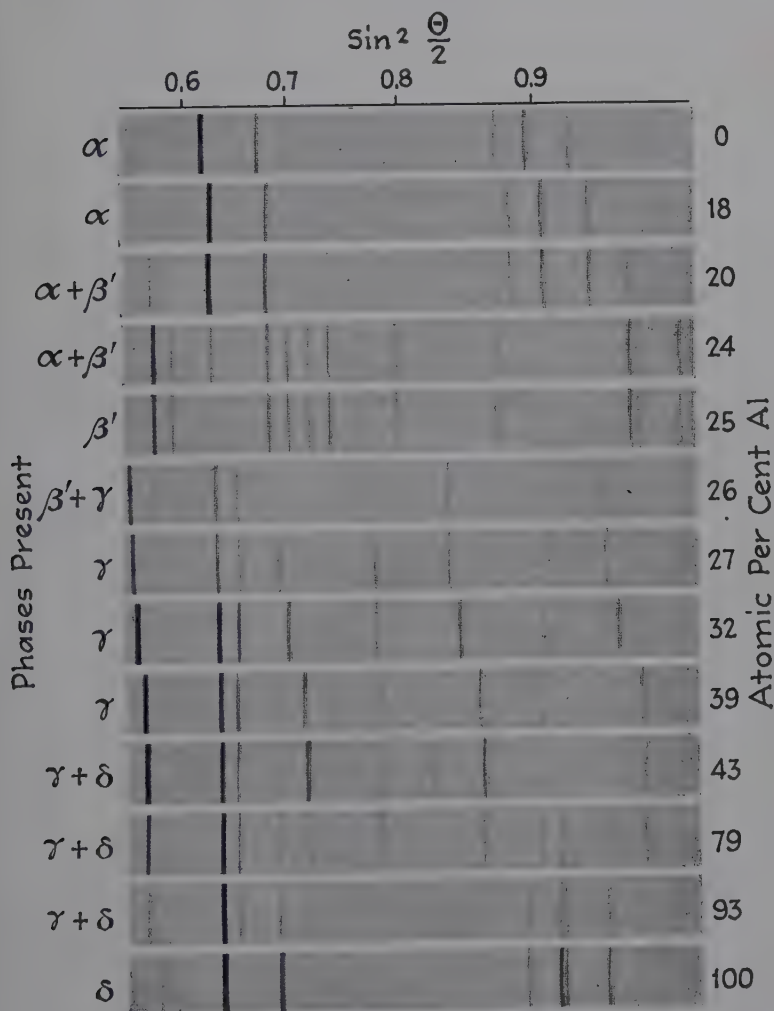


FIG. 192. — Powder patterns of silver-aluminum alloys. (Westgren and Bradley.)

its unit cell. Thus when copper, for example, is combined with zinc, the homogeneity range of this phase corresponds to a formula Cu_5Zn_8 ; for copper and aluminum, it corresponds to Cu_9Al_4 ; and for copper and tin, to $\text{Cu}_{31}\text{Sn}_8$. In all these cases

the ratio of valence electrons to number of atoms is 21:13. Other examples are Cu_5Cd_8 , Cu_5Hg_8 , Cu_9Ga_4 , Cu_9In_4 , $\text{Cu}_{31}\text{Si}_8$, $\text{Na}_{31}\text{Pb}_8$, Ag_5Zn_8 , Ag_5Cd_8 , Ag_5Hg_8 . Phases of the systems Mn-Zn, Fe-Zn, Co-Zn, Ni-Zn, Rh-Zn, Pd-Zn, Pt-Zn, Ni-Cd, etc., all give the same diffraction pattern as γ -brass and with common formulas, typified by $\text{Fe}_5\text{Zn}_{21}$, again corresponding to a ratio 21:13, if zero valence is assigned to manganese and the transition (Group 8) elements. This seems to indicate that only loosely bound electrons in valence shells are involved in the formation of these compounds. Magnetic measurements have proved that no electron contribution is made by these particular metals.

d. The Close-packed Hexagonal ϵ Phase.—An atomic grouping which is connected with a ratio of valence electrons to number of atoms 7:4 is also commonly present in these systems. Examples are CuBe_3 , CuZn_3 , CuCd_3 , Cu_3Si , Cu_3Sn , AgZn_3 , AgCd_3 , Ag_5Al_3 , Ag_3Sn , AuZn_3 , AuCd_3 , AuHg_3 , Cu_5Al_3 , Au_3Sn , MnZn_7 , FeZn_7 .

For these β , γ , ϵ "electron compounds" it is clear that the pattern of atomic positions, and not the actual distribution of atoms, is the significant feature; for example, a CsCl structure would demand the composition CuSn for the body-centered lattice of the β phase, whereas this phase has the composition Cu_5Sn , with the two atoms distributed at random in these proportions. In γ -brass, the 52 atoms in Cu_5Zn_8 are arranged with copper in $8 + 12 = 20$ and zinc in $8 + 24 = 32$ positions, whereas, in Cu_5Cd_8 , copper occupies $8 + 8 = 16$ positions, and the other 36 positions are occupied by $32 \text{ Cd} + 4 \text{ Cu}$ at random. The ratios $\frac{3}{2}$, $\frac{21}{13}$, $\frac{7}{4}$ determine not the chemical properties or chemical analogy but the structures, and hence these may be called "electron" compounds. Jones in 1934 showed that these relationships first established empirically, are well explained by the Brillouin zone theory of metals.

5. *Alloys T-B₂.*—With these systems in which the subgroup metal of Groups 4, 5, and 6 is large and easily polarized there is an increasing tendency toward discrete structures, each approximating to a definite chemical compound and capable of taking up in solid solution only a limited excess of either constituent, but still giving evidence of metallic properties. The most important type of structure is that of nickel arsenide, in which six arsenic atoms are coordinated octahedrally around each nickel atom and

six nickel atoms around each arsenic atom at the corners of a hexagonal prism. Examples: CuSn, AuSn, FeSn, NiSn, PtSn, PtPb, MnAs, NiAs, CrSb, MnSb, FeSb, CoSb, NiSb, PdSb, PtSb, NiBi, PtBi, FeS, CoS, CrSe, FeSe, CoSe, NiSe, CrTe, MnTe, FeTe, NiTe, PdTe, PtTe.

Compounds like FeS₂, pyrites, all show unmistakable homopolar bonds but retain persistence of metallic bonds. The pyrite structure is obtained for -S₂, -Se₂, -Te₂, -As₂, -Sb₂ compounds with the smallest highly polarizing transition metals, whereas the larger T metals form layer lattices of MoS₂ type (Mo, W), or CdI₂ type (Zr, Sn, Pt, Pd).

6. *Alloys A-B₁*.—These structures tend to be ionic. LiZn, LiCd, LiGa, LiIn, NaIn are like NaTl, which is body-centered cubic but with two nearly equal ions alternately at corners and centers; LiHg, LiAl, LiTl, MgTl, CaTl, SrTl are like CsCl but are to be distinguished on account of definite stoichiometric constitution from the β phase of the alloys like brass that form electron compounds. For other compositions structures in this class may be very complex; for example, in Mg₃Al₂ the Al atoms are bound into diatomic molecules, held by ionized Mg²⁺.

7. *Alloys A-B₂*.—These are even more definitely ionic so that NaCl and CaF₂ structures are common. Examples: (Mg, Ca, Ba, Sr, Pb)(S, Se, Te); (Li, Na, Cu)₂(Se, Te); Mg₂(Ge, Sn, Pb).

8. *Alloys of B Subgroup Metals*.—These finally become the most definite chemical compounds of all those with ZnS structures (homopolar) as described in Chap. XVI. Examples: (zinc blende), (Be, Zn, Cd, Hg)(S, Se, Te); AlAs, GaAs, (Al, Ga, In)Sb; wurtzite, MgTe, ZnS, CdS, CdSi.

Interstitial Solid Structures.—In addition to the substitutional solid solutions and compounds already discussed, a series of alloys are recognized in which certain light atoms with small radii (carbon, nitrogen, boron, hydrogen) are held in the interstices between metal atoms on a regular lattice. The most important is the iron-carbon system of which the members possess metallic properties, indeterminate composition, and a sequence of phases and hence class as alloys. Classification is on the basis not of composition but of the metal lattice and the coordination number of the interstitial nonmetal atom. Thus, there are never more of these than are required to fill every

vacancy of one geometric kind, but there may be a deficiency with only some of the equivalent positions occupied; Fe_4N , built on a structure of ideal composition FeN , is such a case. In the dicarbides, two paired carbon atoms appear in interstices,

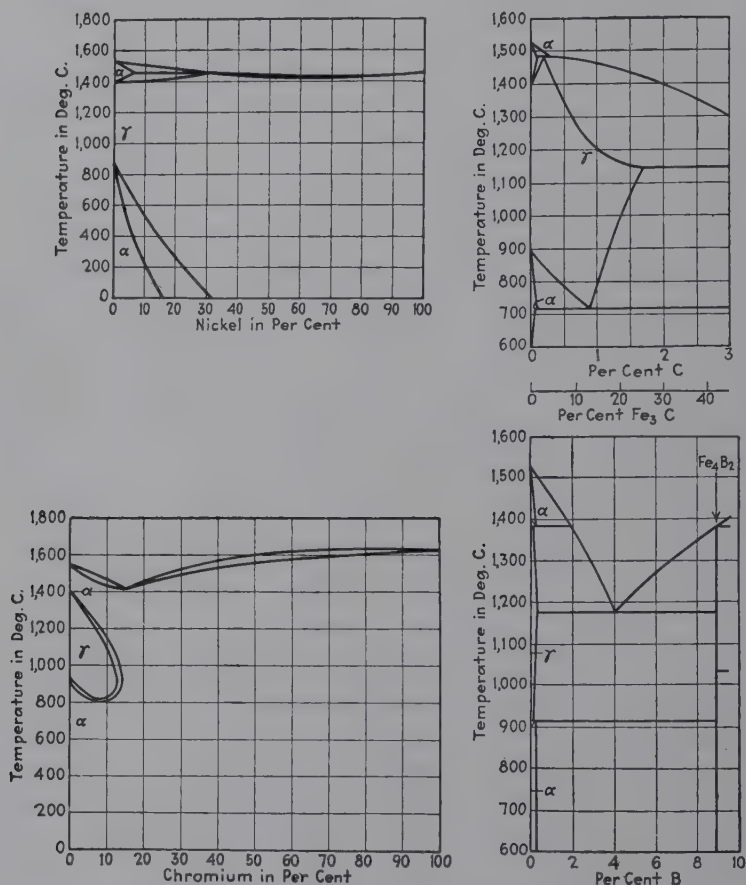


FIG. 193.—Classification of binary iron alloys.

producing distortion from cubic symmetry. In La, Ce, Pr, Nd, U, and V dicarbides, the pairs are parallel to each other and to one edge of the original metal cube (tetragonal $c/a > 1$); in ThC_2 , ZrC_2 , and ZrH_2 , the pairs are parallel to a cube face and with axes in two perpendicular directions (tetragonal $c/a < 1$).

Ubbelohde¹ has demonstrated that hydrogen and deuterium behave as metals in their alloys with palladium, in that they dissolve as alloys and dissociate partly into protons and electrons, and form two solid solutions each with the same structure in equilibrium.

The Systemitization of Iron Alloys.—From the viewpoint of crystal chemical generalizations the iron alloys form a unique series on account of the complications introduced by the polymorphic phases. Sufficient x-ray data are now at hand so that some remarkable relationships have been observed by Wever.²

| | α I b | | α II b | | α III b | | α IV b | | α V b | | α VI b | | α VII b | | α VIII | | b |
|-----|--------------|-----------|---------------|-----------|----------------|------|---------------|-----------|--------------|----------|---------------|------|----------------|-----------|---------------|-----------|-----------|
| I | | | | | | | | | | | | | | 1H | | | 2He |
| II | 3Li ▲ | | 4Be ● | | 5B ○ | | 6C □ | | 7N □ | | 8O | | 9F | | | | 10Ne |
| III | 11Na ▲ | | 12Mg ▲ | | 13Al ● | | 14Si ● | | 15P ● | | 16S ○ | | 17Cl | | | | 18Ar |
| IV | 19K ▲ | | 20Ca ▲ | | 21Sc | | 22Ti ● | | 23V ● | | 24Cr ● | | 25Mn ■ | | 26Fe ■ | 27Co ■ | 28Ni ■ |
| | | 29Cu □ | | 30Zn □ | 31Ga | | 32Ge ● | | 33As ● | | 34Se | | 35Br | | | | 36Kr |
| V | 37Rb ▲ | | 38Sr ▲ | | 39Yt | | 40Zr ○ | | 41Nb ● | | 42Mo ● | | 43Tc | | 44Ru ■ | 45Rh ■ | 46Pd ■ |
| | | 47Ag ▲ | | 48Cd ▲ | 49In | | 50Sn ● | | 51Sb ● | | 52Te | | 53I | | | | 54Xe |
| VI | 55Cs ▲ | | 56Ba ▲ | | 58Ce ○ | 72Hf | | 73Ta ● | | 74W ● | | 75Re | | 76Os ■ | 77Ir ■ | 78Pt ■ | |
| | | 79Au □ | | 80Hg ▲ | 81Tl ▲ | | 82Pb ▲ | | 83Bi ▲ | | 84Po | | 85- | | | | 86Rn |
| VII | 87- | | 88Ra ▲ | | 89Ac | | 90Th | | 91Pa | | 92U | | | | | | |

■ Open γ -Field

□ Expanded γ -Field

▲ Insoluble

● Closed γ -Field

○ Contracted γ -Field

FIG. 194.—Periodic table showing effects of chemical elements in binary iron alloys.

All the many iron alloys may be classified under four types: (a) open γ -field, illustrated by the iron-nickel system in Fig. 193; (b) closed γ -field illustrated by iron-chromium; (c) expanded γ -field (iron-carbon); and (d) contracted γ -field (iron-boron). Figure 194 shows a periodic arrangement of the atoms and the description of which type of binary alloy is formed. The open γ -field for alloys with metals of Group 8, the closed γ -field in the center of the periodic table, and insolubility for elements of Groups 1 and 2 are clearly apparent. That these differences are due primarily to atomic dimensions is shown by Fig. 195. The elements with largest atomic radii are insoluble

¹ *Proc. Roy. Soc. (London)*, **159**, 295 (1937).

² *Ergebnisse tech. Röntgenkunde*, **2**, 240 (1931).

in iron, and those with smallest radii are most soluble and are characterized by open expanded γ -field, whereas intermediate elements narrowed the γ phase. Such generalizations are

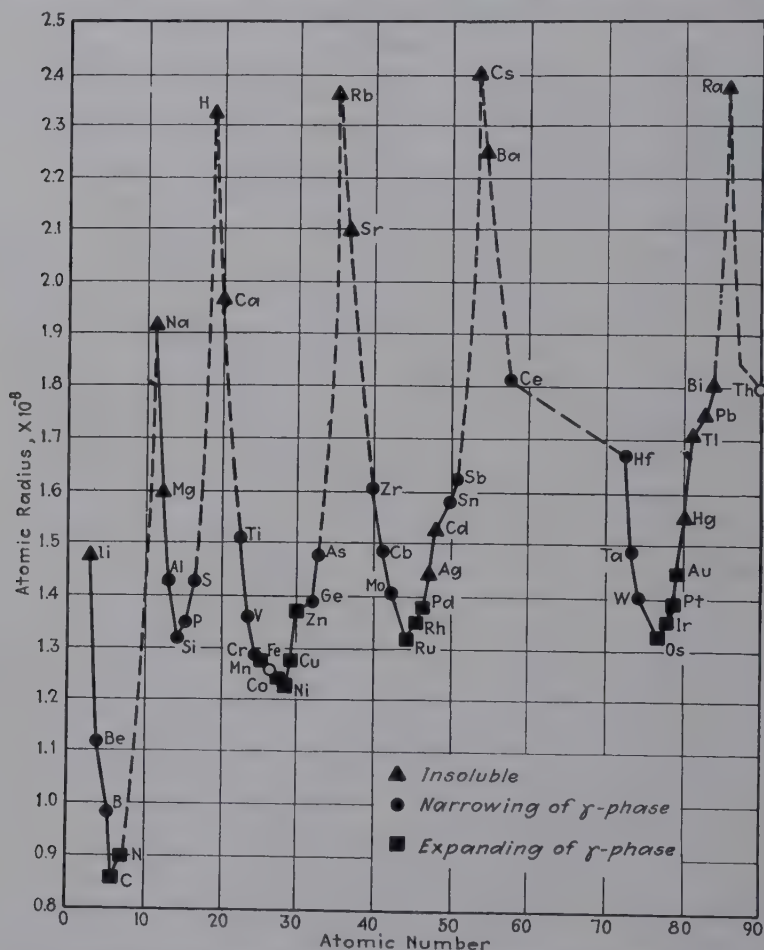


FIG. 195. Relation between atomic radius and formation of binary iron alloy. highly gratifying, and rapid progress may be expected in classifying similarly other systems of binary alloys.

Steel (Fe-C Alloys).—The most important possible application of x-ray analysis to the structure of alloys is, of course, to the series of iron-carbon alloys. There are several reasons for this, aside from the practical utility of steel. The equilibrium

diagram is one of great complexity because of the great variety of forms involving the four allotropic forms of pure iron; hence, there has been among metallurgists for a great many years the widest divergence of opinion concerning the actual constitution of many of the iron-carbon phases. The x-ray has been eagerly sought for a final answer to these moot problems; though it has already given many hopeful signs, the results are still insufficient to more than open the subject.

The facts established by x-ray analysis of steel may be briefly summarized as follows:

1. *Austenite*, formed by quenching Fe-C alloys from above the A_3 transformation point, has the structure of γ -iron (face-centered cubic). Carbon causes an enlargement of the lattice. Westgren and Phragmen found the dimensions of the unit cell to be 3.629 A.U. for a saturated solution (1.7 per cent) quenched from 1100°C. and 3.606 A.U. for a specimen containing 0.9 per cent carbon quenched from 750°C. A specimen containing 12.1 per cent manganese and 1.34 per cent carbon had a parameter 3.624 A.U. As already explained, the carbon atoms are placed interstitially. The carbon may be atomically and irregularly dispersed or the atoms may be more definitely arranged, in the sense that an atom of γ -iron may be replaced by a complex of an iron combined with one or more carbon atoms. In other words, austenite is a solid solution of carbon or Fe_3C (cementite) in γ -iron.

2. *Cementite*.—The only definite compound formed by iron and carbon, Fe_3C , crystallizes in the orthorhombic system. The unit parallelepiped has the dimensions 4.518 by 5.019 by 6.736 A.U. or the axial ratios 0.671:0.753:1. This compound is found in *pearlite* (the eutectoid mixture of α -iron and cementite formed by slow cooling of austenite from the transformation point), *troostite* (α -iron and cementite in colloidal dispersion), and *sorbite* and in the massive spheroidal condition. Meteoric cohenite has the same structure.

3. *Ferrite* has the body-centered cubic structure of pure α -iron. Carbon has a very limited solubility in it (0.06 per cent), since the diffraction lines for the numerous specimens have the same position as for pure electrolytic α -iron. A widening of the lines and the disappearance of the resolution of doublet lines may be taken as an indication of a slight increase (up to 0.3 per cent) in the

lattice, but nonuniformly, since pure iron dimensions are still indicated.

4. *β -Iron.*—There is no x-ray evidence of β -iron, since there is no structural discontinuity between α - and γ -iron.

5. *Martensite.*—Martensite is formed and retained at room temperatures when the γ - α transformation is delayed by sufficiently rapid cooling until a temperature of 300°C. is reached. The austenite \rightarrow pearlite transformation at 200° requires hours; austenite \rightarrow martensite at 100° is instantaneous. The cooling may be slower in the presence of retarding elements such as nickel and manganese. The simple facts were first established that martensite gives the spectrum of α -iron and that the diffraction lines are broad and diffuse.

More careful technique in the preparation of samples and in photographing diffraction spectra have served to clarify the problem. Fink and Campbell¹ found evidence in drastically quenched eutectoid and hypereutectoid steels of a body-centered tetragonal structure. This was not uniform with lower carbon contents, but with 1.5 per cent carbon the value of a was 2.85 A.U. and of c , 3.02 A.U. (body-centered cubic α -iron, $a = 2.86$ A.U.). It was found to be less stable at low temperatures than the γ -iron lattice and disappeared on tempering at 200°C. into ferrite and cementite in the form of sorbite, coarser than pearlite. The martensitic tetragonal structure might represent an arrested stage in transformation from face-centered cubic (γ) to body-centered cubic iron (α). The axial ratio c/a increases with carbon content at constant heating and quenching conditions and with the temperature before quenching at constant carbon content.

It may be concluded that martensite is a supersaturated solid solution of carbon in α -iron and that the intermediate tetragonal structure together with inherent complex strains accounts for hardness. The variable parameters, of course, could account for the very diffuse x-ray diffraction interferences as well as distortion or very small grain size.

The Problem of Hardness.—Six views have been presented² to account for the hardness of martensite: (1) solid solution, (2) supersaturated solid solution, (3) fineness of grains, (4) distorted space-lattice, (5) presence of minute particles of carbide, and (6)

¹ *Trans. Am. Soc. Steel Treating*, **9**, 717 (1926).

² SAUVEUR, *Trans. Am. Inst. Mining Met. Eng.*, **73**, 859 (1926).

internal strains. These reduce to two general phenomena associated with hardness: (1) distortion and (2) slip resistance by the keying action of small particles.

Bernal¹ points out that a pure metal crystal, when stressed, yields not by cleavage or fracture but by the formation of glide planes in which layers of atoms slip over each other with little loss of energy. It is possible that in the ideal case of an absolutely pure metal with infinitely small stress it would lose no energy at all in gliding. Its behavior would, in fact, be that of a liquid, and a pure metal crystal would differ from a liquid only by the regular ordering of its atoms. Actually, however, when a certain amount of gliding has taken place, a hardening sets in which prevents further gliding. This hardening is almost certainly due to a distortion of the lattice elements. What appears to be an exactly similar distortion is produced by the presence of foreign atoms in solid solution. (It is, of course, to these properties of hardening by cold-working and alloying that metals owe their technical importance.) The distortion of the lattice manifests itself in a variety of ways described in Chap. XXI; as well as the mechanical hardening there is always a very large increase in the electrical resistance, but what shows most clearly the nature of the change is the x-ray evidence. In a strained or impure metal crystal the reflection of a monochromatic ray in a crystal plane, instead of occurring extremely sharply over a width of a few seconds of arc, occurs more and more diffusely as the strain is increased. This is an indication that the atoms no longer lie in absolutely plane parallel layers but that there is a more or less irregular displacement of certain atoms from the average planar position. A similar but periodic displacement is produced by the temperature vibration of the atoms, and indeed on looking at an x-ray photograph of a metal that shows very blurred lines it is impossible without further information to know whether they are due to impure crystals, distorted crystals, or hot crystals. It is possible that solid solutions do not represent stable states but metastable ones; that given sufficient atomic mobility, or sufficient time, all solid solutions would separate out into their constituent compounds or form regular superstructures. From this point of view the solid solution is a mere regular form of a glass.

¹ *Trans. Faraday Soc.*, **25**, 370 (1929).

Age-hardening.—Several alloy systems, notably Al-Cu-Si (duralumin), Au-Cu (intermediate state of AuCu), Ag-Cu, Cu-Be, Cu-Fe, low-carbon (armco) iron, etc., are characterized by hardening with time after a heat-treatment. Figure 196 shows the variation of hardness with time of mixed crystals of silver and copper as measured by Agnew, Hanan, and Sachs.¹

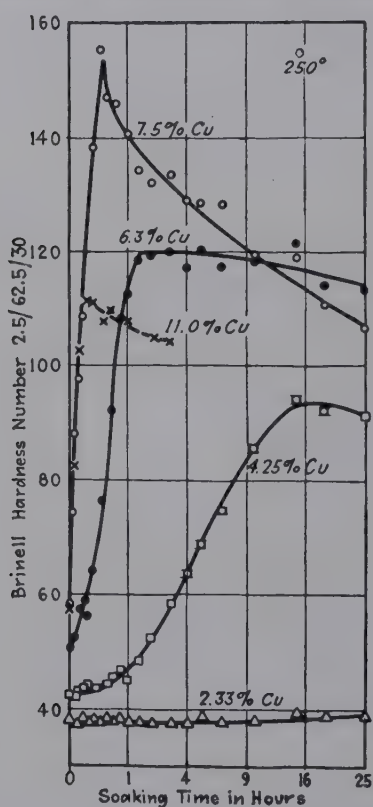


FIG. 196. —Curves showing age-hardening of copper-silver alloys.

The alloy was quenched from 770°C. and then held at a temperature of 250°C. This age-hardening has great technical significance, since an alloy may be fabricated while in easily worked condition and then the product subsequently hardened with aging. Difficulties are, of course, encountered even at room temperatures; for example, if steel sheets are not used for a considerable period after manufacture, they will form far less easily. The phenomenon of age-hardening therefore has been subjected to numerous investigations. If gold-copper mixed crystals containing about 50 atomic per cent gold with entirely random distribution of atoms above 425° are cooled, an intermediate state can be observed from x-ray patterns. The unit cell has the tetragonal form (AuCu) of the final equilibrium state, but in a part of the lattice the copper and gold atoms have definite arrangement and in the remainder are completely random. This inhomogeneous irregularity is to be distinguished from the true homogeneous substitutional solid-solution type. The intermediate state is characterized by great hardness. By long heating under 428° the much softer, entirely definitely

¹ *Z. Physik*, 66, 350 (1930).

arranged tetragonal state is reached. Mild steel-hardening may be due to Fe_4N , FeO , Fe_3C , AlN (in the presence of a trace of aluminum). Diffraction lines for CuAl_2 have been observed after long heat-treatment of duralumin. The theory of hardness has been based on the conception of separation of very small colloidal particles which tend to key slip on planes. However, newer x-ray researches seem to demonstrate that at the point of greatest hardness no new lattice is necessarily observed. There may be a slight broadening of x-ray lines, such as might be produced in very slight deformation, but no change in lattice

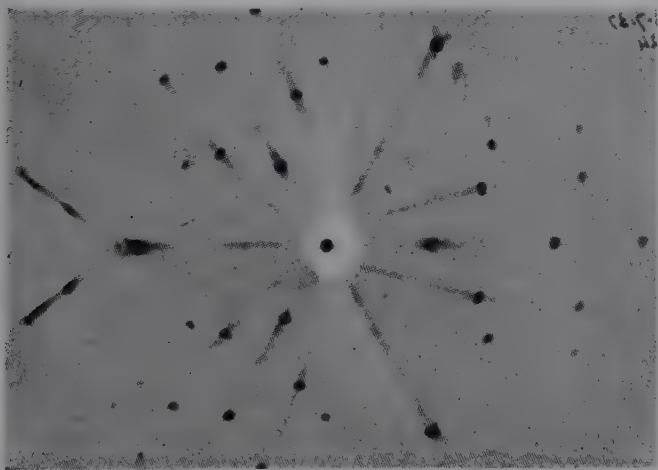


FIG. 197.—Laue pattern showing definite effects (satellite streaks) of age-hardening of aluminum alloy. (*Preston.*)

dimension of the old lattice is observed as ought to be expected from concentration changes, due to separation of a new phase. Upon the basis of magnetic measurements on copper-iron specimens Tammann presented the hypothesis that, before the separation of a new phase, some kind of grouping within the coherent old lattice of the chemically different atoms occurs which in an unknown manner causes increase in hardness. This agrees with the actual observation of inhomogeneous atomic distribution in the intermediate state of AuCu and with the most recent observations on duralumin at maximum hardness by Preston.¹

¹ *Proc. Royal Soc. (London)*, **167**, 526 (1938).

In this classical x-ray investigation with single crystals of Al-Cu alloy compared with pure aluminum, age-hardening is accompanied, before the slightest evidence of CuAl_2 precipitation, by the appearance of satellite streaks resolved into spots diverging to larger angles from each Laue spot (see Fig. 197). These effects are theoretically reproduced by a simple model of a pair of

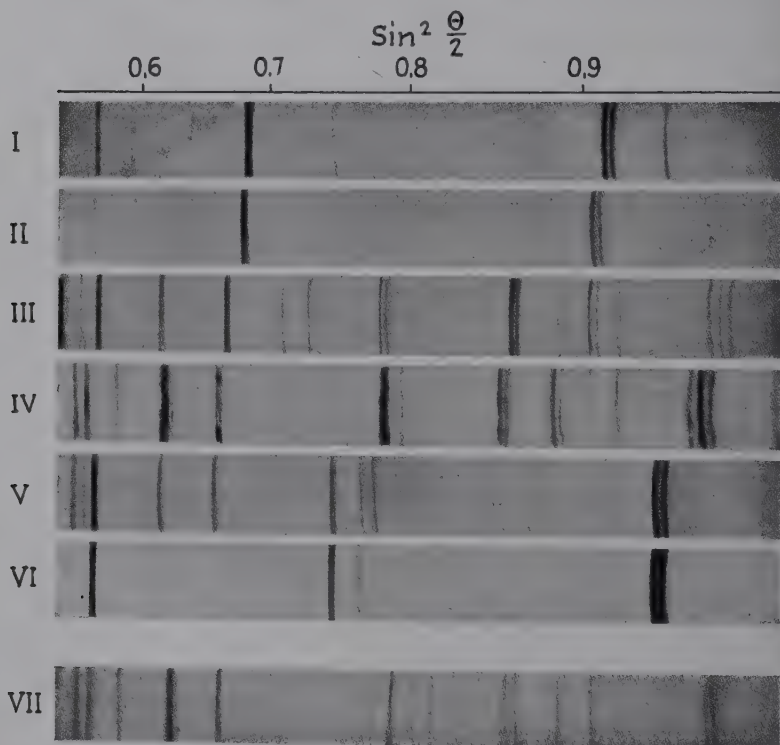


FIG. 198.—Powder patterns of metals and alloys of the iron-tungsten and iron-molybdenum systems. I, Fe; II, Fe, saturated with W; III, Fe_2W ; IV, Fe_3W_2 ; V, $\text{Fe}_3\text{W}_2 + \text{W}$; VI, W; VII, Fe_3Mo_2 .

crossed gratings in two dimensions which leads to the conclusion that age-hardening is associated with the segregation of copper atoms on the 100 planes of the crystal, the quantity still being insufficient to precipitate CuAl_2 as a separate phase. The structural changes in duralumin airplane propellers, studied by the writer and associates, with the accelerating effects of fatigue are described in Chap. XXII.

Polycomponent Alloy Systems.—The complications that are introduced immediately in passing from binary to ternary systems, not to mention more complex systems, are at once apparent. In the x-ray analysis of ternary alloys, there are involved three binary and the whole range of ternary systems represented by all points on the interior of a triangular diagram. As a result only a beginning has been made—but a remarkably brilliant one, particularly in researches at the National Physical Laboratory and the University of Cambridge in England and in the Westgren Laboratory in Sweden. It is not possible here to describe the methods by which a comparatively limited number of specimens and diffraction patterns suffice to establish the essential facts of the entire system.

Of particular significance are the ternary magnetic alloys which are discussed in a succeeding paragraph.

Alloy Steels.—The success attendant upon the complete interpretation of the highly complex x-ray diffraction patterns obtained with alloy steels within the past few years has been truly amazing. A rationally scientific explanation can now be given to the properties of various alloy steels in terms of ultimate constitutions and structure. Ranges of stability of phases are defined, and predictions of the constitution and properties of new alloys are nonempirically made. A very few of all the facts that x-rays have disclosed are enumerated simply as an indication of achievements and possibilities:

1. The identification in the iron-tungsten system of Fe_2W (hexagonal) and Fe_3W_2 (trigonal, 40 atoms per unit cell) and of Fe_3Mo_2 corresponding to Fe_3W_2 in the iron-molybdenum system (Fig. 198).¹
2. Studies of the iron-chromium-carbon system and stainless steel² with the following conclusions:
 - a. Iron and chromium form a continuous series of solid solutions.
 - b. Phases in the iron-chromium-carbon system:
 - α -metal.
 - γ -metal.
 - Cementite, $(\text{Fe}, \text{Cr})_3\text{C}$, in which chromium may rise to 15 per cent.
 - Cubic chromium carbide, $(\text{Cr}, \text{Fe})_4\text{C}$, in which chromium may be substituted by iron up to 25 per cent.
 - Trigonal chromium carbide, $(\text{Cr}, \text{Fe})_7\text{C}_3$, with iron up to 55 per cent.

¹ ARNFELT, "Carnegie Scholarship Memoirs, Iron and Steel Institution," Vol. XVIII, p. 1, 1928.

² WESTGREN, PHRAGMEN, and NEGRESKO, *J. Iron and Steel Inst.*, **117**, 383 (1928).

Orthorhombic chromium carbide, $(\text{Cr}, \text{Fe})_3\text{C}_2$, with only a few per cent of iron substituting.

- c. In annealed ball-bearing steel the chromium is contained in cementite. "Double carbide" causing rejection, due only to unequal distribution of cementite.
 - d. Carbide in stainless steel is cubic chromium carbide saturated with iron (35 per cent).
 - e. Steel for dies (17 per cent nickel, 11 per cent chromium, 2 per cent carbon) contains trigonal chromium carbide with more than half of the chromium substituted by iron.
 - f. Ferrochromium (60 per cent chromium, 5 per cent carbon) peritectic alloy of cubic chromium carbide with iron substituting partially, α -metal, and some trigonal carbide.
3. The identification in high-speed steel of a true double carbide $\text{Fe}_4\text{W}_2\text{C}$, face-centered cubic, $a = 11.04$ A.U., containing 112 atoms per unit cell.
 4. The identification and proof of Fe_4N , important in case-hardening of iron by nitrogen, with the iron on a face-centered cubic lattice, $a = 3.789$ A.U. and the nitrogen at the center.

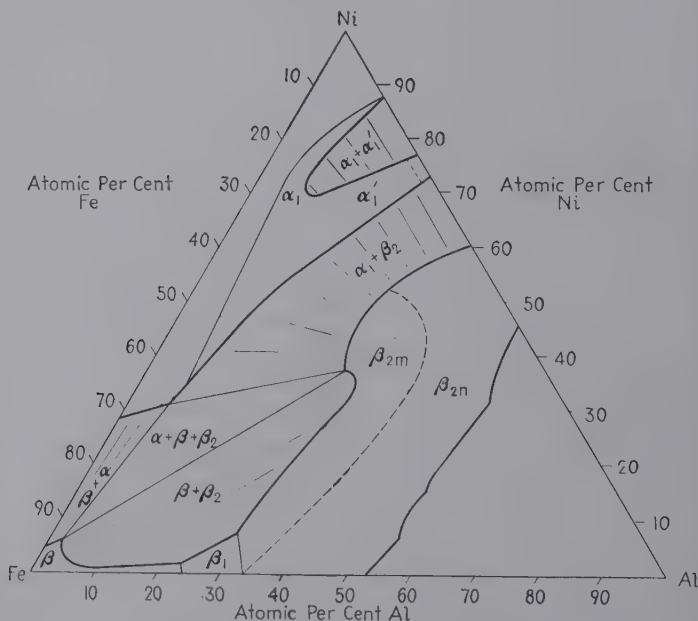
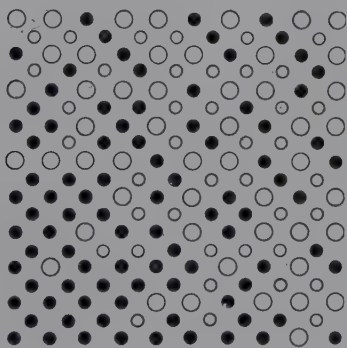
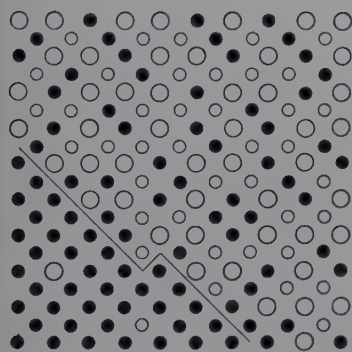
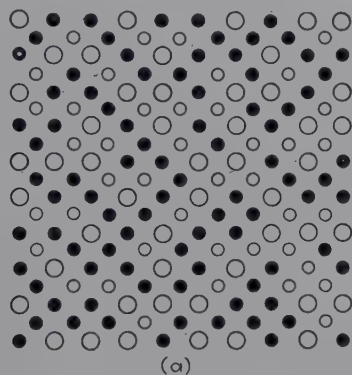


FIG. 199.—Ternary Fe-Ni-Al diagram. (Bradley and Taylor.)

Crystal Structure and Magnetism.—The fact that α -iron is magnetic and β -iron nonmagnetic, though x-rays detect no structural discontinuity between these, seems to indicate that magnetic properties are not functions of the arrangement of atoms

in space. However, Persson in Westgren's laboratory demonstrated that the magnetic Heusler alloys (copper-manganese-aluminum) always show the x-ray diffraction lines of the β phase. In this the basic lattice is body-centered cubic, upon which is superposed a face-centered cubic lattice of aluminum atoms with



● Fe ○ Ni ○ Al

FIG. 200.— Fe_2NiAl after different heat-treatments. (a) Quenched 1200° , one crystal; Fe atoms at random. (b) Slow cooled, two crystals; Fe-rich crystal contracts in volume by 1 per cent. (c) Special heat-treatment for high coercivity, Fe atoms in "island"; no sharp boundary. (*Bradley and Taylor.*)

twice the dimensions of the basic lattice. Hence the unit cube contains 16 atoms, of which 12 are copper + manganese and 4 aluminum. The formula $(\text{Cu}, \text{Mn})_3\text{Al}$ is substantiated by the x-ray results. It is further essential that the concentration of manganese must be above a limiting value for magnetic properties to develop. In other words, the pattern for the

β phase may appear for non-magnetic specimens if manganese is insufficient.

Bradley and Taylor¹ used x-ray patterns in masterly fashion to characterize permanent magnets of iron, nickel, and aluminum. Figure 199 is the ternary diagram established from the structural studies. The two-phase area $\beta + \beta_{2m}$ includes all compositions that are suitable for manufacture of permanent magnets, with Fe_2NiAl (indicated by a dot) typical. The two-phase area is represented with tie lines. An alloy lying on any such line splits up into two constituents, the compositions of which are given by the ends of the lines. For example, Fe_2NiAl which is a single phase at high temperatures breaks up into $\text{Fe}_{38}\text{NiAl}$ near pure iron and into $\text{Fe}_6\text{Ni}_{17}\text{Al}_7$ near the center of the diagrams on slow cooling; thus an iron-rich body-centered cubic constituent β splits off from the main portion β_2 , also body-centered cubic. But the maximum magnetic coercivity is obtained not by (1) quenching of Fe_2NiAl or by (2) slow cooling and separation into two phases, but by (3) a special controlled cooling. In Fig. 200 are shown the atomic arrangements deduced directly from x-ray patterns for these three cases: (1) one lattice, nickel and aluminum atoms in definite positions and iron atoms at random; (2) two lattices (double diffraction lines) for nearly pure iron atoms and for original lattice diminished in iron atoms; (3) one lattice but with non-uniform atomic distribution (indicated by characteristic line broadening). Here the iron atoms have begun to separate, forming only small aggregates without definite boundaries. These small islands of iron cannot break away to form separate crystals when the alloy is cooled at a definite rate. Being still forced to conform to the dimensions of the parent lattice, the iron atoms are held apart under a condition of immense strain—and therein lies the explanation of the remarkable properties of Fe_2NiAl as a permanent magnet.

¹ "Physics in Industry," p. 91, 1937.

CHAPTER XIX

THE CRYSTALLINE AND MOLECULAR STRUCTURES OF ORGANIC COMPOUNDS

The examination of the crystals of organic substances represents the newest phase of the still infant science of x-ray crystal analysis. This hesitancy among experimenters is in one sense surprising, inasmuch as the organic chemist long ago introduced the simplifying and logical conceptions of spatial arrangements of atoms which have been the strength of the science as compared with the great complexities with which inorganic chemists have been confronted. On the other hand, crystallographic examination has shown that the great majority of organic compounds crystallize in the very classes of low symmetry whose diffraction effects are the most difficult to interpret; and good crystals for analysis are usually impossible to obtain. It stands to the matchless credit of Sir William Bragg, always a leader, that he undertook the problems fearlessly. His skill in combining x-ray data with other authentic information, to show that whole molecules instead of atoms are the units placed at the points of the lattice and to arrive at a final solution of structural problems, has given to organic chemistry the solid experimental facts of structure that have been hoped for.

Sir William Bragg¹ speaks of another point of interest in these compounds as follows:

Apart from the interest in determining structures of this kind, there is also the question of the "minor" ties which bind the molecules together; not so much the ties that bind the atoms together in the molecule. The ties which bind molecule to molecule are perhaps of a different and weaker nature and yet must be of immense importance in the constitution of the world, for after all a great deal of nature's work is done at moderate temperatures and simply by the laying of one molecule against another.

¹ *Chem. Ind.*, **45**, 245 (1926).

The Carbon Structures.—The structure of the compounds of carbon must find ultimate prototypes in the structure of crystalline carbon; of this there are two varieties: the diamond, crystallizing in the tetrahedral cubic system with each carbon very definitely at the center of four other equidistant carbons at the corners of a tetrahedron; and graphite, with a lower hexagonal symmetry. "Puckered" six-carbon rings are easily identified in the diamond lattice (Fig. 201). After con-

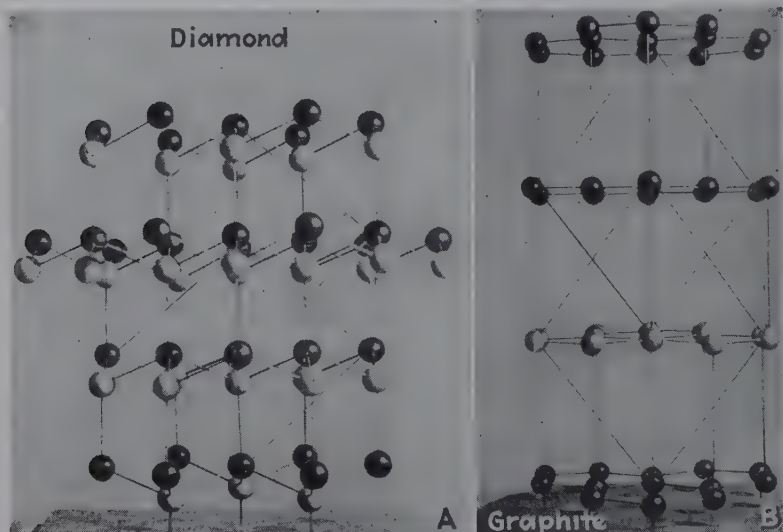


FIG. 201.—Comparison of crystal models of diamond and graphite. (Courtesy Central Scientific Company.)

siderable controversy Bernal¹ succeeded in proving from x-ray data that the carbon atoms in graphite are flattened into a plane so that three of the carbon neighbors remain at somewhat smaller distance from the central atom than in the diamond tetrahedrons (1.42 A.U. as against 1.54 A.U. in diamond) and the fourth is at a greater distance (3.40 A.U.) in the next layer (Fig. 201). In other words, in graphite the atom has three strong bonds coplanar or very nearly so with itself and one weak bond at right angles to these bonds. This bond may be easily ruptured so that one layer will slide over another to account for the lubricating properties of graphite. The peculiar lamellar structure also allows special types of reaction to occur as shown

¹ *Proc. Roy. Soc. (London)*, **106A**, 749 (1924).

by Hofmann and Frenzel.¹ Graphite reacts with alkali metals to form stoichiometric compounds of the type C_8K and $C_{16}K$. X-ray diffraction data show no change in the distance between carbon atoms in the same layers, but the distance between layers increases from 3.38 A.U. in graphite to 5.34 in C_8K . Treatment with mercury regenerates graphite. In graphitic acid this distance between layers is 6 A.U. which increases to 11 A.U. by swelling with water.

One of the most interesting questions in the whole science has been whether the carbon atoms in ring compounds, *e.g.*, aromatic series, lie in one plane, as in graphite and as the organic chemist has represented structures on paper, or are staggered as in diamond. A satisfactory answer to this question has been given only very recently; even yet it cannot be maintained that the shape and dimensions of the benzene ring found for some compounds are necessarily the same in all aromatic compounds. A few of the important steps leading to the final conclusion will be outlined in a later section.

The X-ray Analysis of Organic Molecules.—The general methods of interpretation of x-ray diffraction patterns of crystals outlined in Chap. XIV reach their highest point in the direct delineation of the structure of the organic molecule. The unit cell and the dimensions are evaluated without much difficulty. The intensities give a measure of the extent to which electrons are distributed in the structure. Since the crystal is a periodic structure built up by the repetition of identically arranged molecules in all directions, this periodic medium can be analyzed into a Fourier series of harmonic terms, the periods of which correspond to the spacings of all possible crystal planes. On account of uncertainties introduced by lack of information on phase constants, assumptions and approximations and auxiliary data already described may be necessary, finally leading to a result that is an x-ray picture of the molecules. The complete expression of structure is given by a three-dimensional series whose terms correspond to all possible crystal planes. Such a series is difficult to evaluate numerically owing to the large number of terms; consequently in practice a two-dimensional series is usually employed, which represents a projection of the structure in a given direction. The coefficients in such a

¹ *Kolloid-Z.*, **58**, 8 (1932).

series correspond to the reflections from all the crystal planes that are parallel to the axis along which the projection is made. In such projections of a structure some atoms are often hidden behind others, but the complete structure can usually be worked out by piecing together the results of two or more projections along different crystal axes. The electron density is calculated by summing up the double series at many points taken close together on the projection, and the results are graphically represented by drawing contour lines to pass through points of equal electron density. And the result is the complete contour map of the molecule. The first contour line is usually dotted and represents a density of 1 electron per square angstrom unit. The remaining lines are drawn at unit intervals, so that peaks for usual organic molecules represent 6 or 7 electrons per square angstrom unit. This is the remarkably expressive method now applied for the delineation of the molecule, usually applicable to structures containing closed-ring systems where the possible configurations of the molecule are limited. Figure 214 presents the contour map, plotted as a projection of the double Fourier series for durene, 1,2,4,5-tetramethyl benzene; Fig. 202 shows the unusual structure of oxalic acid dihydrate; and in Fig. 215 appears the crowning achievement of complete analysis, the very large and complex molecule of phthalocyanine, a blue dye. In the simple case of durene the six carbon atoms forming the benzene ring and the four symmetrically attached methyl groups are easily apparent. Thus the structural formula of the organic chemist not only is verified but in a sense is registered by the organic molecule itself. It is recognized at once that sometimes the molecule is inclined at a considerable angle to the plane of projection, and thus the contour map is a foreshortened version of a molecule that may actually be perfectly planar, as determined by projections of other zones of reflection.

Molecular Dimensions.—The x-ray results on these molecular structures involve quite directly interatomic distances, rather than atomic radii, since there is such a variation in unsymmetrical coordination. Experience has shown that the distance between two given atoms linked by a given type of bond is closely constant throughout all organic compounds. It is essential therefore to list these bond lengths, which, when com-

TABLE XLVII.—BOND LENGTHS

| Compound | Bond type | Length, A.U. |
|--------------------------------|-----------------------------|-----------------|
| Diamond..... | C—C aliphatic (true single) | 1.54 |
| Paraffin chains..... | C—C aliphatic (true single) | 1.54 |
| Ethylene..... | C=C (true double) | 1.34 |
| Carbon suboxide..... | C=C | 1.30 |
| Acetylene..... | C≡C (true triple) | 1.20 |
| Tolane..... | C≡C | 1.19 |
| Graphite..... | C—C | 1.42 |
| Benzene..... | C—C aromatic | 1.42 |
| Naphthalene..... | C—C aromatic | 1.41 |
| Anthracene..... | C—C aromatic | 1.41 |
| Chrysene..... | C—C aromatic | 1.41 |
| Dibenzyl..... | C—C aliphatic | 1.58 |
| | C—C aromatic-aliphatic | 1.47 |
| | C—C aromatic | 1.41 |
| Benzoquinone..... | C—C ring | 1.50 |
| | C=C ring | 1.32 |
| Hexamethylbenzene..... | C—C aromatic | 1.42 |
| | C—C aromatic-aliphatic | 1.48 |
| Durene..... | C—C aromatic | 1.41 |
| | C—C aromatic-aliphatic | 1.47 |
| <i>p</i> -Diphenylbenzene..... | C—C aromatic | 1.42 |
| | C—C between rings | 1.48 |
| Diphenyl..... | C—C aromatic | 1.42 |
| | C—C between rings | 1.48 |
| Polyoxymethylene..... | C—O | 1.49 |
| Methyl ether..... | C—O | 1.42 |
| Benzoquinone..... | C=O | 1.14 |
| Urea..... | C=O | 1.25 |
| Oxalic acid dihydrate..... | C—O } resonance | { 1.24 |
| | C—OH } resonance | { 1.30 |
| | O—O H bond | 2.52 |
| | O—O H bond | 2.85 |
| Resorcinol..... | C—OH | 1.36 |
| Pentaerythritol..... | C—OH | 1.46 |
| Urea..... | C—N | 1.37 |
| Thiourea..... | C—N | 1.37 |
| | C=S | 1.64 |
| Hexamethylenetetramine..... | C—N | 1.42 |
| Phthalocyanine..... | C—N } resonance | 1.34 |
| | C=N } resonance | |
| Hexachlorbenzene..... | C—Cl | 1.86 |
| Hexabrombenzene..... | C—Br | 1.94 |
| Iodoform..... | C—I | 2.10 |
| Di-iodocyclohexane..... | C—I | 2.12 |
| | N—O | 1.38 |
| Nitric oxide..... | N=O | 1.15 |
| <i>p</i> -Dinitrobenzene..... | N=O | 1.20 |
| Nitrogen..... | N≡N | 1.06 |

bined with information on bond angles, permit construction of a molecular model. The true single bond between two atoms, for example, —C—C— , has one value, the double bond —C=C— another, the triple bond $\text{—C}\equiv\text{C—}$ another. Thus the measurement of interatomic distances gives direct evidence of the type of binding even in very complex structures where chemical evidence is entirely inadequate. Intermediate bond lengths then represent resonance between two simple types—and we may calculate that a given bond may be, for example, 20 per cent double and 80 per cent single bond. Examples will be illustrated under discussion of specific structures. In Table XLVII are listed the most accurately measured bond lengths in a wide variety of compounds.

Molecular Shape.—Because of rotation around bonds and flexibility of structure it is not always possible from chemical evidence to predict the exact shape of molecules, whether flat or puckered or whether in diphenyl, dibenzyl, etc., the aromatic nuclei are parallel or turned at an angle. Such features must be determined by detailed analysis of the distribution of neighboring molecules in the structure.

Intermolecular Binding.—The third type of information concerning organic crystals, almost unique to the x-ray method and no less important than the information concerning interatomic binding within the molecule, is disclosure of the type of force responsible for molecular coherence in the crystal lattice. This may vary from strengths almost as great as homopolar bonds in hard, brittle high-melting compounds, to the weak residual, or van der Waals, force. For convenience molecular crystals may be classified as in Table XLVIII both in terms of molecular shape and of three types of intermolecular binding force increasing in strength in the order: (1) apolar, or residual; (2) polar linkage between molecules with local dipoles packed so that adjacent dipoles neutralize each other (—OH , =NH , =O groups); (3) ionic (acids, bases, and salts).

The Results of Crystal Analysis of Organic Compounds.—A few years ago all x-ray data on organic compounds could be considered in very little space, and in fact the International Critical Tables, Vol. I, listed only about 15 organic compounds for which space-groups had been assigned. With the great improvements in technique and in methods of interpretation a very large

number of organic compounds have now been analyzed for crystalline and molecular structures with results just as complete and convincing as the examples already cited. Ewald and Her-

TABLE XLVIII

| Molecular shape | Type of intermolecular binding force | | |
|-----------------------------------|--|--|--|
| | Apolar (residual) | Polar ¹ | Ionic |
| Simple symmetrical molecules | Inert gases Diatomic gases Hydrides NH ₃ , CN ₄ , etc. Polyhalides CCl ₄ Simple hydrocarbons Basic beryllium acetate | Urea, thiourea Hexamethylene-tetramine Pentaerythritol | Simple alkyl ammonium salts Oxalic acid ¹ and oxalates Simple amino acids |
| Long molecules | Long-chain aliphatic hydrocarbons Cycloparaffins Plastic sulfur Rubber | Long-chain alcohols, ketones, esters | Fatty acids, soaps Long-chain alkyl ammonium salts Fibrous protein |
| Flat molecules | Rhombic sulfur Aromatic hydrocarbons Phthalocyanines Cyanuric triazide | Halogen, NO ₂ , NH ₂ -derivatives of aromatic hydrocarbons Phenols, quinones Sugars Sterols | Aromatic acids and salts Aromatic bases and salts Methylene blue halides |
| Giant three-dimensional molecules | | | Globular proteins |

¹ Includes structures, especially with OH groups, bonded by hydrogen bridges: pentaerythritol, oxalic acid dihydrate, resorcinol, sugars, etc.

mann have classified these into 64 main types already, with many others still to be fitted into the scheme. Little would be gained in this book by presenting these experimental data, since even tabulation would be greatly extended and since they are to be

found in full in the "Strukturbericht." Consequently only some general conclusions of general interest to the chemist will be considered briefly.

1. *Inorganic Types with Organic Substituted Radicals.*—The alkyl ammonium halides, principally studied by Wyckoff and Hendricks, are the chief representatives. In almost every case a very clear relationship exists between the structure of the compound and the simpler compound in which a metal atom has been replaced by a radical. For example, triethylammonium iodide is like wurtzite, ZnS , with the radical replacing zinc atoms; the length of the chain, of course, causes a large decrease in the axial ratio. Tetramethylammonium iodide is similarly related to phosphonium iodide (type B10), methylammonium iodide to rock salt, and methylammonium chloride to cesium chloride. A very curious result is that in the latter two cases the chains which replace one of the ions in the simple salts evidently appear to be linear rather than zigzag, in order to account for observed symmetry and spacings. The C—C separation is 1.26 A.U. instead of 1.54 expected for an aliphatic chain. However, it is now established that this structure is due to free rotation of the carbon chain around its length and the 1.26 spacing is the projection on the chain axis of the true inclined bond of length 1.54. For at lower temperatures where the rotation does not persist there is a polymorphic transition to a larger unit cell of lower symmetry, consistent with the usual zigzag chain. Several derivatives of hexachloroplatinates and hexachlorostannates, in which these ions are octahedrally coordinated, also have structures that might be predicted from the results on metal ion salts of these complex anions. The chief interest, of course, is in the effect on the symmetry of the ammonium group of substituting various combinations of alkyl groups.

2. *Symmetrical Methane Derivatives.*—The tetrahedral form of these compounds is the point of greatest interest. Methane crystallizes in the face-centered cubic lattice of parallel CH_4 tetrahedra; tetramethyl methane has the diamond cubic structure, and tetraiodomethane is a simple cubic lattice of parallel tetrahedra. X-ray and electron diffraction researches have shown clearly the distortion of the tetrahedra that results when the hydrogen atoms are unsymmetrically replaced by halogens or other groups. Even carbon tetrabromide, which crystallizes in

two modifications with a tetrahedral molecule for the lower temperature modification, loses symmetry at higher temperatures and forms a monoclinic lattice from bimolecules. In tetranitromethane, although cubic, one of the nitro groups evidently differs from the other three in space and the formula is perhaps correctly written $\text{O}=\text{N}-\text{O}-\text{C}(\text{NO}_2)_3$.

Pentaerythritol, $\text{C}(\text{CH}_2\text{OH})_4$, a tetragonal crystal, probably has the distinction of having been investigated more repeatedly than any other organic compound. It illustrates the case in which very slight differences in interpretation of x-ray and optical data lead to widely different molecular structures. In the early work it was concluded that the carbon atoms were all coplanar or formed a flat pyramid. Further work has demonstrated that it is impossible from the x-ray data to distinguish between symmetry classes $\bar{4}$ or 4 (tetrahedral). Researches on crystal growth and solution, etch figures, pyro- and piezoelectricity have given preponderance to the tetrahedral molecule and the space-group $I\bar{4}$. Each OH group is attached to its CH_2 group by a bond that makes a nearly tetrahedral angle with the $\text{C}-\text{CH}_2$ link and is so directed that the four OH groups lie at the corners of a square. Four molecules are linked together by the hydrogen bonds of four OH groups in a square 2.69 A.U. on a side. Besides pentaerythritol, the tetracetate and tetranitrite are also body-centered tetragonal with the same symmetry class, but they differ in the orientation of the center molecule with respect to the molecules at the corners of the unit cell. The compounds $\text{C}(\text{C}_6\text{H}_5)_4$, $\text{Si}(\text{C}_6\text{H}_5)_4$, $\text{Ge}(\text{C}_6\text{H}_5)_4$, $\text{Sn}(\text{C}_6\text{H}_5)_4$, and $\text{Pb}(\text{C}_6\text{H}_5)_4$ all have the same tetrahedral molecular structure and lattice as pentaerythritol tetranitrite.

3. *Unsymmetrical Methane Derivatives without Chain Character.* Chief representatives of this class thus far studied are iodoform, urea and its derivatives, and some formates. In iodoform the iodine atoms form a hexagonal packing of spheres. The carbon and hydrogen atoms enter octahedrally the holes in this lattice, so that the molecules CHI_3 form the unit. In urea, $\text{OC}(\text{NH}_2)_2$, the molecule consists of a central atom circumscribed by an almost equilateral triangle of one oxygen and two nitrogen atoms. There are thus chains of the molecules parallel to the c axis or networks perpendicular. Thiourea is orthorhombic with four molecules per unit cell, instead of tetragonal with two mole-

cules per cell for urea, and the carbon atoms are surrounded by the sulfur and two nitrogen atoms in the form of a flat pyramid. The nitrogen atoms are equivalent, so that the correct formula

in the solid state is $\text{S}=\text{C} \begin{array}{l} \nearrow \text{NH}_2 \\ \searrow \text{NH}_2 \end{array}$ and not $\text{HS}-\text{C} \begin{array}{l} \nearrow \text{NH}_2 \\ \searrow \text{NH} \end{array}$.

4. *Short Aliphatic Chains with Symmetry about a Central C—C Linkage*.—Numerous compounds of this type have been investigated, of chief interest being ethane and its derivatives and oxalic, maleic and fumaric, and tartaric acids and their derivatives. Ethane, C_2H_6 , and diborane, B_2H_6 , crystallize alike with hexagonal cell. The dimensions for the former are $a = 4.46$, $c = 8.19$ A.U., distance C—C in the same molecule 1.55 A.U., C—C, different molecules, 3.5 A.U., distance molecule center to center 4.46 A.U. Of the derivatives C_2Cl_6 , C_2Br_6 , $\text{C}_2\text{H}_4\text{Br}_2$ (two modifications), $\text{C}_2\text{H}_5\text{F}$, $\text{C}_2\text{Cl}_3\text{Br}_3$, and $\text{C}_2\text{H}_4(\text{CH}_3)_2$ (two modifications) are isomorphous-orthorhombic, space-group *Pnma*; $\text{C}_2(\text{CH}_3)_4\text{Br}_2$ and $\text{C}_2\text{Br}_4(\text{CH}_3)_2$ have isomorphous tetragonal structures; $\text{C}_2(\text{CH}_3)_5\text{OH}$ is orthorhombic with eight molecules per unit cell. Further work is required to understand exactly the distortions of carbon tetrahedra caused by substituent groups and the temperature conditions of stability of polymorphic forms.

Fumaric acid is distinguished from its isomer maleic acid in showing six molecules per unit cell, an unusual case of association or polymerization. Outstanding among early work are Astbury's analyses of *d*-tartaric acid and *dl*-tartaric acid (racemic acid).¹ The first is monoclinic, $a = 7.70$, $b = 6.04$, $c = 6.20$ A.U., and $\beta = 100^\circ 17'$, with two molecules to the unit cell; the second is triclinic, $a = 14.82$, $b = 9.74$, $c = 4.99$ A.U., $\alpha = 82^\circ 20'$, $\beta = 122^\circ 50'$, and $\gamma = 111^\circ 52'$, with four molecules to the unit cell. Cleavage occurs in the [100] direction where the OH groups touch.

The power of both crystals and solutions of tartaric acid to rotate the plane of polarized light is to be found in a spiral arrangement of the atoms. In the crystal two such spirals exist, one connected with the four central carbon atoms of the molecule and the second resulting from the way in which the molecules are combined in the crystal unit. These two spirals are in opposite

¹ *Proc. Roy. Soc. (London)*, **102**, 506; **104**, 219.

directions, so that the rotary power of the solid is determined by the difference. In solution, of course, the second spiral structure is absent, and the rotatory power depends only on the central carbon atoms. In racemic acid spirals are exactly balanced, so that there is internal compensation.

5. *Short Aliphatic Chains without Symmetry around a Central C—C Linkage*.—Examples of this classification are metaldehyde, aldehyde ammonia, acetamide, basic beryllium salts of fatty acids, and other metal salts including acetylacetone compounds of trivalent metals. These last are isotrimorphic: α , monoclinic, β , rhombic, and γ , rhombic. The iron compound of the γ -modification has 16 molecules per unit cell of the unusually large dimensions $13.68 \times 15.74 \times 33.0$ A.U.

6. *Special Ring Compounds*.—Hexamethylenetetramine, $C_6H_{12}N_4$, was probably the first organic compound to be subjected to a complete structure determination.¹ It is body-centered cubic with two molecules per unit cell. Each nitrogen atom is bound to three CH_2 groups, and each carbon atom to two nitrogen and two hydrogen atoms, forming so highly symmetrical a structure that dipole effects must be very slight.

7. *Oxalic Acid*.—The structure of oxalic acid dihydrate deserves special consideration as a typical case of successful x-ray analysis (Zachariasen, 1934; Robertson and Woodward, 1936). Figure 202 shows the projected Fourier contour map, the linking of molecules through H_2O , and the planar configuration of the $C_2H_2O_4$ molecule. Of the two oxygen atoms attached to each carbon atom one is at a distance of 1.24 A.U. (type 1) and one at 1.30 A.U. (type 2). This difference is too small to account for a clear distinction between $C=O$ and $C-OH$, and so it represents a partial resonance between the two bindings. The unexpected planar form is explained by the fact that rotation around the $C-C$ axis is restricted by conjugation of double bonds and the short spacing 1.43 instead of 1.54 A.U. Thus this bond has at least 30 per cent double-bond property. This explains why oxalic acid can be oxidized quantitatively with $KMnO_4$ to CO_2 , whereas in other compounds a carboxylic acid is the usual end product. The linking of molecules by water is such that each H_2O molecule is bound to two oxygen atoms of the 1.30 spacing ($C=O$) and one oxygen atom of the 1.24 spacing ($C-OH$), from

¹ DICKINSON, and RAYMOND, *J. Am. Chem. Soc.*, **45**, 22 (1923).

three different molecules. The H_2O —O bond length of the first kind is 2.85 and of the second 2.52 A.U.—the same value usually found to exist between oxygen atoms bound by a hydrogen bond. Thus oxygen atoms of type 1 are bound to only one H_2O as demanded by the hydrogen bond, while the oxygen atoms of type 2 are bound to two H_2O molecules by much weaker forces.

Similarly α and β forms of anhydrous oxalic acid (rhombic and monoclinic) have planar molecules held together by hydrogen bonds, as is also true for potassium and rubidium oxalates. In $(\text{NH}_4)_2\text{C}_2\text{O}_4 \cdot \text{H}_2\text{O}$ Hendricks and Jefferson found that the C—C distance is 1.58 A.U. and that, having no double-bond character, the two CO_2 groups in the molecule are no longer coplanar but inclined 28 deg. to each other.

Long-chain Compounds.—Out of the x-ray studies of the aliphatic series, conducted largely by Müller and Shearer in Bragg's laboratory and by Trillat and Thibaud in de Broglie's laboratory, have come some of the most striking results of the science; these have been achieved in the face of such difficulties as the inability to use the simpler compounds (which are liquid), or to obtain single crystals of the higher members of the series, thus necessitating the use of the powder method except in a few cases.

The great simplifying phenomena discovered in the study of the higher paraffin hydrocarbons, acids, esters, salts or soaps, ketones, etc., were that the unit cells into which the molecules, long pictured by chemists as chains, are packed have one side which is very much longer than the others and that this side grows in a uniformly constant manner as the number of carbon atoms increases. This dimension must, therefore, correspond to the length of the molecule. The other two dimensions remain nearly constant throughout the series; hence, they must correspond to the essentially constant cross section of a chain of carbon atoms.

For the usual diffraction experiments in which single crystals are not obtainable, a small flake of the substance is flattened on a glass or metal backing or melted or poured on a flat surface and placed on an oscillating-type spectrograph. On the film is obtained a single strong line repeated through many orders, corresponding to the long dimension and varying with the number of carbon atoms, and lines corresponding to the smaller side spacings. The x-rays measure the perpendicular distance between

successive identical planes in the crystal; since the principal spacing increases a constant amount for each addition of a CH_2 group, the conclusion is that the molecules are parallel and either perpendicular (in which case the interplanar spacing measures the actual molecule length) or inclined at a constant angle to these reflecting planes. Bragg uses the picturesque analogy of a carpet as a layer, the pile of the carpet as the molecules, and a stack of carpets as the crystal.

This oriented film in a sense, therefore, acts like a single crystal which is oscillated in an x-ray beam so that reflections from

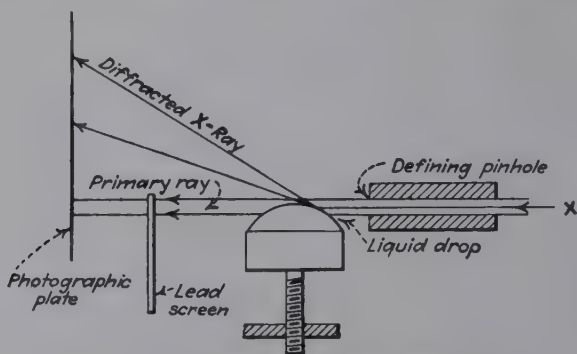


FIG. 203.—The tangent drop diffraction method.

a set of planes are registered by the Bragg method in accordance with $n\lambda = 2d \sin \theta$. The simultaneous appearance of the side spacings proves the powder nature of the specimen. Hence the oriented film consists of many crystal grains oriented exactly alike with respect to one axis but at random *around* this axis.

Another technique which has been used with great success by Trillat and by the writer is the use of a curved surface upon which the molecules of a film may orient. Inasmuch as the x-ray beam may strike this spherical surface tangentially at a whole series of angles, one position will be correct for reflection from the long spacings of the film. Hence oscillation of the specimen is obviously unnecessary. This method is illustrated in Fig. 203. Typical patterns for the same paraffin wax sample, respectively by the method of oscillating a film on a flat plate and of orienting a film on a mercury drop, are illustrated in Fig. 204. Orientation

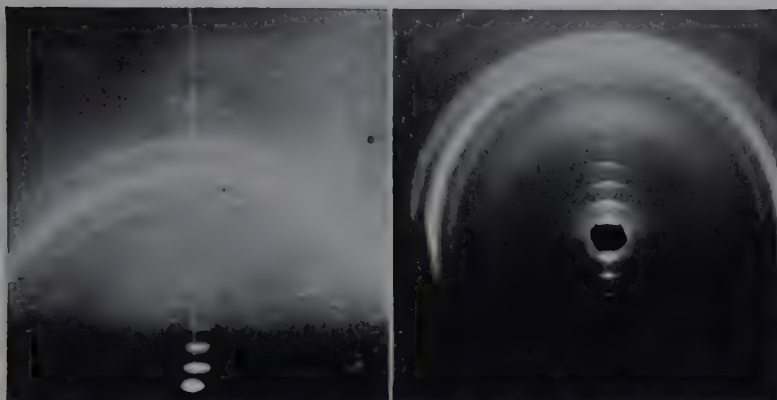


FIG. 204.—Patterns for thin films of paraffin wax. Left, on glass plate and oscillation spectrograph; right, on mercury drop. The short lines or arcs at small angles are interferences in various orders for molecular length, while the long Debye-Scherrer rings correspond to molecular cross section.

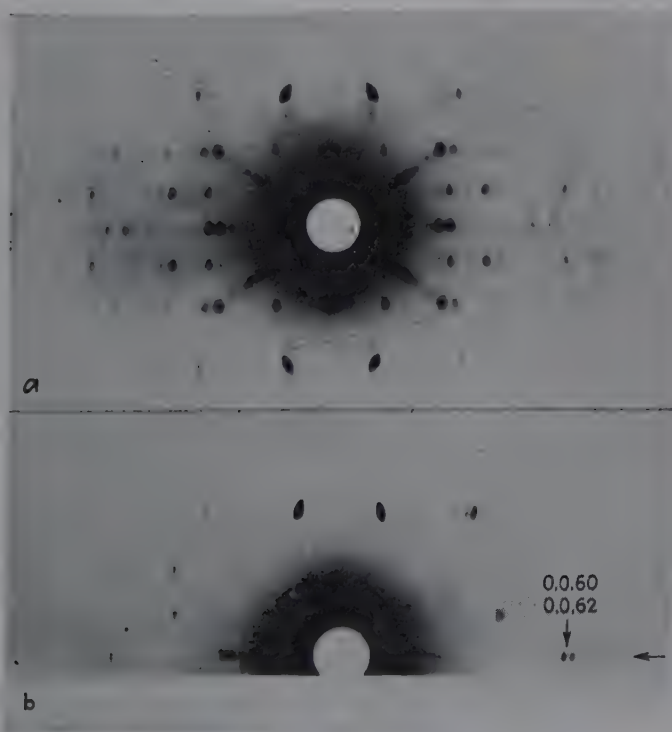


FIG. 205.—Rotation patterns for single crystal of $C_{29}H_{60}$, showing sixty-second-order reflection. (Müller.)

of film on water, metals, molten liquids, etc., will be considered in a later paragraph.

Paraffin Hydrocarbons.—In order fully to understand the results obtained from films of the hydrocarbons, a complete structure determination obviously was necessary, and, of course, this required a single crystal that could be analyzed by the rotation method. Müller¹ succeeded in obtaining a single crystal of $C_{22}H_{46}$ and in completing a remarkably able analysis. A rotation photographic around the a axis and another showing 0, 0.60 and higher reflections are reproduced in Fig. 205. The crystal is orthorhombic with the space-group $Pnma$; the unit cell containing four molecules has the dimensions: $a = 7.45$, $b = 4.97$, $c = 77.2$ A.U. It is evident, therefore, that two molecules with the planes mutually inclined in two different directions so as to produce close-packing end to end are placed along the c axis, since a spacing d_1 of 38.6 A.U. is observed by the powder (thin-film) method together with $d_2 = 4.13$, $d_3 = 3.72$, $d_4 = 2.98$, $d_5 = 2.48$, and $d_6 = 2.35$. These all correspond to the planar indices in the single crystal analysis, respectively, of 002, 110, 200, 210, 020, and 120. The analysis further shows that the CH_2 groups of the chain molecule lie equally spaced on two parallel rows, the lines between successive centers thus forming a zigzag with an angle somewhat less than 92 deg. (slightly distorted tetrahedral angle). The distance between two consecutive scattering centers on either row of the crystal molecule, *i.e.*, from $(CH_2)_0$ – $(CH_2)_2$, is 2.537 A.U., or the increment per CH_2 to the total length is 1.27 A.U. A gap of 3.09 A.U. exists between the ends of two consecutive molecules in the crystal.

Hengstenberg² obtained results also for crystals of $C_{35}H_{72}$ that gave unit-cell dimensions of $a = 7.43$, $b = 4.97$, $c = 46.2$ A.U. (single-chain length). Because of great intensity of the thirty-sixth and thirty-seventh orders, the vertical component of distance between neighboring carbon atoms must be 1.27 A.U. as Müller found.

Of principal interest in these studies is the significance of the zigzag chain in explaining the well-known alternations in properties for substances containing odd and even numbers of carbon

¹ *Proc. Roy. Soc. (London)*, **120A**, 437 (1928).

² *Z. Krist.*, **67**, 583 (1928).

atoms. Müller's interpretation¹ is shown most clearly in Fig. 206. In the odd molecule the pattern repeats itself every second molecule along the direction c , while in the even all successive molecules are identically situated. It would be expected in the actual crystal therefore that two molecules would lie along the c axis for odd-numbered chains and only one molecule in crystals containing even-numbered molecules. This prediction has been fully verified for dicarboxylic acids where the end groups are COOH instead of CH₃ in the paraffins.

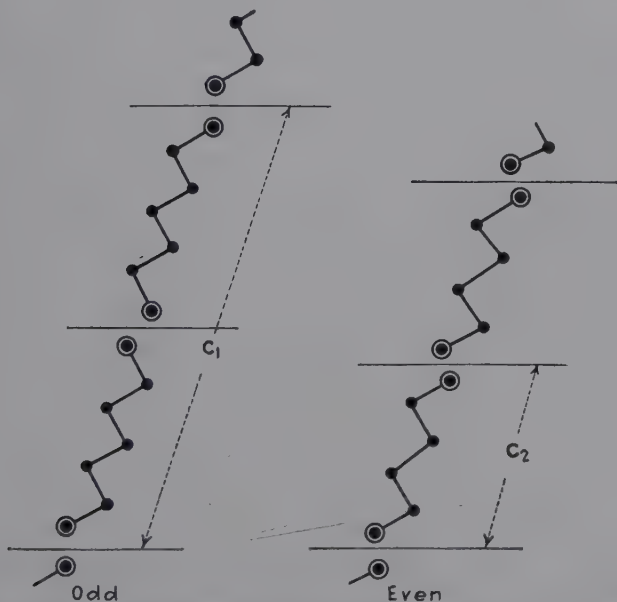


FIG. 206.—Arrangement in layers of long-chain compounds with odd and even numbers of carbon atoms.

In order to test the effect of even and odd hydrocarbons, Müller investigated² a number of normal paraffins ranging from C₅H₁₂ to C₃₀H₆₂ at liquid-air, room, and nearly melting temperatures. The higher members of the paraffin series crystallize in the normal form as found for C₂₉H₆₀, irrespective of whether the carbon content is an even or odd number. Thus for these *long* chains the effects of the end groups are not sufficient to differen-

¹ *Proc. Roy. Soc. (London)*, **A124**, 317 (1929).

² *Proc. Roy. Soc. (London)*, **A127**, 417 (1930).

tiate the two series as predicted from Fig. 206. Differences in the behavior of even and odd members begin to appear, however, when the carbon content decreases. $C_{22}H_{46}$, $C_{20}H_{42}$, and $C_{18}H_{38}$ exist in two alternative structures, the normal one near the melting point and another structure at lower temperatures. The change from the normal form into another one also occurs in the series of odd members between $C_{11}H_{24}$ and C_9H_{20} . The results are expressed graphically in Fig. 207, in which the long spacings, varying from 7.35 A.U. for C_5H_{12} to 40.0 A.U. for $C_{30}H_{62}$, are

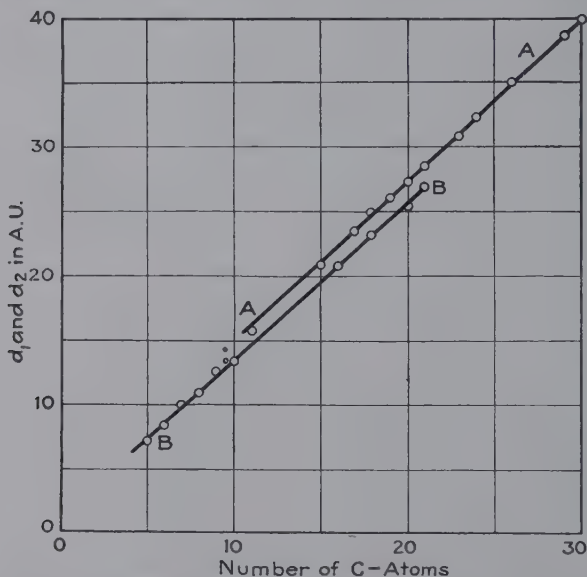


FIG. 207.—Principal spacings for normal paraffin hydrocarbons plotted against number of carbon atoms in chains, showing relationship of two modifications.

plotted against the number of carbon atoms. There are two straight lines, the upper representing the normal crystal structure, the lower the second form appearing at low temperatures. Paraffins tend to become hexagonal at the melting points; in the range C_{21} to C_{29} this state is reached, whereas others melt before becoming hexagonal. This is the result of close packing of freely rotating cylindrical molecules and the crystal becomes optically uniaxial.¹ In spite of this complication, the fact is demonstrated that these chains have a constant increment in length of 1.25 A.U. per carbon atom and that the x-ray pattern

¹ MÜLLER, *Proc. Roy. Soc. (London)*, **138**, 514 (1932).

is a powerful method of identifying any member of an homologous series and of determining molecular weight. Hengstenberg's values of 46.2 A.U. for $C_{35}H_{72}$ and 78.2 A.U. for $C_{60}H_{122}$ are consistent.

Cycloparaffins $C_{12}H_{24}$ to $C_{30}H_{60}$ were studied by Müller in 1933 and found to have the same zigzag form and interatomic distances as the chain paraffins. Cyclohexane forms a regular puckered ring, but the higher members of the series form a double chain, bridged at each end by a small ring of one to three carbon atoms.

X-ray diffraction results with ordinary paraffin waxes are of unusual interest. In spite of the fact that these waxes may contain as many as 18 or 20 different hydrocarbons, both normal and branched-chain isomers, a single diffraction spacing corresponding to molecular length is obtained, together with the usual side spacings. Clark¹ first made x-ray measurements on a series of commercial waxes of varying melting points with these results:

| Wax melting point, degrees Fahrenheit | d_1 | Number of C atoms indicated |
|---|-------|--------------------------------|
| 135 | 39.42 | 29.0 |
| 130 | 38.58 | 28.5 |
| 125 | 35.22 | 26.0 |
| 120 | 34.38 | 25.0 |

The spacing obtained varied, however, depending upon the method of preparing the specimen film (from 36.64 to 40.20 A.U. for the 135° wax) and especially upon the time given for molecular orientation. Furthermore, the presence of addition agents in very small amounts served to change the long spacing. Obviously, possibilities of polymorphism, changing predominance of one molecular species over all others in the mixture and changing tilts of molecules to the diffracting planes may explain the variations.

Clark and Smith² next studied series of samples from carefully fractionated paraffin waxes derived from mid-continent petroleum.

¹ *Science*, **66**, 136 (1929).

² *Ind. Eng. Chem.*, **23**, 697 (1931).

Some representative data are tabulated for one of the series.

| Fraction | A | B | C | D | E | F |
|---|--------|--------|--------|--------|--------|--------|
| Melting point, degrees Centigrade..... | 59.9 | 55.2 | 47.1 | 40.5 | 35.2 | 29.4 |
| Refractive index, 80° C..... | 1.4303 | 1.4306 | 1.4330 | 1.4550 | 1.4359 | 1.4380 |
| Molecular refraction..... | 122.7 | 122.8 | 126.5 | 129.8 | 128.4 | 125.0 |
| Specific gravity..... | 0.770 | 0.773 | 0.779 | 0.783 | 0.786 | 0.792 |
| Solubility in C ₂ H ₄ Cl ₂ (14°, g. for 100 c.c.)..... | 0.115 | 0.218 | 0.82 | 2.4 | 5.7 | 70.3 |
| Molecular weight..... | 366 | 367 | 379 | 389 | 385 | 377 |
| Average value of n in C _n H _{2n+2} indicated..... | 26 | 26 | 27 | 27.6 | 27.4 | 26.8 |
| X-ray identity period, d_1 | 42.3 | 39.2 | 42.3 | 42.3 | 45.8 | 50.3 |
| Number of carbon atoms..... | 31 | 29 | 31 | 31 | 34 | 38 |
| Number of orders of reflection | 6 | 4 | 2 | 2 | 1 | 1 |
| Molecular weight from d_1 | 464.5 | 430.9 | 464.5 | 464.5 | 503.8 | 552.8 |

Some conclusions are as follows:

1. No fraction is a single pure compound.
2. In fractions from the same wax the identity periods corresponding to the predominating molecular length follow no regular order with melting point; thus the largest spacing was obtained with the fraction with lowest melting point.
3. The number of orders of diffraction caused by the oriented molecules varies directly with the melting point of the fraction. This indicates that with the lower melting fractions the degree of perfection of orientation of the molecules becomes less, probably owing to the interference of an increasing number of molecules with lower orienting tendency. Excellent agreement between observed and calculated molecular refractions proves that these molecules must also belong to the paraffin series and are probably branched-chain molecules in view of the small variation in the observed molecular weight compared with large variation in melting point. This is also indicated by the fact that the side-spacing diffraction maxima corresponding to molecular cross sections become increasingly diffuse from A to F.
4. Molecular weights calculated from the x-ray data are about 25 per cent higher than values by the ebullioscopic method. This indicates that besides containing the molecules indicated by the identity period every fraction is also made up of lower molecular weight paraffins, either shorter straight chain or isoparaffins or both.

5. In 16 fractions only five spacings are observed corresponding to the values for pure hydrocarbons with 29, 31, 34, 38, and 42 carbon atoms by interpolation on the straight-line plot of d_1 against n . $C_{38}H_{78}$ and $C_{42}H_{86}$ were recognized as constituents of paraffin wax for the first time.

Aliphatic Acids.—The principal spacings vary from 6.66 A.U. for crystallized acetic acid, $C_2H_4O_2$ (Saville), to 82.0 A.U. for one modification of lacceroic acid, $C_{32}H_{64}O_2$ (Thibaud, powder method). The layers in any one acid have double the spacing displayed by the paraffin with the same number of carbon atoms; hence they are two molecules thick with COOH groups together at the ends of two oppositely turned molecules. Until the remarkable photographs of Prins and Coster, showing as many as 34 orders for palmitic acid, it was believed that the odd orders were generally more intense than the even. These new results prove that this is true to about the ninth order at which point even and odd intensities become equal; beyond this the even orders become more intense, reaching a maximum at the sixteenth. The thirty-fourth-order spectral line is much stronger than any of the adjacent lines, indicating a distinct periodic phenomenon in the fact that the spacing for one molecule (35.6 A.U.) is thirty-four times the increment for a CH_2 group. The precision measurements of Trillat prove that the large lattice spacings (and hence the lengths of the molecules) for the fatty acids vary in proportion to the number of carbon atoms, but group the acids into two series, one for those containing an even number, the other for those containing an odd number of carbon atoms.

In addition the researches of Piper, Malken, and Austin,¹ Thibaud,² deBoer,³ and others have demonstrated that there is a definite polymorphism of the higher fatty acids, each acid from palmitic (C_{16}) up, whether containing even or odd carbon atoms having two forms. One form is obtained by melting the acid and forming a thin layer, the other by evaporating a solution. These are called, respectively, the C or α and the B or β forms. An A or γ form with still larger principal spacing appears very rarely. A graphical representation of the variation of the

¹ *J. Chem. Soc.*, **129**, 2310 (1926).

² *Compt. rend.*, **184**, 24, 96 (1927); **190**, 945 (1930); *Nature*, **119**, 852 (1927).

³ *Nature*, **119**, 50, 635 (1927).

spacings corresponding to molecular length with the number of carbon atoms thus requires at least four curves: odd acids B and C, and even acids B and C. The best data are plotted in Fig. 208. The increase of the chain's length per carbon atom is, respectively, 1.327 and 1.146 A.U. for the B and C forms of the odd acids and 1.21 and 1.10 A.U. for the even acids. The polymor-

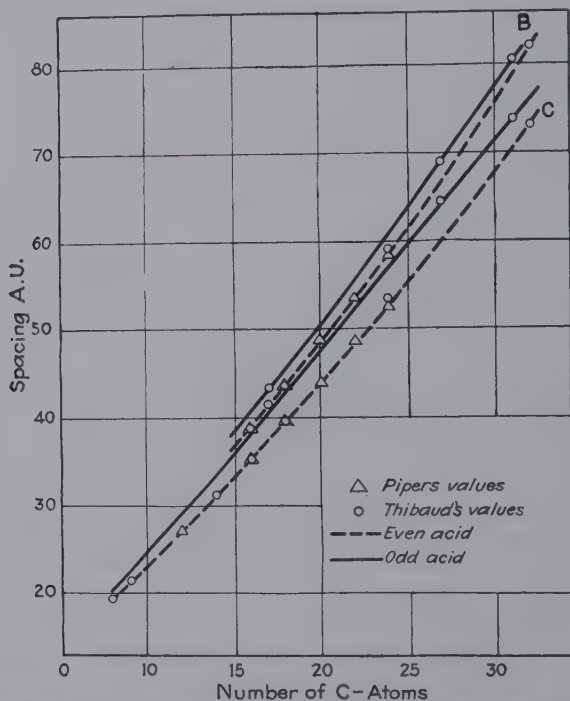


FIG. 208. —Graph for normal aliphatic acids showing effect of even and odd numbers of carbon atoms, and of B and C modifications.

phic transitions occur at definite temperatures and are accompanied by a change not only in spacing but also in refractive index. The different forms are evidently related to the different tilts of the molecules with respect to the diffracting planes. Some representative data are shown in the table on page 437.

Excellent complete analyses of single crystals have been made on stearic acid and derivatives by Müller¹ and on lauric acid by Brill and Moyer,² and partial analyses on several others.

¹ *Proc. Roy. Soc. (London)*, **114**, 542 (1927).

² *Z. Krist.*, **67**, 570 (1928).

Both the C_{12} and C_{18} acids are monoclinic with four molecules per unit cell and with double molecules lying with their long direction almost parallel to the c axis. The zigzag aliphatic acid chain can be represented essentially as an elliptical rod with a ratio of axes of 0.64 as represented in Fig. 209.

Other Acids.—Oleic, with one double bond, linolic with two, and linolenic with three when in thin layers on polished lead, demonstrate according to Trillat how chemical change may be followed

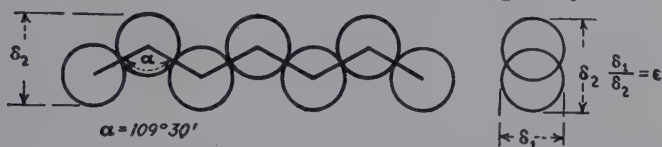


FIG. 209.—Form of zigzag carbon chain and cross section.

by x-ray patterns. New lines appear as oxygen is absorbed at the double bonds. When the latter two become hard and dry, the x-ray spectra disappear as in the case with linseed oil.

| Acid | B Spacing | C Spacing | Transition temperature |
|------------------------------|------------|-----------|------------------------|
| $C_{11}H_{22}O_2$ | 30.1 | 25.4 | 17 (deBoer) |
| $C_{13}H_{26}O_2$ | 35.1, 31.5 | 29.8 | 32 |
| $C_{15}H_{30}O_2$ | 39.7, 35.9 | 34.4 | 44 |
| $C_{17}H_{34}O_2$ | 40.2 | 38.7 | 54 |
| $C_{12}H_{24}O_2$ | 30.6 | 27.4 | 10 (Thibaud) |
| $C_{14}H_{28}O_2$ | 35.0 | 31.2 | 25 |
| $C_{16}H_{32}O_2$ | 39.3 | 35.6 | 40 |
| $C_{18}H_{36}O_2$ | 43.95 | 39.9 | 55 |
| $C_{16} + C_{18}$ acids..... | 41.6 | 37.6 | $40 < T < 55$ |
| $C_{27}H_{54}O_2$ | 69.0 | 64.0 | 82.5 |

Patterson¹ studied a series of phenyl normal saturated fatty acids. Though benzoic acid is a purely aromatic acid, from ϵ -phenyl-caproic acid ($n = 5$) onward, the side chain tends to predominate and the substances tend to be like the aliphatic acids. The lower acids thus represent the stage in which the properties go over from aromatic to aliphatic, and these variations are quite complicated.

The diacids (succinic, adipic, pimelic, suberic, azelaic, etc.) diffract x-rays in the predicted manner from oriented films. Since there are two COOH groups in each molecule, the layers

¹ *Phil. Mag.*, **3**, 1252 (1927).

are only one molecule thick; the spacing of a C_8 diacid, for example, multiplied by 4, gives the observed spacing of the C_{16} fatty acid (with two molecules per layer).

An alternation is observed in the films between chains with even and odd numbers of carbon atoms. Caspari¹ prepared single crystals and found the effect greatly pronounced in complete-structure analyses. In the following table the data are assembled for the unit-cell dimension of the monoclinic unit cell (c) corresponding to molecular length, the number of molecules per cell (z), and for comparison the principal spacings obtained by Henderson from films of the acids:

| Acid | Number of C atoms | c | Z | d (film) |
|-----------------------------|----------------------|-------|-----|------------|
| Adipic..... | 6 | 10.02 | 2 | 6.90 |
| Pimelic..... | 7 | 22.12 | 4 | 7.65 |
| Suberic..... | 8 | 12.56 | 2 | 9.05 |
| Azelaic..... | 9 | 27.14 | 4 | 9.56 |
| Sebacic..... | 10 | 15.02 | 2 | 11.20 |
| Brassylic..... | 13 | 37.95 | 4 | 13.3 |
| Hexadecanedicarboxylic..... | 18 | 25.10 | 2 | |

Part of the discrepancy between single-crystal and film data may be due to polymorphism which has been observed for such diacids as malonic, succinic, and glutaric by Latour.² However, these acids substantiate the theory of Müller as to the effect of even and odd chains on properties.

Alcohols.—Like the acids the alcohols are characterized by an association of molecules in pairs to form double layers, by virtue of the active OH groups. Polymorphism also depends on varying tilts of the molecules to the base of the cell.³ Rotation of the carbon chain is found for $C_{12}H_{25}OH$ which has hexagonal structure at 24° and monoclinic at 16° . The change is irreversible as the temperature is raised on account of a change in molecular tilt as well as rotation.

Esters.—Ordinarily there is a normal decrease in intensity; the layers are one molecule thick; this is true except for acetates, $CH_3COO(CH_2)_nCH_3$, with much greater spacings, suggesting

¹ *J. Chem. Soc.*, **1928**, 3235.

² *Compt. rend.*, **193**, 180 (1931).

³ WILSON and OTT, *J. Chem. Phys.*, **2**, 231 (1934).

doubling from the active double-bonded oxygen atom, while methyl esters, $\text{CH}_3(\text{CH}_2)_n\text{COOCH}_3$, are normal; the increase per carbon atom is 1.22 A.U.

Soaps.—The layers are one molecule thick, and the spacing is independent of the metal for any one acid. By the ingenious method depending upon the fact that the fatty acids on a lead support will form the lead soaps, Trillat has obtained the spectra for a series from the acetate, C_2 , $d = 12.6$ A.U. to the lacceroate, C_{32} , $d = 92.0$ A.U., the largest lattice spacing thus far measured. The increment per carbon atom is 1.3 A.U.

For a whole series of potassium salts, Piper¹ observed two different types with different lattice spacings, one for freshly prepared specimens and one for the same specimen after standing exposed in air which proved to be the acid salt. The acid-salt molecules evidently are perpendicular to the diffracting layer and the neutral-salt chains at an angle of $54^\circ 54'$.

Ketones.—In general for $\text{CH}_3(\text{CH}_2)_m\text{CO}(\text{CH}_2)_n\text{CH}_3$ the layers are one molecule thick; but for ketones with the CO group separated from the end only by a methyl group, double spacings occur, indicating activity of the COCH_3 group comparable with COOH for acids. The compound methyl heptadecyl ketone has double the spacing of the isomeric propyl pentadecyl ketone. The intensities of the normal diketones (oxygen in the middle of the chain) are strong in the odd orders and weak in the even, exactly as with acids, except that one molecule of a ketone acts like two molecules of the acid. If the oxygen atom is one-third along the chain, the third, sixth, ninth, etc., orders disappear. The increase in spacing per carbon atom is 1.3 A.U. A very complete x-ray and thermodynamic study of ketones by Oldham and Ubbelohde² shows that, although the crystal structure is closely similar to that of the corresponding paraffins and independent of the position of the CO group (except methyl ketones), the freezing points depend on this position, being higher when the dipole is near one end of the chain or in the middle. This suggests that the activation energy of melting is supplied by torsional oscillations of the carbon chains.

The following conclusions and practical applications from the x-ray analysis of long-chain compounds may be drawn:

¹ *J. Chem. Soc.*, **1929**, 234.

² *Trans. Faraday Soc.*, **35**, 328 (1939).

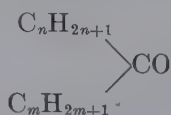
1. *Molecular Form.*—The molecules are confirmed as the long chains known to the chemists. The substances are truly crystalline, since the side spacings are observed, although some of the soaps are obtainable in the mesomorphic smectic state (see Chap. XX). The increments in spacing, per CH_2 group added, are on the average either 1.05 or 1.27 A.U. In diamond an addition of a carbon atom to the zigzag chain lying in one plane increases the length 1.26 A.U. Hence, for paraffins, ketones, etc., the increment is the same as in diamond, and the molecules may be considered as perpendicular to the layers; for acids, etc., with smaller increments, molecules tilted at about 30 deg. may be the explanation. Weight to this explanation is given by the fact that measurements on single crystals of stearic acid show an angle of 30.3 deg. between the c axis and the normal to the c plane in the unit monoclinic prism.

2. *Polymorphism.*—The parallel arrangement of molecules and the tilt may be determined by preparation and working of the samples. Particularly with lower members of the series, depending on whether flakes are pressed on flat surfaces or the substance is melted and solidified in a film, different spacings are obtained. Polymorphism is very common, though previously unsuspected, in many series of compounds.

3. *Molecular Weight.*—The simple x-ray photographs may be used to determine molecular weights by interpolation of the observed spacing on the straight line relating number of carbon atoms to the interplanar spacing. Pure hydrocarbons will give results that fall on the curve whereas mixtures will not; isomers are clearly differentiated as they fall on different curves. This matter is complicated for normal saturated acids with four curves necessary.

4. *Isomerism.*—The position of ketonic oxygen atoms is accurately determinable in any compound from data on the intensities because of its greater scattering power for x-rays and the resultant effect upon the intensities of various orders.

5. *Structural Formula.*—Alternative possible formulas may be tested; for example, the ketones may be



or $C_nH_{2n+1}.COC_mH_{2m+1}$, the length of the first being $n + 1$ or $m + 1$ and of the second $n + m + 1$ carbon atoms; the second is proved correct.

6. *Chemical Analysis*.—Natural materials such as paraffin wax, glyceryl margarate, hydrogenated soybean oil, spermaceti, Chinese wax, ceresin, and lecithin all give lines and may be analyzed. Especially brilliant has been the identification by Chibnall and associates of ketones in complex natural waxes. Mixtures pressed together give lines for all constituents but, when melted together, may give lines for only one constituent which may actually be present in only a minor quantity, as found in paraffin wax. Solid solution over very wide ranges in mixtures of fatty acids has been demonstrated by Slagle and Ott.¹ Binary mixtures often follow Vegard's law in the linear relation of spacing and composition.

7. *Chemical Reactions*.—These long-chain compounds are the best for following the course of chemical reactions. Small quantities of the acids melted on metals show superposed spectra of the acid and the soap formed by interaction with the metal base; the latter spectra are intense with lead, tin, and antimony; less intense with iron, copper, and bismuth; faint with nickel, zinc, and molybdenum; and absent with aluminum, palladium, platinum, and gold. The absorption of oxygen at the double bonds of lead oleate, formed by painting a film of oleic acid on lead, may be followed perfectly by the gradual appearance of new spectrum lines and the disappearance of the oleate lines.

8. *Spectroscopy of Soft X-rays*.—The large spacings characteristic of these stratified organic compounds made possible the spectroscopic measurement of long wave lengths and the bridging of the gap between ultraviolet and x-rays. Ruled gratings are used now more commonly for these researches.

9. *Films and Molecular Orientation at Surfaces and Interfaces*.—Finally, the theory of orientation of molecules at surfaces and interfaces, long well-known as the result of surface-energy studies of Hardy, Harkins, Langmuir, N. K. Adam, and others could be subjected to the most rigorous direct experimental test by the methods discovered for the study of these long-chain organic compounds. In general, the x-ray study of the structure of thin films and surface and interfacial layers has fully substantiated

¹*J. Am. Chem. Soc.* **55**, 4404 (1933).

the conception of definite molecular orientations such as fatty acid molecules at the surface of water standing upright with the polar carboxyl group turned into the water. Obviously, monomolecular films cannot serve as diffraction gratings, but the results obtained with layers only a few molecules thick fully substantiate the picture. A wide variety of experiments has been conducted to show orientation. The excellent results obtained from very thin films on mercury drops have been noted already. Trillat¹ in a second paper reports a whole series of ingenious investigations on the surface structure of entirely solidified

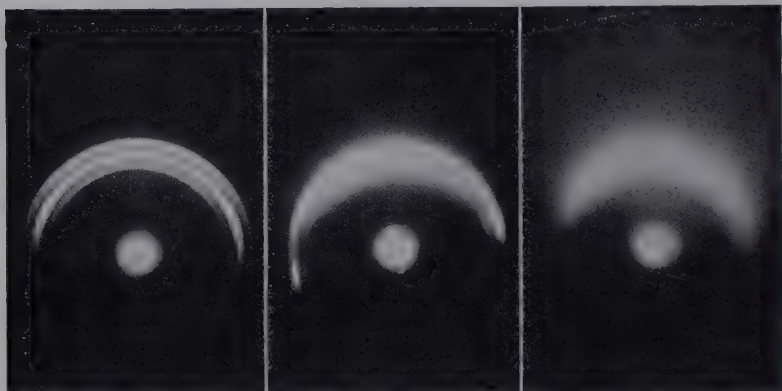


FIG. 210.—Diffraction patterns for drops of paraffin wax. Left, surface of solidified drop; center, surface of molten drop with invisible film cooled by jet of air (molecular orientation indicated by short, sharp arcs near center); right, surface of liquid drop.

drops of fatty acids, diacids, paraffins, and triglycerides, of films of these substances obtained by cooling the surface of a liquid drop, the remainder being molten, and of films obtained by cooling in contact with heated water. An x-ray beam defined by a horizontal slit strikes tangentially upon the surface in each case. The appearance on the diffraction photograph of the interferences in several orders corresponding to the molecular lengths at once proves that the chains must be preferentially oriented at interfaces between solid or liquid substance and air and between water and air. Figure 210 shows a series of patterns for paraffin that was made in the writer's laboratory by J. N. Mrgudich. Especially interesting is the center one made as follows: The paraffin is melted in a small cup by means of a carefully controlled

¹ *Ann. phys.*, **15**, 455 (1931).

current through a resistance wire in contact with the cup. A blast of air is directed on the surface so as to form a transparent film on the molten drop. The pattern shows a liquid halo and in addition sharp interferences for the oriented film. The orientation theories are thus entirely substantiated. Not only is this true of long organic molecules, but even in surface "skins" of other substances. Surface-reflection x-ray photographs have demonstrated conclusively an oriented molecular structure approaching the crystalline condition in the surface of cast-glass cylinders, while a nearly amorphous glass pattern is obtained for the interior. Organization and orientation seem to be inherent tendencies of matter, given the proper conditions of molecular

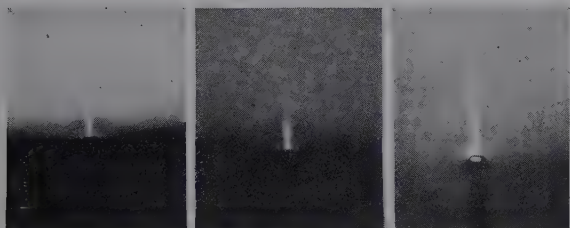


FIG. 211.—Patterns for built-up films from 3, 7, and 50 monolayers of calcium stearate.

mobility, or assisted by some mechanical unidirectional force such as stretching or drawing into a fiber. The orientation of molecules thus observed is true whether in the solid or liquid state. For example, molten lead oleate on metallic lead backing gives nearly as sharp interferences as a solidified film.

The electron diffraction method has proved to be of greatest usefulness in the structural analysis of films too thin for ordinary x-ray technique. The formation of films of oriented molecules of fatty substances on metal surfaces, cellulose, etc., simply by exposure to laboratory atmosphere was proved by Trillat and Metz,¹ when it was discovered that widely different materials were giving the same diffraction patterns from these contaminating and spreading films.

10. *Blodgett-Langmuir Built-up Films*.—This new technique developed by Blodgett and Langmuir for building up films from unimolecular layers or monolayers of long-chain compounds, proteins, etc., spread on aqueous solutions already has proved

¹ *Trans. Faraday Soc.*, **31**, 1127 (1935).

so successful and valuable that it is generally familiar to chemists, biologists, and x-ray analysts. A layer of stearic acid, for example, is spread one molecule deep on a water surface (best containing calcium or barium ions). A glass or metal plate is then lowered through this surface layer; as it is removed a monolayer of the acid adheres to the base with carboxyl groups turned in, and on the next trip down another layer adheres with carboxyl groups turned out. This alternating type is called the Y type. In this way a film of any known number of unimolecular layers is built up. Clark and Leppla¹ made the first x-ray structural studies of such films, obtaining patterns for films of calcium and lead stearate and stearic acid varying in thickness from 3 layers up to 300. Figure 211 illustrates the remarkable patterns obtained for 3, 7, and 50 layers. The measured spacings corresponded with those from melted films or powders (stearic acid 39.7, calcium stearate 49.4, lead stearate 49.6 A.U.). The first direct test was made from the measurements of the theoretical equations for evaluating particle size in the colloidal range from line breadth (see Chap. XXI). In the past three years a large number of papers have appeared describing types of layers, especially Y or alternating, and X in which layers are deposited from alkaline water containing calcium or strontium ions only on the down trip, the effects of pH and temperature, surface potentials, optical measurements, thickness and refractive indices, chemical reactions on the underside of films, formation of skeleton films (mixed barium stearate and stearic acid with stearic acid dissolved out by benzene), adsorption by monolayers of dissolved salts, overturning of layers, and hydrolysis of esters as a function of orientation. References are given in the footnote below² to some of the principal contributions not including the application of the method to the study of proteins,

¹ *J. Am. Chem. Soc.*, **57**, 330 (1935); **58**, 2199 (1936).

² Work at General Electric Research Laboratory (Blodgett, Langmuir, Schaefer), *J. Am. Chem. Soc.*, **56**, 495 (1934); **57**, 1007 (1935); **59**, 1762, 2400 (1937); **60**, 1140, 1513 (1938); *J. Franklin Inst.*, **218**, 153 (1934); *Phys. Rev.*, **51**, 964 (1937); *Science*, **87**, 493 (1938).

PORTER and WYMAN, *J. Am. Chem. Soc.*, **60**, 1083 (1938).

HOLLEY and BERNSTEIN, *Phys. Rev.*, **52**, 525 (1937); **53**, 534 (1938).

SCHULMAN and associates (Cambridge), *Phys. Rev.*, **53**, 909 (1938); *Nature*, **139**, 625 (1937); *Trans. Faraday Soc.*, **34**, 748, 1337 (1938); *Proc. Roy. Soc. (London)*, **161**, 115 (1937); **163**, 170 (1937).

sterols, chlorophyll, pepsin, etc., which will be considered in Chap. XXIII.

11. *Lubricating Films*.—Lubricating films of the "boundary" type are quite thin, and under such conditions it would be expected that a high degree of preferred orientation of paraffin hydrocarbon or soap molecules must prevail. If these molecules were anchored at one end on each of two metal-bearing surfaces, then one metal surface would not rub on another with resultant damage and seizure, but slippage would take place between the CH_3 ends of the molecules of the two oriented lubricant layers. X-ray analyses of lubricating films of oils and greases have fully confirmed this film structure. However, since the usual straight-chain paraffin hydrocarbons have no polar properties, the orienting tendency is comparatively weak. A few years ago Wells and Southcombe discovered that the addition of a small amount of fatty acid reduced the static coefficient of friction and increased the oiliness of a mineral oil to a marked degree. These polar molecules should be preferentially adsorbed at the metal film interface, form double layers considerably more strongly anchored to the metal surface, and indeed improve the orientation of the hydrocarbon molecules. This also has been experimentally proved. Trillat showed that when metal ball bearings are immersed in an oil blended with polar addition agent the surface tension of the liquid changes gradually to that of the pure hydrocarbon oil and oriented layers of the acid are attached to the metal surface. The most comprehensive x-ray studies of lubricants have been made by Clark, Sterrett, and Lincoln.¹ The x-ray evidence of the effects of methyl dichlorostearate used as an addition agent led to the concept of "oil plating." The additional lateral effects of the chlorine atoms on the hydrocarbon chain result in doubling the molecules in each adsorbed layer, while the unchlorinated ester forms only single molecular layers. In fact a reaction with the metal surface and polymerization of the substance results in an adherent *solid* film which resists rupture or abrasion. Acids, esters, and a variety of chlorinated derivatives of aliphatic and aromatic compounds (the last-named having molecules lying flat on the

¹ *Ind. Eng. Chem.*, **28**, 1318, 1322, 1326 (1936); "Chemical and Physical Forces in Lubrication," "The Science of Petroleum," p. 2566, Oxford University Press, New York, 1938.

metal surface) have been subjected to careful study and the x-ray results correlated with measurements of cross-sectional areas of molecules in monolayers under different compressions on the hydrophil balance. Even in viscous lubrication with thick fluid films the effects on molecular regimentation are measured from the liquid diffraction patterns (see Chap. XX). A unique x-ray method of evaluating lubricants in terms of the protection of metal surfaces consists in the use of a fibered metal pin. The degree of preferred orientation of the metal crystals (see Chap. XXI) is determined from the x-ray pattern. A metal



FIG. 212a.—X-ray reflection patterns illustrating method of evaluating protection of fibered metal surface by lubricating film: left, original metal surface; right, surface after wearing by rotating collar.

collar is then rotated around this rod, so that wear will be at right angles to the fiber direction and thus tend to destroy the original arrangement as determined from another pattern at the same position on the pin (Figs. 212a, 212b). Quantitative measurement with the microphotometer before and after wear determines the degree of protection afforded by the lubricant between the surface of the pin and the collar. It is evident that the x-ray diffraction method has made a noteworthy contribution to the very practical problem of lubrication, based upon fundamental structural studies of long-chain carbon compounds.

12. *The Breakdown of High-tension Cables.*—Cables for transmitting high-tension electric currents are constructed from a

paper tape insulation impregnated with pure insulating oil. Occasionally these may fail and cause serious difficulties. Clark and Mrgudich¹ found that such a failure is associated with the formation of one or more crystalline waxes polymerized in corona discharge, which have been identified by x-ray patterns and of which the distribution from core to sheath has been measured. Since cable wax can be detected in very small amounts, x-ray research has led to specifications for insulating oil and cable design that have greatly diminished failures.

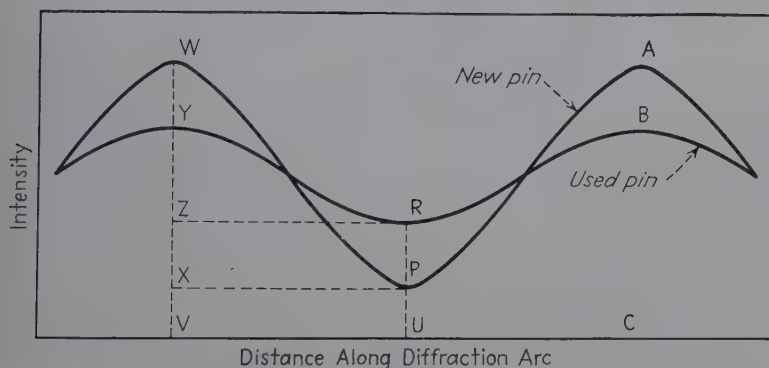


FIG. 212b.—Graphical method of interpreting x-ray patterns in terms of lubricating value.

The Structure of the Benzene Ring and Aromatic Compounds. 1. *Bragg Analysis of Naphthalene and Anthracene.*—The first selections twenty years ago for complete crystal analysis were naphthalene and anthracene, since solid benzene cannot be easily prepared. Bragg found for the dimensions of the unit prisms of these monoclinic crystals, each containing two molecules, the following:

Naphthalene, $a = 8.34$, $b = 6.05$, $c = 8.69$, $\beta = 122^\circ 49'$.

Anthracene, $a = 8.7$, $b = 6.1$, $c = 11.6$, $\beta = 124^\circ 24'$.

The a and b axes are very nearly the same, but the c axis is considerably longer for anthracene than for naphthalene. This difference in the c axis suggested the difference in the length of the two molecules, since anthracene is represented as three contiguous benzene rings and naphthalene as two. Bragg then assumed that the closed rings of six carbon atoms, which were

¹ *Elec. Eng.*, **52**, 101 (1933).

definitely known to exist in diamond, were carried over essentially unchanged into benzene, naphthalene, and anthracene. The difference in length between the two, 3 A.U., was exactly accounted for by the extra ring in anthracene. The constancy of the cross sections of the two cells results from the fact that it is determined not by the length but by the breadth and thickness of a single ring and, hence, is a measure of the space necessary for side-by-side linking of the two molecules in each unit cell. Furthermore, the theoretical length of the naphthalene molecule, 6.65 A.U., agrees with the length of the *c* axis, 8.69 A.U., if allowance of 1 A.U. is made for a hydrogen atom at each end. Further consideration showed that the two molecules in the unit cell were arranged so that one is the mirror image of the other. In the monoclinic prismatic class, there must exist a plane of symmetry, a twofold axis perpendicular to the plane, and, hence, a center of symmetry. If the molecules lack symmetry, then there must be four of them in the cell, one obtained by rotation of another around 180 deg. and the two from the first pair by reflection in the plane of symmetry. Hence, the molecules must have a center of symmetry, since only two are found. The cleavage of these crystals is easily accounted for as coming only in the direction where hydrogen atoms from *different* adjacent molecules touch; in all other directions the strong forces due to the carbon atoms are involved.

2. *The Structure of Hexamethylbenzene.*—The classical research by Mrs. Lonsdale¹ on hexamethylbenzene was the first complete structure determination of an aromatic compound. Even though the rigorous Fourier method was not yet available she demonstrated from x-ray diffraction data that in this compound the benzene nucleus is flat and that the carbon atoms in the methyl group also lie in this same plane. The choice of compound was particularly fortunate, since only one molecule per unit triclinic cell is found and the intensity data may be very directly interpreted. The direct x-ray information on axial lengths and angles is as follows:

$$a = 9.010 \text{ A.U.}, \alpha = 44^\circ 27'.$$

$$b = 8.926 \text{ A.U.}, \beta = 116^\circ 43'.$$

$$c = 5.344 \text{ A.U.}, \gamma = 119^\circ 34'.$$

¹ *Proc. Roy. Soc. (London)*, **A123**, 494 (1929).

The facts that a and b are nearly equal and that the angle between them is nearly $2\pi/3$ immediately suggested hexagonal structure. The factors in the (001) zone should repeat themselves closely throughout the series of planes $(100) \rightarrow (010)$, $(010) \rightarrow (1\bar{1}0)$, $(1\bar{1}0) \rightarrow (\bar{1}00)$. This was tested by a comparison of structure factors which were calculated from the observed intensities by the formula

$$F \propto \sqrt{I} \div \left(\sum f e^{-M} \times \sqrt{\frac{0.15 + \cos^2 2\theta}{\sin \theta}} \right),$$

where $(0.15 + \cos^2 2\theta)$ is the measure of the polarization factor for Mo $K\alpha$ radiation, f is the scattering power of the atoms, and e^{-M} is the temperature factor. Two sets of calculations were made corresponding to f values for diamond (Ponte) and graphite (Bernal), respectively. These proved conclusively the hexagonal arrangement and the graphite arrangement; there was a marked similarity in the intensities of various orders from the (001) cleavage plane and those from the corresponding cleavage plane of graphite. The structure factor was also larger than for any other plane in the crystal and almost independent of the order of reflections, proving that the carbon atoms lay in or near the (001) planes. The factors for planes (340), $(4\bar{7}0)$, and $(\bar{7}30)$ also were very large, and these gave a further clue, since these were small spacing planes and therefore any deviation of the atoms from these planes would cause a more rapid falling off of structure factor than would a similar movement away from a plane of larger spacing. In other words, the carbon atoms must lie at or near the intersections of these planes. There are 36 such intersections and only 12 carbon atoms. Since, however, there is a hexagonal arrangement in the (001) zone, the problem was greatly simplified. Mrs. Lonsdale calculated structure factors for the first six orders of the (100) plane for each possibility, and the true arrangement at once derived.

The immediate deductions are as follows:

1. The molecule exists in the crystal as a separate entity.
2. The benzene carbon atoms are arranged in ring formation.
3. The ring is hexagonal or pseudo-hexagonal in shape. In order to answer the question as to the sizes of the atoms in the rings and the dimensions of the ring itself and whether or not the ring is plane, variations of three kinds are made from the posi-

tions of the atoms established: (1) a variation of atomic dimensions, (2) a variation in directions along which atoms lie (ring rotation), and (3) shifting of atoms perpendicular to the (001) plane, or a puckering of the benzene ring. The effect of each kind of variation upon the structure factors was then determined and compared with experimental results, with the following further deductions.

4. Distance between the nuclear carbon atoms, 1.42 ± 0.03 A.U. Length of the side chain 1.54 ± 0.12 A.U. (diamond).

The aromatic nucleus is therefore exactly like graphite in dimensions.

5. Only the plane ring gives anything like agreement with observations, again as in graphite.

6. The side-chain carbon atoms are attached radially to their respective nuclear atoms and lie in the plane of the ring.

7. Three of the valences of aromatic carbon are coplanar certainly, but no direct information is afforded concerning the fourth except that it must

be so disposed as to give the ring as a whole a center of symmetry. This condition eliminates the Kekule static model with three double bonds.

3. *Further Recent Information Concerning the Benzene Nucleus.* Since the analysis of hexamethylbenzene, renewed interest has been taken in the question of the shape of the benzene nucleus. The fact that in $C_6(CH_3)_6$ it corresponds so closely in structure to the graphite type of ring indicates that very little deformation can have taken place.

In 1932 Cox determined the structure of benzene itself and found the ring to have the same planar hexagonal form with the same interatomic distance of 1.42 A.U. The mutual arrangement of molecules in the orthorhombic unit cell is shown in Fig. 213. They are disposed with their planes parallel to the b axis perpendicular to the plane of the figure but inclined in the other

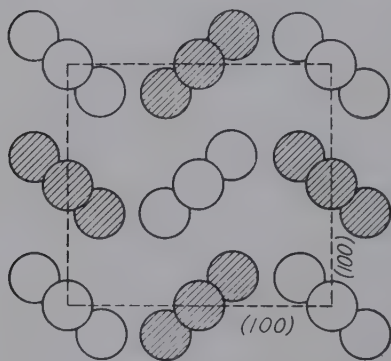
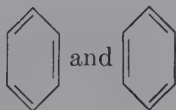


FIG. 213.—The structure of benzene, C_6H_6 . The shaded molecules are displaced vertically relative to the others through one-half of the height of the unit cell.

directions nearly at right angles. The structure is quite loose-knit. The point of chief interest is the light that this molecular structure throws on the chemical valences. A static model of alternate double and single bonds is excluded by the symmetrical form; the constant interatomic distance 1.42 A.U. intermediate between the aliphatic single bond 1.54 and the double bond 1.33 suggests resonance between the two types and between the two Kekule formulas

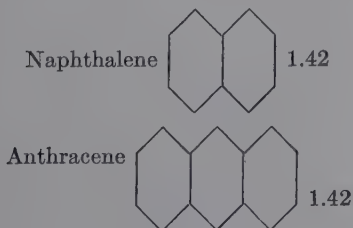


with the Dewar configurations



making a small contribution. With these x-ray results, heats of dissociation and other thermodynamic data are in full accord.

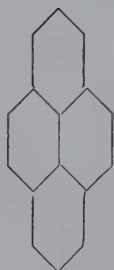
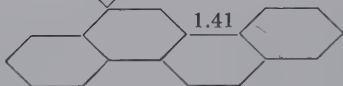
4. *Aromatic Compounds Completely Analyzed*.—A whole series of benzene derivatives has now been subjected to complete x-ray analysis by the Fourier method, in brilliant contributions chiefly from the Davy-Faraday Laboratory of the Royal Institution of which Sir William Bragg is director. All these results confirm the structure of the benzene ring in addition to the establishment of interesting details of each compound. Briefly summarized some of the results are as follows:



Plane regular hexagons; long axis of molecules nearly parallel to *c* axis and planes mutually inclined in two directions, similar to many structures with weak residual forces packing molecules together.

ROBERTSON, *Proc. Roy. Soc. (London)*, **140**, 79; **142**, 674 (1933). ROBINSON, *ibid.*, **142**, 422 (1933); **147**, 467 (1934).

Pyrene

Chrysene,
 $C_{18}H_{12}$ 1, 2, 5, 6 Dibenzanthracene
(5 rings)

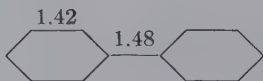
Planar molecules.

Dhar and Guhr, *Z. Krist.*,
91, 123 (1935).

Plane regular hexagons similarly packed in monoclinic cells; dibenzanthracene also has orthorhombic form.

Nature, **132**, 750 (1933);
IBALL, *Proc. Roy. Soc. (London)*, **146**, 140 (1934);
KRISHNAN and BANERJEE, *Z. Krist.*, **91**, 173 (1935).

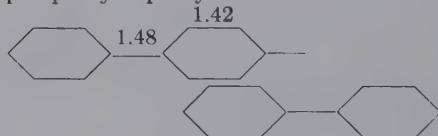
Diphenyl



p-Diphenyl benzene



p-Diphenyl diphenyl



o-Diphenyl benzene



2, 3, or 4 rings in same plane; distance between rings 1.48, shorter than single bond 1.54, showing effect of conjugation; all monoclinic and act like chains.

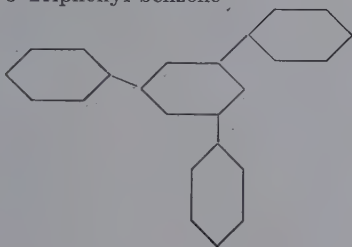
| | a | b | c | β , deg. |
|---|------|------|-------|----------------|
| 2 | 8.22 | 5.69 | 9.5 | 94.8° |
| 3 | 8.08 | 5.00 | 13.59 | 91.9° |
| 4 | 8.05 | 5.55 | 17.81 | 95.8° |

PICKETT, *Proc. Roy. Soc. (London)*, **142**, 333 (1933);
J. Am. Chem. Soc., **58**, 2299 (1936).

Because of close approach of phenyl groups turned 50 deg. out of plane of parent nucleus.

CLEWS and LONSDALE, *Proc. Roy. Soc. (London)*, **161**, 493 (1937).

1, 3, 5 Triphenyl benzene

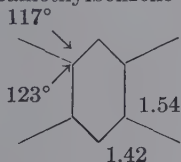


More nearly planar, but packed in layers; three substituent phenyl groups turned 25 deg. from plane of parent nucleus.

ORELKIN and LONSDALE, *Proc. Roy. Soc. (London)*, **144**, 630 (1934).

Durene

1, 2, 4, 5 Tetramethylbenzene



Planar, methyl groups displaced away from each other toward unsubstituted positions. Contour projection, Fig. 214.

ROBERTSON, *Proc. Roy. Soc. (London)*, **141**, 594; **142**, 659 (1933).

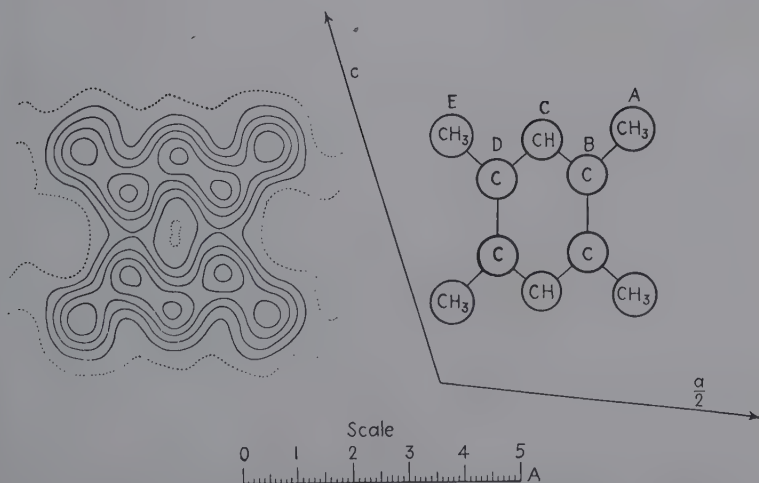
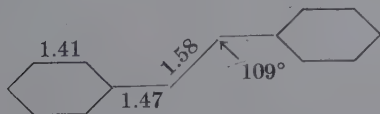
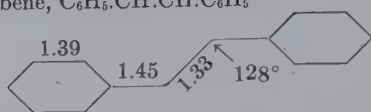


FIG. 214.—Electron density contour map of durene (symmetrical tetramethyl benzene); projection along b axis, and corresponding formula. (Robertson.)

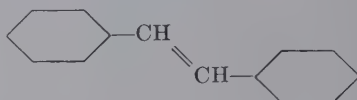
Dibenzyl, $\text{C}_6\text{H}_5\cdot\text{CH}_2\cdot\text{CH}_2\cdot\text{C}_6\text{H}_5$ 

Nonplanar molecule, with two benzene rings parallel but not coincident, at 90 ± 13 deg. to plane of central CH_2 groups linked by purely aliphatic bond at tetrahedral angle.

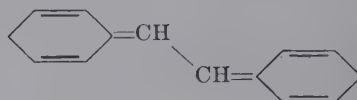
Stilbene, $\text{C}_6\text{H}_5\cdot\text{CH}:\text{CH}\cdot\text{C}_6\text{H}_5$



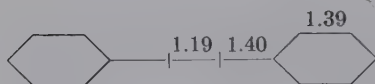
Planar molecule because of no rotation around double bond; 1.45 distance shorter than 1.54 indicates resonance between



and



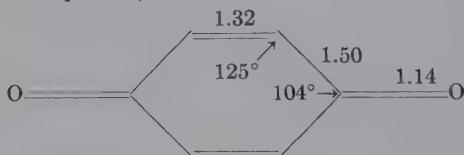
Tolane, $\text{C}_6\text{H}_5\cdot\text{C}\equiv\text{C}\cdot\text{C}_6\text{H}_5$



ROBERTSON and WOODWARD, *Proc. Roy. Soc. (London)*, **154**, 187 (1936); **162**, 568 (1937).

Planar, linear molecule; triple bond length 1.19, single bond length 1.40—unusual contraction in conjugation.

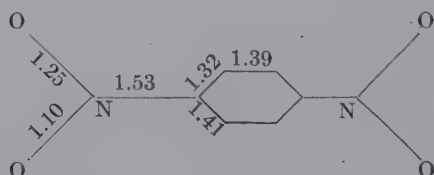
Benzoquinone, $\text{C}_6\text{H}_4\text{O}_2$



Distorted ring arising when resonance excluded—lengthening of bonds next to $\text{C}=\text{O}$ to 1.50 and shortening others to 1.32.

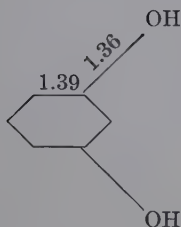
ROBERTSON, *Proc. Roy. Soc. (London)*, **150**, 106 (1935).

p-Dinitrobenzene



Distorted molecule, two oxygen atoms of NO_2 not equivalent; each oxygen atom associated with three CH groups of adjacent molecules in structure of high density.

JAMES, KING, and HORROCKS, *Proc. Roy. Soc. (London)*, **153**, 225 (1935).

Resorcinol (*m*-dihydroxybenzene)

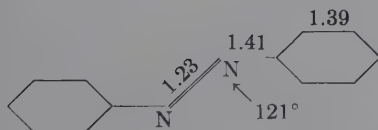
Molecules in spiral arrays about twofold axis, OH groups of successive pairs approaching to 2.7 A.U., indicating hydrogen bond. Structure quite open, density 1.28; at 74° hydrogen bonds "melt" to form β -resorcinol, density 1.33, with more compact grouping (like hydrocarbons).

Orthorhombic *Pna*

| | <i>a</i> | <i>b</i> | <i>c</i> |
|----------|----------|----------|----------|
| α | 10.53 | 9.53 | 5.66 |
| β | 7.91 | 12.57 | 5.50 |

ROBERTSON, *Proc. Roy. Soc. (London)*, **157**, 79 (1936).

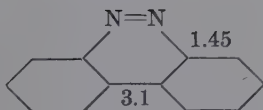
ROBERTSON AND UBBELOHDE, *ibid.*, **167**, 122, 136 (1938).

Trans-azobenzene $C_6H_5.N:N.C_6H_5$ 

Monoclinic, isomorphous with dibenzyl; C—N distance indicates conjugation with N=N. Two independent molecules are present, one flat and in other N=N bond inclined 15 deg. to rings lying in planes 0.32 A.U. apart, causing small changes in dimensions.

DELANGE, ROBERTSON, and WOODWARD, *Proc. Roy. Soc. (London)*, **171**, 398 (1939).

Cis-azobenzene



Orthorhombic, dyad axis of symmetry, benzene rings rotated 50 deg. from planar positions.

ROBERTSON, *J. Chem. Soc.*, **1939**, 232.

mine the unknown phase constant of this resultant wave. On page 321 it was shown that if the structure has a center of symmetry the sine terms in the Fourier equation drop out and the only remaining uncertainty is concerned with the sign of

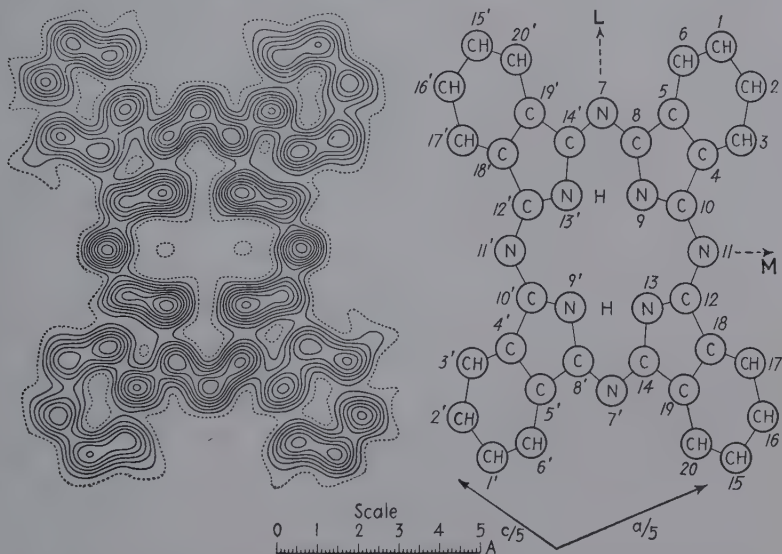


FIG. 215.—Electron density projection along the b axis, showing one complete phthalocyanine molecule. The plane of the molecule is steeply inclined to the plane of the projection, the M direction making an angle of 46° with the b axis, and the L direction 2.3° . Each contour line represents a density increment of one electron per A.U.², the one-electron line being dotted. (Robertson.)

the structure factor coefficient, *i.e.*, whether the wave has a peak or trough at the center of symmetry. Now if one of the scattering particles in the structure is situated exactly at the center, its contribution to the resultant wave will always be a maximum and will correspond to a small wave with a peak at the center of symmetry. Thus a metal atom at the center of symmetry gives a contribution to the resultant reflection that is always a peak, at least for all planes down to those with spacings small compared with the size of the atom. The contribution from all the rest of the molecule may correspond either to a peak or to a trough at the symmetry center, and this question must be decided. In phthalocyanine itself there is no atom at the center of the molecule, but isomorphous derivatives may have a Be, Mn, Fe, Co, Ni, Cu, Pt, etc., atom at this point. The intensity of the x-ray reflection from a given plane in the free compound

and in the metal derivative is noted. If the intensity is greater for the latter and *increases in a series* with the atomic number and atomic structure factor of the central metal atom (*i.e.*, platinum is greater than copper), then it is established that the reflection from the free compound must correspond to a wave with a peak at the symmetry center which has been increased in amplitude by the single peak due to the metal atom. Thus the phase constant is 0 or has a positive sign. If the intensity is less, then the original wave has a trough at the center partly filled up by the metal contribution and the phase constant is π or negative. Thus there is not the slightest uncertainty as to the sign and the Fourier synthesis is carried out directly, and all atoms in the complex molecule except hydrogen are located easily in the projection. Two coordinates X and Z ($h0l$ projection) are located; and Y is found from another projection, although the structure is so regular it is easy to estimate the Y coordinates.

It is at once observed that the inner system of 16 carbon and nitrogen atoms forms a very regular arrangement with a constant interatomic distance of 1.34 A.U. This must represent an equivalence between all C—N bonds and hence a single-double bond resonance, as must also be true for the four equivalent benzene rings and the eight C—C bonds 1.49 A.U. in length linking them to the inner system. The whole molecule is a continuously conjugated system. However, the nitrogen atoms are separated by two distances 2.76 and 2.65, the latter made possible by *internal hydrogen bonds*.

The great importance of this structure is further indicated by the fact that a very similar nucleus with the four outer nitrogen atoms replaced by CH is the basis of the porphyrines—including chlorophyll, haemin, and other important animal and plant coloring agents.

6. *Sugars*.—The principal x-ray research on sugars has been carried on by Hengstenberg and Mark,¹ Sponsler and Dore,² Marwick,³ Astbury and Marwick,⁴ and especially Cox.⁵

¹ *Z. Krist.*, **72**, 301 (1929).

² *J. Am. Chem. Soc.*, **53**, 1639 (1931).

³ *Proc. Roy. Soc. (London)*, **A131**, 621 (1931).

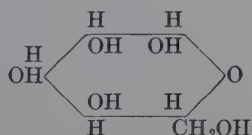
⁴ *Nature*, **127**, 12 (1931).

⁵ *J. Chem. Soc.*, **1935**, 978, 1495.

Essential data are tabulated as follows:

| Carbohydrate | System | Dimensions of unit cell | | | | Density |
|-----------------------------|--------------|-------------------------|----------|----------|----------------|---------|
| | | <i>a</i> | <i>b</i> | <i>c</i> | β , deg. | |
| Natural cellulose..... | Monoclinic | 8.3 | 10.3 | 7.9 | 84 | 1.52 |
| Cellulose hydrate..... | Monoclinic | 8.14 | 10.3 | 9.14 | 62 | 1.56 |
| Cellobiose..... | Monoclinic | 5.0 | 13.2 | 11.1 | 90 | 1.556 |
| Sucrose..... | Monoclinic | 11.0 | 8.7 | 7.65 | 103.5 | 1.588 |
| Mannose..... | Orthorhombic | 7.62 | 18.18 | 5.67 | | 1.501 |
| Glucose (α -d)..... | Orthorhombic | 10.40 | 14.89 | 4.99 | | 1.544 |
| Fructose (d)..... | Orthorhombic | 8.06 | 10.06 | 9.12 | | 1.598 |
| Sorbose..... | Orthorhombic | 6.12 | 18.24 | 6.43 | | 1.654 |

Astbury and Marwick have pointed out that the small variation in density of these saccharoses suggests an approximate close-packing of some molecular unit, and by further calculation of cross-sectional areas it becomes apparent at once that the dimensions of this unit—the sugar ring and its side chain—impress themselves in the various unit cells. For mannose as an example, the ring may be drawn

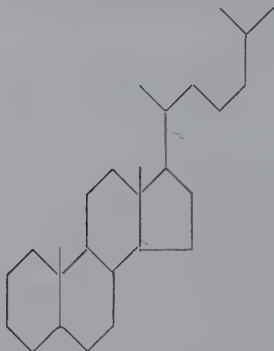


The molecular dimensions so deduced are 7.27, 5.64, and 2×4.58 . Thus probably the sugar ring takes about 4.5 A.U. in thickness or normal to the ring, about 5.5 A.U. across the ring horizontally, and 7.5 A.U. across the ring vertically in the direction of the side chain CH_2OH . All data are consistent with a flat form of pyranose and furanose rings, rather than strainless forms with tetrahedral bond angles.

7. *Carcinogenic Compounds, Sterols, Hormones, Vitamins.*—Reference has already been made to compounds of the type of 1, 2, 5, 6 dibenzanthracene, one of the well-known carcinogenic hydrocarbons.

A significant contribution already has been made by x-ray diffraction methods to the knowledge of the chemical nature of these biologically important compounds which are so complex

that configuration and chemical composition are often unknown. Complete analyses in the sense of those accomplished for the phthalocyanines are not possible as yet, but the x-ray results do suggest probable molecular arrangement. Crowfoot and Bernal have performed a great service in their pioneer efforts. In 1932 the interpretation of studies on ergosterol, calciferol, and other compounds related to vitamin D led to the correction of previously accepted sterol carbon skeletons to the structure



It is not possible here to consider these complex materials, but reference may be made to original papers,¹ largely of Crowfoot and Bernal.

8. *Highly Polymerized Natural and Synthetic Compounds.*—The structures of a great range of compounds with giant molecules, synthetic polymers, cellulose, rubber, proteins, are considered in Chap. XXIII.

Magnetic Measurements on Organic Crystals.—The most valuable of all supplementary methods of determining the structure of organic molecules is the measurement of the magnetic properties of crystals. Since the early experiments of Plücker, Faraday, and Tyndall it has been well known that non-cubic single crystals, even when cut in spherical shape, tend to assume a preferred orientation in a magnetic field. The strength of the effect under constant conditions is characteristic of a given crystalline compound, just as the x-ray diffraction patterns are. Although these general facts were known ninety years ago or

¹ General summary, *Chem. Weekblad*, **34**, January, 1937; *Nature*, **129**, 277 (1932); *Chem. Ind.*, **51**, 259 (1932), **54**; 701 (1935); *J. Chem. Soc.*, **1935**, 93; *Z. Krist.*, **93**, 464 (1936); *Trans. Faraday Soc.*, **29**, 1032 (1933).

more, little was done to correlate magnetic behavior and crystalline structure until the past very few years. Great advances are now being made especially by Krishnan and associates in India and by Mrs. Lonsdale and associates at the Royal Institution in London.¹

The anisotropy of crystals is of two types, diamagnetic and paramagnetic. Any substance placed in a magnetic field experiences a feeble induced opposing magnetization I (magnetic moment per unit volume) proportional to the field H , or $I = \frac{1}{4\pi}KH$, where K is the *diamagnetic susceptibility* per unit volume, is negative in sign, and depends only on distribution of electron density. If the substance is composed of ions, atoms, or molecules having a resultant orbital or spin moment, the tendency of an external magnetic field is to align these molecular magnets in such a way that their potential energy in the field is a minimum.

Complete alignment is opposed by kinetic motion of molecules, by interaction with neighboring molecules or ions, and by the local electric "crystal" field. The induced *paramagnetic* effect is in the same sense as the external field and when it occurs is generally much greater than the universal diamagnetic effect, which is completely masked therefore and is detected only when the elementary particles possess no resultant magnetic moment of their own. The gram-molecular paramagnetic susceptibility χ_m depends on the temperature as follows: $\chi_m = C_m/(T - \Theta)$ where C_m is the Curie constant, T the absolute temperature, and Θ the Curie point. Below Θ the thermal motion is not vigorous enough to overcome the tendency to alignment of the molecular magnets, hysteresis appears, and the substance is ferromagnetic with an intensity, of course, much greater than in paramagnetics.

Ions or molecules showing only a diamagnetic effect are characterized by the presence of closed systems; in other words, these are ions or groups having configurations similar to those of inert gases, with no resultant spin or orbital moment ($j = 0$; see page 119). Almost all organic molecules contain an even number of electrons whose spins are balanced in pairs and orbital moments compensated. Paramagnetism is found chiefly among salts

¹ For the best summarizing accounts see Lonsdale, *Science Progress*, **32**, 677 (1938); *Reports on Progress in Physics*, **4**, 368 (1938); *Proc. Roy. Soc. (London)*, **171**, 541 (1939).

containing ions of transition or rare-earth elements, having incomplete electron groups, and in a few other compounds with molecules containing an odd number of electrons.

Determination of the anisotropy of crystals involves location of principal susceptibility axes and measurement of susceptibility along those axes. These axes correspond to the crystallographic axes in orthogonal crystals (tetragonal, hexagonal, orthorhombic), and in monoclinic crystals one principal axis, χ_3 , coincides with the symmetry axis of the crystal, while χ_1 is the algebraically greater and χ_2 the smaller of two principal susceptibilities in the (010) plane.

The experimental methods involve a technique in which force is exerted on the crystal proportional to the difference of susceptibility in two orthogonal directions. One consists in observation of the change in the period of oscillation of a single crystal, suspended by a vertical torsion fiber, when placed in a uniform horizontal magnetic field. Another, especially useful for very small crystals, consists in suspension from a fine quartz fiber attached to a torsion head which is rotated until the axis of greatest susceptibility in the crystal lies along the field. If the torsion head is rotated from this equilibrium setting by an angle α , the crystal will rotate in the same direction but by a much smaller angle ϕ , the twist on the fiber being balanced by a restoring couple due to the field and the crystal anisotropy, which is a maximum at $\phi = \pi/4$, corresponding to a critical angle of deflection α_c . As this is surpassed by a fraction of a degree, the fiber instantly and rapidly untwists and the crystal spins around. This angle is introduced into the proper equation relating to values of χ .

Since diamagnetism depends only on the electron structure of matter, the mean susceptibility of organic compounds is an additive property, as, for a compound $A_\alpha B_\beta C_\gamma$, $\chi_m = \alpha\chi_A + \beta\chi_B + \gamma\chi_C + \lambda$, where α , β , and γ are the numbers of atoms of susceptibility χ_A , etc., and λ is a small constitutive correction for valence bonds. Thus even in the solid state the mutual influences of neighboring molecules must be negligible, and the anisotropy of the single crystal must be due to that of the unit cell which in turn is the resultant of the component molecules. If the molecule is isotropic magnetically, so also will be the crystal; if the molecule is anisotropic, then the degree to which the crystal reveals that

anisotropy depends on the arrangement of the molecules. If they are more or less parallel as in layer or chain structures, the crystal anisotropy may be as large as that of the molecule but never larger; or the arrangement of molecules may be such as to cancel out the anisotropies as in cubic crystals.

It is at once evident why the most striking magnetic results have been obtained with the aromatic derivatives with the flat benzene ring as described in this chapter. Some susceptibility results are illustrated in the following table for molecular values deduced from crystal susceptibilities and molecular direction cosines:

| Compound | $-K_1 \cdot 10^6$ | $-K_2 \cdot 10^6$ | $-K_3 \cdot 10^{-6}$ |
|--------------------------------------|-------------------|-------------------|----------------------|
| Naphthalene, $C_{10}H_{14}$ | 56.1 | 53.9 | 169.0 |
| Anthracene, $C_{14}H_{18}$ | 75.8 | 62.6 | 251.8 |
| Chrysene, $C_{18}H_{22}$ | 88.0 | 83.3 | 310.8 |
| Hexamethylbenzene, $C(CH_3)_6$ | 101.1 | 102.7 | 163.8 |
| Phthalocyanine..... | 165 | 120 | 98.2 |

Here K_1 and K_2 lie in the planes of the molecules, and K_3 lies perpendicular to that plane. It follows that a measurement of susceptibilities may be the quickest and simplest indication of departures from planar configuration. In this way Lonsdale¹ has shown that symmetrical triphenyl benzene (a *meta* derivative), *orthodiphenylbenzene*, and substituted diphenyl derivatives cannot possibly have planar configuration. A detailed analysis of crystal structure may be tedious or too difficult, but the magnetic susceptibilities of the crystal may well indicate the general shape of the molecule and its approximate position in the crystal framework. In long-chain compounds with no or very few double or triple bonds the maximum diamagnetic susceptibility and maximum refractivity correspond to the length of the molecule; in layer-structure single-bonded molecules (pentaerythritol, etc.) these maxima are in the mean plane of the layer along the direction of greatest length. In chains of conjugated double and single bonds, there is an abnormally large diamagnetic susceptibility normal to the plane of the groups, and the magnetic anisotropy is opposite in sign to that for single-

¹ *Z. Krist.*, **97**, 91 (1937).

bonded molecules and like that of aromatic molecules. Thus valuable information on bond distribution and effects of substituent side groups is immediately available. For these reasons the magnetic apparatus has become a valuable part of the equipment of every laboratory in which research is devoted to analysis of crystal and molecular structures.

CHAPTER XX

THE STRUCTURE OF GLASSES, LIQUIDS, AND OTHER COLLOIDAL AND AMORPHOUS MATERIALS

X-ray Diffraction by Crystalline and Amorphous Substances.—

It is now evident that crystals act as three-dimensional diffraction gratings for x-rays by virtue of the arrangement of the lattice units (atoms, ions, molecules, or groups of these) on sets of equidistant parallel planes. With a beam of monochromatic rays passing through a specimen, a pattern on a photographic plate is obtained, which is absolutely characteristic of the material since it reveals whether that material is crystalline or amorphous, what its crystallographic system and space-group defining coordinates in space and interplanar spacings are, whether it is a single crystal or an aggregate, whether the aggregate has random or preferred orientation of grains, whether it is a single pure substance or is a mixture of two or more individuals or a solid solution, how large the grains or particles are or how thick a film it has, and whether there is distortion or strain. It follows that a truly amorphous substance would be expected merely to scatter x-rays in all directions and produce a general fogging of the photographic plate without evidence of diffraction interference maxima, whereas any kind of arrangement of ultimate units, even though very imperfect, should produce a diffraction pattern characterized by interference maxima. Even a single diffuse broad diffraction ring would seem to indicate at least an elementary tendency toward organization. One of the most remarkable facts from x-ray science is the extreme rarity of the truly amorphous state. Repeatedly it has been found that a specimen which by all ordinary methods of examination appears to be amorphous produces unmistakable evidence of an organized ultimate structure under the searching scrutiny of radiation with wave lengths only $1/10,000$ as long as ordinary light, by means of which microscopic examination is made. Even liquids produce diffraction halos indicative of transient arrangement of molecules governed by distances of nearest

approach in their thermal agitation, or some type of characteristic distribution of neighbors around any given atom. And just now results on diffraction halos from gases have given evidence of the true structure of atoms in the sense of the distribution of diffuse wavelike negative electricity according to Heisenberg and Compton, instead of sharply corpuscular electrons moving in orbits as depicted by the Bohr theory.

Diffraction by Colloids.—A single crystal subjected to analysis by the pinhole method produces a Laue diffraction pattern characterized by a symmetrical array of spots, lying on a series of ellipses. As the size decreases and more individuals lie in the path of the beam, this symmetrical pattern gives way to a random "peppering" of spots. As the size decreases and the number increases still further, these small spots begin to assemble on a series of concentric rings. Finally the spots become so small and numerous that they merge into uniformly intense concentric rings, the so-called "powder" pattern. The maximum range of grain diameter over which these sharp rings are registered is from 10^{-3} to 10^{-5} cm. It is clearly evident that a sharp interference effect can take place only with a certain minimum number of parallel diffracting planes in each particle. As this number falls below the minimum, or, in other words, as the particle size decreases below about 10^{-5} cm., it follows that interference is less perfect and that the diffraction rings (or lines by the Hull-Debye-Scherrer method) will become broader in proportion to decreasing size until in the neighborhood of 10^{-8} cm. atomic dimensions are reached. Conceivably these "halos" might merge and the pattern would then be classed as amorphous. A measurement of line breadth in the colloidal range will therefore allow calculation of particle size as will be illustrated fully in Chap. XXI. The question arises of how small a particle can be and still produce a diffraction pattern upon which maxima may be detected. Levi in his study of metallic catalysts reports that particles only about five times as large as the unit crystal cell (in other words 10 or 15 parallel planes) will produce resolved diffraction maxima, even though these are very diffuse.

Now it must be noted that diffuse diffraction maxima must be the consequence of any crystal grating which is imperfect in the sense of having too few parallel planes or of having these planes, ordinarily sufficient in number, distorted, bent, or imper-

fectly aligned. In other words, it is conceivable that an assemblage of fairly large colloidal particles might yield very diffuse patterns simply because molecules which may themselves be very large are not oriented in regular fashion. This condition is observed in the colloidal gels and is particularly interesting in the light of the prediction that simple mechanical stretching might tend to pull these diffracting units into parallel position and thus permit them to act as a diffraction grating.

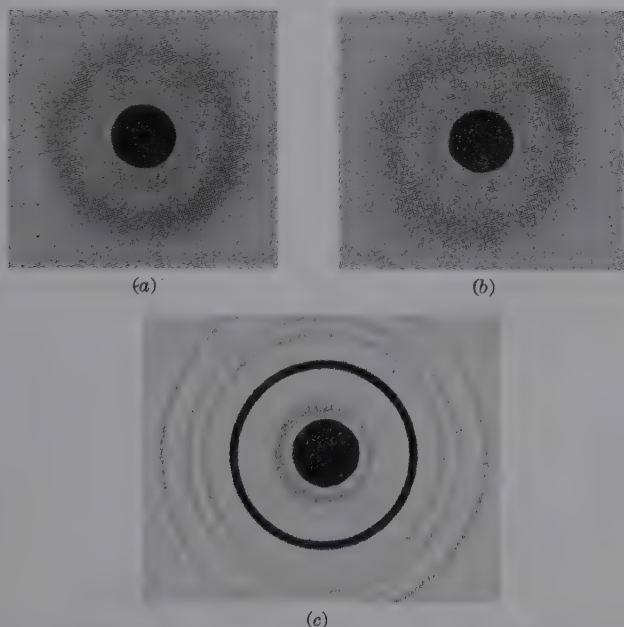


FIG. 216.—Diffraction patterns for glasses and crystalline silica: (a) vitreous silica, $d = 4.32$ A.U.; (b) pyrex glass, $d = 4.26$; (c) β -cristobalite, $d = 4.11$.

Diffraction by Glasses, Liquids, Carbon-blacks, and Other Amorphous Substances.—We have just seen that the crystals may be subdivided into colloidal particles so small that the powder diffraction interferences become broad and diffuse, though they still represent the characteristic spacings of the crystalline lattice. There are substances that cannot be classified as crystalline colloids which also yield patterns of a few broad “halos.” These include all glasses, of which vitreous silica is the simplest example, liquids, and a number of so-called “amorphous” solids, such as the familiar carbon-black. Since crys-

talline silica and silicates have been considered already in Chap. XVII, it is logical to consider first the structure of a glass.

The Structure of Glass.—Diffraction patterns of glass specimens are made by the usual pinhole method with registration on a flat film. Figure 216 illustrates the pattern obtained with the glass formed from molten silica. It is very advantageous on account of the diffuse nature of the pattern to use a strictly monochromatic beam of x-rays reflected from a crystal, such as pentaerythritol, and a vacuum camera by means of which troublesome background fogging is eliminated. To illustrate the general method of interpretation, the simple case of vitreous SiO_2 will be selected from the work of Warren. The two halos, calculated by means of Bragg's law for crystal reflection, correspond to spacings of 4.32 and 1.30 A.U. The two principal theories of interpretation are: (1) The glass is composed of colloidal crystallites of such minute size that the crystal interferences are greatly broadened. (2) The glass is a random network, and x-rays are scattered in this noncrystalline medium.

1. *Crystallite Interpretation.*

a. Favorable data. (1) Vitreous silica, held at 1500° for several hours devitrifies to cristobalite, for which the strong crystalline (111) reflection (Fig. 216) corresponds roughly in angular position to that of the principal glass halo. (2) Cristobalite is the stable crystalline form of SiO_2 in the temperature range through which the vitreous silica solidified. (3) Randall, Rooksby, and Cooper evaluated the particle size upon the assumption of colloidal crystallites as 15 A.U., which seems not unreasonable.

b. Unfavorable data. (1) There is actually a discrepancy of 6 per cent in the spacing of the principal halo, 4.32 A.U., and that of the cristobalite crystal interference, 4.05 A.U. (2) There is no sharp melting point of glass, whereas crystals, even of minute size, would be expected to have a definite value. (3) As glass is annealed, there are no gradual increase in crystal-particle size, as is true for all cases of truly crystalline material, and no sharpening of the diffraction bands; instead, the broad peak of vitreous silica goes over abruptly into the sharp displaced ring of cristobalite. (4) The origin and previous history of the sample have no effect on the pattern of the vitreous state, whereas they should exert an effect in the case of the crystallites. (5)

Cristobalite undergoes a marked volume change between 200 and 300°, whereas vitreous silica has no such change. (6) Precision measurements by Warren¹ prove that the crystal-particle size calculated from the breadths of the halos at points of half maximum intensity is about 7.7 A.U. Since the edge of the unit cell of low-temperature cristobalite is 7.0 A.U., it is necessary to postulate crystals comprising only a single unit cell in order to explain the observed peak width. This has no real significance since the very essence of the crystalline state is regular repetition of the unit cell. (7) The bonding in glass is continuous, rather than a structure in which there are small crystals with a break between them. This is proved by the complete absence of x-ray scattering at small angles on glass patterns, whereas for silica gel there is very strong scattering at small angles, due to the existence of discrete particles (10 to 100 A.U.), with breaks and voids between them. Thus even if a cristobalite crystal is assumed to exist as a center, the scheme of bonding out from this center cannot follow a crystal pattern, for otherwise entirely different widths would be found. Hence x-ray analysis proves that the major part of the material certainly cannot be in the form of cristobalite crystals of sufficient size to have this term mean anything.

2. *Random-network Interpretation.*—The alternative theory of interpretation from a purely descriptive point of view, which we shall see has quantitative mathematical support, retains without change in glass the familiar plan of coordination of four oxygen atoms tetrahedrally around each silicon atom as definitely established in the various crystal forms of SiO_2 . Glass is a form of matter in which the coordination plan is exactly the same as in the crystalline phase but which cooled too rapidly from a viscous melt to permit the orderly construction of any regularly repeating structure; glass, therefore, is a liquid of very high viscosity in which atoms are so tightly bound together in an irregular network that there is no opportunity for the breaking and reforming into crystals. The bonding is continuous even though in a random network. Such a network, as proposed by Zachariasen, is illustrated in Fig. 217. The absence of a sharp melting point and the temperature range of softening are to be explained by the varying energy required to break down each mesh of different

¹ *J. Applied Phys.*, **8**, 645 (1937).

size and arrangement. The tendency of silica to form a glass resides in the tendency to form the SiO_4 coordinated group even in the melt and in the bonding of each oxygen between two silicon atoms. Such linkages stiffen the liquid to a high viscosity so that there is not sufficient mobility to permit crystallization on cooling. And yet the bonding is such that there is still enough flexibility so that the random network is about as stable as the

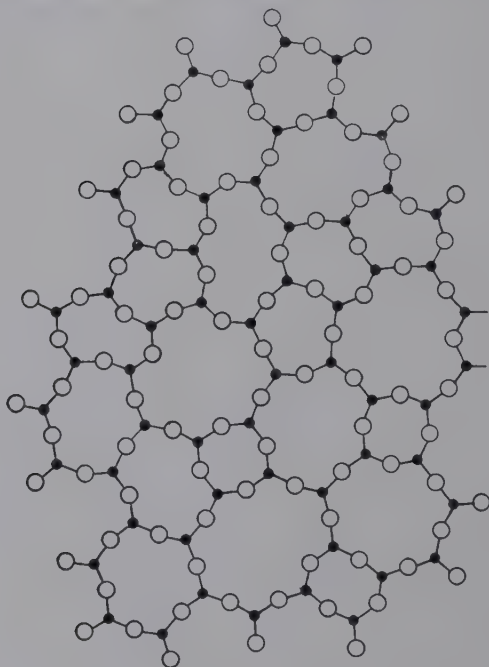


FIG. 217.—Random network of SiO_4 tetrahedra in glass. (Zachariasen.)

crystalline arrangement and so continues to exist; devitrification occurs only at elevated temperatures over considerable time.

Theoretical Calculation of Glass Diffraction Pattern.—If the assumptions of oxygen coordination of silicon and the linking of these tetrahedra in a random network in glass are sound, they may be subjected to mathematical test such that the pattern of halos may be theoretically deduced. The method of calculating the intensity of x-ray scattering on an amorphous solid is based upon the method originated by Zernicke and Prins¹

¹ *Z. Physik*, **41**, 184 (1927).

for liquids and adopted by Warren.¹ The intensity of scattering I , from an array of atoms taking all possible orientations in space, is given by $I = \sum_m \sum_n f_m f_n (\sin sr_{mn})/sr_{mn}$, where $s = (4\pi \sin \Theta)/\lambda$, f is the atomic scattering factor, and r_{mn} is the distance from atom m to n . For SiO_2 ,

$$I = N \left(f_{\text{Si}} \sum_n f_n \frac{\sin sr_{\text{Si}-n}}{sr_{\text{Si}-n}} + 2f_{\text{O}} \sum_n f_n \frac{\sin sr_{\text{O}-n}}{sr_{\text{O}-n}} \right),$$

when N is the effective number of SiO_2 molecules in the sample.

The next step is tabulation of the number of neighbors and their distances about any one atom. For vitreous silica this distribution is as follows:

| | |
|--|--|
| 1 Si surrounded by | 2 O, each surrounded by |
| 1 Si $r = 0$ | 1 O $r = 0$ |
| 4 O $r = 1.60$ | 2 Si $r = 1.60$ |
| 4 Si $r = 3.20$ | $6 \times \frac{1}{2} = 30$ $r = 2.62$ |
| $12 \times \frac{1}{2} = 60$ $r = 4.00$ | 6 SiO_2 $r = 4.00$ |
| 12 SiO_2 $r = 5.20$ | |
| Continuous distribution beyond $R_1 = 6.05$ | Continuous distribution beyond $R_2 = 4.55$ |

This means that out to 5.20 A.U. from each silicon atom the number of neighbors and distances is definite regardless of the orientation of the tetrahedral groups, whereas, beyond this, distances in a random network are indefinite and a continuous distribution of scattering matter is then assumed, equivalent to $-\frac{4}{3}R^3\rho f\phi(sR)$, where ρ is the SiO_2 density and

$$\phi(x) = \left(\frac{3}{x^2}\right) \left(\frac{\sin x}{x - \cos x}\right).$$

Then,

$$\begin{aligned} \frac{I_{\text{unmodified}}}{N} = & f_{\text{Si}} \left[f_{\text{Si}} + 4f_{\text{O}} \frac{\sin 1.60s}{1.60s} + 4f_{\text{Si}} \frac{\sin 3.20s}{3.20s} + \right. \\ & \left. 6f_{\text{O}} \frac{\sin 4.00s}{4.00s} + 12f_{\text{av.}} \frac{\sin 5.20s}{5.20s} - 17f_{\text{av.}}\phi(6.05s) \right] + 2f_{\text{O}} \left[f_{\text{O}} + \right. \\ & \left. 2f_{\text{Si}} \frac{\sin 1.60s}{1.60s} + 3f_{\text{O}} \frac{\sin 2.62s}{2.62s} + 6f \frac{\sin 4.00s}{4.00s} - 8f\phi(4.55s) \right]. \end{aligned}$$

¹ Z. Krist., **86**, 349 (1933); Phys. Rev., **45**, 657 (1934); J. Am. Ceram. Soc., **21**, 49 (1938).

$I_{\text{modified}} = N(I_{\text{Si}} + 2I_{\text{O}})$ where $I = Z - \sum_1^Z (f_n)^2$ where Z is the atomic number.

Now values of $I_{\text{unmodified}} + I_{\text{modified}}$ expressed as electron units per SiO_2 molecule are plotted as a function of $\frac{\sin \Theta}{\lambda} \left(s = \frac{4\pi \sin \Theta}{\lambda} \right)$. This gives an intensity curve (Fig. 218a) that corresponds exactly with the experimental curve from the microphotometer record of the diffraction pattern. Thus a theoretical pattern is deduced, which correctly places the halos (not a continuous fog) and yet assumes no crystalline arrangement whatever beyond about 5 A.U. from any given atom. However, a still more direct method utilizes the experimental intensity curve to calculate distances and number of neighbors at each distance. A radial distribution function is introduced such that $4\pi r^2 \rho(r) dr$ is the number of atoms between distances r and $r + dr$, and a Fourier analysis is carried out.¹ For SiO_2 with two kinds of atoms

$$\sum K_m 4\pi r^2 \rho(r) = \sum K_m 4\pi r^2 \rho_0 + \frac{2r}{\pi} \int_0^\infty si(s) \sin rs ds,$$

where Σ is the summation over molecular composition; K_m is the effective number of electrons in atom m and is equal to f_m/f_e , where f_m is the atomic structure factor and $f_e = \Sigma f_m / \Sigma Z_m$ or average f per electron; $i(s) = \frac{I_{eum} - \Sigma f_m^2}{f_e^2}$ where I_{eum} is the experimental intensity of unmodified scattering in electron units per molecule; ρ_0 is the average number of electrons per unit volume. The quantity $si(s)$ is obtained from the experimental scattering curve which is put on an absolute basis in electron units per SiO_2 by consideration of the fact that at large values of $\sin \Theta$ it must approach the theoretical curve for independent scattering by the atoms. The integration is carried out for different values of r and the values $\Sigma K_m 4\pi r^2 \rho_m$ plotted against r give the radial distribution curve of vitreous silica. This really gives two superposed curves, one for distribution about silicon and one for that about oxygen, as in Fig. 218b. The area under the peaks allows calculation of the number of neighbors at the particular distance. The

¹ WARREN, KRUTTER, and MORNINGSTAR, *J. Am. Ceram. Soc.*, **19**, 202 (1936).

first peak at 1.62 A.U. is to be compared with 1.60 for Si—O distance in crystalline silicates. If there are n oxygen atoms around each silicon atom and $n/2$ silicon atoms around each oxygen atom

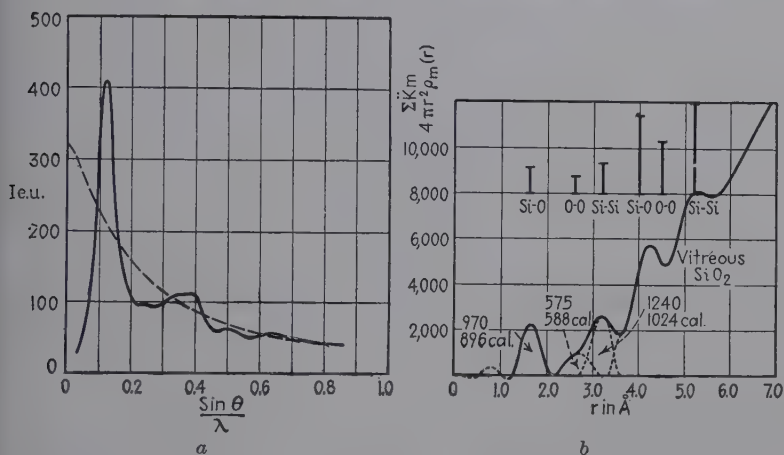


FIG. 218a.—X-ray intensity curve for vitreous SiO_2 in electron units per SiO_2 ; dashed line, independent scattering per SiO_2 .

FIG. 218b.—Radial distribution curve for vitreous SiO_2 . (Warren.)

and, if the values $K_{\text{Si}} = 16$ and $K_{\text{O}} = 7$ are taken, the area under the peak will be

$$A = \underbrace{1 \times 16 \times n \times 7.0}_{\text{Si-O}} + \underbrace{2 \times 7.0 \times \frac{n}{2} \times 16}_{\text{O-Si}};$$

if the measured value of A is introduced, $n = 4$. Similarly the next peak will be due to O—O (2.62), Si—Si (3.20), Si—O (4.00) and O—O (4.5) unresolved at 4.2, Si—Si (5.2) and then a smoothing out for continuous distribution.

The x-ray results on silica glass are completely and quantitatively explained by a random network in which each silicon atom is tetrahedrally surrounded by four oxygen atoms, each oxygen atom bonded to two silicon atoms, the two bonds being roughly diametrically opposite, and a random orientation of the tetrahedra around the Si—O—Si bond.

Every other substance in the glassy state may be treated in analogous fashion. GeO_2 and BeF_2 glasses afford an excellent check on SiO_2 . For soda-silica glass, part of the oxygen atoms are shared between two silicon atoms, and others are bonded to

only one silicon. The double-bonded oxygen atoms build up the continuous framework, in the holes of which the sodium atoms are located at random, with no evidence of compound formation.¹ A complete Fourier radial distribution analysis has been made for soda-boric oxide glass.² In the random network the boron atoms are bonded either to three oxygen atoms in triangles or four tetrahedrally, and the sodium atoms are distributed at random in holes in the boron-oxygen network. Anomalous properties are due to the ability of the boron atom to change to tetrahedral coordination when Na_2O is present to supply the necessary oxygen.

It follows that the tendency of any substance to form large groups of polyhedra will make crystallization difficult and glass formation likely. As examples may be cited, the familiar oxides (acid anhydrides) with non-ionic character: Be_2O_3 , SiO_2 , P_2O_3 , P_2O_5 , GeO_2 , As_2O_3 , As_2O_5 ; similarly BeF_2 (BeO is ionic and forms no glass), H_3PO_4 , $\text{K}_2\text{Mg}(\text{CO}_3)_2$, metallic selenium (chain fragments retained in melts), a large group of organic substances whose melts contain large and irregular molecules, or polymerized groups linked by rather strong forces that retard crystallization.³

The Structure of Amorphous Solids.—By exactly the same radial distribution methods as are employed for glass, it is possible to reproduce theoretically the halo patterns for a whole series of materials that are commonly described as amorphous and thus to account for their structures in terms of the immediate neighbors around any atom. The most familiar examples are the extremely fine powders of the carbon-blacks, amorphous forms of elementary phosphorus, unstretched rubber, etc.

The familiar and commercially important carbon-blacks used as pigments, rubber fillers, etc., have been frequently studied by x-ray diffraction. Usually these give broad halos corresponding to the (002) (basal) and (100) spacings of graphite. The newest measurements by Clark and Rhodes of particle sizes upon such an assumption of minute graphite crystallites are described in the next chapter. Here the interest lies in applying the methods already found so successful for the glass random net-

¹ WARREN and LORING, *J. Am. Ceram. Soc.*, **17**, 249 (1934); **18**, 269 (1935); **21**, 259 (1938).

² BISERE and WARREN, *J. Am. Ceram. Soc.*, **21**, 287 (1938).

³ HÄGG, *J. Chem. Phys.*, **3**, 42, (1935).

works. From the experimental intensity curve the distribution curve $4\pi r^2 \rho(r)$ is derived by a purely mechanical, straightforward method (harmonic analyzer) as already indicated. Four peaks are found as follows:

| Carbon-black | | Single graphite layer (crystal) | | |
|----------------|---|---------------------------------|------------------|-----------------|
| Distance, A.U. | Approximate number of atoms from peak areas | Distance, A.U. | Average distance | Number of atoms |
| 1.5 | 3 | 1.42 | ... | 3 |
| 2.7 | 10 ± 1 | 2.46 } 2.84 } | 2.6 | 6 } 3 } 9 |
| 4.05 | 12 | 3.75 } 4.25 } | 4.0 | 6 } 6 } 12 |
| 5.15 | 12 | 4.92 } 5.11 } | 5.0 | 6 } 6 } 12 |

Allowing for errors and overlapping of peaks it is at once evident that the distribution is that of single graphite layers (Fig. 219) which, therefore, must exist in carbon-blacks. If other layers have a definite position and orientation with respect to a first layer, then graphite is indicated; if they are at random, then at least the carbon-black can be considered to be two-dimensionally crystalline, or *mesomorphic*. From the data a distinction cannot be made. A characteristic feature of carbon-black patterns is very intense scattering at small angles caused by the difference between grain density and average density from loose packing of extremely small grains. Hence the blacks seem to be a heterogeneous mixture of particles ranging from single graphite layers up to graphite crystals several layers thick.¹

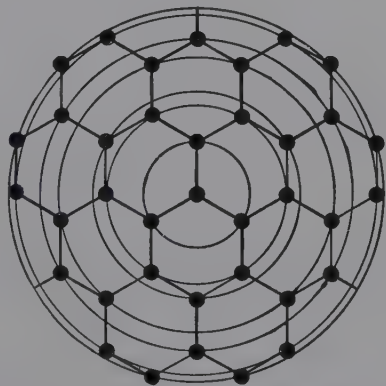


FIG. 219.—Atomic arrangement in a single layer of graphite, with equidistant neighbors shown lying on circles.

¹ WARREN, *J. Chem. Phys.*, **2**, 551 (1934).

Coals, vitrains, durains, charcoals, etc., have been studied, in similar fashion, at least in respect to the graphite halos and small-angle scattering.

The question that naturally arises next is whether or not there is a continuous transition between the crystalline and the amorphous state. From what has been said concerning continuous broadening of lines till these merge and spread over the entire film, such a process would be indicated. Sir William Bragg quotes the experiment by the present writer on carbon. An activated charcoal producing an essentially amorphous pattern had certain characteristic chemical and physical properties which changed over to those of graphite upon brief heating at 1100°C. The x-ray pattern, however, was unchanged since no lines appeared. The great activity of the original charcoal was ascribed to the free valences of disorganized carbon atoms. Upon heating, the solid phase being retained throughout, these began mutually to attach themselves to satisfy these bonds and to form crystal planes of graphite, which were still too few and bent to permit interference of rays, though the properties were typical of graphite. This stage of elementary organization was designated *paracrystalline*. Upon further heating the grains grew in size and the planes in number and rigidity, so that broad diffraction lines for colloidal dimensions finally sharpened to the typical graphite spectrum.

Amorphous red, amorphous black, and *liquid* yellow varieties of phosphorus give remarkably similar patterns and distribution results with three nearest neighbors. In the liquid, P₄ molecules probably exist, but in the high-melting amorphous solids complications are probably introduced by a puckered network as in crystalline black phosphorus.¹

| | Peak 1 | Peak 2 | Peak 3 |
|---------------------------|--------|--------|--------|
| Amorphous red, 50°..... | 2.29 | 3.48 | |
| Amorphous black, 20°..... | 2.27 | 3.34 | |
| Liquid yellow, 48°..... | 2.25 | 3.90 | 5.90 |
| Liquid yellow, 226°..... | 2.25 | 3.90 | 6.10 |

Unstretched rubber gives a typical "amorphous" pattern of broad halos. Again by the same Fourier distribution method

¹ HULTGREN, GINGRICH, and WARREN, *J. Chem. Phys.*, **3**, 351 (1935).

THOMAS and GINGRICH, *ibid.*, **6**, 659 (1938).

it is found that each carbon atom has two carbon neighbors at 1.52 A.U., about 3.4 at 2.68 A.U., and others in its own chain or in adjacent chains at 4.0 and 5.0 A.U. This is in excellent agreement with the concept of a structure of long-chain molecules, whose exact configuration in unstretched rubber, however, cannot be deduced.¹

Synthetic Resins.—All the numerous and familiar commercial plastics or synthetic resins such as bakelite yield halo patterns, and their structures may be represented by the distribution method exactly as in the case of unstretched rubber. These plastics probably having three-dimensional random networks are to be distinguished from the crystalline linear polymers with remarkably rich patterns. No complete analyses have been carried through as yet; from a qualitative point of view, the patterns are often sufficiently distinctive to permit identification of the variety of resin, as indicated in the following table:

| | d_1 , A.U. | d_2 , A.U. | d_3 , A.U. |
|--------------------------------------|--------------|-----------------|-----------------|
| Phenol formaldehyde..... | 3.5 | 4.6 | |
| <i>o</i> -Cresol formaldehyde..... | 3.5 | 5.0 | |
| <i>m</i> -Cresol formaldehyde..... | 3.6 | 5.0 | |
| <i>p</i> -Cresol formaldehyde..... | 3.5 | 4.6 | |
| Xylenol formaldehyde, liquid..... | 4.1 | 5.5 | 17.5 |
| Xylenol formaldehyde, soft..... | 4.2 | 5.5 | 14.7 |
| Xylenol formaldehyde, infusible..... | 4.2 | 5.9 | 15.4 |
| Xylenol formaldehyde, fusible..... | 4.2 | 6.2 | 12.65 |
| Cumarone-indene..... | 2.2 | 5.2 | 9.4 |
| Stearic-glycerol phthalate..... | | 4.55 | 9.32 |
| Half-acid ester..... | 4.05, 4.80 | 6.3 | 14.0 |
| Resin from rosin..... | 2.25 | 5.51 | |
| Glycerol-sulfur..... | | 4.8 | 9.32 |

Patterns and microphotometer curves from the writer's laboratory for a variety of resins are illustrated in the most authoritative treatise.²

Diffraction by Liquids. Older Concepts.—It has been known definitely since 1916 that liquids through which x-rays are passed

¹ SIMARD and WARREN, *J. Am. Chem. Soc.*, **58**, 507 (1936).

² ELLIS, "The Chemistry of the Synthetic Resins," Vol. I, p. 76, Reinhold Publishing Corporation, New York, 1935.

produce diffraction patterns characterized by one or more halos or interference rings, usually somewhat diffuse. A large number of papers dealing with this subject theoretically or experimentally have now appeared. It is not possible here to present the historical development, but only to give the status of experimental results as they now stand. An excellent survey of researches up to 1928 is given in a paper by Drucker.¹

The preponderance of opinion up to 1933 was that the diffraction effects with liquids indicate orderly spatial arrangements of molecules. The phenomenon is understood qualitatively in the same sense that crystal diffraction is understood. Interference effects might be due to periodicities within the atom (electron distribution), within the molecule (atomic distribution), or between molecules. The first must be true for monatomic substances which were investigated by Debye and Scherrer in 1916. Certain halos for other compounds may be due to atomic distribution, but certainly the third cause is predominating in complex molecules, since the chief diffraction maxima are accounted for by a periodicity in the distribution of molecules. This would be particularly true for asymmetrical molecules. In liquids these would have a certain distance of nearest approach side by side or end to end. According to Stewart,²

... if x-rays give evidence of periodic molecular grouping it must not be supposed that these groups are large or that the molecules in any one well defined group remain permanently members of that group. At any one instant these small orderly molecular groups might exist at numerous points in the liquid, the regions between them being not so orderly.

This orderly arrangement in groups was called by Stewart "cybotaxis." There was evidence, therefore, that the Bragg law $n\lambda = 2d \sin \theta$ could be applied to liquid diffraction interferences just as truly as to crystalline solids. Scattering centers at random (*i.e.*, in amorphous material) would produce a large scattering near 0° , but such is not the case for liquids any more than it is for crystals. Furthermore, the integrated intensity in the region of the chief diffraction maximum for equal masses per unit area for a solid and liquid show the same values, again indicating distinct coherence.

The principal work on liquid diffraction up to 1935 was carried out at the University of Iowa by Stewart and associates, who

¹ *Physik. Z.*, **29**, 273 (1928).

² *Rev. Modern Phys.*, **2**, 116 (1930).

used the ionization spectrometer, and by Raman and associates, at Calcutta, who used the photographic method. A brief summary of some experimental conclusions must suffice.

1. In diffraction rings of chain molecules such as *n*-alcohols, *n*-fatty acids, and *n*-paraffins there is always a major intensity maximum corresponding to a spacing of 4.6 A.U. which is evidently the effective diameter of the molecule.

2. Branched-chain isomers invariably increase the effective diameters of the chains in characteristic manner.

3. In polar compounds such as *n*-alcohols a second maximum, whose position depends upon the number of carbon atoms, indicates values of *d* that are twice, or less than twice, the molecular length, indicating a grouping of two polar molecules by attraction of the polar —OH,—COOH, etc., groups. Spacing less than twice molecular length could be accounted for by a tilt with respect to planes, entirely in accord with observations on solid films (see page 438). For isomers in which the polar group is not attached to the end or next to the end carbon atom, doubling does not occur.

4. The carbon atom in these chains occupies a distance of about 1.24 A.U. per atom, indicating probably a zigzag arrangement.

5. Stewart accomplished simultaneous measurement of more than one diameter in a chain in such compounds as 2-methyl hexane (5.25 and 4.84 A.U.) and di-*n*-propyl carbinol (4.85 and 4.5). A third maximum gives the length.

6. Benzene and cyclohexane give sharp rings, indicating a ring structure with thickness of 4.7 and 5.1 A.U. (Stewart), greater than observed for flat rings in crystals. Para derivatives give least thickness.

7. The effect of temperature on diffraction patterns is precisely that which might be predicted upon the basis of crystal data. The intensity maximum is displaced (expansion), and the maximum is diminished in intensity and increased in width (greater disorder due to thermal agitation).

8. Impurities, particularly containing heavy atoms, have a large effect sometimes upon results. The distinction of purity and isomerism constitutes a very useful application.

9. Some apparent discrepancies among the findings of different experimenters were found to be due to the fact that, with an x-ray beam which has not been filtered with greatest care in order to render it monochromatic, halos are produced as an interference

effect of general radiation. With copper radiation and liquid fatty acids this secondary ring is obtained with specimens thicker than 2 mm., according to Thibeaup and Trillat,¹ who further reached the conclusion that inner halos, frequently observed by Stewart and attributed to molecular length, are always due to diffraction of general radiation supposedly by the same spacing as that of the principal halo (cross section). Clark and Stillwell² proved that with molybdenum radiation at a tube voltage of 33 kv. or more the inner ring is produced by diffraction and filtration of general radiation and bears no relation to molecular length, while at voltage below 27 kv. the inner ring is characteristic of the liquid under examination.

10. In many instances the liquid halos correspond approximately in their positions to the principal diffraction maxima for the same substance as a solid.³

11. For totally miscible pairs of organic liquids the pattern exhibits a single major maximum which has an angular position between the maxima for the pure constituents and shifts directly with the concentration.⁴ On the other hand, an emulsion of phenol in water produces the interferences for both constituents. Hence in a solution there exists a single type of cybotactic group to which molecules of both constituents contribute, whereas in the emulsion two types of cybotactic groups exist. This constitutes a fundamental differentiation between solutions and nonsolutions.

12. Stewart and Edwards⁵ showed for a series of 22 octyl alcohols that there is a definite correlation between the coefficient of viscosity and the perfection of grouping in the direction of chain lengths as measured by relative halo intensities. This corresponds with the view that the viscosity within liquid groups is caused by longitudinal slippage. The temperature coefficient of viscosity is negative because the size of groups decreases.

13. An exceptionally careful investigation of water over a range of temperatures was made both by Meyer,⁶ who used

¹ *Z. Physik*, **61**, 816 (1930).

² *Radiology*, **15**, 66 (1930).

³ KRISHNAMURTI, *Ind. J. Phys.*, **3**, Part II, 225 (1928).

⁴ MEYER, *Phys. Rev.*, **38**, 1083 (1931).

⁵ *Phys. Rev.*, **38**, 1575 (1931).

⁶ *Ann. Physik*, **5**, 701 (1930).

a strictly monochromatic x-ray beam obtained by crystal reflection and the photographic method, and by Stewart¹ with his usual ionization method. There was general agreement in finding three interference maxima corresponding to distances 3.13, 2.11, and 1.34 (Meyer), 3.24, 2.11, 1.13 (Stewart). The distance between molecules as scattering centers represented by the most prominent halo decreases with temperature, while the breadth of the halo increases, whereas the distance corresponding to the next most important halo increases. This halo tends to disappear with increasing temperature. There is a quantitative similarity between the periodicities found in the liquid and the three most important periodicities in powdered ice. These results were particularly interesting in the light of theories of molecular association in water. The water diffraction results seemed to indicate periodicities of only one kind of molecular grouping, just as the results on ice indicate one kind of crystal structure only. Hence it appeared that the simple explanation of molecular association is the association in cybotactic groups of a relatively large number of molecules and not in complexes such as di- or trihydrol.

The Modern Interpretation.—It was inevitable that a more quantitative and formal interpretation of liquid diffraction should replace such mechanical pictures as cybotaxis, a theory which was based on a concept that no catastrophic change occurred on melting and that temporary groupings of molecules over small elements of time and space are probable, thus assuming a transient structure closely similar to that of the solid. The basis for this rigorous treatment was given by Debye in 1915 for the intensity of scattering by a noncrystalline liquid and by Zernicke and Prins in 1927 for the Fourier analysis of radial distribution. Today it is unnecessary to postulate any kind of crystalline arrangement, however transient, in a liquid. The diffraction patterns, exactly like those of glasses and amorphous solids, may be theoretically reproduced upon the basis of an arrangement of immediate neighbors around any atom and of a completely random distribution beyond a distance of the order of 5 A.U. Liquid sodium gives a radial density curve $4\pi r^2\rho(r)$ with a peak at 4.0 and another at 2.0 A.U. In the analogy of

¹ *Phys. Rev.*, **37**, 9 (1931).

Warren¹ we may interpret the curve in terms of a box full of ball bearings continuously shaken. About the center of any one ball bearing we shall never expect to find another closer than the diameter of the balls. At about this distance we shall expect to find the centers of several balls, since at any instant there will be a number of balls in approximate contact with the one under consideration. At a somewhat larger distance the number of balls must drop a little since the immediate neighbors described will prevent others from coming into the immediate vicinity of the first ball.

Such is the structure of any liquid—a structure arrived at by the average distribution of neighboring atoms around any one

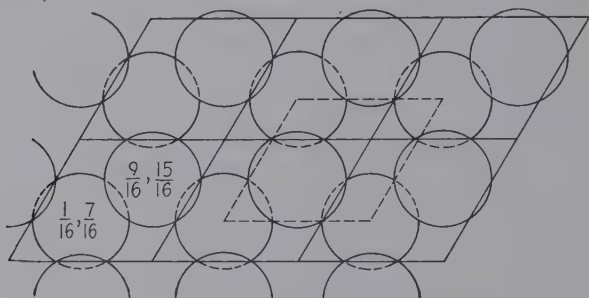


FIG. 220.—The structure of ice, H_2O .

atom. Liquid hydrocarbons have precisely the same treatment as rubber. Peaks represent the distances to the next neighbors, then the next, etc., including neighbors in the next molecule as well as in the same one.

Although there is great similarity between glass and liquid scattering and both are treated alike, there is one important difference: in all glasses the dip following the first peak comes down to the axis, whereas in liquids there is poor resolution in that the dip does not come more than halfway down. The explanation is that in a liquid a molecule does not have permanent neighbors, for some of these are free to move in or out of positions of approximate contact.

The deductions on the structure of water are interesting. The area under the first peak at distance 2.9 to 3.0 A.U. indicates something less than four molecules. The tendency of the water

¹ FARASOV and WARREN, *J. Chem. Phys.*, **4**, 236 (1936).

TRIMBLE and GINGRICH, *Phys. Rev.*, **53**, 278 (1938).

molecule toward tetrahedral coordination, so definite in ice, persists, although on the average less than four neighbors are so bonded. This deficiency is indicated by Raman spectra and explains the latent heat of fusion as a bond-breaking. Water has a greater density than ice in spite of a somewhat greater distance from a molecule to the first neighbors. Ice has an extraordinarily open structure (Fig. 220); when it melts, the second, third neighbors, etc., can fill in between the wide spacings in the solid framework.¹

"Structure" persists for liquids above their critical temperatures, as might also be expected from the radial-distribution interpretation.²

Hydrogen peroxide has peaks on its radial density curve at 3.0 A.U. (12 neighbors) and at 4.25 (6 neighbors); this is precisely a type of face-centered cubic packing of OH groups, which are 0.1 A.U. greater in radius than in water. The correct dipole movement is calculated from such a model.³

Liquid Crystals and Mesomorphic States.—The ability has long been recognized of certain long-chain compounds, such as *p*-azoxyanisol, to form liquid crystals, easily recognized by characteristic anisotropic optical properties. In 1922 Friedel proposed in a classical paper the classification of certain states intermediate between isotropic liquid and crystal as mesomorphic states (Fig. 221). The process on cooling from the transparent liquid is as follows:

Liquid—random distribution of molecules
 ———Discontinuity (definite temperature)

Mesomorphic states:

Nematic (from $\nu\eta\mu\alpha$ thread)—long molecules; oriented in same direction, but not in layers

———Discontinuity (definite temperature)

Smectic (from $\sigma\mu\epsilon\gamma\mu\alpha$, soap)—long molecules; oriented in same direction and in equidistant layers; corresponding to length, but random laterally

———Discontinuity (definite temperature)

Crystal—3-dimensional orientation

Undoubtedly transition phenomena must occur in all cases of solidification of a molten substance, but only in the case of

¹ WARREN, *J. Applied Phys.*, **8**, 645 (1937).

² BARNES, *Chem. Rev.*, **23**, 29 (1938).

³ RANDALL, *Proc. Roy. Soc. (London)*, **159**, 83 (1937).

the certain organic molecules is the temperature range of each state sufficiently extended to permit detection. From the x-ray diffraction point of view it would be predicted that the nematic "liquid crystal" should give a pattern similar to that of the liquid and that the smectic "liquid crystal" should give a sharp interference in several orders corresponding only to the arrangement of oriented long molecules in equidistant layers. The

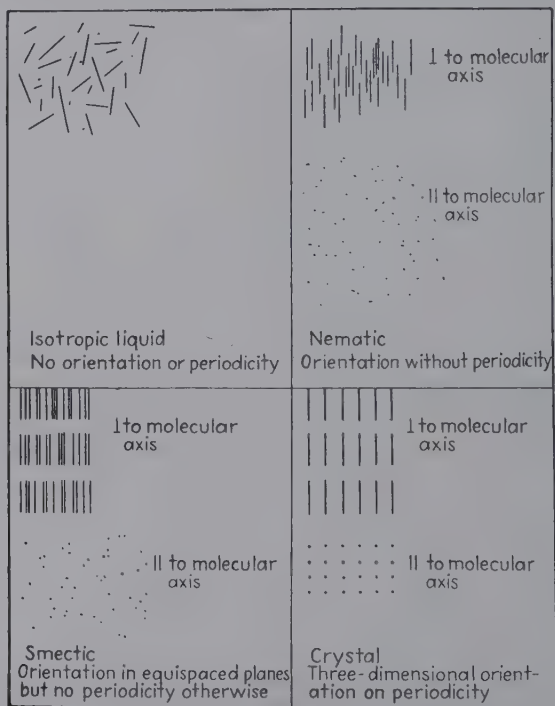


FIG. 221.—Molecular arrangements in liquid, mesomorphic and crystalline states.

crystal, in addition, should give interferences for lateral arrangement. In general, the prediction has been confirmed. Comparison of details of liquid-crystal patterns (intensity, sharpness, and shape of peaks) with those of the isotropic liquid lead to the conclusion that "swarms" of long molecules exist in the liquid crystal of the order of 10^6 molecules with axes parallel and with mobility of the molecules within the swarm much less than they possess in the liquid state.¹

¹ STEWART, *J. Chem. Phys.*, **4**, 231 (1936).

ORNSTEIN and KAST, *Trans. Faraday Soc.*, **29**, 931 (1935).

A logical extension of such researches is the work that has been done on the effect of a magnetic field. There has been cited some evidence of orienting effects on liquid molecules of magnetic fields as disclosed by diffraction patterns, but Stewart found none, a result that he ascribed to the smallness of the cybotactic groups. A marked effect, however, is obtained for the liquid crystalline state, explained better by an anisotropic polarization than by a permanent magnetic moment.

In a magnetic field the directed orientation is indicated on the diffraction rings by localized intensity maxima (fiber pattern). The pattern is markedly sharper in passing from the nematic to the smectic phase in the magnetic field as observed by Hermann and Krummacher. These workers have also proved that, when a melt of a substance which displays mesomorphic phases solidifies in a magnetic field, the crystalline powder is fibered in a direction parallel to the field; the intensity maxima for the pattern correspond in position to those for the liquid crystals in the magnetic field.

Solutions.—Very little quantitative interpretation has been given as yet to diffraction patterns of solutions. The scattering in aqueous solutions does not differ markedly from that of pure water, but two effects are noticeable: (1) a change in sharpness of halos; (2) the appearance of marked scattering at small angles, close to the central undiffracted beam on flat film patterns. Prins¹ found that the principal water halo is markedly sharpened when alkali hydroxides are dissolved, as a result of orientation of the water molecules by the dissolved ions. Solutes also seem to have characteristic effects on changes in sharpness with changes in temperature, *i.e.*, the temperature coefficient of arrangements and number of neighbors around a central molecule. Data on the apparent volume of alkali halides in water solutions are in harmony with the following interpretations: (1) In addition to hydration of Li^+ and Na^+ the ions affect the semiorderly structure of water at distances larger than the atomic radii, the general effect on water being to increase its density or decrease its volume. (2) This structural effect is responsible for variation with concentration of the apparent volume occupied by a pair of ions. (3) The structural effect, though characteristic of the halide, depends more on the alkali than on the halogen. The concepts

¹ *J. Chem. Phys.*, **3**, 77 (1935).

of superstructures (page 394) and of order-disorder (page 395), well known for alloys, have also been applied to solutions.¹ In other words, ions are participants with water in one common or shared structure, different from that of either constituent, but not homogeneous.² Phenomena somewhat akin are found in nonaqueous systems. To illustrate with a single example, Clark, Sterrett, and Lincoln³ found that the presence of a polar compound, such as methyl dichlorostearate in liquid paraffin hydrocarbons in lubricating oils, produced a marked orienting or regimenting effect in that liquid interference maximas are much sharper and remain so at elevated temperatures, at which usual halos become so diffuse that resolution practically disappears. The importance of this "structure" especially in thick films for viscous lubrication is at once apparent.

The other effect in solutions, namely, scattering at small angles, was studied some years ago by Krishnamurti⁴ for aqueous solutions of cane sugar, levulose, and glucose, but more important use has been made of this phenomenon in colloidal solutions.

Colloidal Solutions.—The molecular weight of dextrin calculated by Krishnamurti from the extent of "amorphous" scattering by means of the Bragg formula $n\lambda = 2d \sin \theta$ is 600 and that of gelatin is 3000, which are not improbable values. The solution of sodium oleate produced a ring due to the presence of big groups, or micelles, of sodium oleate in the solution. The extent of the gaseous scattering gave the dimension for the sodium oleate molecule, agreeing with that calculated from molecular weight and density. An excess of scattering directly adjoining the central spot is due to big groups of ionic micelles described by McBain. Aqueous solutions of starch, tannic acid, and gum arabic showed a further scattering at small angles to the primary beam, due to the dissolved molecules or micelles. The molecular weights calculated from the extents of the coronas were 6200, 3134, and 2810, respectively. Thus, a starch molecule contains about 10 dextrin molecules united together, and a tannin micelle contains 10 simple molecules of the formula $C_{14}H_{10}O_9$. The greater importance of these studies is at once

¹ STEWART, *Trans. Faraday Soc.*, **33**, 238 (1937).

² MEYER, *Phys. Rev.*, **38**, 1038 (1931).

³ *Ind. Eng. Chem.*, **28**, 1318, 1322, 1326 (1938).

⁴ *Ind. J. Science*, **3** 209, 307 (1928); **5**, 489 (1930).

apparent, when it is considered that extremely valuable information should be obtained from biological fluids including blood, filtrable virus, etc.

Reference has been made already on page 372 to the structures of sols of the hydrous oxides and oxide hydrates which x-ray analysis has shown to be far simpler than is usually assumed and fully consistent with results on the gels. Particularly significant are x-ray results on streaming sols, *i.e.*, colloidal suspensions forced through fine capillaries under pressure.¹

A 1.4 per cent colloidal solution, or sol, of vanadium pentoxide or a 3 per cent sol of mercury sulfosalicylate produces remarkably clear diffraction patterns indicative of a marked fiber structure, caused by the preferred orientation in streaming of rod-shaped colloidal particles, already observed in polarized light. The same sols at rest in the same capillary tubes produce only faint Debye-Scherrer rings for random arrangement. The spacings for these sols are not the same as for the dry powders of V_2O_5 or the mercury salt, a difference proving hydration; thus the 3.28-A.U. spacing for the sol, completely missing for the powder, is due actually to an oriented water hull on each colloidal particle. The elongated shape of the particles is further indicated by the fact that planes parallel to the long axis and through the smallest dimension of the crystals produce very weak interferences as compared with planes normal to the axis.

A beautifully resolved long spacing of 48 A.U. is found in streaming solutions of sodium oleate, corresponding to the length of two oleate molecules perpendicular to the diffracting planes. This distinguishes the colloidal micelle from the solid crystals of sodium oleate, in which the layer spacing is 41 A.U. and the molecules are inclined at an angle of 60 deg. to the planes. With decreasing concentration of the soap solution the flakelike micelles become thinner down to a limit of a bimolecular layer of oleate molecules, which is actually the structure of the thinnest black areas in soap-bubble films.

The principle of changing colloidal particle size as a function of concentration has been used effectively by Clark and Southard² for measuring capillary-pore diameters in cellulose fibers. The oxazine dye, Nile blue sulfate, in aqueous solution, has a

¹ HESS and GUNDERMANN, *Ber.*, **70**, 1800 (1937).

² *Physics*, **5**, 95 (1934).

varying molecular association as a function of concentration, indicated by potentiometric and spectrophotometric measures and proved by x-ray diffraction patterns. Solutions of the order of one-millionth molar approach obedience to the laws of dilute solutions; in moderate concentrations of the order of $5 \times 10^{-4} M$ the dye molecules associate to micellar structures, and in concentrated solutions the association proceeds to the stage of a colloidal suspension. The principal spacing varies as follows:

| Concentration | d , A.U. |
|---------------|----------------------------|
| 0.0884 | 13.00 (solid powder 13.00) |
| 0.00884 | 11.19 |
| 0.000884 | 10.26 |
| 0.0000884 | 8.14 |
| 0.00000884 | 7.10 |

Between the third and fourth of these solutions, absorption in the capillary pores of cotton fibers increases markedly.

CHAPTER XXI

THE INTERPRETATION OF DIFFRACTION PATTERNS IN TERMS OF GRAIN SIZE, ORIENTATION, INTERNAL STRAIN, AND MECHANICAL DEFORMATION

The Scope of X-ray Diffraction Information.—In the subject matter thus far developed in Chaps. XII to XX, particular application of fundamental principles has been made to the analysis of crystalline constitution, or ultimate structure. It has been shown that such analyses of solids may involve the use of single crystals or of specimens composed of many fine grains usually in random orientation. The various experimental methods employing either single crystals or aggregates have been outlined in Chap. XIII. It has also been indicated that numerous other types of information besides ultimate crystalline structure may be obtained from the interpretation of the x-ray diffraction patterns. It is at once apparent that a whole series of specimens may give identically the same known crystal pattern characteristic of body-centered cubic α -iron, and yet from the standpoint of *practical behavior* these specimens may vary enormously. If, then, x-rays told us only that all the specimens were α -iron, they would perform a notable service but fall far short of the greatest usefulness. Fortunately, by means of these rays it is possible to make fundamental and subtle distinctions between the specimens, which all have the same unit crystal cell, far beyond the powers of any other testing agency, and thus scientifically to account for actual behavior in service and to further rational establishment of manufacturing processes that will ensure a desirable combination of properties in terms of a desirable structure. It is this information concerning grain size, internal strain, fabrication, heat-treatment, etc., which is the newest contribution of x-ray science and at the same time the most important from the actual industrial point of view. In this chapter consideration will be given to the fundamental interpretation of x-ray patterns in terms of some of these properties,

while Chap. XXII will be devoted largely to actual examples and achievements of the x-ray method in metallurgical industry.

Grain Size. 1. *X-ray Evidence of Grain Size.*—In Figs. 130 and 140 are shown the x-ray diffraction patterns for two extremes of grain size of α -iron, respectively, a single crystal grain and a random aggregate of very small grains. The former is distinguished by a symmetrical array of Laue spots, the latter by a series of concentric, continuous Debye-Scherrer rings. Both patterns are definitely characteristic of crystalline α -iron, and, in addition, each characterizes a particular condition of grain size. Of course, there may be every possible gradation in grain size between the extremes and also extending to smaller grain sizes in the colloidal range than those represented by Fig. 140. In general, it may be stated that specimens with grains larger than 10^{-3} cm. in diameter produce a fairly uniform peppering of diffraction spots which grow larger and fewer in number as the grain size increases or the number of grains in the path of an x-ray beam of constant cross section decreases. In the region of 10^{-3} cm. these spots begin to lie on Debye-Scherrer rings as in Fig. 166 if the $K\alpha$ doublet of the radiation is present so as to exceed all other rays in intensity (*i.e.*, approaching monochromatic rays). As the size still further decreases, the spots lying on rings decrease in size and increase in number until individual spots can no longer be distinguished and the diffraction rings appear of continuously uniform intensity and have maximum sharpness. There is a range of particle sizes between 10^{-3} and 10^{-6} cm. as limits which produce these sharp rings and which, therefore, cannot be accurately distinguished. As the grain still further decreases in size below 10^{-6} cm. into the colloidal range, the interference effects become less perfect as the number of parallel reflecting planes falls below a certain value. This manifests itself as a *broadening* of the diffraction rings, so that a measurement of breadth leads directly to an evaluation of grain sizes of colloidal dimensions, as will be illustrated later.

2. *The Measurement of the Size of Submicroscopic (Colloidal) Crystals.*—Since the x-ray method of evaluating particle size was first applied to submicroscopic or colloidal particles from 10^{-6} to 10^{-8} cm., this range will be considered here first.

Debye and Scherrer were the first to derive an equation connecting particle size with an experimental measurement of the

breadth of interferences at points of half-maximum intensities and applicable for the case of a parallel x-ray beam and a sample of negligible absorbing power, as follows:

$$B'_{\text{Scherrer}} = \frac{B}{R} = 2\sqrt{\frac{\ln 2}{\pi}} \cdot \frac{\lambda}{D} \cdot \frac{1}{\cos(\chi/2)} + b'$$

where B' is the measured breadth in radians of a diffraction interference at points of half-maximum intensity (B is this breadth and R the camera radius in millimeters), λ is the wave length, D is the edge length in angstrom units of the crystal considered as cube, χ is the angle of diffraction, and b' is the natural minimum breadth in radians of the Debye-Scherrer diffraction line which is a constant depending upon the particular apparatus and size and absorption of the specimen. Scherrer first determined b' by plotting measured values of B for various interferences against $\frac{1}{\cos(\chi/2)}$ for a sample of colloidal gold. The straight line drawn through the points was then extrapolated to cut the ordinate axis which was the value of b in millimeters and $b/R = b'$, where R is the radius of the camera in millimeters. This equation served for several years though comparatively little work was done on critical experimental tests. Selyakov, by a considerably more straightforward proof, derived the equation

$$B'_{\text{Selyakov}} = \frac{2\sqrt{3 \ln 2}}{\pi} \cdot \frac{\lambda}{D} \cdot \frac{1}{\cos(\chi/2)} + b'$$

which differs from the Scherrer equation by less than 2 per cent. W. L. Bragg by remarkably simple reasoning and calculation utilizing the conception simply of n planes of thickness d arrived at the equation

$$B'_{\text{Bragg}} = 0.89 \frac{\lambda}{D} \cdot \frac{1}{\cos(\chi/2)} + b'.$$

Expressed in the same form,

$$B'_{\text{Scherrer}} = 0.94 \frac{\lambda}{D} \cdot \frac{1}{\cos(\chi/2)} + b'.$$

Thus the particle size is calculated from $D = 0.94 \frac{\lambda}{(B' - b')}$.

$\frac{1}{\cos(\chi/2)}$. According to Warren,¹ however, the correction of broadening to the true value due to particle size alone, $B'_c = B' - b'$, is incorrect and should be represented by $B'_c = \sqrt{B'^2 - b'^2}$. In cases of very broad lines, of course, b' is negligible in comparison with B' .

In 1926, Laue deduced from vector analysis a new equation which in its most general form is free from the limitations of the cubic system and permits size evaluation in different directions and thus the *shape* of a particle. In the simplest rigorous form this equation is

$$\eta = 0.0885 \left[B' \cos \frac{\chi}{2} - \frac{1}{B'} \left(\pi \frac{r}{R} \right)^2 \cos^3 \frac{\chi}{2} \right],$$

where η is a pure number, B' is the measured width of the diffraction maximum at points of half-maximum intensity, in *radians* (actually Laue uses the ratio of total area under the peak to the maximum value of intensity, which for triangular peaks only is equivalent to B'), r is the radius of the cylindrical specimen, R is the radius of the camera and film, and χ is the diffraction angle. The quantity η is related to the size and shape of the particle by the equation

$$\eta = \frac{\lambda}{4\pi} \sqrt{\sum \left(\frac{b_i G}{m_i} \right)^2}, \quad G = \frac{\sum h_i b_i}{[\sum h_i b_i]},$$

where b_i is the ground vector of the reciprocal lattice, h_i are the indices of the reflecting planes, and m_i are numbers that express how many times the elementary cell measurement is repeated in the direction i ;

or

$$\eta = \frac{\lambda}{4\pi a} \sqrt{\frac{(h/m_h)^2 + (k/m_k)^2 + (l/m_l)^2}{h^2 + k^2 + l^2}}$$

for cubic crystals with the unit cell constant a . This equation reduces to $\eta = \lambda/4\lambda m a_i$ for cubic crystals, where $m a_i$ is the extension (or size D) of the crystal particle in the direction a_i , or the magnitude to be calculated with all the other factors known or experimentally measurable. For samples of negligible radius,

¹ *J. Am. Ceram. Soc.*, **21**, 49 (1938).

the Laue expression reduces to the form of the Scherrer equation but with the coefficient 1.46 (Laue's original value 0.90 is in error) instead of 0.94. The necessary conditions for the Laue equation are for a divergent x-ray beam, for absorption in the crys-

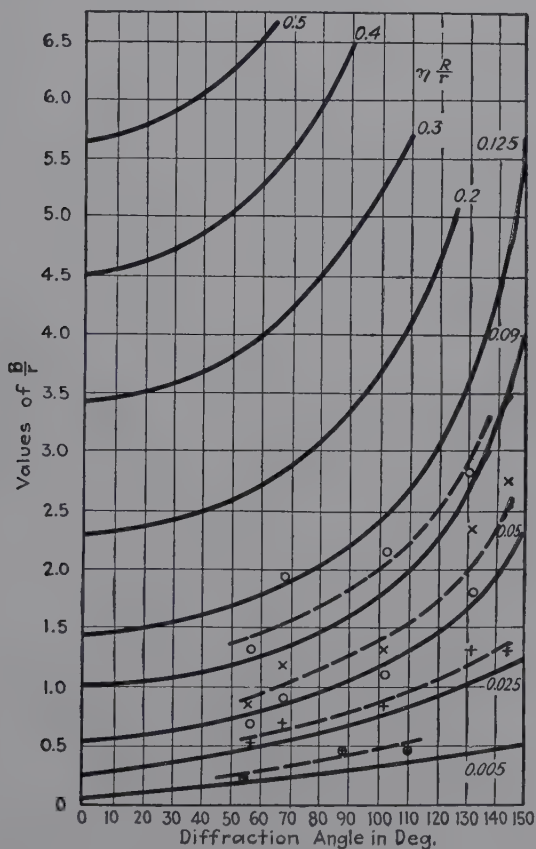


FIG. 222.—Graphical method of determining grain size in the colloidal range. (Brill.)

tal powder which is negligibly small, for completely random orientation, for particles of the same form and size, for undistorted lattices, and for known crystal structures. Patterson extended the theory to the case where the particles have different sizes and showed that the sizes must have a Maxwellian distribution, while Mark favored a symmetrical distribution of the Gauss type.

Without information concerning the distribution function, the average particle size cannot be determined.

Brill¹ extended the theory to the case of substances opaque to x-rays and derived corrections for absorption and for the overlapping of the α -doublet interferences. The equations are so complicated that Brill performed a useful service in presenting a graphical method for the determination of particle size. The standard curves (shown in Fig. 222) derived from the formulas

show the values of $\eta \frac{R}{r}$ as they depend upon $\frac{B}{r}$ and χ . The values B , the interference width at points of half-maximum intensity, r , the specimen radius, and χ , the diffraction angle, are all determined and the point on the chart for B/r against χ is located.

The value of $\eta \frac{R}{r}$ corresponding is found by interpolation between the curves of definite value, from which η and then the particle size and shape are calculated.

The necessary condition of high absorption in the sample is met by preparing powders with a cylindrical core of lead glass; solid wires can be used effectively if the proper wave length is used for high absorption. More recently Brill² has derived satisfactory empirical simplified equations with which direct calculations may be made as easily as for the original Laue conditions of transparent specimens. These are as follows:

$$\frac{B}{r} = \frac{\eta \frac{R}{r}}{0.004 + 0.084 \cos (\chi/2)} + 0.0046 \frac{\chi}{2},$$

$$\eta = \frac{r}{R} \cdot f \left(\frac{B}{r} - f' \right),$$

where $f = 0.004 + 0.084 \cos (\chi/2)$ and $f' = 0.0046 (\chi/2)$.

The previous methods have all been subject to uncertainties concerning the relation between blackening of the photographic film and the intensity of incident x-rays, and the determination of positions of half-maximum intensity of diffraction interferences by means of the photometer. If the specimen under examination is in the form of a hollow cylinder (and thus is

¹ *Z. Krist.*, **74**, 147 (1930).

² *Z. Krist.*, **95**, 455 (1938).

transparent to x-rays and obeys the Laue equations), then over a certain range of particle size each interference will be split into two maxima, the separation of which is a measure of particle size. Instead of measuring breadth at points of half-maximum intensity, the much more direct measurement of the distance between two lines is involved.¹ For such a case the particle size (for the cubic system) must have a value

$$D > \frac{R\lambda\sqrt{2 \cdot 1.8}}{4\eta r \cos^2 \chi/2}.$$

For both large particles yielding sharp interferences and very small particles for which these two maxima become broad and

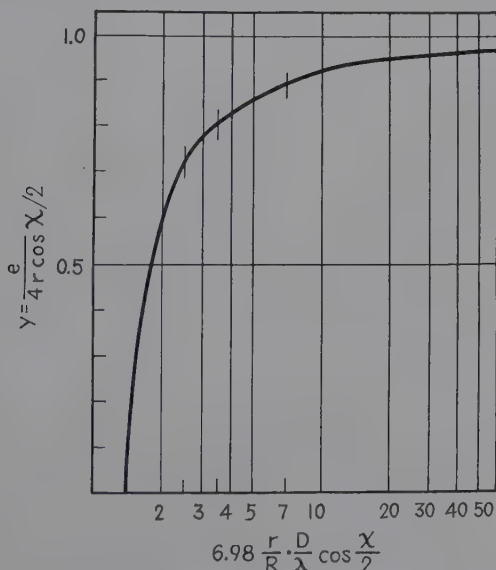


FIG. 223.—Graphical method of evaluating grain size by technique producing split interferences. (Brill.)

overlap, single lines are observed. The simpler equations derived for the particle size involved in the split lines are as follows:

$$(\text{Small}) \quad \eta = \frac{\cos \chi/2}{1.8 \cdot \sqrt{2}} \sqrt{\left(\frac{r}{R} \cos \frac{\chi}{2}\right)^2 - \frac{7}{80} \left(\frac{e}{R}\right)^2},$$

¹ BRILL and PELZER, *Z. Krist.*, **72**, 398 (1929).

$$(\text{Large}) \eta = \frac{1}{1.8} \frac{1}{2} \sqrt{3} \frac{r}{R} \left[\cos^2 \frac{\chi}{2} - \left(\frac{e}{4r} \right) \right],$$

where e is the linear separation of the two maxima. Here again

the best method of evaluation is graphical. The coordinates

are $y = \frac{e}{4r \cos \chi/2}$ and $x =$

$6.98 \frac{r}{R} \cdot \frac{D}{\lambda} \cos \frac{\chi}{2}$ (Fig. 223); y is

calculated for the specimen, x corresponding is read off, and from this D , the particle size, is deduced.

3. *Examples of X-ray Determination of Submicroscopic Grain Size.*—Some examples of diffraction photographs of colloidal materials are shown in Figs. 224, 225, 226. In Fig. 224 patterns for cadmium hydroxide precipitated at 25°,

Fig. 224.—Diffraction patterns for cadmium hydroxide, showing change in line breadths as a function of the temperature of precipitation.

40°, and 100° show clearly that, the lower the temperature, the smaller the particle size and the broader the interferences. In Fig. 225 are presented standard patterns for colloidal gold and

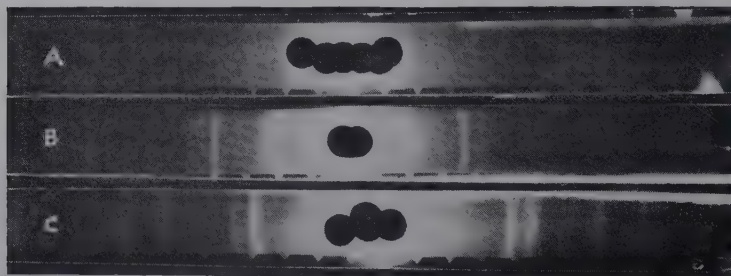
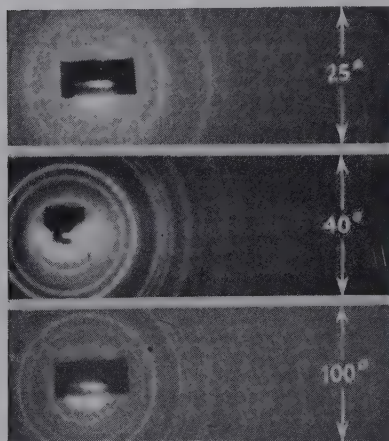


Fig. 225.—Patterns for colloidal metal sols. A, Silver, particle size 21×10^{-7} cm.; B, gold, 13×10^{-7} cm.; C, gold, 2.1×10^{-7} cm.

silver with the following grain sizes: A, silver sol, 21×10^{-7} cm.; B, gold sol, 13×10^{-7} cm.; C, gold sol, 2.1×10^{-7} cm. Figure 226 gives a comparison of grain size of three commercial varieties of tin dioxide used as opacifying agent in enamels.



FIG. 226. — Diffraction patterns of three samples of SiO_2 , with decreasing particle size from left to right.

Brill has compared the Scherrer and Laue equations for several samples of iron as follows:

| Sample | Scherrer | Laue |
|---|----------------------|----------------------|
| Fe from Fe_3O_4 | 2.3×10^{-6} | 2×10^{-6} |
| Heated 10 hr. at 1000° | 4.2×10^{-6} | ∞ |
| Fe from carbonyl I (300°)..... | 7.7×10^{-7} | 1×10^{-6} |
| II..... | 6×10^{-7} | 9×10^{-7} |
| III..... | 1.0×10^{-6} | 1.1×10^{-6} |
| IV..... | 1.2×10^{-6} | 1.0×10^{-6} |
| (1000°)..... | 3×10^{-6} | ∞ |
| Electrolytic iron..... | 2.3×10^{-6} | 2.3×10^{-6} |

There is thus general agreement except for large sizes where the Scherrer equation fails. It is adapted only for small particles in the range and for non-absorbing substances.

The particle size of martensite has been determined several times, Westgren finding 10^{-7} , Wever 10^{-6} , and Selkjakov 2×10^{-6} cm. Clark and Brugmann in studying the structure of case-hardened steel, which is martensite and troostite very largely, estimated a particle size of 10^{-7} .

One of the most important and interesting applications is that of particle size of metal catalysts. Clark, Asbury, and Wick¹ were the first to make a study of particle size as related to the activity of finely divided catalysts. They measured photometrically the line breadths of diffraction spectra from a number of nickel catalysts with identical crystal-lattice type and dimensions, prepared in various ways and differing widely in catalytic activity in hydrogenation and dehydrogenation processes. Most of these catalysts consisted of particles larger than 10^{-6} cm. so that the Scherrer equation did not apply. In general, increase in activity and decrease in particle size did not run parallel as might be expected. There is a more definite relationship for platinized-asbestos catalysts used in the contact sulfuric acid process. Levi² has made several measurements of particle size of the platinum family of metals from the photometered x-ray diffraction spectra, with the result that granules of platinum were twelve to twenty-nine times as large on the side

¹ *J. Am. Chem. Soc.*, **47**, 2661 (1925).

² *Atti accad. Lincei* (6), **3**, 91 (1926).

as the unit crystal cell; palladium thirteen to twenty-nine, rhodium six, iridium four, ruthenium seven to eight, osmium six (latter two hexagonal).

Some of the most interesting particle-size measurements have been made on such non-metallic substances as carbon-black, pigments, colloidal suspensions, rubber, and cellulose. The question is raised of where the discontinuity between crystalline and amorphous states appears and whether or not there is any evidence of amorphous metal at grain boundaries, etc. It is reasonable to suppose that diffraction lines may become so broad that they will coalesce and produce the effect of general fogging of the film, as an amorphous material would be expected to act. From the evidence of carbon-black an amorphous state may show transition to crystalline as judged by changes in physical or chemical properties, while the x-ray pattern is unchanged at first, simply because the crystalline planes are still too few and too distorted to allow sharp interference. It must be realized that temperature oscillations of atoms in a lattice and also distortion both have the effect upon diffraction lines of broadening them, just as small grain size does. These factors must be known, therefore, before adequate interpretation is possible. There is no positive x-ray proof of the amorphous-cement theory of metal aggregates in spite of numerous attempts. Nor can it be said that the theory has been disproved though it seems unlikely.

4. *The Shape of Colloidal Particles.*—An important extension of this method is in the determination of the shape of colloidal particles. If all points for all interferences lie smoothly on the same $\frac{R}{r}$ curve, then a regular shape, *e.g.*, cubic, is immediately indicated. In studies of colloidal nickel prepared electrolytically in the presence of varying sulfur contents Brill found that the B/r values for the (200) plane interferences were all too high. The cause of the discrepancy could be determined by assuming various particle shapes and comparing the breadths for (200) interferences with the standard constant (111) interference breadths in the equation for the cubic system noted under the discussion of the Laue equations. Perfect agreement is obtained when calculations are made for a particle built on the octahedral planes and greatly elongated perpendicular to these planes. For the nickel with 5.8 per cent sulfur the following results are

obtained by assigning the values $m_h = m_k = 9$ and $m_l = 27$, or the edge lengths actually 45 and 165 A.U.:

| Indices | Half value breadth found | Calculated |
|---------|-----------------------------|------------|
| 111 | 0.66 | 0.64 |
| 200 | 0.96 | 0.92 |
| 220 | 1.07 | 1.10 |

For the preparation with smallest particle size only the (111) interference appears, simply because only these planes are present in sufficient number in the tenuous elongated particle to produce visible diffraction effects.

5. *Particle Size and Shape in Carbon-blacks.*—In the preceding chapter several examples have been cited of attempts to explain diffuse halo patterns of glasses and other amorphous solids as arising from very minute crystallites. Since the positions of the halos in vitreous silica correspond to those of crystal interferences from cristobalite, this is a reasonable supposition, but Warren has shown that the values of particle size, 7 to 8 A.U., calculated by the foregoing equations, are too small to have physical significance. As a consequence, the random network and the calculation of radial distributions have come to be the preferred explanation.

The same situation arises for carbon-blacks, all of which yield halo patterns strongly suggestive of colloidal graphite particles. Radial-distribution calculations indicate single graphite layers but uncertainty still remains as to how these layers are combined in larger units. The possibility of particle-size measurement by the Scherrer or Laue equations is, therefore, at least reasonable and not precluded by newer interpretations. Clark and Rhodes¹ have made the most recent and critical study of the structure of a series of commercial blacks used in rubber compounding. Independent patterns were made under conditions conforming to the Scherrer and to the Laue equations, in both cases for non-absorbing materials, the first being extended to the unenclosed wedge-shaped sample used so successfully

¹ *Ind. Eng. Chem., Anal. Ed.*, **12**, 243 (1940).

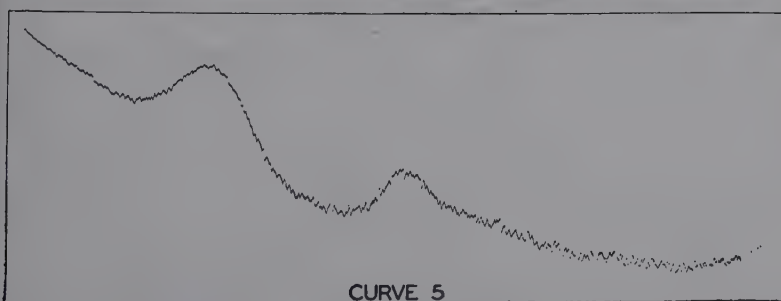


FIG. 227.—Patterns by Laue and Scherrer methods for rubber carbon-blacks compared with graphite (first and fourth); typical microphotometer curve.

in cylindrical cameras (Fig. 142). For the Laue method the samples of necessity have been made into cylinders for which the value of the radius r could be accurately measured. Microphotometer curves were made under extraordinarily carefully controlled conditions, and from these were obtained the breadths at points of half-maximum intensity for the two broad interferences corresponding to the 002 (basal plane) and 100 (prism) interferences of graphite. Typical patterns and curves are shown in Fig. 227. The results are briefly summarized as follows:

1. Excellent checks in particle size were obtained by the Scherrer and Laue methods.

2. The particle size of 18 rubber carbon-blacks was of the order of 20 A.U. for both interferences (at right angles in the hexagonal prisms, assuming graphite structure), and thus the particle shape was essentially equiaxed, though tendency to flake formation ($D_{002} < D_{100}$) is indicated and is reflected in other physical properties.

3. The origin of the black, whether high-temperature or low-temperature channel, is clearly indicated by the particle sizes, which are larger the higher the temperature.

4. The sizes are identical in the black, in the rubber mix (the 100 interference only can be measured since 002 is observed by the rubber halo), or in the black after extraction of rubber from the mix.

5. The x-ray method and the microscopic method of measuring particle size on the same sample gave values of entirely different orders of magnitude:

| Sample | Microscopic size, microns | X-ray diffraction size, A.U. | | Particles per aggregate |
|------------------|---------------------------|------------------------------|---------------|-------------------------|
| | | Altitude | Base diameter | |
| 1..... | 0.045 | 15.4 | 21.6 | 3.2×10^3 |
| 2..... | 0.064 | 15.9 | 18.9 | 9.2×10^3 |
| 3 (thermal)..... | 0.160 | 21.0 | 24.7 | 6.4×10^4 |
| 4..... | 0.025 | 14.4 | 16.4 | 8.1×10^2 |
| 5 (thermal)..... | 1.120 | 18.6 | 25.3 | 2.4×10^7 |

One explanation is that the x-ray method measures only primary particles with the maximum line breadth corresponding to the smallest particles in an undoubtedly heterogeneous mixture of many sizes, whereas the microscopic measures only the aggregate. In any case, though the material is non-uniform in particle size, and distortion may exist in particles in which the single layers are twisted with respect to each other, like cards in a deck, the results on a typically mesomorphic material are of interest and importance.

6. *An Experimental Test of Particle-size Equations.*—It is evident that a direct test of the validity of theories involved in the Scherrer, Bragg, Laue, and Brill equations depends upon specimens in which grain sizes may be evaluated accurately by an entirely independent method. In a few cases known microscopic values have been checked by the x-ray method, though there is always the uncertainty whether the microscopic particle is really a single crystal or an aggregate. The Blodgett-Langmuir technique of building up a film from a known number of layers of a long-chain compound of known molecular length (page 443) provides the means of making a rigorous test through the known thickness of films. Clark and Leppla¹ made the test for the first time with layers of calcium stearate with the following results, comparing breadth measurements observed with those calculated from the simple form of the Laue equation:

| Number of layers | Breadth | |
|---------------------|----------|------------|
| | Observed | Calculated |
| 3 | 0.25 | 0.186 |
| 4 | 0.22 | 0.139 |
| 5 | 0.13 | 0.112 |
| 6 | 0.13 | 0.093 |
| 7 | 0.07 | 0.080 |
| 8 | 0.06 | 0.070 |
| 9 | 0.06 | 0.002 |
| 10 | 0.04 | 0.056 |
| 17 | 0.03 | 0.035 |
| 20 | 0.03 | 0.028 |
| 25 | 0.02 | 0.022 |
| 30 | 0.02 | 0.019 |
| 35 | 0.02 | 0.016 |

¹ *J. Am. Chem. Soc.*, **58**, 2199 (1936).

Considering difficulties the agreement is very satisfactory except for the thinnest films, for which it was demonstrated that distortion plays a considerable role.

7. *Particle-size Measurement from Small Angle Scattering.*—Many colloidal materials produce diffraction patterns with scattering at small angles, in addition to the halos corresponding to crystal planes. Reference has been made to Krishnamurti's measurement of particle sizes in colloidal solution and to the small angle scattering of silica gel as contrasted with none for glass. An extensive study of the theory and application has been made by Guinier.¹

Treated similarly to scattering by gases, the fundamental formula is derived as follows:

$$\frac{I}{I_e} = Mn^2e^{\frac{-4\pi^2}{3\lambda^2}R^2\epsilon^2}$$

where I is the intensity; I_e the intensity scattered by an electron at a small angle; M the number of particles; n the total number of electrons in a particle; R the "ray of gyration," or size function related to volume as $V = \frac{4}{3}\pi(\sqrt{\frac{5}{3}})^3R^3$; and ϵ the diffraction angle. A curve drawn of $\log I$ as a function of ϵ^2 , extrapolated to zero angle, gives $\log Mn^2I_e$. For a spherical particle the equation reduces to $I/I_e = N^2e^{\frac{-4\pi^2}{5\lambda^2}R^2\epsilon^2}$. For elongated or flake-like particles, also, suitable graphical methods are employed. The following results have been obtained for R : ovalbumin, 20.3 A.U.; rubber, 35 A.U.; colloidal silver, 64 A.U.; Raney nickel catalyst, 23 A.U.; graphite, diameter 400 A.U.; cellulose, cylinders of diameter 30 A.U.

The measurement of very long crystal spacings at small angles by direct diffraction, which leads to evaluation of giant molecule sizes, is considered in Chap. XXIII.

8. *Particle-size Measurement in the Microscopic Range.*—A method of evaluating grain size to supplement and check microscopic measurement of grains of the order of 10^{-3} to 10^{-2} cm. in diameter has long been needed, particularly if some information can be obtained about grains below the surface of a polished specimen. X-ray patterns are now filling this require-

¹ Theses presented to the Faculté des Sciences de l'Université de Paris, 1939.

ment. It has been demonstrated already that with grain sizes of 10^{-3} cm. or larger the diffraction interferences are no longer

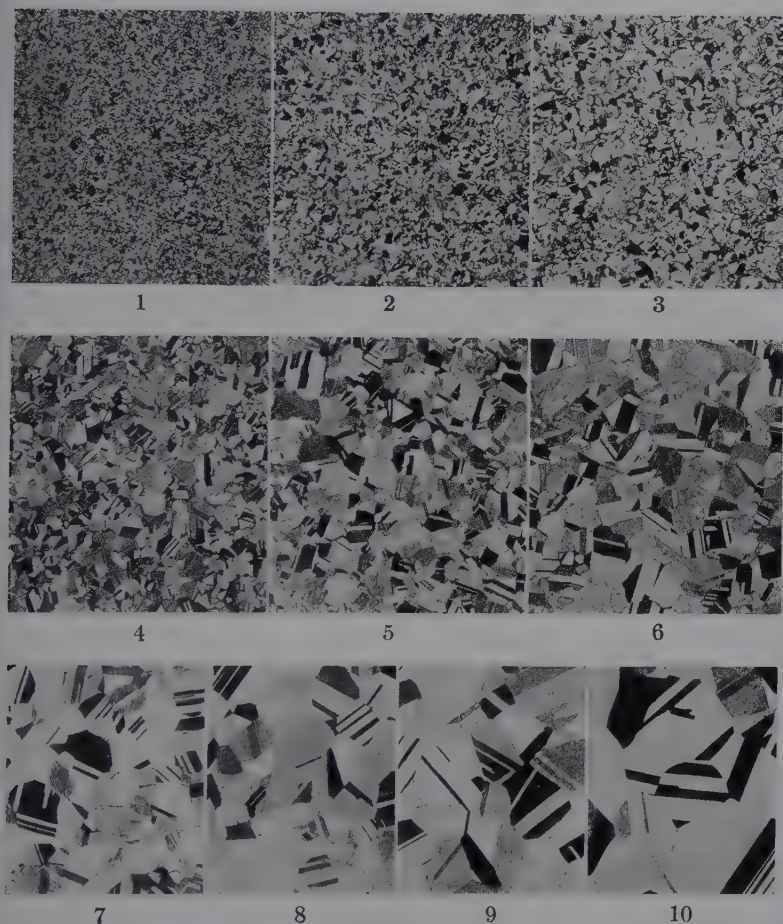


FIG. 228a.—Grain-size standards (A.S.T.M.) for the estimation of the diameter of average grain of annealed materials, particularly non-ferrous alloys such as brass, bronze, and nickel-silver. $\times 75$. Average grain diameter as follows:

- | | |
|--------------|---------------|
| 1. 0.010 mm. | 6. 0.065 mm. |
| 2. 0.015 mm. | 7. 0.090 mm. |
| 3. 0.025 mm. | 8. 0.120 mm. |
| 4. 0.035 mm. | 9. 0.150 mm. |
| 5. 0.045 mm. | 10. 0.200 mm. |

uniform and continuous circles or lines. These interferences show individual spots, and as the size increases the Debye-Scherrer rings disappear and a uniform "peppering" appears.

The size of the spots depends upon the divergence of the primary x-ray beam, the size and shape of the focal spot on the target of the x-ray tube, and the extent of the crystal in the plane of the reflecting face. Consequently, the size of the interference spot on the photographic film from a grain increases with increas-

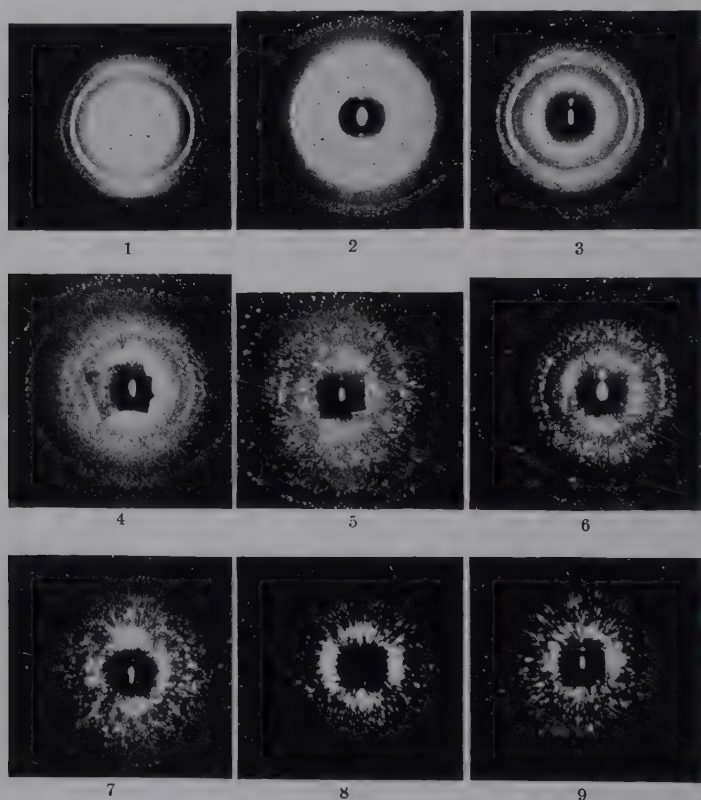


FIG. 228b. —Standard x-ray diffraction patterns for increasing grain size in the microscopic range (compare Fig. 228a).

- | | | |
|--------------|--------------|--------------|
| 1. 0.009 mm. | 4. 0.033 mm. | 7. 0.065 mm. |
| 2. 0.012 mm. | 5. 0.037 mm. | 8. 0.085 mm. |
| 3. 0.020 mm. | 6. 0.045 mm. | 9. 0.095 mm. |

ing grain size as long as the cross section of the crystal perpendicular to the ray to be reflected is smaller than the cross section of the impinging bundle of rays. Mark and Boss have shown a linear relationship between the size of interference spots for particles between 10 and 100 microns (10^{-3} to 10^{-2} cm.) and the

grain size measured microscopically. The slope of the straight lines depends upon the experimental conditions and apparatus; but, once known, grain sizes may be directly read off for any specimen from a measurement of the interference spots.

Clark and Zimmer have greatly extended these results, using the brass samples from which standard A.S.T.M. grain-size photomicrographs were prepared (Fig. 228*a*). The corresponding standard x-ray patterns photographed in most carefully con-

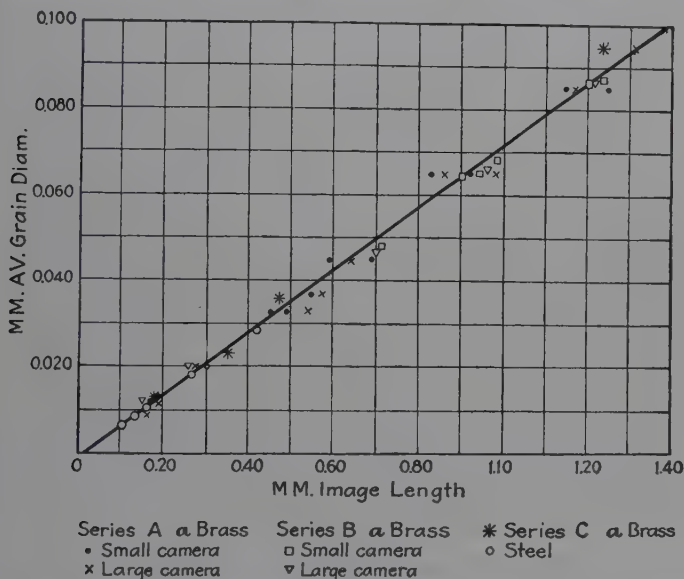


FIG. 229.—Graphical correlation between image lengths of x-ray diffraction interferences and average grain diameters in microscopic range. (Clark and Zimmer.)

structed cylindrical cameras are shown in Fig. 228*b*. When the microscopic measurements are plotted against the lengths of the x-ray diffraction images, the straight-line plot of Fig. 229 is obtained. The results with two other series of brass samples, steel, carborundum, silica, etc., all lie on this same curve, so that it undoubtedly represents a universal relationship. It is essential, however, that the annealed metal sample shall not show residual preferred orientation or fibering. It is essential that the grains should have uniform size, since otherwise the x-ray measurement will give the average only of the largest particles, the small particles producing no individual sharp interferences. The

effect of size distribution is very clearly demonstrated in Fig. 230. Two specimens of silica with the same average particle size as prepared and measured by Drinker and Hatch at the Harvard School of Public Health were subjected to x-ray analysis by Aborn and Davidson. The difference is remarkable. In *a* the deviation from the average was very small, whereas in *b* it was large. Without a knowledge of the fact that the average particle sizes were the same, and of the distribution, the mistake would be made of assigning a considerably larger particle size to *b* in which the large grains producing individual interferences are balanced by grains too small

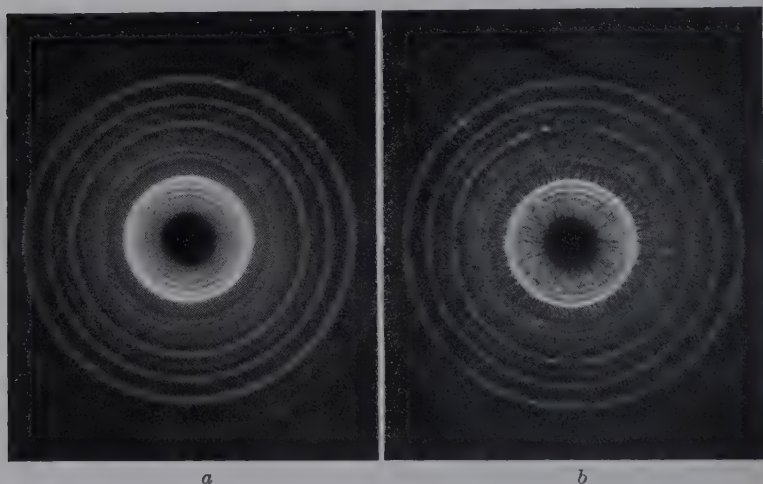


FIG. 230.—Diffraction patterns for two samples of silica with the same average particle size but differing widely in the distribution of sizes. *a*, average size 4.4 microns, distribution (standard deviation) 1.341; *b*, 4.5 microns and 2.166, respectively.

to produce distinguishable spots. Microphotometric curves are reproduced in Fig. 231 for grain sizes of 4.4 microns, standard deviation 1.34; and 36 microns, standard deviation 1.28. These were made by turning the film around an axis so that one of the diffraction circles was continuously registered. Obviously there are no equations comparable with those for colloidal particles for calculating particle size of large grains from a measured quantity such as diffraction interference breadth. Hence the microphotometric curves were measured, including number of peaks per unit length, average height of peaks, area per peak, and the total area under peaks per unit length. When for specimens with

nearly the same size distribution the last-named quantities are plotted on log paper against average particle size, the points lie on a straight line. For specimens with widely different distribution but the same average size, the points do not lie on this line. This work on silica is of great importance in laying the foundation for further work on metal grain sizes. It is evident that considerable care and skill are required in deducing accurately grain size for the region in question.

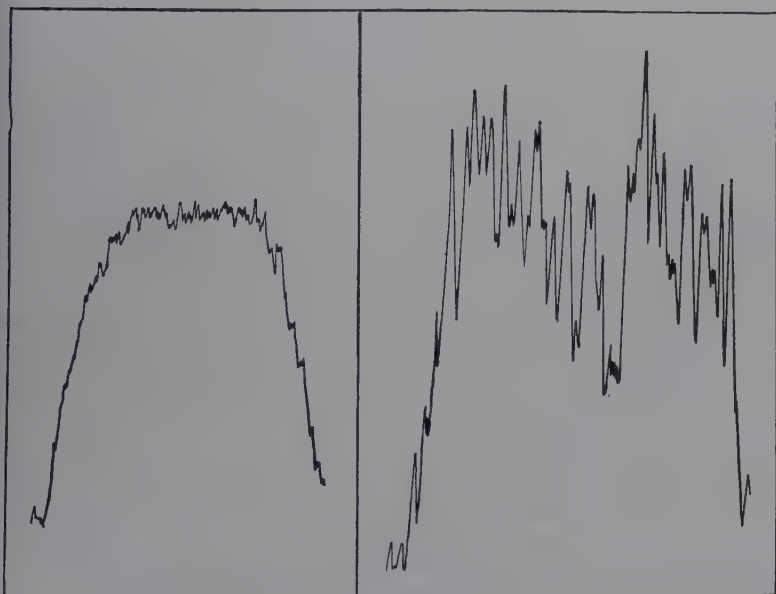


FIG. 231.—Microphotometric curves for diffraction rings of silica samples. Left, average size 4.4 microns; right, average size, 36.0 microns.

9. *Examples of Measurement of Size of Microscopic Particles.*—

It is needless to point out the very great importance of grain size in terms of practical behavior of commercial materials. Practically all annealing operations following mechanical work involve grain growth. Magnetic permeability and hysteresis loss in electric steels are certainly dependent upon grain size. The life of electrical contact points is a function of optimum grain size. Even the enameling of steel, corrosion, electrodeposition, and numerous other phenomena depend upon grain size. Many of these will be illustrated in the next chapter, devoted to

heat-treatment and to practical applications of x-ray methods to commercial metals. The control of grain size in metallurgical products is one of the great achievements of the science. Another typical application has been reached on the reuse of plaster of Paris molds. These deteriorate very rapidly on reuse, the tensile strength becoming much less on each successive recalcination. X-ray photographs show that the gypsum particles grow larger as strength decreases. The addition of $\frac{1}{4}$ per cent Al_2O_3 increases strength by decreasing grain size. A basic patent on bright nickel, formed by electrodeposition, and of great commercial importance not only in nickel plating but also in undercoating for bright chrome plating, specifies a grain size less than 0.0001 mm. The x-ray method of grain size evaluation has been used repeatedly in developing processes and in tests for infringement.

Orientation of Grains.—Many research and practical problems arise in which a knowledge of orientation of crystal planes in a single metal crystal or of single grains in an aggregate is highly desirable. It has been demonstrated in Chap. XIV that the x-ray goniometer is a powerful method of ascertaining orientation. Single metal crystals are made frequently by cooling a melt in a quartz tube by extremely slow and careful cooling, as first devised by Prof. Bridgman. Obviously, no planar faces are developed and recourse must be had to goniometric establishment of orientation of planes with respect to one direction or another before physical data may be properly interpreted. There are frequent references to x-ray goniometry of this kind in the literature, especially with respect to the presence or absence of twinning. Again, a strip or sheet of metal may be polycrystalline and yet have certain properties dependent upon just how the individual grains (of course, large) are oriented with respect to the surface. This is especially true of electric or magnetic properties, which may differ widely for two specimens, say, of silicon steel, with the same apparent grain size and general structure. In this case the Laue method of crystal analysis may be employed. Standard Laue photographs for body-centered and face-centered cubic and hexagonal close-packed metals in every possible and known orientation with respect to the x-ray beams are to be found in the literature. All that is necessary, therefore, is to compare a Laue pattern for a grain in a sheet, to the surface of which the x-ray beam is perpendicular, with the standard

patterns in order to establish easily the orientation of the lattice planes of the grain in question with respect to the surface.

Sir William Bragg has indicated another field in which knowledge of orientation is of practical importance. The wearing properties of jewel bearings for watch movements depend upon how they are cut from original sapphires. Figure 232 shows Laue patterns for two such bearings with different crystallographic orientations and different resistance to wear.

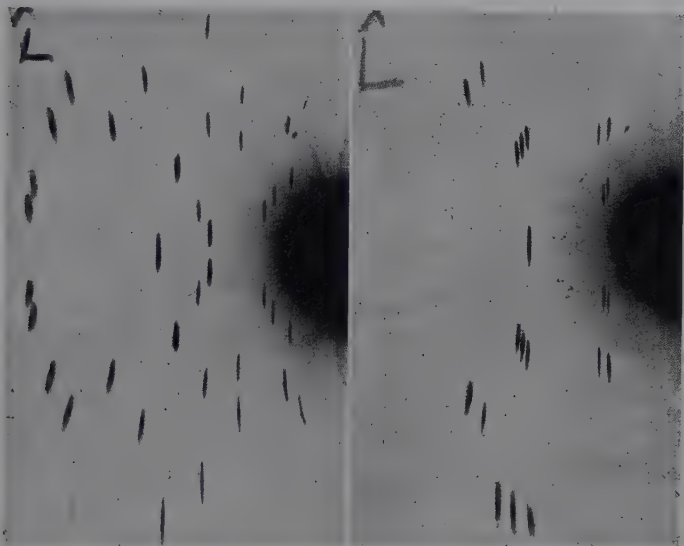


FIG. 232.—Patterns for artificial sapphires used in jewel pivots of watch movements with same structure but different orientations and different wearing properties. (*Sir William Bragg.*)

Internal Strain.—Many metal structures fail because of gross defects which may be detected readily by radiographic examination. But many metal objects may appear radiographically perfectly sound and still fail. The cause here is far more deep-seated and is concerned with residual internal strain or lattice plane distortion. Strain in transparent objects is readily ascertained by interference colors when examined in polarized light. In this manner glass apparatus is tested. Dirigible models of transparent celluloid have been studied under all conditions of stress. The writer has even detected strain in linseed-oil and patent-leather films in this way. But for opaque objects such

as metals the method is precluded. The use of gage marks for detecting strain in metals is well known. For example, the diameter of a cylinder of metal is very carefully measured. Successive layers from the inside of the cylinder are then removed on a lathe and the changes in the outside diameter with the relief of strain observed. There are many modifications of this technique that have been widely employed, but there are serious objections and limitations. In the first place, the dimensional changes may be too small to measure accurately. Again, the direction of the strain may be such as to be missed entirely by the gage-mark method. In all of metallurgy there has been no problem that has so urgently required an adequate method. To

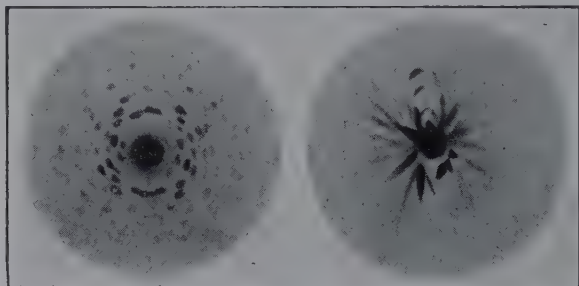


FIG. 233.—Laue patterns of a normal and of a bent crystal of gypsum, illustrating asterism. These are the first patterns ever made. (*Czochralski*.)

the detection and even quantitative estimation of internal strain x-ray diffraction science has made a great contribution, although the application still requires much fundamental research and standardization.

X-ray Evidence of the Effect of Stresses and of Residual Strain in Specimens.—Depending on the texture of any material, single crystalline or aggregate, and the type and extent of stress or deforming force applied to this specimen above and below the elastic limit, x-ray diffraction patterns provide a number of manifestations of change. These will be enumerated first and then further consideration given to some of the more important.

1. *Radial streaks*, or “asterism,” on Laue patterns for bent or distorted single crystals and on large-grained aggregates. Figure 233 shows what happens to the Laue diffraction pattern of a single crystal (gypsum) when it is bent. The spots are elongated to radial streaks, or “asterism striations” (polychromatic radi-

ation), caused by the reflection of different wave lengths by one set of distorted planes in which lattice orientation has been

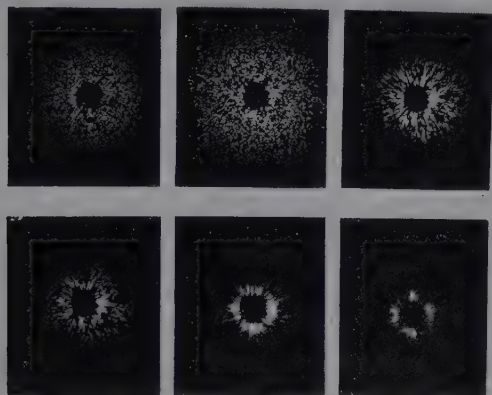


FIG. 234.—Effects upon diffraction pattern of successive loadings of specimen of silicon steel, illustrating asterism striations as evidence of internal strain.

changed by elastic or plastic deformation. Any pattern, even for a polycrystalline material, that shows these radial streaks is an indication of internal strain.

The crystal planes are distorted so that reflection takes place as though cylindrical mirrors had replaced plane mirrors. Figure 234 shows how a strain pattern can be synthesized by loading successively a strip of iron while the exposure is made. Even under the elastic limit there is clear evidence of strain; at higher loads slipping on planes occurs and rupture accompanied by fibering of the metal in many cases. Figure 235 shows the strained condition

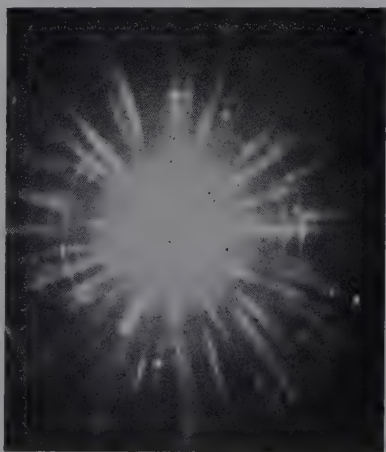


FIG. 235.—Pattern for chilled cast steel, showing internal strain.

of a block of cast steel which has been rapidly chilled. The distribution of strains of a large casting determined solely by

x-ray patterns is shown in Fig. 236. The world-wide interest in this figure, since its original publication several years ago, is an interesting side light upon the value of this method in affording information heretofore impossible. Other examples are presented in the next chapter.

2. *Shift in Positions of Spots*.—Within the elastic limit and before deformation of Laue spots begins, the application of small stresses may cause rearrangement of spots by rotation of grains with approximate reversible recovery of original positions, although permanent change may accompany greater stresses. From the work of Clark and Dunn,¹ enlarged portions of patterns show this rearrangement (Figs. 281 and 282). Attendant changes

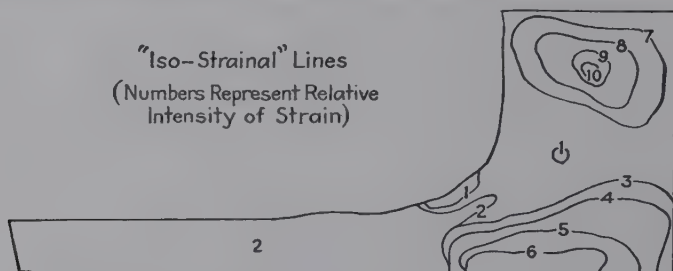


FIG. 236.—Distribution of internal strains in the cross section of a large steel casting, determined solely from x-ray diffraction patterns.

in magnetic properties are described in the next chapter. In this work double exposures on the same film though from identically the same position for unstressed and stressed conditions show the doubling of spots.

3. *Peripheral Widening of Spots*.—For specimens with a range of grain sizes for which the Debye-Scherrer rings are made up of distinct sharp spots, a very sensitive and accurate method of evaluating distortion is the effect of stress in causing these spots to elongate or blur, and even to fuse together. For this method the back-reflection method has been employed usually so that large specimens may be utilized and high-angle diffraction rings registered. In fatigue studies of metals Gough and Wood derived a formula by which the change in orientation of a reflecting plane may be calculated from the elongation of spots in the peripheral direction. Barrett devised a camera in which specimen and film oscillate together. A band instead of a narrow ring

¹ *Phys. Rev.*, **52**, 1170 (1937).

is registered, consisting of a series of rings, laid side by side, each being registered from a slightly different position of the specimen. This greatly enhances the chances of observing blurring and elongation of spots in one or more directions, as shown in Fig. 297. There is no difference in the mechanism of deformation of grains whether the deformation is brought about by fatigue stressing in the safe or in the unsafe range or by static loading, such as straight tension. This deformation results from a rotation of parts of a grain with respect to each other about one or more axes. In fatigue tests slip takes place on crystallographic planes by plastic flow as indicated by x-ray patterns, slip lines, relief of internal strains introduced by quenching by alternating fatigue stresses, increase in hardness, raising endurance limit, and anomalous heating.

4. *Fragmentation of Grains*.—One of the necessary consequences of stress is a fragmentation of large grains, easily apparent on a series of patterns with increasing stress. This is especially true for rolling deformation. A certain size is evidently required before rotation and slip can proceed. Clark and Beckwith found a periodicity in fragmentation at about each 3.3 per cent reduction, leading finally to preferred orientation of grains. Figure 267 shows how fragmentation proceeds from distinct spots to a nearly smooth series of powder lines.

5. *Displacement of Debye-Scherrer Interferences*.—In the case of a homogeneous elastic deformation applied to specially prepared specimens so that over many crystals there is a uniform displacement of atoms out of their normal positions in the lattice, the direction of the x-ray interferences is changed and the lines are shifted in position while remaining essentially unchanged in sharpness. The amount of displacement is proportional to the elastic stress. For this work where utmost precision is required to detect the very small changes, the back-reflection method must be used. For an iron or steel specimen under stress, gold foil is closely attached to the surface so that the gold interferences may serve as a standard of calibration. The change in lattice constant a with that in the radius of the Debye-Scherrer ring r is given by the equation

$$\frac{da}{dr} = \frac{a}{2A} \cot \theta \cos^2 2\theta,$$

where A is the distance from specimen to film. Extensive measurements have been made by Dehlinger and Glocker,¹ by whom the theory and equations have been developed. From line shifts, measurement can be made of the total or directional stresses, as follows: With $2r = 50.0$ mm., for a gold diffraction ring as standard, a $\frac{1}{10}$ -mm. shift of the line of the stressed material means the following changes in lattice constants and stress:

| Metal | Radiation | Change in lattice constant A.U. | Change in single stress, kg. per sq. mm. | Stress sum, kg. per sq. mm. |
|----------------------|-----------|------------------------------------|---|-----------------------------------|
| Al..... | Cu | 0.000461 | 0.94 | 2.41 |
| Duralumin..... | Cu | 0.000426 | 0.91 | 2.30 |
| Fe..... | Co | 0.000349 | 3.04 | 9.18 |
| Cu..... | Co | 0.000397 | 1.60 | 4.04 |
| α -Brass..... | Co | 0.000603 | 1.47 | 4.21 |

6. *Broadening of Debye-Scherrer Interferences.*—Under the more usual conditions in which lattice stresses are not so uniformly applied, as in bending so that different parts of the volume through which x-rays pass have different changes in lattice constants, the line is broadened rather than displaced (Fig. 237). This effect is, therefore, the same as that which resides in diffraction by colloidal crystals. A consequent effect is the fusion of $K\alpha$ doublet lines into an unresolved broad interference.

7. *Increase in Background Fogging.*—Strained specimens tend to scatter x-rays to a greater degree than normal lattices. If less than half the atoms in a stressed specimen are displaced from normal positions, the interference line will not broaden, but the scattering increases at the expense of interference intensity.

8. *Decrease in Intensities of Interferences.*—A more nearly quantitative method of measuring internal strain is concerned with the diminution in intensity of lines particularly at large angles (high orders). Hengstenberg² has made an investigation of KCl crystals, with the interesting results shown in Fig. 238 for intensity changes for 6 00, 8 00, and 10 00 reflections. Such

¹ GLOCKER, "Materialprüfung mit Röntgenstrahlen," 2d ed., p. 304, Verlag Julius Springer, Berlin, 1936.

² "Fortschritte der Röntgenforschung," p. 139, 1931.

relationships have been observed qualitatively also for cold-worked and annealed metals, the ratio I_{200}/I_{400} , for example, being much greater for the cold-worked specimens.

9. *Fibering*.—A final consequence of a unidirectional stress of sufficient magnitude is to align favorably sized grains in a

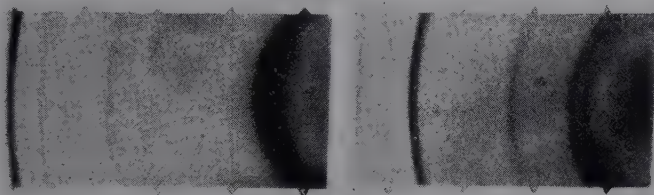


FIG. 237.—Effect of strain or distortion in broadening diffraction interferences. Left, strained; right, unstrained.

preferred orientation or fiber structure (Fig. 168). The interpretation of such patterns is considered in the next section.

The Meaning of Strain.—The exact mechanism involved in strain is still not well understood. It is to be distinguished

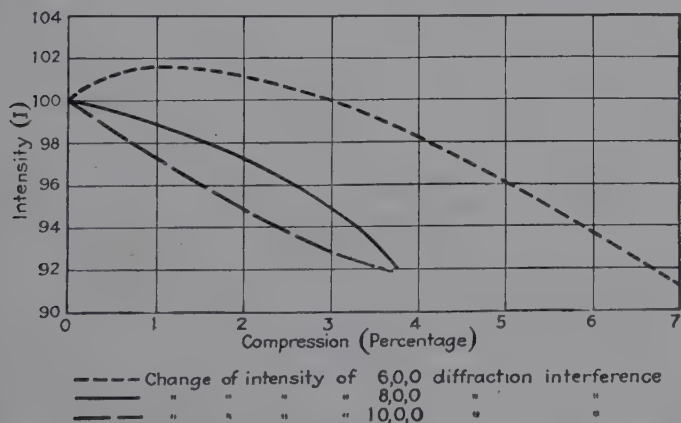
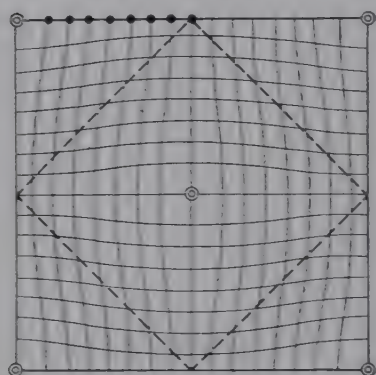


FIG. 238.—Changes in intensity of high-order reflections with deforming force. (Hengstenberg.)

clearly from the effect of a uniform deforming force which produces slipping on lattice planes. Hengstenberg has calculated for the condition of strain that, for a certain degree of deformation of 4 per cent change in length of an edge parallel to the direction of compression, 3 per cent of the atoms are displaced from their

normal positions to a maximum of one-eighth the distance between atoms. Strain must represent a condition of localized failure on the glide planes. In contrast to this irregularly distributed strain, plastic deforming forces on the surfaces of whole glide blocks do not change the lattice constants. The high-order lines remain perfectly sharp, so that the $K\alpha$ doublet is perfectly resolved. Consequently, whole blocks of the crystal at least 600 A.U. in dimensions must slip relative to each other, since deviations of the lattice constant of only 0.5 per cent or the formation of glide blocks smaller than 600 A.U. would cause inevitably an increase in breadth of the diffraction lines.



• Atoms of dissolving substance
 ○ Atoms of dissolved substance
 FIG. 239.—Distortion of lattice by introduction of foreign atoms.

Lattice distortion can be produced not only by mechanical deformation but also by the introduction of foreign atoms which form solid solutions. These effects may be expressed quantitatively by the intensity changes, as has been done by Hengstenberg. The intensity of a mixed crystal reflection according to Laue is

$$\Psi^2 \sim (p_1\Psi_1 + p_2\Psi_2)^2$$

(pure crystal $\Psi^2 \sim \Psi_1^2$) where p is the atomic per cent of each component and Ψ is the scatter-

ing power of the atoms which is proportional to the atomic number at reflection angle 0. This expression has been experimentally verified for silver-gold alloys. The fact that all the diffraction interferences varied in intensity in the same way as compared with pure silver proved conclusively that the gold atoms with about the same size as silver atoms had negligible distorting effect in the silver lattice. An opposite effect is characteristic of mixed crystals with lattice distortion, such as duralumin. The intensity data are as follows:

Quenched: $(p_1\Psi_1 + p_2\Psi_2)^2 = (0.02 \times 20 + 0.98 \times 13)^2 = 177.7$
 (copper 2 atomic per cent)

Tempered: $(p_1\Psi_1)^2 = (0.949 \times 13)^2 = 161.0$
 (CuAl₂ separated)

The 111 and 200 reflections for the quenched duralumin are actually more intense in the proportion above, but with increasing diffraction angle the ratio diminishes and for (420) reflections the intensity is 10 per cent smaller. The explanation is to be found in lattice distortion, as exemplified in Fig. 239, caused by the presence of copper atoms in the aluminum lattice.¹

THE X-RAY ANALYSIS OF FIBER DIAGRAMS AS RELATED TO THE FABRICATION OF METALS AND ALLOYS

1. Fiber Diagrams.—It is now a familiar fact that metal powders or random aggregates yield pinhole diffraction patterns on flat photographic films consisting of concentric uniformly intense



FIG. 240.—Diffraction patterns for cold-rolled aluminum foil showing fibering or preferred orientation. Left, x-ray beam perpendicular to rolling direction; right, beam parallel to rolling direction.

rings. Whenever a piece of drawn wire or thin rolled foil are used as specimens, perpendicular to the primary beam, the diffraction rings are very intense in localized intensity maxima as though more crystal grains are contributing reflection effects in certain directions, whereas in other positions few, if any, crystal grains are available for reflection, and there is little or no blackening on the film. Thus the rings observed for random arrangement of grains become series of symmetrical segments in the case of directed or preferred orientation. This type of pattern for worked metals, generally designated fiber diagrams, has been illustrated in Fig. 168 for aluminum wire and Fig. 240 for aluminum sheet.

¹ The copper atoms are smaller than aluminum; hence Fig. 239 actually represents an opposite case.

Drawn wires and rolled sheets represent different types of preferred orientation. In wires the same pattern is obtained with any orientation as long as the x-ray beam passes perpendicular to the wire axis, whereas in rolled sheets different-appearing fiber patterns are obtained with the beam perpendicular or parallel to the rolling plane.

These are fiber structures in the same sense as cellulose, stretched rubber, or asbestos fiber. None of these materials is a single crystal; all are built up of many crystal grains, but these are arranged so that a definite crystallographic axis is parallel to the axis of the fiber. In an aluminum wire that has not been annealed after drawing, the x-ray pattern demonstrates that the body diagonals, or [111] direction, in all the grains, each of which is a single crystal built up from unit face-centered cubes, lie parallel to the wire axis. Evidently, therefore, this common orientation has been induced in the process of mechanical working; the particular position is evidently that which will present maximum resistance to further deformation. It will be noted that no other limitation has been put on preferred orientation in an aluminum wire, for example, than that the [111] direction is parallel to the wire axis, or direction of drawing. Hence any grain may be turned anywhere through 360 deg. around a body diagonal as an axis and still fulfill conditions, and thus the outer form of grains in the wire may appear perfectly irregular with any kind of face in the surface. Herein lies the difference in the orientation of grains in a rolled sheet or foil, for in this case a definite crystallographic direction lies parallel to the direction of rolling *and, also*, a definite crystallographic plane in all the crystal grains lies parallel to the plane of rolling. For example, in strongly rolled iron or steel a *face* diagonal [110] direction lies parallel to the direction of rolling, and a cube face parallel to the plane of rolling. On account of this added limitation in rolled structure, which does not apply in drawn wires or complete fiber structure, this is called limited fiber structure.

In the foregoing discussion ideal cases of exact arrangements have been implied. In practice these cases are never realized, since the orientations are never perfect, though the greater the deforming force, the more nearly do the grain positions approach the ideal. As will become apparent, it is possible to determine

from the x-ray patterns, the departures from limiting ideal orientations.

As previously explained, the Laue or monochromatic pin-hole method is almost exclusively used in the study of worked metals, since it affords a pattern 360 deg. in azimuth. It is necessary only to mount a wire or sheet specimen over the outer pinhole so that the beam will pass perpendicular to the wire axis or rolling direction. The pattern is registered on a flat photographic film.

2. The Interpretation of Complete Fiber Patterns (Drawn Wires).—Of first concern is the pattern of the Debye-Scherrer rings which defines the particular metal. All the lattice planes with the same lattice spacing d reflect rays on the same diffraction ring, which is continuous in the case of random orientation or segmented into spots or arcs for fibered materials. It is useful

| Body-centered cubic | | Face-centered cubic | |
|---------------------|--|---------------------|--|
| Indices | $a_0/d_{hkl} = \sqrt{h^2 + k^2 + l^2}$ | Indices | $a_0/d_{hkl} = \sqrt{h^2 + k^2 + l^2}$ |
| (110) | 1.41 | (111) | 1.23 |
| (200) | 2.00 | (200) | 2.00 |
| (112) | 2.45 | (220) | 2.83 |
| (220) | 2.83 | (113) | 3.32 |
| (130) | 3.16 | (222) | 3.46 |
| (222) | 3.46 | (400) | 4.00 |

to list again for the body-centered and face-centered cubic lattices the planar indices corresponding to the rings that appear, passing from the innermost outward.

In this fashion it is possible to determine the planar indices for each ring.

Next to be found are the positions of the intensity maxima upon the rings. One of the sets of parallel reflecting planes may be imagined rotated 360 deg. around an axis perpendicular to the primary x-ray beam. In the course of this rotation it will pass four times through the proper angle for reflection in accordance with Bragg's law and produce upon a photographic plate placed behind the specimen a four-point pattern which is symmetrical with respect to a vertical line on the plate

parallel to the rotation or fiber axis and also with respect to a horizontal line. In other words, these maxima are, for example, at the clock hour-hand positions of 1:30, 4:30, 7:30, and 10:30 (see Fig. 241). If this particular reflecting plane in a special case is parallel to the axis of rotation (or fiber axis), then only two spots are produced on the ring on the horizontal line (three and nine o'clock). No reflection occurs, of course, if this plane is exactly perpendicular to the rotation axis. Two spots occur on the vertical line (twelve and six o'clock) if the angle of the reflecting plane with respect to the rotation (fiber) axis is equal to the

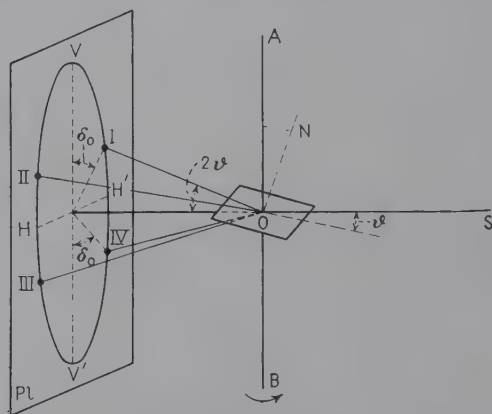


FIG. 241.—Analysis of the ideal four-point fiber diagram, with x-ray beam perpendicular to the fiber axis. *SO*, x-ray beam; *AB*, fiber axis.

angle of incidence of the x-ray beam. It is at once clear, therefore, that the positions of intensity maxima on a given ring on the photographic plate may be measured and used directly to deduce the positions of lattice planes in the wire in a very simple manner. If α is the angle between the normal to the set of reflecting planes and the rotation (fiber) axis and δ is the angle measured on the film between a radius drawn through a particular intensity maximum and the vertical line *VV'* (which is known to be parallel to the rotation or fiber axis), then

$$\cos \delta = \frac{\cos \alpha}{\cos \Theta},$$

where Θ is the angle of incidence. At small reflection angles, such as are true for the most important diffraction circles for

metals, $\cos \theta$ is approximately 1. Hence $\delta = \alpha$. Thus a simple angle measurement on the film is also the value for the angle between the normal to a set of reflecting planes and the fiber axis.

In any cubic lattice the angle between the fiber axis with indices uvw and a lattice plane hkl is given by

$$\cos \alpha = \frac{uh + vk + lw}{\sqrt{u^2 + v^2 + w^2} \sqrt{h^2 + k^2 + l^2}}.$$

In aluminum wire the $[111]$ direction is the fiber axis. The innermost ring registers the reflection from all the octahedral planes (111) , $(\bar{1}11)$, $(1\bar{1}1)$, $(\bar{1}\bar{1}1)$ and the other four parallel to these. Hence α , and consequently δ , on the film will be 0° for (111) , which means that the (111) planes are perpendicular to the fiber axis $[111]$ (as by definition) and cannot reflect. For the others $\alpha = 71^\circ = \delta$ (see Fig. 242).

Further data for aluminum wire calculated in this way are presented at the top of page 524.

Since there is agreement between the calculated positions and those found experimentally for drawn aluminum (Fig. 168), the

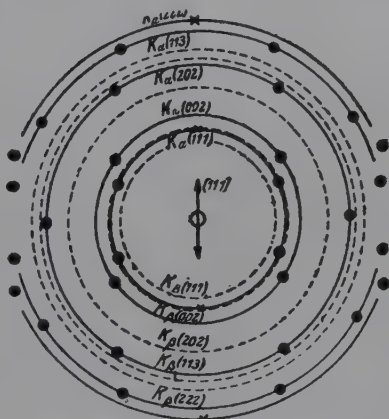


FIG. 242.—Theoretical fiber diagram for aluminum wire with $[111]$ parallel to wire axis (see Fig. 168).

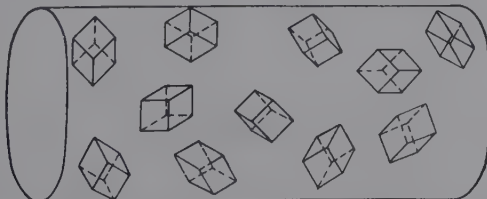


FIG. 243.—Diagram showing unit crystal cubes in aluminum wire with cube diagonals parallel to wire axis, but oriented at random around this axis.

assumption of the $[111]$ fiber axis is correct and the wire structure may be represented as shown in Fig. 243, with the unit crystal

| Ring number | Planes | Number cooperating | α , degrees |
|--------------------|--------------------|--------------------|--------------------|
| { 1(111) 5(222) | ($\bar{1}11$) | 6 | 71 |
| | ($1\bar{1}1$) | | |
| | ($11\bar{1}$) | | |
| { 2(200) 6(400) | (100) | 6 | 55 |
| | (010) | | |
| | (001) | | |
| 3(220) | (110) | 6 | 35 |
| | (101) | | |
| | (011) | | |
| | ($\bar{1}10$) | | |
| | ($\bar{1}01$) | | |
| 4(113) | ($0\bar{1}1$) | 6 | 90 |
| | 113, etc. | 6 | 30 |
| | $\bar{1}13$, etc. | 12 | 59 |
| | 113, etc. | 6 | 80 |
| | | | |

cubes oriented with cube diagonals parallel to the wire axis, but at random around these diagonals as axes.

For body-centered cubic wires like iron (Fig. 244) the assumption may be made that the [110] direction is parallel to the wire axis, and this is then tested.

| Ring | Planes | Number cooperating | α , degrees |
|--------------------|--|--------------------|--------------------|
| { 1(110) 4(220) | (101) | 8 | 60 |
| | ($10\bar{1}$) | | |
| | (011) | | |
| | ($01\bar{1}$) | | |
| 2(200) | (100) | 4 | 45 |
| | (010) | | |
| | (001) | | |
| 3(112) | (211), (121), etc. | 2 | 90 |
| | (112), ($11\bar{2}$), etc. | 8 | 30 |
| | ($2\bar{1}1$), ($\bar{1}21$), etc. | 4 | 55 |
| | ($1\bar{1}2$), ($\bar{1}\bar{1}2$), etc. | 8 | 73 |
| | (130), (310), etc. | 4 | 90 |
| 5(130) | (301), (031), etc. | 4 | 27 |
| | ($\bar{1}30$), ($3\bar{1}0$), etc. | 4 | 48 |
| | (103), (013), etc. | 4 | 63 |
| | (111), ($11\bar{1}$) | 12 | 77 |
| | ($1\bar{1}1$), ($\bar{1}\bar{1}1$) | 4 | 35 |
| 6(222) | | 4 | 90 |

As a matter of fact, the intensity maxima lying on the Debye-Scherrer rings are not sharp spots but are really arcs of 10 deg. in cases of extreme cold work, or more (Fig. 245). This means, of course, that all the crystal grains are not perfectly oriented and that there is a "scattering" in a cone around an average or ideal position which is the wire axis itself. The scattering angle or apex of this cone is obviously half the arc length of the intensity maxima. Every possible gradation of preferred orientation may be practically observed in metal specimens from sharp spots to continuous rings for random arrangement.

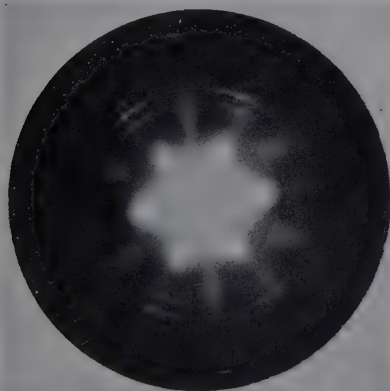


FIG. 244.—Fiber pattern for hard-drawn steel wire.

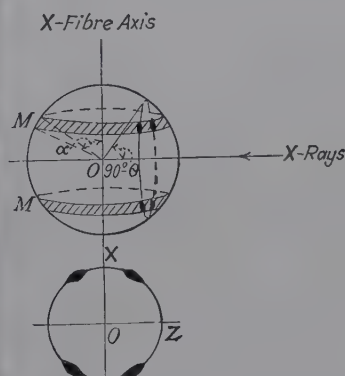


FIG. 245.—Analysis of true fiber diagram. Compare with ideal four-point diagram in Fig. 241.

The arc lengths of the maxima are, therefore, a measure of the amount of cold work and preferred orientation or fibering in a given specimen, either directly produced or residual after heat-treatment.

In many cases of examination of fabricated metals it may be impossible or undesirable to orient the specimen with the fiber axis perpendicular to the primary x-ray beam. If, then, the specimen is placed at an oblique angle, a pattern is obtained with exactly the same Debye-Scherrer rings as before but the four-point diagram is changed when two of the points move apart on a ring and the other two together, still retaining symmetry with respect to vertical and horizontal lines on the film. Instead of one angle δ to be measured for the four spots, there are now two angles δ and δ' evaluated by

$$\cos \delta = \frac{\cos \alpha - \cos \beta \sin \Theta}{\sin \beta \cos \Theta}$$

and

$$\cos \delta' = \frac{\cos \alpha - \cos (180^\circ - \beta) \sin \Theta}{\sin (180^\circ - \beta) \cos \Theta}$$

where α is the same as before, β is the angle between the fiber axis and the direction of the primary beam, and Θ is the angle of incidence (Fig. 246).

For evaluation of the indices of the fiber axis in a drawn metal, two or three methods are available:

1. Trial and failure method by assuming indices, calculating the intensity maxima to be expected on the various rings,

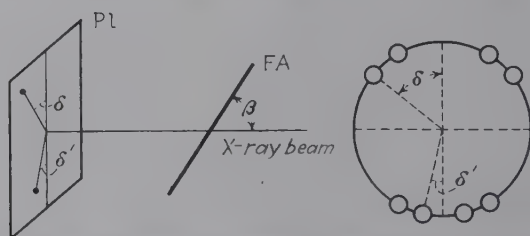


FIG. 246.—Effect upon diffraction pattern of tilting fiber axis (FA) at angle β to x-ray beam.

as illustrated above for aluminum and iron, and comparing with experimental film.

2. Use of patterns for obliquely oriented fiber axis with a series of values for the angle β . If the crystal lattice plane perpendicular to the fiber axis (Polanyi's diatropic planes) reflect a beam of wave length λ incident at the angle Θ , then, when $\beta = 90^\circ - \Theta$, an intensity maximum will appear at the twelve o'clock position on one of the Debye-Scherrer rings due to (hkl) planes. For cubic crystals the evaluation of the (hkl) indices for the ring upon which the intensity maximum appears gives at once [hkl] the fiber axis, since the normal to these planes is the same as the axis.

3. Sometimes only two or three intensity maxima are necessary to evaluate the fiber axis. Glocker and Kaupp¹ give the example of electrodeposited copper with maxima on the (111) and (200) [or (100), second order] rings. Since

¹ Z. Physik, **24**, 121 (1924).

$$\cos \alpha = \frac{uh + vk + lw}{\sqrt{u^2 + v^2 + w^2} \sqrt{h^2 + k^2 + l^2}},$$

where $[uvw]$ is the fiber axis and (hkl) a set of planes, then for the (111) and (100) planes, respectively,

$$\cos \alpha_1 = \frac{u + v + w}{\sqrt{3} \sqrt{u^2 + v^2 + w^2}},$$

$$\cos \alpha_2 = \frac{u}{\sqrt{u^2 + v^2 + w^2}}.$$

Intensity maxima appear on both rings at 90 deg.; hence $\delta_1 = \alpha_1 = \delta_2 = \alpha_2$; furthermore, substituting the values of $\cos \alpha_1$ and $\cos \alpha_2$, $0 = u + v + w$ and $0 = u$, or $v = -w$. The fiber axis is therefore $[0\bar{1}1]$.

X-ray patterns taken with the beam parallel to the fiber axis are characterized by uniform Debye-Scherrer rings indicative of random orientation.

3. Multiple-fiber Structures in Drawn Wires.—Sometimes more than one preferred orientation is observed as a multiple-fiber structure. This is true of face-centered cubic metals in which both $[111]$ and $[100]$ directions serve as fiber axes. The distribution of grain orientations between these two varies depending on the metal. This has been studied quantitatively by Schmid and Wassermann.¹ Diffraction patterns shown in

| Metal wire | Per cent crystals with | | Half length of interferences on (200) ring | |
|---------------|-------------------------------------|-------|---|--------|
| | [100] | [111] | | |
| | Parallel to direction of drawing | | [100] | [111] |
| Aluminum..... | 0 | 100 | | 3° 30' |
| Copper..... | 40 | 60 | 7° | 3° |
| Gold..... | 50 | 50 | 8° 30' | 4° 30' |
| Silver..... | 75 | 25 | 7° 30' | 3° |

Fig. 247 were registered on a cylindrical film instead of the usual flat film, so that the layer-line diagrams characteristic for fibers

¹ *Z. Physik*, **42**, 779 (1927).

are more prominently shown. The data obtained for the percentage of crystals in the [100] and [111] orientations and for the half length of interferences on the (200) ring as a measure of the exactness of fibering are as follows:

The scattering around the [100] preferred orientation is evidently twice as great as around the [111] axis. The presence of a double-fiber structure with varying proportions of each and variations in scattering around a fixed position have great prac-

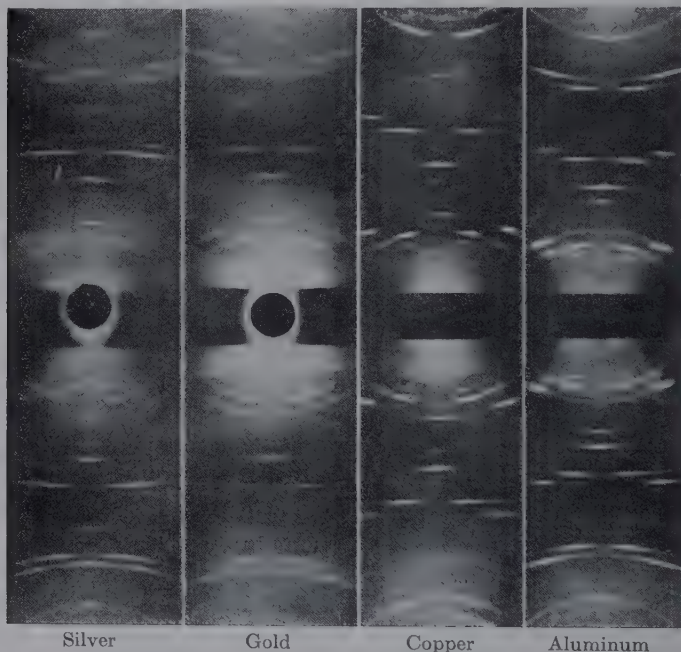


Fig. 247.—Debye-Scherrer patterns for hard-drawn wires. (*Schmid and Wassermann.*)

tical significance in differentiating drawing, annealing, and physical properties of aluminum, copper, gold, and silver.

W. M. **4. The Zonal Structures of Hard-drawn Wires.**—An interesting structural phenomenon in hard-drawn wires is illustrated in Fig. 248 for copper wire. A beam of monochromatic x-rays defined by a slit was reflected from the surface of a cold-drawn copper wire about 0.5 mm. in diameter. The pattern in (a) shows a nearly random arrangement of grains in spite of the prediction concerning fibering. The wire was then etched down in successive steps and an x-ray examination made. The structure of

the innermost core of the wire in (b) is characterized by extreme fibering. Hence, wires drawn through dies have distinctly zonal structures with the grains becoming more perfectly oriented the nearer to the wire axis considered as a line at the exact center.

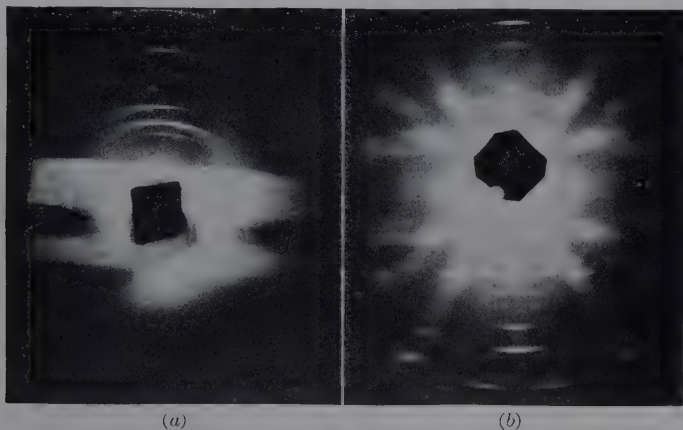


FIG. 248.—Patterns illustrating zonal structure in copper wire: (a) surface; (b) innermost core.

In other words, in the passage through the die, the flow of metal exactly in the direction of drawing occurs only in the middle of the wire, whereas in the walls the metal is flowing inward as well as along the length of the wire and the crystal grains are thus disposed at an angle to the core.

Ordinary powder diffraction spectra (Hull method) also show the zonal structure. Figure 249 (upper) shows the pattern of the

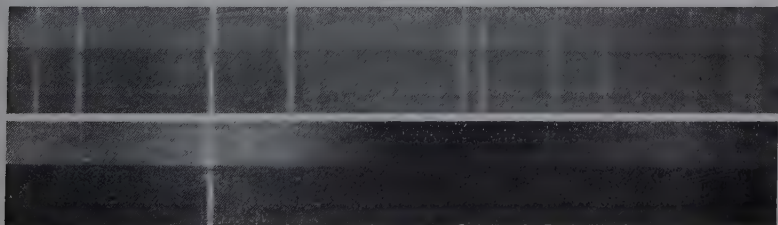


FIG. 249.—Hull diffraction patterns showing zonal structure of copper wire. Upper, outer mantle; lower, core.

original copper wire, which is really the structure of the outer mantle of the wire. The intensities of the various diffraction lines are just about those to be expected from a somewhat random orientation. Figure 249 (lower) is the pattern for the core of this wire after etching down to a diameter of about 0.13 mm.

A surprising change has occurred since the (111) line has entirely disappeared, the (200) line is about the same, the (220) line is about doubled in relative intensity, the (311) line is about half as intense, etc. This illustrates the error which might be made in the interpretation of such patterns if the facts were not known. The phenomena here observed agree with a [100] direction for the fiber axis but not so well with the [111].

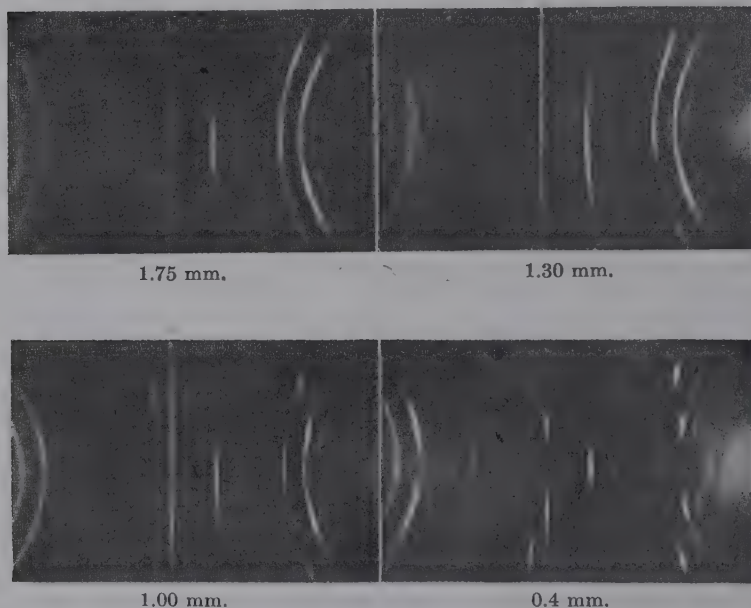


FIG. 250.—Patterns for copper wire showing zonal structure with decreasing diameter.

This condition of a central linear zone and a conical mantle, of course, is of primary importance in affecting the texture of the wire and in the proper interpretation of diffraction patterns. The zonal structure of wires has also been studied by Schmid and Wassermann. In Fig. 250 are reproduced patterns from their work on copper wire with the diameters 1.75, 1.3, 1.0, and 0.4 mm. Not only does the sharpness of fibering shown by the shorter interference maxima increase as layers are removed, but there is also evidence of unsymmetrical interferences. From these the inclination of the fiber axis [111] to the wire axis in different zones is determined as follows:

| Distance of Layer from Center, Millimeters | Inclination Angle, Degrees |
|---|-------------------------------|
| 1.75 (outer skin) | <2 |
| 1.6 | 9 |
| 1.3 | 6 |
| 0.9 | 4 |
| 0.4 | 0 |

This indicates that, in the outermost skin of the wire, the effect of the die has been to keep the grains which are oriented nearly parallel to the direction of drawing, but slightly below this the conical flow is evident.

The texture of a hard-drawn wire, therefore, may be represented in Fig. 251. Schmid

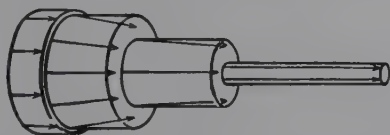


FIG. 251.—Zonal texture of hard-drawn wires.

and Wassermann report tests of tensile strengths in kilograms per square millimeter corresponding to zones for two specimens of hard-drawn copper wire, as follows:

| | Tensile Strength |
|-----------------------------------|------------------|
| 1. Original diameter 4.85 mm..... | 38.3 |
| Etched to 3.20 mm..... | 41.3 |
| Drawn to 3.20 mm..... | 45.2 |
| 2. Original diameter 1.75 mm..... | 46.1 |
| Etched to 1.00 mm..... | 52.8 |
| Drawn to 1.00 mm..... | 51.0 |

It is evident that the core zone of a wire has the highest tensile strength in keeping with its parallel preferred orientation. This anisotropic or zonal structure is an inherent property and improvement in the superficial zones is not gained by increasing the amount of cold work.

5. Summary of X-ray Results on Deformation Structures of Drawn Wires.—All body-centered cubic metals when drawn are characterized by a [110] direction parallel to the direction of drawing; all face-centered cubic metals have a [111] direction in the wire axis, with a second orientation of [100], the proportion of crystal grains in the various metals varying as explained above. An exception in the case of copper wire recrystallized at 1000°C. has been noted. Only the core of these wires and perhaps the outermost skin approximate these orientations, since in the mantle zones the fiber axis is inclined to the wire axis. In answering

the question why a particular crystallographic direction becomes parallel to the direction of deformation it may be noted that the most thickly populated atomic planes in the body-centered cubic lattice are the (111) planes, with the (100) planes next most densely populated. It is a general drawing phenomenon, there-



FIG. 252.—Pinhole pattern for rolled sheet metal (high carbon steel) with nearly random grains.

fore, that the most densely populated planes take up positions perpendicular to the wire axis and that these orientations are such as to present maximum resistance to further deformation.

6. Interpretation of Fiber Patterns for Rolled Sheets (Limited Fiber Structure).—It is possible for cold-rolled sheet metal to

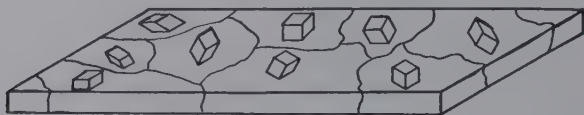


FIG. 253.—Texture of sheet metal with randomly oriented grains.

produce a diffraction pattern indicating nearly random orientation of grains, as in Fig. 252. The structure of the sheet could then be diagrammatically drawn as in Fig. 253. But in general, as explained above, crystal grains in a rolled sheet not only take up positions with a certain crystallographic direction parallel

to the direction of rolling but are further limited by having certain crystallographic planes parallel to the plane of rolling and to the transverse direction. Thus the diffraction pattern for rolled sheet steel in Fig. 254 indicates clearly the structure of the



FIG. 254.—Pinhole pattern for usual type of rolled sheet steel with preferred orientation of grains.

sheet with preferred orientation of grains as pictured in Fig. 255. The diffraction patterns allow the evaluation of the indices of these three characteristic directions (*i.e.*, rolling direction, the normal to the rolling plane, and the transverse direction lying in the rolling plane at right angles to the rolling direction) and also

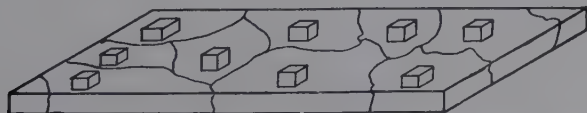


FIG. 255.—Texture of rolled sheet metal (steel) with preferred orientation of grains.

with remarkable accuracy the departure, or scattering, from the theoretically ideal orientation as is always observed in practical cases. The rolling direction may be readily ascertained by the methods outlined above for drawn wires, although all the diffrac-

tion interferences will not be present on account of the further limitation in rolling. For the determination of the crystallographic indices of the transverse direction and the normal to the plane of rolling, a further step must be taken. The first method is that of Glocker, explained in detail in his book:¹ a single metal crystal is considered to rotate through 360 deg. around the known fiber axis, and the reflection angle 2θ of the x-ray beam, impinging at right angles to the axis of rotation, on the different lattice planes of the crystal is plotted as a function of the angle of rotation. The result is a series of rotation curves which are extremely useful in interpreting results on rolled sheets or foils. Glocker gives curves for fiber axis [112], [001], and [111], with octahedral (111), cubic (100), dodecahedral (110), and (113) planes for each. He considers in detail the case of rolled silver in which [112] is parallel to the rolling direction and (110) planes are parallel to the rolling plane.

7. Detailed Analysis of Pattern for Rolled Steel.—To show in detail how a diffraction pattern (Fig. 254) of commercial rolled sheet may be completely interpreted, the example of low-carbon sheet steel is selected. By the usual methods of powder-pattern analyses, the Debye-Scherrer rings upon which the arcs appear are identified from the center outward as 110, 200, and 210 reflections of body-centered cubic iron. The inner broad band is caused by the polychromatic or white radiation reflected by the planes of greatest spacing (110). The inner edge is determined by the short wave length of the white radiation, which is determined by the peak voltage across the x-ray tube (here 36,768 volts). The outer edge is caused by an absorption edge due to the silver of the film emulsion, which occurs at a wave length of 0.485 A.U.

| Planes | Azimuth, Degrees |
|-------------|------------------|
| 110 | 0 |
| $\bar{1}10$ | 90 |
| 101 | 60 |
| 100 | 45 |
| 001 | 90 |
| 112 | 55 |
| $\bar{1}12$ | 90 |
| 121 | 30 |
| $\bar{1}21$ | 73 |

¹ "Materialprüfung mit Röntgenstrahlen," pp. 312-324, Berlin, 1927.

With $[uvw]$ as $[110]$, the equation on page 523 simplifies to

$$\cos \alpha = \frac{h + k}{\sqrt{2}\sqrt{h^2 + k^2 + l^2}}.$$

With this equation the theoretical azimuth of spots on the various rings is as shown on page 534.

These diagrams should be symmetrical along both a vertical and a horizontal axis; for every spot at angle δ on the right there is one at δ on the left, and one on the right and left at $(180^\circ - \delta)$.

In comparing this theoretical complete fiber diagram with the actual diffraction patterns the fiber axis is assumed to be perpendicular to the x-ray beam which practically may not be exactly true. This will tend in some cases to shift the positions toward one pole or the other and cause fiber spots that originate from planes at high angles from the fiber axis to appear with less rotation than would be expected, as will be discussed in the next section.

In Fig. 254 the following experimental interferences are observed:

| INNERMOST SHARP RING (110) | | |
|----------------------------|--|---------|
| 0° | | Present |
| 60° | | Missing |
| 90° | | Present |
| SECOND SHARP RING (100) | | |
| 45° | | Present |
| 90° | | Missing |
| THIRD SHARP RING (211) | | |
| 30° | | Present |
| 55° | | Missing |
| 73° | | Present |
| 90° | | Missing |

The broad band can have the same intensity maxima as the sharp (110) ring:

| | |
|-----|---------|
| 0° | Present |
| 60° | Missing |
| 90° | Present |

Since this orientation takes care of all the spots appearing on the diffraction pattern but calls for spots that do not appear, it is evident that the assumption of a $[110]$ axis is correct but that there is a further limitation of orientation in a rolled sheet.

The other condition of a cube face lying parallel to the surface of a sheet that is usually given will be taken as the zero position, and angular rotation about the face diagonal fiber axis necessary to cause the appearance of various spots will be calculated. Then, by the presence or absence of certain spots, the degree of perfection of the fulfillment of this condition can be determined on each film. If this orientation were perfect, only a very few spots would appear on any ring, and the ring itself would be missing.

The calculation of this angle of lateral rocking to one side and the other about the zero position necessary to cause the appearance of each spot is very involved in most cases, and a complete solution of this problem of a cubic lattice rotating about a [110] axis has been worked into the series of rotation curves by Glocker, mentioned above. These curves were used in investigating how great an angle of rotation of the cube about the [110] fiber axis from the zero position of the (100) face in the sheet is necessary in order that a diffraction spot may occur by having fulfilled the law specifying the angle of diffraction.

It will be seen that in the special case of any planes containing the x-ray beam the necessary angle of rotation about any axis perpendicular to the beam will directly equal the angle Θ given in the diffraction equation.

The presence of spots on the two (110) rings at the twelve and six o'clock positions can be explained only by another type of imperfection in orientation. This is a *tipping* of planes, which in a perfect orientation would contain the x-ray beam and be perpendicular to the fiber axis, about an axis perpendicular to both

| Necessary angle of rotation | Ring | Radiation | Azimuth, degrees |
|-----------------------------|------|-----------|------------------|
| 4 | 110 | White | 90 |
| 9 | 112 | $K\alpha$ | 73 |
| 10 | 110 | $K\alpha$ | 90 |
| 18 | 112 | $K\alpha$ | 30 |
| 18 | 110 | $K\alpha$ | 60 |
| 20 | 100 | $K\alpha$ | 45 |
| 22 | 110 | White | 60 |
| 45 | 112 | $K\alpha$ | 90 |
| 70 | 112 | $K\alpha$ | 55 |

the beam and the fiber axis. This is actually an *inclination of the fiber axis to the surface of the sheet*, and its calculation falls in the special case mentioned in the last paragraph. The angles of rotation necessary for the appearance of the various spots on the several rings arranged in the order of their appearance with increasing rotation were found to be as shown on page 536.

The angle of inclination of the fiber axis to the sheet necessary to cause the appearance of spots at the six and twelve o'clock positions on the rings will be calculated. These reflections can originate only from (110) planes, and the inclination is directly equal to the angle of incidence given by the Bragg equation for this set of planes.

| Ring | Radiation | Wave length | Inclination angle |
|-------|-----------------------|-------------|-------------------|
| (110) | M α K α | 0.710 A.U. | 10° 18' |
| (110) | White | 0.336 | 4° 45' |

Inclination of the fiber axis to the surface of the sheet in both directions with respect to the direction of the last pass will have the effect of causing the spots to extend over a wider angle on the circles and will cause spots to appear at slightly smaller rotation angles than those calculated to be necessary. If more grains are inclined in one direction than in the other, which in general seems to be the case, the intensity maxima will be displaced in one direction of azimuth and there arises a possibility of the appearance of spots on one side of the equator for which there are no corresponding spots on the other side.

8. Deformation Structures of Magnesium Alloys.—The growing industrial importance of magnesium and its alloys also lends particular interest to the mechanism of its deformation. Figures 256 to 261 show diffraction patterns and theoretically calculated diagrams, respectively, for forged and extruded DOWMETAL (nearly pure magnesium alloy). The analysis of the patterns proves that the forged magnesium alloy possesses a fiber axis parallel to the [001] direction, whereas the extruded alloy shows a [210] fiber axis in the direction of extrusion at low temperatures and a [110] direction at high temperatures, a curious change in glide direction with temperature. Schmid working with single crystals found translation on the basal planes with the diagonal



FIG. 256.—Pattern for forged Dowmetal (magnesium alloy).

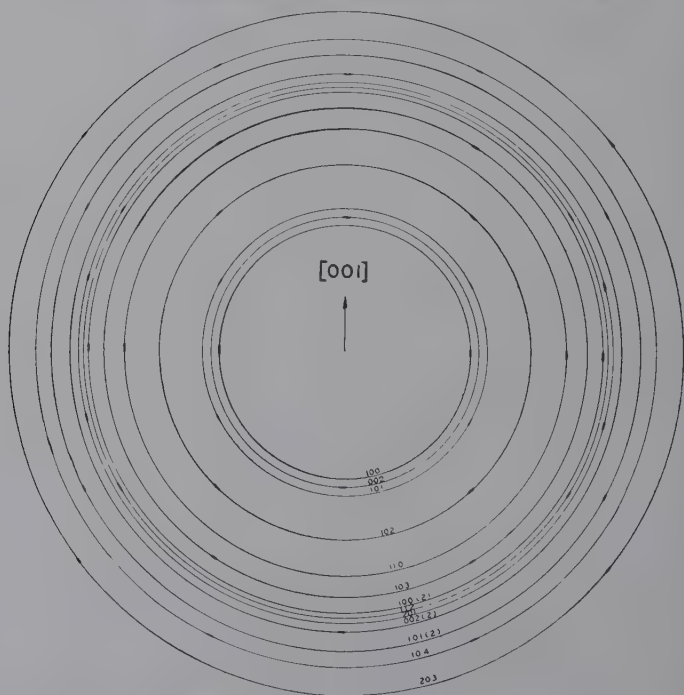


FIG. 257.—Theoretical fiber pattern for $[001]$ parallel to fiber axis, hexagonal system, with which the actual pattern in Fig. 256 agrees.

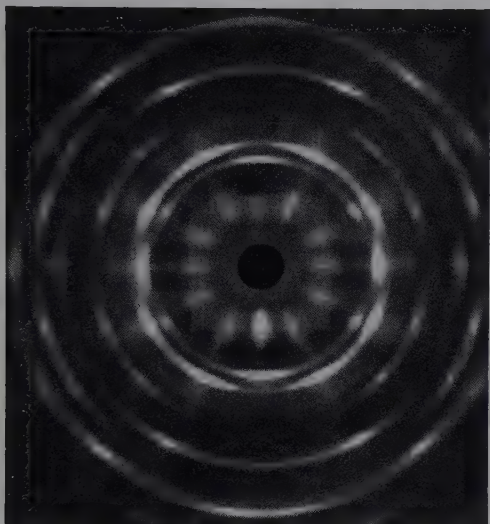


FIG. 258.—Pattern for Dowmetal extruded at ordinary temperatures.

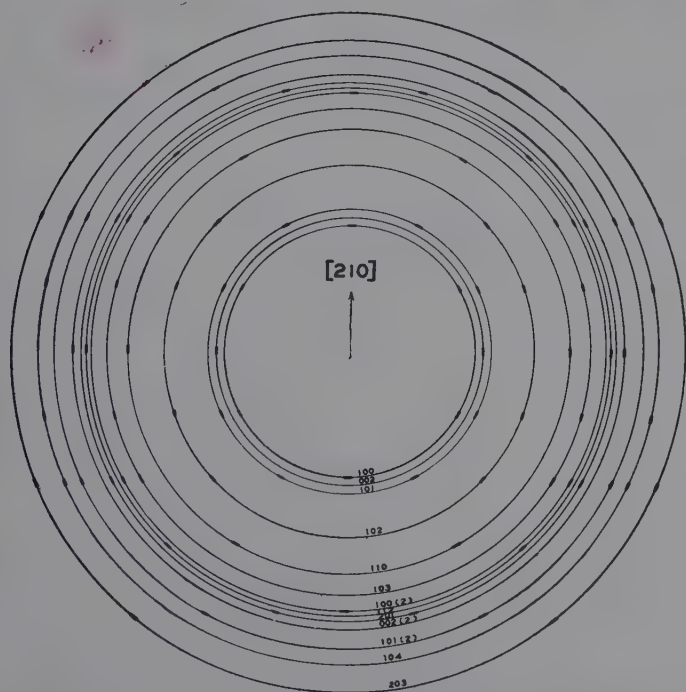


FIG. 259.—Theoretical fiber pattern for $[210]$ parallel to fiber axis, hexagonal system, with which the actual pattern in Fig. 258 agrees.

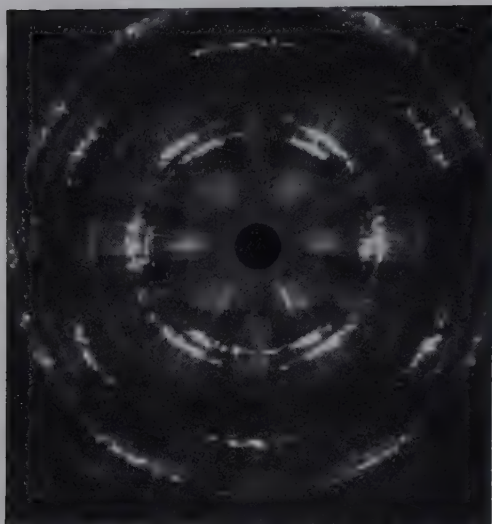


FIG. 260. —Pattern for Dowmetal extruded at high temperatures. Note, in comparison with Fig. 258, the effect in changing preferred orientation, and greatly increasing grain size.

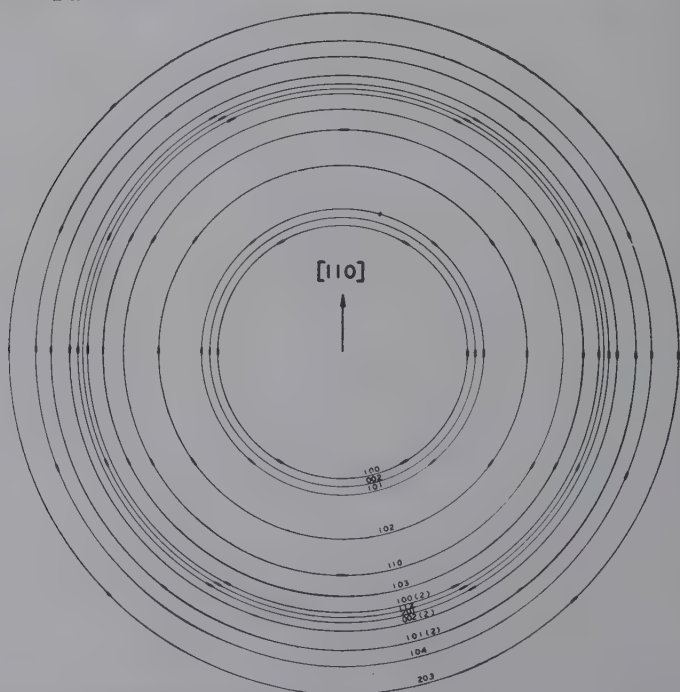


FIG. 261.—Theoretical fiber pattern for $[110]$ parallel to fiber axis, hexagonal system, with which the pattern in Fig. 260 agrees.

axis of the first kind as glide direction. Above 225° translation on the pyramid faces occurs with the same glide direction. In many important respects, therefore, magnesium differs in behavior from zinc and cadmium.

9. Pole Figures.—The generally accepted method of graphical expression of orientation of crystallites in fibered materials, and the statistical deviation around the ideal preferred positions, is the pole figure for the normals of the reflecting planes. Several diffraction patterns are made for a specimen with the primary x-ray beam at various angles to directions of drawing, rolling, etc., and to planes in sheet specimens. For each important set of lattice planes the position of planes is represented by a stereographic projection (page 287). The pole sphere and method of projection upon a plane are shown in Fig. 262*a*. For rolled sheets, for example, the plane of rolling is chosen as the plane of projection. From 15 patterns the projections in Fig. 262*b* for rolled α -brass were determined by von Göler and Sachs. These three pole figures give the positions of the normals to (100), (111), and (110) planes with respect to the direction of rolling. The crosshatched areas represent the greatest densities of positions of the normals, and the corresponding crystallite positions are predominant. Around these regions lines enclose wider areas corresponding to more widely scattered orientations. Thus the distribution of crystallites may be described as a scattering around an ideal orientation with a (110) plane parallel to the plane of rolling, a rolling direction [112], and a cross direction [111]. These ideal orientations are projected as dots on the figures. The correctness of interpretation is shown by the following: The point in the center of Fig. 262 *b(c)* means the normals that definitely identify the (110) rolling plane; the points where the equator in Fig. 262 *b(b)* cut the circle indicate normals to (111) planes or the [111] direction. And so the rolling direction must be [112]. It is necessary only to project the ideal position for the arrangement on the (100), (111), and (110) planes and compare with this the pole figure from the diffraction patterns. Perhaps a second or third orientation will be required to account for all the observed interferences. The whole graphical projection is simplified by the fact that there is mirror symmetry about the vertical *W.R.* and horizontal *Q.R.* lines, and hence a quarter of the projection suffices to complete the entire figure. Thus the pole figure as a terse

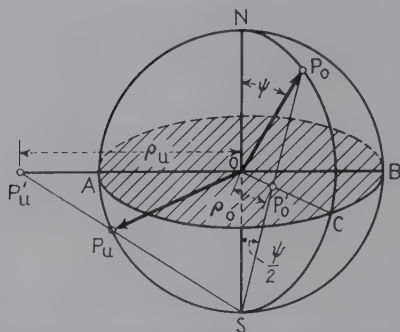


FIG. 262a.—Derivation of pole figure by stereographic projection. P_o and P_u are two face poles; with the eye at S (south pole) the projection of P_o on the shaded equatorial plane is P'_o ; that of P_u in the lower hemisphere is on the extended line at P'_u .

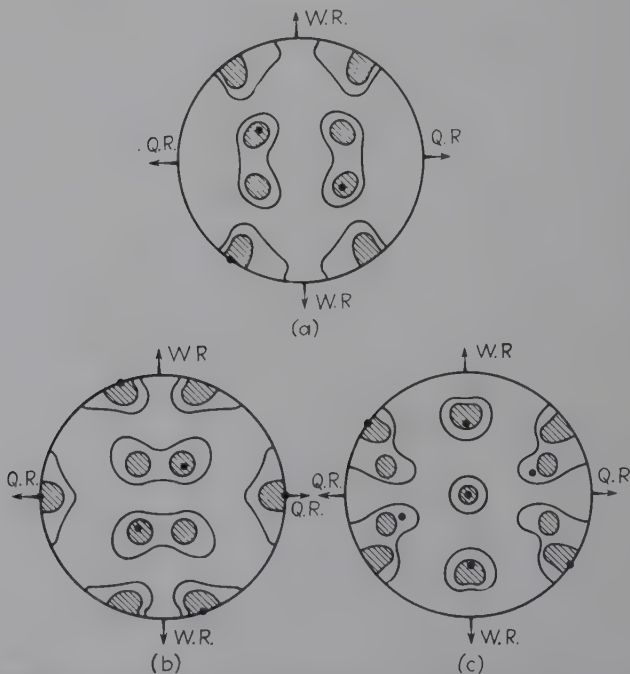


FIG. 262b.—Pole figures for rolled brass; $W.R.$, rolling direction; $Q.R.$, cross direction. (a) (100) plane; (b) (111) plane; (c) (110) plane, which is parallel to the plane of rolling. (von Göler and Sachs.)

representation of all orientations has superseded all other methods of interpretation of fiber patterns. As a formal means of comparison of cellulose and other natural-material-fiber orientations it is commonly applied. The accuracy increases with the number of patterns at different angles. In the example cited for rolled α -brass, the areas of most common normal distribution are correct within 5 deg.

10. Summary of Deformation Textures of Metals.

| Deformation and metal | Lattice type | Directions and planes parallel to force |
|--|--------------|--|
| 1. Drawing: | | |
| Ag, Al, Au, Cu, Ni, Pd. | F.c.c. | I [111] II[100] } distribution (see p. 527) |
| α -Fe, Mo, W..... | B.c.c. | [110] |
| Mg, Zr..... | Hexagonal | (0001)—ring fiber |
| Zn..... | Hexagonal | (0001), inclined 18°—spiral fiber |
| 2. Swaging, hammering (depends on direction of flow): | | |
| Al, Cu..... | F.c.c. | [100] |
| α -Fe..... | B.c.c. | { [111] [100] (weak) |
| Mg..... | Hexagonal | [0001] |
| 3. Rolling: | | |
| | | Rolling plane |
| Ag, α -brass, tin-bronze | F.c.c. | [112] (110) |
| Pt..... | F.c.c. | I[112] I(110) |
| | | II[100] II(001) |
| Al, Au, Cu, Ni..... | F.c.c. | I[112] } or I(110) } or II[111] } [335] II(112) } (135) |
| Mo, Ta, W..... | B.c.c. | [110] (001) |
| α -Fe..... | B.c.c. | I[110] I(001) |
| | | II[110] II(112) |
| | | III[112] III(111) weak |
| Cd..... | Hexagonal | (0001) inclined at 30° |
| Mg, Zr..... | Hexagonal | (0001) |
| Zn..... | Hexagonal | [1120] (0001) inclined at 20° |

11. The Mechanism of Plastic Deformation.¹—The properties of metals that permit plastic deformation under the stresses

¹ See ELAM, "Distortion of Metal Crystals," University Press, 1935; Hoyt, Preprint, American Society for Metals, October, 1936.

of drawing, rolling, forging, compression, torsion, etc., are the basis of all commercial processes of fabrication. It is of greatest importance, therefore, to have some knowledge as to the mechanism by which deformation and extension take place. The single crystal subjected to the tensile test is obviously the most direct method of evaluating fundamentally the processes involved in elastic behavior, plastic yielding, deformation, and rupture. The results on the far more common polycrystalline metals differ in that the test on these materials is the summation of the behavior of individual grains and grain boundaries such that the specimen reacts as an isotropic material and the deformation is governed by the applied stress system. The single crystal, however, behaves anisotropically, or entirely differently in one direction than in another. Instead of a conical necking and fracture it may neck down to a chisel edge or fracture on a cleavage plane. The lattice geometry rather than the stress is the determining factor. There is the further difference that the single crystal is weaker and under the proper conditions far more ductile than the fine-grained aggregate.

The mechanism of plastic deformation is probably most easily exemplified by the hexagonal close-packed metals such as zinc, cadmium, and magnesium, upon which very extensive studies have been made by numerous investigators. In these metals there is only one densest packed plane, the basal plane (0001), so that a crystal may be represented as a pack of cards. It is a general rule that with greatest precision the parallel densest packed planes support slip and the densest packed direction is the direction of slip. Therefore, when the basal planes in zinc are at an angle to the wire axis, a tensile pull stretches the wire by slip along these planes, which tilt still more toward the long axis during extension, as shown in Fig. 263. This causes the wire to stretch out into a thin ribbon, or band, with elliptical cross section. As soon as the angle of these planes reaches 70 to 80 deg., the crystal usually fails by cleavage on the basal or one of the three prismatic planes. If the basal planes are parallel or perpendicular to the axis of the wire and the direction of tensile pull, no slip can occur and the specimen fails by brittle cleavage. Thus plastic deformation can occur only when the basal planes start out a few degrees from parallel or perpendicular position, the latter being best for display of great ductility and elongation.

The slip ellipses on the zinc crystal are distinct, and the changing angle of tilt during deformation may be followed optically, but best of all by x-ray patterns. Slip along the (0001) planes is restricted to one of the three diagonal axes such as [1010], and with these three assuming any position in the slip plane the one selected will be that which most closely coincides with the direction of maximum resolved shear or the major axis of the elliptical section. The basal planes tend to rotate about the hexagonal axis so that the slip direction may come into coincidence with the direction of maximum shear with the result that the cross section widens and becomes eccentric. At the ends of the

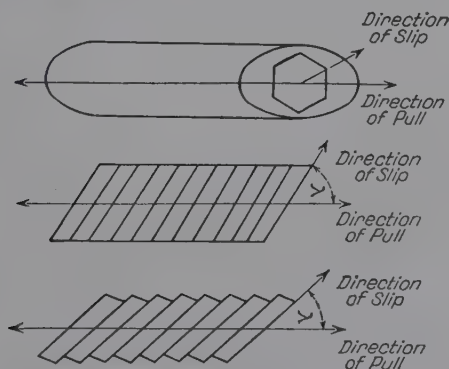


FIG. 263.—Mechanism of deformation of zinc.

specimen held in grips this behavior disappears; it is also clear that at a transition zone between grip ends in initial condition and the plastically extended center section the basal planes must be bent through a very considerable angle.

In this whole process, complete correlations have been made with the stress-strain diagrams, for as soon as slip begins the resistance to further slip increases. After the crystal wire has elongated to a thin elliptical ribbon during primary elongation, it may deform locally in a new place by marked constriction of the ribbon in the direction of the major axis. This results in formation of a fine "after-elongation" cylindrical thread, representing extension of several hundred per cent and a fifty-fold strengthening. Matthewson and Phillips proved that twinning about a pyramidal plane (1012) brings the basal planes into position for slip again.

In face-centered cubic metals the (111) planes are most densely packed, and upon these slip occurs. There are four equivalent sets, each with 3 directions along which slip can take place, or 12 directions of slip in all. This starts on one set first, causing rotation of the lattice in order to line up slip planes and directions with the crystal axis or the direction of pull. But this brings another set of the (111) planes into position for slip, with the result that the crystal necks down locally to a chisel-edge fracture.

The body-centered cubic metals such as tungsten, molybdenum, and chromium have low ductility as might be predicted from their structural geometry. The (110) planes and [111] direction are most densely packed, but the usual predictions on slip are not fulfilled for the plane of slip since this may be (112) or some other plane. Iron is a general exception in this group, but in spite of extensive study the mechanism of deformation is not well understood. This important metal is characterized by curved or wavy slip bands which render identification of the slip planes exceedingly difficult. Thus (110), (112), and (123) singly or in pairs have been reported, with probably best evidence for the last-named. Barrett has shown very recently that a special type of fragmentation results in the formation of deformation bands. The lattice within a band rotates away from the parent orientation and to a position with the [110] direction parallel to the axis but with the bands curved.

The foregoing descriptions apply to the gross features of deformation and fabrication of metals, many of which are visible. Attendant upon these are certain microchanges detected usually only by the x-ray pattern as a distortion, the evidences of which (primarily asterism on Laue patterns) have been considered on page 512. By following the changes of individual spots of a Laue pattern it is found that slip in one direction produces a greater change in the lattice in that direction than in other directions. As in bending a mica plate, the metal lattice becomes bent about an axis that lies in the slip plane and at right angles to the direction of slip. Actually the lattice is acting in "blocks" or "fragments," based upon many observations of "terraced" surfaces after deformation; but these are curved, the thickness and degree of curvature being consistent with any observed change in spacings for interferences on patterns. This is Polanyi's concept of "flexural slip" (*Biegeleitung*) which in its

main features still gives the best explanation of the x-ray evidences of distortion. Thus, though there is a remarkable preservation of crystalline structure even in most severe deformations, there is a modification such that motions along slip planes must occur in approximately whole numbers of unit lattice distances and such that the planes are no longer "smooth." From this has arisen in its various aspects the slip-interference theory to account for strengthening and hardening of metals during cold working (see page 406).

Typical changes in x-ray diffraction patterns of aluminum crystals subjected to tensile deformation are illustrated in the work of Clark and Beckwith.¹ Figure 264 shows the device for applying tensile stress to thin sheet specimens in position on the diffraction apparatus; Fig. 265 shows selected patterns for the behavior of a single crystal under increasing loads; Fig. 266 shows the effect of stress on a combination of a single large crystal and many small ones; and Fig. 267 the characteristic behavior for a uniform polycrystalline sample. Fragmentation as indicated by the gradual emergence of smooth Debye-Scherrer rings from a pattern of spots at random with increasing stress is particularly striking. Rotation of these fragments with still greater stress results in preferred orientation indicated by localized intensity maxima on the rings.

12. Preferred Orientations, in Electrodeposited Metal Sheets. In the preceding sections the production of a directed crystal orientation by means of mechanical work has been considered in

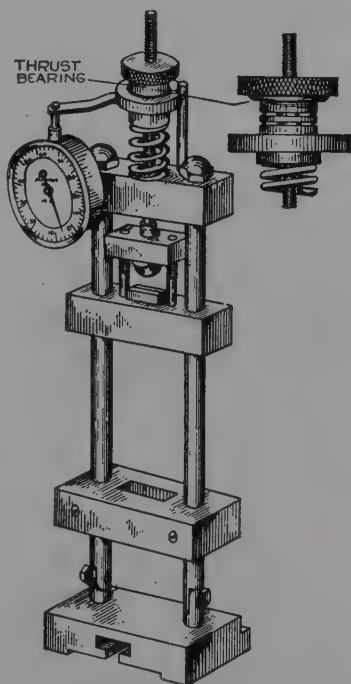


FIG. 264.—Device for applying tensile stress to thin sheet specimens while they are being subjected to x-ray diffraction analysis.

¹ *Trans. Am. Soc. Metals*, December, 1937, p. 1207.

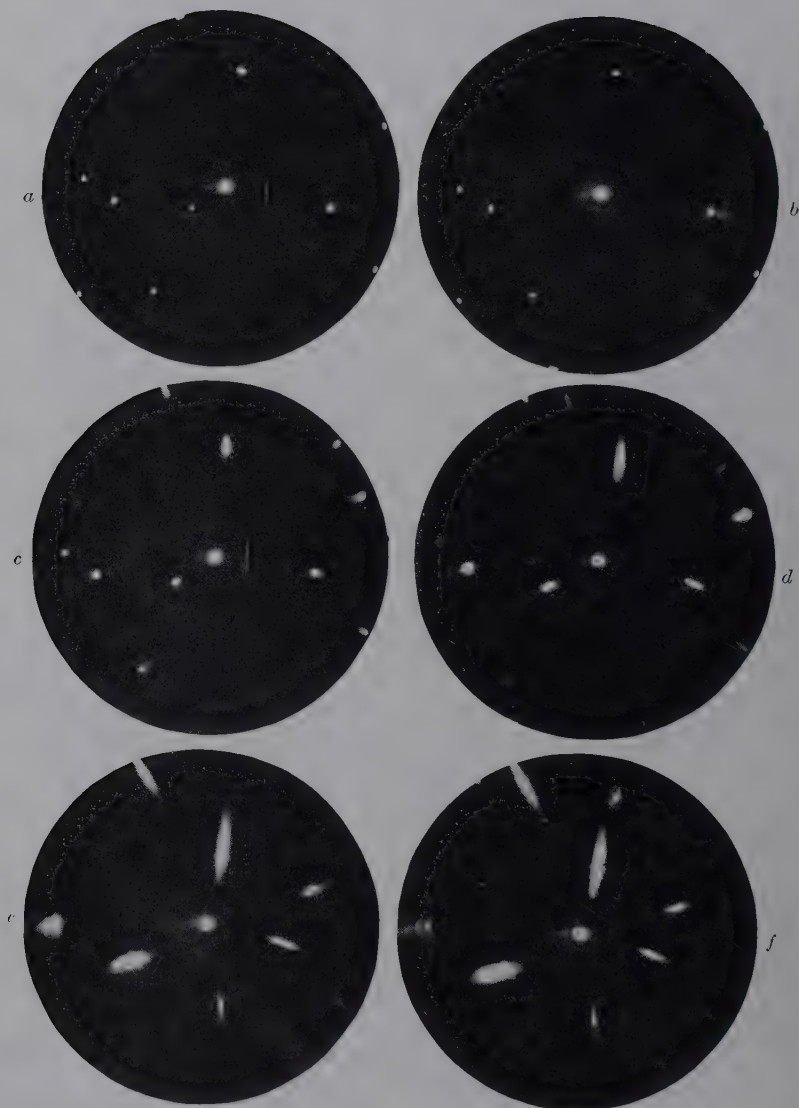


FIG. 265.—Patterns for single aluminum crystal under increasing stress in apparatus shown in Fig. 264.

| Pattern | Stress, lb. per sq. in. | Elongation, per cent |
|----------|----------------------------|-------------------------|
| <i>a</i> | 0 | 0 |
| <i>b</i> | 3,000 | 0.8 |
| <i>c</i> | 6,000 | 2.67 |
| <i>d</i> | 9,000 | 7.5 |
| <i>e</i> | 12,000 | 25.0 |
| <i>f</i> | After fracture | — |

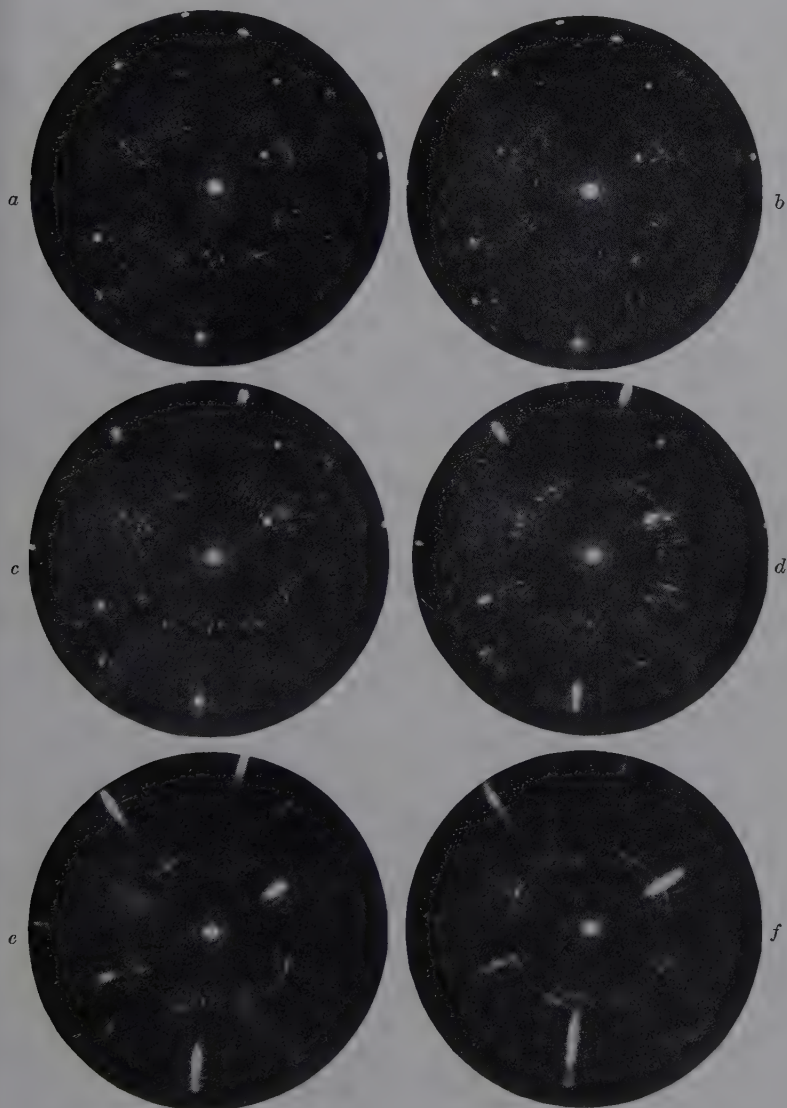


FIG. 266.—Patterns for aluminum sheet specimen consisting of one large single crystal and several small ones, subjected to increasing tensile stress.

| Pattern | Stress, lb. per sq. in. | Elongation, per cent |
|----------|----------------------------|-------------------------|
| <i>a</i> | 0 | 0 |
| <i>b</i> | 2,000 | 0.5 |
| <i>c</i> | 4,000 | 1.5 |
| <i>d</i> | 6,000 | 3.3 |
| <i>e</i> | 8,000 | 6.5 |
| <i>f</i> | 10,000 | 14.3 |

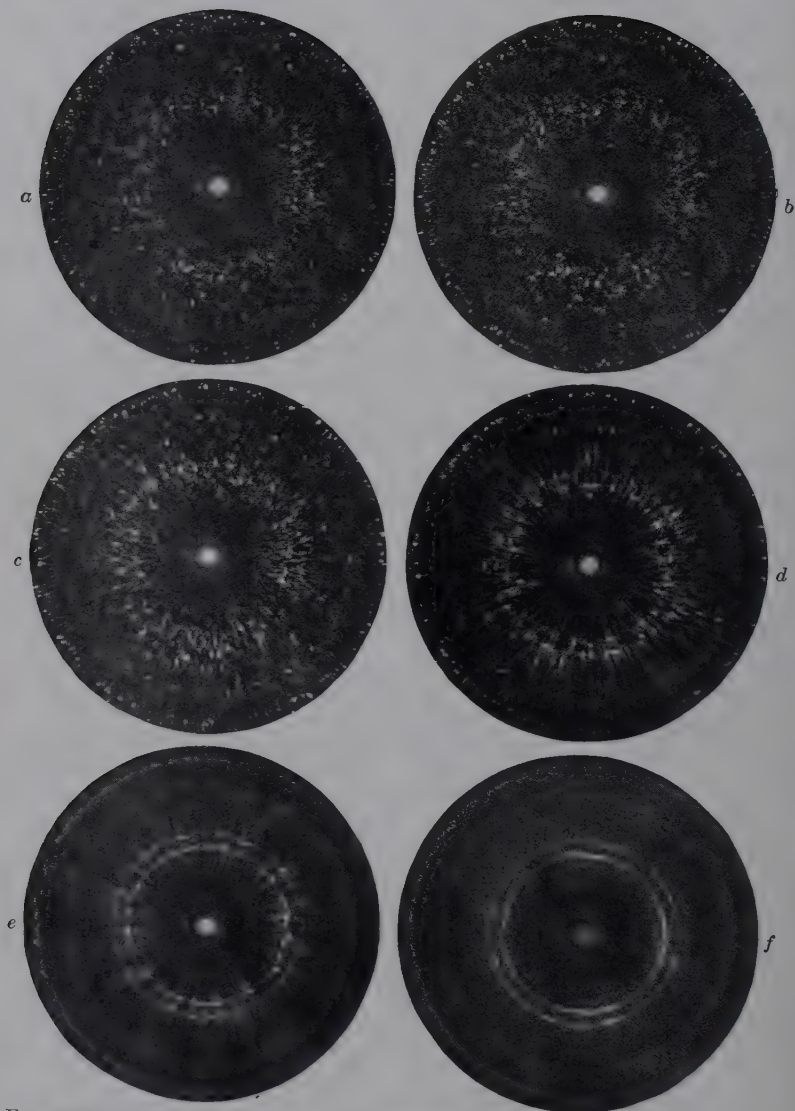


FIG. 267.—Patterns for aluminum sheet specimen with uniform small grains subjected to increasing tensile stress.

| Pattern | Stress, lb. per sq. in. | Elongation, per cent |
|---------|----------------------------|-------------------------|
| a | 0 | 0 |
| b | 3,000 | 0.5 |
| c | 6,000 | 1.0 |
| d | 9,000 | 3.2 |
| e | 12,000 | 10.0 |
| f | After fracture | — |

detail. The question naturally arises of whether or not crystals may actually *grow* in such a way as to have a common crystallographic direction parallel to the axis of growth. Experiment proves that electrodeposited metal films show a fiber structure similar to that of drawn metals and that the grains grow out parallel to the stream lines of the current or perpendicular to the surface of the electrode. The interpretation of the fiber patterns leading to an evaluation of the indices of the fiber axes proceeds exactly as outlined for wires. Of course, the fiber axis is parallel to the cross section or thinnest dimension of the deposited sheet. If, then, an x-ray beam impinged at right angles upon the surface of such a sheet, it would pass parallel to the fiber axis. As demonstrated for wires, the pattern is always indicative of ran-



FIG. 268.—Theoretical patterns for bright nickel electrodeposited films with various assumed crystallographic directions parallel to the fibering direction; $\beta = 82$ deg.; D (distance from specimen to plate), 1.5 cm.

dom orientation, since the crystal units may be oriented anywhere through 360 deg. around the fiber axis. It is necessary, therefore, to have films thick enough to pass the beam perpendicular to the fiber axis or to use the method of inclining the fiber axis at an oblique angle β to the primary beam. Bozorth¹ has published curves for graphical analysis of patterns so obtained with the formula

$$\cos \delta = \frac{\cos \alpha - \cos \beta \sin \Theta}{\sin \beta \cos \Theta}.$$

Figure 268 shows theoretical patterns for bright nickel deposits at $\beta = 82$ deg. all of which have been found, depending on variables of deposition. Many excellent papers have been published on detailed studies involving effects of electrolytes, current density, temperature, concentration, stirring, orientation as a function of thickness, effect of base electrode metal, recrystallization, presence of small amounts of addition agents, pH, electrode potential, etc.

¹ *Phys. Rev.*, **26**, 310 (1925).

| Element | Lattice | Solution | Current density, amperes per square centimeter | Fiber axis | Observer |
|---------------|----------|---|--|--|---------------------------|
| Silver..... | F. C. C. | Cyanide | 0.007 | Random | Glocker and Kaupp |
| Silver..... | F. C. C. | 0.1 <i>N</i> AgNO ₃ | 0.010 | [111], [001] | Glocker and Kaupp |
| Silver..... | F. C. C. | 0.1 <i>N</i> AgNO ₃ | 0.022 | Random | Glocker and Kaupp |
| Copper..... | F. C. C. | 0.1 <i>N</i> CuSO ₄ | 0.03 | [011] | Glocker and Kaupp |
| Nickel..... | F. C. C. | $\left\{ \begin{array}{l} \text{Ni(NH}_4\text{)}_4\text{SO}_4 \text{ or} \\ 0.1 \text{ } N \text{ NiCl}_2 + \\ 0.9 \text{ } N \text{ NiSO}_4 \end{array} \right.$ | 0.005 | [001] | Bozorth |
| Nickel..... | F. C. C. | NiSO ₄ + boric acid | 0.10 | [001] [011] (on underlying copper) | Clark and Frolich |
| Nickel..... | F. C. C. | 0.9 <i>N</i> NiCl ₂ + 0.1 <i>N</i> NiSO ₄ | 0.005 | [211] | Bozorth |
| Lead..... | F. C. C. | Pb(ClO ₄) ₂ or fluosilicate | 1.0 | [211] | Clark, Frolich, and Aborn |
| Chromium..... | B. C. C. | Grube | | [111] | Glocker and Kaupp |
| Iron..... | B. C. C. | 10 per cent Fe(NH ₄) ₄ SO ₄ | 0.001 | [111] | Glocker and Kaupp |
| Iron..... | B. C. C. | 10 per cent Fe(NH ₄) ₄ SO ₄ | 0.015 | Random | Glocker and Kaupp |
| Iron..... | B. C. C. | 50 per cent FeCl ₂ | 0.001 | [111] | Glocker and Kaupp |
| Iron..... | B. C. C. | 50 per cent FeCl ₂ at 100° C. | 0.1 | Random | Glocker and Kaupp |
| Iron..... | B. C. C. | Same + CaCl ₂ | 0.1 | [112] | Glocker and Kaupp |
| Tin..... | B. C. T. | | | [111] | |

13. Deposition of a Metal from Solution by Displacement.—

Metallic silver deposited from a solution of silver nitrate by introducing a small piece of copper has a fibrous structure with the axis [110] which makes an angle of 30 deg. with the direction of growth. The microcrystals show a rotation around this axis with an angle of ± 11 deg. As the (111) planes of the silver crystals lie parallel to the flat surfaces of the deposited metal, the direction of growth of the deposited silver lies nearly parallel to the [112] axis.¹

¹ TSUBOI, *Kyoto Coll. Sci. Memoirs*, **11**, 271 (1928).

14. Properties of Mirrors and Sputtered Films.—Very thin films of metals have been frequently studied. Foils of platinum, nickel, and copper 7 to 18 microns thick produced by cathodic sputtering and thermal evaporation show a structure. The support upon which the film is deposited and the presence of gas have a profound effect upon the crystal arrangement.

15. Growth Texture of Castings.—Superficial observation alone discloses the regularity of grain orientations and directions of growth in castings. In both body-centered and face-centered cubic metals the orientation is such that (100) planes lie parallel to the long axis of the crystal grain. In white tin (110), in the hexagonal close-packed metals (magnesium, zinc, cadmium) ($10\bar{1}0$), with (0001) perpendicular, and in bismuth (111) planes lie parallel to this direction. It is obvious that these preferred arrangements in commercial metal castings are of great significance in determining the possibility of machining operations and the tensile strength. For example, a zinc casting with radially arranged dendritic crystal grains has a modulus of elasticity of 800 kg. per square millimeter and a coefficient of expansion of 38×10^{-6} ; if the crystallization is controlled so that the orientation is parallel to the long dimension of the casting, the modulus of elasticity is 12,000 kg. per square millimeter and the coefficient of expansion is 14×10^{-6} . On the other hand, with the basal planes (cleavage) parallel to the long axis of the crystallites, profound splitting may ensue during rolling of the billet. It is possible therefore by means of x-ray analysis of structures of specimens cut in a certain way from castings prepared by a given technique to ascertain what crystallographic directions correspond to the dimensions of the unit.

CHAPTER XXII

PRACTICAL APPLICATIONS OF X-RAY DIFFRACTION TO PROBLEMS OF THE METALLURGICAL INDUSTRY

In preceding chapters the fundamentals of x-ray metallography have been outlined. The interpretation of diffraction patterns has been presented in terms of the characteristic crystal structures of pure metals and alloys and in terms of important technical properties such as grain size, internal strain, and effects of mechanical deformation. The immediate practical industrial significance of these fundamental facts has been pointed out in part, and other applications are obvious to anyone acquainted with metallurgical problems. It is now the purpose to enumerate briefly some of the actual problems of practical metallurgy, aside from the structure and constitution of alloys, and to illustrate some of the results of approach to these problems by the x-ray method. This list is merely one selected somewhat at random and is in no sense a complete record of achievement. Most of the examples have been selected from among the investigations in the writer's own laboratory.

In general, the x-ray method has been called upon to decide upon the proper method of manufacturing technique, to ensure constant properties, and to make a fundamental distinction between metal or alloy commodities with satisfactory and unsatisfactory behavior. For commercial metals the scientific methods of interpretation derived for pure materials as presented in preceding chapters are applied, although every new metal specimen is a new subject for research in itself. Gradually, metallurgical industry is coming to the realization, on the one hand, that there is nothing mysterious in x-rays or magic in the searchings of ultimate structures and, on the other hand, that these rays are not a panacea for all troubles unsolvable by other methods even though a brilliant record of achievement is already written. X-rays allow the observation of the interior of solid objects for gross inhomogeneities, and they extend the scope of

fine-structure analysis far beyond the microscope down to the ultimate architectural pattern of atoms in space. Without undue enthusiasm it may be stated as a fact that the contributions of x-ray research to metallurgical science *over so few years* surpass the record of all other experimental methods. The growing interest and confidence in a great research tool are demonstrated by the number of experimental installations in the research laboratories of metallurgical manufacturers and universities.

1. The X-ray Analysis and Control of Heat-treatment and Recrystallization of Cold-worked Metals. *The Province of Heat-treatment.*—When metals are worked by rolling or drawing, they become fibered. In other words, aggregates in which the crystal grains have random orientation assume in the process of mechanical deformation a structure in which the grains assume a definite orientation with respect to a common direction—that of rolling or drawing. The analysis of the mechanism from x-ray patterns is given in the preceding chapter. These sheets or wires are now characterized by strongly directional properties, and it is the province of heat-treatment in general to cause a recrystallization of the grains while retaining the form of the sheet or wire, so that a random nondirectional orientation is again obtained as is absolutely required, for example, in forming steels. Again internal strains introduced by rapid chilling in castings, etc., are relieved by heat-treatment. The x-ray method finds powerful practical use in discovering just how completely the fiber structure or the internal strain has been removed. In its sensitiveness as such a control method it far transcends the microscopic or other physical tests.

It is the purpose of the present section to consider in a more quantitative manner the mechanism of recrystallization during heat-treatment of single relatively pure metals, principally aluminum, silver, and copper. The information that has been derived from x-ray researches, chiefly by Glocker, Kaupp, and Widmann,¹ on these metals is astonishing in its scope.

Heat-treatment of Cold-rolled Foils.—There are three possible effects of heat-treatment of cold-rolled foils: (1) The directed orientation of grains is completely lost, and the new grains are

¹ *Z. Physik*, **45**, 200 (1927); *Z. Metallkunde*, **17**, 354 (1924); GLOCKER, "Materialprüfung mit Röntgenstrahlen," p. 332, Berlin, 1927.

in random arrangement from the outset of recrystallization. (2) Between the states of fiber structure and final random arrangement there is an intermediate step consisting of a directed arrangement different from that produced in rolling, which goes over into the random type of temperatures in the neighborhood of the melting point. (3) The new recrystallization or intermediate directed orientation persists to the melting point.

a. Recrystallization of Aluminum Sheet.—At all degrees of rolling, even up to 98 per cent reduction, aluminum recrystallizes with a random orientation of grains. Heating for 15 min.

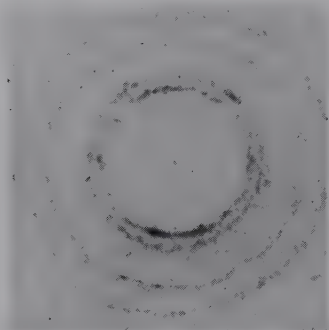


FIG. 269.—Pattern for cold-rolled aluminum foil after annealing, showing recrystallization in random arrangement.

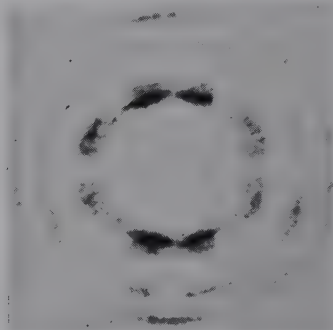


FIG. 270.—Pattern for cold-rolled silver foil after annealing at 225 to 750°C., showing recrystallization in new preferred orientation.

at 265°C. does not destroy the fiber pattern of the rolled sheet (Fig. 240), but at 275°C., or above, this is lost. The pattern consists now of concentric rings with a spotted appearance indicative of a random arrangement of larger grains (Fig. 269). This is the type of structure that might be generally expected, and for all the metals with degrees of rolling below 90 per cent reduction, including silver and copper, this is observed. Aluminum thus represents the first of the possible effects of heat-treatment.

b. The Recrystallization of Silver.—Glocker was the first to observe that with strongly rolled silver (97 per cent) the recrystallization did not take place with chaotic arrangement of grains, but with a new crystallographic orientation (Fig. 270) with the (113) planes in the plane of rolling instead of the (110) planes as in the original rolled structure. This structure is maintained even after 10 days or more of heating at 300°C., but at higher tempera-

tures (rapidly at 850 to 900°C.) the random orientation results, together with a considerable increase in grain size. These facts illustrate the very important fact that long annealing at low temperatures does not necessarily produce the same effect as annealing for a short time at high temperatures, in spite of common belief and practice in metallurgical circles.

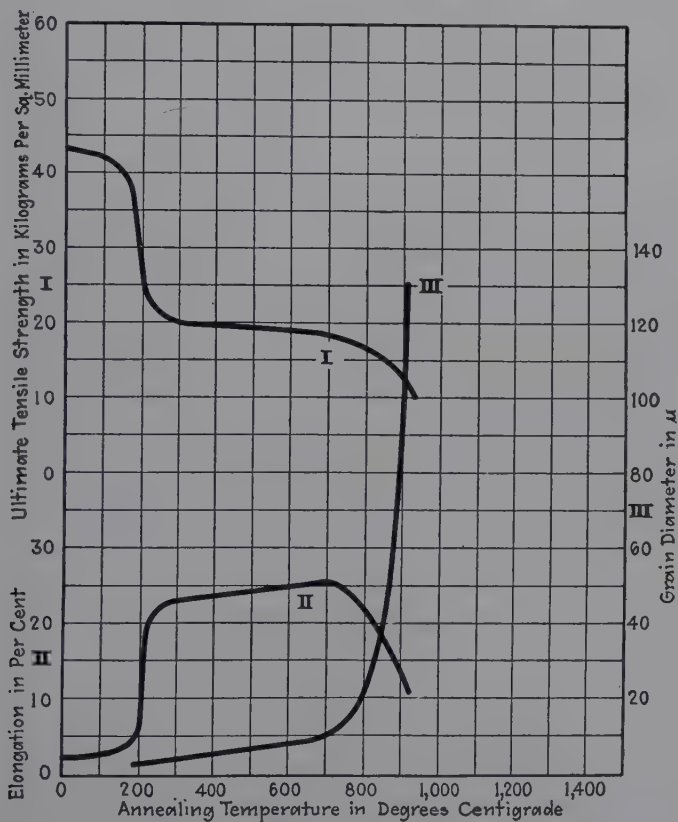


FIG. 271. —Tensile strength, elongation, and grain size of rolled sheet steel after annealing as functions of annealing temperature. (Glocker and Widmann.)

The sequence of events during recrystallization as interpreted from the x-ray patterns may also be tested and compared with the results of technological tests on tensile strength, elasticity, and grain size. Widmann's data as plotted in Fig. 271 show distinctly the breaks occurring with the appearance of the new directed position at 200°C. and with random orientation at 800°C.

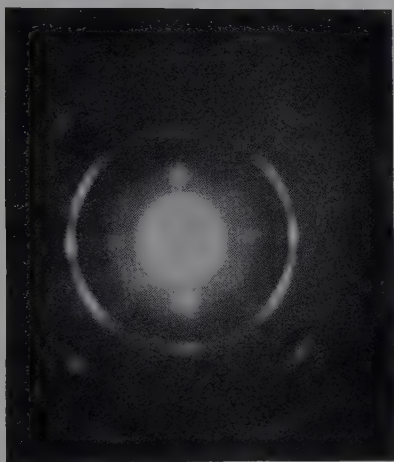
The very curious fact also was found that if the silver is reduced only partially in one rolling operation, is heated at 700°C., and is again rolled down to final thickness, then the properties are distinctly different from those of the silver reduced in one rolling only. In the former case the x-ray patterns indicated that the sheet begins to recrystallize at room temperature. Consequently annealing produces abnormally large grains and loss of tensile strength, the metal is characterized by mixed, very large and very small grains, and is difficult to handle practically.

c. Impurities Change Recrystallization Temperature.—The effects of small amounts of impurities on the recrystallization temperature of silver may be determined far more accurately from the x-ray patterns than from microscopic analysis. Widmann's studies of this subject have been fully substantiated by the present writer. In the following table are listed the data on the effects of impurities.

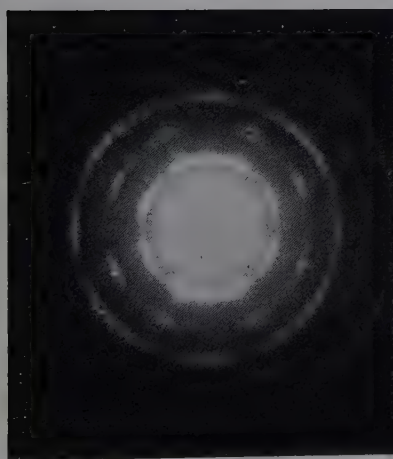
| Element | Impurity | | Recrystallization temperature, degrees Centigrade |
|------------------|------------------|------------------|---|
| | Weight, per cent | Atomic, per cent | |
| Pure silver..... | | | 150 |
| Copper..... | 0.303 | 0.51 | 230 |
| Copper..... | 0.12 | 0.20 | 200 |
| Copper..... | 0.073 | 0.123 | 175 |
| Aluminum..... | 0.2 | 0.93 | 190 |
| Zinc..... | 0.119 | 0.195 | 145 |
| Lead..... | 0.059 | 0.03 | 145 |
| Nickel..... | 0.1 | 0.15 | 137 |
| Gold..... | 0.1 | 0.054 | 112 |
| Gold..... | 0.2 | 0.11 | 110 |
| Palladium..... | 0.1 | 0.10 | 112 |
| Iron..... | 0.035 | 0.068 | 110 |
| Iron..... | 0.055 | 0.107 | 20 |
| Iron..... | 0.065 | 0.126 | 20 |

It is clear that copper and aluminum raise the temperature, whereas all other elements, particularly iron, lower it. Five hundredths of 1 per cent of iron is sufficient to lower the temperature of recrystallization of silver to room temperature. Ancient as is the metallurgy of silver, this fact has been discovered

only recently by means of x-rays. It is safe to conclude that silver, except of the highest purity, always has contained at least this trace of iron. Why then has not recrystallization



(a)



(b)



(c)

FIG. 272.—Recrystallization of low-carbon steel shim stock. (a) Original rolled structure; (b) recrystallized in new preferred orientation; (c) heated above upper critical point to produce random arrangement of grains.

served to ruin, practically speaking, cold-rolled silver articles? The answer is that copper also is universally present and in amounts of 0.1 per cent or less completely compensates for the

powerful effect of 0.05 per cent iron. In the same way aluminum compensates for gold which also lowers the recrystallization temperature of silver. It is interesting to note, however, that the temperature of 150°C . for pure silver does not hold for the very purest silver (considerably less than 0.0005 per cent iron and 0.00002 per cent lead) possible to prepare. Very pure silver recrystallizes at room temperature. Copper has little effect on grain size and on the appearance of the intermediate directed orientations of silver; iron, nickel, and especially lead increase grain size, and zinc decreases it. The recrystallization positions of grain are not so perfectly directed in the presence of the

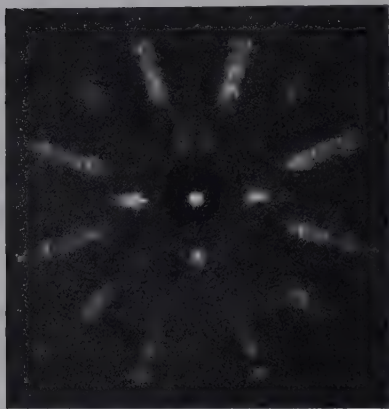


FIG. 273.—Pattern for recrystallized copper sheet showing very high degree of preferred orientation.

metals. Thus, for the first time is it possible to have a quantitative idea of the metallurgical importance of very small amounts of impurities. In every case addition of larger amounts has little or no effect as compared with the introduction of the first traces.

d. The Recrystallization of Iron.—Both brass and iron (body-centered cubic) behave somewhat similarly to silver when rolled and annealed. For iron rolled to a reduction in gage of 97 per cent and

heated above 600° there is an orientation so that the $[350]$ direction is parallel to the rolling plane, while the cold-rolled metal is characterized by a $[110]$ direction. Figure 272 shows a series of patterns for low-carbon steel subjected to various heat-treatments; of particular interest are the new recrystallization orientation and the fact that random orientation is obtained only after heating above the upper critical point. Silver, brass, and iron, therefore, represent the second of the three recrystallization mechanisms.

e. The Recrystallization of Copper.—When strongly rolled copper (99 per cent) is annealed, a new phenomenon is observed. The recrystallization structure shows a new orientation of grains with the cube faces parallel to the rolling plane. Copper of

ordinary purity, after complete reduction by cold rolling, tends to recrystallize with a chaotic arrangement of grains; but if a first reduction of 50 per cent is made with hot rolls at 600°C., followed by cold rolling, the cubic recrystallization arrangement is so nearly perfect that the x-ray diffraction pattern indicates practically a single crystal (Fig. 273). The further remarkable

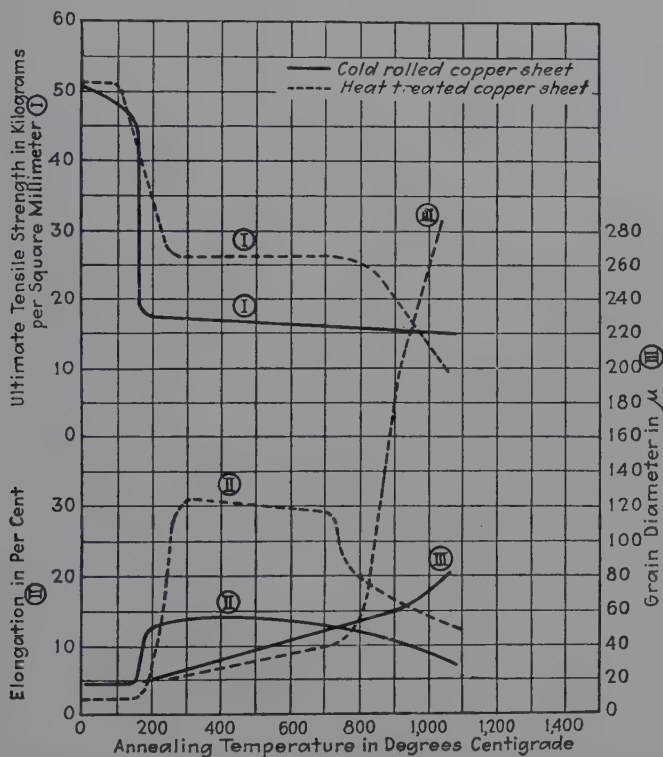


FIG. 274.—Tensile strength, elongation, and grain size of cold-rolled copper sheet (full lines) and of a sheet reduced 50 per cent by hot rolling and 50 per cent by cold rolling (dotted lines) as functions of annealing temperature. (Glocker and Widmann.)

fact is that this structure persists clear to the melting point. Not only does copper differ from silver (dependent, of course, on the method of rolling) in an entirely different recrystallization orientation, but also in the fact that this never goes over to the random structure. It follows, therefore, that such a sheet has greatly different properties from one in which the grains are in disordered arrangement.

A comparison of the tensile strength, elasticities, and grain sizes of the two kinds of copper sheet is given in Fig. 274. Both the strength and elasticity of the sheet with cube-face (oriented) grains are smaller than those of the random sheet. Czochralski has found that these properties are minimum in the direction of the cube edge, as is true here, whereas physical properties of the ordinary sheet are an average (higher) of all directions. The oriented sheet, however, is more resistant to corrosion than the random.

The effects of impurities as ascertained by Widmann from x-ray patterns are as shown in the accompanying table.

| Element | Impurity | | Recrystallization temperature, degrees Centigrade |
|---------------------------------|------------------|------------------|---|
| | Weight, per cent | Atomic, per cent | |
| Electrolytic copper, unmolten.. | | | 205 |
| Electrolytic copper, melted.... | | | 250 |
| Tin..... | 0.24 | 0.129 | 375 |
| Silver..... | 0.24 | 0.14 | 340 |
| Lead..... | 0.15 | 0.046 | 325 |
| Manganese..... | 0.23 | 0.267 | 320 |
| Phosphorus..... | 0.36 | 0.73 | 325 |
| Cadmium..... | 0.19 | 0.108 | 300 |
| Antimony..... | 0.06 | 0.032 | 280 |
| Sulphur..... | 0.21 | 0.42 | 275 |
| Arsenic..... | 0.14 | 0.119 | 250 |
| Nickel..... | 0.28 | 0.302 | 250 |
| Gold..... | 0.20 | 0.065 | 250 |
| Silicon..... | 0.06 | 0.13 | 245 |
| Zinc..... | 0.33 | 0.32 | 220 |
| Bismuth..... | 0.027 | 0.008 | 200 |
| Iron..... | 0.21 | 0.24 | 190 |
| Aluminum..... | 0.12 | 0.28 | 150 |
| Cuprous oxide..... | 18.0 | 8.33 | 150 |

f. The Recrystallization of Silver-copper Alloy.—In the light of the foregoing results with pure silver and copper, it is interesting to compare the x-ray results on sheets of an 80:20 silver-copper alloy.¹

¹ GLOCKER and WIDMANN, *Z. Metallkunde*, **20**, 129 (1928).

The tensile strength of a strip rolled down to 98 per cent reduction is 90 kg. per square millimeter as against 40 for silver and 50 for copper. After annealing at 800° the strength is only 30. Elongation of the alloy becomes noticeable only above 300°C. but approaches that of silver (20 per cent) after treatment at 800°C. Although the softening and recrystallization lies in a range of only about 20°, the range in the alloy lies between 200 and 700°C. Mixed crystals, embedded in the eutectic and richer in copper, are brought out when the specimen is heated nearly to the melting point. Even heating for hours at 780°C. shows only a few of these crystals because the grains are smaller than 2 microns; at 800°C. the grains are five times larger but show no preferred orientation. The first evidence of recrystallization in the x-ray photographs appears at 400°C., when some diffuse lines become sharply resolved into doublets. Unless the specimen is heated for hours above 780°C., x-rays give the typical diagram of rolled silver.

The Recrystallization of Wires.—The drawing of metals into wires represents also a fibering of the grains but with a different mechanism which is somewhat simpler as previously explained. For all face-centered cubic metals (silver, copper, aluminum, gold, lead, etc.) a [111] direction, or cube body diagonal, is parallel to the wire axis with every possible orientation of the cubes (360 deg.) around the diagonal; for body-centered cubic metals (α -iron, molybdenum, tungsten, etc.) a [110] or cube-face diagonal is parallel to this axis. In general, there are no intermediate new orientations of grains during recrystallization by heat-treatment. Instead, the sharply localized intensity maxima in the diffraction patterns for the wires gradually become more indistinct with increasing temperature. The last traces of fibering are remarkably persistent, and an entirely random arrangement is attained only after annealing near the melting point.

| | Kilograms per Square Millimeter |
|------------------------------|------------------------------------|
| Original..... | 24.4 |
| 150°, $\frac{1}{2}$ hr..... | 18.7 |
| 200°, $\frac{1}{2}$ hr..... | 14.3 |
| 250° | 11.0 |
| 350° } $\frac{1}{2}$ hr..... | |
| 550° } | |

Sachs and Schiebold¹ have compared the x-ray diagrams and the tensile strength of a cold-drawn aluminum wire (1.18 mm.) after various annealing treatments. The treatments and tensile strengths are as shown on page 563.

The x-ray diagrams show a gradual increase in particle size with dots appearing on a continuous background of the diffraction rings at 250 and 300°C.; at 550°C. there appear large spots, far fewer in number but still lying on rings. At 150°C. the interference maxima broaden, indicating a departure of the oriented particles from perfect alignment, but even after annealing at 550°C. strong evidences of fiber structure remain.

An exception to the general effect of annealing, however, is observed with very pure aluminum wire.² It has been found that, on heating hard aluminum wire (0.35- or 0.8-mm. diameter, 99.95 per cent pure) at 600° for 3 hr., recrystallization occurs with perfect unidirectional orientation of the grains with a [111] direction parallel to the wire axis. This orientation is the same as in the original cold-drawn wire, so that aluminum differs from copper in this respect and, of course, from aluminum of lesser purity. The texture of the wire seems very nearly unchanged by the treatment, but the tensile strength has decreased from 20.6 kg. per square millimeter to 3.5, and the elongation has changed from 1 to 5 per cent (single crystal wires 20 per cent). Here it is clear that the grain orientation is not the only factor governing elastic properties.

For aluminum-silicon alloy wires, the strength decreases from 26.5 to 15.6 kg. per square millimeter after heat-treatment, the elongation increases from 2 to 17 per cent, but the grain orientation and texture indicated by the x-ray pattern are unchanged.

The single case of intermediate-recrystallization preferred orientation is with deeply drawn copper wire annealed above 1000°C.³

The new orientation is with a [112] direction, instead of [111] parallel to the wire axis. This observation is further substantiated by Tammann and Meyer who counted in a cross section the following orientations of faces: (111) 27 per cent, (101) 12 per cent, (100) 61 per cent, whereas theoretically for

¹ *Z. Metallkunde*, **17**, 400 (1925).

² SCHMID and WASSERMANN, *Z. tech. Physik*, **9**, 106 (1928).

³ SCHMID and WASSERMANN, *Z. Physik*, **40**, 451 (1926).

chaotic arrangement the proportions are, respectively, 38, 40, and 22 per cent. Such a wire acts as a single crystal as compared with ordinary wires with random orientation. Following are the comparative data:

| Treatment | Tensile strength, kilograms per square millimeter | Elasticity, per cent |
|------------------------------|---|-------------------------|
| Original..... | 49.3 | 1 |
| 300°..... | 24.4 | 30 |
| 800°..... | 23.9 | 23 |
| 1000° (3 hr., oriented)..... | 21.3 | 17 |

In general the x-ray study of wire annealing is not quite so satisfactory as that of rolled foils. Studies on crystalline wires of zinc and tin by Polanyi and his associates prove that often the change in mechanical properties and recrystallization evidence in x-ray patterns do not run parallel, since under certain conditions of original cold working and annealing these crystals may soften without evidence of recrystallization.

2. Annealing of Cast Steel.—Figure 275 shows the structures of cast steel as cast with large internal strain, of the steel annealed according to commercial practice, and of the same steel with an ideal structure obtained by the selection of correct temperature and time of heat-treatment through the agency of x-ray diffraction patterns. One of the manufacturers of castings was annealing large steel pieces for 6 hr. at a somewhat indefinite temperature. A short x-ray investigation proved beyond question that the correct temperature of annealing could be determined within $\pm 10^\circ$ and that under these conditions a greatly improved structure was obtained not in 6 hr. but in $\frac{1}{2}$ hr. The economic value of such a single discovery is at once evident in speeding production twelvefold without additional expense. Such examples in this general field of heat-treatment for the removal of strains and directional properties might be multiplied many times.

3. Magnetic Properties as a Function of the Structure of Silicon Electric Steels.—Figures 276*a* to *f* reproduce again the first series of pinhole diffraction patterns ever made for silicon steel strips with varying magnetic hysteresis loss as noted. If the

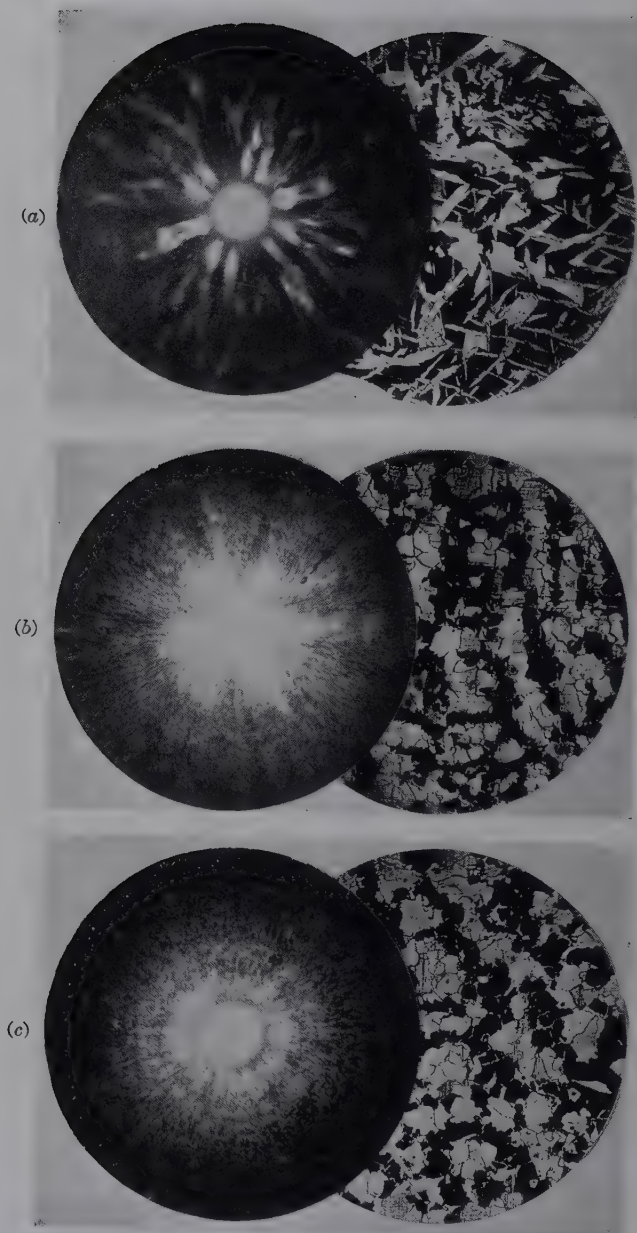


FIG. 275.—Diffraction and microscopic studies of annealing of cast steel. (a) Original structure, as cast, showing internal strain; (b) commercial anneal, showing incomplete removal of detrimental structure; (c) ideal annealed structure of same steel.

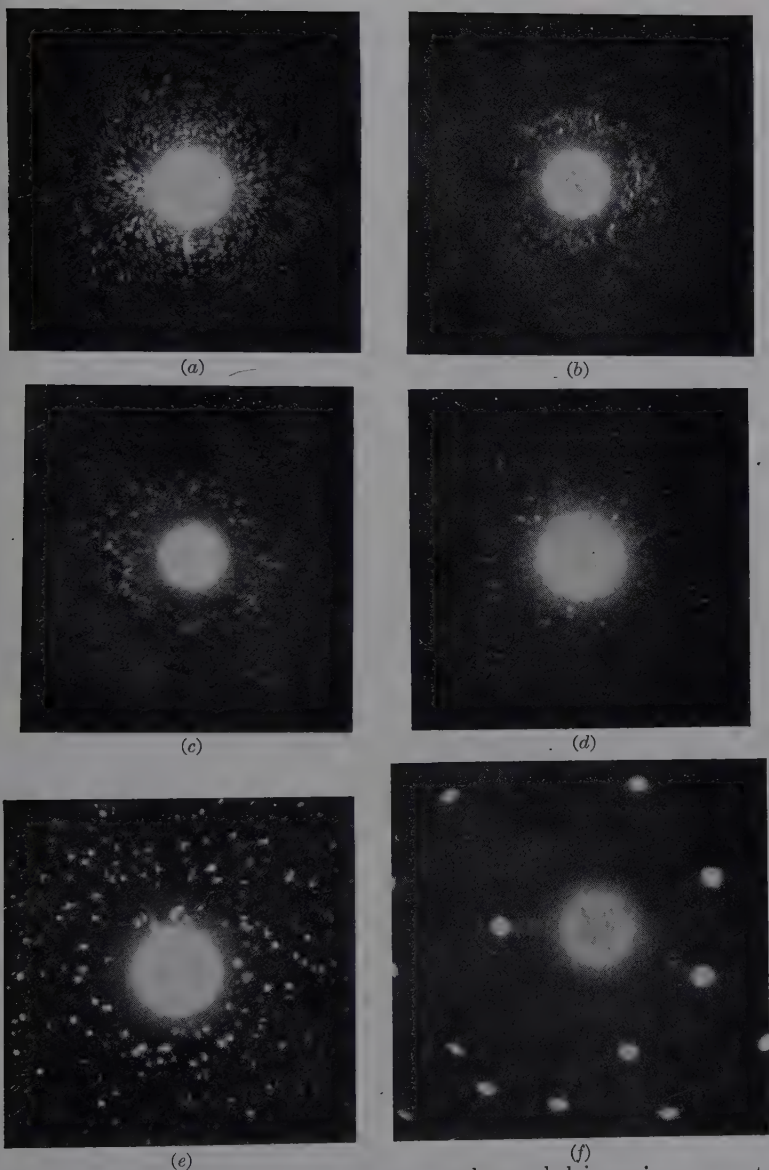


FIG. 276.—Patterns for silicon transformer steel annealed in various ways, to show effect of grain size on magnetic hysteresis loss:

| | Watts per Pound |
|----------|-------------------------|
| (a)..... | 0.8636 |
| (b)..... | 0.8181 |
| (c)..... | 0.8068 |
| (d)..... | 0.7727 |
| (e)..... | 0.6931 |
| (f)..... | 0.5535 (single crystal) |

grain boundaries have not been unduly thickened by overheating in the annealing furnace, the magnetic loss may be calculated empirically from the number and size of diffraction spots on a given area of the various patterns. Occasionally some strips may be unusually brittle and have unaccountably high loss. In every case an x-ray examination proves that the large single grains have an extraordinary orientation of crystallographic planes with respect to the surface of the sheet due to an uncontrolled factor in the rolling or annealing operation. In the ordinary case it will be remembered that iron grains in a rolled

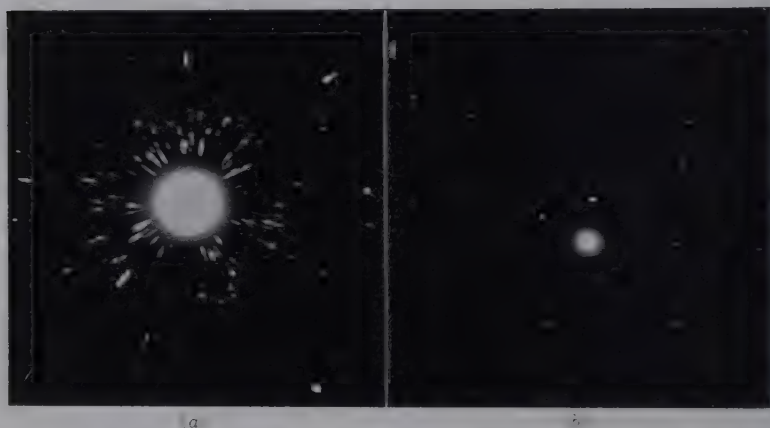


FIG. 277.—Comparison of grain perfection in silicon electric steel. (a) Supposedly superior grade as now produced commercially showing imperfect grains; (b) specimen free from strain produced by simple technique.

sheet are oriented with a $[110]$ direction parallel to the direction of rolling and (100) planes in the surface of the sheet. The Epstein test for measuring magnetic loss usually employs 100 or more strips, and an average value is, of course, measured. On several occasions in the writer's laboratory it has been possible by single patterns to separate a bundle into at least five groups, two with a lower loss, two with a higher, and one with the same average loss of the whole original bundle.

More important from the standpoint of magnetic properties than grain size is grain perfection, *i.e.*, freedom from all strain. This has been amply demonstrated in recent extensive experiments in the writer's laboratory. The x-ray pattern is the only guide to establishment of the correct rolling and heat-treatment

that will ensure grain perfection. Figure 277*a* shows the pattern of supposedly highest quality silicon steel commercially produced in 1932, while Fig. 277*b* shows the result of remarkably simple technique, derived with the help of x-ray control, from the same raw material. The magnetic properties of the latter as well as ductility are markedly superior; and scientific control of production is easily possible by regulation of the silicon content, percentage cold reduction, without intermediate anneal, time and temperature of annealing, extent of a further pinch pass, and final heat-treatment. New mills with small rolls allow cold rolling of the silicon steel successfully for the first time. Since silicon steels represent large-grained aggregates, the x-ray diffraction patterns are characterized by a random peppering of spots rather than definite rings. Hence it would appear to be impossible to discover by ordinary diffraction methods whether or not there is any tendency toward preferred orientation of these large grains throughout a sheet. Recourse is then had to the simple devices of slowly moving the specimen in its own plane across the pinhole by a suitable mechanical device during the exposure. The resultant pattern is an integration over a large number of grains instead of the few contained in only a certain area traversed by the x-ray beam in the stationary sample. If there is a preponderance of orientations in any one direction, a definite concentration of spots will appear, just as localized intensity maxima indicated preferred orientation on the interference rings for small-grained specimens. The indications are that some such preferred orientation may actually be beneficial for certain magnetic properties.

In 1935 Clark and Beckwith¹ derived a modulus from measurements on diffraction patterns of 4 per cent silicon steel to express residual distortion. Annealed strips, producing sharp Laue spots, were subjected to rolling reductions from 1 to 10 per cent, thus producing marked evidence of asterism, and then heat-treated at 700, 800, and 900°C. The modulus has the form $M = RQ/36$, where R is the average radial distance in millimeters of the spots from the center, 36 is the radius of the circle in millimeters in which spots are measured (or any other selected value), and Q is the average ratio of the longest to the shortest dimension

¹ *Z. Krist.*, **90**, 392 (1935).

of the Laue spots, measured by projecting the pattern on a screen, being larger the greater the distortion. Thus a specimen

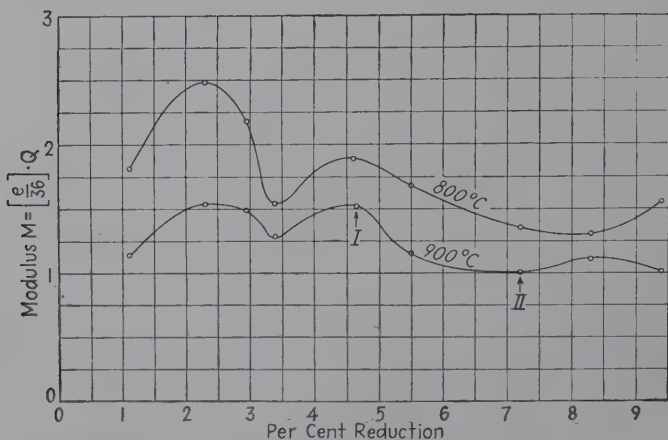


FIG. 278.—Relation between rolling reduction, annealing temperature, and residual distortion modulus for silicon steel.

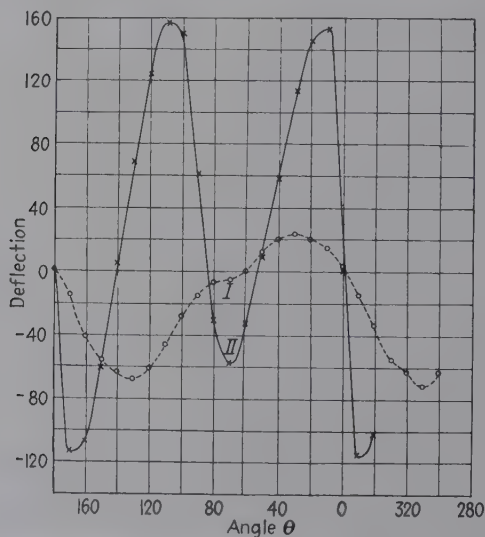


FIG. 279.—Magnetic curves for silicon-steel specimens with distortion moduli. 1.0 (II) and 1.89 (I).

reduced 7.20 per cent and annealed at 900°C. has $M = 1.0$ and perfectly sharp spots (Fig. 277a), while one reduced 2.30 per cent and annealed at 800° has $M = 2.48$ (Fig. 277b). Curves

relating reduction, annealing temperature, and residual distortion modulus are shown in Fig. 278; and the very large effect on magnetic properties is shown in Fig. 279 for specimens with

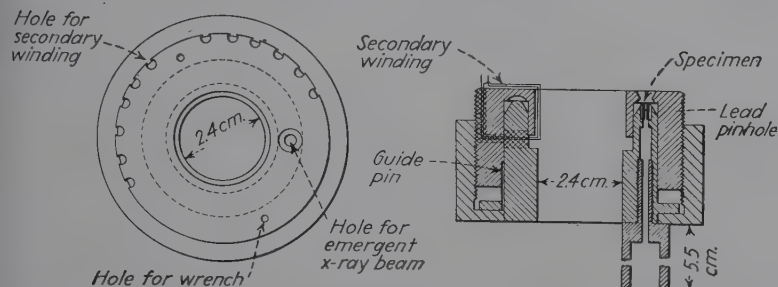


FIG. 280.—Apparatus for producing strains and for holding specimens during magnetic measurements and x-ray diffraction exposure.

moduli 1.0 and 1.89 (the best available commercial grade). A more quantitative correlation was made in 1937 by Clark and Dunn.¹

Flat rings cut from sheet silicon steel by grinding and etching were clamped between dies that bent them into cupped form to fit over a toroidal plunger. In the same apparatus shown in Fig. 280, the specimen is held and deformed, the diffraction pattern photographed, and, serving as the secondary winding, the circumferential magnetization measured by means of a specially constructed primary winding.²

As the bending strains increase, the permeability decreases. At light loads the deformation is elastic; after release the permeability is restored and the displacement of Laue spots shown in Fig. 281 also is reversible.



FIG. 281.—Pattern illustrating shift in positions of diffraction spots for unstressed silicon-steel specimen when subjected to slight deformation in apparatus shown in Fig. 280.

¹ *Phys. Rev.*, **52**, 1170 (1937).

² DUNN and CLARK, *op. cit.*, p. 1167.

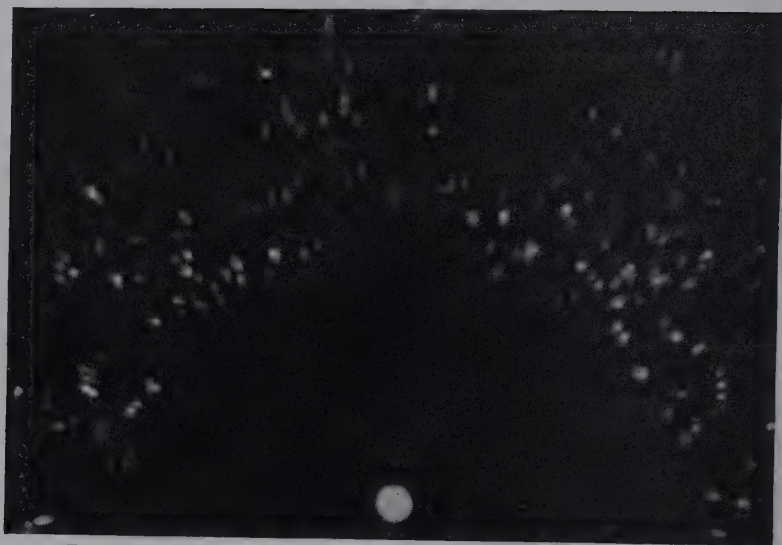


FIG. 282a. —Enlarged pattern for unstressed silicon-steel specimen.

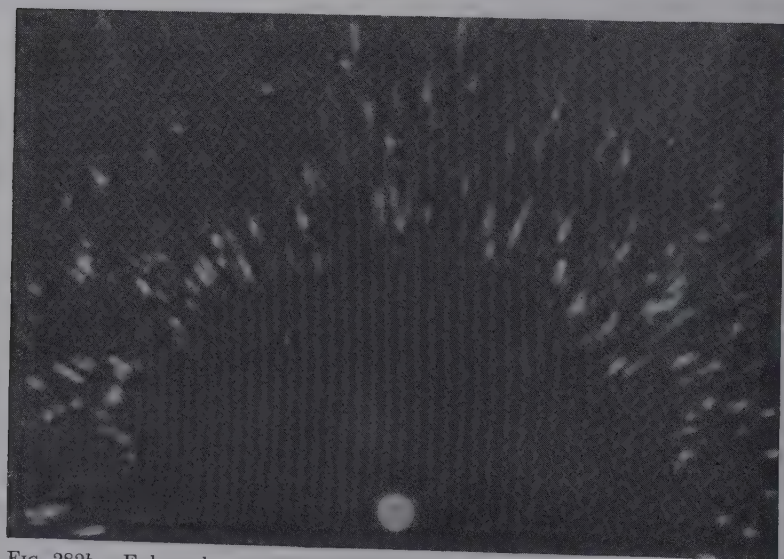


FIG. 282b. —Enlarged pattern through identically the same portion of specimen, highly strained.

After greater bending strain, there is only partial recovery to the initial state. Similarly the Laue spots are permanently displaced and distorted. Figures 282*a* and *b* show enlarged patterns for a specimen respectively unstressed and highly strained with 75.2 per cent drop in magnetic induction. The changes in the shape of Laue spots agree at all stages with bending of strained crystals about axes lying in the original plane of the sheet.

These studies have led to the commercial production of electric steel of superior quality. They illustrate convincingly the value of correlation of structures with fundamental physical, mechanical, and even chemical properties.

4. The Stages of Reduction and the Effects of Variables in Commercial Cold Rolling of Sheet Metals.—The fundamental investigations of the types and degrees of preferred orientation produced in metal sheets by cold rolling have been considered in the preceding chapter. However, the *course* of changes in crystal fragmentation and orientation during successive stages in the rolling process and the effect of variables in the raw material and in the technique of rolling upon the establishment of the ultimately attained preferred orientation are of greater commercial significance. Clark and Sisson made a long series of studies of these problems for various metals as follows:

1. Percentage reduction and its relation to various factors.
 - a.* Structure.
 - b.* Power requirements.
 - c.* Hardness.
 - d.* Amount of distortion as disclosed by the resolution of the x-ray $K\alpha$ doublet.
 - e.* Type and degree of orientation.
2. Effect of variables in original material on structures.
 - a.* Grain size.
 - b.* Thickness.
 - c.* Carbon content.
3. Effect of rolling variables upon structure.
 - a.* Roll diameter.
 - b.* Speed of deformation.
 - c.* Reversal of strip.
 - d.* Percentage reduction per pass.
4. Effect of deformation due to combined tension and compression.
 - a.* Applied tension during rolling.
 - b.* Effect of stretching followed by rolling.
 - c.* Drawing of flat sheets.
 - d.* Rolling of drawn wires.
 - e.* Rolling at various angles.

The scope of these data is obviously far too extensive to permit presentation of results here except for a few points of especial interest.

1. *Structural Changes with Successive Reductions.*—The change in x-ray patterns with successive reductions is best reported by Fig. 283a to g for low-carbon steel, selected from a series of 84 samples. Here the x-ray beam passed perpendicular to the rolling direction and to the surface of the sheet.

| Figure | Pass | Gage, inches | Percentage reduction | Pattern |
|-----------|------|-----------------------------|----------------------|---|
| 283a..... | 0 | 0.158 (hot-rolled strip) | 0 | Large random grains |
| b..... | 1 | 0.1475 | 7 | Fragmentation below 35μ and appearance of rings |
| c..... | 9 | 0.084 | 47 | Nearly complete fragmentation, random |
| d..... | 14 | 0.046 | 71 | Appearance of six-point fiber pattern characteristic of drawing |
| e..... | 19 | 0.023 | 85.5 | Passing from six- to four-point pattern |
| f..... | 21 | 0.0165 | 90 | Typical rolling pattern |
| g..... | 30 | 0.005 | 97 | Perfect orientation |

From a whole series of steel samples the following average results were obtained:

| Appearance of | Per Cent Reduction |
|---------------------------------------|--------------------|
| Continuous rings (fragmentation)..... | 27 |
| Sharp rings..... | 38 |
| Six-point fiber pattern..... | 54 |
| Four-point fiber pattern..... | 76 |

Such values, of course, are greatly dependent on type of mills, chemical composition, thickness, grain size, and orientation in the original material.

These results confirm those of Tammann who found that in rolling two clearly defined changes in crystal orientation can be distinguished: (1) that in which the force due to rotation of the rolls acts as a stretching force (six-point x-ray pattern); (2) that

in which the action of the rolls is similar to that of simple compression and exerts the greatest influence on the final orientation in cases of large reductions.

2. *Effect of Initial Grain Size.*—Grain size has considerable influence upon the structure of cold-rolled steel during early

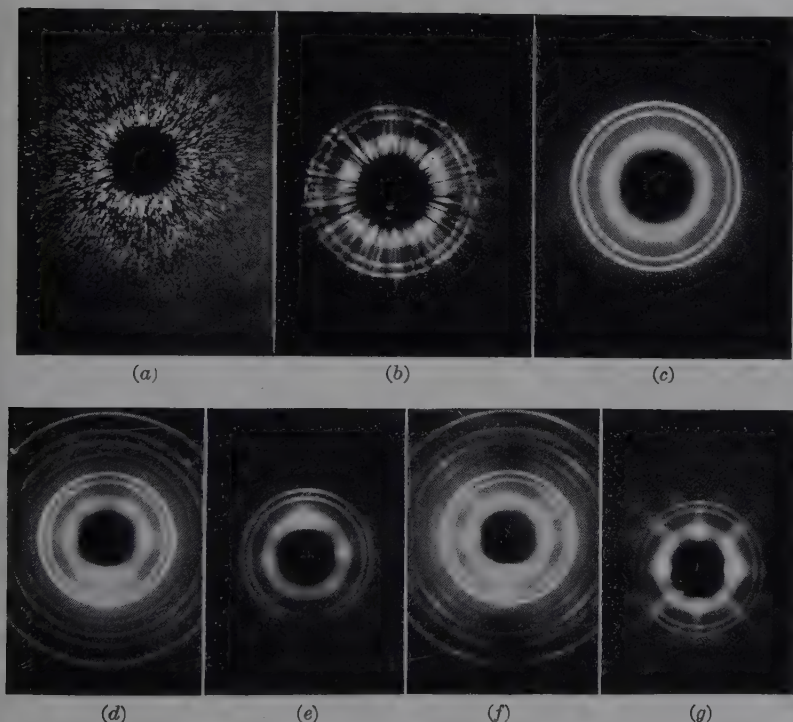


FIG. 283.—Changes in structure with steps in rolling of low-carbon sheet steel. (a) Hot-rolled strip; (b) one pass, 7 per cent reduction; (c) 9 passes, 47 per cent reduction; (d) 14 passes, 71 per cent reduction; (e) 19 passes, 85.5 per cent reduction; (f) 21 passes, 90 per cent reduction; (g) 30 passes, 97 per cent reduction.

stages of reduction, but after large reductions the effect is lost. The smaller the initial grain size, the less cold work is required to produce fibering (Fig. 284).

3. *Effect of Initial Strip Thickness.*—The degree of fibering depends not only on the percentage reduction but also on the initial strip thickness. A sample reduced from 0.08 to 0.01 in. does not show the same degree of preferred orientation as one

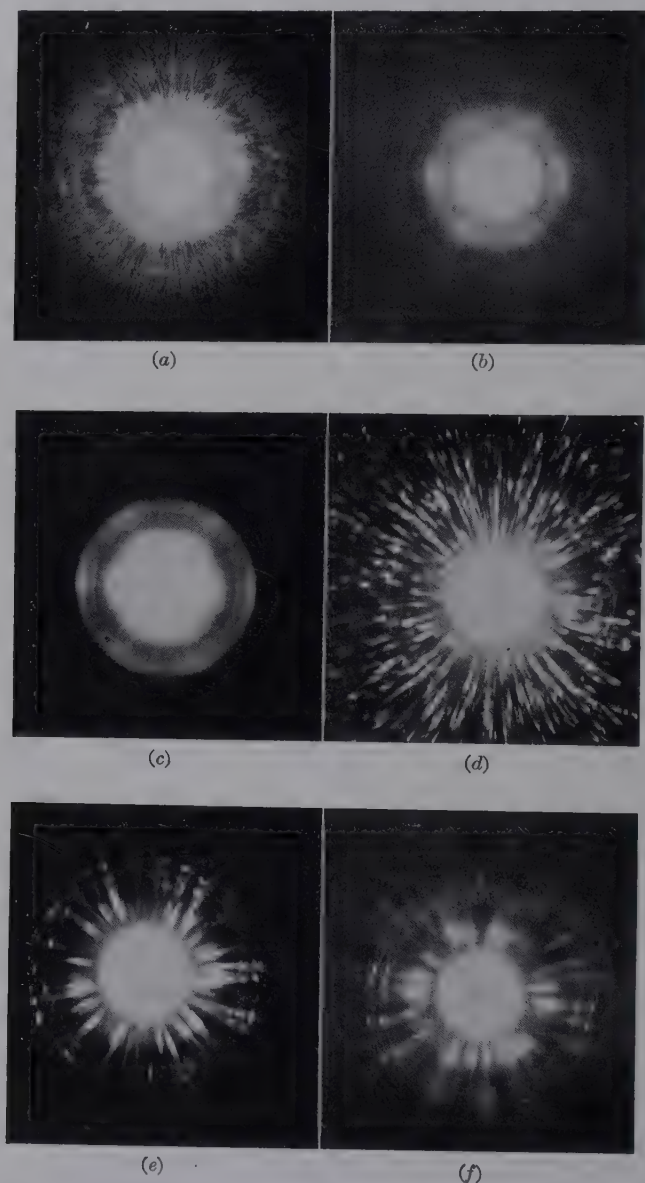


FIG. 284.—Comparison of effects of drawing reduction on steel with small and large initial grains. (a) Original (small grains); (b) after 5 per cent reduction; (c) after 15 per cent reduction; (d) original (large grains); (e) after 5 per cent reduction; (f) after 15 per cent reduction. Compare (a) and (d), (b) and (e), (c) and (f).

reduced from 0.04 to 0.005 in., although both have received 87.5 per cent reduction.

4. *Effect of Carbon Content.*—Most of the previous work on preferred orientation in cold-rolled sheets has been carried out on pure metals. In steels the pearlite is hard and more brittle than ferrite and concentrates at the junctions of the ferrite grains with the result that when pearlitic steel is cold-rolled gliding takes place only in the ferrite. During the rolling process the pearlite is dispersed while the soft ductile ferrite forms a plastic bond that is not oriented, so as to form a straight fiber structure, but is curved around the pearlite particles. The x-ray pattern, therefore, gives the appearance of random arrangement for high-carbon steels (Fig. 252).

5. *Effect of Rolling Variables.*—1. The roll diameter has less effect on final structure than the total percentage reduction. The smaller the rolls, the greater is the angular divergence of the grains laterally in the rolling plane from the ideal preferred direction, while large rolls tend to produce more divergence normal to the *rolling* plane. Numerous other small differences may also be quantitatively ascertained, particularly for early and intermediate stages of reduction.

2. With small rolls the same structure is obtained at speeds from 70 to 800 ft. per minute, and with unidirectional or reversed passes through the rolls.

3. Various combinations of tension and compression of the sheets have been studied in detail, both experimentally and with vector theory. Fiber structures are ultimately obtained, but the appearance of the four-point pattern characteristic of compression can be greatly delayed by application of tension.

4. Interesting results are obtained by rolling metals in all directions (random), at 90 deg. (very perfect fibering), 60 deg. (six-point instead of four-point patterns), etc.

5. An x-ray method of determining the amount of cold rolling to which a sheet has been subjected. By the usual method of taking x-ray diffraction patterns of cold-rolled sheets, the x-ray beam passes perpendicular to both the rolling direction and the plane of rolling. Preferred orientation may appear only after 60 to 70 per cent reduction, depending on the type of mill and original material variables. If the beam is made to pass through the material perpendicular to the rolling direction

and *parallel* to the rolling plane (edge on of the sheet), evidence of preferred orientation is obtained after 15 to 30 per cent reduc-

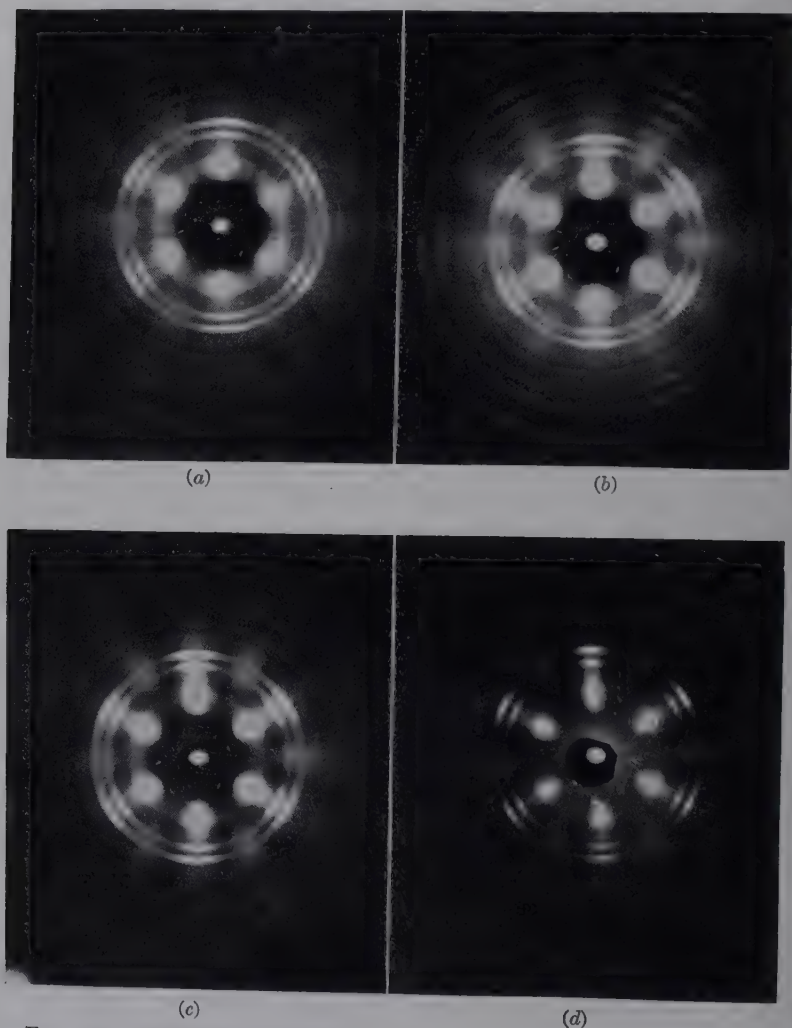


FIG. 285.—Patterns for sheet steel, made with x-ray beam perpendicular to rolling direction and parallel to rolling plane, from which amount of cold work may be calculated. Percentage reductions: (a) 16; (b) 36.5; (c) 53; (d) 85.

tion, depending upon the above-mentioned variables. This orientation gives a six-point fiber pattern similar to that for cold-drawn wires. Instead of the pattern changing to a fourfold

pattern upon further reduction as is the case when the beam is normal to the rolling plane, the type of pattern remains the same. However, as the percentage reduction increases, the intensity maxima become sharper, as illustrated in Fig. 285 for 16, 36.5, 53, and 85 per cent reduction. If the percentage reduction is plotted against the sine of the angle of arc formed by the intensity maxima on the broad inner band of the pattern, a straight line is obtained. For a large number of specimens this relationship has been found accurate within a maximum of 10 per cent.

In certain cases it has been possible even to determine very small amounts of cold work such as roller leveling after annealing,

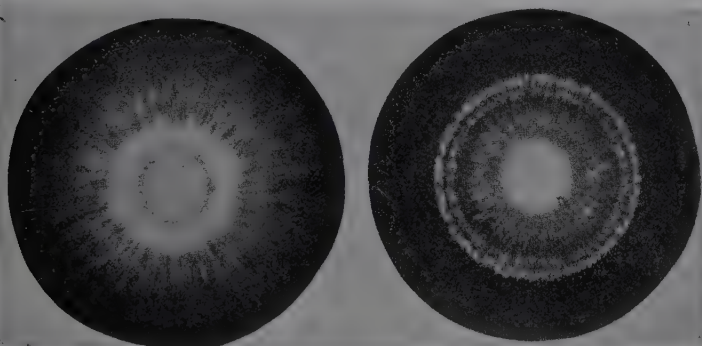


FIG. 286.—Patterns showing comparison of steel welds. Left, ordinary arc method; right, hydrogen-atmosphere method.

by careful examination of the x-ray patterns (elongation and splitting of interference spots).

5. Structure of Welds.—Figure 286 shows the comparison of a weld of the same steel made by the ordinary arc method and by the hydrogen-atmosphere method. The former is characterized by very small, highly distorted grains (radial striations) and the latter by much larger, random unstrained grains with requisite strength and ductility.

6. Forming Steels.—One of the great contributions has been to define specifications in terms of structure for forming steels, especially since unstrained and random properties are essential. Patterns and photomicrographs for supposedly four grades of forming steel, soft, quarter hard, half hard, and hard, demonstrate that there are only two grades essentially. Satisfactory

and unsatisfactory forming steels are easily differentiated by the patterns in Fig. 287. The latter retains a residual preferred orientation of grains introduced in the original rolling; hence the annealing has been entirely inadequate, and failure in the forming operation can be predicted definitely from such a pattern.

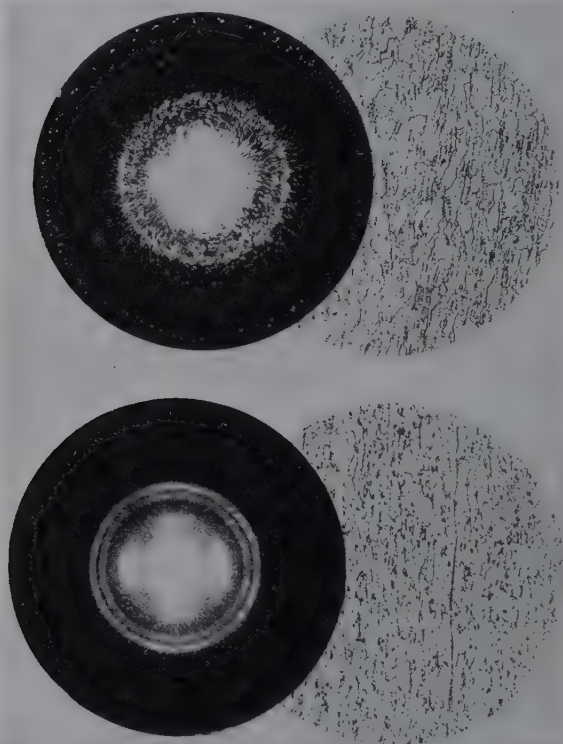


FIG. 287.—Diffraction patterns and photomicrographs for satisfactory (above) and unsatisfactory (below) forming steels. Note residual rolling structure in the latter.

Figure 288 demonstrates the structure of a sheet after successful forming and explains why another sheet failed.

7. Forming Copper.—Phillips and Edmunds have demonstrated that hard-rolled copper has a pronounced fiber structure with $[\bar{3}53]$ as the fiber axis, instead of $[112]$ as found by others, and (110) planes in the surface. A preferred orientation is found in the annealed sheet which forms ears on cupping, whereas

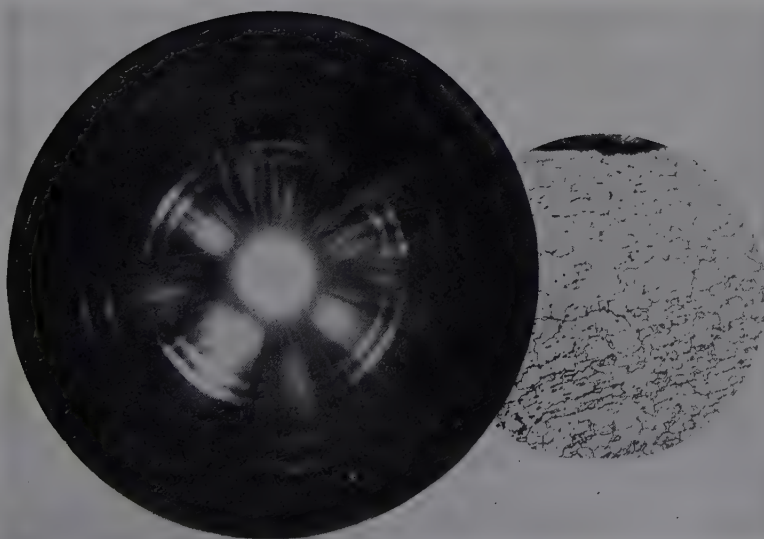
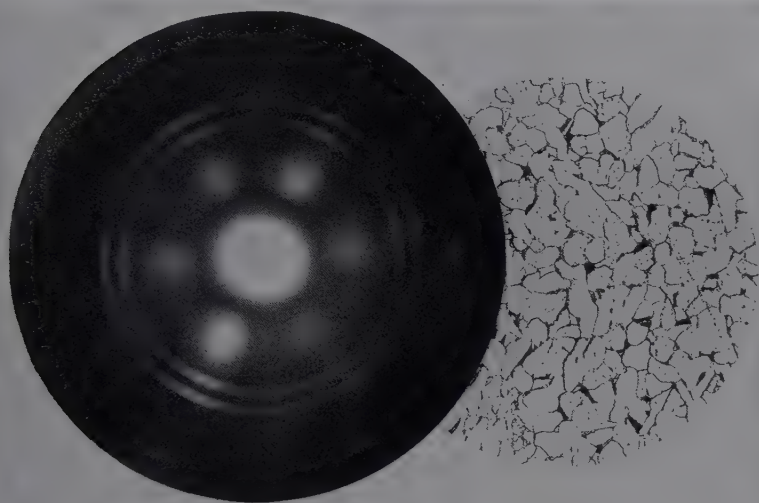
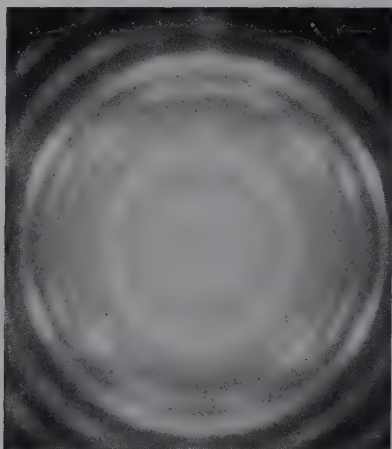
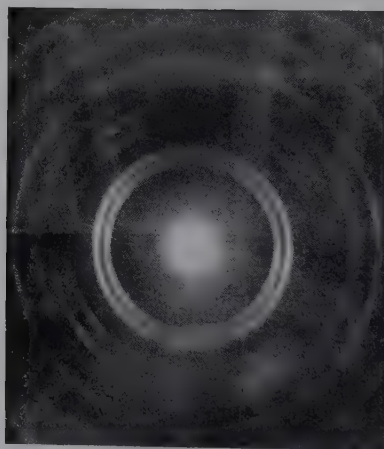


FIG. 288.—Structures of forming steels after forming. Above, satisfactory; below, unsatisfactory.

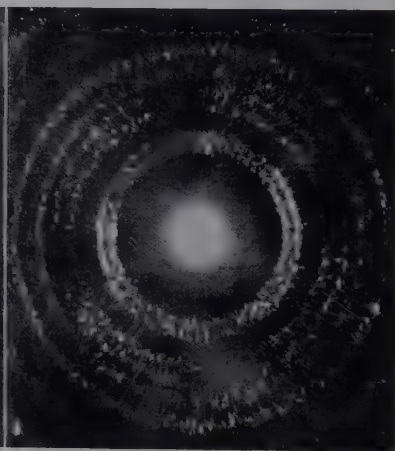
that which forms without ears has random orientation. The formation of ears in drawn copper is avoided by the limitation of rolling reduction to 65 per cent and annealing at 500 to 600°C.



(a)



(b)



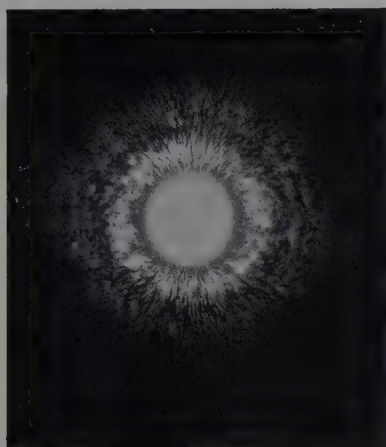
(c)

FIG. 289.—Patterns for molybdenum ribbon used in electric resistance furnaces. (a) Cold rolled in the United States; (b) cold rolled, German process; (c) ribbon after use in furnace, showing marked grain growth.

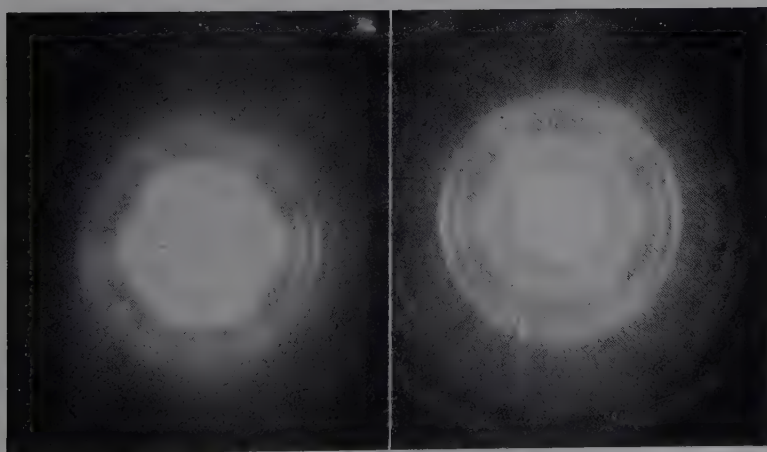
In general, all sheet metals that fail in forming operations show evidences, by the extremely sensitive diffraction method, of residual fibering, which the annealing treatment has not removed,

or a new recrystallization orientation, such as is commonly found for copper shown in Fig. 273.

8. Changes in Electric-furnace Resistor Ribbon.—Figure 289 shows the patterns of two types of cold-rolled molybdenum



(a)



(b)

(c)

FIG. 290.—Patterns showing effects of twisting and bending on steel wire.
(a) Original; (b) after 38 twists; (c) after 10 bends.

ribbon used in resistance furnaces and another that demonstrates what happens after short usage—a very large growth of grains.

9. Comparison of Effects of Twisting and Bending Steel Wires. (0.60 per cent carbon, annealed at 1200°F.).—The original structure of the wire is shown in Fig. 290 together with the patterns, respectively, after 38 twists and 10 bends. Grain fragmentation begins with the first twist and reaches a maximum

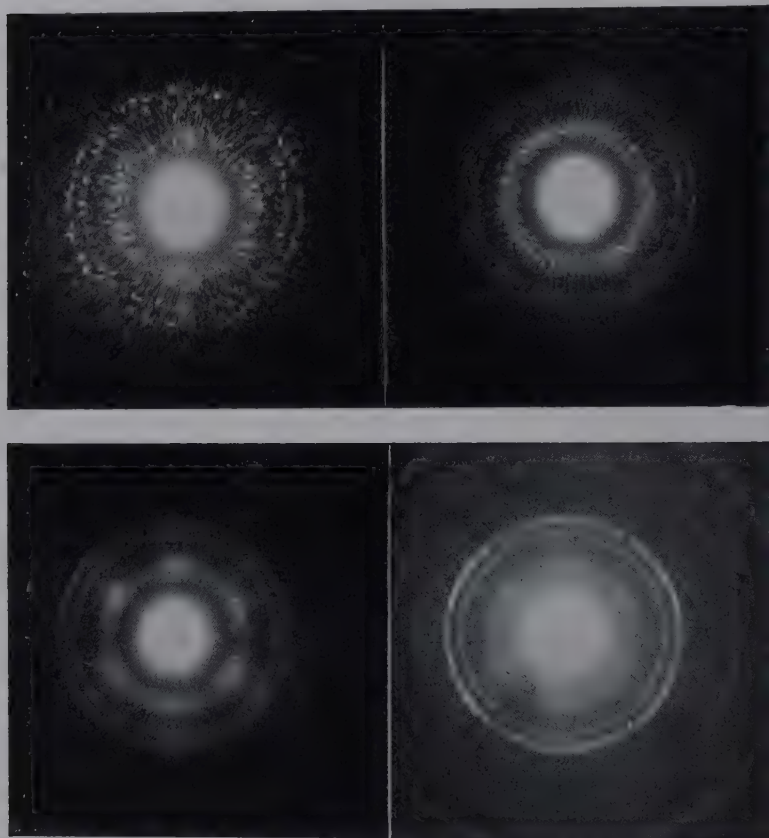


FIG. 291.—Patterns from specimens in same lot of 0.10 per cent carbon Bessemer continuous mill rod, showing non-uniformity of structure.

between 3 and 5 twists, followed by a much more gradual effect. After 13 twists the beginning of fibering or preferred orientation is evident, and this is quite marked for the case of 38 twists.

For the bending tests the wire was bent through an angle of 90 deg. and returned to its original position. The next bend was made in the opposite direction, the third like the first, etc.

Severe grain fragmentation begins with 1 bend, since the pattern is more diffuse. Two bends were equivalent to 13 twists in this respect; 3 bends introduces preferred orientation which becomes more perfect up to the breaking point. The bending test, therefore, is much more severe. These tests are of the utmost importance for suspension-bridge cables.

10. Effect of Carbon Content on Annealing.—X-ray studies of 0.06, 0.19, and 0.34 per cent carbon steel wires drafted similarly and annealed at the same temperatures for the same length of time prove that increasing carbon increases sluggishness in recrystallization, causes smaller but less distorted grains. In a similar way it has been possible to define in every case the temperature at which recrystallization begins after a given drafting or reduction in area by cold work, the temperature at which good annealing occurs, with removal of strain and directional properties due to original cold work, the grain size resulting from a given treatment, etc.

11. Non-uniformity of Production.—Many examples of this might be presented. In Fig. 291 are shown the patterns for four samples of Bessemer steel and from the same continuous mill, selected from various coils. The differences require no comment.

12. The Relation between Reduction, Temperature of Annealing, and Structure.—Two series of patterns are reproduced. Figure 292 is for a constant annealing temperature of 1200°F. with successive reduction of low-carbon sheet of 2, 5, 10, 15, 20, 40, 60, and 80 per cent. Figure 293 is for 1500°F. temperature of annealing for the same specimens. The most marked effect is the difference between the temperatures of 1200 and 1500° on the specimen reduced in cross-sectional area by 2 per cent. At the lower temperature no recrystallization occurs, whereas at the higher so great is the change that only a single grain of iron is in the beam.

Relationship between these three variables can best be shown by a three-dimensional diagram such as is represented in Fig. 294 which shows readily how research on a given metal can lead to a thorough scientific method of heat-treatment rather than to an entirely empirical one. In this figure, the variable that may be determined from x-ray data in this case is grain size, though any other property might also serve. It proves that the final annealed structure of a sheet which has been cold-

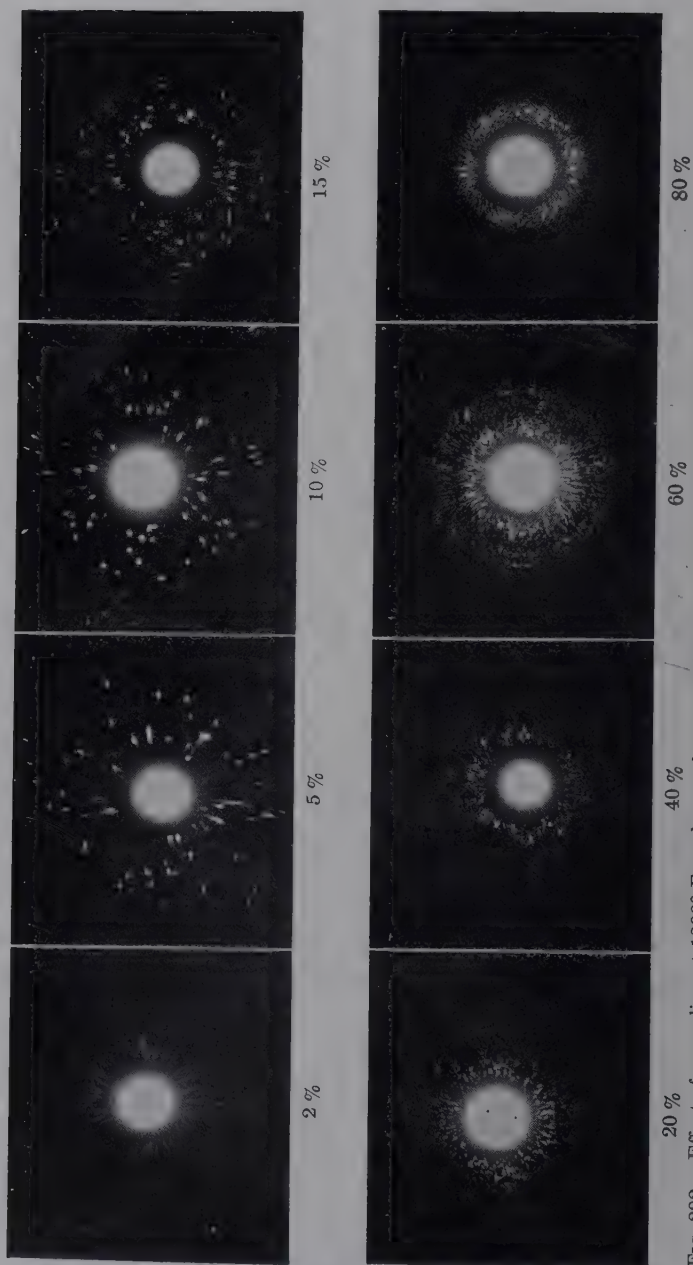


FIG. 292.—Effect of annealing at 1200° F. on low-carbon steel sheet with various reductions by cold work (compare with Fig. 293).

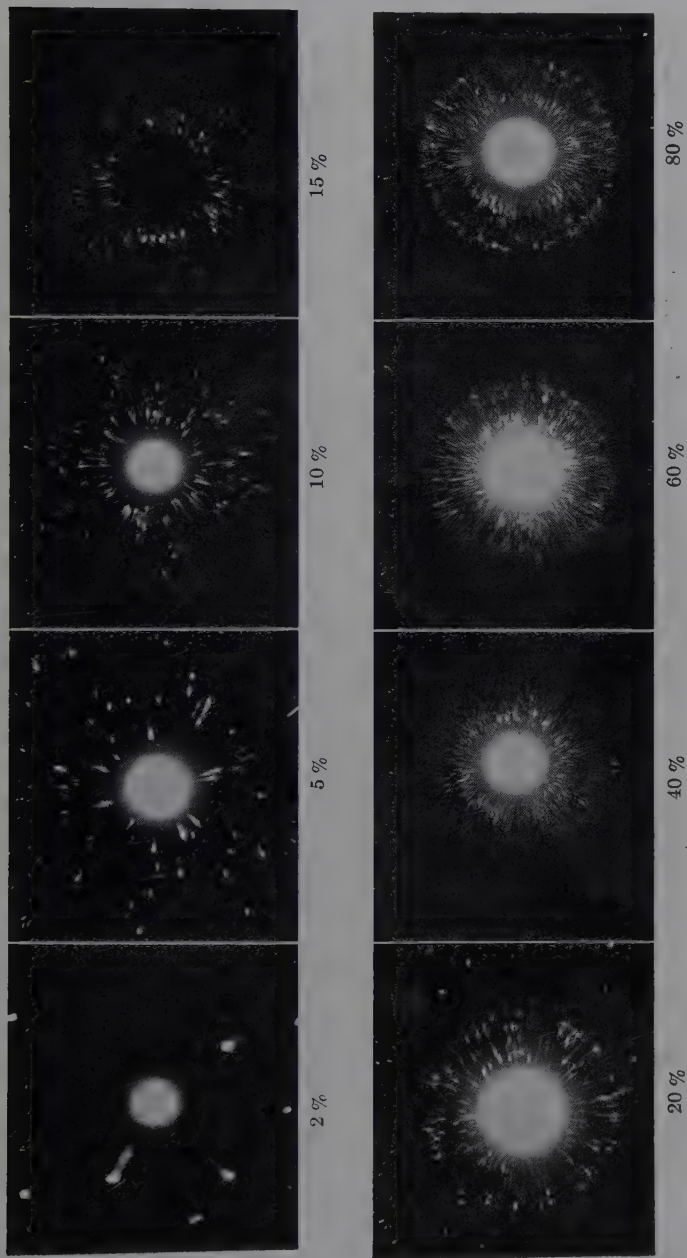


FIG. 293.—Effect of annealing at 1500° F. on low-carbon steel sheet with various reductions by cold work (compare with Fig. 292).

rolled to 90 per cent reduction without intermediate anneals must be different from that of the sheet which has been rolled down in steps with intermediate anneals. Each of these in effect places the specimen back at 0 per cent reduction. The diagram shows also that if very large grains are desired, following a complete cold reduction, the specimen is annealed, giving the size characteristic for the reduction at the right of the diagram, then given a pinch pass or very small cold reduction so that the conditions on the left of the diagram are realized, and then again heat-treated.

13. Problems of Fatigue of Metals.—Comprehensive work in combining x-ray research with fatigue tests has not yet been

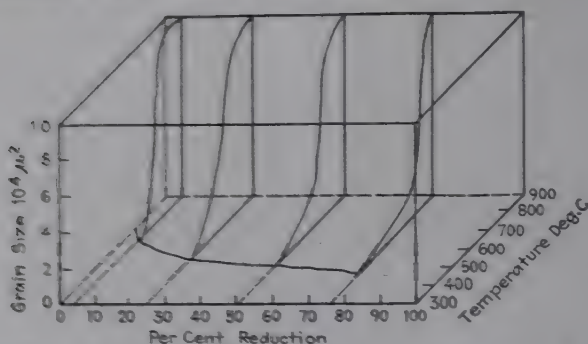


FIG. 294.—Three-dimensional diagram illustrating scientific control of recrystallization of cold-worked metals.

completed, although progress has been made and more should be expected. The chief difficulty has been in providing specimens sufficiently thin for x-ray analysis. As an example of such research some preliminary results are presented in Fig. 295 for steel rails, the diagram in Fig. 296 showing the location of samples. The ideal structure shown by No. 14 may be contrasted with No. 26 for example, which shows strain and actual preferred orientation of grains. In such an area fissures usually occur, largely as a result of the varied structure in contiguous portions of the rail.

In a classical investigation by Barrett,¹ x-ray patterns made by oscillating specimen and film together (page 514) convincingly demonstrate that in fatigue stressing there is cold work by plastic

¹ *Metals and Alloys*, January, 1937.

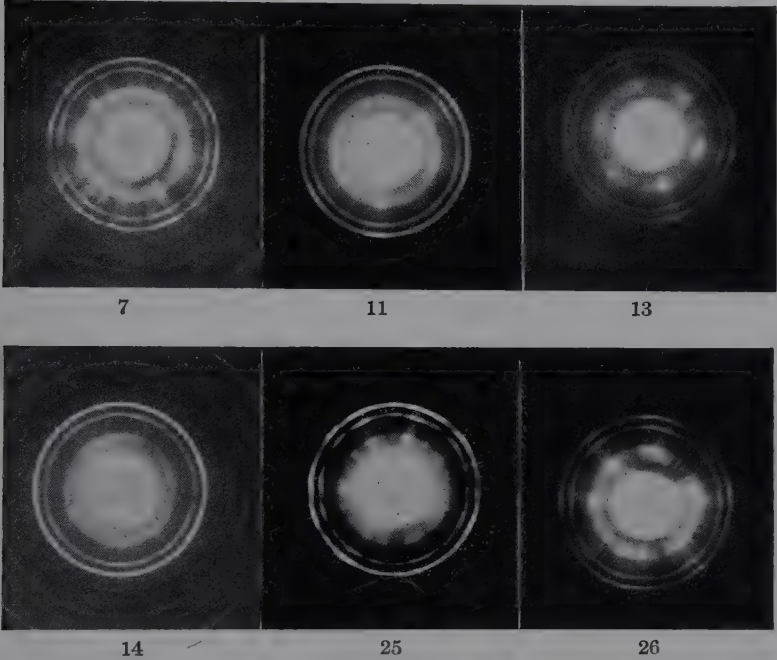


FIG. 295.—X-ray study of structure of steel rails, with numbers referring to location in rail in Fig. 296.

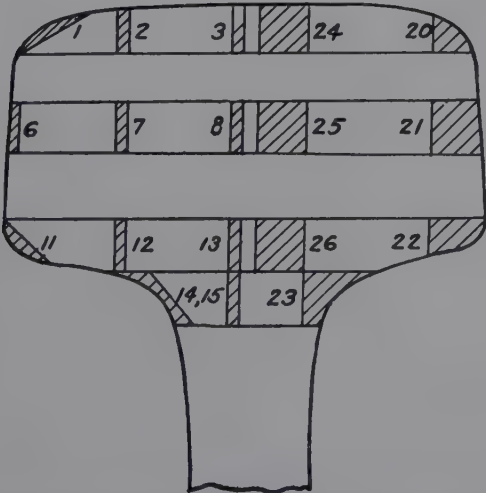


FIG. 296.—Diagram showing location of specimens subjected to x-ray examination for fine structure, some of which are presented in Fig. 295.

flow of the lattice along slip planes practically indistinguishable from that of static stressing. Figure 297 represents the effect of cold work below the endurance limit for a commercial 2S-O aluminum specimen placed in the Moore rotating-beam fatigue machine. The pattern on the left is for the unstressed specimen; the pattern at the right is for the same specimen after it had withstood 505,000,000 cycles without breaking. Spots have become

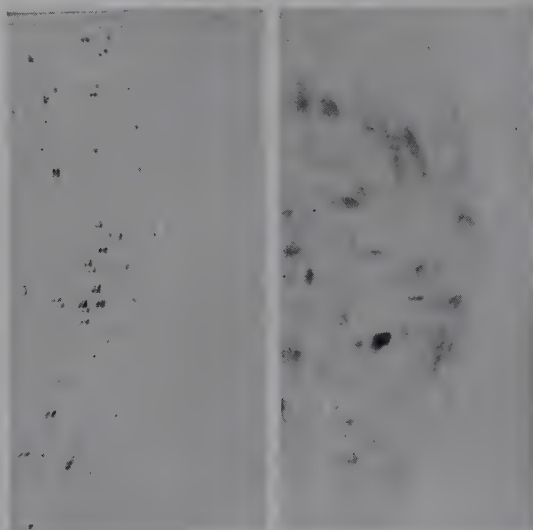


FIG. 297.—Patterns by Barrett technique (oscillation of specimen and film, spreading out narrow area into band) for commercial aluminum [$\text{Fe } K\alpha$ radiation; (400) reflection]. Left, unstressed; right, after fatigue stressing without failure, withstanding 505,000,000 cycles, with structural change due to cold work in safe range of stress. (Courtesy Charles S. Barrett.)

blurred or elongated in one or more directions, as evidence of cold work *without damage* below the endurance limit. This result is one of many which have led Barrett to conclude that damage is not registered on the x-ray patterns and hence that fatigue failure cannot be safely predicted from evidences only of cold work, which may be actually beneficial.

From a study covering two years devoted to structural changes in duralumin airplane propellers, typical patterns are selected in Fig. 298 for the alloy in initial condition, after 900 hr. use on a plane, and after 1,400 hr. After detailed study of all parts of a blade, the surface area near the hub, which seems to be a focus

of component stresses, is located, and a reflection pattern made at different times. The amazing increase in grain size and evidences of distortion by vibrational stresses in this age-hardening alloy are self-evident, and failure seems an inevitable result. Improvements in propeller design and in the composition and properties of the alloy within the past few years have greatly reduced such profound and dangerous changes.

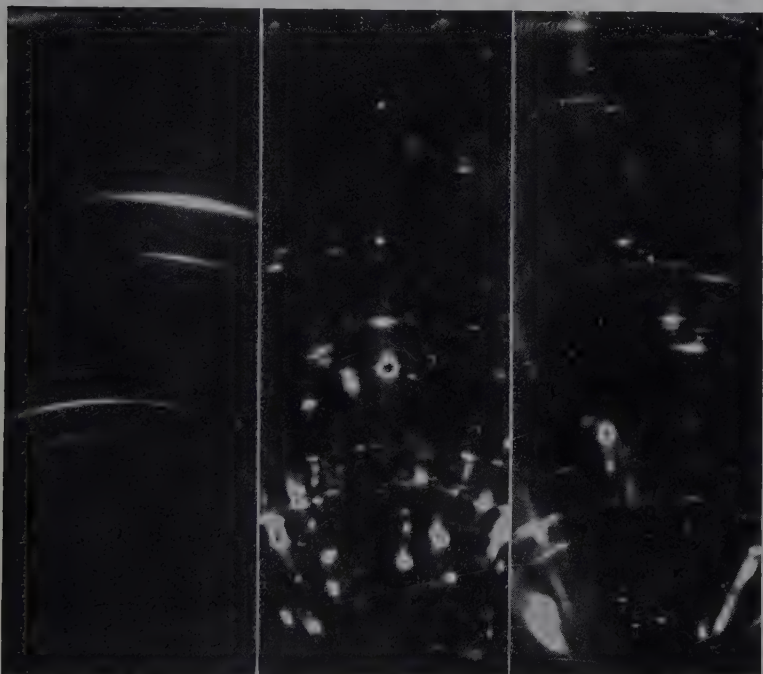


FIG. 298.—Patterns for aluminum-alloy airplane propellers. Left, unused propeller; center, propeller used on plane after 900 hr. flying; right, same after 1,400 hr. Grain growth and distortion with increasing use are indicated.

The Heat-treatment of Watch Springs.—The manufacture of mainsprings for watches that have satisfactory properties and endurance against breakage presents an extraordinarily difficult control problem. The springs are annealed in baskets in electric furnaces, but even springs from the same basket differ markedly, for some have “slow-motion” action, some “fast-motion,” and some are satisfactory. The first type seems to be associated with metal that is too soft, the second with brittle metal that

breaks easily. The three patterns show convincingly the differences: the soft spring has been annealed, until grains have grown to a point where they register spots on the Debye-Scherrer ring; the hard spring is incompletely annealed, and the preferred orientation of the original rolled-steel strip persists; the satisfactory spring lies between these two extremes, with smooth continuous rings of uniform intensity indicative of removal of preferred orientation, but maintenance of fine grains—possible only within an extremely narrow range. Several hundred new and untested springs were classified by single x-ray patterns into the three groups, and subsequent behavior in watches was accurately predicted.

CHAPTER XXIII

POLYMERS—SYNTHETIC AND NATURAL MATERIALS WITH GIANT MOLECULES

The Importance of Polymers.—Upon this fascinating and immeasurably important subject it would be far easier to write an entire book than a single chapter. For, if this is the chemical age, it is primarily the polymer hour of synthetic resins, plastics, chloroprene, nylon, and countless commercial products produced by man in his attempt to follow the pattern of nature in the building by living processes of cellulose, rubber, chitin, proteins, or the living cell.

No better tribute could be paid to the late Dr. W. H. Carothers, outstanding authority in the chemistry of polymerization, than to quote his sincere appraisal¹ of the peculiar significance of polymers in the world of today:

The most important peculiarity of high polymers is that they alone among organic materials manifest to a significant degree such mechanical properties as strength, elasticity, toughness, pliability, and hardness. Weight for weight cellulose and silk are stronger than steel; rubber exhibits a combined strength and elastic extensibility that is not even remotely approached by anything in the inorganic world; while diamond is harder than any other material. The practical uses of high polymers depend almost entirely on these mechanical properties: our clothing and furniture, and much of our shelter are made of such materials. The names cellulose, wool, rubber, and silk suggest at once the great importance of the non-chemical uses of natural high polymers.

Probably the bulk of the organic matter in living beings is made up of high polymers. The necessity of this lies in the fact that living organisms must have physical form and coherence, and polymers are the only organic materials capable of supplying these properties. The variability of living matter also requires a high degree of structural complexity, and the possibilities of high polymers in this connection are indicated by Fischer's well-known calculation that 20 different amino acids may form 2.3×10^{18} different polypeptides of 20 units. Another pertinent

¹ *Trans. Faraday Soc.*, **32**, 39 (1936).

fact is that the physical properties of high polymers are profoundly affected by their physical history: the melting points of certain polyesters can be reduced several degrees by the mere application of stress, and their strength in the direction of stress is, at the same time, increased manyfold. Finally, reactions of polymerization also appear to be uniquely adapted to the chemistry of vital growth, because they are the only reactions that are capable of indefinite structural propagation in space.

To the still incomplete knowledge of the structures and building plan of these manifold materials with giant molecules, x-ray diffraction methods have made, are making, and will continue to make an indispensable and brilliant contribution, supplementing, and perhaps even surpassing, the results of chemical synthesis and analysis, microscopic examination, measurements of viscosity, fractionation and molecular-weight evaluation in the ultracentrifuge, and all other tests applied to colloidal materials.

Definition of Polymerization.—Polymers are built up into what may be termed giant molecules or macromolecules from one or more monomers, or simple compounds of low molecular weight. Conventionally, it has been assumed that polymerization consists in self addition and is limited to unsaturated compounds, and that a monomer and its polymer or polymers have identical compositions. Today the connotation of the term polymerization is far broader. It is an intermolecular combination that is functionally capable of proceeding indefinitely, or leading to molecules of infinite size. Polymers need not have a composition identical with the parent monomer; polymerization may proceed as addition and condensation; it may involve participating molecules that are not alike, thus to form products like the sensational substitute for natural silk, nylon; and it may apply to unsaturated compounds, cyclic compounds, or polyfunctional compounds, in general, x - R - y , where x and y are capable of mutual reaction (Carothers).

Classification of Polymers.—Macromolecular substances are classified in several ways: (1) according to natural or synthetic origin; (2) according to the probable mechanism of formation, discussed in the next section. (3) Polymers are further classified into two groups depending upon whether they form linear chains or three-dimensional networks, usually random. In the first

group belong protein fibers, rubber, cellulose and its esters and ethers, and many synthetic materials, such as polyoxymethylenes from formaldehyde, polystyrene, polyethylene oxide, polyvinyl alcohol, chloride, acetate, etc., polyacrylester, polyphosphornitrylchloride, thiokol (organic polysulfide), and elastic sulfur. These are generally crystalline solids producing fiber diffraction patterns. The three-dimensional networks, such as hard rubber, most synthetic resins like bakelite (phenol aldehyde), vinyl resins (safety glass), hydroxy dicarboxylic resins (glyptal), methyl methacrylate (lucite), linoxyn, etc., yield amorphous patterns usually like felted fibers, the interpretation of which has been considered in Chap. XX. (4) The linear polymers are further classified according to length, which in turn determines important properties. Staudinger distinguishes the following:

1. Hemicolloids. Molecular weight up to 10,000 with chain lengths of 50 to 250 A.U.; powdery, dissolving without swelling in solution of low viscosity.

2. Mesocolloids. Molecular length 250 to 2500 A.U.; intermediate properties.

3. Eucolloids. Threadlike molecules over 2500 A.U. in length up to 1 micron or more; characteristic for familiar natural fibers, some elastic, dissolving with swelling to solutions of high viscosity. It is only this type that may be spun into textile fibers. It is generally true that a given material, especially of natural origin, is a mixture of many molecular lengths, which may be determined by ultracentrifuge analysis. A complete theory and calculation of molecular-size distribution in linear condensation polymers, based on the work of Carothers and coordinated with ultracentrifuge results, have been derived by Flory.¹ Molecular-weight analysis of mixtures by sedimentation equilibrium is given by Lansing and Kraemer² and in a long series of papers by Wyckoff, applied especially to viruses to which reference will be made in a later paragraph.

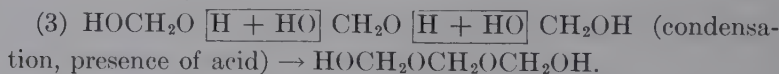
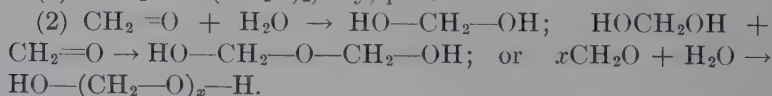
Relation between Natural and Synthetic Polymers.—It is a singular fact that many types of synthetic polymer can be made, but no naturally occurring polymerization has been exactly duplicated in the laboratory. Polyacetals, polyamides, and

¹ *J. Am. Chem. Soc.*, **58**, 1877 (1936).

² *Ibid.*, **57**, 1369 (1935).

polyprenes have been synthesized in large numbers, but not the polyacetal cellulose, the polyamide proteins, or the polyprene rubber, though, in the last case, polyprenes like chloroprene have been made which equal natural rubber in strength and elastic extensibility and surpass it in some respects. The α -amino acids or esters can be polymerized in vitro to a cyclic dimer (diketopiperazine), whereas in the living organisms the polyamide is always linear, probably because of control of orientation by adsorption at interfaces. Nevertheless, the same basic principles of structure prevail, and it is reasonable to expect that some of the natural environmental conditions of reaction may be artificially approached. Another fundamental difference lies in the fact that in natural fibers the molecules grow in length and into fibrils, possibly through an intermediate state of particles, or micelles, as a biological process. For synthetic fibers the macromolecules are first formed by polymerization; this material is then spun into artificial fibers from viscous solutions, or melts. Textile fibers, sheets, etc., are also manufactured in similar fashion from natural materials dispersed in solution: dispersed cellulose regenerated as rayon fibers and cellophane sheets; artificial wool fibers (lanital) from casein dispersions; etc.

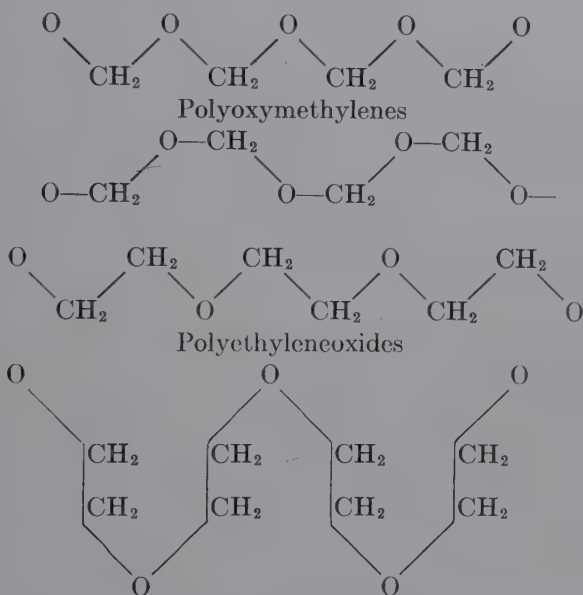
Examples and Mechanisms of Polymerizations.—1. A very familiar polymerization frequently studied as a structural model with x-rays is that of formaldehyde to form the polyoxymethylenes and derivatives. The possible mechanisms are:



A half-dozen varieties of polyoxymethylenes, with various end groups (α , β —OH; γ —OCH₃; δ -diacetate; etc.) and with molecular weights up to 100,000 have been analyzed by x-rays. Ott¹ has claimed direct diffraction measurement of chain lengths (c axis) of 45 A.U. for δ -polyoxymethylene (24 formaldehyde groups); 113.4 A.U. for γ -polymer (60 CH₂O groups); 60 A.U. for para-

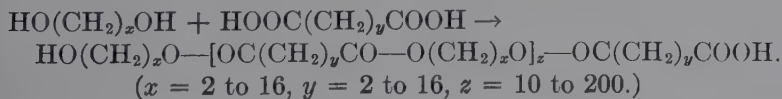
¹ *Z. physik. Chem.*, **B9**, 378 (1930).

formaldehyde (32 CH₂O groups). But Sauter¹ has denied the existence of "inner" interferences, the identity period being 17.3 A.U. There is still some uncertainty which of the following forms the chains have:

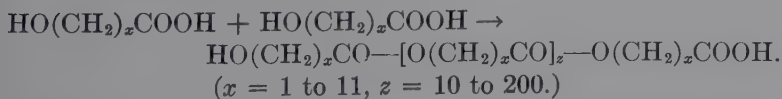


2. Other well-known examples from the work of Carothers and associates, involving reactions by the same chemical process, monomer with monomer, monomer with polymer, and polymer with polymer, are as follows:

a. Polyesters from glycols and dicarboxylic acids:

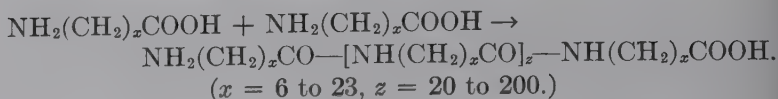


b. Polyesters from hydroxy acids:



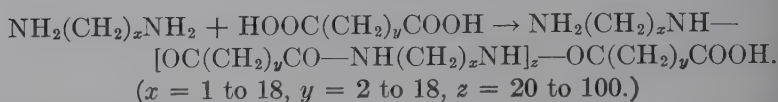
¹ *Ibid.*, B18, 417 (1932); B21, 186, 161 (1933); B37, 403 (1937).

c. Polyamides from amino carboxylic acids:

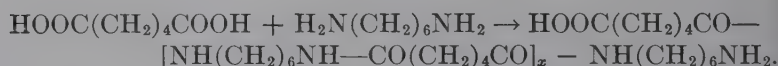


With this is to be compared natural silk $—\text{NH}—\text{R}—\text{CO}—\text{NH}—$
 $\text{R}'—\text{CO}—\text{NH}—\text{R}—\text{CO}—\text{NH}—\text{R}'—\text{CO}—$.

d. Polyamides from diamines and dicarboxylic acids:



The most famous representative of this class is the sensational *nylon*, now being manufactured by the du Pont Company, as a substitute for natural silk fibers. It is produced from the mutual reaction and polymerization of adipic acid and hexamethylenediamine:



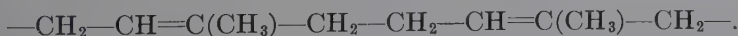
Benzene, C_6H_6 , is the starting commercial material and the successive steps are phenol, $\text{C}_6\text{H}_5\text{OH}$, \rightarrow cyclohexanone, $\text{C}_6\text{H}_{10}\text{O}$, \longrightarrow adipic acid \rightarrow adipamide \rightarrow adiponitrile \rightarrow hexamethylenediamine. The condensation of adipic acid and hexamethylenediamine is carried out by dissolving both in a high-boiling solvent, such as cresol or xylenol, and heating them at 200°C . until the requisite viscosity and degree of polymerization are reached. The polyamide is, of course, a mixture of chains of different lengths and of polymer homologs, but its valuable properties seem to arise from the unusual regularity of the molecules, which permits the well-crystallized structure. Because of low solubility and high stability of the polymer, nylon fibers are spun, not from viscous solution, but from the melt at 270 to 280°C ., under conditions of tension such that the solidifying filament is extended three- to fivefold. This promotes the unusual degree of preferred orientation, as shown by the x-ray pattern in Fig. 299 and displayed in the physical and mechanical properties that are shown in tables in comparison with those of natural fibers. The uses of nylon in the manufacture of stockings and toothbrush bristles (Exton) are familiar to everyone. It is

interesting to note that nylon has a comparatively low molecular weight and degree of polymerization—far lower than might be predicted for the properties that it has. Staudinger has shown that the strength of fibers does not increase in proportion to the degree of polymerization as measured by viscosities of comparable solutions; a “eutectic region” is reached at a polymerization degree (the number of monomer groups in a chain) of 700 to 800, at which tensile-strength curves flatten out to nearly constant value even though viscosities increase rapidly. Use can be made generally of this observation in avoiding the great difficulties in handling fluids of very high viscosity.

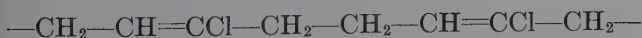
3. Although natural rubber has not been synthesized, there have been produced a number of related “synthetic” rubbers, many of which possess the characteristic elastic properties. It is possible to distinguish by x-ray patterns of stretched samples every one of these products from natural rubber; for, as a matter of fact, only one or two of the synthetic samples give any crystal pattern at all on stretching. If any polymer is ever synthesized which produces a pattern identical with that of natural rubber, to be discussed in a later paragraph, then it is safe to identify that polymer as truly synthesized rubber. The best known examples of “synthetic” rubber are:

(1) From butadiene: $-\text{CH}_2-\text{CH}=\text{CH}-\text{CH}_2-\text{CH}_2-\text{CH}=\text{CH}-\text{CH}_2-$ (Buna).

(2) From isoprene (probably the monomer of natural rubber in strictly uniform combination, but always in mixed 1, 2 and 1, 4 combination in synthetic products):



(3) From β -chlorobutadiene:



Chloroprene, duprene.

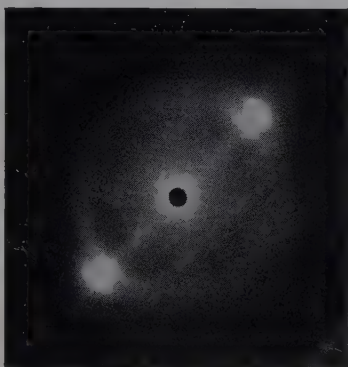
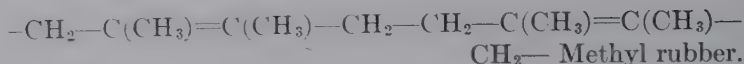
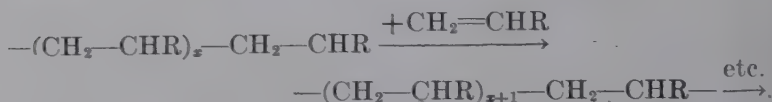


FIG. 299.—Diffraction pattern of nylon fibers (x-ray beam perpendicular to fiber axis).

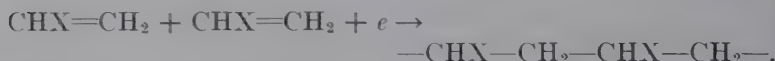
d. From dimethylbutadiene:



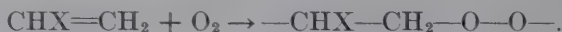
4. Vinyl polymerizations (including not only vinyl alcohol derivatives, but all polymerizations involving olefinic double bonds) are chain reactions in which the chain is propagated through successive addition of monomer molecules to a free radical:



These processes have been extensively studied from the standpoint of kinetics, heats of reaction, and mechanisms of chain initiation, propagation, transfer, and termination. Thus initiation may be the result of thermal energy:



Or it may result catalytically by impurities or on walls, thus lowering activation energy:¹



Or it may be brought about photochemically:



Principles of distribution and probability, steric factors, and side reactions govern termination of their growth. In the last case, multimembered rings (Ruzicka and associates) may form by bending of two ends of a chain together (x-ray identification, page 433); or a hydrogen atom may wander along the chain and saturate one end (such isomerization reactions have been experimentally verified); or stabilizers such as hydroquinone in polymerizing styrenes may by side reactions with the free valences at chain ends terminate the chain.

Most vinyl polymers have a "head-to-tail" structure, as proved by Marvel² and associates. Familiar examples are:

¹ FLORY, *J. Am. Chem. Soc.*, **59**, 241 (1937).

² *Op. cit.*, **60**, 1045, 280 (1938); **61**, 3241 (1939).

a. Polyvinylalcohol: $\text{—CH}_2\text{—CHOH—CH}_2\text{—CHOH—CH}_2\text{—CHOH—}$.

The diffraction pattern of the polymer as a fiber is illustrated in Fig. 300.

Numerous derivatives with various substituent side groups have been synthesized and are used for safety-glass plastics, etc. These substituent groups seem to be attached along the chains at random, with the result that the x-ray patterns are no longer indicative of sharply oriented macromolecules.

b. Polyvinylacetate:

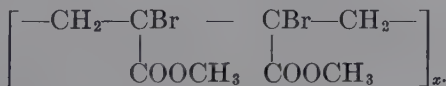


c. Polyvinylchloride: $\text{—CH}_2\text{—CHCl—CH}_2\text{—CHCl—CH}_2\text{—}$ (PC fibers and sheets, common in Europe; Koroseal).

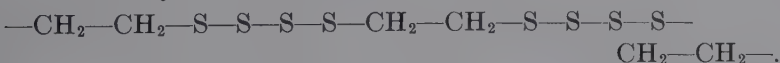
Closely related are the commercially prominent polystyrenes:



In contrast, alkyl α -haloacrylates, polyacrylyl chloride, etc., have "head-to-head tail-to-tail" structure, again as shown by Marvel¹ and associates:



5. Sulfur often plays an important role in polymerizations. In fact, elastic sulfur itself consists of long-chain molecules in contrast with the S_8 rings in orthorhombic sulfur. A sulfur fiber, made from the reaction of sodium thiosulfate and nitric acid, produced the remarkably rich pattern in Fig. 302a. Thiokol, a linear polymer of commercial value, is formed by the reaction of dichlorethylene and Na_2S_4 with splitting out of NaCl :



The polysulfones, extensively studied by Marvel² and associates at the University of Illinois, are formed by the reactions

¹ *Ibid.*, **61**, 3244, 3156 (1939).

² *Ibid.*, **60**, 2622 (1938); **61**, 2709, 2710 (1939).

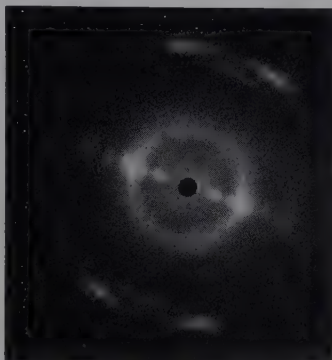
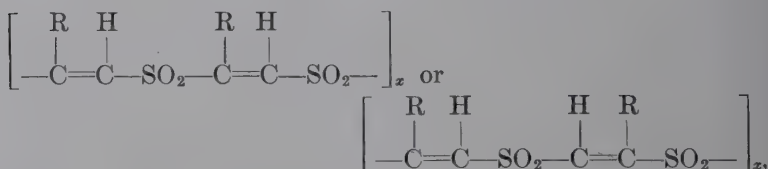


Fig. 300.—Fiber pattern of polyvinylalcohol.

of olefin and acetylene derivatives with SO_2 . The general reaction is a combination in the ratio 1:1, but vinyl chloride and bromide are unique in that two olefin units combine with one SO_2 unit in the presence of peracetic acid as catalyst to give the polysulfone: $-\text{[SO}_2\text{CHClCH}_2\text{CHClCH}_2\text{]}_x-$. Acetylene itself does not react, but $\text{RC}\equiv\text{CH}$ combines with SO_2 to give polymers



or both. These can be drawn into fibers that yield remarkably clear x-ray patterns, exemplified by Fig. 301 for pentyne polysulfone, and changing progressively in spacings with change in the R group.

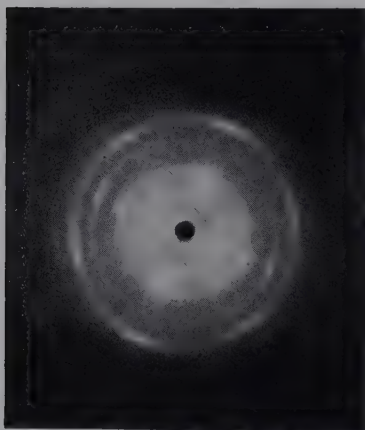
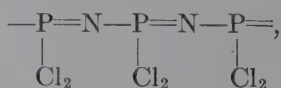


FIG. 301.—Fiber pattern of pentyne polysulfone (synthesized by Marvel and associates).

6. A purely inorganic polymer with typical rubberlike properties is polyphosphornitrylchloride



or, better, a resonance¹ form



This is distinctly crystalline, with unit orthorhombic cell and dimensions of $a = 11.07$, $b = 4.92$, $c = 12.72$ A.U. and containing eight molecules of PNCl_2 (Fig. 302b).

The Relation between Polymer Structure and Chain Length and Properties.—In Table XLIX are compiled by Mark general relationships between structures of high polymers (chemical

¹ MEYER, LOTMAR, and PARKOW, *Helv. Chim. Acta*, **19**, 930 (1936).

nature of monomer, chain length, chain flexibility, and netting number or cross linkages) and properties (heat, oil, and water resistance, impact and abrasive strength, and reversible elasticity).

Table L gives average data experimentally accumulated by Staudinger¹ for comparison of fibers of native and regenerated



FIG. 302a.—Pattern for sulfur fibers, made by spinning product of reaction of sodium thiosulfate and nitric acid.

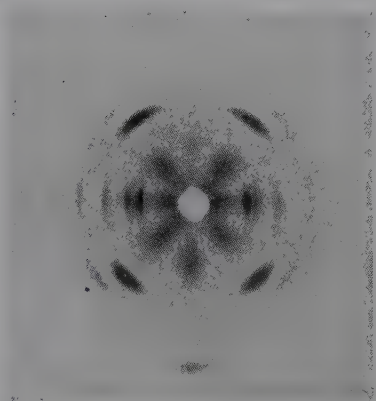


FIG. 302b.—Fiber pattern of polyphosphornitrylchloride. (Meyer, Lotmar, and Parkow.)

cellulose, natural and regenerated protein, and purely synthetic polymers. Carothers and Hill² were the first to prove experimentally that a useful degree of strength and pliability in artificial fibers from synthetic linear-condensation superpolymers requires

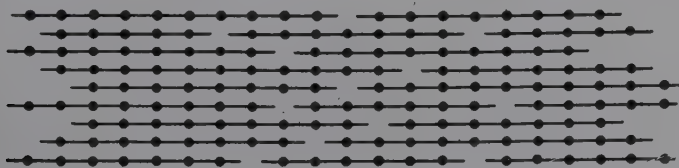


FIG. 303.—Lattice from polymer molecules of unequal length.

a molecular weight of at least 12,000 and a molecular length not less than 1000 A.U. The macrocrystalline lattice is pictured in Fig. 303.

¹Über makromolekulare Verbindungen CCXXVI, *Melliand Textilber.*, 9, Heidelberg, 1939.

²*J. Am. Chem. Soc.*, **54**, 1579 (1932).

TABLE XLIX.—RELATIONSHIP BETWEEN STRUCTURE AND PROPERTIES OF HIGH-MOLECULAR POLYMERS

| | Heat resistance | | Oil resistance | | Water resistance | | Impact strength | | Abrasive strength | | Reversible elasticity | |
|----------|----------------------|--|---|---|---|--|-----------------------------|--|--|--|----------------------------|--------------------------------------|
| | Dec. | Inc. | Dec. | Inc. | Dec. | Inc. | Dec. | Inc. | Dec. | Inc. | Dec. | Inc. |
| <i>a</i> | <i>x</i> | <i>x</i> | By CH ₃ , OCH ₃ , and fatty groups | By OH groups and O-bridges | By OH, NH ₂ , OCH ₃ , HSO ₃ , COOH groups | By CH ₃ , C ₆ H ₅ , and fatty groups | <i>x</i> | <i>x</i> | By CH ₃ or fatty groups | By OH groups | <i>x</i> | <i>x</i> |
| <i>b</i> | By short chains | By long chains | <i>x</i> | <i>x</i> | <i>x</i> | <i>x</i> | When chains are short | By long chains | By short chains | By long chains | By short chains | By long chains |
| <i>c</i> | <i>xx</i> | <i>xx</i> | By very flexible chains | When chains are not too flexible | When chains are very flex- ible | By rigid chains | <i>x</i> | <i>x</i> | <i>x</i> | <i>x</i> | By rigid chains | Very much by flexi- ble chains |
| <i>d</i> | Low net- ting dex | Very much by high netting index | By low netting index | Very much by high netting index | When net- ting dex is very low | By high netting index | By low netting index | Very much by high netting index | By low netting index | Very much by high netting index | By low netting index | By low netting index |

a = chemical nature of the monomeric molecule.*b* = length of the chains.*c* = flexibility of the chains (*e.g.*, cellulose, very low; polyvinyl alcohol, medium; polybutadiene, very high).*d* = netting number or cross linkages (*e.g.*, cellulose, rubber, 0; polystyrene, low, 3 to 5; polybutadiene, medium, 5 to 10; hard rubber, buna, high, 10 to 20; bakelite, very high, 50).*x* = little effect.*xx* = no effect.

TABLE L.—AVERAGE STRENGTH AND DEGREE OF POLYMERIZATION OF FIBERS

| Fiber | Degree of polymerization (D.P.) | Number of chain members | Titer, deniers | Tensile strength, grams per denier, dry | Breaking elongation, dry | Bending strength |
|--------------------------|---------------------------------|-------------------------------|----------------|---|--------------------------|------------------|
| Cellulose: | | | | | | |
| Egyptian cotton..... | 3,000 | 15,000 | 1.85 | 3.6 | 13.1 | 16,000 |
| Ramie..... | 3,000 | 15,000 | 4.1 | 6.7 | 4.1 | 3,500 |
| Viscose rayon..... | 290 | 1,450 | 1.4 | 2.35 | 16.0 | 150 |
| Cuprammonium rayon... | 560 | 2,800 | 3.9 | 1.97 | 26.0 | 175 |
| Nitrorayon..... | 170 | 850 | 6.5 | 1.75 | 17.5 | 50 |
| Protein: | | | | | | |
| Silk..... | | | 1.25 | 5.8 | 21.5 | 3,000 |
| Wool..... | | | 5.5 | 1.5 | 41.4 | 40,000 |
| Leucital (casein)..... | | | 3.3 | 0.9 | 84.2 | 70 |
| Synthetic: | | | | | | |
| PC, polyvinylchloride... | 2,000 | 4,000 | 4.1 | 1.4 | 24.0 | 1,200 |
| Nylon..... | | 900 (molecular weight 12,500) | 3.2 | 4.25 | 16.2 | 40,000 |

Cellulose. Composition.—Polymers of dehydrated glucose residue represented by the formula $(C_6H_{10}O_5)_x$; 1—4 glucosidal linkage through oxygen bridge; cellobiose the repeating unit along macromolecular chains (Fig. 304).

Occurrence.—The principal framework of plants as fibers of the commercially important wood, cotton, jute, sisal, hemp, ramie (Fig. 305), flax; sheets in the single-celled *Valonia*; in the green algae *Halicystis*, in membranes formed by the action on glucose, fructose, sucrose, glycerin, etc., of *Acetobacteri xylinus*, and in the marine animal tunicin. Cellulose dispersed in viscose and cuprammonium solutions regenerated as rayons.

Polymorphic Forms.—At least three: cellulose I, native, the usual form from all natural sources except in *Halicystis*; cellulose II, mercerized or hydrate, the native form in *Halicystis*¹ and formed from cellulose I by treatment with alkali solutions of requisite strength followed by complete washing out of alkali; cellulose II transformed to cellulose I by heating in glycerin at 250°C.; cellulose III by slow removal of ammonia from cellulose I or II swollen in liquid NH_3 ; reverted to cellulose I or II.²

¹ Sisson, *Science*, **87**, 350 (1938).

² Clark and Parker, *J. Phys. Chem.*, **41**, 777 (1937).

Crystal Structures.—For native cellulose (I) several structures based on x-ray diffraction data have been proposed since the first crystal model in 1926 of Sponsler and Dore. The now generally accepted structure is that of Meyer and Misch,¹ confirmed in a rigorous test by Gross and Clark:²

Monoclinic, space-group P_{21} ,

$a = 8.35$ A.U.,

$b = 10.3$ A.U. (fiber axis),

$c = 7.95$ A.U.,

$\beta = 84^\circ$.

$Z(C_6H_{10}O_5 \text{ groups per cell}) = 4$.

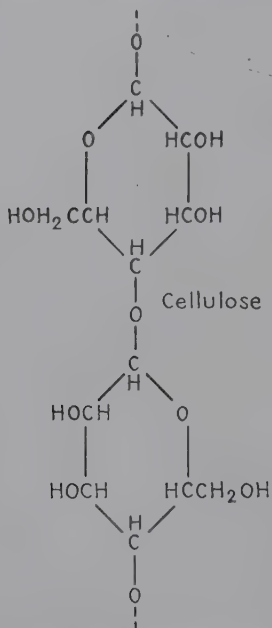


FIG. 304.—Structural formula of repeating cellobiose unit in cellulose.

Figure 306 shows the disposition in the unit cell of cellobiose units along the macromolecules and the fact that the β -glucose residues are pointing alternately in opposite directions. Without considering the details of alternative interpretations by Sauter and Sponsler, Gross and Clark calculated the nine patterns for highly oriented cellulose preparations to be expected for each of the Meyer and the Sauter structures, for the three experimental techniques, transmission, rotation, and goniometer (equatorial layer line), each in three directions (Fig. 307). Then, with

stretched, highly oriented specimens of bacterial cellulose, *Valonia*, and tunicin, nine patterns were made and compared with those theoretically deduced—with complete substantiation of the Meyer structure. Typical patterns are shown in Fig. 308.

Unit cell data for the other polymorphic forms of cellulose are as shown in the table on page 608.

The greater monoclinic angle and more open structure easily account for the ease in dyeing and processing the mercerized form of cellulose.

Orientations in Cellulose Fibers and Sheets.—With the cellulose chain and unit cell common to all materials, each natural

¹ *Helv. Chim. Acta*, **20**, 232 (1937).

² *Z. Krist.*, **99**, 357 (1938).

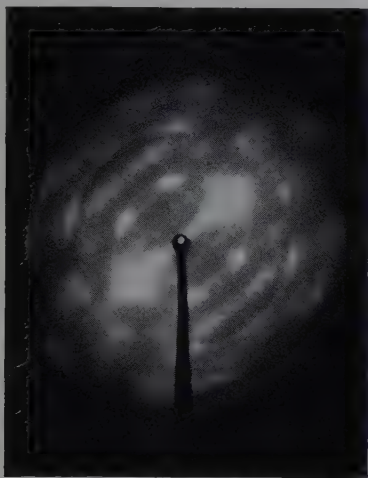


FIG. 305.—Fiber pattern of ramie, a natural source of cellulose.

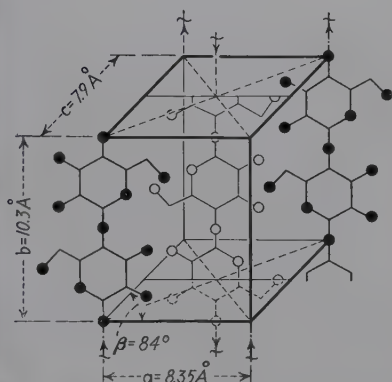
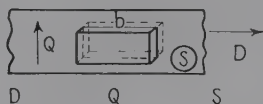
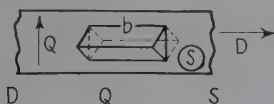


FIG. 306.—The crystal unit cell of cellulose.



Transmission Patterns



Rotation Patterns



Goniometer Patterns



FIG. 307.—Theoretical diffraction patterns for alternative interpretations of cellulose structure. Left, Meyer-Mark patterns; right, Sauter patterns. D is the direction of stretching; Q , the direction perpendicular to D and lying in the surface of the membrane; S , the direction normal to the surface of the membrane. Transmission patterns are made with the beam passing through the sample parallel to the direction indicated by the column heading. Rotation and goniometer patterns are obtained by rotating the sample about an axis parallel to the direction indicated by the column heading. (Gross and Clark.)

fiber or membrane is distinguished by a typical diffraction pattern and a typical orientation of macromolecules or crystal-

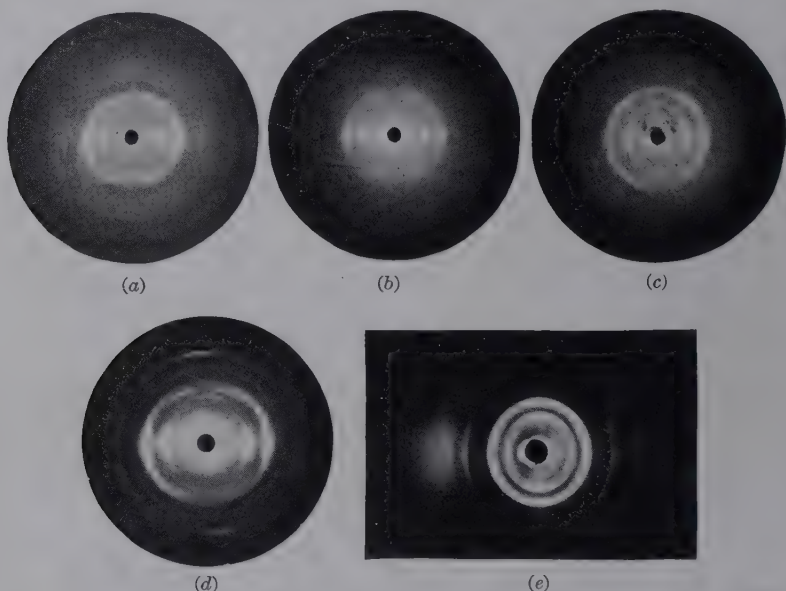


FIG. 308. --Typical patterns for highly oriented cellulose preparations, used for comparison with theoretical patterns for alternative interpretations in Fig. 307. (a) Bacterial cellulose, transmission; (b) tunicin, transmission; (c) Valonia, transmission; (d) bacterial cellulose, goniometer; (e) bacterial cellulose, rotation.

lites. Orientation is characterized by type and degree; this has been extensively studied in a series of papers by Sisson and Clark and by Sisson.¹ The x-ray method for quantitative comparison of

| Unit cell dimensions | Cellulose II (mercerized or hydrate) | Cellulose III |
|----------------------------|--|-------------------|
| <i>a</i> | 8.14 A.U. | 7.48 A.U. |
| <i>b</i> | 10.3 A.U. | 10.3 A.U. |
| <i>c</i> | 9.14 A.U. | 8.61 A.U. |
| β | 62° (Fig. 309) | 58° (Fig. 310) |

¹ *Ind. Eng. Chem., Anal. Ed.*, **5**, 296 (1933); *Ind. Eng. Chem.*, **27**, 51 (1935); *J. Phys. Chem.*, **40**, 343 (1935); *Contrib. Boyce Thompson Inst.*, **9**, 239 (1938).

crystallite orientation in cellulose fibers is based on the assumption that the distribution around the pencil of x-rays is proportional to the distribution of intensity around the (002)



FIG. 309.—Fiber pattern of mercerized (hydrate or II) cellulose.



FIG. 310.—Fiber pattern of cellulose III.

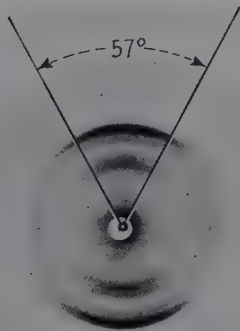


FIG. 311.—Diffraction pattern and photomicrograph of cotton fiber, showing correlation of fibril spiral angle. (Courtesy W. A. Sisson.)

diffraction ring. In cotton, for example, submicroscopic crystalline structure revealed by x-rays usually runs parallel to visible configuration such as fibrils (Fig. 311). Intensity measurements are made with a microdensitometer equipped with a rotating

stage. Curves are thus constructed, the value at each point representing the relative percentage of the total crystallites over a 5-deg. angular range. The orientation of the cellulose structural units varies widely in different fibers and in the same fiber. The influence upon physical and chemical properties has been

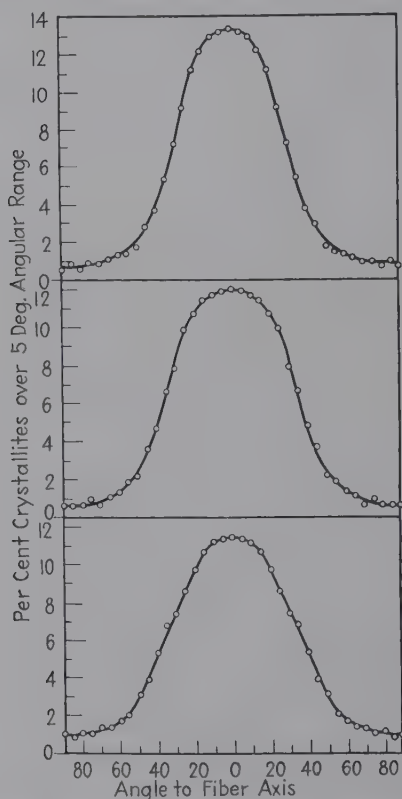


FIG. 312.—Curves illustrating microphotometric method for comparison of chain or crystallite orientation in fibers from x-ray patterns. Top, Egyptian cotton; center, Eastern cotton; bottom, irrigated cotton.

established with reference to degree of mercerization, tensile strength, classification (the x-ray method is now used by the United States government), elasticity and dyeing properties of cotton; the swelling elasticity, tensile strength, dyeing properties, resistance to enzymatic decomposition, gloss, creasing resistance, refractive index of rayons; and the density, tensile strength, expansion, and shrinkage of wood. The general method can be

illustrated by three varieties of cotton, as in Fig. 312; and the methods for expressing differences in orientations are illustrated in the following table:

| | Irrigated | Eastern | Egyptian |
|--|-----------|---------|----------|
| Tensile strength of cord (kg./sq. mm.).... | 17.6 | 18.3 | 20.0 |
| Height of mode (mm.)..... | 11.4 | 12.0 | 13.35 |
| Percentage of orientation..... | 45.06 | 49.94 | 52.86 |
| Cosine summation factor..... | 85.38 | 87.79 | 88.58 |
| Median..... | 17.83° | 16.41° | 14.38° |
| Mean..... | 27.27° | 25.51° | 24.10° |
| Standard deviation..... | 32.40° | 29.30° | 28.40° |

Thus, the last six types of measurement from the curves run parallel with the practical property of tensile strength. Cotton fibers younger than 25 days show random orientation of cellulose chains. For these very young fibers, even five days old, crystalline cellulose is present, though the patterns may be obscured by effects due to waxes which may be removed by extraction.

X-ray data prove that in cellulose fibers the *b* axes of the crystallites (*i.e.*, the direction of the chains) approach an orientation in the cell wall either parallel to or at some spiral angle to the fiber axis. The types of preferred orientation, always assuming deviation from ideal 100 per cent arrangement, are described by Sisson, specifically for fibers made from bacterial cellulose membranes but generally applicable, as follows:

1. Random.
2. Uniplanar: *b* axes parallel to a plane but at random otherwise.
3. Selective uniplanar (ring fiber): *b* axes parallel to but otherwise at random in a plane; (101) planes have a selective orientation parallel to plane.
4. Uniaxial: *b* axes parallel to fiber axis but planes at random.
5. Selective uniaxial: *b* axes parallel to fiber axes and (101) planes parallel to plane containing fiber axis.

The designation of the three principal interferences for cellulose, and the position of (101) planes, are given in Fig. 313. There are illustrated in Figs. 314*a,b,c,d*, and *e* the sample orientation and directions *A,B,C*; the pole figures (see page 541) with

dotted areas representing projection of b axes, and crosshatched the $[101]$ directions; and the patterns for the three inner interferences (101) , $(10\bar{1})$, (200) from the center out.

By such methods the structures of many fibers and of sheets both natural and deformed have been determined, largely by

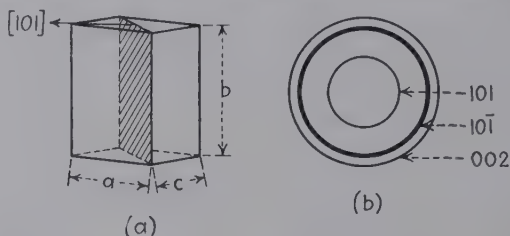


FIG. 313.—The cellulose unit cell with the (101) plane shaded, and the three principal diffraction rings appearing on patterns.

Sisson; for example, in spiral native fibers there is a non-selective orientation, adequately proved by the synthesis of theoretical patterns. Especial attention has been directed to *Valonia* in order to discover the mechanism of cell-wall deposition.¹ It has

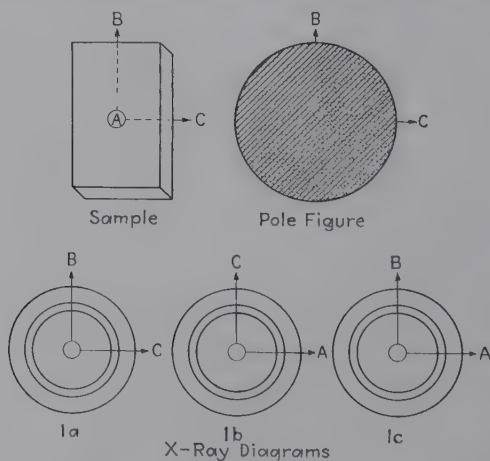


FIG. 314a.—Random orientation in cellulose specimens.

layers in which cellulose chains in any one layer are inclined to those of preceding and subsequent layers at an angle of about 80° ; the chains of one set form a system of meridians in the

¹ ASTBURY, MARWICK, and BERNAL, *Proc. Roy. Soc. (London)*, **109**, 443 (1932); PRESTON and ASTBURY, *ibid.*, **122**, 76 (1937).

roughly spherical cell wall, and those of the other set a spiral closing down on two "poles" (apex and base). The (101) plane of spacing 6.1 A.U. is approximately parallel to the cell wall. It

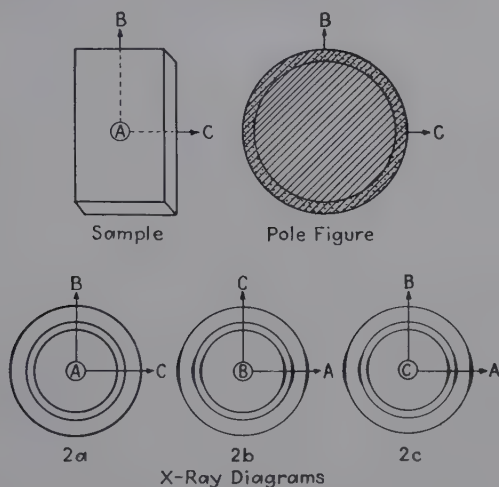


FIG. 314b.—Uniplanar orientation in cellulose specimens.

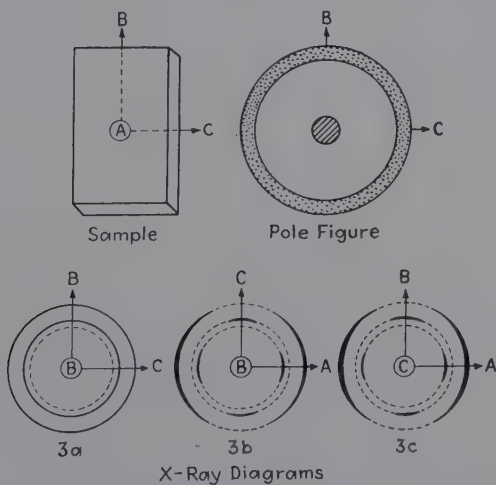


FIG. 314c.—Selective uniplanar orientation in cellulose specimens.

is a general rule that in any sample elongated in one direction the *b* axes are oriented parallel to that direction, and if the sample is constricted in one direction the (101) planes are oriented normal to that direction. Both elongation and shrinkage are

involved in coagulated cellulose (rayons and cellophane): random, swollen state or shrinkage along three axes; uniaxial, by shrinkage along two axes or by elongation on one axis and shrink-

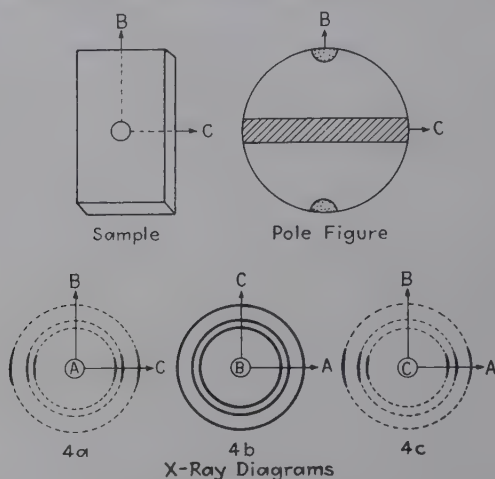


FIG. 314d.—Uniaxial orientation in cellulose specimens.

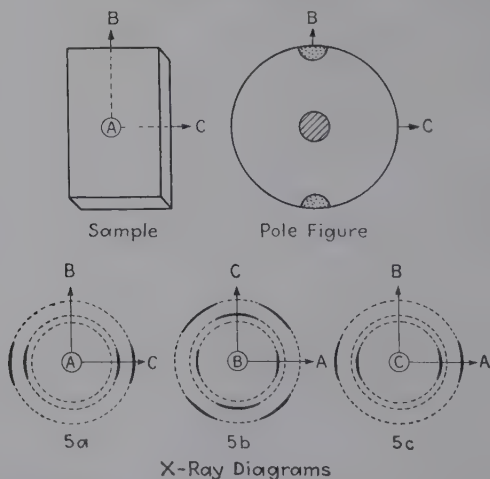


FIG. 314e.—Selective uniaxial orientation in cellulose specimens.

age along two axes; uniplanar, by shrinkage on one axis or elongation on two axes and shrinkage on one axis; biaxial, shrinkage on one and elongation on one. In cellophane, shrinkage occurs perpendicular to the sheet and gives a pattern for selective uni-

planar orientation. Shrinkage is actually more important than stretching elongation in establishing the structure of rayons. Viscose, if spun without tension, has a selective orientation with reference to the fiber surface, rather than the previously considered, highly oriented "skin." The control of the degree of orientation, guided by x-ray patterns, has resulted in vast improvement in the tensile strength, dry and wet, and in other properties of present-day rayon. Figure 315 compares the patterns of old and new products, with the greatly increased degree of fibering.

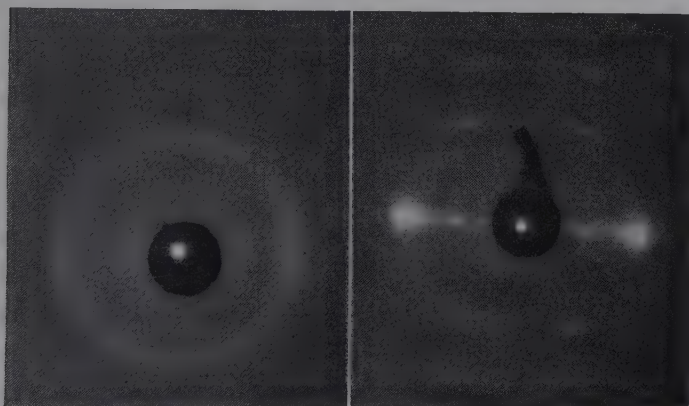


FIG. 315.—Patterns for old (left) and new (right) varieties of rayon, showing great increase in degree of preferred orientation in latter, introduced by tension during coagulation.

Orientation in wood is of great significance since it determines the properties of strength, splitting, swelling, shrinkage, etc. Wood is really two interpenetrating systems of cellulose fibers and of incrustants such as lignin. The crystallites, or chains, of cellulose may be parallel to the fiber axis (producing the usual fiber pattern with intensity maximum on the equator) or at a constant slope to the axis and parallel to each other (producing a "four-point" pattern); or they may deviate considerably from either position, usually the latter. Figure 316 shows typical patterns. The orientation depends on the species of wood, the season of growth (summer wood is denser and more perfectly oriented than spring wood), and the position of growth. Compression wood on the leaning side of trunks or underside of

branches is more perfectly oriented. Ritter and Stillwell¹ have shown that the orientation is random for 1 ft. or more from a growing tip and that complex transition structures occur at junctions with parent branches.

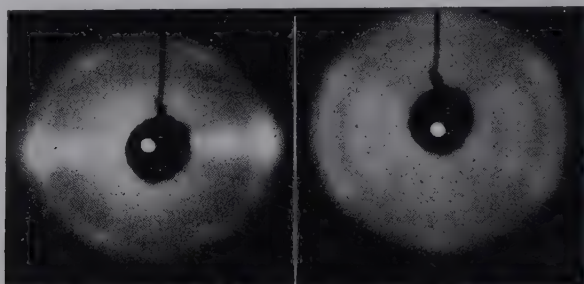


FIG. 316. —Typical patterns for wood, showing wide variations. Left, high-density yellow poplar; right, compression structure on leaning side of tree trunks.

The correlation has been established that woods with cellulose chains parallel to the fiber axis split easily, have high tensile strength, and undergo little longitudinal shrinkage: for example,

| | Average slope, degrees | Average longi- tudinal shrink- age, per cent |
|--------------------|---------------------------|--|
| Redwood: | | |
| Spring wood..... | 30 | 0.3 |
| Summer wood..... | 12 | 0.04 |
| Loblolly pine..... | 40 | 1.2 |

The most recent determination of orientation is that of the minute ray cell.² Instead of orientation of chains parallel with the longer longitudinal dimensions as expected, they deviate 30 deg. from the vertical crosswise direction, thus explaining the considerable swelling and shrinkage in longitudinal and tangential directions.

The orientation of wood fibers in violins is significant in terms of tone. Spruce in the tops is definitely fibered; instruments with the best tone quality show almost complete lack of orientation

¹ *Paper Trade J.*, **98**, 277 (1934); *Physics*, **4**, 167 (1933).

² GROSS, CLARK, and RITTER, *Paper Trade J.*, Dec. 7, 1939.

in the wood used for the back, in contrast with a high degree of preferred orientation in instruments with a harsh tone quality and weak response.¹ A major research project relating structure, aging, varnish, etc., with tone quality is now in progress at Harvard University.

Particles, Micelles, and Fringes.—The structure of cellulose as considered thus far has related primarily to the giant primary-valence molecular chains of the polymer cellulose. The question then very naturally arises as to the next step in organization in the series culminating in the visible fiber or sheet. Four theories will be considered:

1. *Macromolecular Theory.*—As illustrated in Fig. 303 the cellulose fibril, or filament, is a lattice of macromolecules with no

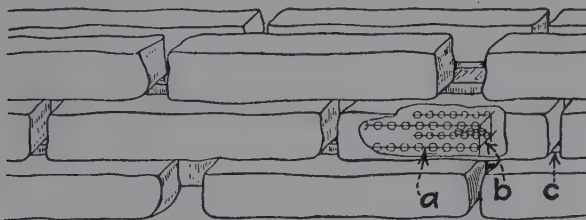


FIG. 317.—The micellar, or crystallite, model of cellulose fiber structure (Seifriz-Meyer-Mark). *a*, Primary-valence chains; *b*, secondary-valence forces holding chains in bundle; *c*, tertiary forces (and cementing material) between micelles.

intermediate stages of aggregation; probably best applicable to synthetic polymers.

2. *Micellar Theory.*—A parallel bundle of cellulose chains undoubtedly would possess crystalline properties. The size of such a bundle would be expected to be within the colloidal range and constitute the micelle (a familiar term introduced initially by von Nägeli in 1858), or crystallite. This concept, the earliest to explain x-ray results on cellulose introduced by the botanist Seifriz and by Meyer and Mark, is illustrated in Fig. 317. Utilizing the Laue equation for particle-size evaluation from the breadths of interferences, Hengstenberg and Mark² determined that the micelle, or crystallite, should be greater than 600 A.U. long and 55 A.U. thick—in other words, should consist of a bundle of chains each with about 100 dehydrated glucose residues.

¹ LARK-HOROWITZ, and CALDWELL, *Nature*, **134**, 23 (1934).

² HENGSTENBERG and MARK, *Z. Krist.*, **69**, 271 (1928).

Primary-valence forces hold the glucose residues in the form of a chain; secondary-valence forces (perhaps hydrogen bonds) hold the chains alongside each other; and tertiary forces or amorphous cementing material between micelles hold them together in a fiber. This structure accounts for a number of the properties of cellulose fibers, particularly the tensile strength conditioned by

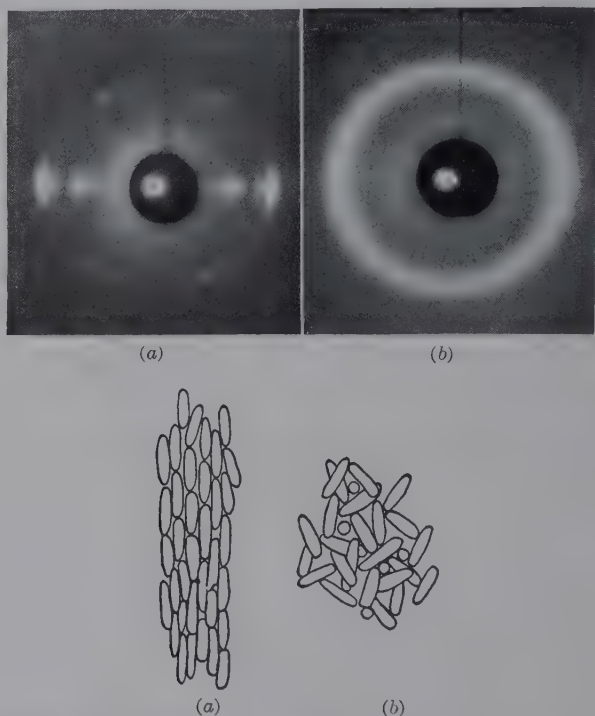


FIG. 318.—Effect of arrangement of micelles on diffraction patterns of cellulose.
(a) Fiber (improved rayon); (b), cellophane sheet.

the pulling apart of the “bricks” rather than by the very high strength residing in the primary-valence bond. Swelling is also explained, for many fibers and sheets can swell in suitable liquids and still produce an unchanged diffraction pattern (intermicellar swelling), while other reagents cause a change in spacings because of penetration between the chains themselves, thus affecting the unit cell (intramicellar swelling). Cellulose is considered to be dispersed in solution in the form of micelles by solution of the

intermicellar material; if the treatment is drastic, the micelles may be broken into fragments, even into single chains which may be greatly shortened, thus lowering viscosity and molecular weight. The disarrangement of micelles into a brush heap is easily distinguished in the x-ray pattern (Fig. 318).

3. *Particle Theory*.—In 1933 Farr and Eckerson announced the isolation of uniform ellipsoidal cellulose particles 1.5 microns long and 1.1 microns in cross section (Fig. 319). X-ray analysis proved that these particles are truly cellulose and that there is no direct evidence of smaller subunits, since the Debye-Scherrer

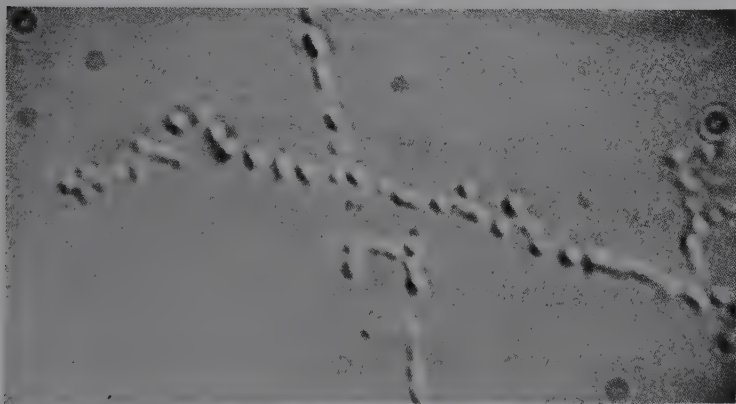


FIG. 319.—Disintegration of cotton fibril into uniform ellipsoidal particles of crystalline cellulose. (Farr and Eckerson.)

rings are sharp and compatible with these particles as single true crystalline entities. Actually it is possible to explain the differential breadths of interferences in fiber patterns used by Hengstenberg and Mark in other ways than as an indication of micellar size. If the particle, as observed in the cytoplasm of very young cotton fibers or from the disintegration, for example, in concentrated hydrochloric acid of a wide variety of mature plant materials, is the unit particle, then the maximum molecular length could be 1.5 microns, corresponding to a molecular weight of about one-half million which agrees with ultracentrifuge measurements on native fibers. A comparison of magnitudes is given in Table LI.

The isolation of these particles and their dispersion in viscose and cuprammonium solutions, in which the particles retain their

identity, as also in regenerated rayons, are a matter of solution of the cementing pectinlike substance, which in turn seems to be largely responsible for the viscosity of cellulose solutions. The existence and significance of these microscopic particles have been the subject of considerable controversy, particularly from the standpoint of observed smaller dimensions in certain growth lamellae. Mrs. Farr in December, 1939, gave evidence for the origin of these particles from the disintegration of rings formed within the plastid, a disk-shaped organ in plant protoplasm. Thus fully formed cellulose particles are discharged into the cytoplasm by the rupture of the membrane of the plastid (usually four particles from each ring), either in the presence or in the absence of chlorophyll and in either native or mercerized form (the latter in the algae *Halicystis*). These particles then form chains end to end, and by compression the cylindrical fibril deposits on the cell wall. Whether or not there are subunits of the uniform particle corresponding to micelles is still uncertain.

TABLE LI

| Units | Glucose residue | Cellobiose residue | Unit cell | Micelle | Particle |
|---------------------------------------|------------------|--------------------|-------------------|------------------|------------------------|
| Glucose..... | 1 | | | | |
| Cellobiose..... | 2 | 1 | | | |
| Unit cell..... | 4 | 2 | 1 | | |
| Micelle..... | 6,000 | 3,000 | 1,500 | 1 | |
| Particle..... | 84×10^8 | 42×10^8 | 21×10^8 | 14×10^8 | 1 |
| Length A.U..... | 5.15 | 10.3 | 10.3 | 500 | 15,000 |
| Cross section A.U..... | | | 8.35×7.9 | 50×50 | $11,000 \times 11,000$ |
| Number glucose residues in chain..... | 1 | 2 | 2 | 100 | 3,000 |
| Molecular weight (single chain)..... | 162 | 324 | 324 | 16,000 | 480,000 |

4. *Net and Fringe Structure*.—The newest theory is in a sense a compromise, but one that has found wide acceptance. As a result of the work of Mark, Kratky, and Frey-Wyssling especially, the "brick" structure representing regular termination of cellulose chains is discarded in favor of an essentially continuous network of longer chains. Over occasional areas these chains may be nearly parallel to form ordered regions corresponding to crystallites, or micelles, which therefore are not discon-

tinuous "bricks" but are bound together with the same long cellulose chains in disorder (Fig. 320).

Various chemical and physical methods, namely, the determination of end groups, osmotic measurements, studies with the ultracentrifuge, viscosities, and x-ray investigations have in

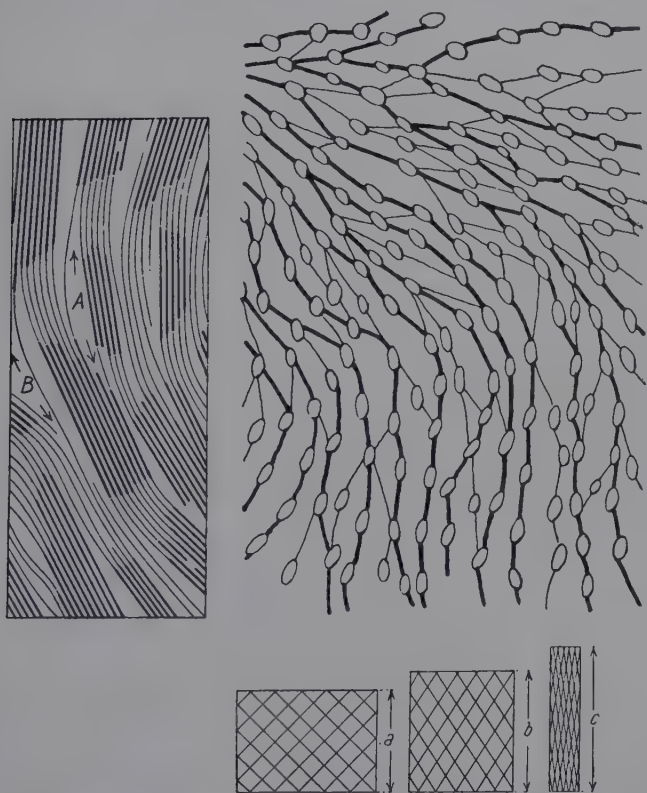


FIG. 320.—Fringe and network structure of cellulose showing ordered regions of parallel molecules and disordered regions corresponding to flexible joints; and the mechanism of extension of a network. (Mark, Kratky, and Frey-Wyssling.)

all cases pointed to the conclusion that the principal valence chains in native cellulose reach a degree of polymerization of at least 2,000. If the chains are assumed to be stiff, they would have a length of 1.5 microns and a diameter of about 7 A.U. If they are considered to be wound into a ball, the diameter would be about 100 A.U. It has been well established experimentally that every technical treatment of native cellulose

causes a certain amount of degradation. Several investigators agree that in the precipitated material of technical threads and films, consisting of cellulose, the degree of polymerization lies between 150 and 500.¹

A rough classification can be established so that it may be stated that samples which consist mainly of chains with a degree of polymerization of 200 or less may be expected to show very poor technical properties, such as tenacity, elasticity, and pliability. An increasing degree of polymerization is accompanied by rapid improvement in the quality until at a chain length above 700 or 800 (see page 599) there seems to be no further direct influence on the tensile strength of the material. In order to explain more fully these observations it is useful first to consider the cellulose sample as built up from chains of infinite length into an ideal material. In order to tear this fiber or film, it is necessary to rupture all the single chains contained in a given cross section. It is possible to estimate the energy required to do this, if the tensile strength of the principal valence bond is known.²

The modulus so calculated is 800 kg. per square millimeter. It is an interesting fact that Meyer and Lotmar have measured very carefully the modulus of elasticity for different fibers and have found actually several specimens, which gave values corresponding very closely with the figures for an ideal sample of infinite chain length. It is difficult to understand why chains of finite length should have properties so closely in agreement with an ideal cellulose built up of infinitely long molecules. Every chain in the real sample must have an end somewhere, and obviously this point should be a weak spot potentially where a break may take place without a rupture of the primary-valence chain itself. This paradoxical situation is explained diagrammatically in Fig. 320. In considering two molecule ends it is apparent that if they are not inside a crystallized region in the material, under the influence of a stress, they might be separated from each other quite easily inasmuch as they are held together only by weak molecular forces. The work required to separate them would be small, and consequently the tensile

¹ KRAEMER, *Ind. Eng. Chem.*, **30**, 1200 (1938).

² MARK, "Physik und Chemie der Cellulose," p. 59, Berlin, 1932.
MEYER and LOTMAR, *Helv. Chim. Acta*, **19**, 68 (1935).

strength of the sample should be low. On the other hand, when the ends of the two molecules lie inside a crystallized region of one micelle, then they are kept in their positions not only by the forces between the ends, but also by the van der Waals forces along the two lengths. In order to separate the two molecules, it is necessary to pull them out of the lattice and to overcome all the forces along the length with which they are held inside the crystallized region. If the parts of the main valence chains, which belong to the micelle, are long enough, then the total energy required to pull them out of this range will be great, because the two ends of the chains are entirely concealed in the center of the micelle and do not form on this account a potential weak spot for the rupture of the filament. In this way, the micelles in the cellulose may play a role similar to that of carbon-black particles in rubber, which pick up the loose ends of the rubber hydrocarbon chains on their surfaces and thus fortify the structure, which might be otherwise potentially very weak.

It is clear that, if the length of the chains approaches the length of micelles, it will frequently occur that the end of a chain will coincide with the end of a micelle, with the result that the tensile strength of the sample will be determined by the weak secondary-valence forces.

It may now be asked at what length the chain will coincide with the linear dimensions of the micelle. The measurements on the length of the crystallized regions in cellulose have been deduced by Hengstenberg and Mark¹ from the widths of interferences on x-ray diffraction patterns. For the samples of cellulose under stress, the average length was found to be larger than 600 A.U.

Very recently Kratky and Mark² have applied the method of Frey-Wyssling to elucidate this problem further. In this method small metal crystals, usually gold, are deposited inside cellulose fibers, which are then subjected to x-ray diffraction analysis. These patterns are distinguished by the evidence of blackening of the photographic film at very small angles in the neighborhood of the primary beam. The marked intensity of scattered radiation at very small angles close to the primary beam indicates that something like a lattice with very large

¹ *Op. cit.*

² *Protoplasm*, **25**, 261 (1936); **26**, 75 (1936); **27**, 372, 563 (1937).

spacings is built up in the process of distribution of the heavy metal particles in the cellulose fiber. From this intensity distribution, it is possible to derive approximately the dimensions of the micelle in the material under stress. These measurements give values for the crystallized regions of 700 to 1000 A.U. in length, on the average, and 50 to 70 A.U. as the diameters. As mentioned above, a definite drop in tensile strength is observed if the degree of polymerization falls below about 200. A single glucose residue has a length of about 5 A.U. so that a degree of polymerization of 200 means a chain length of about 1000 A.U. A comparison of this value with the average length of the micelle proves at once that the decrease in tensile strength takes place when the average length of the cellulose chains equals the average length of the crystallized regions. When the chains are five times longer (polymerization degree 1,000), then the chain ends have a greater probability of being concealed inside the micelles and, consequently, the tensile strength approaches the maximum value as measured by Meyer and Lotmar.

It may now be concluded that the crystallized portions of the structure are the reinforcing backbone of the structure while the unordered regions may be regarded as the weak spots. If a film is soaked with water, the x-ray evidence shows that there is no change in the crystallized regions and that the water penetrates only the amorphous material which is built up by the fringes of the micelles. If chain ends occur, as they frequently do, in these swollen areas, then tensile strength will be a very sensitive function of swelling. The wet strength of cellulose fibers depends, therefore, to a large degree upon the average length of the chains; for the longer the chains are, the larger the amount of crystallized material and the smaller the chance of chain ends occurring in the unordered network of the fringes.

From this point of view, instead of distinguishing between intermicellar and intramicellar swelling, it is better to speak of entrance of water into the fringes or into the crystallized regions or micelles themselves.¹

This conception of cellulose structure indicates that the *physical properties*, tenacity, elasticity, etc., are functionally

¹ HERMANN, *Kolloid-Z.*, **81**, 143, 300 (1937); **82**, 58, 83, 71 (1938).

related to the amount of crystalline material, whereas the *reactivity* of the fiber, swelling, drying, ease of chemical reactions, etc., is to be associated with the amorphous parts. The relative frequency and the length of the micelles depend upon the average chain length; hence, this in turn determines in large measure both physical and chemical properties.

The question now arises of what molecular changes accompany a macroscopic deformation of a film or filament. In commercial practice a cellulose material is formed in a swollen state. The water between the chains in the fringe areas gives to these regions between the stiffer crystallized micelles the role of joints which impart to the whole system a certain amount of flexibility. Thus, it is justifiable to visualize a swollen fiber as a flexible network in which the crystallized regions represent the stiff links and the fringe ranges, the bendable joints (Fig. 320). Kratky¹ has shown that increasing preferred orientations of mechanically treated films and fibers can be followed closely with calculations based upon such an assumption. Recently Hermanns² has obtained further experimental checks in studies of the extension of cellulose hydrate filaments.

One of the outstanding consequences of the conception of a flexible fringe work is the fact that a threadlike system built up by such a structure can undergo, at the maximum, an extension of 100 per cent, whereas a film cannot be extended more than 57 per cent. In fact, hydrate cellulose films and sheets that have been investigated have never exceeded this limiting value for their extensibility. By following up the continually rising parallel orientation of the micelles by means of x-rays and polarized light, the plastic deformation of swollen fibers can be explained by the conception of a flexible network.

In order to understand the mechanical behavior of high molecular-weight systems, it is not sufficient to believe that more or less extended and tightly constructed elongated particles are present. Nor is it sufficient to assume that homogeneously dispersed long-chain molecules undergo the flow of plastic deformation. It is necessary to visualize a *mixture of both*, a combination of crystallized ranges with many chain ends emerg-

¹ *Kolloid-Z.*, **64**, 213 (1933); **68**, 347 (1934); **70**, 14 (1935); **80**, 139 (1937); **84**, 149 (1938).

² *Ibid.*, **86**, 245 (1939).

ing from their surface so that they are embedded in an amorphous movable medium formed by the flexible fringes.

The total behavior of the system is influenced by the following:

1. The relative amounts of crystallized and amorphous fractions.
2. The ratio between the average length of the main valence chains and the average length of the crystallized regions.
3. The flexibility of the fringe and its sensitivity to swelling and chemical reactions.

Diffraction of X-rays at Very Small Angles by Celluloses and Rayons.—From the writer's laboratory have been reported the measurements of very large spacings for a number of natural materials. These include 171 A.U. in living nerve,¹ 440 A.U. in collagen, 48 A.U. for radially oriented natural wax in intestinal wall collagen,² 81 A.U. in keratin, 58 A.U. in gel rubber, and 75 A.U. in chitosan.³

By extending the experimental technique to its fullest possibilities, attempts have been made to resolve interferences at very small angles corresponding to very large spacings in cellulose and its derivatives. In most of these cases there is a definite but somewhat diffuse scattering at very small angles. Equatorial maxima run out from this halo like small arrowheads; but in spite of ingenuity in obtaining the very sharpest possible patterns, it has been impossible to resolve these equatorial streaks into a series of individual spots. There are, however, some very interesting characteristics of this phenomenon.⁴

Figure 321a is a diagrammatic representation of the innermost part of a diffraction pattern for native ramie. A continuous streak runs along the equator from the central spot of the pattern, which is widest at the smallest angles and tapers gradually to a nearly constant width of blackening on the film. The greatest intensity seems to be reached at a spacing of about 40 A.U., followed by a rapidly diminishing intensity down to about 20 A.U. The obvious explanation of this pattern seems to be that a whole range of lateral spacings between macromolecules, crystallites, or micelles occurs. The greater this spacing is,

¹ *Radiology*, **25**, 131 (1935).

² *Radiology*, **27**, 339 (1936).

³ *J. Am. Chem. Soc.*, **57**, 1509 (1935); *J. Phys. Chem.*, **40**, 863 (1935).

⁴ CLARK and PARKER, *Science*, **85**, 203 (1937).

i.e., the smaller the angle, the less perfect is the longitudinal arrangement along the length of the chains in the crystallites so that the resulting diffraction effect is increasingly more diffuse or wider.

In Fig. 321*b* is represented the innermost part of the pattern of mercerized cellulose dried under tension so that the greatest preferred orientation can be gained. The same equatorial streak can be observed as with the original native ramie, but now it is very sharp and uniform in width until it merges with the trace of the undiffracted beam. The marked effect, therefore, of

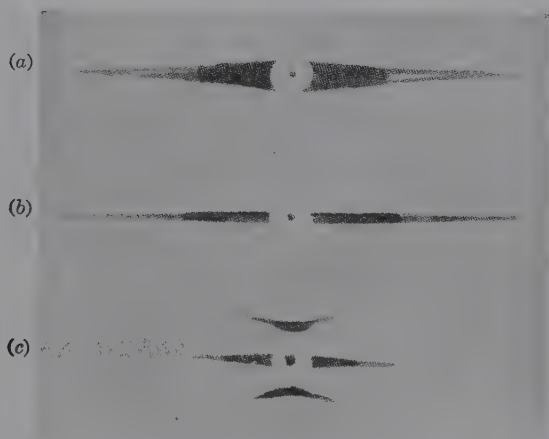


FIG. 321.—Diagrams of diffraction effects at very small angles of fiber pattern. (a) Native ramie; (b) mercerized ramie dried under tension; (c) regenerated cellulose rayons (nitro, cuprammonium, viscose).

pulling the chains more nearly parallel to each other is directly indicated.

Figure 321*c* represents an entirely new finding for rayon. With the most careful technique involving very small pinholes, careful blocking of the primary beam, vacuum camera, and similar details, we find for all regenerated cellulose rayons, including nitro, cuprammonium, and viscose, the production of a very sharp equatorial streak and very definitely a first layer line on either side from which can be measured a fiber identity period of 154 A.U. Acetate rayons do not give this pattern but only a fairly diffuse general scattering around the central spot. The progression in regularity of structure from native ramie to

mercerized ramie when dried under tension and then to commercial rayons seems to be clearly indicated by these curious unresolved diffraction maxima at very small angles.

Topochemical Reactions of Cellulose as Revealed by X-rays.—

Mercerization of cellulose is the first example of a topochemical reaction, *i.e.*, the conversion of one crystal form into another in a fiber without destroying or indeed even seriously affecting the fiber in over-all structure or strength. Now almost all reactions of cellulose are topochemical in the same way. This, of course, is exactly what should be expected for crystal particles that are embedded in a usually less resistant matrix.

At the present time a large amount of work is being done on *changes* in structure of cellulose—a familiar process in chemistry for a system concerning which for a given steady state there is a limited amount of information. Nitration and acetylation, important commercial processes, are topochemical reactions in that the original fibrous form of cellulose may be retained without disintegration during esterification. Another point of interest shown by x-ray patterns is the irreversibility of some reactions. When an attempt is made to determine the point of equilibrium in chemical treatment of a fiber by an approach from both sides (building up and decomposing or concentrating and diluting a reagent in contact with cellulose), a very considerable hysteresis effect is shown. Starting with cellulose and hydrazine, the former will be in equilibrium up to 38 per cent solutions of hydrazine and still show only the cellulose pattern. In decomposition of the cellulose-hydrazine complex, the interferences show the structure of the complex from 63 to 20 per cent solutions. Hess has shown that mercerized cellulose gives the pattern of natroncellulose III in NaOH solutions under 11 per cent; natroncellulose I, 12 to 26 per cent; and natroncellulose II, above 28 per cent. In dilution experiments the last pattern appears down to 2.16 per cent solutions. These and similar experiments have thrown considerable light on the mechanism of these crystallite-heterogeneous reactions. In the building up of a cellulose compound the molecules of the reagent must pass into the interior of the crystallite, or micelle, *through* layers of the solid reaction product, whereas in dissociation by dilutions of the outer reagent the transport from the interior of the crystallite of the dissociated molecules corresponding to the original reagent must take place

through layers of the solid disintegration product. This micellar-heterogeneous reaction is illustrated in Fig. 322. The surface layers are too thin to allow registration on diffraction patterns. Although mono- and diesters should be expected as intermediate products, they usually are not identified by x-ray patterns. The chemical action on the three hydroxyl groups of cellulose to a final triester is entirely completed in a given layer before the reagent reaches the next molecular layer. Intermediate products would appear then only at interfaces and on geometric grounds

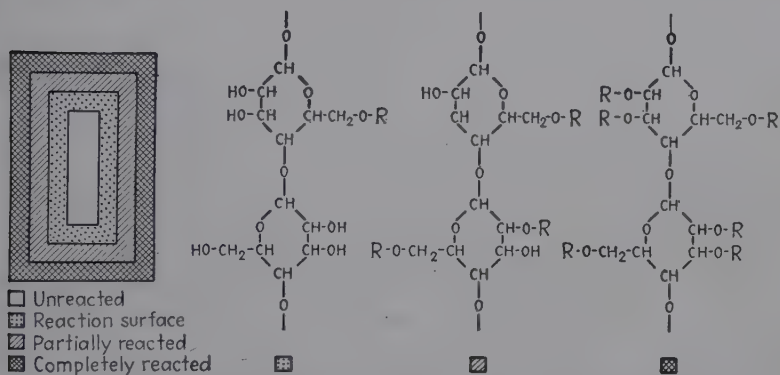


FIG. 322.—Diagram of a heterogeneous micellar reaction. The cross section of a micelle, in which the reaction has progressed to a greater degree on the outside layers, and the probable degree of reaction of the cellulose chain in the different layers are illustrated.

could not be roentgenographically expected. On the other hand, if the ratio of speed of diffusion of the reagent into the cellulose particle to the speed of reaction is high, then intermediate products might be formed in second, third, fourth, etc., molecular layers before reaction is completed in the first layer. Only recently, therefore, distinctive patterns have been obtained for the hemimethylate of cellulose ($10\text{CH}_3/2\text{C}_6$) and dinitrocellulose. In some cases, especially for substituted products lower than triderivatives, very diffuse patterns are obtained. Hess has shown that one reaction product may be separated from another (for example hemimethylate from trimethyl cellulose) by extraction, so that both fractions then give characteristic sharp patterns. Stretched films of "amorphous" nitrate or acetate may yield evidence of fibering, called pseudocrystalline; actually a proportion of randomly oriented crys-

tallites, undetected before stretching, are brought into more easily detected parallel orientation.

Polymorphism of Cellulose Derivatives.—The x-ray method is making possible the identification of a growing list of polymorphic compounds (usually dimorphic). The formation in the fibrous state depends on the choice of conditions of temperature, concentration of reacting compounds, etc.; once formed a given modification in fibrous form cannot in general be converted into another form. For example, fibrous acetylcellulose I is formed under 35°C., acetylcellulose II above 50°C., and a mixed diffuse pattern for the product at 35 to 50°C. These facts may be considered a proof that even in solution the particles are present in colloidal dispersion and that reactions are of the heterogeneous type mentioned above. The dimorphism may be of a type of certain keto-enol tautomeric relations for organic compounds which depend on the nature of the solvent for the equilibrium point. Dimorphism has been found not only for cellulose (when native cellulose goes over to so-called cellulose hydrate through a series of intermediate compounds) but for the HClO_4 compound, copper-alkali cellulose, acetone nitrocellulose, a complex with a solvent or swelling agent, acetylcellulose and many others. A whole series of new compounds has been made possible from the complexes with solvents (ketones especially). Thus, xylol will not combine with nitrocellulose directly but will displace acetone in acetone nitrocellulose or will react in the presence of acetone acting as a catalyst. All these identifications have been made possible by the roentgenographic method. In general one form is related to native cellulose, the other to mercerized cellulose. There are four forms of so-called natroncellulose. With 11 to 18 per cent NaOH cellulose gives form I (with 6 H_2O water of crystallization); above 22 per cent form II, anhydrous, is identified. Form I when dehydrated does not give II, but another form III. Form III, as previously stated, is produced when mercerized cellulose is treated with less than 11 per cent solution of NaOH .

The compound $1\text{NaOH}/2$ glucose has been classed as pseudo-stoichiometric since only the micellar-surface hydroxyl groups (about 50 per cent) are first affected. Many other reactions are considered in a thorough summary by Sisson¹ of the x-ray diffraction behavior of cellulose derivatives.

¹ *Ind. Eng. Chem.*, **30**, 530 (1938).

The Swelling of Cellulose.—The great contributions of x-ray diffraction to classification of swelling phenomena already have been mentioned. Four types of swelling have been described:

1. Intermicellar. No change in x-ray pattern as cellulose + water.

2. Intramicellar. The interferences shift in position, a fact indicating a change in spacing with penetration of the agent into the lattice. Ammonia produces a great swelling and increase in the (101) spacing from 6.1 A.U. in native cellulose to 10.3. Quaternary ammonium hydroxides with still larger molecules increase this spacing as high as 16.7 A.U., the *b* (fiber-axis) spacing remaining always constant at 10.3 A.U. Swelling of intercrystalline material is responsible for marked increase in fiber diameter.¹

3. Permutoid. A complex formation that completely changes the pattern as inulin or agar + water. This might easily be classed as a special case of (2).

4. Osmotic. The swelling agent diffuses through a skin or membrane into the interior giving an essentially amorphous pattern, as for some proteins such as nerve fibers and copper-alkali cellulose, and Brownian motion of the semifluid interior.

Some interesting special cases of swelling are the formation of the Knecht compound with nitric acid (oxonium combination on the oxygen bridge); and reaction with LiSCN. In swelling in LiSCN/H₂O = $\frac{5}{1}$, an identity period is obtained that is ten times the 5.1-A.U. length of a C₅H₁₀O₅ group. This means either short molecules or some peculiar regulatory principle in the addition of groups to the long cellulose chains which gives a repeating identity along the fiber.

Starch.—Native starches give one of three types of powder diffraction pattern called *A*, *B*, and *C*, though *C* is probably a combination of *A* and *B*. All efforts to orient starch molecules by pressure or by drawing out fibers have been unsuccessful; consequently it has not been possible as yet to derive a reliable interpretation of structure. Starch is a rather low condensation product of α -glucose forming rings, whereas cellulose is formed linearly from β -glucose.

On precipitation by alcohol from water all starches give a *V* pattern, varying from very diffuse interferences to a sharper

¹ CLARK and PARKER, *J. Phys. Chem.*, **41**, 777 (1937).

SISSON and SANER, *ibid.*, **43**, 687 (1939).

pattern for starch paste after drying. Samples of starch from various organs of the same plant species may show different types of the *C* or *B* pattern; a solution of starch gives instead of *V* the *B* pattern on evaporation at 20°C., *A* at 60°C., and *C* at intermediate temperatures. The spacings, intensities, and types of starch giving each pattern are as follows:

| A | B | C |
|----------------|----------------|---------------|
| 5.79 <i>m</i> | 15.77 <i>s</i> | 11.6 <i>w</i> |
| 5.02 <i>s</i> | 8.34 <i>vw</i> | 7.05 <i>m</i> |
| 4.42 <i>m</i> | 6.25 <i>m</i> | 4.5 <i>m</i> |
| 3.76 <i>s</i> | 5.79 <i>m</i> | |
| 3.40 <i>w</i> | 5.15 <i>s</i> | |
| 2.62 <i>vw</i> | 4.52 <i>m</i> | |
| 2.33 <i>vw</i> | 4.04 <i>m</i> | |
| 2.07 <i>vw</i> | 3.69 <i>m</i> | |
| 1.90 <i>vw</i> | 3.38 <i>w</i> | |
| | 2.87 <i>w</i> | |
| | 2.58 <i>vw</i> | |
| | 2.33 <i>vw</i> | |

Intensities: *s*, strong; *m*, medium; *w*, weak; *vw*, very weak.

The types of starch giving each pattern are:

A: Wheat, maize, rice, rye, millet, ipomoea tjalappa (tropical morning glory), *Arum escul.*

B: Potato, *Canna indica*, *Canna edulis*, fritillaria, *Curcuma angustifolia*, *Musa paradisiaca* (type of banana), *Dioscorea alata*, *Arracacia escul.*, *Jatropha manihot*, *Araucaria brasil*, xuxu (Brazilian cucumber), edible chestnut.

C: Sago, maranta, cassava, pea, bean, lentil, sweet potato, *Arenga pinnata*, *Colocasia escul.*, *Manihot utiliss.*, *Arum maculatum*.

Other Polysaccharides.—Xylan, mannan, inulin, agar, glycogen, lichenin, pectin, etc., have all been subjected to diffraction study, but in the absence of single-crystal or good fiber patterns no molecular interpretations have been possible as yet. Humidity and swelling have a marked effect. Pectin forms films on drying with a marked selective orientation indicating crystallites in the form of thin tablets 22 A.U. thick.

Lignin.—This complex substance, which plays so important a role in wood structure, gives in all cases a very diffuse pattern

mental vital process that is so little known, the protoplasmic secretion.

Chitin.—Chitin is the compound that makes up most of the organic part of the skeletons of Arthropoda. In the animal kingdom, to which it is limited with very few exceptions, it occurs only in the invertebrates. In addition to forming the exoskeletons of insects, Crustacea, etc., it is the major constituent of the lenses of the eyes, the tendons, and the linings of the respiratory, excretory, and digestive systems.

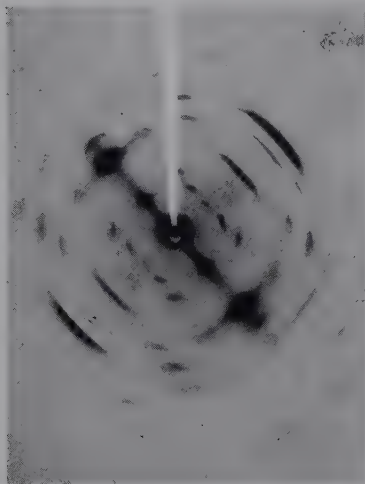


FIG. 324.—Fiber pattern for chitin, comprising the mandibular tendon of lobster.

Chitin is remarkably similar to cellulose in formation of long carbohydrate chains except that it contains nitrogen, thus moving a step toward the familiar proteins of the vertebrate world. Figure 323 shows the formula of the acetylglucosamine residue

which is to be compared with cellulose in Fig. 304.

Chitin produces very rich fiber diffraction patterns (Fig. 324) from which is deduced the crystal structure.¹ This is probably orthorhombic with the unit cell dimensions (Fig. 325).

$$\begin{aligned}a &= 9.25 \text{ A.U.}, \\b &= 10.46 \text{ A.U.}, \\c &= 19.25 \text{ A.U.}\end{aligned}$$

As laid down in sheets the only orientation is that the b axes are parallel to the surface. At a temperature of 200°C. chitin forms a definite addition compound with lithium thiocyanate, while at lower temperatures intramolecular swelling occurs. Various fractions of chitin nitrate have different average lengths of the carbohydrate chain. Chitin nitrate is orthorhombic with

¹ CLARK and SMITH, *J. Phys. Chem.*, **40**, 863 (1936).

MEYER and MARK, *Ber.*, **61**, 1936 (1928).

MEYER and PANKOW, *Helv. Chim. Acta*, **18**, 589 (1935).

$$a = 9.2 \text{ A.U.},$$

$$b = 10.3 \text{ A.U.},$$

$$c = 23.0 \text{ A.U.}$$

A whole series of compounds is formed with sodium hydroxide, but it is difficult to isolate pure compounds and to obtain sharp patterns because of hydrolysis.

Chitosan is the compound formed by hydrolysis of half the acetyl groups in chitin. When formed from a sheet it undergoes a change to a more restricted orientation such that the 002 planes

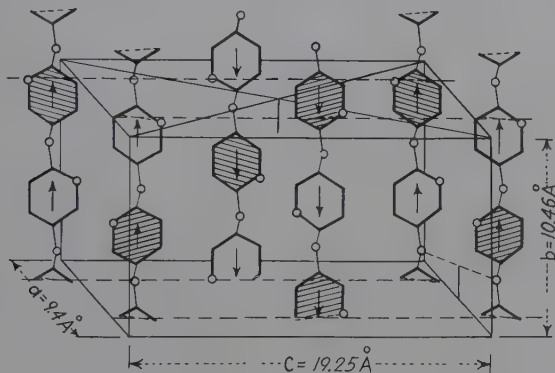


FIG. 325.—The crystal unit cell of chitin.

become parallel to the surface of the sheet. The unit cell of chitosan (monoclinic) has the dimensions

$$a = 8.9 \text{ A.U.},$$

$$b = 10.25 \text{ A.U.},$$

$$c = 17.0 \text{ A.U.},$$

$$\beta = 88^\circ.$$

Like chitin, chitosan forms a long series of interesting addition compounds with distinctive patterns. While chitin gives a continuous series of long equatorial spacings like cellulose, chitosan produces resolved maxima in several orders corresponding to a definite lateral spacing between molecular chains or crystallites of 75 A.U. This spacing increases markedly upon swelling in dilute alkali.

Rubber.¹—When unstretched rubber is examined by x-rays, it produces a blurred ring, the halo that is typical of the amorphous

¹ From a paper by the author, *Ind. Eng. Chem.*, **31**, 1397 (1939).

or liquid state. Its behavior when stretched was first reported by Katz¹ who observed interference spots at 80 per cent elongation. Their intensity increased with increasing elongation, and at 400 per cent a definite fiber diagram was observed. Consequently, rubber when extended was considered to be crystalline, and the Joule effect to result from an actual formation of crystals (Fig. 326).

The behavior of stretched rubber between 80 and 1,000 per cent elongations was investigated by Hauser and Mark² who made a more accurate study of the positions and intensities of the

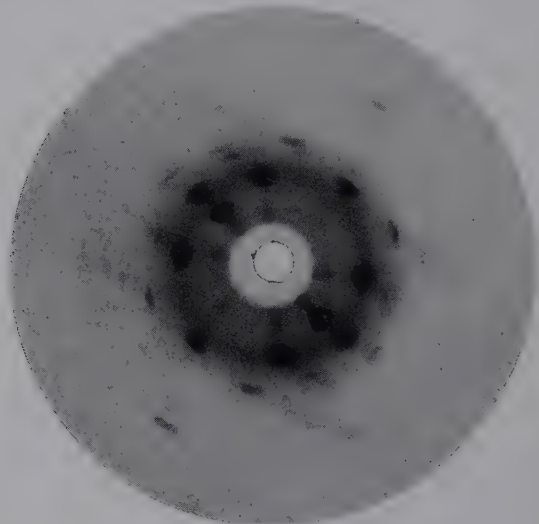


FIG. 326.—The crystal fiber pattern of stretched rubber.

interferences. The positions of the interferences were found to be independent of the degree of stretching, but their intensities increased proportionally with it. The position of the amorphous ring remained unchanged during extension, but its intensity decreased with continued elongation. Therefore, an amorphous or liquid phase in unstretched rubber was supposed to be changed to a crystalline phase when it was stretched. The positions of the interferences, which depend on the dimensions of the unit cell, did not change with continued stretch, and consequently a definite space lattice was indicated. Other evidence showed that

¹ *Kolloid-Z.*, **36**, 300; **37**, 19 (1925).

² *Kolloidchem. Beihefte*, **22**, 63 (1926).

new crystalline units were constantly produced during elongation and that the major axis of the crystalline phase was oriented parallel to the direction of stretch. The interferences in stretched rubber disappeared at 60°C. When rubber was maintained in an extended condition for some time, the interference spots vanished. If rubber was milled or swollen by solvents before stretching, the interference spots did not appear.

Three-dimensional or "higher" orientation in rubber can be produced in sheet specimens¹ in which the width decreases less than the thickness on stretching. With this additional information a recent paper by Lotmar and Meyer² reports accurate measurements of the structure of crystallized rubber. The unit cell was derived by the graphical method of Sauter, is monoclinic, and has the following axes:

$$\begin{aligned}a &= 8.54 \pm 0.05 \text{ A.U.}, \\b &= 8.20 \pm 0.05 \text{ A.U. (fiber axis)}, \\c &= 12.65 \pm 0.05 \text{ A.U.}, \\\beta &= 83^\circ 21'.$$

Volume of unit cell = 880 A.U.³ approximately.

They report 7.6 molecules per unit cell, and this value is based on the highest value of density (0.965) reported in the literature. Eight molecules are assumed to be present. By an elimination of possible space-groups, there remains the probable one $P2_1/c$ and the chains are presumed to have the symmetry of a twofold screw axis. The crystallite is said to be a molecular racemate of right and left spiral molecules.

Sauter³ in Staudinger's laboratory disagreed with the assignment of indices to interferences in the patterns of Lotmar and Meyer, as was also the case with cellulose. Sauter assigned the following values for the rubber unit cell:

$$\begin{aligned}a &= 8.91 \text{ A.U.}, \\b &= 8.20 \text{ A.U. (fiber axis)}, \\c &= 12.60 \text{ A.U.}, \\\beta &= 90^\circ \text{ (orthorhombic)}.$$

¹ MARK and VON SUSICH, *Kolloid-Z.*, **46**, 11 (1900); *Z. physik. Chem.*, **4**, 431 (1929).

CLEWS and SCHLOSSBERGER, *Proc. Roy. Soc. (London)*, **164**, 491 (1938).

GEHMAN and FIELD, *J. Applied Phys.*, **10**, 564 (1939).

² *Monatsh.*, **69**, 115 (1936).

³ *Z. physik. Chem.*, **B36**, 405, 427 (1937).

A pattern made on Sauter's conical camera is reproduced in Fig. 327.

This proposal was disproved in the laboratory of Meyer in Geneva. The correctness of the Lotmar and Meyer proposed structure for rubber has been verified in the writer's laboratory by the same conclusive methods as were employed in the test of the alternative structures proposed for cellulose.

Crystal interferences in frozen, unstretched smoked sheet were found by Hauser and Rosbaud.¹ They were indicated

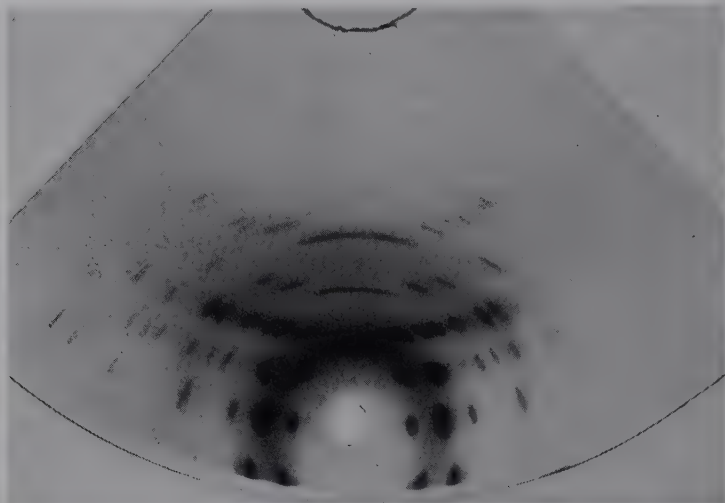


FIG. 327.—Pattern for stretched rubber on conical film by Sauter technique, permitting rapid indexing of interferences.

by Debye-Scherrer rings. Later von Susich constructed a melting curve from the behavior of patterns of frozen rubber at different temperatures. With unstretched rubber the powder pattern disappeared completely at approximately 35°C. and with stretched rubber at about 90°C. Above 90°C. the pattern was that of an amorphous material. Indices were assigned to four rings in the frozen-rubber pattern, but no spacings or calculations were mentioned.

Subsequent to the work of Lotmar and Meyer, Barnes² examined two samples of frozen crude rubber, one of which

¹ *Kautschuk*, **3**, 17 (1927).

² *Can. J. Research*, **15**, 156 (1937).

had remained frozen for 22 years and the other for at least 11 and probably for 30 years. They lost their opacity at approximately 41°C. The measurements of Barnes agree excellently with those reported by Lotmar and Meyer for stretched rubber. Identical patterns were obtained from each specimen.

In cooperative researches between the National Bureau of Standards and the x-ray laboratory at the University of Illinois, patterns have been made under extraordinarily careful conditions for sol, gel, and total rubber, both unstretched and stretched and when crystallized by freezing and from solutions.¹ For the latter specimens, temperatures below -80°C. were maintained in the x-ray cameras during exposures. Total rubber when stretched and exposed to an x-ray beam produced the characteristic crystal fiber pattern. Stretched sol rubber produced no evidence of this pattern even at 1,000 per cent elongation. With stretched gel rubber, the pattern was formed above 100 per cent elongation and at 200 per cent was sharp and intense. A large interplanar spacing of 54 A.U. (or $2 \times 54 = 108$ A.U.) found in the unstretched gel was absent in the sol. The patterns obtained with stretched gel (crystal fiber), with frozen sol, gel, and total rubber (Debye-Scherrer rings indicating small randomly oriented crystals), and with gel and sol crystals produced from solution all gave the same crystal-structure results, in excellent agreement with those reported by Lotmar and Meyer. The general conclusion from all these experiments and many others not specifically mentioned is that rubber consists of long chains of isoprene units. In the stretched state these molecules are extended and oriented in parallel fashion and thus produce crystal fiber patterns. In the non-extended state rubber behaves as a liquid, and its diffraction pattern is that of a liquid (page 476). But the question remains unanswered of whether the molecules themselves are folded or like springs in the unstretched state so that the extensibility of rubber is the result of the extensibility of these springs or whether they are fully extended and extensibility results from the bending and flexing of a tangled aggregate of chains. Another related question is whether molecules act separately or in bundles, or crystallites. Simple spirals, distorted spirals, or some form of folding have been proposed frequently and have principal

¹ *J. Research Nat. Bur. Standards*, **19**, 479 (1937); **22**, 105 (1939).

support from the analogy of proteins shown by Astbury to exist in folded, extended, and supercontracted forms. Thus folding of protein chains accounts for the noncrystalline diffraction halos for globular proteins which in the process of denaturation tend to unravel and unfold and approach the condition of elongated molecules. During elongation these molecules must first orient properly in order to extend in the direction of elongation. A considerable difficulty arises in explaining on this basis how the spirals become elongated in unstretched frozen rubber to form definite randomly oriented crystals with the same fundamental lattice dimensions as those derived from the fiber crystal patterns of stretched rubber.

Another proposal by Hermann and Gerngross¹ considered rubber to be bundles of extended molecules that run almost parallel over part of their length as a network and through curved and disorganized fringes in other parts. Elasticity and pliability would reside in these fringes. This allows for preexisting crystallites, or bundles, though not detected by x-rays in unstretched rubber except after standing at low temperatures. This picture described in detail on page 620 was recently applied with great power to the structure of cellulose by Mark, but of course cellulose is crystalline and composed of extended chains in the natural unstretched fibers.

One of the earliest concepts was a tangled snarl of long thread-like molecules in ordinary liquid rubber which can be pulled into parallel alignment. This has been subjected with some success to thermodynamic and mechanical analysis. There are numerous modifications of kinked chains in random orientation from thermal agitation, although an explanation of long-range elasticity of rubber is lacking.

The most extensive theory of structure proposed after the advent of the x-ray data was that of a two-phase system. Gel rubber forms a three-dimensional network soaked with liquid sol rubber of lower molecular weight. These micelles, or crystallites, of bundles of chains then preexist in unstretched rubber, but swelling and distortion destroy the possibility of crystal interferences until extension squeezes out the sol phase. That rubber can be fractionated into a gristly ether-insoluble gel phase and an easily extensible ether-soluble sol phase cannot be denied.

¹ *Kautschuk*, **8**, 181 (1932).

The chief objection which has been raised to this rubber model is that it begs the issue as to what is the cause of long-range extensibility in the solid network, though nothing is to prevent slipping of adjacent crystallites in the semifluid phase as a lubricant.

The observation by Clark, Warren, and Smith¹ that pure sol rubber prepared at the National Bureau of Standards and protected against oxidation by extraordinary precautions fails to produce a fiber pattern even at 1,000 per cent elongation, whereas gel rubber and total rubber indicate crystalline organization at less than 200 per cent elongation, seems a significant point in favor of the two-phase concept.

If crystallites, or micelles, exist in rubber, then it should be possible to ascertain something about the size and shape from the measurement of the breadth of the x-ray crystal interferences. It is well known that these interferences broaden as particle size decreases in the colloidal range and that Scherrer, Laue, Brill, and others have provided the necessary fundamental formulas which are theoretically sound and have been verified by direct experiment. By this means Hauser and Mark² first determined that the length of the lattice in the fiber axis and thus the average length of crystallites was 300 to 600 A.U. and that the breadth and thickness were as high as 500 A.U., in contrast with the narrower bundles (50 A.U.) in cellulose; thus they correspond to 80,000 to 150,000 isoprene units in a crystallite. The breadths do not change (sharpen) with increasing elongation and intensity, which proves that particles do not enlarge but that new crystallites are formed with increasing extension.

Vulcanized Rubber.—1. Crystalline sulfur or additional new crystalline compounds formed by the vulcanizing agent and rubber in adequately cured stock are not indicated on diffraction patterns by the appearance of new rings or spots. Even in hard rubber with high sulfur content this is true. The only diffraction effects not due to rubber itself are due to excess crystalline vulcanizing agent or to crystalline fibers.

2. Vulcanized rubber unstretched produces an amorphous halo, and when sufficiently stretched, a crystal fiber pattern.

¹ *Science*, **79**, 433 (1934).

² *Kolloidchem. Beihefte*, **22**, 63 (1926).

Three-dimensional, or "higher," orientation can also be attained by proper stretching conditions (Gehman and Field).

3. The positions of halos and of crystal interferences are identically the same for crepe or smoked sheets and for vulcanized rubber. Hundreds of measurements with the aid of the best microphotometers have detected no shift in positions, alterations in relative intensities, missing or additional interferences. This simply means that vulcanization produces no measurable changes in intermolecular spacings or lattice arrangement of polymerized isoprene molecules. There is no evidence of solid solution, compound formation, separate crystalline phase (if the mix is heated sufficiently to remove crystalline sulfur), or any other structural changes in terms of the unit crystal cell.

4. The crystal fiber pattern appears only after a considerably greater elongation after vulcanization than is required for crude rubber. For the latter the crystal pattern appears at 80 per cent extension and increases in intensity with further extension. Crude rubber that has been subjected to mastication must be stretched above 80 per cent (depending on the extent of the treatment). Vulcanized rubber (about 5 per cent of sulfur) must be stretched to 225 to 250 per cent elongation. Thus there is considerably greater resistance in vulcanized rubber to the parallel arrangement of molecules or crystallites, but once formed the crystal pattern indicates a lattice structure identical with that of stretched crude rubber. In the ebonite, or hard-rubber, state the pattern is obviously that of a non-parallel arrangement of molecular chains and crystallites in keeping with the very high viscosity and nonelasticity. A mix of rubber with 30 per cent sulfur and 1 per cent accelerator must be heated at least 1 hr. at 132°C. before all evidences of excess crystalline sulfur are removed.

5. The sharpening of interferences for vulcanized rubber, if observed, would mean an increase in crystallite size, as if more molecules were bonded together laterally as by bridges or lengthened by catalyzed chain polymerization. Increased breadth or diffuseness of interferences would mean breakdown of particles to smaller fragments and depolymerization. This, however, can also mean an increased distortion within particles of the same size. Katz and Bing observed that for stretched

vulcanizates with 25 per cent sulfur at 132°C. for 120 min. the interferences were diffuse and broad. However, for ordinary vulcanized rubber of maximum elasticity and strength these breadths are at least as narrow and in many cases slightly sharper when compared with crude rubber patterns at high elongations. This observation has been made many times in the course of twelve years at the University of Illinois.

6. Definite hysteresis effects are observed for vulcanized rubber. When a specimen is stretched rapidly to 250 per cent, crystal interferences appear at once which are much more intense than the patterns for a specimen stretched 250 per cent very slowly.¹ When this is allowed to retract slowly, the crystal interferences remain visible down to 130 per cent. Furthermore, photometric analysis proves that the amorphous halo which is perfectly uniform for unstretched samples shows differential intensity of the equator compared with the poles for elongations of 100 per cent. This indicates that, even before reaching the critical elongations, rubber molecules bearing sulfur are being directed toward a parallel arrangement within the amorphous, mesomorphic, or liquid crystal state. In April, 1940, Clark, Blaker, and Ball presented complete crystallization hysteresis loops determined from diffraction patterns made at various stages of elongation and retraction of rubber specimens. These loops were quantitatively correlated with stress-strain hysteresis loops and with the important practical property of resilience.

7. Rubber vulcanized in the stretched state loses completely its crystal fiber structure, thus proving the disorganizing effect of the vulcanizing agent.²

8. Experiments on vulcanized sol and gel rubber in the writer's laboratory seem highly significant. Pure sol rubber does not tend to form crystal fibers even at 1,000 per cent elongation, as though the material were a fluid or the molecules too short to maintain a preferred orientation in the fiber once formed. Total rubber behaves normally in that greater elongations are required; vulcanized gel is quite similar to the untreated gel on the elongation required; but vulcanized sol rubber crystallizes and forms fibers at about 200 per cent, far below the value

¹ IGUCHI and SCHOSSBERGER, *Kautschuk*, **12**, 193 (1936).

² HAUSER, *India Rubber World*, **101**, 1 (1939).

for the unvulcanized phase and nearly the same as the vulcanized gel. This seems to indicate that the primary action of the vulcanizing agent is to solidify and strengthen the sol phase in which the gel phase may be dispersed. Under the same experimental conditions the vulcanized-sol interferences are appreciably broader than those of vulcanized gel at the same elongation, which can mean that the degree of polymerization and the number of molecules in the crystallite are still below the values for the gel. Years ago Ostromislensky compared vulcani-

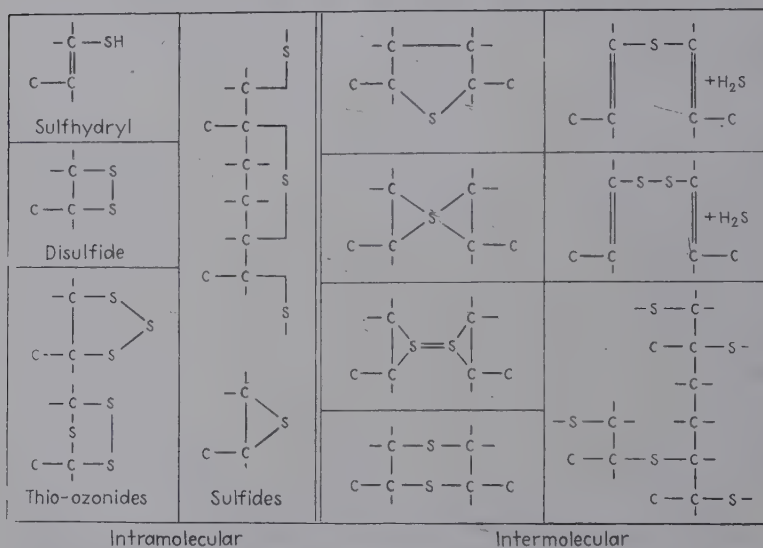


FIG. 328. —Possible types of sulfur combinations in vulcanized rubber. (Hauser.)

zation with a swelling in which sulfur-containing rubber serves as the swelling medium for unchanged rubber and is mechanically stronger than rubber itself. And yet the reversible stretching still maintained after vulcanization demands that the inner crystallite structure and the ability of the molecules to fold up again on release of tension must be retained, and so the crystal interferences are unchanged in position. After all, as Katz stated in his original paper, the remarkable fact is not that a crystal pattern is produced upon stretching, but that this pattern reverts immediately upon the release of tension to the liquid halo.

Thus the mechanism of vulcanization still remains an open question, largely because the presence of sulfur is not directly

indicated by x-ray methods. Preponderance of evidence and of opinion favors chemical combination by one of the possibilities represented in Fig. 328 by Hauser.¹

Gutta Percha, Balata, and Chicle.—There has been a very considerable disagreement concerning the structures of gutta percha and balata which are, like rubber, polymers of isoprene. The discrepancies have at last been explained in the work of Hopff and von Susich² and of Stillwell and Clark.³ These two substances produce diffraction patterns different from rubber,

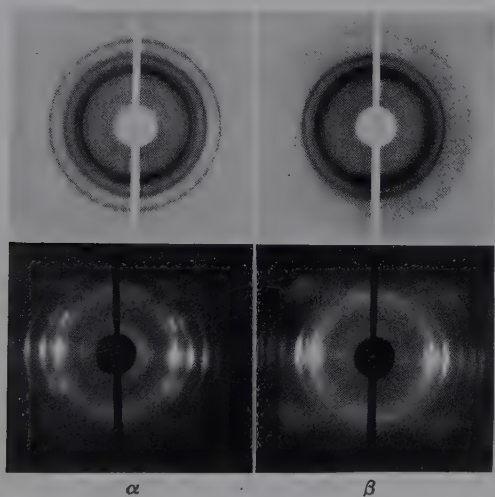


FIG. 329.—Patterns for unstretched and stretched α -gutta percha (left) and β -gutta percha (right).

but probably like each other. There are two modifications, the α which is stable below 60°C. and the β produced by heating above 60°C., giving different patterns in the unstretched as well as the stretched state. Stillwell and Clark have found balata in ordinary commercial form to differ from ordinary gutta percha, in the same way that von Susich's α -modification differs from β -gutta percha (Fig. 329).

Chicle has been studied by Stillwell and Clark. The hydrocarbon constituent here is identical with gutta percha. The

¹ *Ind. Eng. Chem.*, **30**, 1291 (1938).

² *Kautschuk*, **11**, 234 (1930).

³ *Ind. Eng. Chem.*, **23**, 706 (1931); *Kautschuk*, **5**, 86 (1931).

resins, calcium oxalate, and other substances constitute the remainder of this product.

Rubber, gutta percha, balata, and chicle all are built from hydrocarbon chains of the same constitution. The difference comes in a *cis* configuration for rubber where the identity period is 8.4 A.U. and a *trans* form in the gutta percha, or zigzag chains with an identity period of 8.8 A.U.

Proteins.—Since the beginning of this century and as a result of the work of Emil Fischer and others, proteins have been

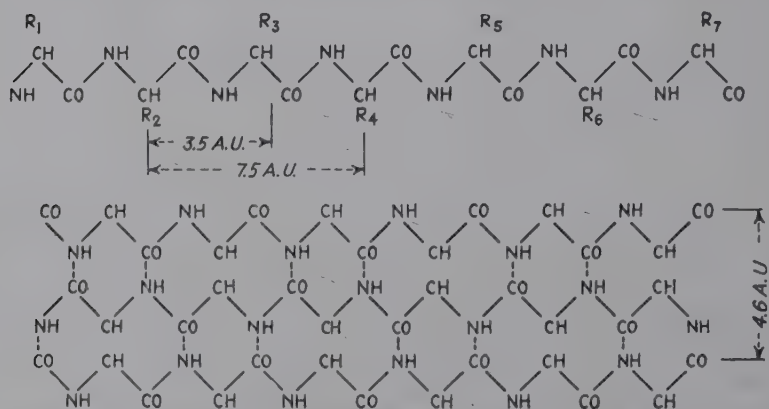
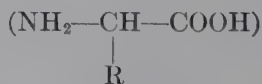


FIG. 330. The backbone polypeptide chain in proteins (above), and the cross-linking of chains.

considered to be long chains formed from repeated condensations of α -amino acids



to a configuration of the type represented in Fig. 330.

Thus a more or less common backbone is characteristic of all protein molecules (at least in fibers). Proteins are classified as fibrous (crystalline) and nonfibrous, globular, or corpuscular (not obviously crystalline). They differ in R groups; and they exist naturally in specific folded configurations. The four principal states of the polypeptide chains in fibrous proteins are illustrated in Fig. 331.

Silk Fibroin.—Silk fibroin, a natural crystal fiber, is distinguished by stability and simplicity since it yields on hydrolysis

principally glycine and alanine. Thus its R groups are almost entirely hydrogen and CH_3 . The x-ray pattern (Fig. 332)

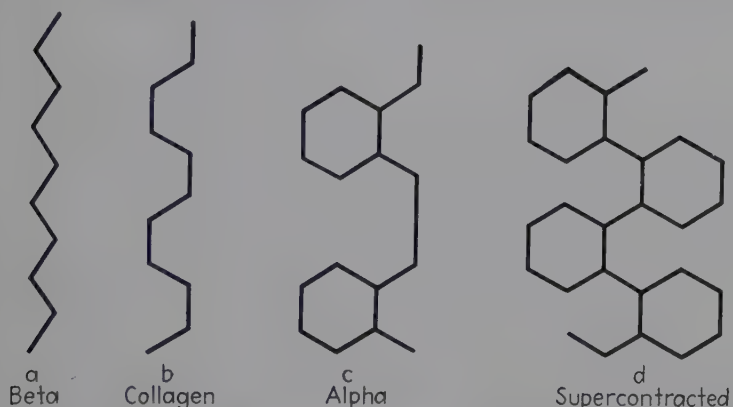


FIG. 331.—The four principal configurations of molecular chains by which all proteins may be classified. (*Astbury.*)

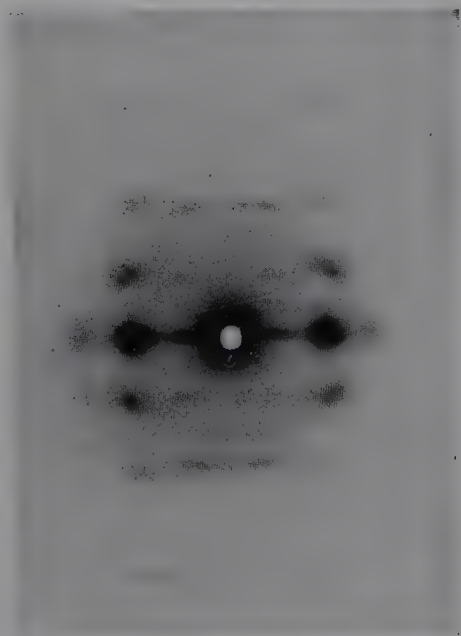


FIG. 332.—Fiber pattern of the protein fibroin constituting natural silk.

is fully consistent with the foregoing concept of a fully extended polypeptide chain. The unit monoclinic cell has the dimensions

$$\begin{aligned}
 a &= 9.68 \text{ A.U.}, \\
 b &= 7.00 \text{ (2 amino acid residues of 3.5 A.U.)}, \\
 c &= 8.80 \text{ A.U.}, \\
 \beta &= 75^\circ 51'.
 \end{aligned}$$

Stretching has no effect on the pattern; hence, the crystallites, being already stretched to the fullest extent, merely slide over one another. Slight variations are observed for silk fibroin from different sources.

Keratin (Mammalian Hair).—To Astbury is due the present extensive knowledge of keratin, or the protein of hair, wool, horn, etc. When stretched these produce patterns of β -keratin similar to silk fibroin; but in the normal unstretched state, a completely different pattern for α -keratin (Fig. 333) indicates some regularly folded condition of the backbone of the molecule from which it may be pulled out straight in the presence of moisture and to which it returns upon release of tension. Thus the molecular configurations of the normal and stretched hair may be represented as in Fig. 334.

The β -keratin then forms a grid, built up by interactions and combinations between the R groups of neighboring main chains. The crystal particle consists of a series of parallel grids. The dimensions roughly are

| | |
|--|-----------|
| Amino acid residue along main chain..... | 3.5 A.U. |
| Side-chain spacing..... | 10.0 A.U. |
| Spacing between grids..... | 4.5 A.U. |

Since β -keratin is the prototype of proteins with fully extended chains, it is useful to tabulate the details of the fiber pattern:

| | Plane | Spacing | Intensity |
|-------------------|-------|---------|-----------|
| Equator..... | 001 | 9.7 | <i>s</i> |
| | 200 | 4.65 | <i>vs</i> |
| | 400 | 2.4 | <i>w</i> |
| 1-layer line..... | 111 | 4.7 | <i>m</i> |
| | 210 | 3.75 | <i>s</i> |
| | 410 | 2.2 | <i>w</i> |
| 2-layer line..... | 020 | 3.33 | <i>s</i> |
| | 220 | 2.7 | <i>w</i> |
| 3-layer line..... | 030 | 2.2 | <i>w</i> |
| | 230 | 2.0 | <i>w</i> |

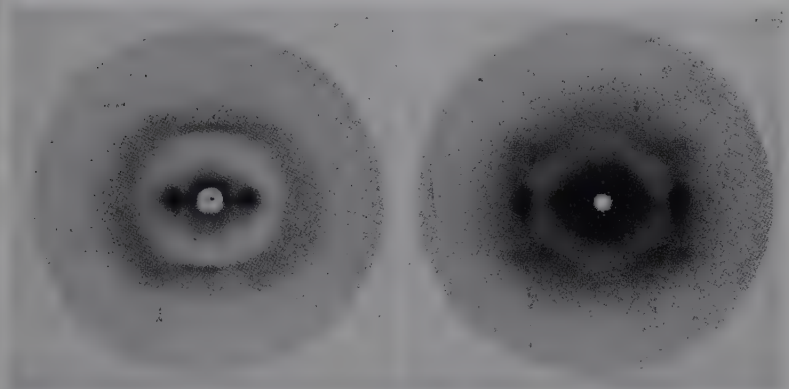


FIG. 333.—Fiber patterns of keratin, the protein of wool, hair, horn, spines, etc.
(a) α -form, unstretched; (b) β -form, stretched.

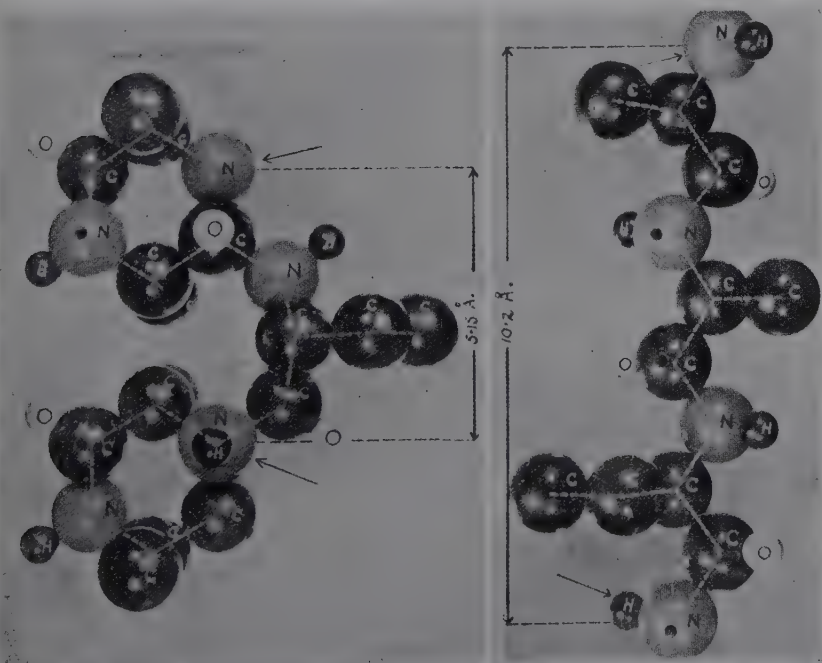


FIG. 334.—Molecular models for α - and β -keratin deduced from patterns in Fig. 333.

Thus the orthorhombic unit cell has the dimensions $a = 9.3$, $b = 6.66$, $c = 9.7$ A.U. This form may be permanently set when the hair or wool is steamed in the stretched state, simply because cross linkages are hydrolyzed and reformed in a configuration that will prevent return to the folded α -state. The pattern is characterized by a smearing along the layer lines exactly as observed by the writer years ago for asbestos (Fig. 167), indicating an irregular breakdown confined only to the direction of the side chains. Lateral pressure selectively orients the side-chain spacing perpendicular and the backbone spacing parallel to the plane of flattening, so that the β -keratin crystallites seem



FIG. 335.—The pattern of feather keratin.

to be ribbon-shaped, longest in the direction of the main chains and thinnest in the direction of the side chains, which means that there are comparatively few main chains per grid but many grids piled on top of one another.

The natural unstretched form of the protein common to hair, wool, spines, nails, horn, etc., has α -keratin as the prototype with main chains folded so that the grids are buckled. The orthorhombic cell has the di-

mensions $a = 27$, $b = 10.3$, $c = 9.8$ A.U. Half the length of the b axis corresponds to the folded length in the direction of the fiber axis of three amino acid residues; 9.8 A.U. is again the side-chain spacing. Keratin can be treated by steam or alkali in the extended state so that upon release the fibers exhibit supercontraction to a length shorter than normal. Thus the α -folding is further elaborated to about one-third the length of β -keratin as indicated on the patterns.

Feather keratin produces the richest protein pattern known (Fig. 335), but it is based fundamentally on the same β -structures with patterns greatly elaborated and approaching some of the crystallized proteins. Most of the quill has polypeptide chains parallel to the length with a thin outer layer in which they run at right angles to the

ing for the remarkable strength. The periodicity along the fiber axis may be as high as 304 A.U., while the length of the amino acid residue is only 3.08 instead of 3.33 A.U. as in β -keratin, but the quill may be pulled out to the latter value. Such is the protective covering of birds and reptiles, as contrasted with the mammalian keratin; and the identity of the constitution and structure of feathers, beaks, claws, tortoise shell, and reptilian scales is remarkable and irrefutable evidence of the common ancestry of birds and reptiles.

Muscle.—All the observations on diffraction patterns, structure, behavior on stretching, and supercontraction in keratin have now been duplicated by Astbury for the protein in muscle, namely, myosin. The photograph of washed and dried muscle, and indeed of living muscle, if the presence of water is taken into account, is remarkably like that of α -keratin; that of stretched myosin is also like that of β -keratin. Hence, myosin possesses folded chains in the condition at rest, which are further folded upon supercontraction. Since keratin possesses a much higher sulfur content from its cystine constituent, the side linkages between neighboring chains may be through the —S—S—groups, so that a hair may be considered as a “vulcanized” muscle fiber with reduced elastic sensitivity and increased resistance to chemical attack.

Similarly, fibrous proteins of the epidermis (skin of a cow's nose), fibrin, and even denatured “globular” proteins, demonstrate in their diffraction patterns a very close relationship with α -keratin (extended), α -keratin (folded), and super-
 Conjugen.—The principal constituent of vertebrate tendons and tissues is the protein collagen, which, upon hydrolysis, yields gelatin. Surgical catgut ligatures are collagen fibrils from the walls of sheep. An extended x-ray study

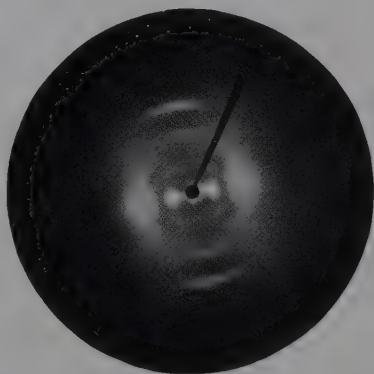


FIG. 336.—Pattern of well-oriented catgut ligature.

of catgut in the writer's laboratory has led to greatly improved processing of the ligatures with respect to uniformity and enhanced tensile strength. This was achieved largely through improved preferred orientation of protein crystallites under combined swelling and tension,¹ as shown in Fig. 336.

Collagen and gelatin, being made up of 15 or more amino acids of widely different functional groups and molecular weights, have previously not given patterns with sufficient orientation and

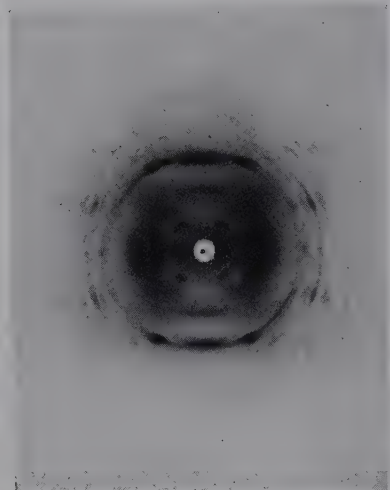


FIG. 337.—Pattern for rattail tendon collagen.

number of interferences to lend themselves readily to analysis. Long-chain molecules are rather easily oriented by tension but lack sufficient organization of amino acid residues to produce a well-defined lattice. The existence of a halo, which shows indication of partial orientation, superimposed upon a faintly sharp interference pattern indicates a "pseudo-crystalline" structure. On the pattern appear inner equatorial arcs for a spacing of 10.4 to 17.0 A.U., depending on the amount of water held by the protein and meas-

uring the distance between main chains, or the length of cross linkages; a spacing of 4.5 to 6.1 A.U. corresponding to the thickness of the grid; and a fiber axis identity period of 9.75 A.U., or three times an amino acid residue length of 3.25 A.U. Another spacing of 2.84 A.U., thought by Astbury to be a contracted residue length, might be due to planes that are not perpendicular to the fiber axis. Both collagen and stretched gelatin ribbons give essentially this same type of ordinary pattern (Fig. 337).

Clark, Parker, Schaad, and Warren² first reported the existence of a spacing along the fiber axis in collagen of 432 A.U. or twice

¹ CLARK and ZIEGLER, *The X-ray in the Study of the Catgut Ligature, Surgery, Gynecology and Obstetrics*, **58**, 578 (1936); CLARK, FLEGE, and ZIEGLER, *Surgical Ligatures, Ind. Eng. Chem.*, **26**, 440 (1936).

² *J. Am. Chem. Soc.*, **57**, 1509 (1935).

this value (Fig. 338) (one of the longest ever directly measured) which is completely missing in gelatin. This gives a remarkable clue to the organization of collagen in contrast with gelatin. This spacing indicates a regularly repeating residue along the chains or an over-all length of the molecules themselves. The spacing 432 A.U. decreases to 408 A.U. for chromicized gut without further evidence of interaction of the chromicizing solution with collagen. With these and other data Astbury in his Procter lecture¹ has given the most complete picture of the collagen molecular chain built up from a multiple of 72 amino acid residues in the configuration shown in Fig. 331.

Collagen seems to form addition compounds with NaOH. This reaction is reversible since the original collagen pattern is regained after treatment of the alkali addition compound in a buffered solution at the isoelectric point pH 4.78. Addition compounds with entirely different structures and patterns are formed with KOH, LiOH, RbOH, and CsOH. Astbury believes that these changed patterns are due to the alkalis, entrapped as oriented crystals in the collagen. Further research will clarify the problem. This may be a new method of crystal structure analysis of substances like the alkalis about which little is known on account of lack of single crystals.

The peculiar behavior of the 48-A.U. equatorial interferences appearing on intestinal-wall but not tendon collagen patterns on treatment of the fibers with hot water, alkali solution, salts, and various organic solvents led to the discovery by Clark and Schaad of a waxlike substance whose molecules are radially oriented on collagen fibrils in these wall tissues and serve both as a lubricant and as a protection against enzyme digestion of the collagen. Analysis indicates an empirical formula of $C_{14}H_{28}O_2$ or a multiple and that the compound may be related to cholesterol derivatives

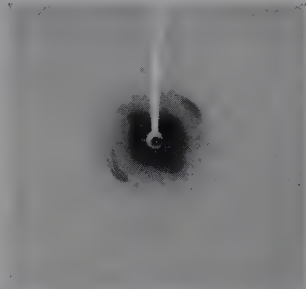


Fig. 338.—Interferences at very small angles (long spacings) for collagen. The meridional interferences (diagonal, upper left to lower right) represent several orders of the spacing 432 or 864 A.U.

¹ *Nature*, **145**, 421 (1940).

rather than an ordinary ester. It is evident that this substance, which is completely absent in tendon, is synthesized or adapted by the body for this very specific purpose. The power of the x-ray diffraction method in biological research is clearly indicated by this example.

Collagen fibers contract in hot water above definite temperatures to as much as three-quarters of the original length. In this state they display long-range elasticity like that of keratin and myosin and diffraction halos corresponding to side-chain and backbone spacings. Elastin from the ligamentum nuchae (the very elastic neck ligament) is actually collagen in this supercontracted form.

Globular Crystalline Protein.—The obvious limit of the idea of folding and twisting protein chains is to be found in the so-called globular proteins such as egg albumin, hemoglobin, edestin, etc. These substances may actually be crystallized in a sense far different from the fibers just discussed. It would appear that they are built in a very delicately balanced fashion of somewhat spherical units which have been shown so brilliantly in the work of Svedberg with the ultracentrifuge to have molecular weights of 35,000 or a multiple. X-ray work by Bernal and Crowfoot¹ on pepsin and insulin crystals (Table LII) have definitely confirmed this contention. Clark and Shenk² have made an extensive study of crystallized and denatured egg albumin. In the usual case the patterns for these proteins consist essentially of two halos corresponding to the two principal distances between main chains, 10 and 4.5 A.U. By boiling and other methods of denaturation, the pattern resembles even more strongly that of powdered or disoriented β -keratin, showing that a highly specific and delicately balanced configuration in the original globular protein is broken down. By stretching, Astbury has succeeded in orienting denatured albumins and globulins so that fiber patterns are produced. Thus denaturation actually liberates polypeptide chains from crystalline proteins and permits their conversion into visible fibers which, on stretching, are found to be structurally analogous to stretched wool and unstretched silk.

¹ *Nature*, **133**, 794 (1934); **135**, 591 (1935); **141**, 521 (1938); **144**, 1011 (1939).

Proc. Roy. Soc., (London), **A164**, 580 (1938); **B127**, 36 (1939).

² *Radiology* **28**, 144 (1937).

TABLE LII.—PROTEIN SINGLE CRYSTALS¹

| Protein | Cell dimensions | | | | Space-group | Molecules per cell | Molecular weight | Remarks |
|----------------------------|-----------------|--|----------|---------|--|--------------------|----------------------------------|--|
| | <i>a</i> | <i>b</i> | <i>c</i> | β | | | | |
| Insulin: | | | | | | | | |
| Dry..... | 74.8 | | 30.9 | | <i>R</i> 3 | 1 | 37,600 | Most complete Patterson-Harker Fourier analyses |
| | 44.4 | $\alpha = 114^\circ 48'$ (rhombohedral) | | | | .. | | |
| Wet..... | 83.0 | | 34.0 | | | .. | 52,400 (20% H ₂ O) | |
| Excelsin..... | 86 | | 208.2 | | <i>R</i> 3 | 1 | 305,800 | |
| Lactoglobulin | | | | | | | | |
| Tabular: | | | | | | | | |
| Wet..... | 63.5 | 63.5 | 145.0 | | <i>P</i> 222 | 8 | 36,500 | Complete patterns down to small spacings only with crystals wet with mother liquor |
| Dry..... | 59 | 59 | 105 | | ? | 8 | | |
| Needles: | | | | | | | | |
| Wet..... | 63.5 | 63.5 | 125.0 | | <i>P</i> 4 ₂ 2 ₁ | 8 | | |
| Dry..... | 54 | 54 | 125 | | ? | 8 | | |
| Chymotrypsin: | | | | | | | | |
| Wet..... | 49.6 | 67.8 | 66.5 | 102° | <i>P</i> 2 ₁ | 4 | 32,000 | |
| Dry..... | 45 | 62.5 | 57.5 | 112° | <i>P</i> 2 ₁ | 4 | | |
| Hemoglobin: | | | | | | | | |
| Wet..... | 109 | 63.2 | 54.2 | 112° | <i>C</i> 2 | 4 | 69,000 | |
| Dry..... | 102 | 56 | 49 | 134° | <i>C</i> 2 | 4 | | |
| Pepsin, wet..... | 116 | 67 | 460.8 | | | | | |
| Tobacco-seed globulin..... | 123 | 123 | 123 | | Cubic | 4 | 325,000 | |

Bence-Jones protein: spacings, 2.2, 3.4, 4.8, 10.1, 11.1, 14.8, 25, 28, 41 A.U.

¹ Compiled by Astbury and Bell, *Tabulae Biologicae*, 17, 90 (1939).DENATURED PROTEINS¹

| Protein | Side spacing | | Backbone spacing | |
|--------------------|--------------|-----|------------------|------|
| Edestin..... | 11.0 | ... | 4.55 | 3.6 |
| Pepsin..... | 11.5 | 6.5 | 4.59 | 3.6 |
| Egg albumin..... | 10.23 | ... | 4.75 | 3.67 |
| Serum albumin..... | 9.6 | ... | 4.48 | 3.6 |
| Zein..... | 9.82 | ... | 4.64 | |
| Casein..... | 10.23 | ... | 4.59 | |
| Trypsin..... | 9.82 | ... | ? | |
| Ascaridine..... | 10.0 | ... | 4.6 | |

¹ Patterns like disoriented β -type.

Clark and Shenk have shown that denatured hemoglobins give diffraction patterns very similar to those of egg albumin. X-ray studies were made of rat and horse oxyhemoglobin and horse and pig carbon monoxide hemoglobin. The two horse hemoglobins with a maximum spacing of 48.2 A.U. seem to be the same, but the patterns are different for blood from different animals. The color constituent of hemoglobin, hemin, chlorohemin, potassium oxyhemin, and other derivatives are all identical from all sources. Patterns are illustrated in Figs. 339 and 340.

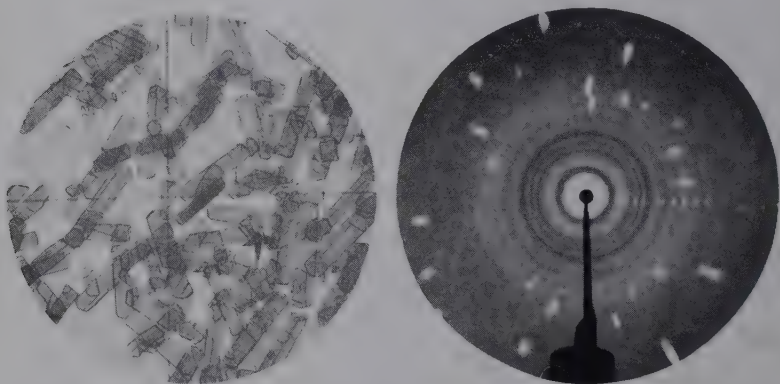


FIG. 339.—Photomicrograph and x-ray pattern for crystalline oxyhemoglobin from rat blood.

Of greatest recent interest has been the x-ray analysis of crystallized tobacco mosaic virus protein, isolated first by Dr. W. M. Stanley of the Rockefeller Institute for Medical Research. The significance lies in the attempt to explain how this material, placed in the proper environment, is able to produce more of itself and how closely a crystalline protein comes to the process of life. Wyckoff and Corey, Bernal and associates, and Clark and Parker have all studied this virus.¹ Bernal has found a maximum spacing of 152 A.U. for the dry gel, 210 A.U. for the wet gel (hexagonal close-packed), and 300 to 470 A.U. for liquid preparations. A second interference appears at 75 to 80 A.U., which has been found by the other workers also. More than 20 interferences appear on some patterns, some for spacings *within the single*

¹ *J. Biol. Chem.*, **116**, 51 (1936).

Nature, **138**, 1051 (1936).

molecule. The molecules are 150 A.U. wide and at least 1000 A.U. long, made up of subunits of the dimensions $11 \times 10 \times 10$ A.U. (Bernal).

Casein and Aging of Cheese.—In a study just completed in the writer's laboratory the diffraction pattern of casein shows two

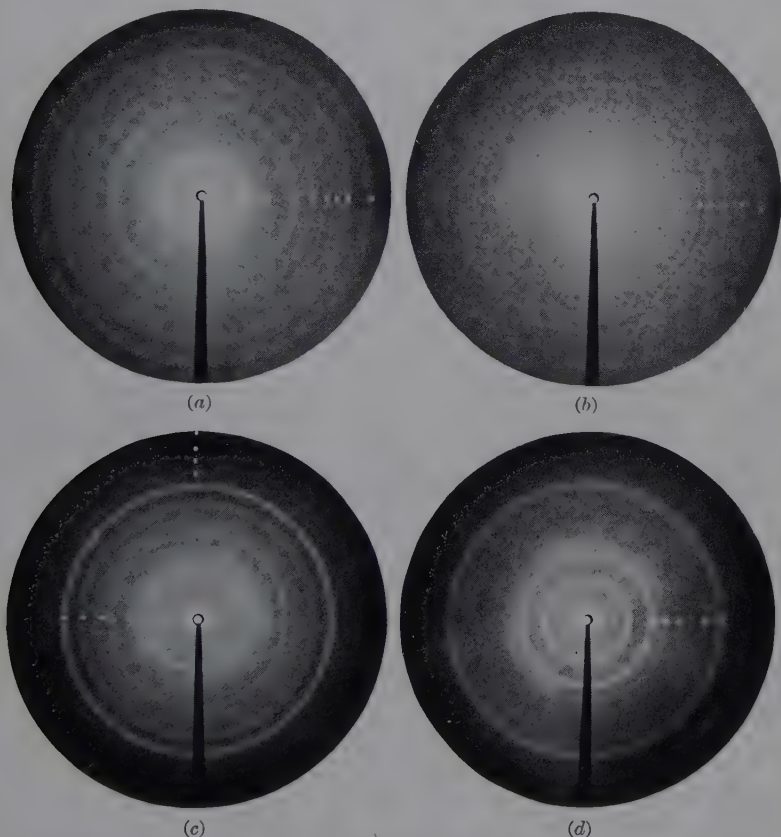


FIG. 340.—Patterns for color constituent of hemoglobin. (a) Formic acid extracted hemin; (b) acetic acid extracted hemin; (c) chlorohemin; (d) potassium oxyhemin.

halos at calculated spacings of 9.8 to 10 and 4.6 A.U., similar to those of other proteins and corresponding, respectively, to side-chain spacings and the perpendicular distance between layers of polypeptide chains. Upon treatment with formaldehyde again sharp interferences appeared for 3.83- and 2.6-A.U. spacings. But, strangely enough, cheddar cheese, upon ripening,

produces sharp interferences for 3.83 and 2.6 A.U. Since cheese ripening is essentially a hydrolysis of proteins into amino acids, it is not unlikely that these diffraction effects are due to liberated amino acids. Of 19 amino acids examined, only three gave corresponding interferences, as follows:

| | d_1 , A.U. | d_2 , A.U. |
|--------------------|--------------|--------------|
| Isoleucine..... | 3.84 | 2.61 |
| Aspartic acid..... | 3.86 | 2.64 |
| Proline..... | 3.87 | 2.62 |

Analysis has proved that crystalline amino acids are actually formed on aging. A long spacing of 39.8 A.U. is found in cheese which corresponds rather well with the value 41.7 A.U. calculated by Svedberg as the radius of a casein particle.

Monomolecular Films of Proteins.—Langmuir, Schaeffer, and Wrinch¹ have developed the method by which many proteins capable of existing in water as large spherical molecules can be spread on water surfaces, giving elastic solid monomolecular films having great two-dimensional compressibility. Such monofilms may be transferred from a water surface onto solid surfaces; thus the total number of layers may be determined and the thickness measured by optical or x-ray methods. This work has demonstrated that, if films are transferred to a solid backing by pushing into the water and then pulling out the plate, one surface of the protein film is predominantly hydrophilic. A careful study of all the properties of these films has led these workers to the view that the protein monolayer is a two-dimensional network held together by strong elastic springs and is not in accord with a structure consisting of polypeptide chains. Added interest in the whole problem, which still requires much experimental work, is based upon the theory proposed by Dr. D. M. Wrinch of a further elaboration of the folding of protein chains into a cyclol pattern. This gives to a protein sheet a framework upon which may be superposed a large number of physiologically active compounds, including the carcinogens, sterols, bile acids, sex hormones, and heart poisons. The cyclol pattern depends upon the assumption that amino acids can condense by means of single, double, or triple peptide links. When such a cyclol pattern is formed, all the side chains emerge

¹ *Science*, **85**, 76 (1937).

from one surface whereas the other surface is free from side chains. Hence, it is possible for proteins with the most diverse chemical composition to share one common surface pattern, namely, that on the surface free from side chains. The extension of this concept of the use of large molecules of various types, including proteins, as templates is promising as an interpretation of many biological mechanisms. The theory based on x-ray results on insulin and Patterson-Harker Fourier projections by Crowfoot has been the subject of an extraordinary controversy.

Astbury measured a thickness of a monolayer of egg albumin by x-ray by micrometer, and optically as 9.5 A.U.—the side spacing of fibrous protein. Therefore, the formation of a monolayer is another example of denaturation by unfolding of chains.

The Plan of Synthesis of Proteins.—The present conclusion from an integration of structural information on all proteins is that there is no real distinction between fibrous and corpuscular proteins other than the configurations of straight or folded polypeptide chains. In addition there is now a clear glimpse of the possibility that proteins are synthesized according to a common plan. Bergmann and Niemann in a series of masterly researches have concluded that the total number of residues in any protein and the numbers of each of the different kinds of residue are expressible in the form $2^n 3^m$. For example, in the silk fibroin mentioned in an earlier paragraph, the proportions of residues are: glycine $\frac{1}{2}$, alanine $1/2^2$, tyrosine $1/2^4$, arginine $1/2^3 3^3$, lysine $1/2^3 3^4$, histidine $1/2^5 3^4$. From such fractions the minimum number of residues required to make up a molecule and the minimum molecular weight follow—and are found to agree with ultracentrifuge results. If this remarkable synthetic plan is sound, then the egg albumin group is made of 288 residues, hemoglobin 576, etc. Keratin seems to have the proportions: glutamic acid $1/2^3$, arginine $1/2^4$, aspartic acid $1/2^4$, tyrosine $1/2^5$, lysine $1/2^4 3^1$, tryptophane $1/2^5 3^1$, histidine $1/2^6 3^1$. Gelatin probably is built from the amino acids glycine $1/2^3 3^1$, proline $1/2^1 3^1$, hydroxy-proline $1/2^0 3^2$, alanine $1/2^0 3^2$, arginine $1/2^1 3^2$, leucine $1/2^1 3^2$, lysine $1/2^3 3^1$.

Nerve.—The diffraction patterns of fresh and dried medullated and non-medullated nerves are described in a paper by Schmitt, Bear, and Clark.¹ Medullated nerves are represented by the

¹ *Radiology*, **25**, 131 (1935).

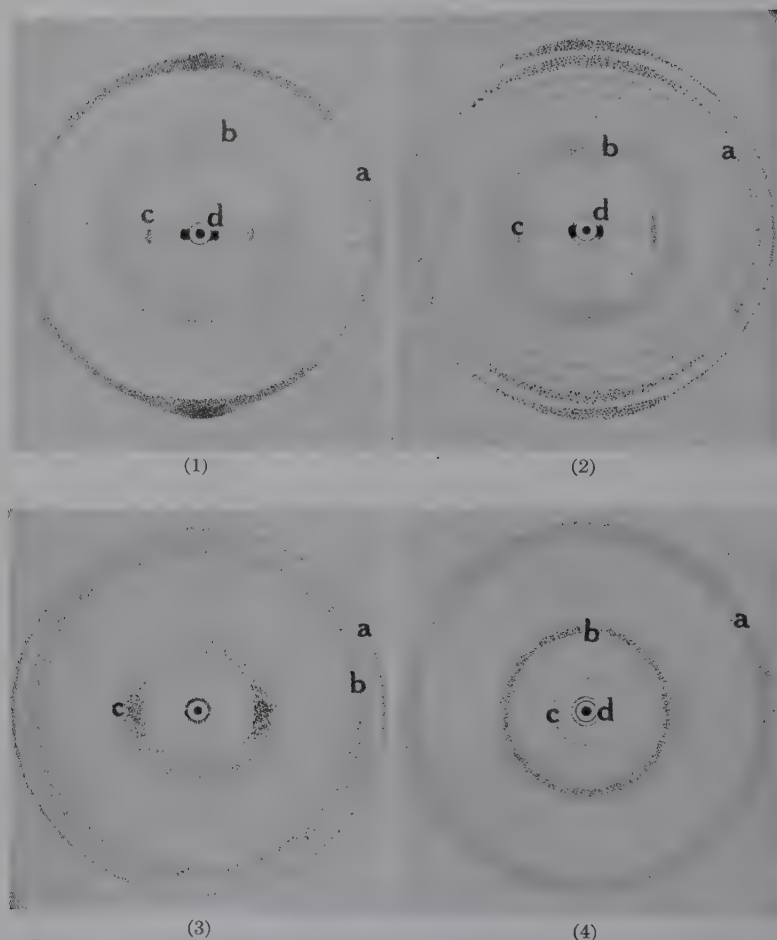


FIG. 341.—Sketched patterns for living nerve, dried nerve, and nucleoprotein artificial fiber. (1) Fresh medullated nerve. *a*, 4.7 A.U. meridionally sickled rings; *b*, 9.4 A.U., meridional spot; *c*, 15.5 A.U. equatorial point; *d*, large-spacing equatoria points. (2) Stretched and dried medullated nerve. *a*, meridionally accentuated rings at 4.20, 4.67, 5.20, and 5.8 A.U.; *b*, 10 A.U. meridionally accentuated ring; *c*, 11.5 A.U. equatorial point; *d*, large-spacing equatorially accentuated rings. (3) Lobster or crab claw or leg nerves dehydrated in alcohol under tension. *a*, 4.2 A.U. ring; *b*, 4.8 A.U. ring; *c*, 11.5 A.U. equatorial sickle. (4) Artificial fiber made by spinning nucleoprotein solutions (neutral-soluble extract or neurostromin from dried lobster nerves or cow spinal cord) into alcoholic acetic acid. *a*, 4.8 A.U. ring; *b*, 9.1–11.5 A.U. ring; *c*, 23 A.U. ring; *d*, 48 A.U. ring.

sciatic, motor, and sensory roots of the frog and cat and by the corpus callosum of the cat; non-medullated nerves by the claw and leg nerves of the lobster and crab.

Diffraction patterns were made in 5 min. while the specimens were kept fully alive. Diagrams of these patterns are illustrated in Fig. 341.

The pattern of fresh medullated nerve is probably due entirely to oriented fluid crystals of the myelin sheath, for it can be reproduced fairly completely in preparations made by rubbing up a benzene extract of spinal cord with water. The fundamental aggregate of these fluid crystals appears to have dimensions of $4.7 \times 9.4 \times 171$ A.U., the various lipoids being associated in a mixed crystal fashion. The c spacing lies radial and perpendicular to the long direction of the axon. This means that in thinly myelinated fibers the myelin sheath is composed of but relatively few layers of these oriented lipoids associated end to end.

With the exception of the equatorial sickles at 11.5 A.U. (15.5 to 17 A.U. in fresh nerve), the patterns of dried medullated nerve can be reproduced by dried extracted lipoids. Rings with spacings characteristic of phosphatides and of cholesterol can be identified in the pattern of dried nerve. Drying disorients certain of the components of the myelin, leaving others fairly well oriented.

Heating frog sciatics causes a disorientation of the lipoids that appears to occur at or about the same temperature at which the action potential is extinguished. Higher temperatures, which cause maximal shortening, have little further effect on the x-ray patterns.

Patterns of frog sciatics treated with cyanide until the action potential was blocked departed little from the normal.

To study the structure of the axis cylinder, lobster- and crab-leg and -claw nerves were used. These nerves have in the past been assumed to represent pure axis cylinder, containing little or no connective tissue or lipoids. This assumption has been shown to be incorrect by chemical analysis and by histologic investigation. The lipid content may be as high as from 25 to 30 per cent of that of the white matter of mammalian brain. Connective tissue is by no means negligible; there is interfibrillary connective tissue as well as fibrous material closely adherent to each fiber. There is also a sheath that appears to be comparable to the Schwann sheath. These facts greatly complicate the

analysis of the axis cylinder since the proteins of the axis cylinder give spacings similar to those of collagen of the connective tissue.

Artificial fibers spun from the nucleoproteins of lobster nerves, though fairly strongly positively birefringent, indicate no orientation in their diffraction patterns. A ring of 9.1 to 11.5 A.U. represents the proteins. Even though these fibers were spun from fat-extracted protein, rings at 48, 23, and 4.8 A.U. represent the lipid components.

Alcohol-dried lobster nerves show equatorial sickles at approximately the same spacing as that given by the nucleoprotein of the axis cylinder. This fact was originally interpreted as showing that the axis cylinder contains oriented protein micelles. This conclusion must be qualified in view of the demonstrated presence in these nerves of collagenous material which might be responsible for at least a part of the orientation.

Although lipids are present in very appreciable quantities in lobster nerve, they give rise to no pattern in fresh nerve. However, if the nerve is treated with glycerin, which changes the birefringence from positive to negative, patterns may be obtained which demonstrate that the lipids have become oriented. Preliminary experiments indicate that cholesterol and perhaps also the phosphatides are involved in the effect.

The nerve of the squid represents the nearest approach to a pure giant axon yet found. This material, though displaying weak birefringence, presents an essentially amorphous pattern. It is estimated that only about 8 per cent of the long-chain protein molecules in the axis cylinder have actually any preferred orientation.

Nucleic Acids and the Chromosomes.—Two kinds of structure pertaining to the very source of life are the chromosomes and the viruses, both of which have the power of reproducing themselves and an organization based on association of proteins and nucleic acids. These are made up of nucleotides, which are double rings, one of purine or pyrimidine base and the other a sugar with phosphoric acid attached. In the chromosomes is thymonucleic acid, located in the dark bands and rising and falling corresponding to the cycle of cell division. The description of the structural features is given partly in the words of the experimenter himself, Prof. W. T. Astbury:¹

¹ *Science Progress*, **133** (1939).

Sodium thymonucleate is a fibrous material with an x-ray pattern showing a repeating spacing of 3.34 A.U. along the fiber axis. The properties indicate long rod-like particles of molecular weight up to a million. Hence they are columns of flat nucleotides 3.34 A.U. apart, or a pile of 2,000 plates. The spacing 3.34 A.U. is the same as that between successive side chains in a fully extended polypeptide. The logical conclusion is a matching of intramolecular patterns which nature has adapted to the processes of chromosome division. During mitosis and meiosis the chromosomes pass through a cycle of length changes, and the moment of full extension must be decided by this critical period

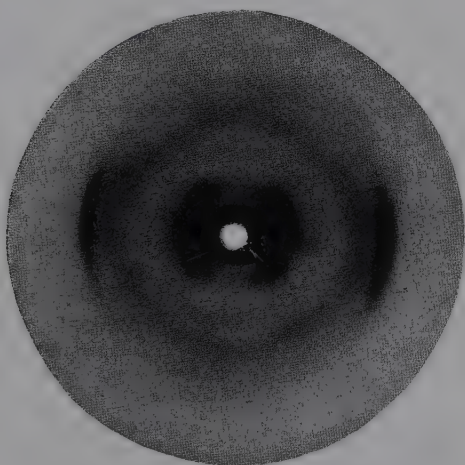


FIG. 342.—The pattern of clupein thymonucleate. (*Astbury.*)

between the nucleotides. To test these possibilities further Astbury has combined clupein, a simple polypeptide from sperm, with thymonucleic acid through the reaction of basic arginine side-chains with the phosphoric acid groups down the side of the acid column. This fibrous material (Fig. 342) resembles very closely the protein-nucleic acid compounds in the chromosomes, which seems strong evidence that the polypeptide chains must run along the length of the chromosomes. Since the genes form a linear sequence along the length of the chromosomes, here is an experimental beginning to contribute to the science of genetics. The proteins are the most important molecules in life: it may be that the patterns of life are only the patterns along polypeptide chains. The nucleotide is also directly indicated as the subunit within the giant molecules of viruses. This then is the building stone of the simplest "living" thing.

INDEX

A

Absorption, 134
 coefficients, 134
 edges, 98, 123, 131
 of high-voltage radiation, 141
 mechanism of, 137
 practical applications of, 150
 spectra, 95, 120
 Acceleration law in Bohr theory, 115
 Acids, aliphatic, 435
 Age-hardening, 408
 Aircraft parts, testing of, 166, 172
 Alcohols, 438
 Alkyl ammonium halides, 422
 Alloys, 390
 classification, 391
 polycomponent, 411
 Aluminum crystals, deformation of, 547, 550
 Aluminum ion in silicates, 377
 Alums, 371
 Ammonium nitrate, modifications of, 369
 Amorphous solids, diffraction by, 465, 474
 Analysis, chemical, by x-rays, 126, 128
 Anisodesmic crystals, 342
 Annealing, of cast steel, 565
 of sheet steel, 585
 Anthracene, 447, 451
 Apparatus, for chemical analysis, 126
 multiple diffraction, 274-276
 Aromatic compounds, x-ray analysis, 451
 Atomic structure, Bohr theory of, 113
 modern theory of, 118
 Auger effect, 123, 144

Automotive parts, testing of, 172
 Axes, crystal, 235

B

Back-reflection method, 271-273
 Bacteria, effect of x-rays on, 198
 Balata, 645
 Balmer series, 114
 Barium chloride dihydrate, space-group, determination of, 285
 Battery, high-voltage storage, 44, 45
 Beevers and Lipson, method of, 322
 Bending of wires, 584
 Benzene crystal structure, 450
 β -rays, 143
 Binary compounds, types of, 332, 333
 Binary intermetallic systems, classification of, 391
 Binding force, intermolecular, in organic compounds, 421
 Biological effects of x-rays, 198
 mechanism of, 216
 Blackening, photographic, 75
 Blodgett-Langmuir films, 443
 test of particle size by, 503
 Bohr theory, 113, 117
 Bond, chemical, 125
 Bond lengths in organic compounds, 419
 Bonds, classification of, 338
 covalent, homopolar, 343
 hydrogen, 348
 ionic, 338, 340
 ionic-covalent, 345
 metallic, 347
 single-double, 346
 van der Waals, 349
 Bracken series, 114
 Bragg and Peirce, law of, 136

Bragg diffraction law, 81, 82
 departures from, 88
Bragg method, 257, 260
Bragg-Williams theory of super-
 lattices, 395
Brass, 396
 pole figures of, 542
Brillouin zones, 391
Bromine, crystal structure of, 330
Bucky diaphragm, 159
Bunsen law, 76

C

Cables, high-tension, break-down,
 446
Cadmium hydroxide, grain size of,
 496
Calcite, and aragonite, 366
 as standard crystal grating, 83
Cameras for powder diffraction, 269
Cancer, 219
Cancer therapy, 223
Carbon, effect on annealing, 585
Carbon-black, particle size and
 shape of, 500
 structure of, 474
Carbon structures, 416
Carcinogenic chemicals, 221
Carcinogenic compounds, structure
 of, 452, 459
Casein, 657
Castings, growth texture of, 553
 radiographic examination of, 166
Catalysts, particle size of, 498
Catgut ligatures, 652
Cell, normal, effect on, 206
 radiosensitiveness, 209
Cellulose, composition, 605
 crystal structures, 606
 diffraction at small angles, 626
 occurrence, 605
 orientations in fibers and sheets,
 606
 polymorphic forms, 605, 630
 swelling, 631
 topochemical reactions of, 628
Cement, 387

Ceric salts, reduction of, 190
Charcoal, structure of, 476
Cheese, aging of, 657
Chemical analysis by x-rays, 126
Chemical effects of x-rays, 77, 194,
 215
Chemical reaction mechanism, 185
Chicle, 645
Chitin, 634
Chitosan, 635
Chromosomes, effect of x-rays on,
 203
 structure of, 662
Circuits for x-ray machines, 49
 Bouwers, 55
 cascade, 54
 Gratz, 50
 Greinacher, 51
 Villard, 51
 voltage multiplying, 51
 Witka, 51
Clay and soil minerals, 383
Close-packing, 326
Clupein thymonucleate, 663
Coal, radiography of, 174
Cobaltamines, 374
Collagen, 651
Colloids, diffraction by, 466, 486
 flocculation of, 193
Coloration by x-rays of glass and
 minerals, 196
Combination principle, 112, 124
Complex coordination compounds,
 374
Compton effect, 139
Concrete, as protection against
 x-rays, 149
Condenser discharge tube, 38
Conductivity, effects of x-rays on,
 69
Constants, lattice, for elements, 327
Contour map, electron density, 321
Coolidge tube, 23, 29
 for quantitative analysis, 130
Cooling, 32
Coordination number, 341, 350, 352
Copper sulfate pentahydrate, 370
Copper-zinc alloys, 396

Corrosion of alloys, 393
Counterfeit coins, 151
Covalent bonds, 343
Crystal chemistry, 357
Crystal systems, 235
Crystallography, fundamentals of, 233
Crystals, classification of, 338, 340
 x-ray diffraction, 82
Cubic body-centered structure, structure factor of, 316
Cubic face-centered structure, structure factor of, 316
Current, measurement of, 58
Cybotaxis, theory of, 478
Cyclol structure of proteins, 658
Cycloparaffins, 433

D

Debye-Waller intensity correction, 315
Defect structures, 362
Deformation textures of metals, 531, 543
Denaturation of proteins, 654, 655
Density of crystals, 279
Diagnosis, medical, 153
Diamond and copper space-groups, 243
Diamond structure, 416
Diatomic molecules in solids, 330
Diffraction, by crystals, 7, 81
 of electrons, 10
 by fibers, 311
 of hydrogen atoms, 11
 interferences, 81, 254
 by liquids, 477
 methods, 256
 by powders, 267
 tubes for, 40
Diffraction analysis, apparatus for, 256, 257
 information from, 254
 methods of, 256, 257
 steps in, 249, 278
Discovery of x-rays, 1
Disorder in the solid state, 362
Distortion, residual, in silicon steel, 570
Dosage, measurement of, 62
Dosimeters, biological, 200
Doublets, 113
Drosophila, eggs as dosimeter, 200
Duane and Hunt, law of, 92, 93
Duane ionization chamber, 65
Durene, 453
Dusts, diffraction analysis of, 381

E

Eder's solution, 194
Effective wave length, 146
Electric steel, structure and magnetic properties of, 565
Electrical conductivity, 69
Electrical precautions, 60
Electrodeposited metals, texture of, 552
Electrodes, insulation of, 25
Electromagnetic waves, 6
Electrometer, 86
Electron compounds, 397
Electron density, Fourier analysis of, 320
Electrons, back diffusion of, 26
 dual nature of, 10
Elements, crystalline structure of, 324
 constants for, 327
 discovery of, 111
 lattice types of, 325
Embryos, effect on, 205
Energy-level diagram, 122
Energy relation, photochemical, 191
Erythema, 211
Esters, 438
Exposure charts, 160
Extinction, corrections for, 318
Extinctions, determination of space-group from, 284

F

Fatigue of metals, 588
Fiber diagrams, 519

Fiber pattern, 257, 311
Filament, double, 35
 line focus, 33
 spiral, 23
Films, 441
Filters, 108
Filtration, 144
"Fingerprint" of crystals, 309
Fluorescence, 71
 biological use of, 73
Fluorescent characteristic x-rays,
 138
Fluorescent coefficient of absorption,
 136
Fluorescent screen, 72
Fluoroscopy, 157
Focal spot, 22, 30
Formaldehyde polymers, 596
Forming copper, 580
Forming steels, 579
Formulas, interplanar spacing, 281,
 283
Fourier analysis, in radial distribu-
 tion functions, 472
Fourier method of analysis, 319, 320
Frequency law in Bohr theory, 115
Frey-Wyssling method, 623
Fringe and net structure of cellulose,
 620
Fruits, fluoroscopic inspection of,
 168

G

Gage, uniformity of, 151
 γ -rays, 9, 184
Gelatin, 652
Generation of x-rays, 5
Genetics and x-rays, 202
Glasses, 388, 468
 coloration of, 196
 diffraction by, 467
 examples of, 474
 structural theories of, 468
Glide planes, 242, 247
Globular proteins, 654
Gnomonic projection, of Laue pat-
 terns, 288

Gold-copper alloys, 394
Goniometer, patterns, 267
 Schiebold-Sauter, 264, 362
 Weissenberg, 263, 264
Grain size, colloidal, 490
Graphite, structure, 416
Gratings, 89
Grid-biased tube, 35
Gutta-percha, 645
Gypsum, 372

H

Hafnium, 112, 131
Half-value thickness, 134
Hardness, of alloys, 406
 of crystals, 341
Hearing, effect of rays on, 215
Heat-treatment of cold-rolled foils,
 555
Hemoglobins, 656
Hereditary material, effect of x-rays
 on, 201
Hexamethylbenzene, 448
Homopolar bonds, 343
 single-electron, 344
 three-electron, 344
Hormones, 459
Hydrates, types of, 370
Hydrogen atom, diffraction of, 11
Hydrogen bond, 348
 in oxalic acid crystals, 425
 in pentaerythritol, 423
Hydrogen peroxide, liquid, 483
 reactions involving, 190
Hydrous oxides, 372
Hysteresis in crystallization of rub-
 ber, 643

I

Ice, structure of, 483
Illinium, 112
Indices, Miller, 234
Industrial diagnosis, 156
Insulation of electrodes, 25
Insulin, 655
Intensifying screens, 72, 162

- Intensities of x-ray interferences,
 laws of, 313-323
 structure factor, 317
 Intensity, measurement of, 62
 biological method, 78
 chemical method, 77
 coloration method, 196
 fluorescent method, 72
 heat method, 62
 ionization method, 63
 photographic method, 74
 selenium-cell method, 70
 Intermetallic compounds, 397
 β -phase, 397
 β' -phase, 398
 γ -phase, 399
 ϵ -phase, 400
 Inversions, rotary, 247
 Iodates, structure of, 361
 Ionic bond, 338, 340
 in crystals, 342
 Ionization by x-rays, 63
 Ionization chambers, 65
 Iron alloys, binary, 403
 Isodesmic crystals, 342, 361
 Isomorphism, 360
- J
- Jewel pivots in watch movements,
 511
- K
- K* series, 99
 Kenotron, 47
 Keratin, 648
 Ketones, 439
 Klein-Nishina formula, 142
 Kronig theory of fine structure, 124
- L
- L* series, 102
 Laue equation for grain size, 492
 Laue method and patterns, 256, 257
 interpretation of, 286
 projection of patterns, 287
 symmetry effects of, 287
- Layer lattices, 354
 Layer lines, 293
 Lead, colloidal, as protection against
 x-rays, 148
 Lead compounds, powder patterns
 of, 310
 Leather, 150
 Lignin, 632
 Lindemann glass, 42
 Liquid crystals, 483
 Liquids, conductivity of, 70
 diffraction by, 477
 Long-chain compounds, 427
 Lubricating films, 445
 Luminescence, excitation of, 70
 Lyman series, 110, 114
- M
- M* series, 103
 Magnesium alloys, deformation
 structures of, 537
 Magnetic alloys, 412
 Magnetic field, effect on liquid
 crystals, 485
 Magnetic measurements on organic
 crystals, 460
 Manganese, β , structure of, 329
 Mass absorption, coefficient, 135
 Measurement of diffraction films,
 279
 Mechanism of biological action, 216
 Medical diagnosis, 153
 Mesodesmic crystals, 342
 Mesomorphic states, 483
 Metal radiography, 173
 applications of, 173
 tubes for, 15
 Metallic bond, 347
 Metallic state, properties of, 390
 Metastability, effect of x-rays upon,
 196
 Methane, derivatives, 422
 Methods of diffraction analysis, 256
 Micas, 386
 Micellar theory, 617
 Microphotometer, 77
 Microradiography, 180

Microscope, ultraviolet, 10
 Microsymmetry, elements, 242, 284
 Miller indices of planes, 234
 Minerals, coloration of, by x-rays, 196
 Mixed oxides, 361
 Mixtures, determination of composition, 151
 Modulus for residual distortion, 569
 Molecular bond, 349
 Molecule, importance of, in solids, 233
 Momentum law in Bohr theory, 115
 Monochromatic x-rays, 107
 Montmorillonite, 384
 Morphotropism, 360
 Morphotropy of A_2BO_4 , 368
 Moseley law, 109, 110, 124
 Multiple diffraction apparatus, 274–276
 Muscle protein, 651
 Mutations, produced by x-rays, 203
 Myosin, 651

N

N series, 103
 Naphthalene, 447, 451
 Nematic state, 483
 Nerve structure, 659
 Nickel, bright deposits, 510
 Nickel electrodeposited films, 551
 Nile blue sulfate solutions, 488
 Nucleic acids, 662
 Nylon, 598

O

Optical properties of crystals, 369
 Orbits, electron, 115
 Order-disorder transformations, 395
 Organic compounds, decomposition of, by x-rays, 192
 Organic molecules, x-ray analysis, 417
 Orientation, of grains, 510
 molecular, 441
 Oxalic acid, dihydrate, 425

P

Paintings, radiographic examination of, 177
 Paracrystalline state, 476
 Paraffin hydrocarbons, 430
 Paraffin wax, 433
 Particle size, colloidal, 490
 in microscopic range, 504
 from small-angle scattering, 504
 Particles, cellulose, 619
 Paschen series, 114
 Patterson-Harker synthesis, 322
 Pauli exclusion principle, 120
 Pauling rules, 376
 Penetrometer, Benoist, 146
 Pentaerythritol, 423
 Perovskite structure, 361
 Peroxides and dioxides, 365
 Phosphorus, amorphous and liquid, 476
 Phosphorus pentachloride, structure of, 374
 Photochemistry, 185, 215
 Photoelectrons, 186
 Photographic effect of x-rays, 74, 160
 Photon, 10
 Phthalocyanines, 456
 Planck action constant, 92
 Planck-Einstein quantum equation, 92
 Planes in crystals, indices of, 234
 Plastic deformation, mechanism, 543
 Point groups, 240
 Polarization, 345, 353
 Pole figures, 541
 Polyamides, synthetic, 598
 Polyesters, synthetic, 597
 Polyethyleneoxides, 597
 Polymerization, definition of, 594
 examples and mechanisms, 596
 Polymers, classification of, 594
 importance of, 593
 natural and synthetic, 595
 relation of properties and chain length, 602

- Polymorphism, 324, 360
 in long-chain compounds, 431, 436, 440
 Polynuclear anions, nuclear, 367
 Polyoxymethylenes, 597
 Polyphosphornitrylchloride, 602
 Polyprenes, synthetic, 599
 Polysaccharides, 632
 Polysulfones, 602
 Pore size, from dye solutions, 488
 Porosity, 151
 Potassium persulfate, decomposition of, 187
 Potentials, critical excitation, 121
 Powder diffraction, 267
 interpretation of, 305
 practical use of, 309
 typical examples of, 300
 use of reciprocal lattice in, 307
 Preston spots on Laue patterns, 290
 Prism, refraction in, 89
 Production of x-rays, efficiency of, 79
 Projections of space-groups, 248, 249
 Propellers, airplane, 590
 Properties, prediction of, 341
 of x-rays, 11
 Protection from x-rays, 147
 Protein single crystals, 655
 Proteins, 646
 monomolecular films of, 658
 synthesis of, 659
- Q
- Qualitative analysis, 130
 Quality, measurement of, 80, 146
 Quantitative analysis, 130
 Quantum numbers, 116, 118
 Quantum theory, 116
- R
- r*-meter, 65, 66
r unit, 67
 Radial distribution calculations, 472
 Radicals, anion, in solids, 365
 Radii, atomic, 358
 of atoms and ions, 354
 covalent, 355
 ionic, 358
 van der Waals, 359
 Radiography, 152
 applications of, 173
 industrial diagnosis by, 156
 medical diagnosis by, 153
 tubes for, 15
 Radiopathology, 218
 Radius ratios, 350
 Rails, structure of, 588
 Random network structure of glasses, 469
 Rating of tubes, 32, 34, 37
 Ray cell, 616
 Rays, β , 143
 cathode, 3, 6
 γ , 184
 Grenz, 15
 Hertzian, 7
 radio, 9
 Roentgen, 4
 ultraviolet, 9
 visible, 9
 Reactions, chemical, 77, 194, 215
 Reciprocal lattice, 294
 analysis of urea for, 303
 goniometer patterns in, 302
 interpretation of rotation patterns in, 299
 powder patterns for, 307
 Recoil electrons, 187
 Recovery from radiation, 211
 Recrystallization of aluminum sheet, 556
 of copper, 560
 effect of impurities on, 558, 562
 of silver, 550
 of silver-copper alloy, 562
 of wires, 563
 Rectification, 49, 50
 Rectifiers, 46, 47, 49
 Reflection, total, 88, 89
 Refraction, 88
 Resins, synthetic, 477
 Resistor ribbon, 583
 Resonance, 346
 Resonance transformer, 56, 58

Rhenium, 112
 Richardson equation, 24
 Rock salt, structure of, 340
 Rolled sheets, fiber structure of, 532
 Rotation in the solid state, 368
 Rotation method and patterns,
 257, 260
 interpretation of, 291
 reciprocal lattice interpretation of,
 299, 300
 Rubber, frozen, 638
 sol and gel, 639
 stretched, 635
 theories of structure, 639
 unstretched, 476
 vulcanized, 641
 Rule of $8 - n$, 330
 Rydberg constant, 112

S

Satellites, 110, 123
 Scattering of x-rays, 134, 138
 Scherrer equation for colloidal grain
 size, 491
 Schiebold-Sauter goniometer, 264,
 362
 Screw axis, 242, 246
 Selenium, crystal structure of, 331
 Shape of colloidal particles, 499
 Sheet metals, stages in reduction by
 cold rolling, 573
 Sheets, recrystallization of, 556-562
 Shockproof equipment, 61
 Silica, forms of, 380
 Silicates, 375
 classification of, 378
 defect structures in, 378
 Silicosis, diagnosis of, 381
 Silk fibroin, 646
 Silver mercuric iodide, 364
 Sloan generator, 55
 Smectic state, 483
 Soaps, 439
 Sodium bronze, structure of, 361, 362
 Sodium oleate micelle, 487
 Soil profiles, 386
 Solid solutions, interstitial, 401
 substitutional, 392, 394
 Solid state of matter, 231
 structure of, 232
 Sols, grain size in, 496
 Solutions, diffraction by, 485
 Space-group notation, 243
 Space-groups, 242
 determination from extinctions,
 284
 notation for, 250
 projections of, 248, 249
 Space-lattice, 236, 238
 Spacing, interplanar, 281, 283
 Spectra, absorption, 95, 98, 120
 chemical analysis from, 126
 continuous, 92
 crystals for, 82
 emission, 94, 99, 119
 K series, 99
 L series, 102
 M and *N* series, 103
 ruled grating, 89
 Spectrograph, 128
 Spectrometer, double, 87, 107
 ionization, 84
 Spectrometry, 257, 260
 Spinel structure, 361
 Starch, 631
 Steel, alloy, 411
 analysis of texture of rolled sheets,
 534
 carbon, 404
 Stereographic projection of Laue
 pattern, 287
 Sterols, 459
 Stimulation by x-rays, 214
 Storage battery, high-voltage, 44
 Strain, internal, 511, 512
 mechanism of, 517
 Streaming sols, structure of, 487
 Stresses from line shifts, 515
 Structure factor, atomic f_0 , 314
 crystal, F , 315
 examples of, 316
 relation to intensities, 317
 Strukturbericht, 324
 Sugars, 458

- Sulfur, conductivity of, 69
 fibers of, 602
Sulfur oxy-acids, 367
Sulfur trioxide, transformations of, 196
Superstructures, superlattices, 394
Supervoltage therapy, 225
Surfaces, molecular orientation in, 441
Susceptibilities, magnetic, 460
Swelling, types of, 631
Symmetry in crystals, 240
 axes, 241, 245
 center, 24
 glide plane, 242
 plane, 241, 247
 screw axis, 242, 246
Synthetic polymers, 595
Synthetic rubber, 599
- T
- Tangent drop method, 428
Targets, rotating, 36
 stationary, 32
 thin plate, 24
Therapy, supervoltage, 225
Thiokol, 601
Tin, crystallography of, 236
Tissues, effect of x-rays on, 210, 211
Tolerance dose, 148
Topochemical reactions of cellulose, 628
Transformers, 45, 56
Tubes, x-ray, 15
 Aminco-Ksanda, 19
 Baird, 20
 cascade, 30
 condenser discharge, 38
 Coolidge, 23, 29
 deep therapy, 15, 26
 demountable, 42
 design of, 25
 diagnostic, 42
 diffraction, 40, 42
 double focus, 35
 electron, 15, 23
 Tubes, x-ray, gas, 15
 grid-biased, 35
 Hadding-Siegbahn, 18
 high-intensity, 38
 ion, 15
 Lauritsen, 29
 life of, 24
 line-filament, 33, 35
 metal radiographic, 15
 Metalix, 27, 28, 42
 miniature, 20
 Ott-Selmayr, 42
 radio tube as, 20
 rating of, 32, 34
 Roentgen's, 16, 17, 37
 rotating anode, 36
 Seemann, 18
 self-shielding, 40
 Shearer, 19
 shockproof, 39, 41
 Siemens-Pantix, 26
 supervoltage, 27, 29, 30
 XP, 35
Tungsten, filaments, 23
Twisting of wires, 584
- U
- Ultramarines, 377
Unit cell, 237
Urea, goniometer pattern and interpretation, 303
- V
- Vacuum, Coolidge, 23
Valence, and x-ray spectra, 105
Valve-tube rectifier, 47, 48
Van de Graaf generators, 29, 54
van der Waals bond, 349
Vector model of atom, 118
Vegard's additivity law, 393
Vinyl polymers, 600
Violins, wood structure in, 616
Viruses, 656
Vitamins, 460
Voltage, measurement of, 58
Vulcanization, 644

W

- Watch springs, 591
- Water, 370
 - reactions of, 189
 - structure of, 481, 482
- Wave lengths, effect on intensity, 68
 - measurements of, 80, 103
- Weissenberg goniometer, 263, 264
- Welds, soundness of, 171
 - structure of, 579
- Wires, fiber structure of, 521, 527
 - recrystallization of, 563
 - zonal structure of, 528
- Wood structure, 615

X

- X-rays, biological effects of, 198
 - chemical effects of, 77, 194, 215

- X-rays, effect on tissues, 210
 - and genetics, 202
 - ionization by, 63
 - monochromatic, 107
 - photographic effect of, 74, 160
 - physical effects of, 62
 - properties of, 11
 - protection from, 147
- X-unit, 8

Z

- Zeolites, 372, 377
- Zinc, mechanism of deformation, 545
- Zinc sulfide, structure factor for, 316
- Zonal structure of wires, 528
- Zone, crystal, 236
- Zone theory of metals, 391

UNIVERSITY OF ILLINOIS-URBANA



3 0112 068721619